Design and synthesis of new potential drugs for the treatment of Human African Trypanosomiasis

A Thesis submitted to the University of Wales for the Degree of

Doctor of Philosophy

by

Alessandro Baliani

November 2005

Supervisor: Professor Ian Gilbert

ProQuest LLC
789 East Eisenhower Parkway
P.O. Box 1346
Ann Arbor, MI 48106-1346

Dedicated to my parents, my brother Luca
for believing in me and
to my beloved grandmother that will
always have a special place in my heart.

***

Dedicata ai miei genitori e a mio fratello,
per tutta la fiducia, l'amore e il supporto
ed in particolare a mia nonna,
per l'amore ed i momenti indimenticabili
che resteranno sempre vivi nel mio cuore.

Abstract

Parasitic protozoa are the cause of most widespread diseases known to man and include malaria, toxoplasmosis, African sleeping sickness and Leishmaniasis. Human African trypanosomiasis (sleeping sickness) is caused by two subspecies of *Trypanosoma brucei*, *T. brucei gambiense* and *T. brucei rhodesiense,* which are transmitted by tsetse flies. Adverse side effects and drug resistance have led to a re-emergence of African trypanosomiasis in sub-Saharan Africa and therefore new drugs are urgently needed.

The rational approach toward the development of new potential chemotherapeutics focuses on differences in biochemistry and metabolism between the human host and the causative agent. The P2 transporter is a nucleoside transporter which is unique to the protozoan parasite *Trypanosoma brucei*. It has been shown that the transporter transports some structural motifs not recognised by other transporters. The P2 transporter was considered as a possible target to exert a selective effect against parasites but not against host cells. The principal of this rational approach is to attach P2 recognition motifs (e.g. the melamine unit) to cytotoxic agents.

A series of nitroheterocyclic compounds was designed with linkages to melamine groups which are known substrates of the P2 transporter in African trypanosomes. The compounds were prepared from the 2,4-diamino-6-chlorotriazine by displacement of the chlorine by hydrazine and then condensation with the appropriate nitrofuraldehyde.

A series of nitroheterocycles were also designed with linkage to benzamidine as P2 recognition motif. The chemistry and the solubility of these compounds hindered the establishment of a valid synthetic procedure in order to link the nitroheterocycle to the benzamidine.

All the compounds were assayed for their ability to inhibit adenosine uptake by the P2 transporter. *In vitro* toxicity against intact bloodstream form trypomastigotes of *T.b. brucei* and *T. b. rhodesiense* was also measured. Several compounds showed *in vitro* trypanotoxicity with IC_{50} concentrations in the nanomolar range. Compound **6** and compound **54** showed an IC_{50} against *T. b. rhodesiense* line of 25 nM and 18 nM respectively. Two compounds retained their trypanocidal effect in mice curing all the mice infected with a STIB 795 *T. b. brucei* model of infection. One compound cured also 1 mouse of 4 infected with the more stringent model STIB 900 *T. b. rhodesiense*. The comet assay showed that the compound is not genotoxic at the doses tested, indicating that this is a good drug lead against HAT.

Acknowledgements

First of all I would like to thank the Welsh School of Pharmacy for funding this project in Cardiff and the Wellcome Trust, UNDP/World Bank/ WHO special Programme for Research and Training in Tropical Diseases for funding.

A very special thank to Professor Ian Gilbert, my supervisor, for being helpful, patient, encouraging and for giving me the chance to work in UK.

Thanks for their collaboration to Dr. Michael P. Barrett and his group at the University of Glasgow, Institute of Biomedical and Life Sciences, Division of Infection & Immunity.

Thanks to Dr. Reto Brun and his group for their collaboration at the Swiss Tropical Institute, Basel, Switzerland.

Thanks to Dr. Simon Croft and his group at the London School of Hygiene and Tropical Medicine, London.

A very special thank to Ron Edwards for all his help with the mass spectrometer and all the laboratory technicians for their help and technical support.

I would like to thank all the member and ex member of my group, Silvia, Didier, Simon, Christophe, Cyrille, Toba, Gian Filippo, Ludovic, Shane, Corinne, Federica, Orlagh, Salvatore, Alessandro S., Olivier, and Valery for being encouraging and helpful whenever I needed them and for the wonderful atmosphere in the laboratory.

I would like also to thank some friends, members of the School, Betty, Federica, Francesca, Jérome, Felice, Giovanna, Abdel, Nurol, Malina, Cristina, Thet Thet, for the wonderful time in Cardiff.

A special thank to my friends in Italy, Daniele, Maurizio, Tatiana, Francesco and Roberto.

Also a special thank to my aunt Sandra and to my cousins Sabrina and Barbara for all their support and kindness.

Publications

Part of this thesis has been published in the following journals:

- Stewart, M. L.; Bueno, G. J.; Baliani, A.; Klenke, B.; Brun, R.; Brock, J. M.; Gilbert, I. H.; Barrett, M. P. **Trypanocidal activity of melamine-based nitroheterocycles.** *Antimicrob. Agents Chemother.* **2004**, *48*, 1733-1738.

- Baliani, A.; Bueno, G. J.; Stewart, M. L.; Yardley, V.; Brun, R.; Barrett, M. P.; Gilbert, I. H. **Design and synthesis of a series of melamine-based nitroheterocycles with activity against trypanosomatid parasites.** *J. Med. Chem.* **2005**, *48*, 5570-5579.

The full articles are referred in the Appendix 2.

Table of Contents

1. Introduction:

2. The P2 transporter:

5. Results and Discussion III:

6. Biological results:

7. Conclusions: 185

8. Experimental I:

Triazine Derivatives

9. Experimental Section II:

Amidine Derivatives

Abbreviations & Acronyms

Ac	Acetyl
Ado	Adenosine
AT1	Adenosine transporter type 1
Bn	Benzyl
Boc	1,1-Dimethylethoxycarbonyl (*tert*-butoxycarbonyl)
BSA	Bovine serum albumin
bsf	Blood stream form
BZ	Benznidazole
cat.	Catalytic
Cbz-Cl	Benzyloxycarbonyl-chloride
cDNA	recombinant DNA
CNS	Central nervous system
d	Doublet
Da	Dalton
dATP	Deoxyadenosine triphosphate
DCC	Dicyclohexylcarbodiimide
DCM	Dichloromethane
dCTP	Deoxycytidine triphosphate
DFMO	Difluoromethylornithine
dGTP	Deoxyguanosine triphosphate
DHAP	Dihydroxyacetone Phosphate
DFMO	Difluoromethylornithine
DIPC	Diisopropylcarbodiimide
DIPEA	Diisopropylethylamine
DIPU	Diisipropyl urea
DMAP	Dimethylaminopyridine
DMAPP	Dimethylallyl Pyrosphosphate

DMF	Dimethylformamide
DMSO	Dimethylsulfoxide
DNA	Deoxyribonucleic acid
ED_{50}	Effective dose for 50% reduction of organisms
EDC	1-(3-Dimethylaminopropyl)-3-ethylcarbodiimide hydrochloride
EDTA	Ethyl diamino tetra acetic acid
Endo III	Endonuclease III
eq.	Equivalent
ES	Electrospray ionisation
Et	Ethyl
FBS	Fetal bovine serum
FPG	Formamido Pyrimidine DNA-glycosylase
FPPS	farnesyl-pyrosphosphate synthase
G3P	Glycerol-3-Phosphate
h	Hour
HAPT	High Affinity Pentamidine Transporter
HAT	Human African Trypanosomiasis
hENT	Human Equilibrative Nucleoside Transporter
HOBt	1-Hydroxybenzotriazole
HRMS	High resolution mass spectrometry
Hz	Hertz
IC_{50}	Concentration required for 50% inhibition
IMBI	Irreversible mechanism based inhibitor
IPP	Isopentenyl Pyrophosphate
IR	Infrared spectroscopy
iPr	Isopropyl
J	Coupling constant
Kb	Kilobase
kDa	Kilodalton
kDNA	Kinetoplastid DNA
Ki	Inhibition constant
L-6 cells	rat skeletal myoblasts
LAPT	Low Affinity Pentamidine transporter
LHMDS	Lithium 1,1,1,3,3,3-hexamethyldisilazane
LRMS	Low resolution mass spectrometry

m	Multiplet
M	Molar concentration
Me	Methyl
MED	Minimal effective dose
min.	Minute
Mp	Melting point
MS	Mass spectroscopy
MSA	Methansulfonic Acid
mRNA	Messenger ribonucleic acid
ms	Milli-second
MS	Mass spectrometry
MST	Mean survival time
MW	Molecular weight
NAC	N-acetyl-glucosamine
n-but	*normal*-Butyl
NMR	Nuclear magnetic resonance spectroscopy
n-Pro	*normal*-Propyl
ODC	Ornithine decarboxylase
PBS	Phosphate buffered saline
PCR	Polymerisation chain reaction
PG	Protecting group
Ph	Phenyl
ppm	Part per million
Pr	Propyl
Pyr	Pyridine
q	Quadruplet
quint	Quintuplet
R	Substituent
R_f	Retention factor
RNA	Ribonucleic acid
r.t.	Room temperature
s	Singlet
SM	Starting material
SOD	Superoxide dismutase
t	Triplet
TBAF	Tetrabutylammonium fluoride

tBu	*tert*-Butyl
TBDMS	*tert*-Butyldimethylsilyl
TBDPS	*tert*-butyl-chlorodiphenyl-silane
TBTU	2-(1*H*-Benzotriazol-1-yl)-1,1,3,3-tetramethyluronium tetrafluoroborate
TEA	Triethylamine
TFA	Trifluoroacetic acid
THF	Tetrahydrofuran
TL	Total Length
TLC	Thin layer chromatography
TbNT	*T. brucei* nucleoside transporter gene.
UV	Ultraviolet spectrometry
VSG	Varian Surface Glycoproteins
WHO	World health organisation

1. Introduction:

Human African Trypanosomiasis

Parasitic protozoa infect hundreds of million of people and are responsible for some of the most important diseases and around the world such as malaria, toxoplasmosis, leishmaniasis and human African trypanosomiasis. Comparatively little research is done in the field and the funds available for further investigations reflect by no means the number and the seriousness of cases. The research described in this thesis focused on human African trypanosomiasis.

1.1 Introduction

Human African Trypanosomiasis (HAT) or sleeping sickness represents a serious public health threat in Africa. 60 million people in 36 countries of sub-Saharan Africa are at risk of contracting the disease and only three to four million inhabitants are under reasonably regular medical surveillance[1]. The 45000 new cases reported in 1999 to the World Health Organisation (WHO) do not reflect the reality of the situation, but simply show the absence of detection and underscore the inadequacy of the current campaign against this disease. 300,000-500,000 people are estimated to be infected with HAT[2]. The disease is difficult to diagnose and

[1] Bouteille, B.; Oukem, O.; Bisser, S.; Dumas, M. Treatment perspectives for human African trypanosomiasis. *Fundam. Clin. Pharmacol.* **2003**, *17*, 171-181.

[2] WHO; Report on Global Surveillance of Epidemic-prone Infectious Diseases - African trypanosomiasis; WHO Press Release, 2001.

treat even in regions where medications are available. The clinical and the therapeutic management of the disease is complicated by multiple factors such as political and economical realities together with the complexity of the disease itself[1].

HAT is caused by subspecies of *Trypanosoma brucei*, a parasitic protozoa transmitted in Africa by tsetse flies. There are two forms of human African trypanosomiasis caused by two sub-species of *T. brucei*: a chronic form of infection caused by *Trypanosoma brucei gambiense* and a more acute infection caused by *Trypanosoma brucei rhodesiense*[3]. The distribution of the two forms of sleeping sickness differs substantially: the chronic form is distributed in Central and West Africa whereas the acute form is distributed in South and East Africa. Infection with either subspecies is fatal if untreated.

A third subspecies of Trypanosoma, *Trypanosoma brucei brucei*, is responsible of the animal trypanosomiasis also known as "Nagana" and is not infectious to human beings.

African countries can be divided in four different categories (as shown on figure 1.1) in terms of prevalence of the disease[4]:

1) epidemic;
2) highly endemic;
3) low endemicity;
4) at risk.

[3] Kuzoe, F.; Jannin, J.; Brun, R.; Ndungu, J.; Büscher, P.; Miaka Bilenge, C.; Van Nieuwenhove, S.; Doua, F.; Mbulamberi, D.; Burri, C.; Aksoy, S. Human African trypanosomiasis. *Nat. Rev. Microbiol.* **2004**, *2*, 186-187.

[4] http://www.who.int/inf-fs/en/fact259.html. World Health Organisation; African trypanosomiasis or sleeping sickness. *WHO Fact Sheet* 259 [online], **2001**.

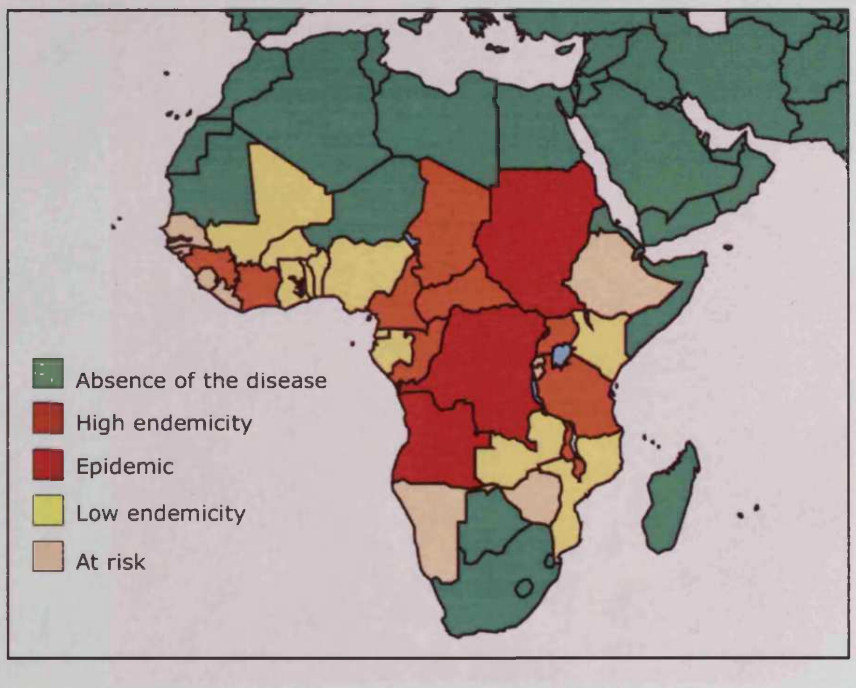

Figure 1.1: distribution of the human African trypanosomiasis. The different colours show the different prevalence of the disease[3].

1.2 The parasite and the vector:

The genus *Trypanosoma* is responsible for many parasitic diseases affecting man and other vertebrates which are the final hosts[5]. Trypanosomes are usually parasites of the blood stream even if there are some species that can adapt to an intracellular existence.

The Trypanosome species can be divided into two major groups on the basis of their development in vertebrates:

- ***Stercoraria*** (e.g. *Trypanosoma cruzi*): *Stercoraria* Trypanosomes (*Trypanosoma cruzi*, American trypanosomiasis) live in the blood and in the muscles of the heart and gut. Transmission of the parasites from the vector to the vertebrate host is through vector faecal contamination.
- ***Salivaria*** Salivarian trypanosomes (e.g. *Trypanosoma b. gambiense*, *T. b. rhodesiense* and *T. b. brucei*) live in body fluids including the blood and in late stages the cerebrospinal fluid, where

[5] Dinah, M. J.; Gilles, H. M. Human Antiparasitic drugs: Pharmacology and usage; Wiley, 1985.

they grow and divide by binary fission. Transmission in most cases involves insect vectors (tsetse flies) by blood feeding[6].

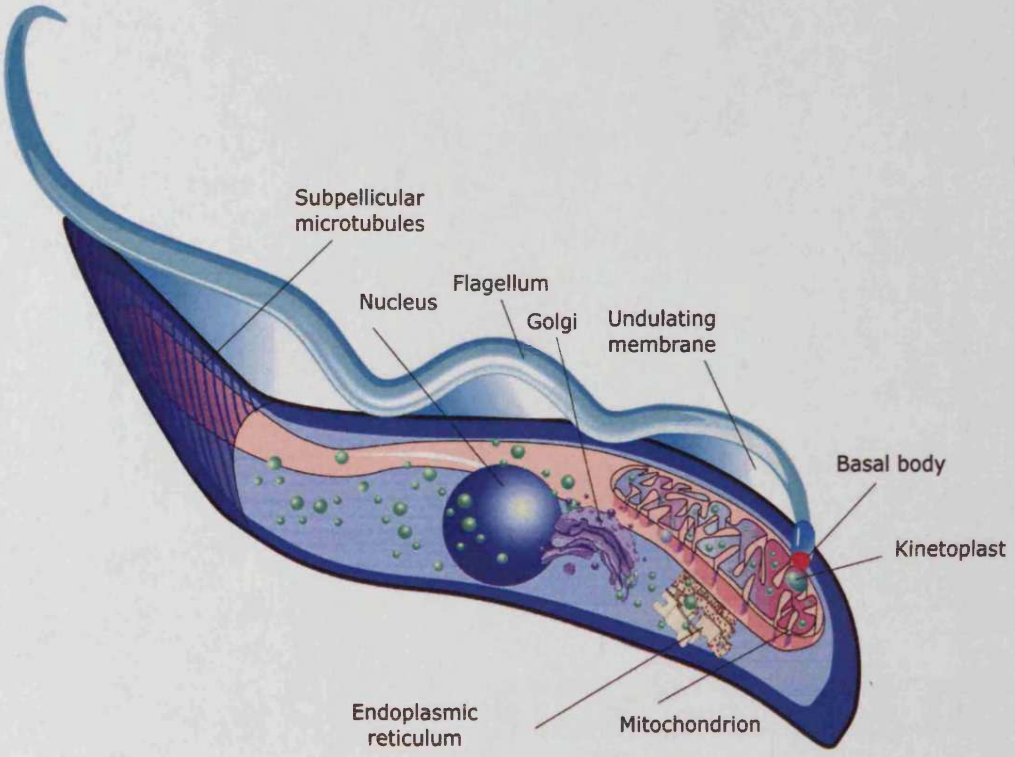

Figure 1.2 Structure of a *Trypanosoma brucei* (bloodstream form).

The genus *Trypanosoma,* together with the Leishmania is included in the protozoan order Kinetoplastida. The kinetoplastids are a widespread group of single cell-eukaryote flagellated protozoa. The main feature of this group of protozoa is an organelle known as kinetoplast which is a staining oval body smaller and distinct from the nucleus[7]. The organelle is near the base of the flagellum (or occasionally near a basal body). As the name suggests, its original function was believed to be involved with the motility of flagellum[8]. Actually it represents a distinct region of the mitochondria that contains extranuclear DNA (kinetoplastid DNA). Kinetoplastid DNA is relatively abundant and consists of concatenated mass

[6] Cross, G. A. M. *Ann. Rev. immunol.* **1990**, *83.*

[7] Molyneaux, D. H.; Ashford, R. W. The biology of Trypanosoma and Leishmania, parasites of man and domestic animals; 1st ed.; Taylor & Francis Ltd: London, 1983.

[8] Fries, D. S.; Fairlamb, A. H. Antiprotozoal Agents. *Burger's Medicinal Chemistry and Drug Discovery*; Sixth ed.; John Wiley & Sons, Inc, 2003; pp 1033-1088.

of mini and maxi-circles[8]. The maxi circles are present in few copies and encode for mitochondrial genes whereas mini circles are present in many copies and their function is less clear.

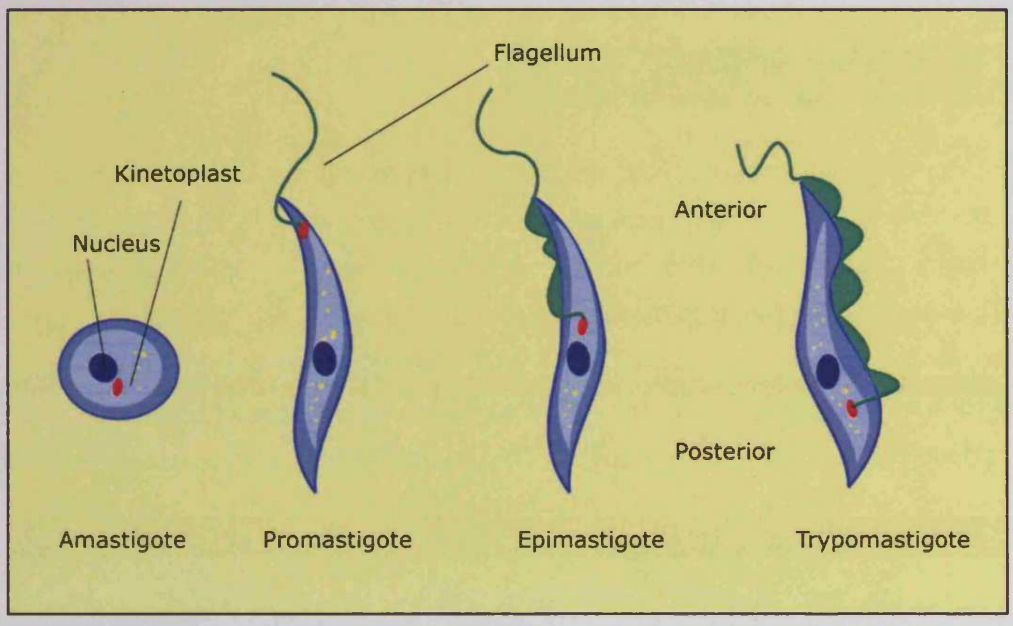

Figure 1.3 Different morphological forms of Trypanosomes.

The various kinetoplastid species exhibit different morphological forms (picture 1.3) that are distinguished by the position of the kinetoplastid in relation to the nucleus and the presence or absence of an undulating membrane[5]:

- **Trypomastigote**: the kinetoplastid is located posterior to the nucleus. The flagella folds back along the body of the parasite forming an undulating membrane which runs the entire length of the cell;
- **Epimastigote**: the kinetoplast is located more centrally, usually just anterior to the nucleus. This results in a shorter undulating membrane;
- **Promastigote**: the kinetoplast is between the nucleus and the anterior end and no undulating membrane is formed.
- **Amastigote**: form found as intracellular stage (*T. cruzi*). The parasite is more rounded and has no flagella;

- **Metacyclic trypomastigote**: represents the end of the invertebrate cycle. These resemble the blood forms but they are smaller and infective to vertebrates.

1.3 The Life cycle of *T. brucei*:

The entire life cycle of African trypanosomes is represented by extracellular stages and can be divided into tsetse fly stages and human stages (figure 1.4). The human stages start when an infected tsetse fly (genus *Glossina*) injects metacyclic trypomastigotes into skin tissue during a blood meal in the mammalian host. The parasites enter the lymphatic system and pass into the bloodstream where they transform into bloodstream trypomastigotes[9]. The bloodstream trypomastigotes are carried to other sites throughout the body, reach other blood fluids (e.g., lymph, spinal fluid), and continue the replication by binary fission. The tsetse fly stages start when a tsetse fly takes a blood meal with bloodstream trypomastigotes on an infected mammalian. In the infected fly's midgut, the parasites transform into procyclic epimastigotes, multiply by binary fission, leave the midgut, and transform into epimastigotes. The epimastigotes reach the fly's salivary glands and continue multiplication by binary fission[9]. The cycle in the fly takes approximately 3 weeks.

After cessation of division, the epimastigote starts to express a dense variable surface glycoprotein coat (VSG coat) and this expression leads to detachment and maturation as non-dividing, infective metacyclic trypanomastigotes[6]. The VSG coat accounts for about 10 % of the total protein of the bloodstream forms of *T. brucei.* The variability lies in the fact that the parasite can shed its coat and build a new one by expressing another surface glycoprotein[6]. The sequential expression of VSGs results in an ever-changing antigenic pattern. Antigenic variation, in the manner and to the extent that it occurs in the African trypanosomes, is unique to the parasites and appears to be the primary mechanism for evasion of the hosts' immune responses[6]. Humans are the main reservoir for *Trypanosoma brucei gambiense* but this species can be also found in

[9] http://www.dpd.cdc.gov/dpdx Parasites and Health. African Trypanosomiasis. Pubblic Information Fact sheet, 2 August 2004.

animals. Wild game animals are the main reservoir of *T. brucei rhodesiense*[9].

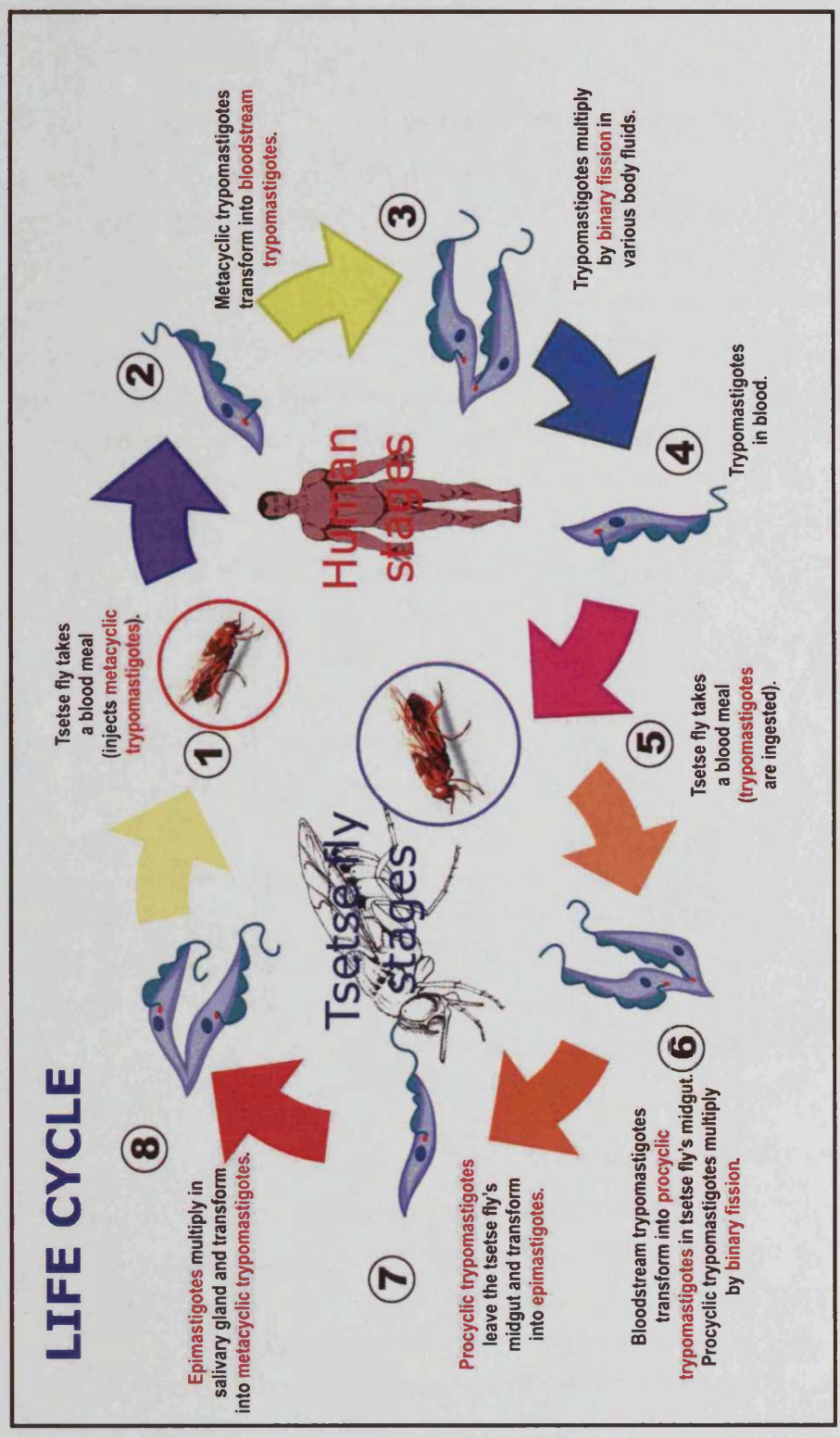

Figure 1.4: Life cycle of *Trypanosoma brucei*.

1.4 Pathology:

The disorder can be distinguished in two stages depending on whether the parasites have become manifest in the cerebrospinal fluid:

1.4.1 Stage 1 (haemolymphatic stage):

After their inoculation, the parasites proliferate at the site of infection leading to an inflammatory nodule or ulcer also called trypanosomal chancre (figure 1.5). The chancre appears in about 50% of the *rhodesiense* infections but rarely in *gambiense* infections[10]. After 3–4 weeks, the chancre heals and the parasites spread to the draining lymph node and reach the bloodstream, initiating the haemolymphatic stage of the disease[10]. This stage is characterised by general malaise, headache, and fever of an undulating type[10].

The *rhodesiense* infection, with its more acute course, is characterised by pancarditis with congestive heart failure, pericardial effusion, and pulmonary oedema can cause fatalities at this early stage. The gambiense infection, in contrast to the *rhodesiense* infection, shows more insidious development that is frequently unrecognised or misdiagnosed. A typical sign of gambiense human African trypanosomiasis is generalised lymphadenopathy that develops after several weeks, frequently in the posterior triangle of the neck[10].

Figure 1.5. Trypanosomal Chacre[10].

1.4.2 Stage 2 (CNS stage):

In this stage the parasites invade internal organs such as the CNS. This usually happens within few weeks in the *T. b. rhodesiense* infection and can take several months and sometimes years in *T. b. gambiense* infection. The stage 2 is characterised by immunosuppression and as it progresses severe headache and sleep disorders appear (figure 1.6). The

[10] Barrett, P. M.; Burchmore, R. J. S.; Stich, A.; Lazzari, J. O.; Frasch, A. C.; Cazzulo, J. J.; Krishna, S. The trypanosomiases. *The lancet* **2003**, *362*, 1469-1479.

name sleeping sickness was coined because of early recognition of diurnal somnolence and nocturnal insomnia. Together with these manifestations there are personality changes and impairing of the mental functions. Progressive CNS involvement culminates in coma and death in untreated cases[10].

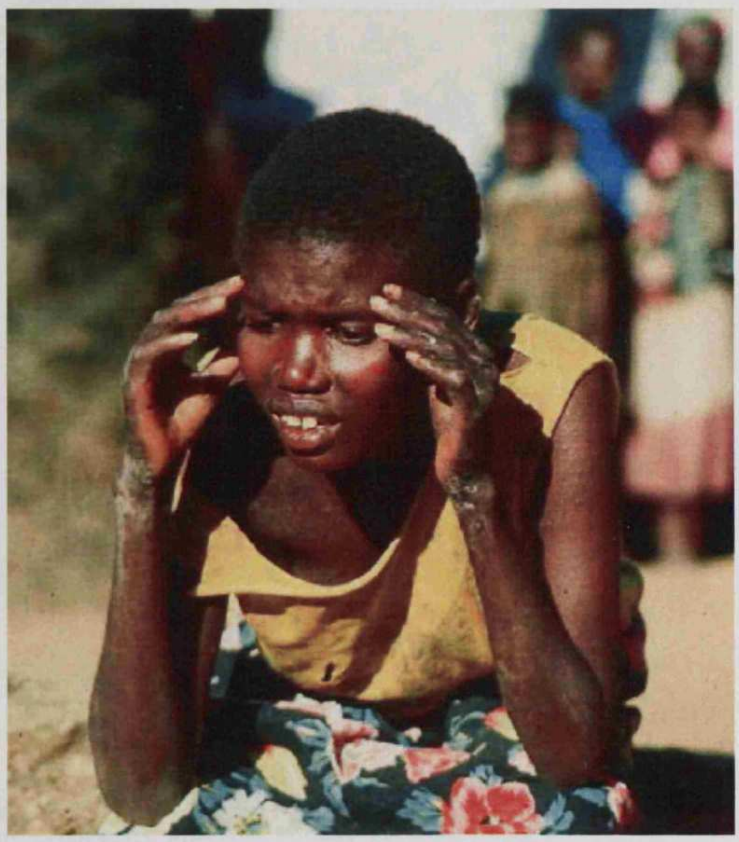

Figure 1.6 Patient with stage 2 HAT[10].

1.5 Vector control:

Apart from drug treatment of infected patients the disease is generally fought via its vector, the tsetse fly. The flies pass most of their time at rest in shaded places in forested areas. The preferred sites are the lower woody parts of vegetation; many tsetse flies hide in holes in the trunks of trees and between roots.

Traps and screens are an effective means of tsetse control. They are cheap, easy to transport, and completely safe for the user and the environment. Once a suitable trap or screen has been developed for a given area, no special expertise is needed in order to use it. This method is

therefore ideally suited for anyone seeking to provide cheap and effective community protection[11]. The flies search for blood-meals or resting places partly or wholly by sight, and are attracted by large objects that move or contrast with the landscape. Certain colours, especially blue, attract many tsetse flies.

1.5.1 Biconical trap

The biconical trap (figure 1.7) was one of the earliest models to be designed. It is not used in large-scale control operations because of its relatively high price and complicated structure. However, it is still used to monitor the effectiveness of tsetse fly control activities. The lower cone is made of electric-blue cotton or synthetic cloth. The inner part is divided into four compartments by four segments of black cloth. Four openings allow the flies to enter the blue cone. The upper cone is made of mosquito netting, and flies are caught in the top part, by a simple trapping device[11].

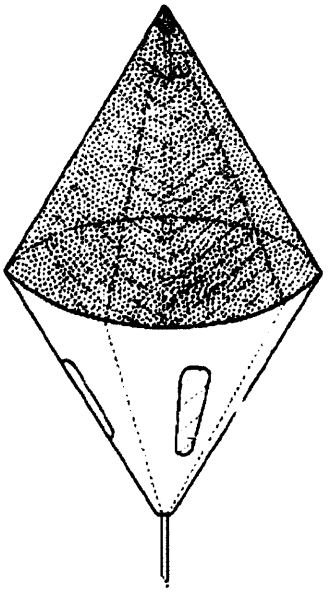

Figure 1.7 The biconical trap. The cones are separated into four compartments by four segments of black cloth[11].

1.5.2 The pyramidal trap:

The pyramidal trap consists of a pyramid of transparent white mosquito netting surmounting two black and two blue screens arranged in the form of a cross (Fig.1.8). It was developed in the Congo[12] and is currently being extensively used in Uganda. If provided with a catching device at the top this trap can be used without an insecticide and is then suitable for areas with high rainfall. In large-scale programmes it offers the advantage that it is very compact for storage.

[11] www.who.int/publications chapter 2.Tsetse flies; WHO, 1997; pp 178-192.

[12] Power, J. In *TDR news,*, 1989; pp 3.

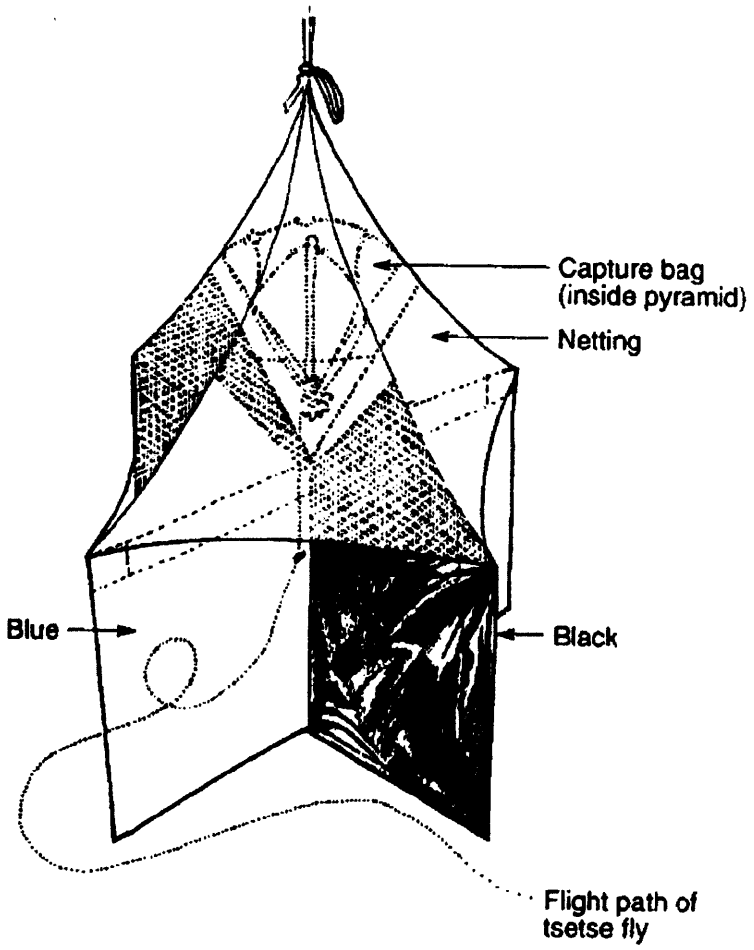

Figure 1.8 Scheme of a pyramidal trap[11].

1.5.3 Impregnated screens

Unlike traps, screens are effective in killing tsetse flies only when impregnated with an insecticide. The most commonly used screen consists of a strip of electric-blue material made of cotton and polyester or plastic with a strip of black nylon sheeting on either side, giving a total size of about $1m^2$. The screen is attached to two wooden laths and suspended from a branch by means of a rope or from a metal support driven into the earth[11].

1.6 Drug Targets:

A number of different drug targets that could be considered in order to have a selective action of the drug. Genetic manipulation methods are now available to validate these targets[13, 14].

1.6.1 Glucose metabolism:

African trypanosomes are dependent on glycolysis for energy production[10]. In bloodstream *T. brucei*, the first seven steps of glycolysis occur in glycosomes which are organelles similar to peroxisomes. The NADH produced during glycolysis inside the glycosomes is reoxidised within the organelles by molecular oxygen via dihydroxyacetone phosphate (**DHAP**): glycerol-3-phosphate (**G3P**) shuttle combination with a terminal G3P oxidase in the mitochondrion. The high activity and specificity for G3P of the oxidase is sufficient to account for the high rate of respiration of bloodstream trypanosomes[15, 16]. The trypanosomal glycolytic enzymes have some differences compared to the mammalian ones and could therefore considered as another chemotherapeutic targets[17,18].

---

[13] Clayton, C. E. Genetic manipulation of kinetoplastida. *Parasitol. Today* **1999**, *15*, 72-78.

[14] Kelly, J. M.; Taylor, M. C.; Rudenko, G.; Blundell, P. A. Transfection of the African and American trypanosomes. *Methods Mol. Biol.* **1995**, *47*, 349-359.

[15] Opperdoes, F. R.; Bakker, B. M.; Westerhoff, H. V. Metabolic control analysis of glycolysis in trypanosomes as an approach to improve selectivity and effectiveness of drugs. *Mol. Biochem. Parasitol.* **2000**, 106, 1-10.

[16] Michels, P. A. M.; Hannaert, V.; Bringaud, F. Metabolic aspect of glyosomes in trypanosomatidae - New data and views. *Parasitol. Today* **2000**, *16*, 482-489.

[17] Verlinde, C. L. M. J.; Hannaert, V.; Blonski, C.; Willson, M.; Perie, J. J.; Fothergill-Gilmore, L. A.; Opperdoes, F. R.; Gelb, M. H.; Hol, W. G. J.; Michels, P. A. M. Glycolysis as a target for the design of new anti-trypanosome drugs. *Drug Resist. Updates* **2001**, *4*, 50-65.

[18] Aronov, A. M.; Suresh, S.; Buckner, F. S.; Van Voorhis, W. C.; Verlinde, C. L. M. J.; Opperdoes, F. R.; Hol, W. G. J.; Gelb, M. H. Structure-based design of submicromolar, biologically active inhibitors of trypanosomatid glyceraldehyde-3-phosphate dehydrogenase. Proc. Natl. Acad. Sci. U. S. A. **1999**, *96*, 4273-4278.

1.6.2 Lipid and isoprenoid metabolism:

Trypanosomes survive in the human bloodstream by virtue of a dense cell surface coat made of variant surface glycoproteins (VSGs). The VSG of bloodstream African trypanosomes is anchored to the cell surface by a GPI that contains myristate as its only fatty acid component[19]. African trypanosomes can produce myristate for use in GPI anchor remodelling. Inhibition of myristate biosynthesis has recently been considered since the relationship with a trypanocidal effect[20].

Protein farnesyl transferases are also being investigated as targets[21, 22].

1.6.3 Polyamines metabolism:

The polyamines putrescine and spermidine play an essential role in cell differentiation and proliferation[19, 23]. Ornithine serves as the principal precursor in their synthesis. Ornithine decarboxylase, S-AdoMet decarboxylase and spermidine synthase have crucial functions. Compounds interfering with polyamine biosynthesis[24,25] such as D,L-α-

[19] Keiser, J.; Stich, A.; Burri, C. New drugs for the treatment of human African trypanosomiasis: research and development. *Trends Parasitol.* 2001, 17, 42-49.

[20] Paul, K. S.; Jiang, D.; Morita, Y. S.; Englund, P. T. Fatty acid synthesis in African trypanosomes: A solution to the myristate mystery. *Trends Parasitol.* **2001**, *17*, 381-387.

[21] Buckner, F. S.; Yokoyama, K.; Nguyen, L.; Grewal, A.; Erdjument-Bromage, H.; Tempst, P.; Strickland, C. L.; Xiao, L.; Van Voorhis, W. C.; Gelb, M. H. Cloning, heterologous expression, and distinct substrate specificity of protein farnesyltransferase from Trypanosoma brucei. *J. Biol. Chem.* **2000**, *275*, 21870-21877.

[22] Ali, B. R. S.; Pal, A.; Croft, S. L.; Taylor, R. J. K.; Field, M. C. The farnesyltransferase inhibitor manumycin A is a novel trypanocide with a complex mode of action including major effects on mitochondria. *Mol. Biochem. Parasit.* **1999**, *104*, 67-80.

[23] Schechter, P. J.; Barlow, J. L. R.; Sjoerdsma, A. *Inhibition of polyamine metabolism*; Academic Press, Inc.: New York, 1987; 345.

[24] Muller, S.; Coombs, G. H.; Walter, R. D. Targeting polyamines of parasitic protozoa in chemotherapy. *Trends Parasitol.* **2001**, *17*, 242-249.

difluoromethylornithine (**DFMO**) have been used as therapeutic agents and will be described separately in this chapter.

1.6.4 Thiol metabolism:

The existence of trypanothione reductase represents one of the fundamental metabolic differences between host and parasite. In fact, in trypanosomes trypanothione reductase replace the role of glutathione reductase in mammals. Therefore trypanothione is a good target candidate and its inhibition is expected to compromise the redox defences of the parasite and to increase sensitivity to drugs unbalancing the redox equilibrium of the parasite[19].

1.6.5 Membrane transporters:

Since parasites take nutrients from their host, they have membrane transporters specialised for the uptake of essential metabolites. Blockage of these vital transporters represents another good drug target and will be described separately on chapter 2.

1.6.6 Topoisomerases:

Topoisomerases are enzymes involved in the topological control of the kinetoplast DNA (kDNA) during replication, transcription and recombination. The inhibition of these enzymes is another promising theoretical approach for new antitrypanosomal drugs[26]. However, because kDNA is not essential for the parasite survival, nuclear rather than mitochondrial topoisomerases might be the main drug targets[27].

---

[25] Bacchi, C. J.; Nathan, H. C.; Hutner, S. H.; McCann, P. P.; Sjoerdsma, A. Polyamine metabolism: a potential therapeutic target in trypanosomes. *Science* **1980**, *210*, 332-334.

[26] Wang, J. DNA topoisomerases as targets of therapeutics: an overview. *Adv. Pharmacol.* **1994**, *29A*, 1-19.

[27] Burri, C.; Bodley, A. L.; Shapiro, T. A. Topoisomerases in kinetoplastids. *Parasitol. Today* **1996**, 12, 226-231.

1.7 Treatment of human African trypanosomiasis:

The surface of the parasite is shrouded by a glycoprotein coat. There are up to a thousand genes encoding antigenically distinct version of this coat; this antigenic variation process gives the parasite the capacity to avoid the immune-response by the host[28]. This process represents the main problem for potential vaccines against the parasite.

Three of the four currently approved drugs for the treatment of HAT were developed over 50 years and all the current therapies are unsatisfactory for different reasons[29]: serious side effects, poor efficacy, undesirable routes of administration and increasing of drug resistance[30]. Therefore new drugs are urgently needed.

The WHO and Médecins Sans Frontières finally obtained commitments from the Aventis Pharma, Bristol-Myers Squibb and Bayer pharmaceutical companies to provide stocks of all trypanocides for at least 5-year period[31]. However, there is a constant threat that production of the currently used drugs will be interrupted because is not profitable[19].

Currently there are only few trypanocidal drugs in Phase I-III of clinical development. Considering that it takes at least 6 years to get approval for a compound after the first application to humans (Table 1.1) it is very unlikely that any new trypanocidal drug will be registered in this decade[19].

The treatment of the HAT depends on the clinical stage of the disease: the haemolymphatic stage is treated with pentamidine (Pentacarinat®; Aventis), suramin (Germanin®; Bayer). Diminazene aceturate (Berenil®; Intervet) is used only for veterinary. The neurological stage relies on the use of melarsoprol (Arsobal®; Aventis) although it does

---

[28] Fairlamb, A. H.; Borst, P. Surface receptors and transporters of *trypanosoma brucei*. *Annu. Rev. Microbiol.* **1998**, *52*, 745-778.

[29] Fairlamb, A. H. Chemotherapy of human African trypanosomiasis: current and future prospects. *Trends Parasitol.* **2003**, *19*, 488-494.

[30] Fairlamb, A. H.; Barrett, M. P. The biochemical basis of arsenical-diamidine crossresistance in African trypanosome. *Parasitology Today* **1999**, *14*, 136-140.

[31] WHO; (www.who.int/inf-pr-2001/fr/cp2001-23.html) L'organisation Mondiale de la Santé et Aventis annoncent une initiative majeure pour intensifier la lutte contre la maladie du sommeil. *Communiqué OMS/23, 3 May*, **2001**.

not meet current standards for approval because its toxicity. The use of other trypanocidal drug DL-α-difluoromethylornithine (DFMO, Ornidyl®; Bristol-Myers-Squibb) still has problems related to cost, supply and difficulty of administration under African health care conditions. By 1989 700 cases of *Trypanosoma brucei gambiense* infections have been treated in Phase III trials with a 95% cure rate. The drug was approved in 1990 by the US FDA and registered in Europe in 1991 and postmarketing testing is still ongoing[19]. Nifurtimox (Lampit®; Bayer) has been also recognised for its effectiveness but it has never received marketing authorisation for *T. b. gambiense* HAT and its use is reserved for cases that are refractory to all the other available treatments[1].

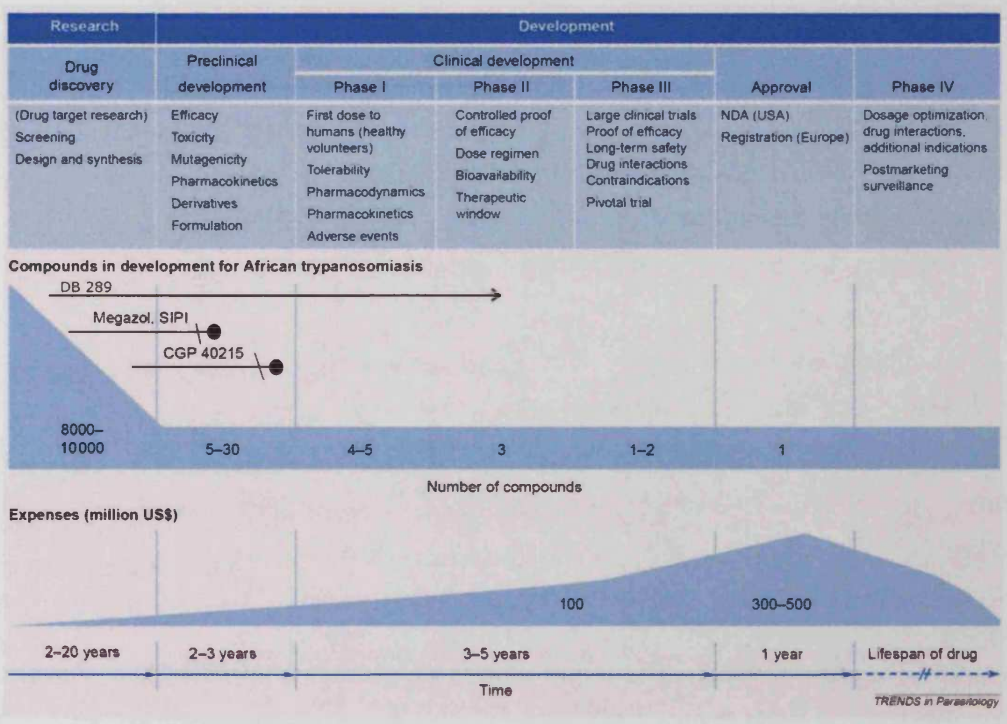

Table 1.1 Stage of drug research and development and HAT[19].

1.8 Suramin

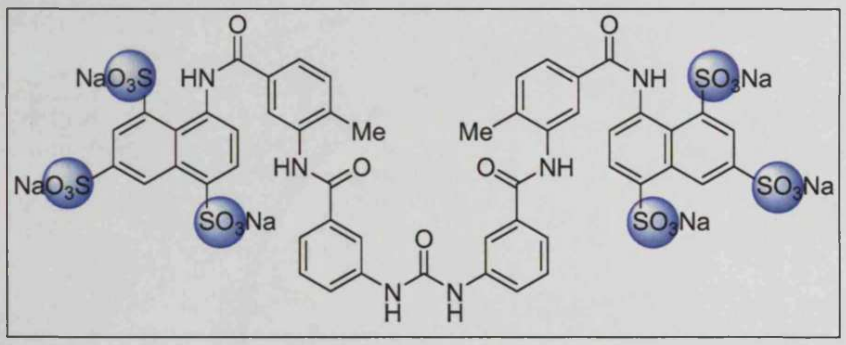

Scheme 1.1 Structure of Suramin.

Suramin (Germanin®;Bayer) was introduced in the early 1920s and today is still the drug of choice for treatment of the early stage of *T.b. rhodesiense* infections. Suramin is a symmetric polyanionic sulfonated naphthylamine (scheme 1.1), negatively charged at physiological pH, structurally related to Paul Ehrlich's trypan red with *in vivo* trypanocidal activity[32]. Suramin is absorbed by endocytosis and has a slow trypanocidal effect[33]. In the trypanosome is thought to inhibit several enzymes mainly involved in the glycolysis. The mode of action of the drug is still unclear. It is known that the drug is bound in serum with albumin and low density lipoprotein (LDL). LDL is also thought to be involved in the uptake of the drug via receptor mediated endocytosis (figure 1.9)[34].

Because of its ionic nature, the drug does not penetrate the CNS and is therefore used only in the primary stage of *T.b. rhodesiense* infections. The dosage for adults is usually 1g (for children is 20 mg/Kg) by i.v. injection on days 1, 3, 7, 14, and 21. Suramin is also effective in *T.b. gambiense* infection, but because of the risk of sudden shock in case of infection by *Onchocerca volvulus*, pentamidine should be preferred to it[1].

---

[32] Mansour, T. E. Antitrypanosomal and Antileishmanial Targets. *Chemotherapeutic Targets in Parasites*; University Press, Cambridge, **2002**; pp 90-128.

[33] Fairlamb, A. H.; Bowman, I. B. R. Uptake of the trypanocidal drug suramin by bloodstream forms of Trypanosoma brucei and its effect on respiration and growth rate in vivo. *Mol. Biochem. Parasit.* **1980**, *1*, 315-333.

[34] Vansterkenburg, E. L. M.; Coppens, I.; Wilting, J.; Bos, O. J. M.; Fischer, M. J. E.; Janssen, L. H. M.; Opperdoes, F. R. The uptake of the trypanocidal drug suramin in combination with low-density lipoproteins by *Trypanosoma brucei* and its possible mode of action. *Acta Trop.***1993**, *54*, 237-250.

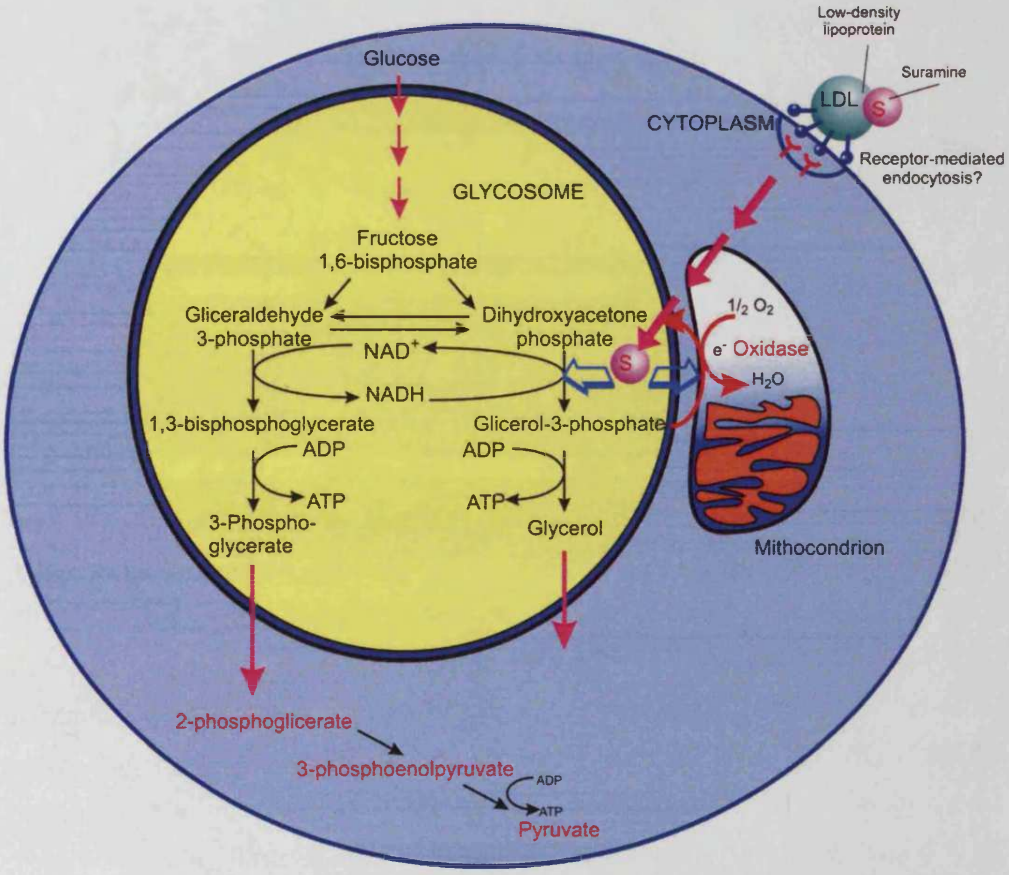

Figure 1.9 Representation of the supposed mechanism of action of suramin

The most serious and common side effect of suramin is that on the kidney[5]. The side effect usually becomes manifest after a few days of treatment and is the result of the irritant effect resulting from drug accumulation in the epithelia cells of the proximal convoluted tubules. Other side effects are fever, mucocutaneous eruptions, nausea, vomiting, haematological toxicity.

1.9 Pentamidine:

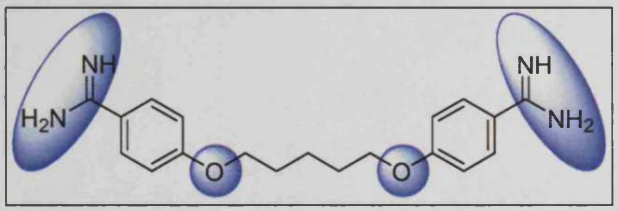

Scheme 1.2 Structure of pentamidine

Pentamidine (Lomidine®; Aventis) is an aromatic diamidine (scheme 1.2) introduced in 1940. The drug is still a drug of choice for the treatment of early stage infection of *T.b .gambiense* infections. The drug is highly protonated at physiological pH and therefore has a poor oral bioavailability.

The intramuscular administration (4 mg/Kg/d for 10 days) is preferred because of the severe hypotensive reaction that can occur after intravenous administration.

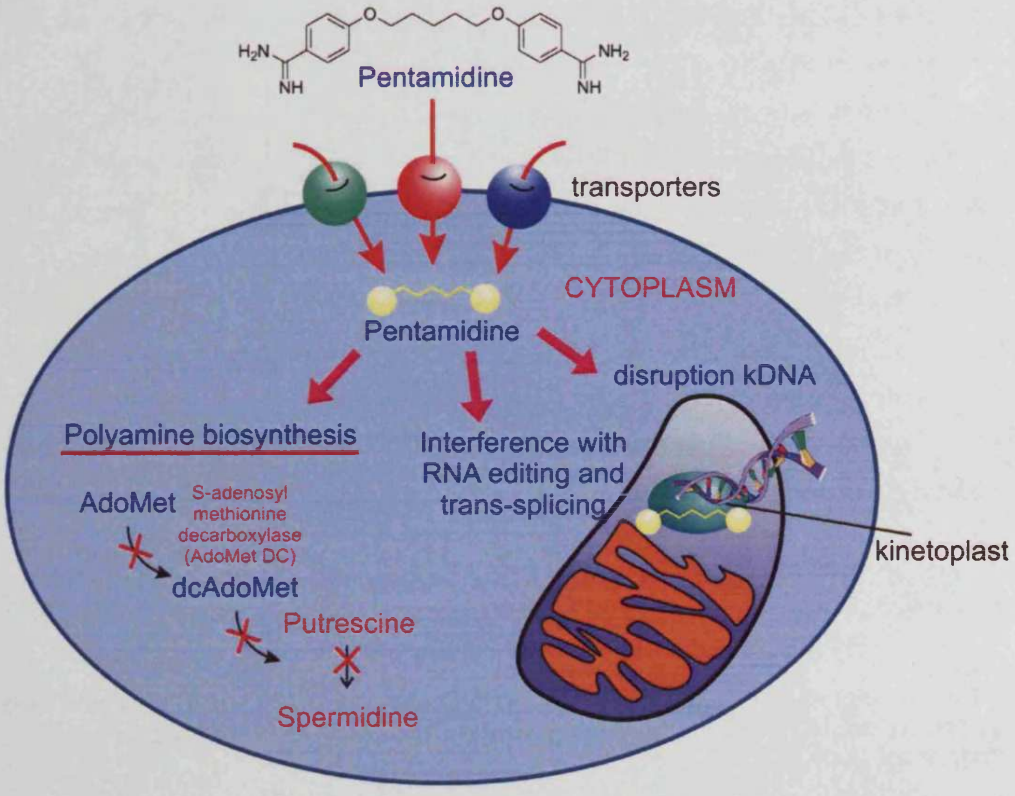

Figure 1.10 Mechanism of action of pentamidine.

The mechanism of action is still unclear. It is known that the drug is accumulated into the cell by at least three transporters (to be discussed later)[35],[36].

Pentamidine is thought to bind to negative charged cellular components such as phospholipids and nucleic acids, and disrupts the structure of the kinetoplast DNA (kDNA), by inhibiting topoisomerases II[37]. Another possible mechanism involves the interference with the polyamine biosynthesis by inhibiting the enzyme S-adenosylmethionine decarboxylase (AdoMet DC) that catalyse the formation of decarboxylated AdoMet that is required for the conversion of putrescine into spermidine (figure 1.10).

1.10 Melarsoprol:

Melarsoprol (Mel B, Arsolbal®; Aventis) was introduced in 1949 for the treatment of late stage of HAT either by *T.b. rhodesiense* or *T. b. gambiense*. Paul Ehrlich first introduced arsenicals as drugs for use against HAT at the beginning of the last century[38].

Chemically melarsoprol combines a trivalent organic derivative of arsenic called melarsen oxide with a heavy metal chelating agent called BAL (British Anti-Lewisite or dimercaprol). The combination reduces the toxicity of the drugs without reducing the pharmacological effect.

Melarsoprol is accumulates into the parasite through an unusual amino-purine transporter, P2 transporter, the loss of which leads to drug resistance[38].

As for the previous drugs, the mode of action of melarsoprol is not clearly understood. The drug acts as a pro-drug: once administered is

[35] Fairlamb, A. H.; Carter, N. S.; Berger, B. J. Uptake of Diamidine Drugs by the P2 Nucleoside Transporter in Melarsen-Sensitive and -Resistant *Trypanosoma-Brucei-Brucei*. *J. Biol. Chem.* **1995**, *270*, 28153-28157.

[36] De Kooning, H. P. Uptake of Pentamidine in *Trypanosoma brucei brucei* is Mediated by Three Distinct Transporters: implications for Cross-Resistance with Arsenicals. *Mol. Pharmacol.* **2001**, *59*, 586-592.

[37] Shapiro, T. A.; Englund, P. T. Selective cleavage of kinetoplast DNA minicircles promoted by antitrypanosomal drugs. *Proc. Natl. Acad. Sci. U. S. A.* **1990**, *87*, 950-954.

[38] Denise, H.; Barrett, M. P. Uptake and mode of action of drugs used against sleeping sickness. *Biochem. Pharmacol.* **2001**, *61*, 1-5.

rapidly converted into its active form or **melarsen oxide** which binds reversibly to serum proteins. Trivalent arsenicals are known to inhibit a wide number of enzymes or substrates that contain thiol groups. The selective toxic action of the drug is therefore related to the "selective uptake" into the parasite through the P2-purine transporter[35].

Melarsoprol reacts with trypanothione, a cofactor in oxidation-reduction mechanism in the trypanosome, to form a reversible but stable adduct called **Mel T.** The adduct acts as a competitive inhibitor of trypanothione reductase, an enzyme essential for maintaining the correct intracellular thiol-redox balance[39] (figure 1.11).

The overespression of a multidrug resistance protein (MRPA, a putatite thiol conjugate transporter) resulted in a tenfold greater resistance to melarsoprol[29].

Historically, it was thought that the mechanism of action of melarsoprol was related to its ability to inhibit enzymes essential for glycolysis (e.g. pyruvate kinase) in African trypanosomes. This is now known to be an immediate consequence of loss of cell integrity rather than a direct cause of cell lysis[40].

The drug is water insoluble and it is given intravenously (3.6 mg/Kg for 3-4 days series at 7-days intervals) dissolved in propylene glycol (highly irritant to tissues). The main side effect of melarsoprol is a serious reactive encephalopathy that occurs in 5-10% of cases. Other side effects are vomiting, abdominal colic, peripheral neuropathy, arthralgia and trombophlebitis.

---

[39] Fairlamb, A. H.; Henderson, G. B.; Cerami, A. Trypanothione is the primary target for arsenical drugs against African trypanosomes. *Proc. Natl. Acad. Sci. U. S. A.* **1989**, *86*, 2607-2611.

[40] Van Schaftingen, E.; Opperdoes, F. R.; Hers, H. G. Effects of various metabolic conditions and of the trivalent arsenical melarsen oxide on the intracellular levels of fructose 2,6-bisphosphate and of glycolytic intermediates in *Trypanosoma brucei*. *Eur. J. Biochem.* **1987**, *166*, 653-661.

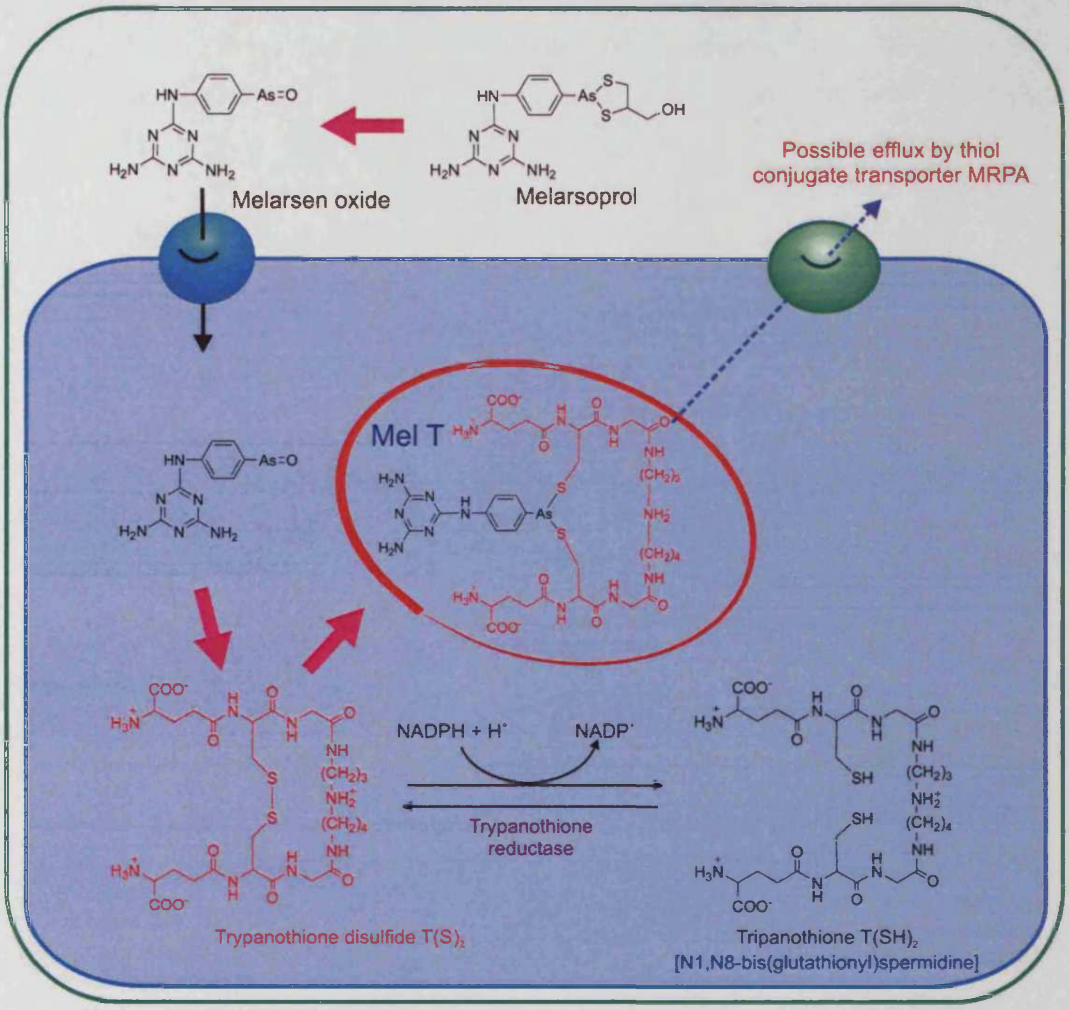

Figure 1.11. Mode of action of melarsoprol.

1.11 Eflornithine (DFMO):

Eflornithine was developed in 1977 as anticancer compound but it was ineffective and so abandoned for this use. Later it was found to be active *in vivo* against trypanosomes. Eflornithine is also known as DFMO or DL-α-difluoromethylornithine and represents a drug of choice for the treatment of late stage of *T. b. gambiense*. *T. b. rhodesiense* poorly responds to eflornithine.

The mechanism of action of DFMO is based on its irreversible and specific inhibition of **ornithine decarboxylase** (**ODC**) in trypanosomes

(figure 1.12 and 1.13). Decarboxylation of ornithine is a crucial step in the polyamine biosynthesis which is essential for the differentiation and the division of the parasite. **DL-α-difluoromethylornithine** is a so-called irreversible mechanism based inhibitor (**IMBI**). When ODC decarboxylases DFMO, an irreversible inhibitor is formed (figure 1.12) that reacts with the catalytic site of the enzyme[41].

The reason for its efficacy is not fully understood because DFMO is equally effective suicide inhibitor of mammalian ODC. A possible reason that can explain the selectivity in the parasite is the pronounced differences in turnover rates between the host and the parasite[42]. The inhibition of ODC induces:

- loss of putrescine and decrease of spermidine levels;
- decrease of trypanothione level;
- alteration of the AdoMet metabolism;

As consequence of the inhibition of ODC there are a series of effects:

- decrease of DNA, RNA, protein synthesis;
- reduced synthesis of variant surface glycoprotein;
- morphological and biochemical changes.

DFMO presents a pronounced synergic effect with melarsoprol (and other trivalent arsenicals) since they both induce depletion of intracellular trypanothione levels by reducing the synthesis and promoting the efflux[42]. Treatment with DFMO is expensive and it is also difficult to administer. The dosage is usually 400mg/Kg per day in 4 daily infusions over 2 h for 7 or 14 days which equates to a total dosage of approximately 3-6 g/Kg [29].

[41] Poulin, R.; Lu, L.; Ackermann, B.; Bey, P.; Pegg, A. E. Mechanism of the irreversible inactivation of mouse ornithine decarboxylase by alpha-difluoromethylornithine. Characterisation of sequences at the inhibitor and coenzyme binding site. *J. Biol. Chem.* **1992**, *267*, 150-158.

[42] Heby, O.; Roberts, S. C.; Ullman, B. Polyamine biosynthetic enzymes as drug targets in parasitic protozoa. *Biochem. Soc. T.* **2003**, *31*, 415-419.

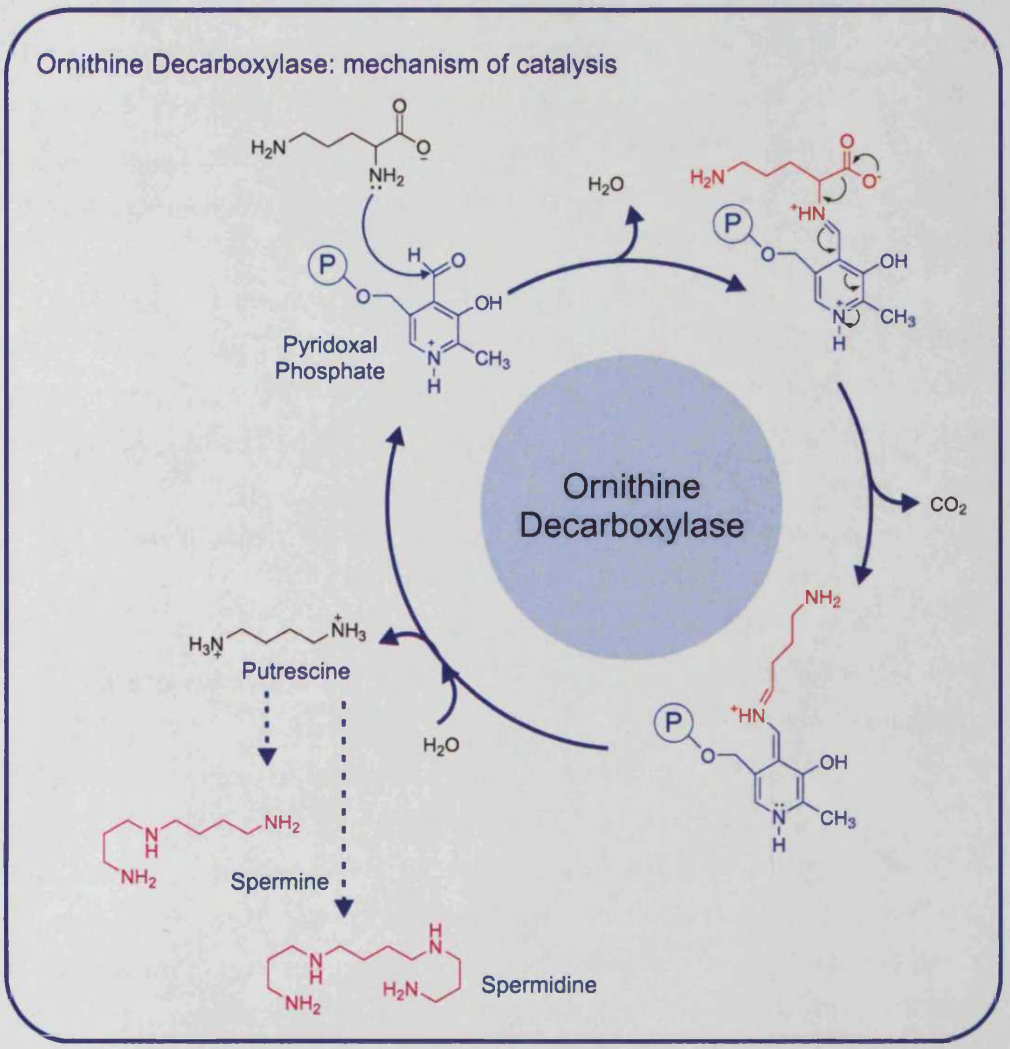

Figure 1.12 Mechanism of catalysis of Ornithine Decarboxylase (ODC).

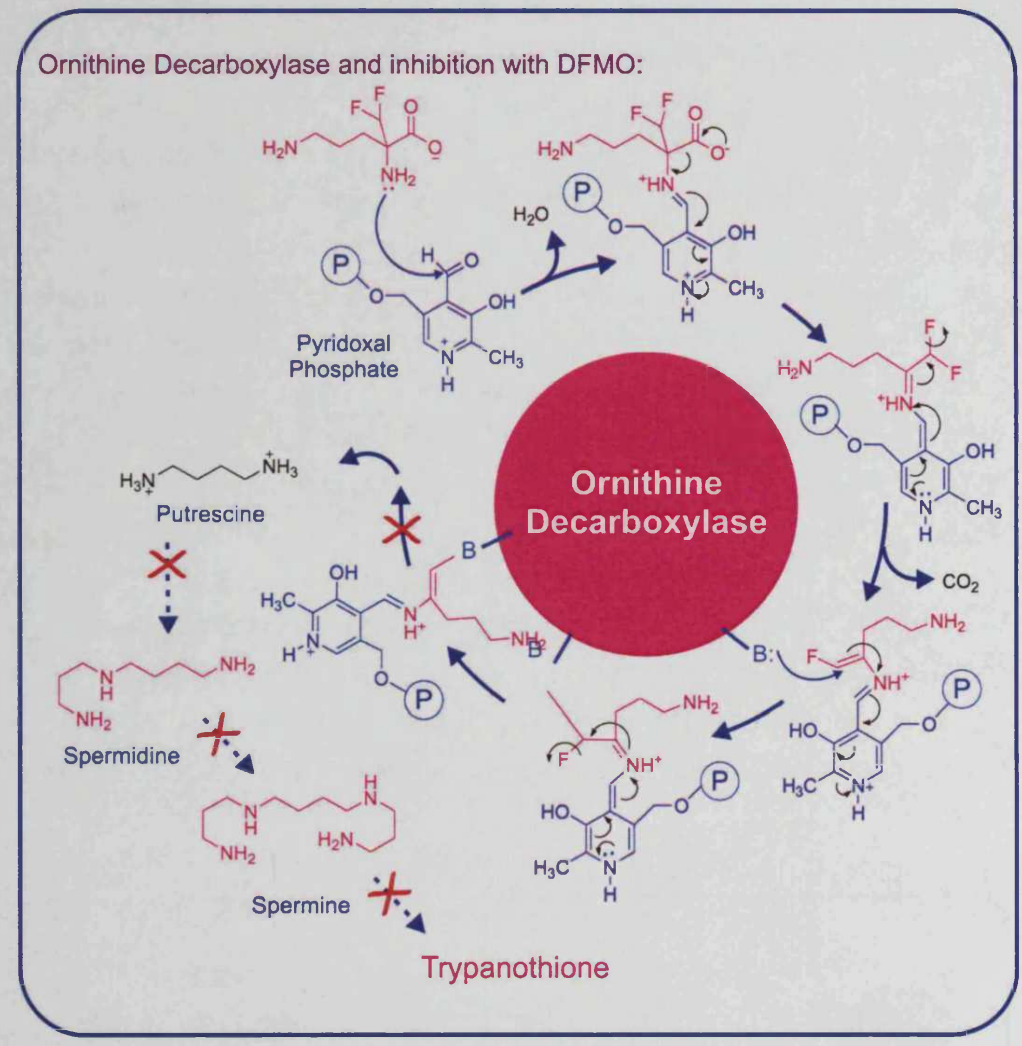

Figure 1.13 Suicide inhibition of Ornithine Decarboxylase (ODC) by DFMO.

1.12 Nifurtimox and 5-nitrofurans:

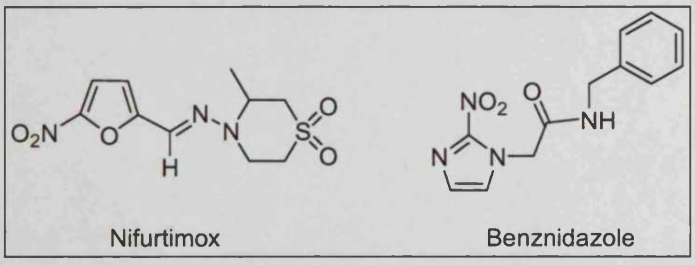

Scheme 1.3 structure of nitrofuran nifurtimox and nitroimidazole benznidazole.

Nifurtimox (Lampit®; Bayer) is a 5-nitrofuran derivative (scheme 1.3) that was introduced in 1976 for the treatment of American

trypanosomiasis (Chagas' Disease). Side effects are very common and in most of the cases it is not possible to complete a full course of treatment. However, the drug has been also used for the treatment of late stage HAT (*T. b. gambiense* infections) where eflornithine and melarsoprol are ineffective[29].

The mechanism of action of nifurtimox and other nitrofurans and nitroimidazoles (e.g. nitroimidazole, scheme 1.3) compounds remains uncertain. It is known that nifurtimox requires one electron reduction to form the nitro ion radical. NADH and NADPH can act as electron donors in this contest, but the enzyme(s) involved in the catalysis is still unknown (figure 1.14). The nitro ion radical is thought to reduce molecular oxygen to superoxide anion regenerating the original nitro-compound[8]. The cell is unable to cope with overproduction of superoxide anion; the superoxide is converted into other reactive oxygen species such as cell hydroxyl radical and hydrogen peroxide. These species together with the superoxide anion induce damage to DNA, proteins and membrane and culminate in cell death.

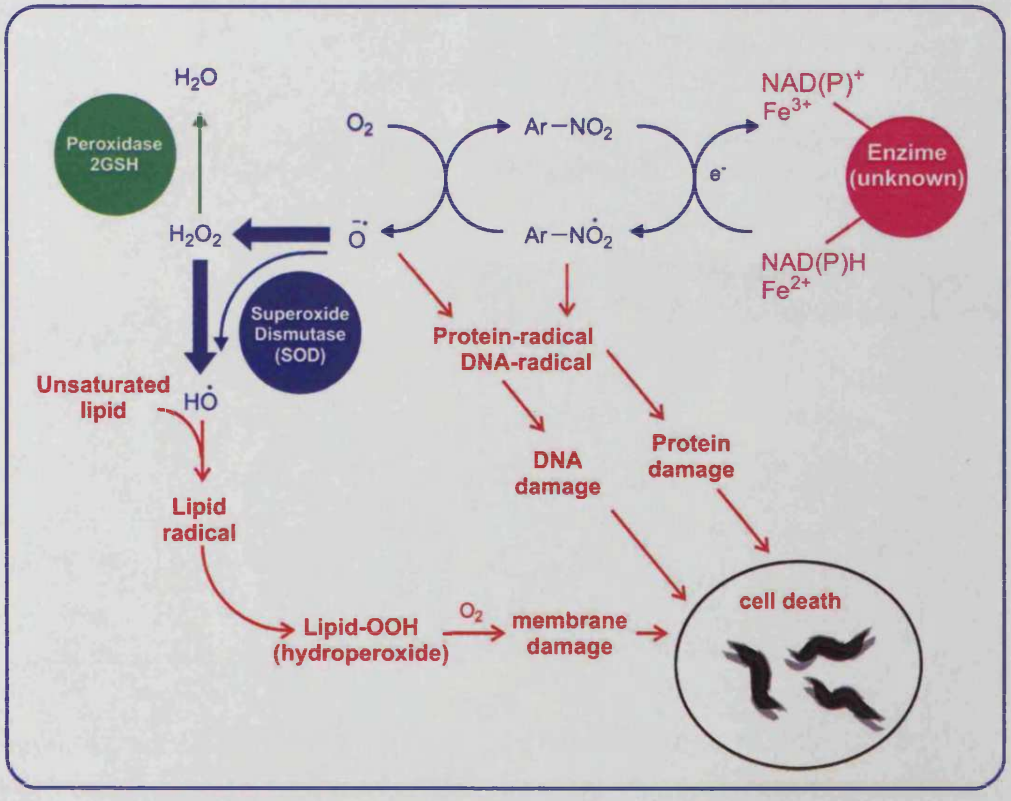

Scheme 1.14 Mechanism of action of nitroimidazole and nitrofurans.

2. The P2 transporter:

A drug target for chemotherapy.

Kinetoplastid parasites such as *Trypanosoma brucei*, lack the ability to synthesise important nutrients including purines; they are auxotrophs for these and must salvage the compounds from their hosts[43]. Purines are essential for the growth, multiplication, and survival of these organisms. In order to import these metabolites they have specialist nucleoside and nucleobase transporters[44]. The nucleoside/nucleobase transporters play an important role in chemotherapy since they represent an ideal way for the delivery and the internalisation of new drugs.

2.1 Nucleoside/nucleobase transporters in *T. brucei*:

Different nucleoside transporters were characterised in *Trypanosoma brucei* by Carter and Fairlamb, 1993[35, 45]. A **P1 type** system mediates the uptake of the purine nucleosides adenosine, inosine and guanosine and a **P2 type** system mediates the uptake of adenosine and

[43] Sanchez, M. A.; Tryon, R.; Green, J.; Boor, J.; Landfear, S. M. Six related nucleoside/nucleobase transporters from *Trypanosoma brucei* exhibit distinct biochemical functions. *J. Biol. Chem.* **2002**, *277*, 21499-21504.

[44] Baliani, A.; Bueno, G. J.; Stewart, M. L.; Yardley, V.; Brun, R.; Barrett, M. P.; Gilbert, I. H. Design and synthesis of a series of melamine-based nitroheterocycles with activity against trypanosomatid parasites. *J. Med. Chem.* **2005**, *48*, 5570-5579.

[45] Carter, N. S.; Fairlamb, A. H. Arsenical-resistant trypanosoma lack an unusual adenosine transporter. *Nature* **1993**, *361*, 173-175.

adenine. The P2 transporter is only expressed in bloodstream form (**bsf**) of the parasite, whilst the P1 transporter is found in both bsf and procyclic forms (figure 2.3)[43]. In addition to these two transporters four nucleobase transport activities have also been identified: **H1**, **H2** and **H3** that mediate the transport of hypoxantine, guanine and adenine[46, 47]. H1 is found in procyclic forms (**PF**) while H2 and H3 are found in bfs. Also a **U1** transporter mediates the transport of uracil in procyclic forms of *T. brucei*[43].

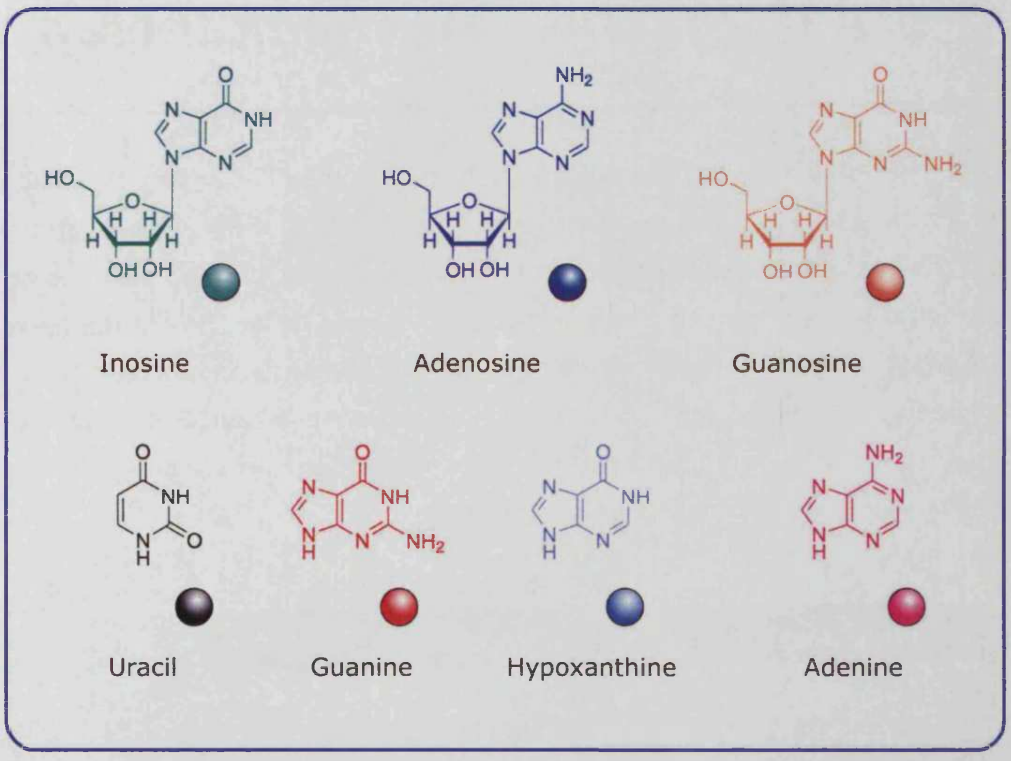

Figure 2.1 Structure of some nucleosides and nucleobases.

[46] De Koning, H. P.; Watson, J.; Jarvis, S. M. Characterisation of a nucleoside proton symporter in procyclic *Trypanosoma brucei brucei*. *J. Biol. Chem.* **1998**, *273*, 9486-9494.

[47] De Koning, H. P.; Jarvis, S. M. Hypoxanthine uptake through a purine-selective nucleobase transporter in *Trypanosoma brucei brucei* procyclic cells is driven by protonmotive force. *Eur. J. Biochem.* **1997**, *247*, 1102-1110.

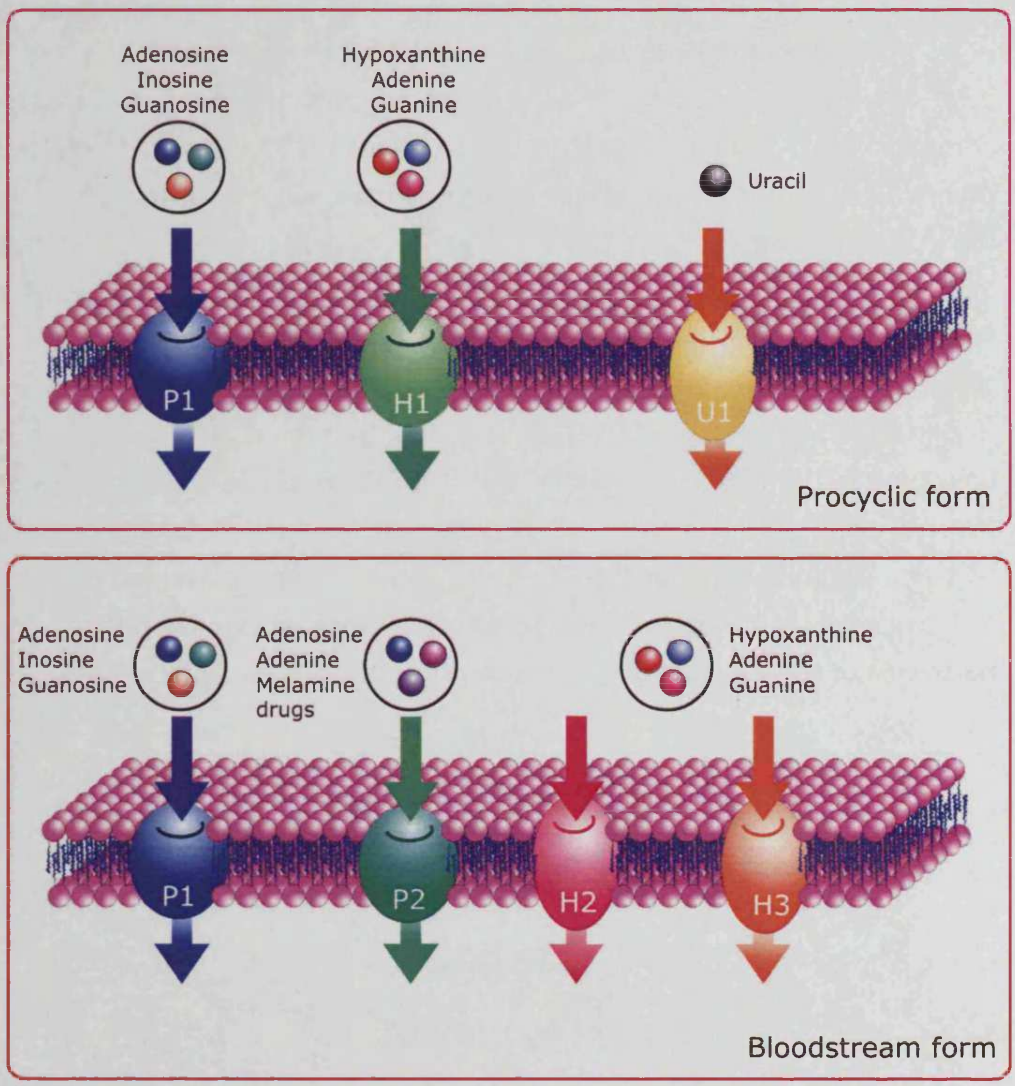

Figure 2.2 Transporters in T. *brucei* procyclic and bloodstream form.

2.1.1 "P1-like" transporters:

In order to understand the biological role of the purine transporters in survival and adaptation of *T. brucei* in different environments functional and biochemical characterisation has been carried out in the past few years. The first *T. brucei* nucleoside transporter gene cloned was the transporter 2 gene, ***Tb*NT2**, which encodes a P1 type transporter expressed only in bfs[43]. Later it was found that the *Tb*NT2 gene was a member of a multigene family (*Tb*NT2 like genes) that encodes six distinct transporters (TbNT2, TbNT3...TbNT7). To clone *TbNT2* like genes Sanchez

et al.[48] searched the *T. brucei* genome data base using the TbNT2 amino acid sequence as a query. The genes of the family are all clustered in chromosome II separated by intergenic regions. The six predicted TbNT proteins have very similar amino acid sequences suggesting that they are nucleoside isoforms[43]. The predicted amino acid sequences showed high identity to TbNT2 (81-96%)[43]. The gene that predicted a protein with the highest identity (96%) was designated ***TbNT2/927*** (T. *brucei* nucleoside transporter 2/927). The other P1 type genes, as already mentioned, were designated *TbNT3* through *TbNT7*. Multiple alignment between two human equilibrative transporters, hENT1 and hENT2, a Leishmania nucleoside transporter, LdNT1.1, and TbNT2 revealed that only 32 amino acids are out of 464 residues present in TbNT2 are conserved[48]. The conserved residues are likely to be important either for the biochemical function of the permease or for the folding of the protein into the active conformation[48].

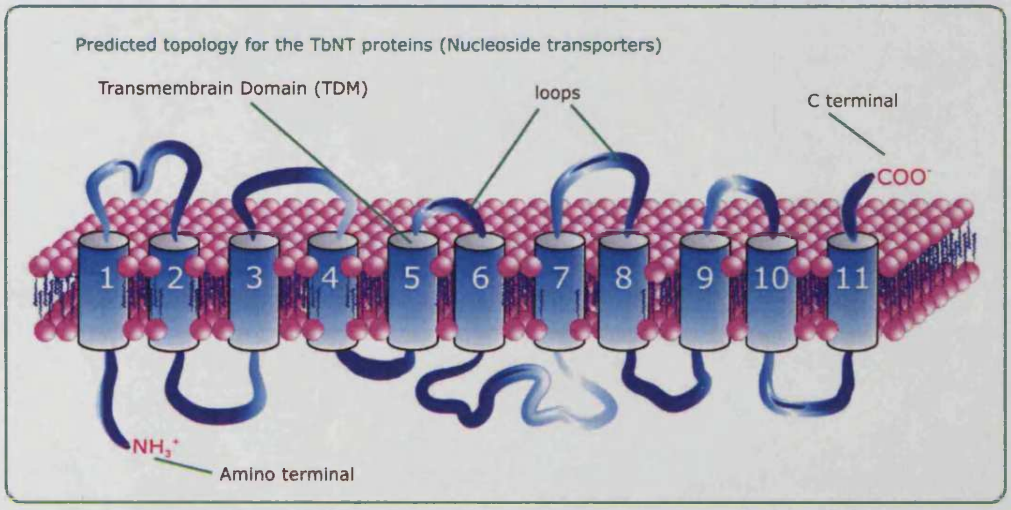

Figure 2.3 Predicted topology of a TnTP protein.

The predicted topology indicated that the secondary structure is similar to the human equilibrative nucleoside transporter 1 (**hENT1**) with 11 transmembrane domains (TMD) as shown in figure 2.3. The topology proposed for this family of transporters, with some exceptions, places the NH_2- terminal hydrophilic domain and the large hydrophilic loop between transmembrane domain 6 and 7 on the cytoplasmic side of the membrane,

[48] Sanchez, M. A.; Ullman, B.; Landfear, S. M.; Carter, N. S. Cloning and functional expression of a gene encoding a P1 type nucleoside transporter from *Trypanosoma brucei*. *J. Biol. Chem.* **1999**, *274*, 30244-30249.

whilst the COOH-terminal hydrophilic tail is on the extracellular surface[48]. The conserved residues mentioned above are present both within and outside of predicted transmembrane domains but none of them was observed to occur within the large hydrophilic loop between TMD 6 and 7[48].

2.1.2 P2-transporter:

The *TbAT1* gene encoding the P2 transporter (TbAT1) was identified by functional expression cloning in *Saccharomyces cerevisiae* (Mäser and Kaminsky[49]). An *S. cerevisiae* strain incapable of adenosine uptake cloned with a T. *brucei* cDNA library acquired the ability to grow on this substrate. When expressed in yeast, *TbAT1* not only enabled adenosine uptake but conferred also susceptibility to melaminophenyl arsenicals[49].

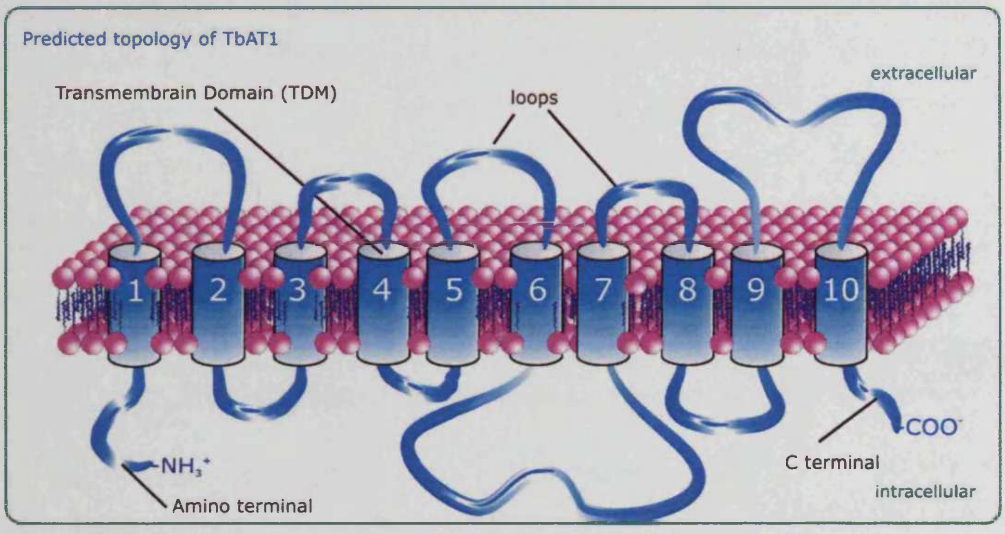

Figure 2.4 Predicted topology of TbAT1.

Sequencing of the cDNA revealed that the P2 transporter is represented by a protein of 463 amino acids with a predicted structure of 10 transmembrane domains (α-helices), cytosolic amino and carboxy terminals and a large, negatively charged cytosolic loop between transmembrane domains 6 and 7 (figure 2.4) [49, 50]. TbAT1 shows

[49] Maser, P.; Sutterlin, C.; Kralli, A.; Kaminsky, R. A nucleoside transporter from *Trypanosoma brucei* involved in drug resistance. *Science* **1999**, *285*, 242-244.

[50] Carter, N. S.; Barrett, M. P.; De Koning, H. P. A drug resistance determinant in *Trypanosoma brucei*. *Trends Microbiol.* **1999**, 7, 469-471.

substantial homology to the **human equilibrative nucleoside transporters** hENT1 and hENT2[51, 52].(35% and 33% respectively).

Further studies at the molecular level, like cloning of **TbAT1** (P2 type nucleoside transporter)[49] and of **TbNT2** (P1 type nucleoside transporter) genes showed that other **ENT** families[53] like TbAT1, human ENT2 are able to transport some nucleobases with higher K_m values than for nucleosides. Sanchez *et al.*[48] used functional expression of *TbNT2/927* through *TbNT7* in *Xenopus oocytes* to identify the substrate specificity of the *TbNT2/927* family. Initial studies showed that oocytes injected with *TbNT2/927*, *TbNT5*, and *TbNT7* cRNA were able to transport adenosine, inosine and guanosine whilst the oocytes injected with *TbNT3* and *TbNT4* cRNA did not mediate the uptake of any purine nucleosides[48]. In order to characterise the affinity of these transporters for adenosine and inosine, Sanchez *et al.*[48] calculated the K_m values from the saturation curves. TbNT2/927, TbNT5, and TbNT7 were high affinity adenosine/inosine transporters (K_m values <5μM)[43]. In intact *T. brucei* parasites the transport of nucleosides is dependent upon the transmembrane proton motive force, suggesting that these permeases are active proton symporters[43].

2.2 Substrate recognition motifs and affinity:

De Koning and Jarvis formulated a structure activity relationship for the binding of nucleosides/nucleobases to the P1 and the P2 adenosine transporters based on the inhibition data collected from a series of

---

[51] Griffiths, M.; Yao, S. Y. M.; Abidi, F.; Phillips, S. E. V.; Cass, C. E.; Young, J. D.; Baldwin, S. A. Molecular cloning and characterization of a nitrobenzylthioinosine-insensitive (ei) equilibrative nucleoside transporter from human placenta. *Biochem. J.* **1997**, *328*, 739-743.

[52] Griffiths, M.; Beaumont, N.; Yao, S. Y. M.; Sundaram, M.; Boumah, C. E.; Davies, A.; Kwong, F. Y. P.; Coe, I.; Cass, C. E.; Young, J. D.; Baldwin, S. A. Cloning of a human nucleoside transporter implicated in the cellular uptake of adenosine and chemotherapeutic drugs. *Nat. Med.* **1997**, *3*, 89-93.

[53] Griffith, D. A.; Jarvis, S. M. Nucleoside and nucleobase transport systems of mammalian cells. *Biochim. Biophys. Acta* **1996**, *1286*, 153-181.

potential substrates[54]. The inhibition was assessed by evaluating the ability of the substrate to inhibit the uptake of radiolabeled adenosine ([^{3}H]-adenosine) in P1 and P2 transporters. The affinity constants (K_i) are values related to the binding with the transporter even if they do not indicate that the ligands are transported through the membrane. The binding and the affinity was determined as free Gibbs energy (**ΔG°**) calculated from the K_i value:

$$\Delta G° = -RT\ln(K_i)$$

where R is the gas constant and T is the absolute temperature[54].

2.2.1 P1 transporter recognition motifs[54]:

Table 2.1 shows some K_i values determined for the P1 transporter by de Koning *et al.*[54] The yellow area highlights the high affinity for purine nucleosides compared to the other class of inhibitors evaluated.

Compound	P1 Transporter K_i (μM)
Purine nucleosides	
Adenosine	0.36 ± 0.05
Inosine	0.44 ± 0.10
Guanosine	1.8 ± 0.3
2'-Deoxy-Adenosine	0.19 ± 0.02
3'-Deoxy-Adenosine	210 ± 48
5'-Deoxy-Adenosine	100 ± 7
2'-Deoxy-Inosine	0.34 ± 0.11
Pyrimidine nucleosides	
Uridine	830 ± 86
Thymidine	44 ± 10
Purine nucleobases	
Adenine	NE, 250
Hypoxanthine	>1000
Xanthine	>250
Pyrimidine bases	
Thymine	NE, 500
Uracil	NE, 500
5-fluorouracil	NE, 500

Table 2.1 Ki values for potential inhibitors of P1 mediated adenosine uptake in T.*brucei* bloodstream forms[54]. NE, no effect at the indicated concentration.

[54] De Koning, H. P.; Jarvis, S. M. Adenosine transporters in bloodstream forms of *Trypanosoma brucei brucei*: substrate recognition motifs and affinity for trypanocidal drugs. *Mol. Pharmacol.* **1999**, *56*, 1162-1170.

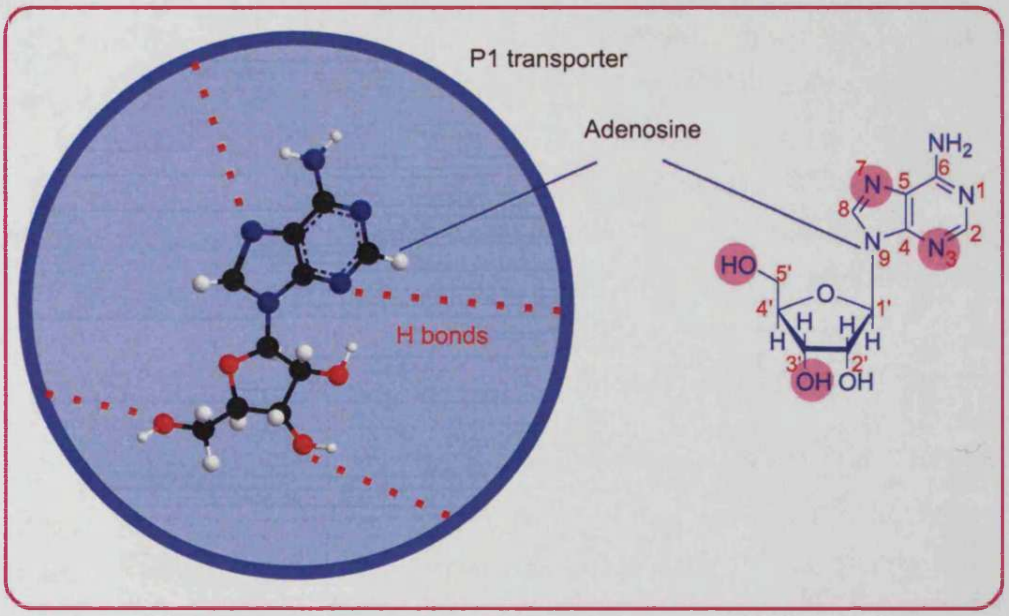

Figure 2.4 recognition motifs of P1 *T. brucei* transporter.

- The P1 transport function is not inhibited by pyrimidine or purine nucleobases and by acyclic nucleosides analogues but it is potently inhibited by a wide number of purine nucleosides indicating that the ribose moiety is essential for binding to P1 (table 2.1).
- 3′ and 5′ hydroxyl groups of ribose are involved in the interactions with the transporter;
- The P1 transport showed strict selectivity for purines over pyrimidines (table 2.1);
- The group at position 6 of the purine ring is not involved in the binding;
- The nitrogen at position 3 of purine ring is essential for high affinity binding and hydrogen bond might be involved in the interaction;
- Part of the imidazole ring of the purine ring is also involved in the binding through a hydrogen bond.

2.2.2 P2 transporter recognition motifs[54]:

Table 2.2 shows some K_i values determined for the P2 transporter by de Koning *et al.*[54] The blue area indicates the selectivity for purine over pyrimidines.

Compound	P2 Transporter K_i (μM)
Purine nucleosides	
Adenosine	0.91 ± 0.29
Inosine	NE, 100
Guanosine	NE, 250
2'-Deoxy-Adenosine	0.23 ± 0.04
3'-Deoxy-Adenosine	ND
5'-Deoxy-Adenosine	ND
2'-Deoxy-Inosine	170 ± 23
Pyrimidine nucleosides	
Uridine	NE, 500
Thymidine	NE, 500
Purine nucleobases	
Adenine	0.30 ± 0.02
Hypoxanthine	>500
Xanthine	110 ± 10
Pyrimidine bases	
Thymine	NE, 500
Uracil	NE, 500
5-fluorouracil	NE, 500

Table 2.2 Ki values for potential inhibitors of P2 mediated adenosine uptake in T.*brucei* bloodstream forms[54]. ND, not determined. NE, no effect at the indicated concentration.

- The P2 does not require the presence of the ribose moiety for ligand binding (table 2.2);
- Strict selectivity for purines over pyrimidines (table 2.2);
- The amino group in position 6 of the purine ring is essential for interaction and substituents at this position reduce the affinity;
- The nitrogen residue at position 1 is part of the P2 binding motif;
- The main motif for the P2 transporter is $H_2N\text{-}C_6(R_1)=N\text{-}R_2$ with N1 acting as a potential H-bond acceptor and the amine as a possible donor of two H-bonds;
- The aromaticity of the ring is also important and interact with the transporter via π-π-interaction;

- The lone pair of electrons at N9 are delocalised into the π-system of the pyrimidine ring creating a partial positive charge that can interact with the transporter via polar interactions.

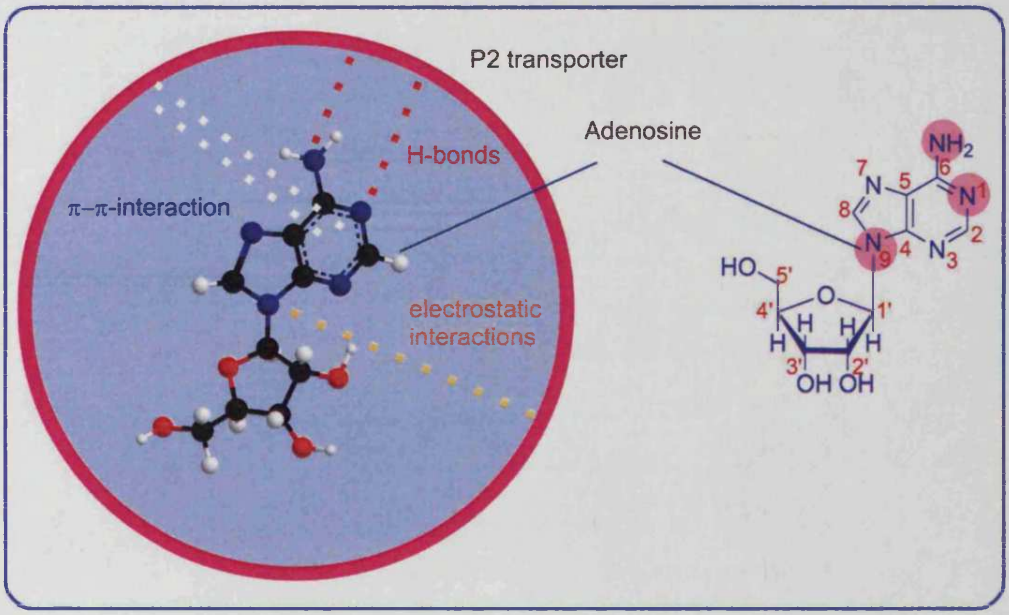

Figure 2.5 recognition motifs of P2 *T. brucei* transporter.

2.3 Human nucleobase transporters:

In mammalian cells there are two nucleoside transporter gene families: the equilibrative nucleoside transporters (**ENTs**) and the concentrative nucleoside transporters (**CNTs**). The cloned transporters within each family share significant sequence homology[55]. The ENTs are facilitated carrier proteins and the CNTs are Na^+ dependent secondary active transporters (Figure 2.6)[55]. Within each major class there are multiple subtypes with different substrate specificity and inhibitor sensitivity.

The equilibrative nucleoside transporters mediate facilitated diffusion of nucleosides across membranes. The concentration gradient

[55] Kong, W.; Karen, E.; Wang, J. Mammalian Nucleoside Transporters. *Curr. Drug. Metab.* **2004**, *5*, 63-84.

determines the direction of the nucleosides flux through the transporter that therefore function bidirectionally[55]. hENT1 transports both purine (adenosine, guanosine, inosine) and pyrimidines (uridine, cytidine, thymidine). The *T. b. brucei* transporters previously described despite the human transporters are proton symporters[47].

The hFNT1 transporter is closely related to the TbNT family and appears to be the most ubiquitous human nucleobase transporter[56]. The predicted secondary structure for hENT1, as well as described for the tbNT (figure 2.4), shows 11 transmembrane domains with an intracellular N-terminus and a short extracellular C-terminus)[55]. The predicted secondary structure for hCNT1 shows 13 transmembrane domains with a long intracellular N-terminus and a long extracellular C-terminus[55].

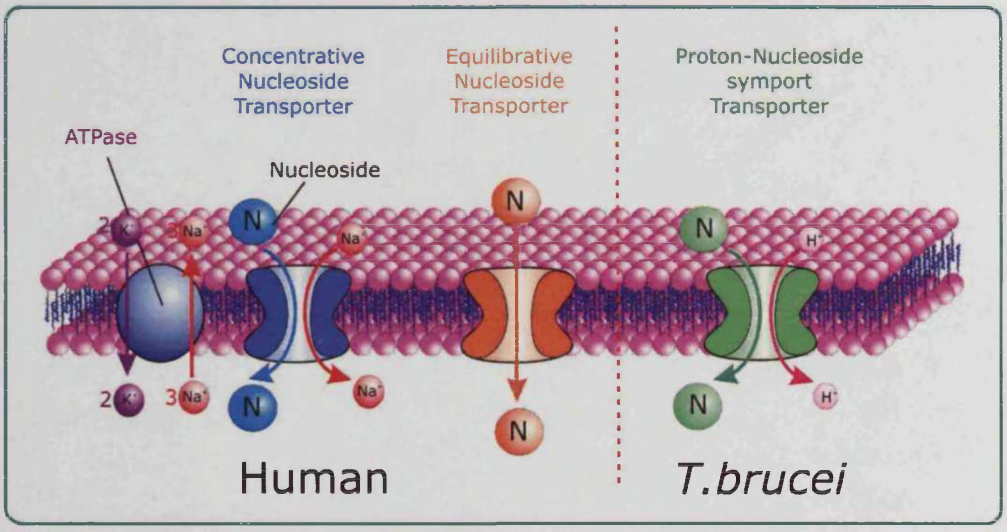

Figure 2.6. Nucleosides/nucleobases transporters in human and in *T.b. brucei*

Wallace and De Koning have formulated a structure activity relationship for the binding of several ligands to the human erythrocyte facilitative nucleobase transporter as well as for the *Trypanosoma* P1 and P2 transporters[56].

Table 2.3 shows some K_i values determined for hENT1 by de Koning *et al.*[56] The green area highlights the high affinity for purine nucleobases compared to the other class of inhibitors evaluated.

[56] Wallace, L. J. M.; Candlish, D.; De Koning, H. P. Different Substrate Recognition Motifs of Human and Trypanosome Nucleobase Transporters. *J. Biol. Chem.* **2002**, 277, 26149-26156.

Compound	hFNT1 K_i (μM)
Purine nucleosides	
Adenosine	NE, 1000
Inosine	NE, 1000
Guanosine	NE, 250
Pyrimidine nucleosides	
Uridine	NE, 1000
Thymidine	ND
Purine nucleobases	
Adenine	16 ± 4.5
Hypoxanthine	290 ± 21
Xanthine	>150
9-methylguanine	7.4 ± 2.0
9-Deazaguanine	8.0 ± 2.5
Pyrimidine bases	
Thymine	>1000
Uracil	NE, 1000
Cytosine	NE, 1000

Table 2.3 Ki values for inhibition of ^{3}H-permeant uptake in hFNT[47]. ND, not determined. NE, no effect at the indicated concentration.

The results achieved from the structure activity relationship for the human transporter can be summarised as follow:

- The transporter was described as purine-specific high affinity[56] (table 2.3);
- The imidazole ring plays an important role in the interaction explaining the preference of purine over pyrimidines[56];
- π-π stacking of the aromatic purine ring interact with one or more aromatic residues in the transporter stabilise the binding of the permeant[56];
- An unprotonated "pyrimidine type" N1, as present in aminopurines, is necessary for an optimal binding[56];
- Strong H-bond interaction with N3 (unprotonated in all natural purines) [56].

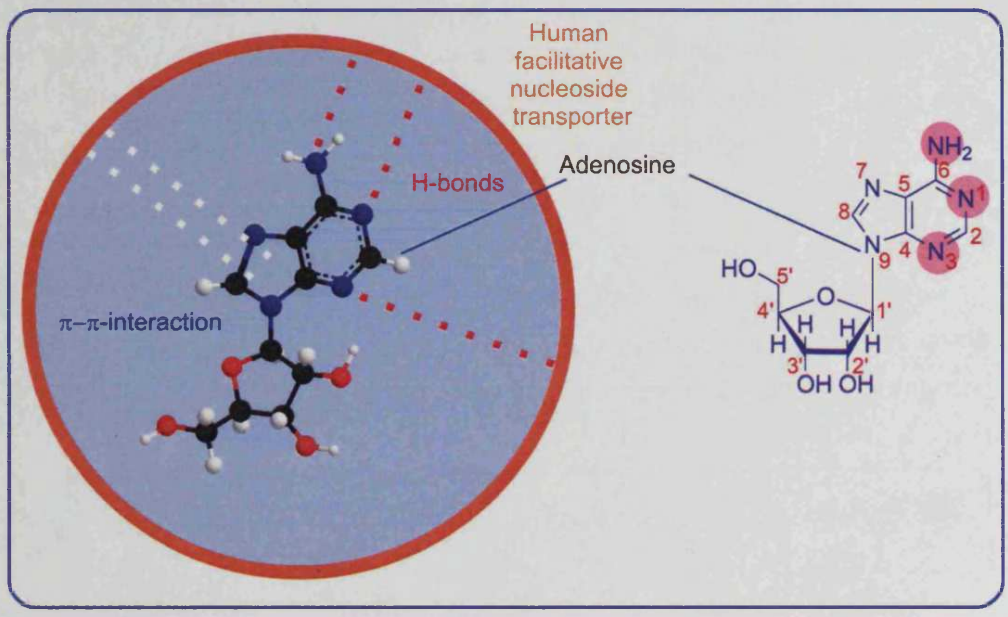

Figure 2.7 recognition motifs in human facilitate nucleoside transporter.

2.4 Uptake of trypanocidal drugs through P2 transporter:

The substrate recognition model previously analysed explains the primary role of P2 transporter in the uptake of some important trypanocidal drugs[30, 45, 54]. The P1 transporter displays a 50 to 100 fold lower affinity for these compounds and therefore has not been implicated in the drug uptake[54].

Williamson[57] in 1959 discovered that melamine-containing molecules could antagonise the trypanocidal action of melaminophenyl arsenicals and the diamidines. He proposed that a "melamine receptor" was involved in the competition on the trypanosome surface. Today we know that the "melamine receptor" is represented by the P2 transporter.

Considering the structure activity relationship studies by De Koning and Jarvis[54] previously analysed it is possible to summarise the main requirements of P2 transporter in order to have an optimal binding:

1) Presence of an amidine group that may be integrated into a pyridine or pyrimidine ring[54];

[57] Williamson, J. Drug resistance in trypanosomes; selective interference with trypanocidal action. *Brit. J. Pharmacol.* **1959**, *14*, 431-442.

2) Presence of aromatic ring associated or integrated with the amidine group[54];

3) Electronegative group attached to the aromatic ring, para to the amidine and able to contribute to the π-system with a lone electron pair[54].

It is clear that nucleobases (6-aminopurines), melamine-based arsenicals and diamidines share a common structural motif to allow recognition by the P2 transporter[30] (figure 2.8).

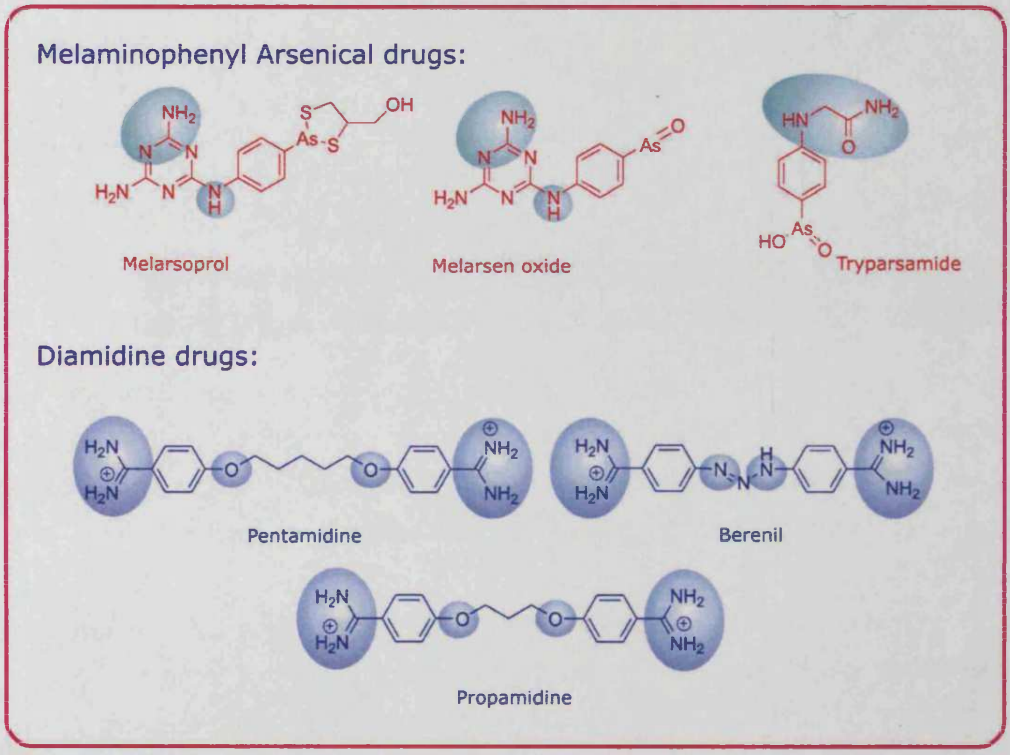

Figure 2.8 Structure of some trypanocidal drugs and their common structural motifs.

The structure of melarsoprol fulfils all the requirements for the high affinity binding to the transporter and the large phenylarsenical group does not seem to affect the binding. Pentamidine shows the same affinity for the transporter suggesting that the amidine group does not need to be integrated in the aromatic ring and also that the amino group in para position can be replaced by an ether group[54].

Carter and Fairlamb[45] proved that the melaminophenylarsenical drugs and diamidines are transported into the cell through the transporter. In fact, adenosine and adenine but not inosine were able to protect the

bloodstream form from the melarsenoxide-induced lysis *in vitro*. This observation was also supported by the finding that P2 transporter activity was absent in melarsoprol-resistant strain[45].

2.5 Pentamidine receptors and resistance in *T. brucei*:

Melaminophenyl arsenical and pentamidine are still the main chemotherapeutic treatment for the sleeping sickness. Since the treatment has not changed in the last 50 years resistance to these agents is undermining the treatment of this disease. Many cases of stage 2 sleeping sickness are refractory to treatment with the melaminophenyl arsenical melarsoprol[50]. It is therefore essential to understand the mechanisms behind this growing problem.

The analysis of the results of the cloning and expression of the *TbAT1* gene encoding the P2 transporter can help to understand the mechanism behind the resistance. The first important step was achieved by constructing a *TbAT1* knockout clone to investigate whether *TbAT1* alone contributes to P2 activity in *Trypanosoma brucei brucei*. Mäser and Kaminsky found that ***TbAT1*** gene encodes an adenine-sensitive adenosine transporter when expressed in yeast (*Saccharomyces cerevisiae*)[49] but the formal proof that *TbAT1* encodes the P2 activity was achieved after the gene deletion studies carried out by Matovu and De Koning[58].

The total absence of P2-type transporter in tbat1-null bloodstream form trypanosomes proved that TbAT1 is the P2 transporter. Loss of TbAT1 reduced the sensitivity of trypanosomes to melarsoprol but only by approximately 2 fold. However, even a small reduction of sensitivity is important, since the level of melarsoprol in the cerebrospinal fluid of patients has to be within certain levels in order to kill all the parasites in the central nervous system. The therapeutic ratio index of melarsoprol is very low and a small reduction in sensitivity can render the drug ineffective.

[58] Matovu, E.; Stewart, M. L.; Geiser, F.; Brun, R.; Maeser, P.; Wallace, L. J. M.; Burchmore, R. J.; Enyaru, J. C. K.; Barrett, M. P.; Kaminsky, R.; Seebeck, T.; de Koning, H. P. Mechanisms of arsenical and diamidine uptake and resistance in *Trypanosoma brucei*. *Eukaryot. Cell* **2003**, *2*, 1003-1008.

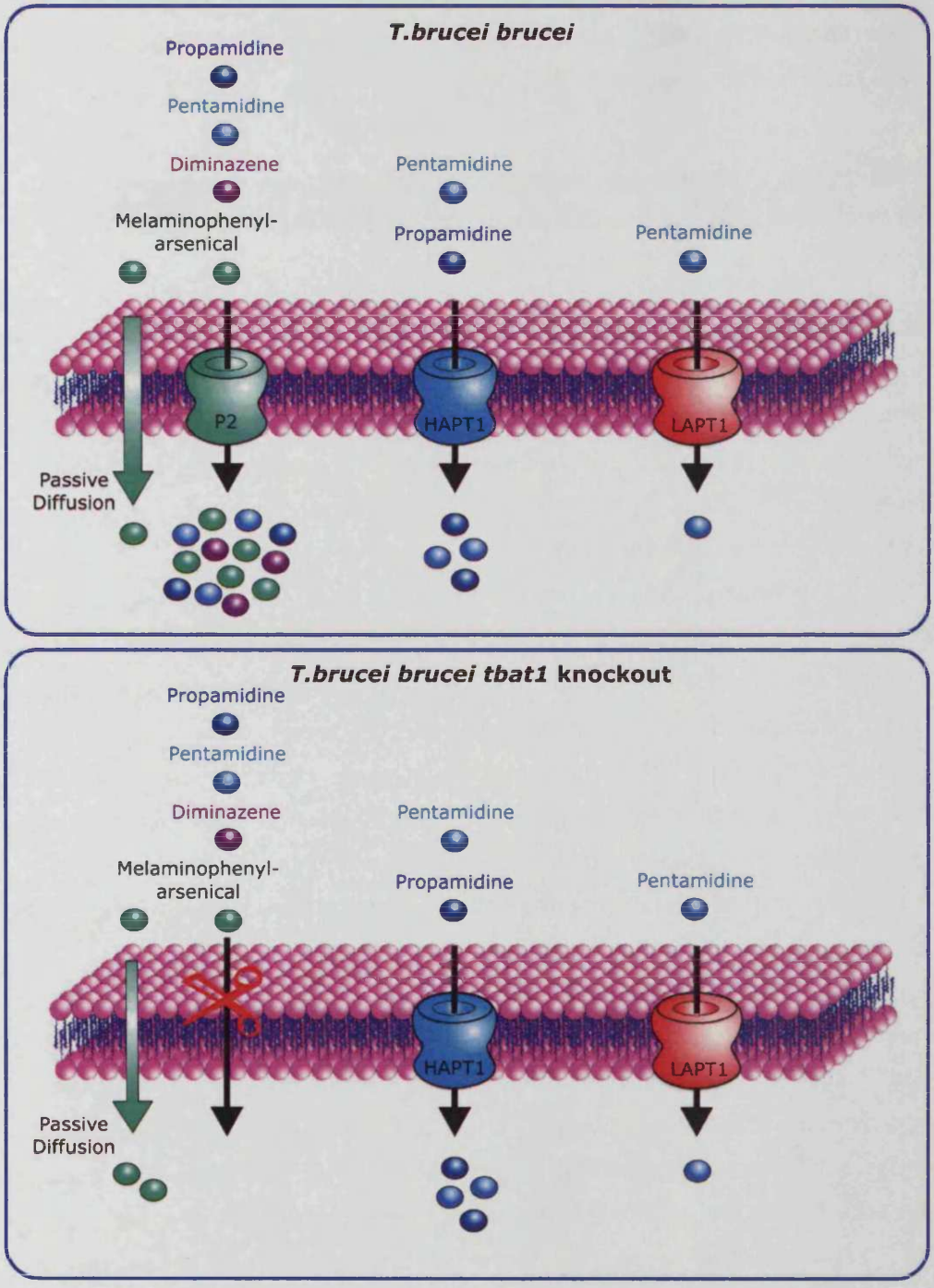

Figure 2.9 Mechanism of transport in *T. brucei brucei* wild and knockout types.

The P2 transporter, as previously described, exerts high affinity also for diamidines like pentamidine. However the transport of [^{3}H]-pentamidine is only partially blocked by adenosine in *T. brucei* and also ***TbAT1*-null** trypanosomes are only slightly more resistant to pentamidine compared to the wild type[58]. Another important observation was that

TbAT1-null parasites showed a more pronounced resistance to diminazene, another important diamidine related to pentamidine, used for treating cattle. De Koning and Matovu proposed the presence of two additional adenosine-insensitive transporters specific for pentamidine: the high-affinity pentamidine transporter (**HAPT1**; K_m= 36 ± 6 nM) and the low-affinity pentamidine transporter (**LAPT1**, K_m= 56 ± 8 μM)[59] (figure 2.9). Both the transporters are still active in *TbAT1*-null mutants (figure 2.9) explaining why treatment with pentamidine is not likely to give rise to resistance whilst resistance to diminazene occurs rapidly[49, 59]

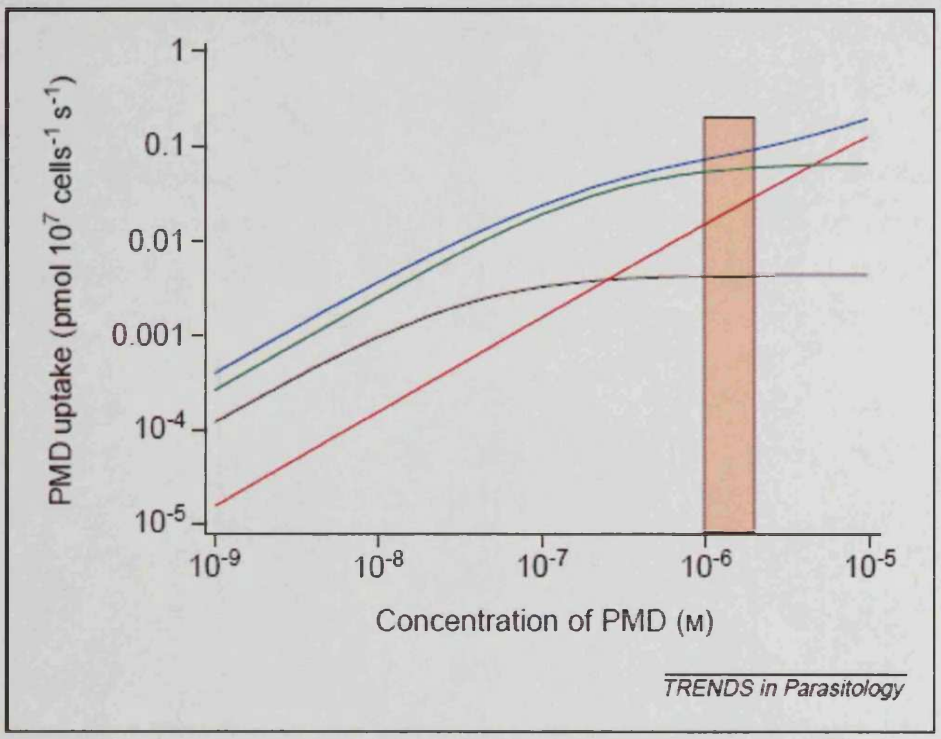

Figure 2.10 Pentamidine uptake rates operated by the various transporters. Black line: HAPT1; blue line, combined uptake of HAPT1, LAPT1 and P2; green line, P2; red line, LAPT1. The orange bar indicated the maximum plasma concentration of pentamidine in patient[60].

The three pentamidine transporters show different kinetic parameters and therefore the relative contribution of each to the total flux

[59] De Koning, H. P. Uptake of Pentamidine in *Trypanosoma brucei brucei* is Mediated by Three Distinct Transporters: Implications for Cross resistance with Arsenicals. *Mol.Pharmacol.* **2001**, *59*, 586-592.

is dependent on the extracellular concentration of pentamidine (figure 2.10)[60]. The P2 transporter mediates 50-70% of the pentamidine uptake. The high affinity transporter (K_m= 36 ± 6 nM) is saturated at low concentration and therefore contributes relatively little to the total flux of pentamidine (figure 2.10)[60]. Diminazene, though structurally related to pentamidine, does not appear to be a substrate of the adenosine-insensitive transporters explaining the higher level of resistance in the null mutant clone (figure 2.10)[59]. However the level of cross-resistance between diminazene and melarsoprol is inconsistent and suggests that melaminophenyl arsenicals, as well as described for some diamidines, have a secondary route of entry into the trypanosome[60].

It is likely that together with the loss of TbAT1 there are more processes involved in resistance. In fact, some laboratory strains of *T. brucei*, selected for arsenical resistance after prolonged exposure to subcurative doses, are deficient in TbAT1 activity and exhibit high level of resistance to melaminophenyl arsenicals[59].

[60] Bray, P. G.; Barrett, M. P.; Ward, S. A.; de Koning, H. P. Pentamidine uptake and resistance in pathogenic Protozoa: Past, present and future. *Trends Parasitol.* **2003**, *19*, 232-239.

2.6 Aims and Objectives:

The P2 transporter recognises common chemical features among its different substrates. The amidine-like moiety appear essential for the recognition and can be normally found in a P2 substrate as free amidine group or incorporated in a heterocyclic ring such as in a purine or in a triazine. The differences previously described between the *T. brucei* P2 transporter and the related human nucleoside transporters are substantial to exploit this route to selectively deliver cytotoxic agents to the parasite.

As melamine derivatives are both uncommon transporter recognition motives and are easily accessible they seem to be ideally suited to act as transport/recognition unit.

The aim of the work carried out and presented in the following chapters is to synthesise new melamine and benzamidine derivatives with trypanocidal activity. For simplicity, the modifications can be subdivided into two main groups: modifications of triazine derivatives and of benzamidine derivatives.

New triazines derivatives can be achieved generating different group of compounds A, B, C, D, E and F. The different derivatives have the common feature of having a trypanocidal moiety attached to a recognition moiety through a linker. The modification can be summarised as follow:

- Modification of the melamine recognition unit by introducing alkyl substituents (**A**, scheme 2.1) or by introducing functionalised chains (**B**, scheme 2.1);

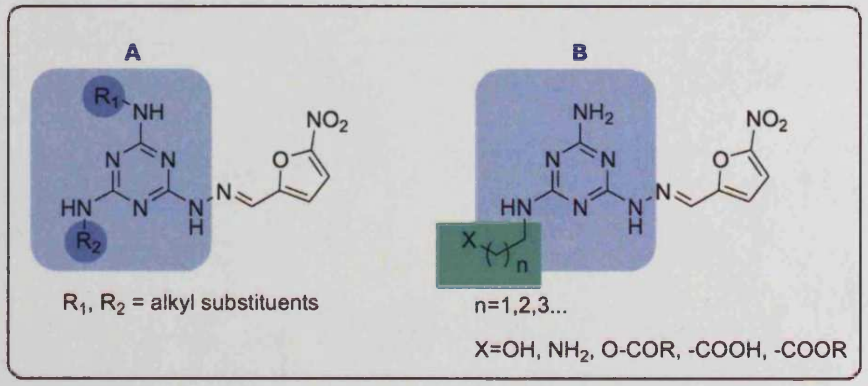

Scheme 2.1 Modifications of the triazine moiety.

- Replacement of the furan ring with other nitroheterocycles (**C**, scheme 2.2) or with nitro-homoaromatics (**D**, scheme 2.2);

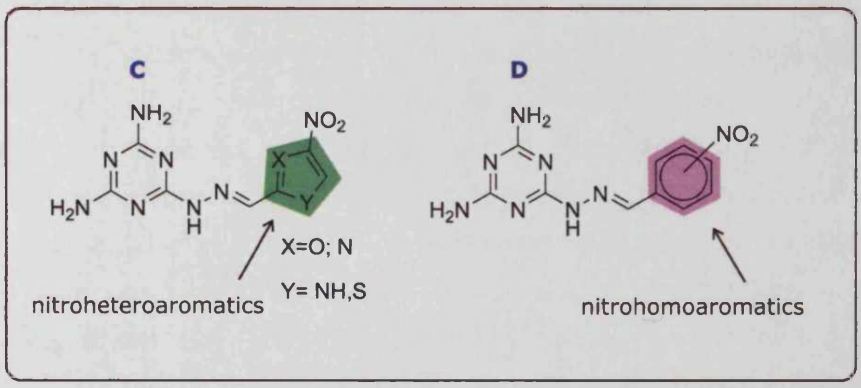

Scheme 2.2 Modifications of the nitroheterocycle unit.

- Complete removal of the nitro group or replacement with other Michael acceptors (**E**, scheme 2.3) ;

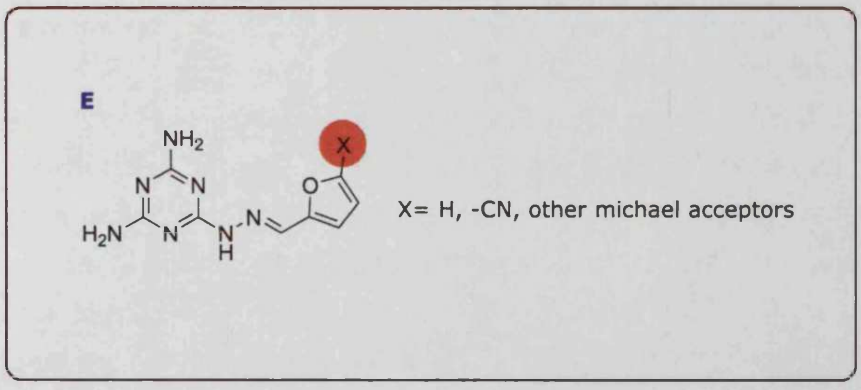

Scheme 2.3 Modifications of the nitroheterocycle unit.

- Introduction of different linkers with different length and chemical functionality (**F**, scheme 2.4);

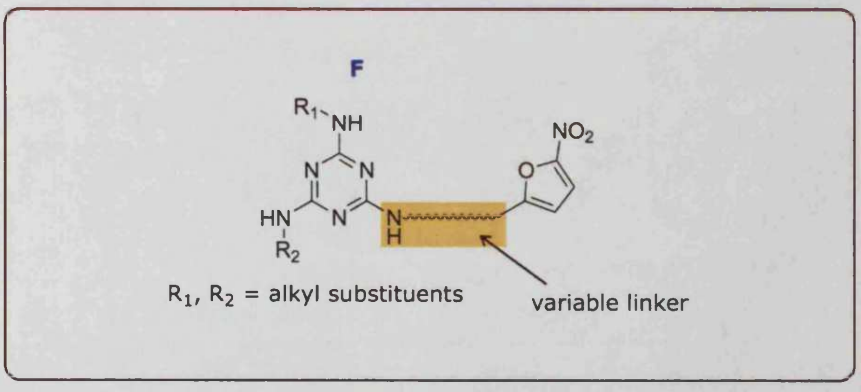

Scheme 2.4 Modification of the spacer linker.

Benzamidine derivatives can be generated by attaching the benzamidine moiety to a nitrofuran ring through a variable spacer linker (**G**, scheme 2.5). The nitrofuran ring, as well as described for the triazine derivatives, can be replaced with other nitroheterocycles structures (**H**, scheme 2.5).

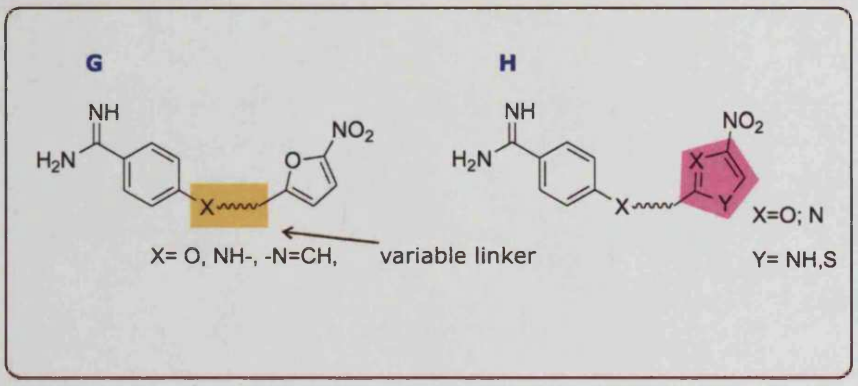

Scheme 2.5 Modification of benzamidine structures .

Prodrugs related to the previous structure have been also investigated and will be separately described in chapter 5.

The modifications above summarised will be separately discussed in the chapters that will follow. All new compounds have been tested for their ability to interact with the P2 transporter in *Trypanosoma brucei* species. Cytotoxic activities against *T. brucei* species and related parasites as well as against mammalian cell lines have been also tested and will be separately described in chapter 6.

3. Results and Discussion I:

Triazine derivatives

The substrate specificity of the P2 transporter represents an opportunity for drug design. Together with the natural substrates, adenine and adenosine, other motifs such as melamines and benzamidines have shown to be good substrates for this transporter. Following a rational drug design approach, a series of new potential drugs have been designed by linking trypanocidal agents to groups known to be substrates of the P2 transporter, in order to selectively target the toxic effect to the parasite. This chapter focuses mainly on the coupling of melamine groups to a different series of nitroheterocycle compounds.

3.1 Drug design approaches:

Nearly 100 years ago Paul Ehrlich developed the **haptophore-toxophile biphasic theory** of drug action (figure 3.1). The theory described the "**haptophore**" as a component of a molecule directed toward a specific cell receptor while the "**toxophile**" or "poisoner" was responsible for the cytotoxic activity by chemically combining with the target[30, 61]. The drug design approach that we consider today is to some extent related to Ehrlich's theory. We know that we can extend the term "receptor" to encompass different cellular components such as membrane transport systems and intracellular targets such as enzymes and other

[61] Ehrlich, P. The collected papers of Paul Ehrlich. Volume I. *Histology, Biochemistry and Pathology.*; Pergamon Press, 1959; pp 596-618.

components[30]. However, at the same time, it is clear that non-covalent forces such as hydrogen bonds, electrostatic interactions and hydrophobic interactions are also extremely important for drug action.

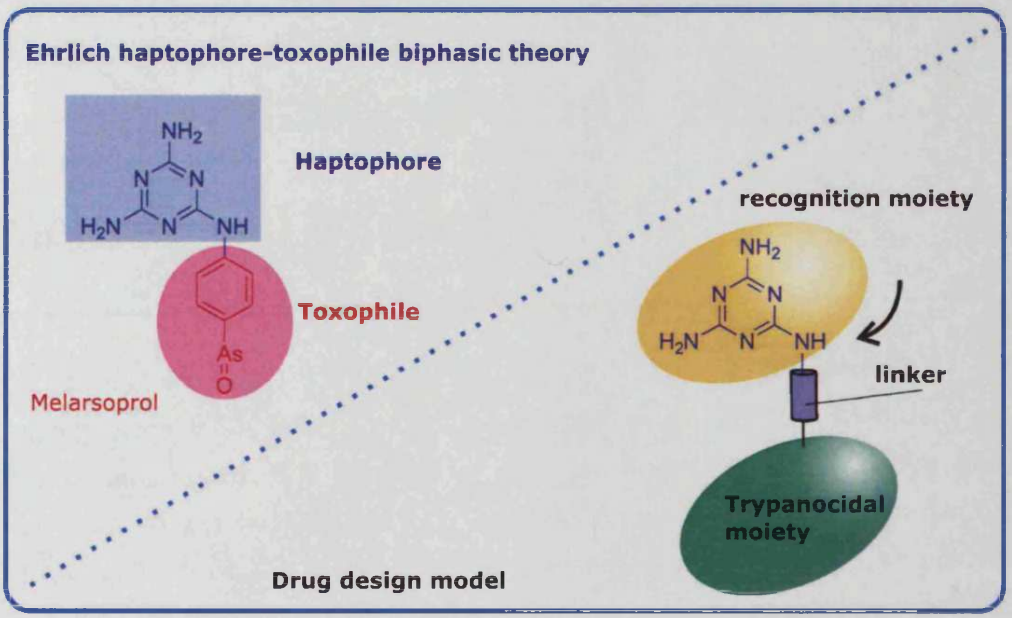

Figure 3.1 Models of drug design from the Ehrlich's theory.

Our model is based on a recognition moiety being linked to a trypanocidal moiety, with or without a linker between the two units. The recognition moiety chosen is the [1,3,5]-unsubstituted triazine unit. The 1,3,5-triazines are generally not recognized by mammalian nucleoside transporters and should therefore offer excellent selectivity between host cells and parasites[30, 54]. Moreover trybizine (scheme 3.1), containing a 2,4-diamino-[1,3,5]-triazinyl moiety, was reported as a new trypanocidal compound by Kaminsky and Brun[62]. Trybizine showed *in vitro* activity against *T. brucei rhodesiense* and *gambiense*. However, further studies indicated that the compound had a poor ability to cross the blood brain barrier and was not able to cure the mice model[62].

[62] Kaminsky, R.; Brun, R. *In vitro* and *in vivo* activities of trybizine hydrochloride against various pathogenic trypanosome species. *Antimicrob. Agents Chemother.* **1998**, *42*, 2858-2862.

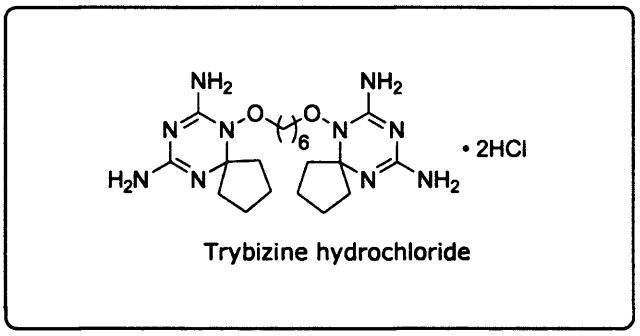

Trybizine hydrochloride

Scheme 3.1 Chemical structure of trybizine hydrochloride.

☞ *The work described in the following sections 3.2 and 3.4 is work carried out by previous members of the group. This work is only being discussed herein to provide sufficient background to facilitate the understanding of our project and the work carried out by the author.*

3.2 Polyamines as cytotoxic agents:

In the initial project carried out by Klenke *et al.*[63] in our laboratory, the melamine unit was linked to polyamines, chose as the toxophile. The importance of polyamines in most eukaryotes[19] has been discussed already in the previous chapter. They are essential cell components and are involved in cell differentiation and proliferation[19, 64, 65, 66]. Polyamine analogues have shown promise as anticancer agents, antiparasitic agents, antidiarrhoeals, anti-HIV agents, metal chelators, and as gene delivery agents[63, 67].

---

[63] Klenke, B.; Stewart, M. L.; Barrett, M. P.; Brun, R.; Gilbert, I. H. Synthesis and Biological Evaluation of s-Triazine Substituted Polyamines as Potential New Anti-Trypanosomal Drugs. *J. Med. Chem.* **2001**, *44*, 3440-3452.

[64] Karigiannis, G.; Papaioannou, D. Structure, Biological Activity and Synthesis of Polyamine Analogues and Conjugates. *Eur. J. Org. Chem.* **2000**, *1841-1863.*

[65] Kuksa, V.; Buchan, R.; Lin, P. K. *T.* Synthesis of polyamines, their derivatives, analogues and conjugates. *Synthesis* **2000**, 1189-1207.

[66] Marton, L. J.; Pegg, A. E. Polyamines as targets for therapeutic intervention. *Annu. Rev. Pharmacol. Toxicol.* **1995**, *35*, 55-91.

[67] Tye, C.-K.; Kasinathan, G.; Barrett, M. P.; Brun, R.; Doyle, V. E.; Fairlamb, A. H.; Weaver, R.; Gilbert, I. H. An approach to use an unusual adenosine transporter to selectively deliver polyamine analogs to trypanosomes. *Bioorg. Med. Chem. Lett.* **1998**, *8*, 811-816.

With this in mind, polyamine metabolism was initially chosen as our target in African trypanosomes. The known anti HAT compound DL-α-difluoromethylornithine (DFMO) represents an inhibitor of the first step of polyamine synthesis, as catalysed by the enzyme ornithine decarboxylase.

Since the parasites lack a polyamine transporter, the P2 transporter system has been exploited as a means to deliver and target these polyamines analogues[67].

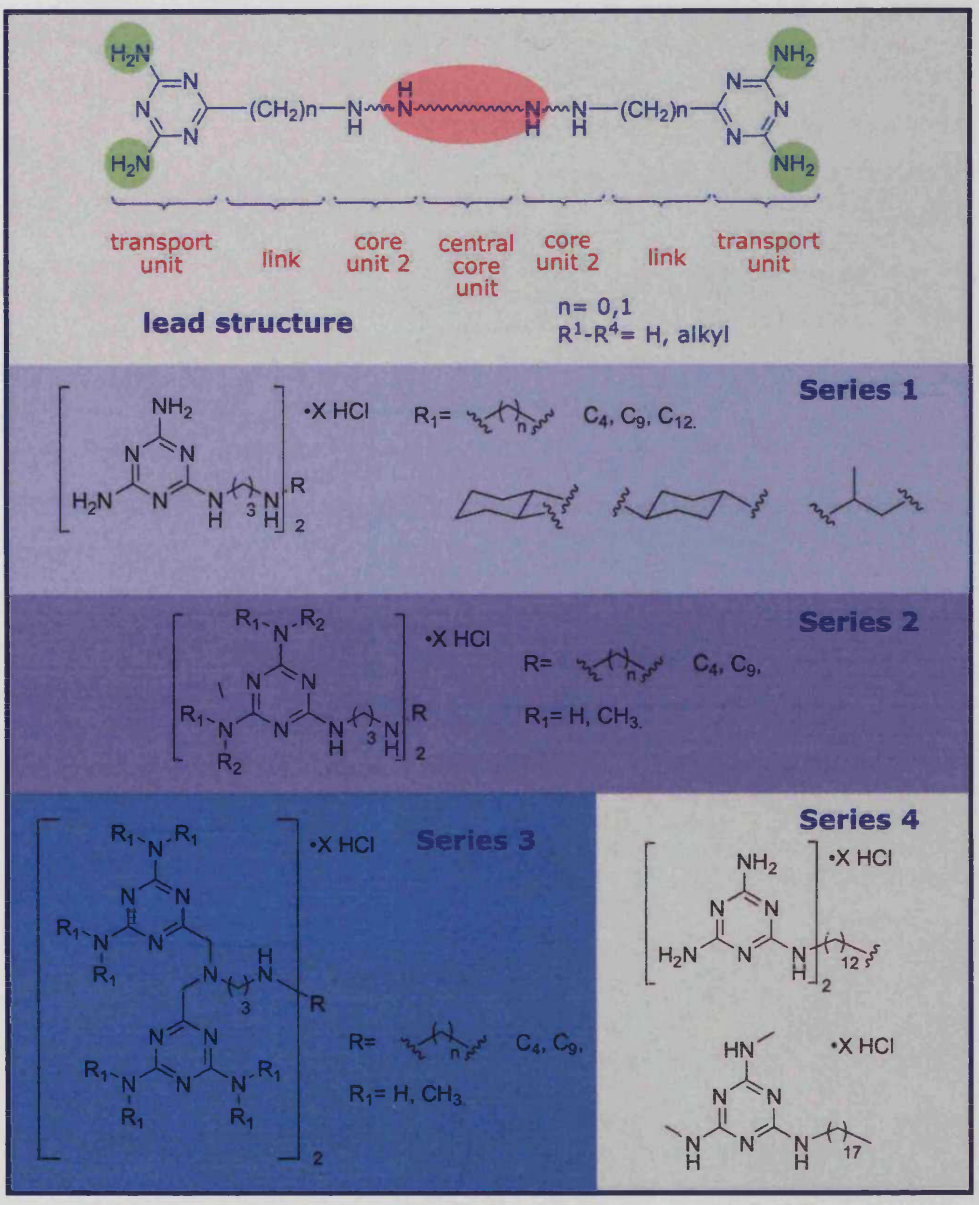

Scheme 3.1 Lead structure (on the top) considered for the generation of different series of substituted polyamines.

A series of substituted polyamines were designed and synthesised by Klenke *et al.*[63] carrying 1,3,5-triazine units. The structure, as shown on scheme 3.1, represents the lead structure that was used as starting point to generate four different series of compounds. The main modifications carried out are represented by the variation of the central core structure and by modification of the transport unit by addition of methyl substituents on the 1,3,5-triazine units[67]. Some of the compounds of the series synthesised by Klenke B. *et al.*[63] in our laboratory were highly active against both *T. brucei rhodesiense* values (e.g. compounds a, b and c of series 2 showed respectively IC_{50}=0.57 μM, IC_{50}=0.44 μM, IC_{50}=0.18 μM) and *T. brucei brucei in vitro* and selective on a cellular level but host toxicity precluded the full evaluation of these compounds *in vivo*[67]. However, these initial *in vitro* results were very encouraging and suggested that the triazine moiety does play a crucial role in the mode of action of these drugs.

3.3 Nitrofurans as cytotoxic agents:

As biological studies of the polyamine derivatives proved toxic for mammal we therefore decided to focus our attention on alternate cytotoxic motifs to couple to the P2 transporter motifs. We become interested in nitroaromatic compounds as they have long been known to be effective against trypanosomes[68]. Nitroheterocyclics such as nifurtimox and benznidazole (Scheme 3.2) are known to be potent trypanocidal compounds. Nifurtimox is a nitrofuran derivative that is currently licensed for the American Trypanosomiasis (Chagas' Disease)[69] and is under clinical

[68] Stewart, M. L.; Bueno, G. J.; Baliani, A.; Klenke, B.; Brun, R.; Brock, J. M.; Gilbert, I. H.; Barrett, M. P. Trypanocidal activity of melamine-based nitroheterocycles. Antimicrob. Agents Chemother. 2004, 48, 1733-1738.

[69] Maya, J. D.; Bollo, S.; Nunez-Vergara, L. J.; Squella, J. A.; Repetto, Y.; Morello, A.; Perie, J.; Chauviere, G. *Trypanosoma cruzi*: effect and mode of action of nitroimidazole and nitrofuran derivatives. *Biochem. Pharmacol.* **2003**, *65*, 999-1006.

trial for the African HAT and particularly for the treatment of arseno-resistant *Trypanosoma brucei gambiense* HAT[70, 71].

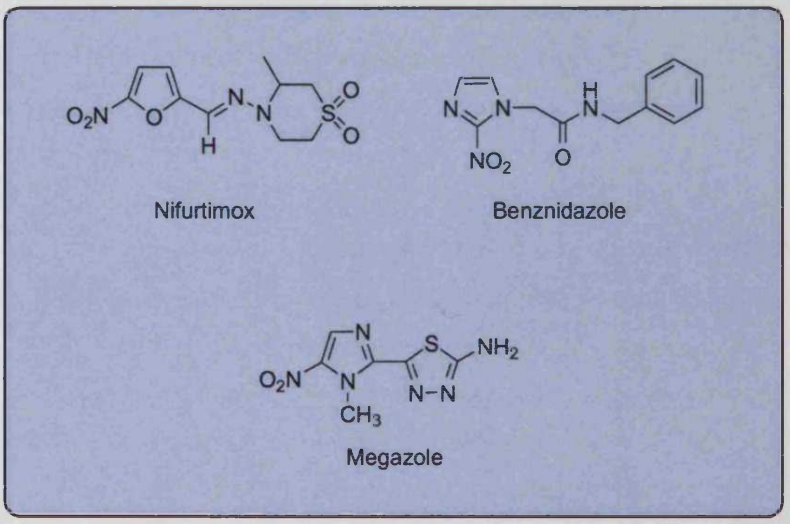

Scheme 3.2 Structure of some known anti-Chagas nitroheterocycles.

Megazole, a nitroimidazole derivative, was also recently investigated for its trypanocidal activity[72, 73] but toxicity issues prevented further development[74].

The coupling of nitroheterocycle moieties to the P2 recognition motifs have been undertaken in order to aim a selectively cytotoxic effect at the trypanosomes. Our approach should selectively deliver/concentrate

[70] Legros, D.; Ollivier, G.; Gastellu-Etchegorry, M.; Paquet, C.; Burri, C.; Jannin, J.; Buscher, P. Treatment of human African trypanosomiasis - present situation and needs for research and development. Lancet Infect. Dis. 2002, 2, 437-440.

[71] Pepin, J.; Milord, F.; Meurice, F.; Ethier, L.; Loko, L.; Mpia, B. High-dose nifurtimox for arseno-resistant *Trypanosoma brucei gambiense* sleeping sickness: an open trial in central Zaire. *T. Roy. Soc. Trop. Med. H.* **1992**, *86*, 254-256.

[72] Bouteille, B.; Marie-Daragon, a.; Chauviere, G.; De Albuquerque, C.; Enanga, B.; Darde, L.; Vallat, J. M.; Perie, J.; Dumas, M. Effect of megazol on T*rypanosoma brucei brucei* acute and subacute infections in Swiss mice. *Acta Trop.* **1995**, *60*, 73-80.

[73] Enanga, B.; Keita, M.; Chauviere, G.; Dumas, M.; Bouteille, B. Megazol combined with suramin: a chemotherapy regimen which reversed the CNS pathology in a model of human African trypanosomiasis in mice. *Trop. Med. Int. Health* **1998**, *3*, 736-741.

[74] Poli, P.; Aline de Mello, M.; Buschini, A.; Mortara, R. A.; Northfleet de Albuquerque, C.; Da Silva, S.; Rossi, C.; Zucchi, *T.* M. Cytotoxic and genotoxic effects of megazol, an anti-Chagas' disease drug, assessed by different short term tests. *Biochem. Pharmacol.* **2002**, *64*, 1616-1627.

nitroheterocycles in the parasite increasing the potency and also allowing a lower dosage, minimising effects on human host. Although the mechanism of action of nitrofurans is still under investigation, as previously described, it is thought that they interfere with the redox system in trypanosomes that are essential for their survival. Nifurtimox and related compounds act as redox cyclers[69] and experiments suggest that intracellular reduction of nifurtimox, followed by redox cycling, gives the formation of oxygen radical anions ($O_2^{\cdot -}$) and hydrogen peroxide (H_2O_2) molecules which are responsible for damage to proteins, lipids and DNA which lead to cell death of the parasite (see chapter 1). It is thought that benznidazole does not act via this mechanism but through covalent binding to macromolecules[69]. Megazole also acts by oxygen redox cycling, but its main mechanism of action is thought to be protein synthesis inhibition[69] (figure 3.2).

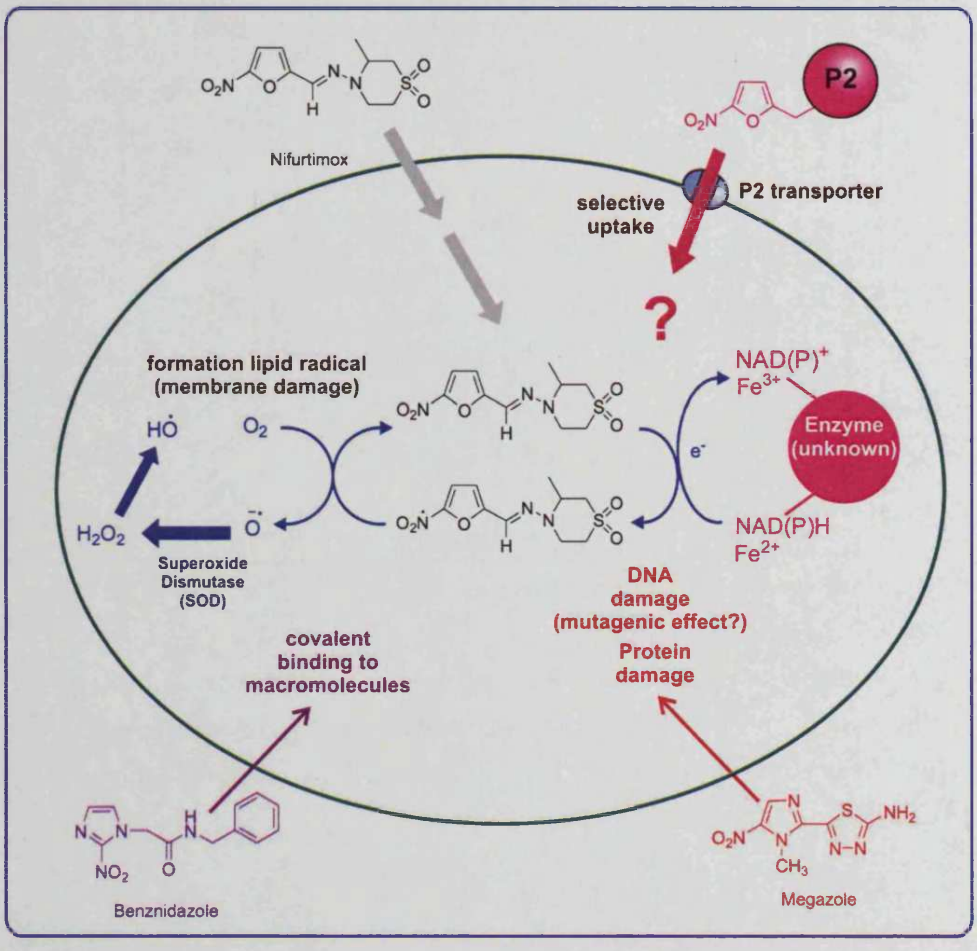

Figure 3.2 Possible mechanisms of action of different nitroheterocycles. The nitrofuran derivatives proposed bearing the P2 motif could have a similar mechanism of action as shown for nifurtimox.

3.4 N- and O-alkylation and arylation of nifurazone and nifuroxime:

Having decided to use nitrofurans as the toxic moiety to be delivered to the parasite, we next focused on a possible way to link the toxic unit to the P2 transporter moiety. 5-nitrofuraldehyde (**1**) represented a good and versatile starting material for this purpose as the aldehyde function can be further functionalised or directly attached to the triazine unit.

Previous workers in our group, Jimenez-Bueno and Klenke initially decided to convert the nitrofuraldehyde into the corresponding nifurazone (**2**) using hydrazine hydrate in methanolic solution to yield compound 2 (scheme 3.3). Arylation of compound **2** using 6-chloro-2,4-diamino-1,3,5-triazine (**4**) was then attempted (Jimenez-Bueno, G., Klenke, B., unpublished data).

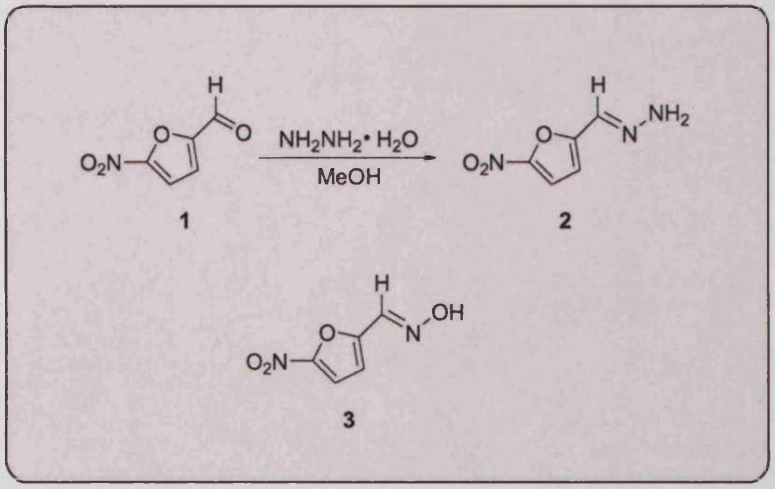

Scheme 3.3 Preparation of nifurazone and structure of nifuroxime.

O- direct arylation was also attempted using the commercially available nifuroxime derivative (**3**). Both arylations were attempted using K_2CO_3/KI in acetonitrile (scheme 3.4) but the formation of the product was not observed.

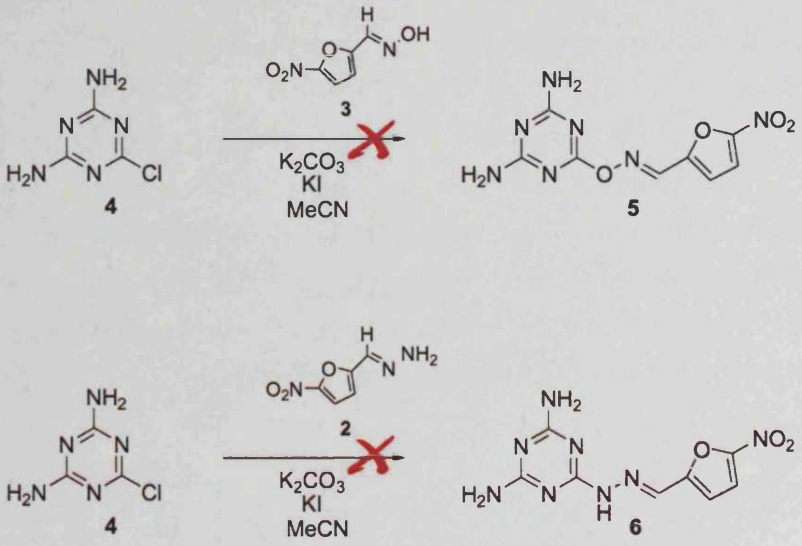

Scheme 3.4 (A) Attempted N and O direct arylations.

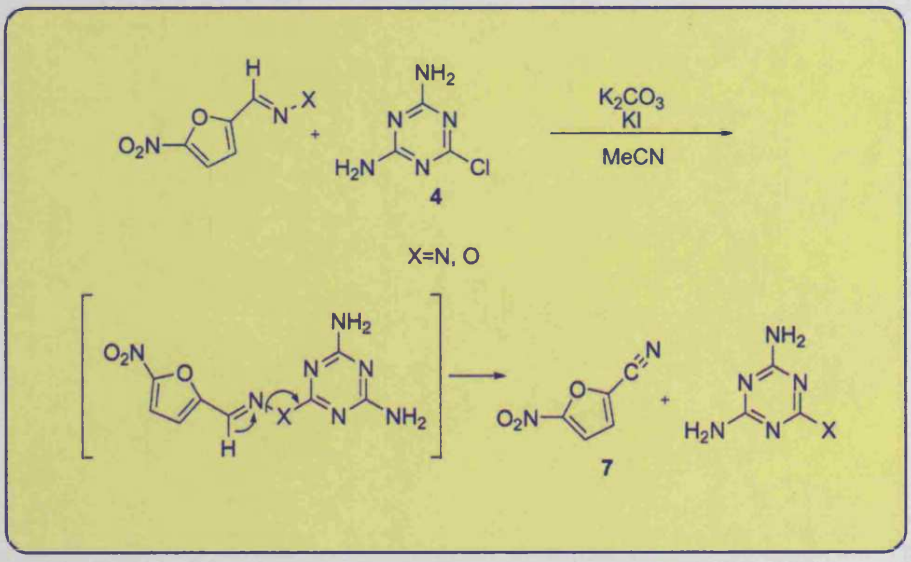

Scheme 3.4 (B) possible mechanism involved in the N and O arylation.

The mass spectrometric analysis of the reaction mixture suggested that the formation of the 5-nitro-2-cyanofuran (**7**) may have occurred after possible decomposition of the desired products as following proton abstraction by the base as proposed in scheme 3.4B. In fact, 1,3,5-triazines act as strongly electron withdrawing substituents and could further activate the oxime or the hydrazone. This property has been

exploited to activate carboxylic acids in peptide coupling reactions and ester formations[75].

In order to reduce this electron withdrawing effect of the triazine, Bueno J. G. replaced the 6-chloro-2,4-diamino-1,3,5-triazine with 6-bromomethyl-2N-methyl-2,4-diamino-1,3,5-triazine (**8**) (scheme 3.5). The experiments were conducted using two different solvents. However analysis suggested that the product may have been formed and probably also decomposed by a similar mechanism (scheme 3.6).

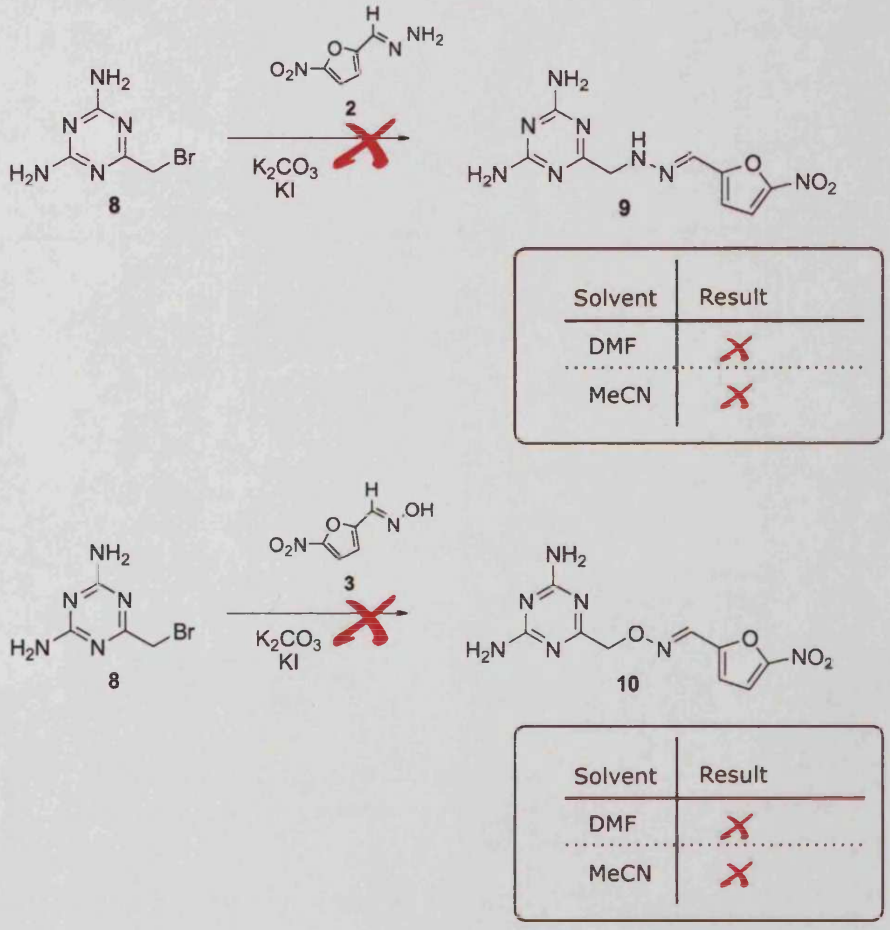

Scheme 3.5 Attempted N and O-alkylation of nifuroxime and nifurazone.

The difficulties encountered in the synthesis of these initial derivatives forced us to find other routes for linking the two units. Our initial idea was to attach the hydrazine function to the triazine ring instead

[75] Kaminska, J. E.; Kaminsky, J. Z.; Gora, J. 2-Acyloxy-4,6-dimethoxy-1,3,5-triazine - A new reagent for ester synthesis. *Synthesis* **1999**.

of to the nitrofuran (scheme 3.6). The commercially available 6-chloro-2,4-diamino-1,3,5-triazine (**4**) was converted to the hydrazine derivative by refluxing the starting material with hydrazine hydrate in water solution[76]. The 1,3,5-triazinyl-hydrazine intermediate obtained (**11**) was then successfully coupled to the 5-nitrofuraldehyde to give the corresponding first hydrazone final product (**6**).

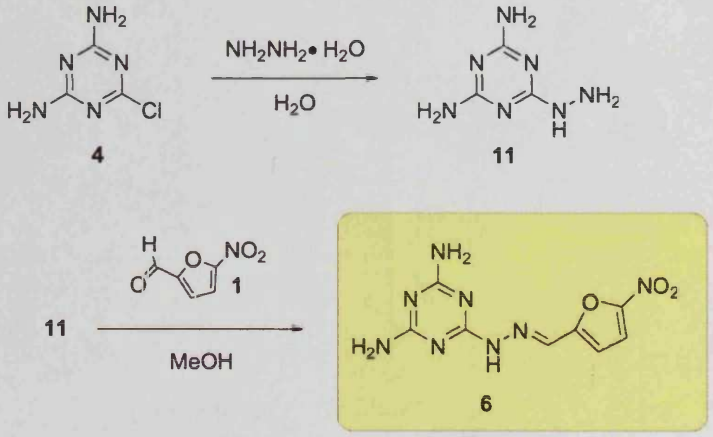

Scheme 3.6 Synthesis of the first lead hydrazone.

The product obtained gave one of the first interesting biological assay results. In fact, *in vitro* screening of the compound against a model of *T. b. rhodesiense* infection had shown an activity in the sub micromolar range and this result was very encouraging. One of the problems encountered during the preparation of compound **6** was its low solubility, which made its purification problematic.

Compound **6** represented our first lead structure. With this in mind, a different series of compounds were generated by modifying this structure. This work represents the main part of the project carried out in our laboratory throughout my PhD studentship.

☞ *The work described from this part onwards is that carried out by the author to fulfil the requirements of the degree award.*

[76] Simmonds, R. J.; Stevens, M. F. G. Triazines and Related Products .25. Methods for the Attachment of Sugar Residues to Cyto-Toxic 1,3,5-Triazines. *J. Chem. Soc.-Perkin Trans. 1* **1982**, 1821-1825.

3.5 Design and synthesis of new hydrazones compounds:

The figure 3.3 below summarises the main modifications that were introduced in our lead structure (**6**) and that are described in the following paragraphs.

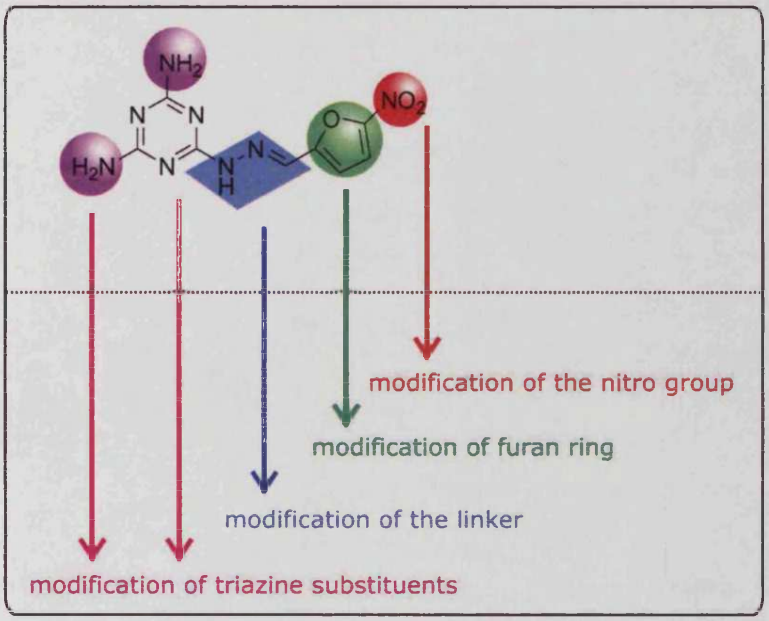

Figure 3.3 Representation of the possible modifications of the lead structure.

The main modifications carried out, based on our lead compound (**13**) included:

- modification of the furan ring and replacement with other heterocyclic rings or homoaromatic rings;
- modification of the nitro group and elimination of the group;
- modification of the linker;
- modification of the substituents of the triazine ring.

Before starting to carry out this series of modifications we decided to further characterise and analyse our lead compound. The product was synthesised following the same procedure carried out by Bueno-Jimenez in our laboratory. The synthesis was successfully achieved with 36% yield and purification was performed by recrystallisation with water-methanol (95/5).

The ^{1}H-NMR of the product is very interesting with a characteristic signal of the hydrazone function (-NH-) that falls around 11 ppm and a signal of the –CH- of the imino function that falls around 8 ppm (figure 3.4). We have also noted that this compound is insoluble in most of the organic solvents except DMSO. This insolubility represents an issue for this class of compounds and some of the modifications we have carried out are aimed at improving this property as greater solubility will facilitate their development as drugs.

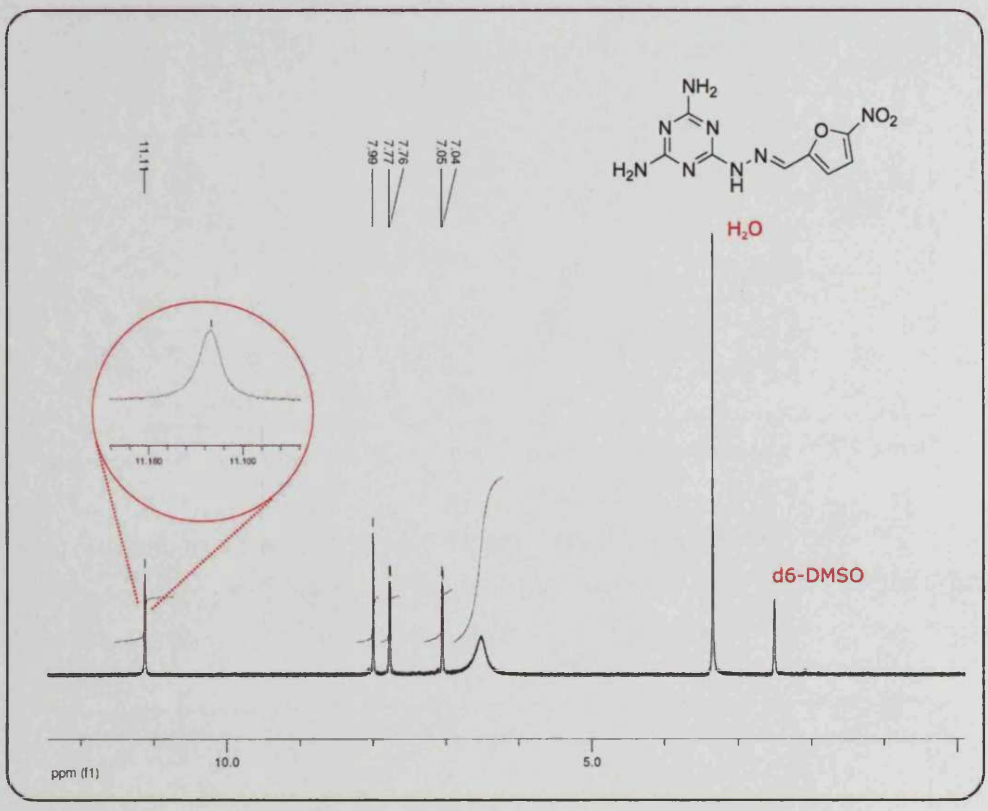

Figure 3.4 ^{1}H-NMR of compound **6**.

3.6 Modification of the furan ring:

3.6.1 Replacement of furan ring with a thiophene ring:

The first change we decided to carry out was the replacement of the furan ring with a thiophene ring. The introduction of a thiophene not only allows us to understand the importance of the furan ring for the trypanocidal activity but we also thought that this could be a strategy to improve the solubility of the product in organic solvents and thus the

pharmacokinetic properties. Another important reason for having a thiophene derivative is related to its possible different redox potential compared to the lead compound. It is well known that the biological activity of several nitroheterocycles is dependent upon the nitro group reduction process (scheme 3.8)[77]. The mechanism of action of megazol, for instance, is still unknown but it has been proved that its reduction is a key step for that mechanism[77]. The single electron reduction of megazol by trypanosome microsomes has been confirmed by enzymatic reduction studies. Although the mode of action of these nitrofuran derivatives is not yet known, redox recycling cannot be ruled out[78].

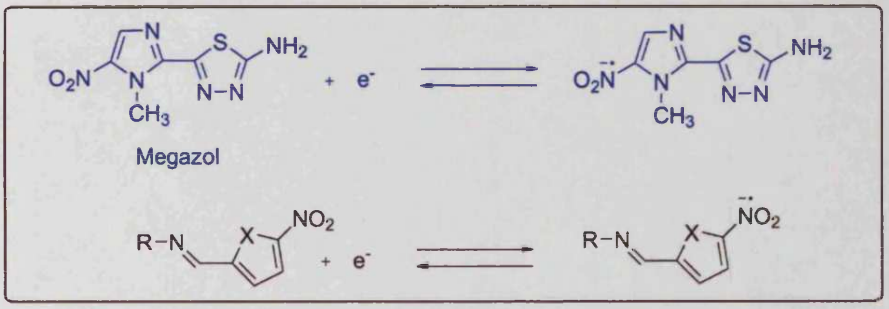

Scheme 3.7 reduction equation of megazol and of a general nitroheterocycle derivate.

The commercially available 5-nitrothiophen-2-carboxaldehyde (**12**) was reacted with the triazinyl-hydrazine derivative (**11**) giving the 5-nitrothiophene-carboxaldehyde hydrazone derivative (**13**) in 25 % yield.

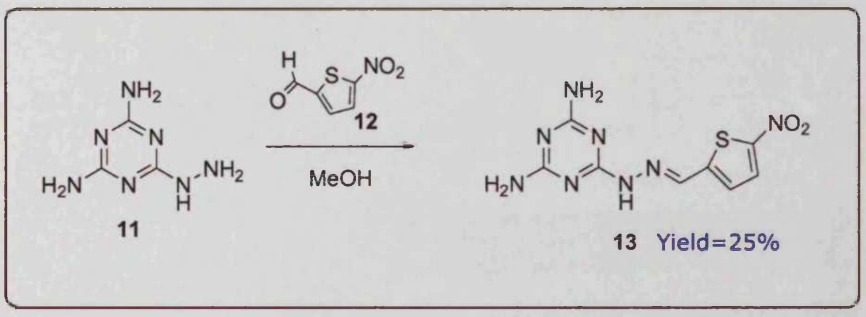

Scheme 3.8 Synthesis of hydrazone derivate of the 5-nitro-thiophene-2-carboxaldehyde.

[77] Bontà, M.; Chauviere, G.; Perie, J.; Nunez-Vergara, L. J.; Squella, J. A. Nitro radical anions from megazol and related nitroimidazoles in aprotic media. A father-son type reaction triggered by an acidic proton. *Eletrochim. Acta* **2002**, *47*, 4045-4053.

[78] Viode, C.; Bettache, N.; Cenas, N.; Krauth-Siegel, R. L.; Chauviere, G.; Bakalara, N.; Perie, J. Enzymatic reduction studies of nitroheterocycles. *Biochem. Pharmacol.* **1999**, *57*, 549-557.

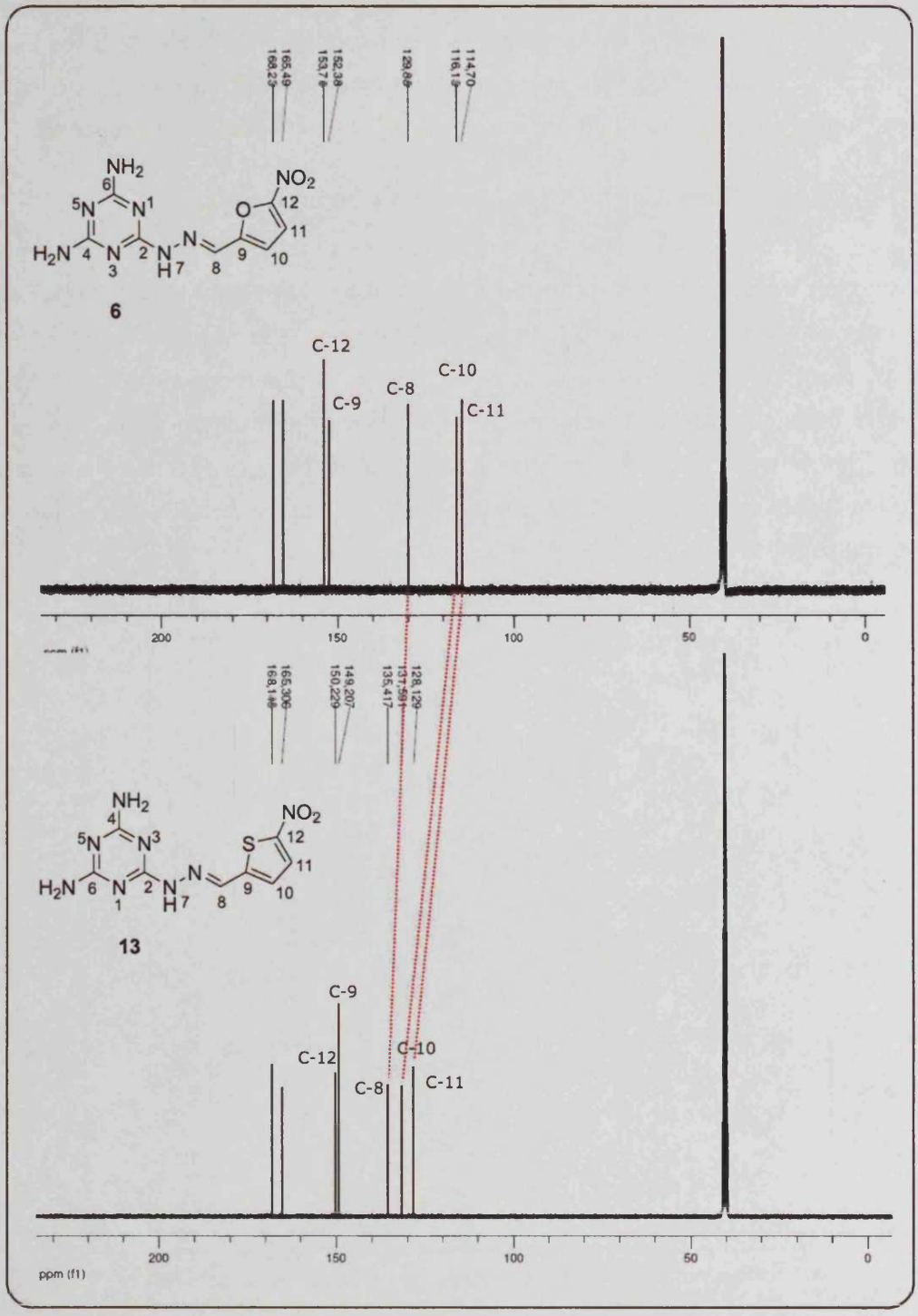

Figure 3.5 ^{13}C-NMR of new hydrazone compounds.

It is interesting to compare the ^{13}C-NMR of compound **6** with the thiophene analogue (**13**). Replacement of the O with a S significantly changed the chemical shifts of the –CH- of the thiophene ring but does not

affect the chemical shifts of the triazine carbons. The peaks corresponding to -CH- of the thiophene ring are shifted to higher values compared to those of the furan. The -CH- of the imino function of the thiophene analogue also falls at a higher value but the difference is less significant.

3.6.2 Replacement of furan ring with a phenyl ring:

In order to evaluate the importance for the activity of the nitrofuran function we decided to synthesise a series of derivatives in which the furan ring has been replaced with a homoaromatic ring. The reaction was carried out reacting the hydrazine derivative (**11**) with the three isomers of the nitro-benzaldehyde (**14**, scheme 3.9)[44]. The yields obtained were different for the different hydrazones: recrystallisation of the orto and meta isomers gave yields below 20% whilst the para isomer was recrystallised to give a significantly improved yield of 77%.

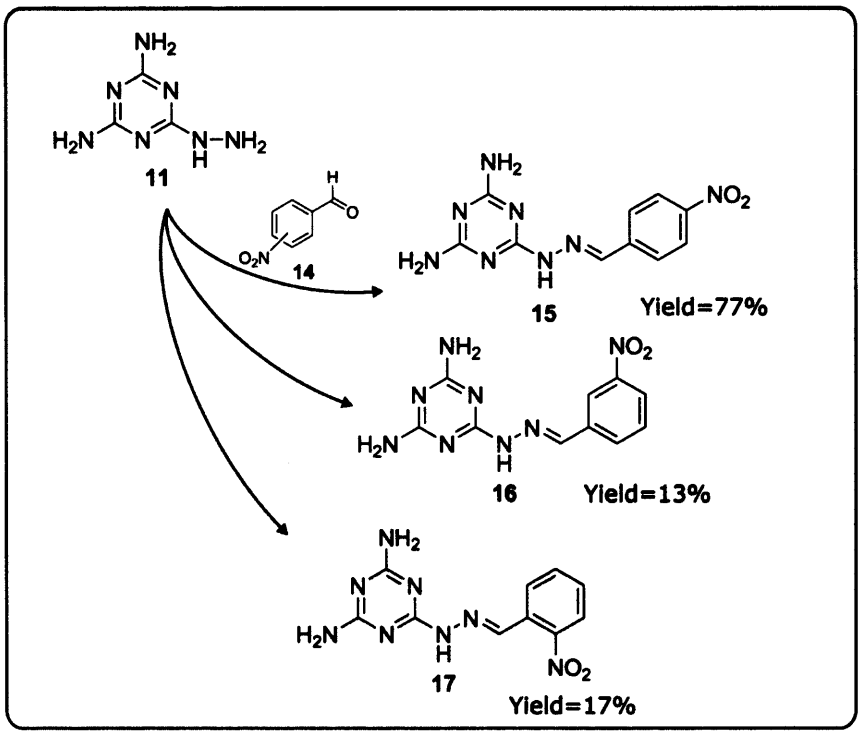

Scheme 3.9 synthesis of hydrazones of the nitrobenzaldehyde.

3.7 Modification of the nitro group:

One of the main issues in the development of new trypanocidal nitroheterocycles concerns their possible genotoxic effects[72]. Some studies

have shown that the mechanism of megazol is associated with DNA damage[79]. Moreover megazol was found to give a positive Ames test[80] and to be mutagenic in mammalian cell tests[72]. It is extremely important to determine whether this unwanted effect is dependent on a particular chemical functionality. It is also important to determine if the mechanism behind the trypanocidal activity is the basis of this mutagenic effect. The role of the nitro group was therefore investigated.

3.7.1 Removal of the nitro group function:

One of the first changes we decided to consider was the removal of the nitro group. Even though the mechanism of action of nitrofuran derivatives is still unclear, the role of the nitro group in their mechanism seems essential. Therefore hydrazone derivatives, without the nitro function, were designed in order to evaluate the role of this group for the activity. Considering the first two hydrazone nitroderivatives (**6** and **13**) of our series, we synthesised their corresponding analogues without the nitro group function using respectively 2-furaldehyde (**18**) and 2-thiophene-carboxaldehyde (**20**) to yield compounds **19** and **21** respectively.

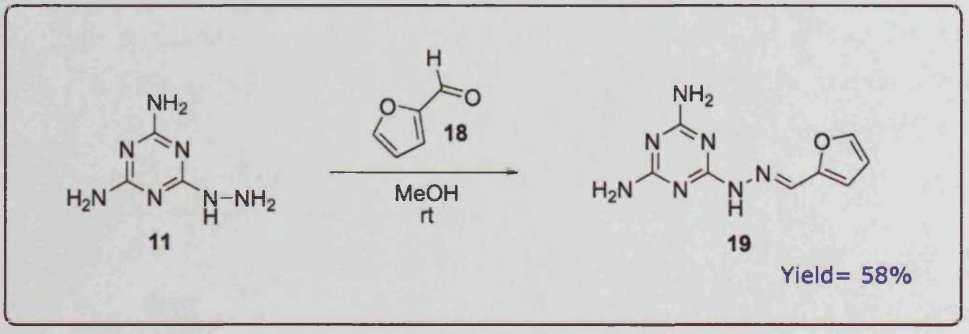

Scheme 3.10 Synthesis of hydrazone derivative of the 2-furaldehyde

[79] Enanga, B.; Ariyanayagam, M. R.; Stewart, M. L.; Barrett, M. P. Activity of megazol, a trypanocidal nitroimidazole, is associated with DNA damage. *Antimicrob. Agents Chemother.* **2003**, *47*, 3368-3370.

[80] Ferreira, R. C.; Ferreira, L. C. CL 64,855, a potent anti-*Trypanosoma cruzi* drug, is also mutagenic in the *Salmonella*/microsome assay. *Mem. I. Oswaldo Cruz* **1986**, *81*, 49-52.

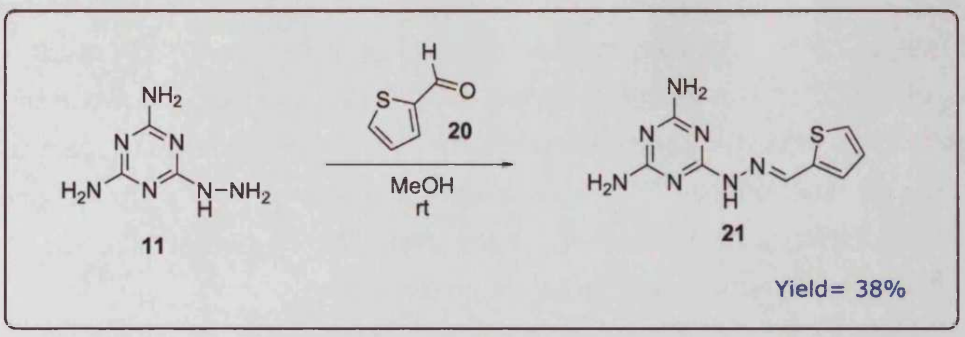

Scheme 3.11 Synthesis of hydrazone derivative of the thiophene 2-carboxaldehyde.

3.7.2 Replacement of nitro group: synthesis of cyanoderivate analogue:

Another interesting modification we carried out was the replacement of the nitro group with a nitrile function. This modification was carried out to determine whether the properties of this group are entirely dependant upon the electronic properties of the nitro group. For this purpose the nitro group was replaced with another electron withdrawing group, the nitrile group. In order to carry out this modification, 5-cyano-2-furaldehyde (**23**) was needed. During the synthesis of **23** we encountered some difficulties which we think were probably related to the electron withdrawing effect of the nitrile group. Therefore different routes to **23** were investigated. The first reaction attempted was the formylation of the 2-cyano-furan (**22**) via the **Vilsmeier reaction**.

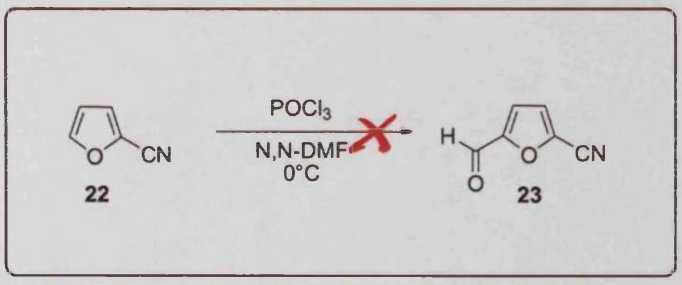

Scheme 3.12 Attempted synthesis of 5-cyano-2-furaldehyde.

The mechanism proceeds through the formation of the Vilsmeier reagent via addition of the phosphorous oxy-trichloride to the N,N-DMF. It was expected that the highly reactive intermediate would react with the cyanofuran via electrophilic aromatic substitution, as shown in scheme 3.13, to give 5-cyano-2-furaldehyde (**23**).

Treatment of **22** with $POCl_3$ under the standard conditions at 0°C using DMF as both solvent and source of formyl group was carried out[81]. MS analysis showed the formation of the expected product but the attempt to isolate it from the complex mixture failed. ^{1}H-NMR analysis of the mixture showed a weak signal of the aldehyde and it is likely that the amount of product formed was negligible.

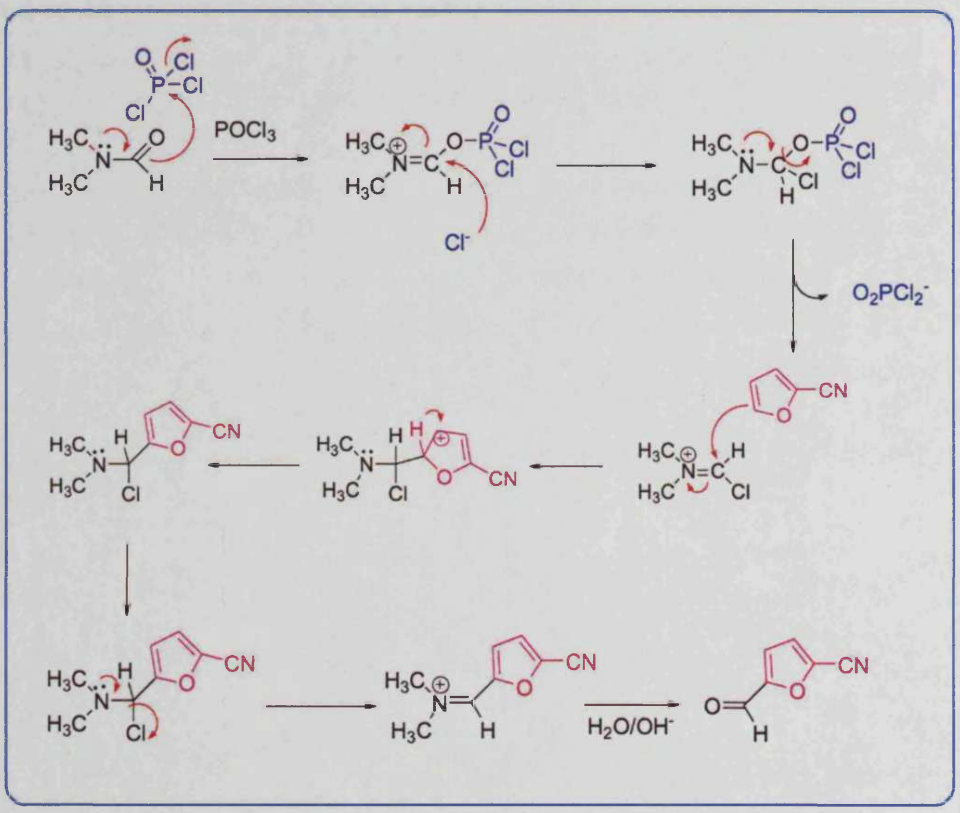

Scheme 3.13 Mechanism of Vilsmeier reaction[81].

A possible explanation of the low reactivity of the cyanofuran could be due to the electron withdrawing effect of the nitrile group that exerts a deactivating effect on the furan ring. In fact, as shown on the following resonance structures (scheme 3.14), the positive charge in one of the structures falls on the carbon that is directly involved in the electrophilic attack.

[81] Downie, I. M.; Earle, M. J.; Heaney, H.; Shuhaibar, K. F. Vilsmeier Formylation and Glyoxylation Reactions of Nucleophilic Aromatic-Compounds Using Pyrophosphoryl Chloride. *Tetrahedron*. **1993**, *49*, 4015-4034.

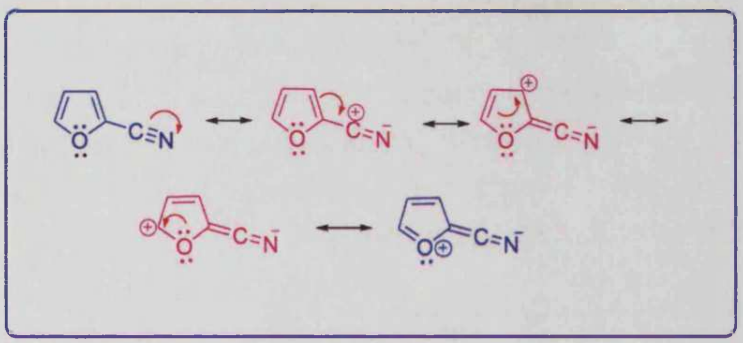

Scheme 3.14 Resonance structures of 2-cyanofuran. The resonance structures of major importance are represented in blue.

The problems associated with scheme 3.12 led us to propose scheme 3.15 as an alternative route. 5-hydroxymethylfuraldehyde (**24**) was used as the starting material. The aldehyde was converted to the corresponding aldoxime (**25**) by nucleophilic addition of hydroxylamine hydrochloride at 0°C.

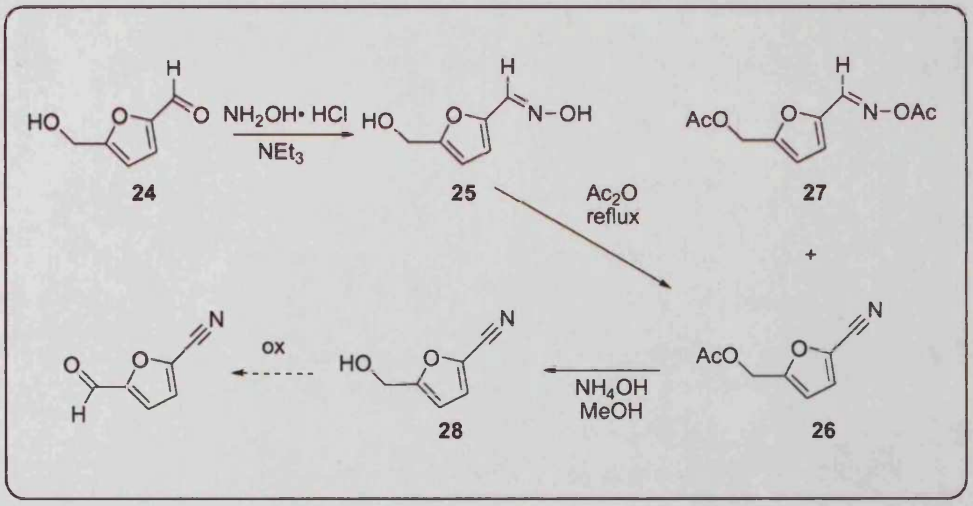

Scheme 3.15 Alternative route attempted for the synthesis of 5-cyano-furaldehyde.

The oxime was successively refluxed with acetic anhydride giving the corresponding acetylated nitrile[82] (**26**) together with the bis-acetylated aldoxime (**27**) as unwanted byproduct. The nitrile (**26**) was hydrolysed to

[82] Chauviere, G.; Bouteille, B.; Enanga, B.; de Albuquerque, C.; Croft, S. L.; Dumas, M.; Perie, J. Synthesis and biological activity of nitro heterocycles analogous to megazol, a trypanocidal lead. *J. Med. Chem.* **2003**, *46*, 427-440.

the corresponding alcohol (**28**) using a solution of ammonia in methanol[83]. However as only a negligible amount of compound **28** was obtained the oxidation could not be performed.

At this point we found a "one pot method" in the literature for the conversion of aldehydes into nitriles (scheme 3.16)[84]. The procedure was carried out using hydroxylamine hydrochloride and phthalic anhydride in anhydrous acetonitrile[84]. However, analysis of the reaction suggested that polymerisation may have occurred and the desired product was not obtained.

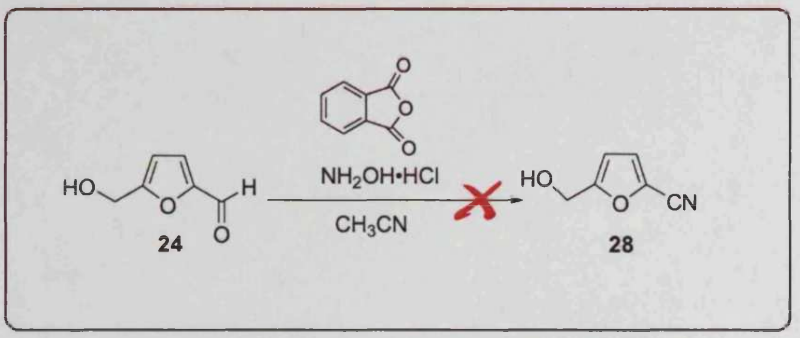

Scheme 3.16 Attempted direct conversion of aldehyde to nitrile.

Transformation of **24** to the desired product **28** was successfully achieved using iodine in ammonia-water and THF using the method of Talukdar *et al.*[85]. The mechanism proposed (scheme 3.18) involves the nucleophilic addition of the ammonia to the aldehyde to give the corresponding aldimine which is subsequently oxidised with iodine to give an N-iodo-aldimine intermediate. The subsequent elimination of HI gives the correspondent nitrile (**28**). The formation of the nitrile can be easily monitored since the dark solution turns to a colourless solution after complete reduction of the iodine to iodide.

---

[83] Floyd, A. J.; Kinsman, R. G.; Roshanali, Y.; Brown, D. W. Direct Cyanation of the Furan Nucleus by Chlorosulfonyl Isocyanate. *Tetrahedron,* **1983**, *39*, 3881-3885.

[84] Wang, E. C.; Lin, G. J. A new one pot method for the conversion of aldehydes into nitriles using hydroxyamine and phthalic anhydride. *Tetrahedron Lett.* **1998**, *39*, 4047-4050.

[85] Talukdar, S.; Hsu, J. L.; Chou, *T.* C.; Fang, J. M. Direct transformation of aldehydes to nitriles using iodine in ammonia water. *Tetrahedron Lett.* **2001**, *42*, 1103-1105.

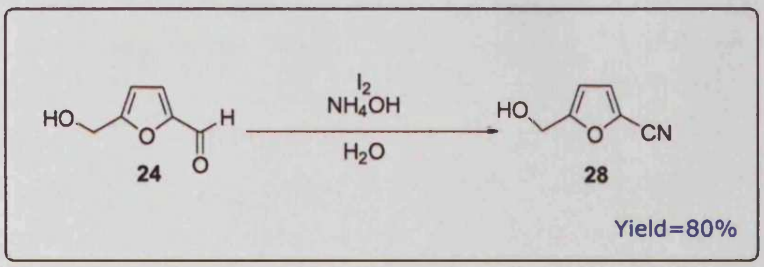

scheme 3.17 conversion with Iodine.

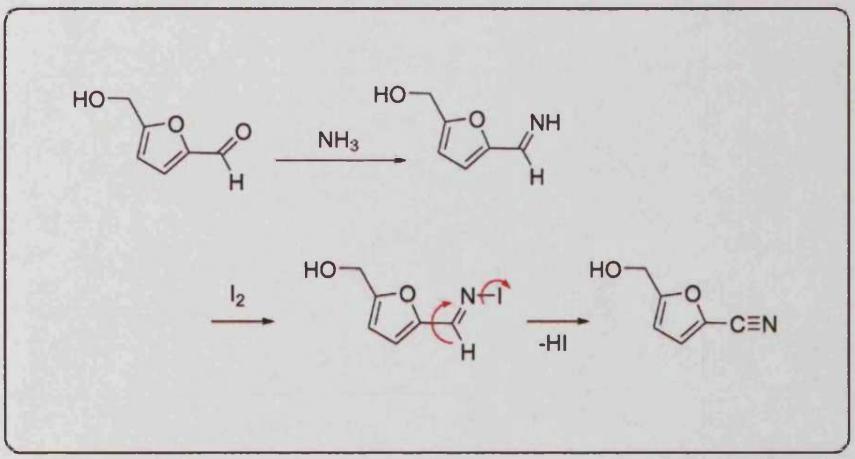

Scheme 3.18 mechanism of conversion of aldehyde to nitrile via Iodine.

Oxidation of the alcohol (**28**) to the aldehyde (**23**) was carried out using the standard procedure of pyridinium chlorochromate (PCC) in DCM (scheme 3.19). However, the yield of the reaction was very low and the amount of aldehyde recovered after purification was negligible.

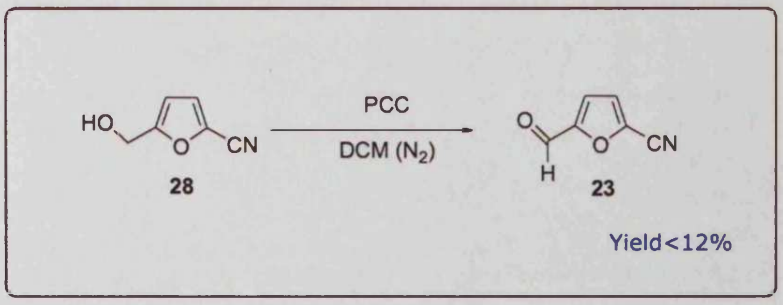

scheme 3.19 Oxidation with PCC in DCM.

The oxidation of the alcohol **28** was achieved in higher yield via the **Swern oxidation**[86]. The mechanism described (scheme 3.20) is characterised by the nucleophilic attack of DMSO on the oxalyl chloride. Nucleophilic acylic substitution is followed by decarboxylation to generate the highly reactive chlorosulfonium intermediate which reacts with the alcohol (**28**). Proton abstraction by Et_3N catalyses the elimination of the dimethylsulfide and the oxidation of the alcohol to aldehyde (**23**, scheme 3.20).

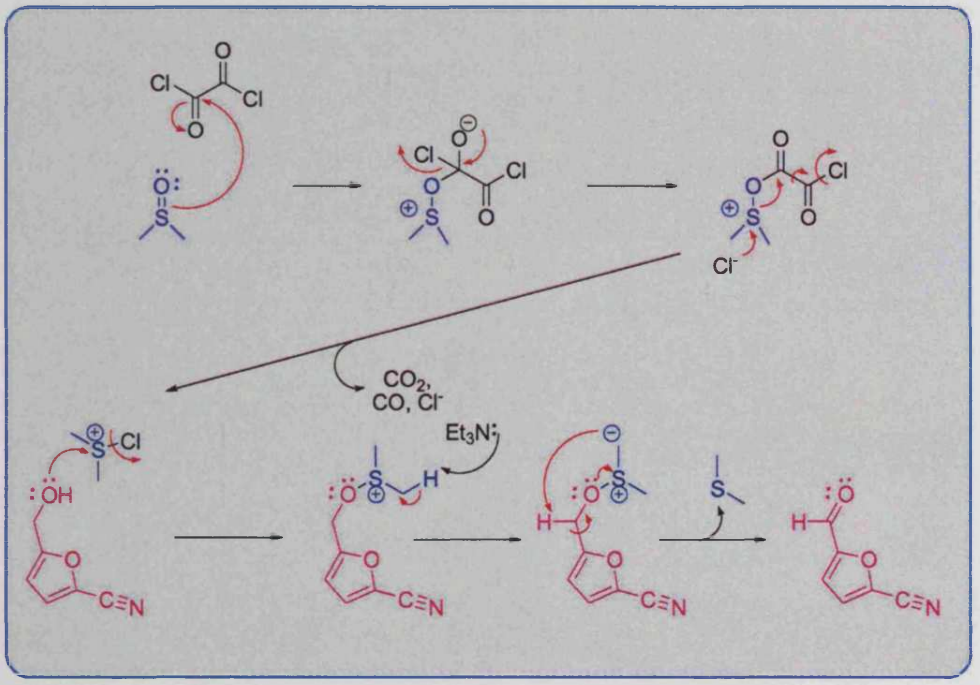

Scheme 3.20 Mechanism of Swern oxidation[86].

The aldehyde **23** was subsequently coupled with the hydrazine intermediate **11** to give the corresponding hydrazone (**29**) as shown on scheme 3.21.

[86] Omura, K.; Swern, D. Oxidation of alcohols by "activated" dimethyl sulfoxide. A preparative, steric and mechanistic study. *Tetrahedron*, **1978**, *34*, 1651-1660.

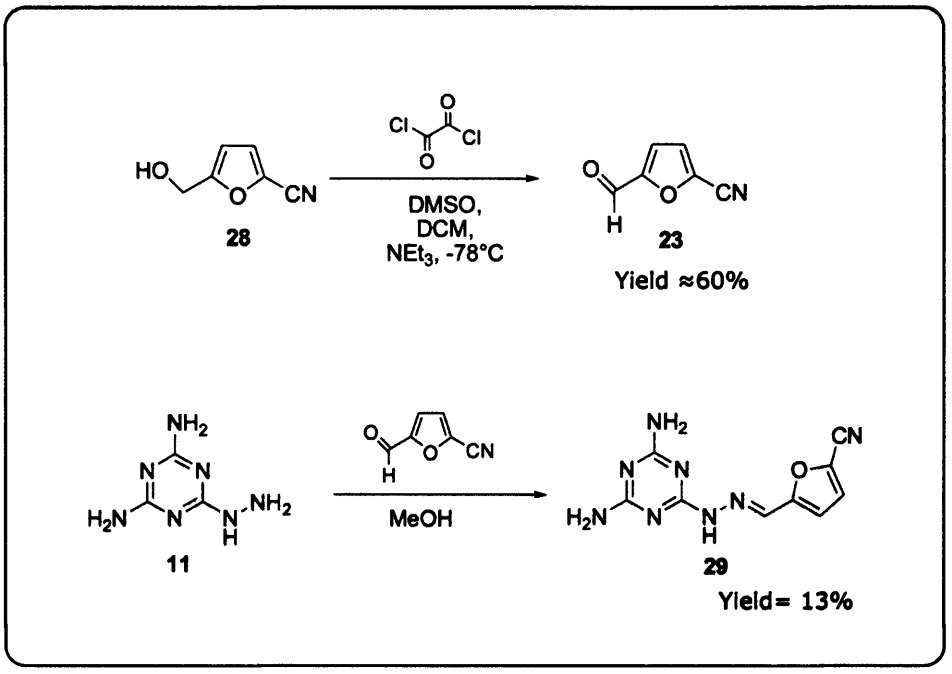

scheme 3.21 Oxidation of alcohol via Swern oxidation and formation of the hydrazone derivative of 5-cyano-2-furaldehyde.

3.8 Nitrothiazole as cytotoxic unit and nitazoxanide:

We have already discussed that mutagenicity is a possible issue for the clinical development of nitrofuran derivatives. Noteworthy also is the latest data regarding nitazoxanide. The nitazoxanide is a redox-active prodrug chemically consisting of nitrothiazolyl-salicylamide (scheme 3.7). The drug is known for its antiprotozoan, antihelmintic and antibacterial properties against *Helicobacter pylori*[87]. Studies of mutations to give rifampicin resistance have indicated that nitazoxanide is not mutagenic[87]. Although the mechanism of action of this drug is still unclear, it is known that, its possible action is related to the presence of the nitrothiazole ring. It was thought that substitution of the nitrofurans with the nitrothiazole may dissociate the trypanocidal effect from the mutagenic effect. Therefore several attempts were performed in order to prepare compounds such as that detailed below in scheme 3.7.

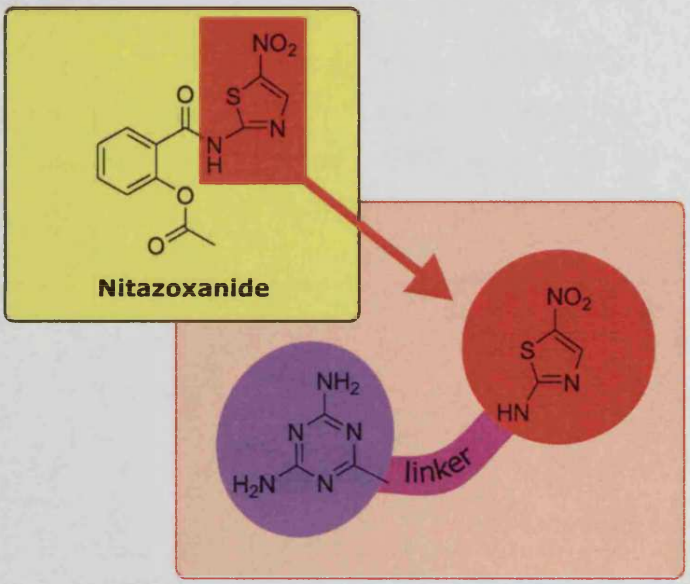

Figure 3.7 Structure of nitazoxanide and design of melamine nitrothiazoles.

Two different routes were attempted, based on the nucleophilic aromatic substitution of the halogen. In the first route we attempted the

[87] Sisson, G.; Goodwin, A.; Raudonikiene, A.; Hughes, N. J.; Mukhopadhyay, A. K.; Berg, D. E.; Hoffman, P. S. Enzymes associated with reductive activation and action of nitazoxanide, nitrofurans, and metronidazole in Helicobacter pylori. *Antimicrob. Agents Chemother.* **2002**, *46*, 2116-2123.

nucleophilic aromatic substitution on the triazine ring by the amine of the nitrothiazole **30** (scheme 3.22) and 6-chloro-2,4-diamino-[1,3,5]-triazine (**4**) was chosen as first substrate for the displacement with 2-amino-5-nitrothiazole (**30**) as shown on scheme 3.22. After 24 hrs at reflux, the formation of the desired product (**31**) was not observed by TLC and MS analysis of the reaction mixture.

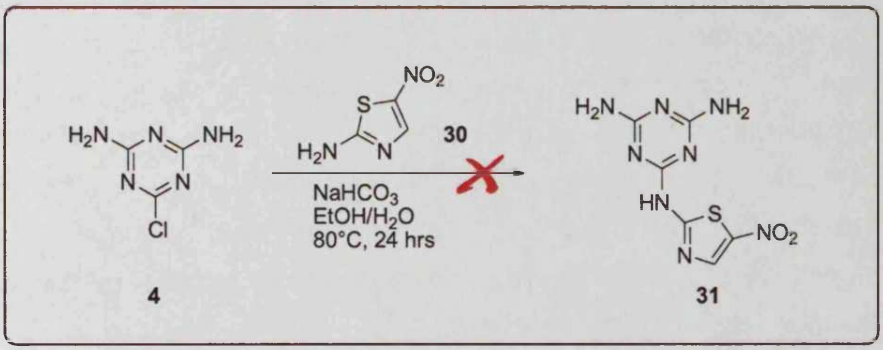

Scheme 3.22 attempted synthesis of melaminyl-5-nitro-thiazole.

It is possible that the amino group attached to the thiazole ring is deactivated by the presence of the nitro group, as shown on the following resonance structures, and this would explain the poor nucleophilic character of the amino group.

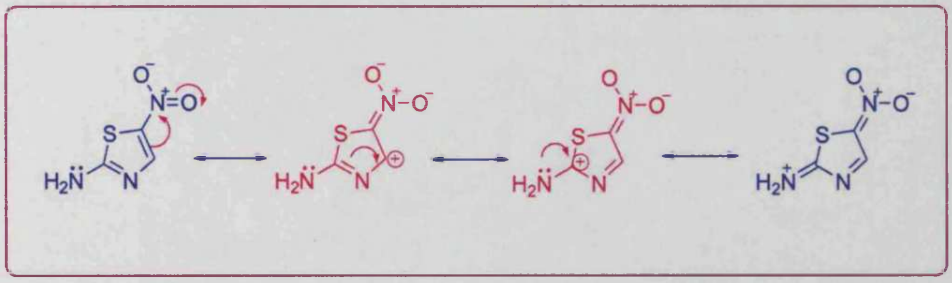

Scheme 3.23 resonance structures of 2-amino-5-nitrothiazole (**32**). The resonance structures of major importance are represented in blue.

After this observation, we proposed to move the halogen to the thiazole ring, which should activate for nucleophilic aromatic substitution by the nitro group. A series of substrates with varying nucleophilic character was chosen, as shown in scheme 3.24, but unfortunately none of the reaction gave the desired product, as confirmed by TLC, MS and NMR

analyses. These results suggest that the 5-nitro-thiazole ring is probably not activated enough for the nucleophilic aromatic substitution.

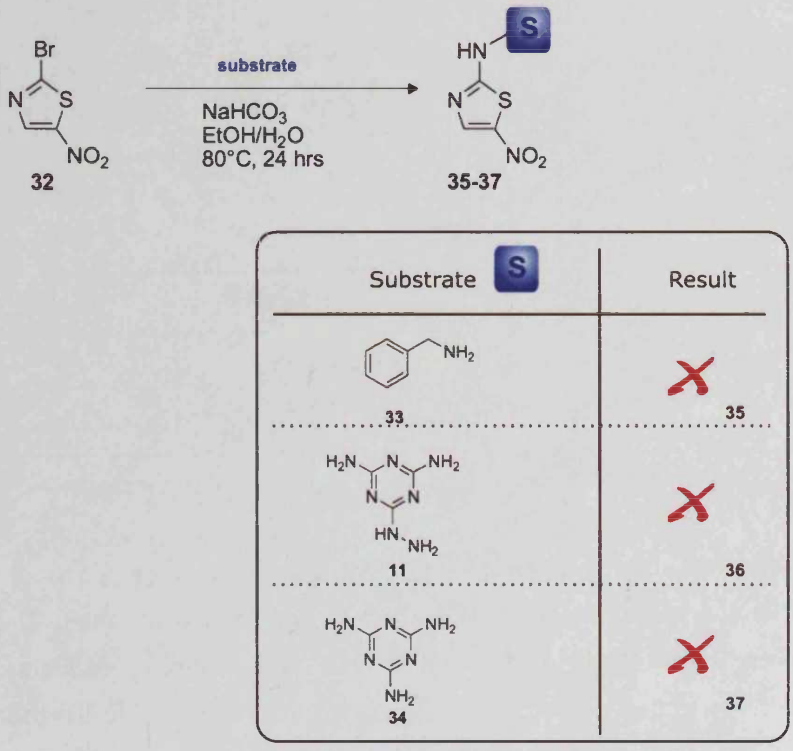

Scheme 3.24 Attempted synthesis of some nitrothiazole compounds.

3.9 Modification of linker function: reduction of the hydrazone

One of the modifications of the hydrazone linker we investigated involves the reduction of the hydrazone to hydrazine. The hydrazone lead compound **11** was chosen for reduction. However, the product showed high resistance to all the different reduction conditions attempted. We can propose that the hydrazone function maintains the conjugation of the aromatic rings and generates a highly conjugated and stable system. Several attempts were carried out to reduce the hydrazone function (scheme 3.25 A and B) using two different starting materials. In the first two attempts the reduction was attempted on hydrazone (**6**) prepared *in situ* from compound **11** (scheme 3.25 A). In both cases $NaBH_4$ in dry methanol was used. In a second attempt the solvent was concentrated

after the formation of the hydrazone to remove any water generated in situ and then dry MeOH was added.

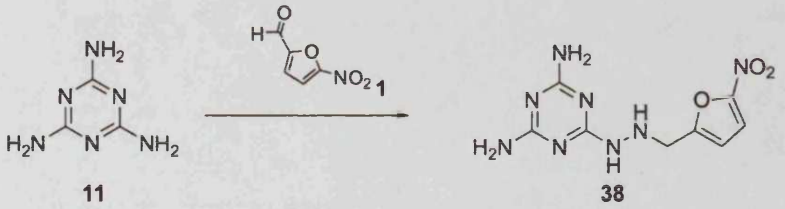

Reagent/Solvent	Result
$NaBH_4$/ MeOH	✗
$NaBH_4$/ readdition of fresh dry MeOH	✗

Scheme 3.25 A Formation *in situ* of **6** and subsequent reduction.

The last two attempts (scheme 3.25 B) were carried out on recrystallised hydrazone **6** using $NaBH_4$ in dry MeOH or $LiAlH_4$ in dry THF respectively. The starting material proved to be inert to reducing agents and as well as observed in the previous two attempts the hydrazone **6** was recovered from the reaction mixture with no other products.

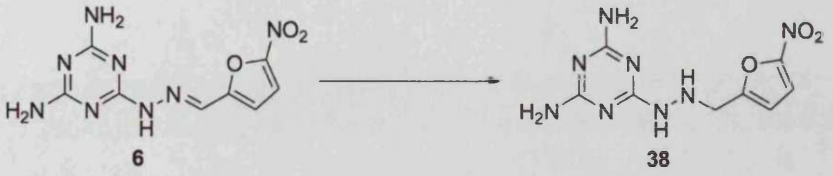

Reagent/Solvent	Result
$NaBH_4$/ MeOH	✗
$LiAlH_4$/ THF	✗

Scheme 3.25 B Attempted reductions of the hydrazone **6**.

An alternative route to access the hydrazine derivative **38** is shown on the scheme above. We proposed that the hydrazinyl-triazine **11** should attack 2-bromomethyl-5-nitrofuran by nucleophilic substitution to give the desired hydrazone derivative **38**.

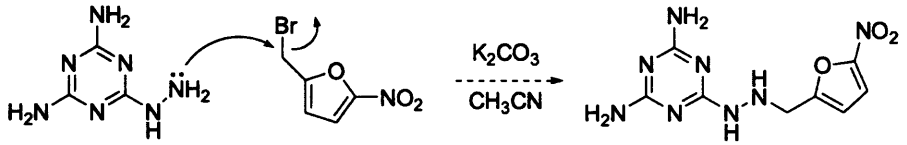

11 **39** **38**

Scheme 3.26 Alternative route for the synthesis of the hydrazone compound **38**.

3.10 Modification of the triazine moiety:

3.10.1 Methyl substituted triazinyl-hydrazines:

In order to alter the lipophilic properties of our lead compound **6**, our initial modifications to the triazine moiety were based on the introduction of methyl substituents to the melamine unit. The starting material used for this purpose is represented was cyanuric chloride. The formation of aminochloro-s-triazines has not been generally studied and only a few references can be found in literature. However, some reactions of cyanuric chloride with ammonia and few amines have been reported by Fierz-David and Matter[88].

We have prepared novel substituted alkylamino-triazines through modifications of the standard procedure. Most of the reactions were carried out in a suspension of water. The cyanuric chloride was finely suspended in water by pouring an acetone solution of it into ice-water[89]. The use of an aqueous system allowed the product to be isolated in high yields[90] and at the same time increased the reactivity of the cyanuric chloride. Triazine derivatives were prepared fresh for subsequent use as

[88] Fierz-David, H. E.; Matter, M. Azo and anthraquinonoid dyes containing the cyanuric ring. *J. Soc. Dyers Colour.* **1937**, *53*, 424-436.

[89] Goi, M. Reactivities of cyanuric chloride derivative I. Displacement reactions of substituted 2,4-bis(anilino)-6-chloro-s-triazines with benzylamine. *Yuki Gosei Kagaku Kyokaishi* **1960**, *18*, 332-336.

[90] Thurston, J. *T.*; Dudley, J. R.; Kaiser, D. W.; Hechenbleikner, I.; Schaefer, F. C.; Holm-Hansen, D. Cyanuric Chloride Derivatives I. Aminochloro-s-triazines. *J. Am. Chem. Soc.* **1951**, *73*, 2981-2983.

they can decompose on storage and cause purification problems for subsequent products[91].

The chlorine atoms of cyanuric chloride can be replaced successively by substituted or non substituted amines via nucleophilic aromatic substitution (scheme 3.27) activated by the triazine ring.

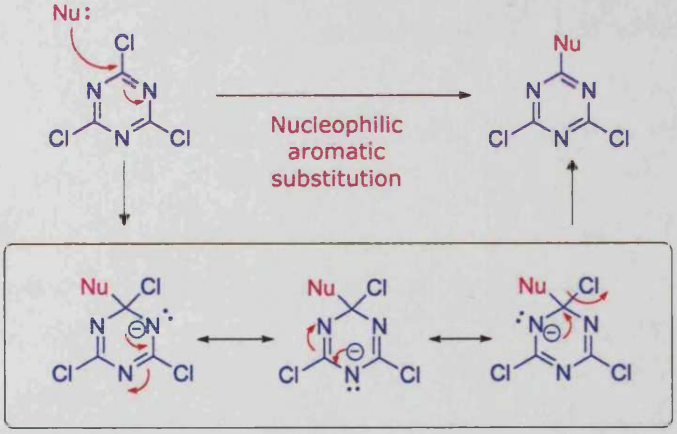

Scheme 3.27 Nucleophilic aromatic substitution of cyanuric chloride.

After the first displacement, the following displacements of chlorine become sequentially more difficult. However, nucleophiles can selectively displace the three different chlorines of cyanuric chloride by controlling the reaction temperature. In general the first substitution can be achieved by keeping the temperature below 0°C. The second chlorine can be displaced by increasing the temperature to room temperature and the third at above 70 °C[92] (scheme 3.28). Together with these factors it is also important to consider the reactivity of the nucleophiles. In the last two chlorines the reactivity varies greatly with the degree of substitution and with the nature of the nucleophile[90]. In general, when different amino groups are to be introduced the least reactive amine is introduced first[44].

[91] Pearlman, W. M.; Banks, C. K. Substituted chlorodiamino-s-triazines. *J. Am. Chem. Soc.* **1948**, *70*, 3726-3728.

[92] De Hoog, P.; Gamez, P.; Driessen, W. L.; Reedijk, J. New polydentate and polynucleating N-donor ligands from amines and 2,4,6-trichloro-1,3,5-triazine. *Tetrahedron Lett.* **2002**, *43*, 6783-6786.

The use of water as a reaction medium does not cause hydrolysis of the chlorotriazine but simplifies the isolation of the products that precipitate clearly from solution[93].

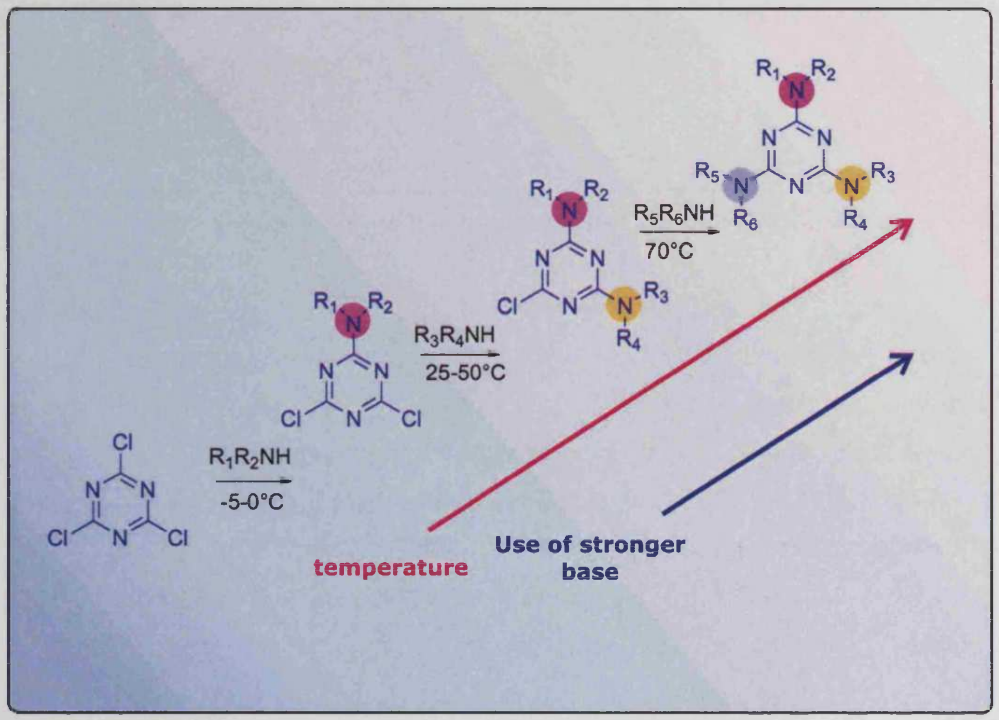

Scheme 3.28 Effect of temperature and of base on substitution of cyanuric chloride.

The first monoamino substituted 4,6-dichlorotriazines were obtained by reaction of cyanuric chloride with ammonia, methylamine and dimethylamine hydrochloride respectively[94,95]. The hydrochloride amine salts were neutralised with NaOH and the products precipitated from solution to give the desired intermediates **41-43** in high yields[44].

[93] Kaiser, D. W.; Thurston, J. *T.*; Dudley, J. R.; Schaefer, F. C.; Hechenbleikner, I.; Holm-Hansen, D. Cyanuric chloride derivatives. II Substituted melamines. *J. Am. Chem. Soc.* **1951**, *73*, 2984-2986.

[94] Diels, O. "Zur Kenntnis der Cyanurverbindungen". *Ber. Deut. Chem. Ges.* **1899**, *32*, 691-702.

[95] Koopman, H.; Daams, J. Investigations on herbicides. I. 2-(Substituted amino)-4,6-dichloro-1,3,5-triazines. *Recl. Trav. Chim. Pay-B.* **1958**, *77*, 235-240.

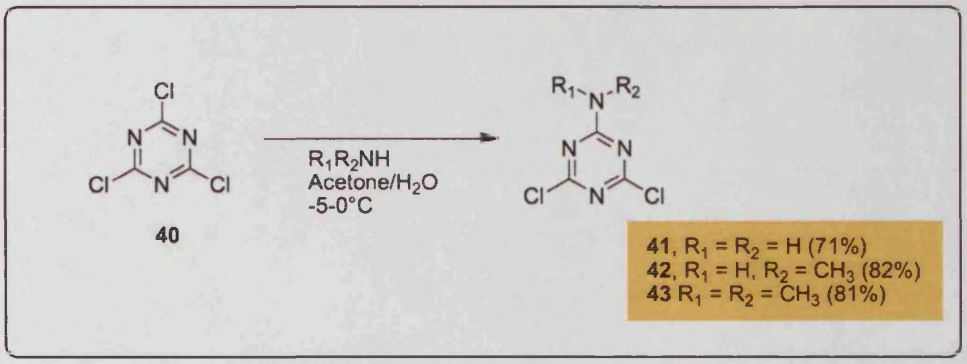

Scheme 3.29 Synthesis of methyl substituted monoamino dichlorotriazines

The 2,4-disubstituted-6-chloro-1,3,5-triazines were obtained by reaction (scheme 3.30) of a further amine with the previously synthesised 2-monosubstituted-4,6-dichloro-1,3,5-triazines (**41**-**43**). NaOH 2N (in excess when the amine was used as hydrochloride salt) or $NaHCO_3$ was used as the base. The fine suspension was formed at 0°C with ice water and the temperature is usually left to rise to room temperature[44]. The products precipitated from solution and were also isolated as high yields (shown in brackets on scheme 3.30).

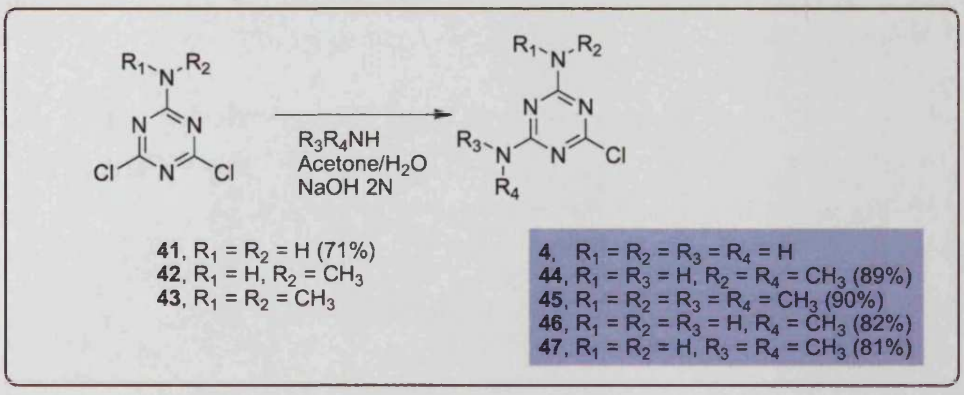

Scheme 3.30 Formation of 2,4-disubstituted-6,chloro-1,3,5-triazines.

The displacement of the last chlorine, as previously mentioned, is the most difficult, but by using hydrazine hydrate as the nucleophile this was achieved without difficulty by simply heating the 2,4-disubstituted-6-chloro-1,3,5-triazine at 85°C[96] to yield the desired intermediates **11**, **48**-**51** (scheme 3.31).

[96] Simmonds, R. J.; Stevens, M. F. G. Triazines and Related Products .25. Methods for the Attachment of Sugar Residues to Cyto-Toxic 1,3,5-Triazines. *J. Chem. Soc.-Perkin Trans. 1*,**1982**, 1821-1825.

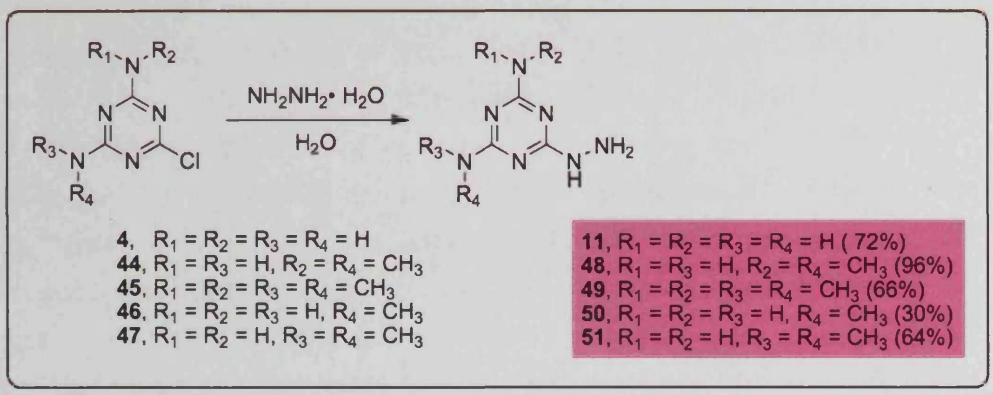

Scheme 3.31 Formation of Triazinyl-hydrazines.

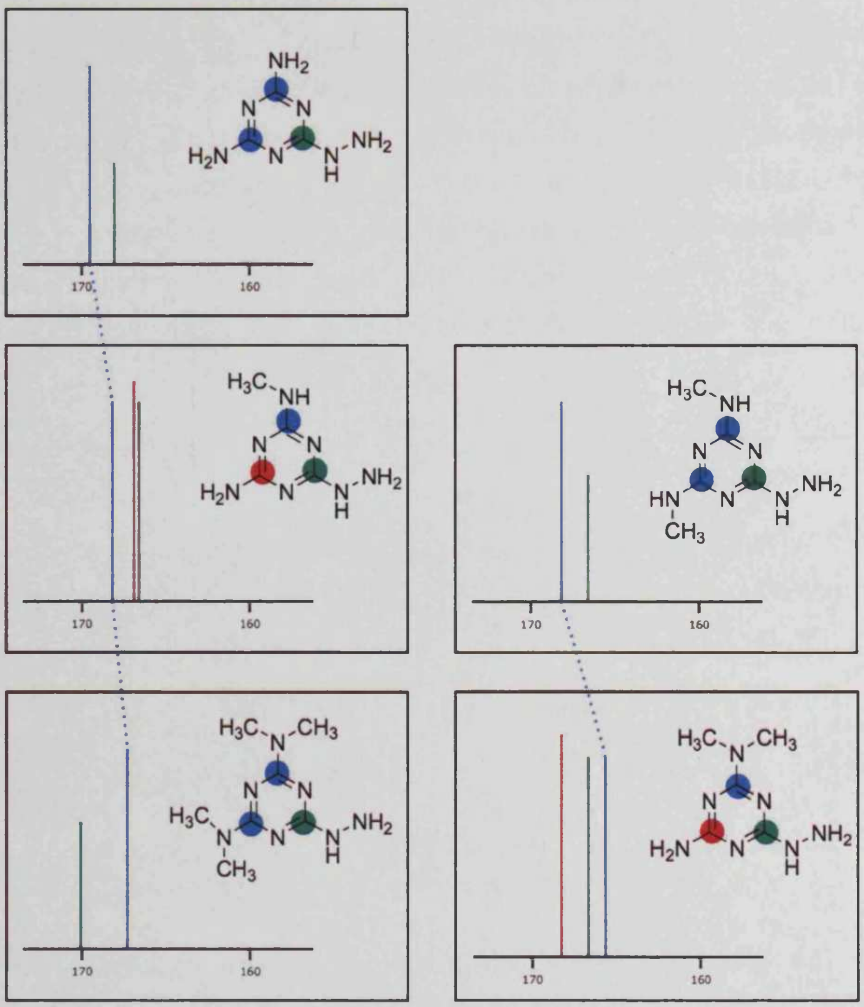

Figure 3.8 ^{13}C-NMR of the triazinic carbons; the NMR spectra have been drawn from the original NMR spectra. The scale is in ppm. The dots in cyan show the decrease of chemical shift with the increase of the substitution of the amino groups. The chemical shifts were assigned with ACD Labs software vers. 2.3.

The analysis of these simple triazine products presented some difficulties. Reversed phase TLC analysis of the reaction mixtures was not clear. MS analysis and ^{13}C-NMR are usually the most reliable way to analyse when the solubility of the products allows us to use these techniques. The ^{13}C-NMR is more useful than the ^{1}H-NMR where the signals corresponding to the N-H of the amino and hydrazino groups are variable and often fall at the same chemical shift. The triazine carbon attached to chlorine usually shows lower chemical shifts compare with the ones attached to a nitrogen and the chemical shift of the triazine carbon attached to the amino group decreases to lower field with the addition of methyl group substituents (figure 3.8).

The hydrazines obtained were reacted with 5-nitro-2-furaldehyde (**1**) in methanol to give the corresponding hydrazones (**52-55**) as shown in scheme 3.32. Hydrazones **52** and **55** were previously synthesised by Jimenez-Bueno and were found to be active in submicromolar range against *T.brucei rhodesiense*[44]. The synthesis of compound **55** was repeated and purification by recrystallisation was performed to increase purity.

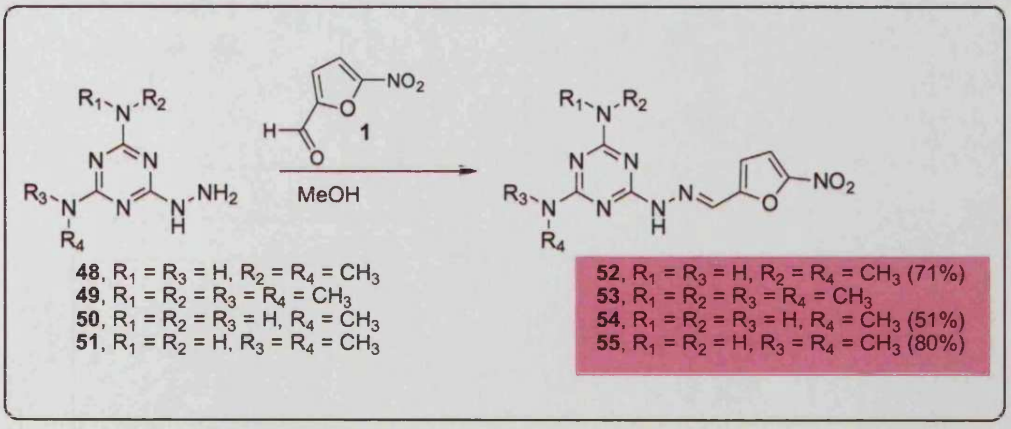

Scheme 3.32 Synthesis of methyl substituted hydrazones.

The different combinations of methyl substituents were carried out in order to evaluate if small variations of lipophilicity can affect the *in vitro/in vivo* activities of the compounds.

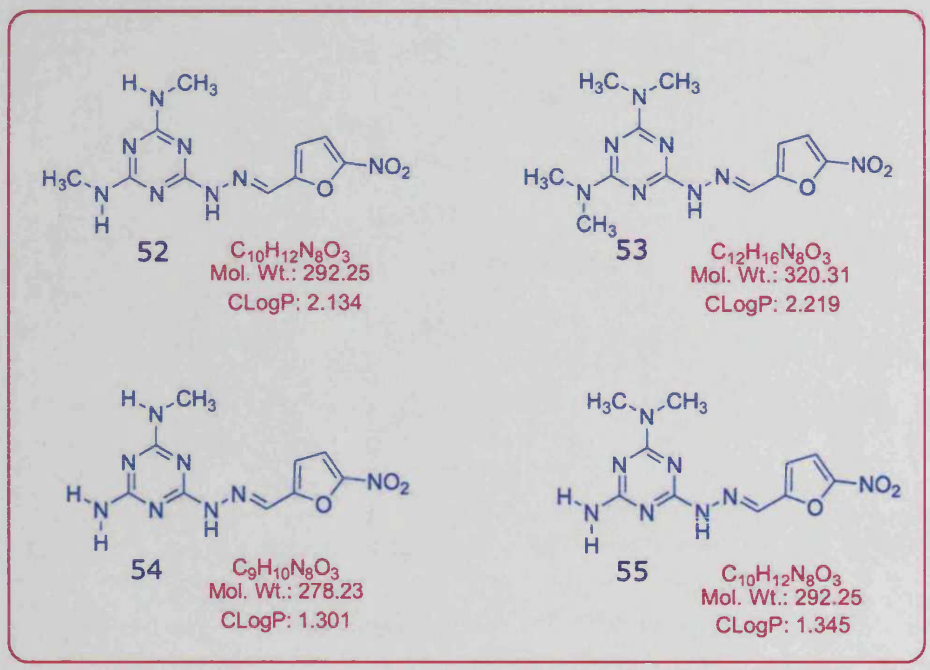

Scheme 3.33 Predicted ClogP values for methyl substituted hydrazones. The ClogP was obtained with Chemdraw ultra 8.0 software.

Scheme 3.33 shows the variations of the ClogP values with the variation of methyl substitution. If, for instance, we consider the predicted ClogP (chemdraw ultra 8.0 software) values of compound **52** and **55** we can see a significant difference of ClogP occurs by moving a methyl group from one amino group to another.

3.10.2 Introduction of alkyl substituents:

Together with the synthesis of methyl substituted triazinyl-hydrazones we also decided to investigate the effects of introduction of bulkier amino-alkyl groups onto the triazine. As a first model, we considered three main groups: *n*-propyl, *iso*-propyl and *n*-butyl substituents. The 4,6-dichlroro-2-amino-1,3,5-triazine (**4**) was used as the starting material (scheme 3.34) and the second chlorine was displaced using the standard procedure of using NaOH as base at room temperature after the formation of the fine suspension at 0°C.

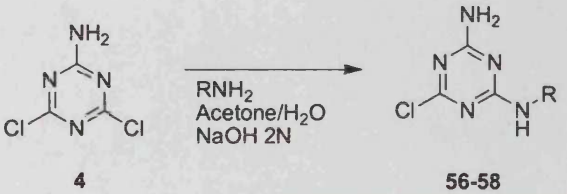

4 **56-58**

Substituent (R)	Result	Yield
n-propyl (**56**)	✓	76 %
iso-propyl (**57**)	✗	—
n-butyl (**58**)	✓	94 %

Scheme 3.34 Synthesis of alkyl 2-monosubstituted 2,4-diamino-6-chloro-1,3,5-triazines.

As shown in scheme 3.34, the synthesis of the *n*-propyl (**56**) and *n*-butyl (**58**) derivatives were successfully achieved in high yields. The synthesis of the *iso*-propyl derivative (**57**) was more problematic and the outcome was unclear. The corresponding hydrazines were obtained by refluxing the triazines with hydrazine hydrate as shown on scheme 3.35. Reaction of the crude product **57** was also attempted but the negative outcome of this next step confirmed that the formation of the isopropyl derivative had probably failed. However, at this point intermediate **57** was found to be commercially available and therefore the final step was repeated to give the desired compound **60** in 73% yield.

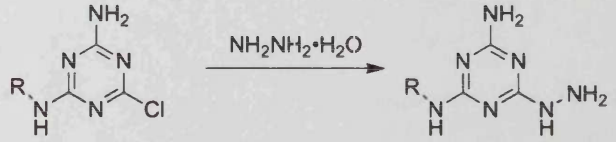

56, R= *n*-propyl
57, R= *iso*-propyl
58, R= *n*-butyl

59, R= *n*-propyl
60, R= *iso*-propyl
61, R= *n*-butyl

Substituent (R)	Solvent	Result	Yield
n-propyl	H_2O	✓	52 %
iso-propyl (crude product)	H_2O	✗	—
iso-propyl (Aldrich)	EtOH	✓	73 %
n-butyl	H_2O	✓	52 %

Scheme 3.35 Synthesis of alkyl 2-monosubstituted 2,4-diamino-1,3,5-triazinyl-hydrazines.

The syntheses were carried out in water suspension, except for the iso-propyl derivative (**60**) where ethanol was used because of solubility problems. The hydrazines (**59**-**61**) were finally coupled with 5-nitro-2-furaldehyde to yield the desired hydrazones (**62**-**64**) as shown on scheme 3.36.

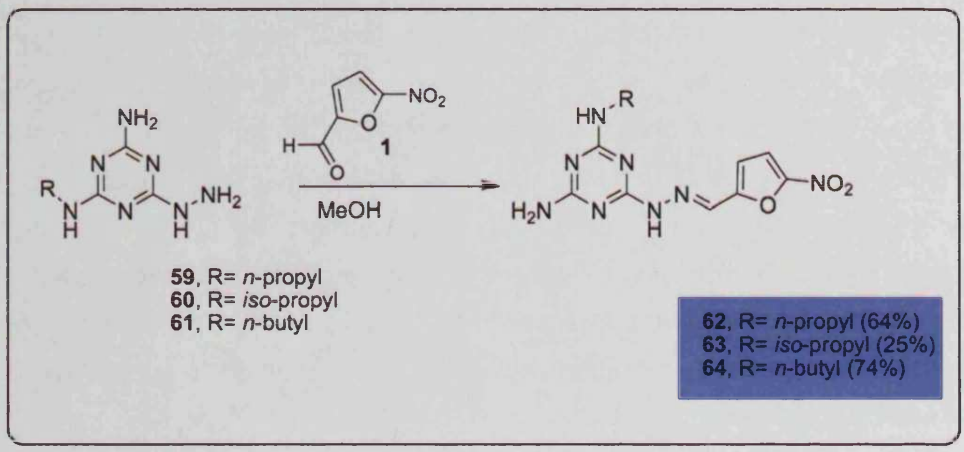

Scheme 3.36 Synthesis of alkyl-monosubstituted triazinyl-hydrazones

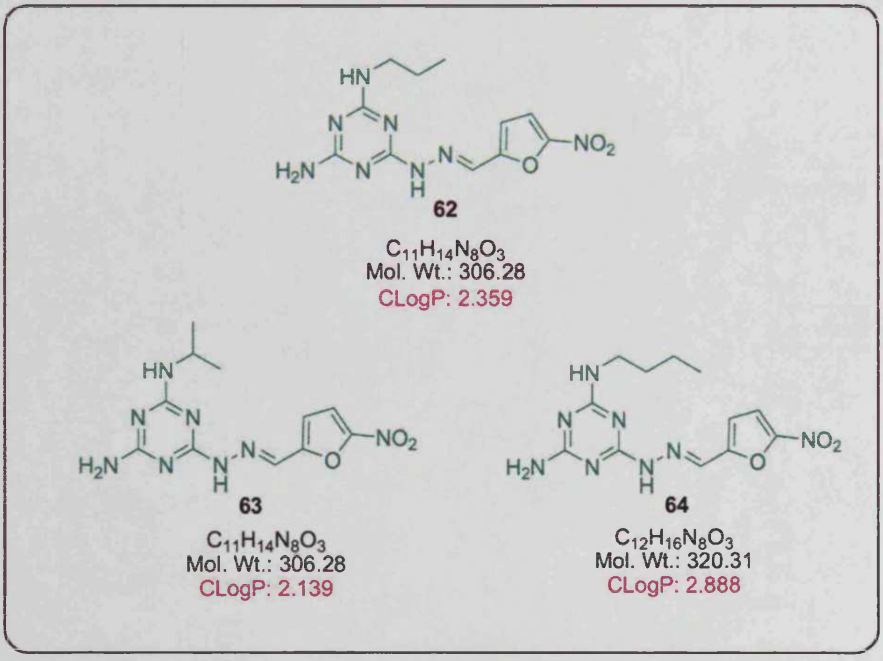

Scheme 3.37 Predicted ClogP values for alkyl substituted hydrazones.

As for the previous methyl substituted derivatives, the ClogP was also predicted for these hydrazones (scheme 3.37). The higher values obtained (2.88 if we consider the n-butyl derivative) compared to the

previous hydrazones should give us interesting data when correlated to their activity.

3.10.3 Introduction of functionalised chains:

The introduction of functionalised chains represents another modification of the lead we carried out. Functional groups such as hydroxyl, amino or carboxyl groups can be used as a further strategy to obtain a series of derivatives with a wide range of lipophilic/hydrophilic values. At the same time the presence of a functional group in the chain offers the possibility to perform further modifications and a possible way to synthesise interesting prodrugs with improved pharmacokinetic characteristics (figure 3.9). Figure 3.9 shows a different series of products that can be achieved though a series of modifications. The insertion of a functionalised chain can dramatically modify the solubility properties of this class of compounds.

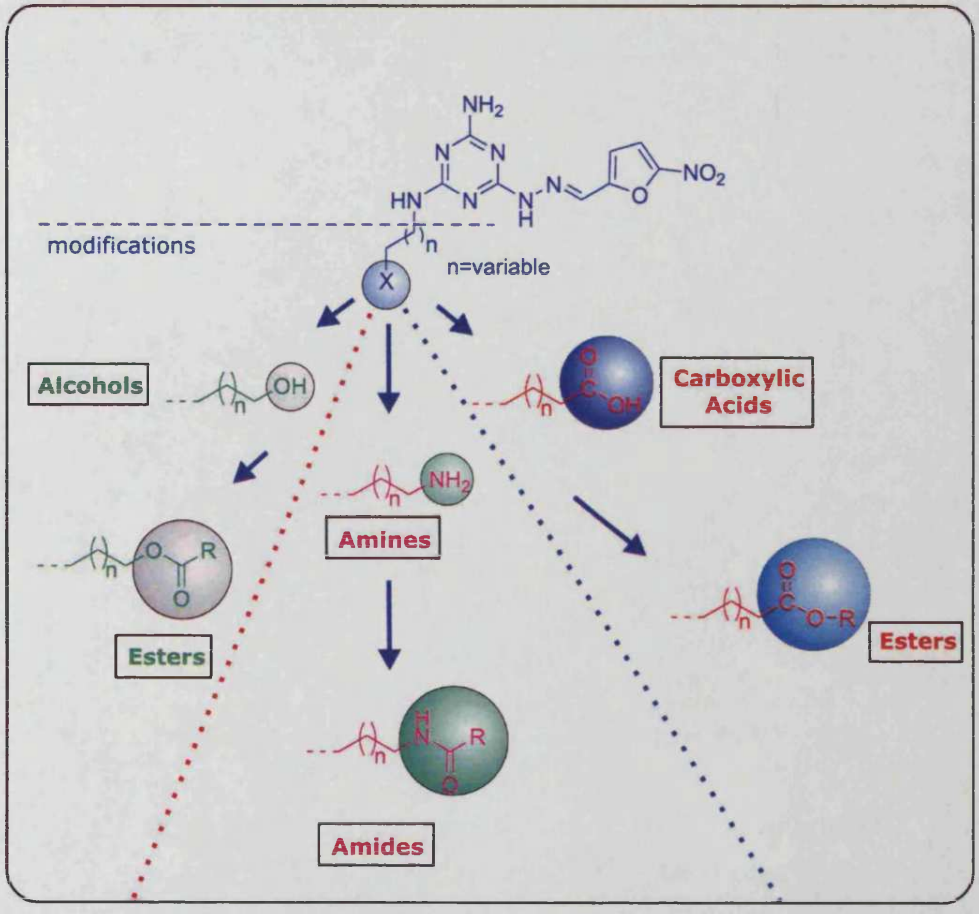

Figure 3.9 Introduction of functionalised chains.

3.10.3.1 Insertion of amino-alkyl-alcohols:

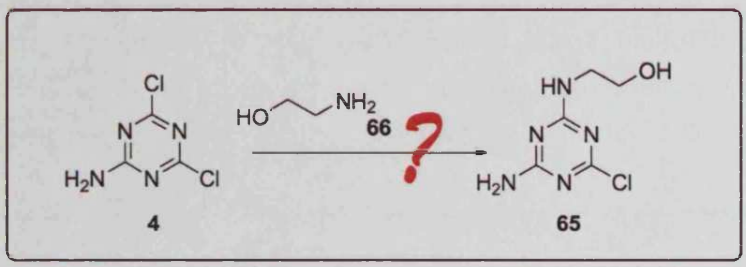

Scheme 3.38 Attempt of insertion of ethanolamine.

The first functional group we decided to insert is the hydroxyl group, however whilst carrying out this modification we encountered several difficulties. The chain we decided to insert on the triazine ring was the ethanolamine. The first procedure followed was the standard methodology of acetone-water suspension using NaOH as base but the outcome was unclear (scheme 3.38). MS electrospray analysis appears to be an unsuitable technique for this class of compounds and at the same time, the presence of extra peaks on the NMR spectra, hindered the monitoring of these experiments. The reaction was also carried out by maintaining the pH over the range of 10-11, where the nucleophilicity of the amino group is optimal (figure 3.10). However, as observed for the previous experiment, the outcome of this reaction was not clear.

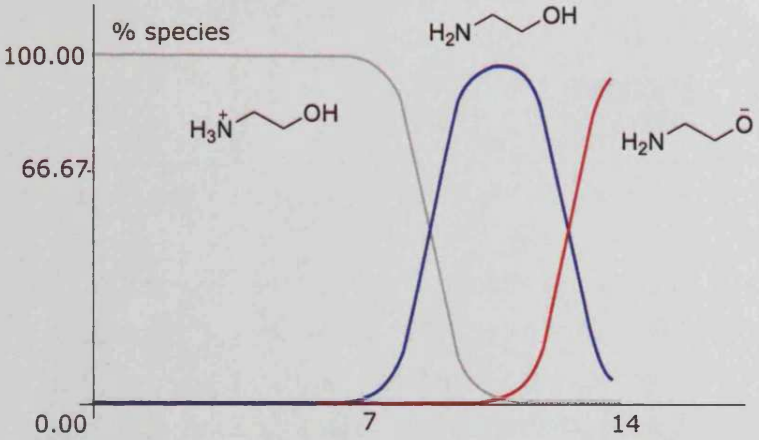

Figure 3.10 Diagram of ethanolamine (**66**). The % of the different species varies with the pH.

After efforts to purify the product failed we decided to follow an alternative route and to protect the hydroxyl group of the ethanolamine with a more lipophilic group before its insertion on the triazine ring. The insertion of the more lipophilic group was thought to be a strategy as polarity and hydrophilicity seemed to cause a problem with these compounds.

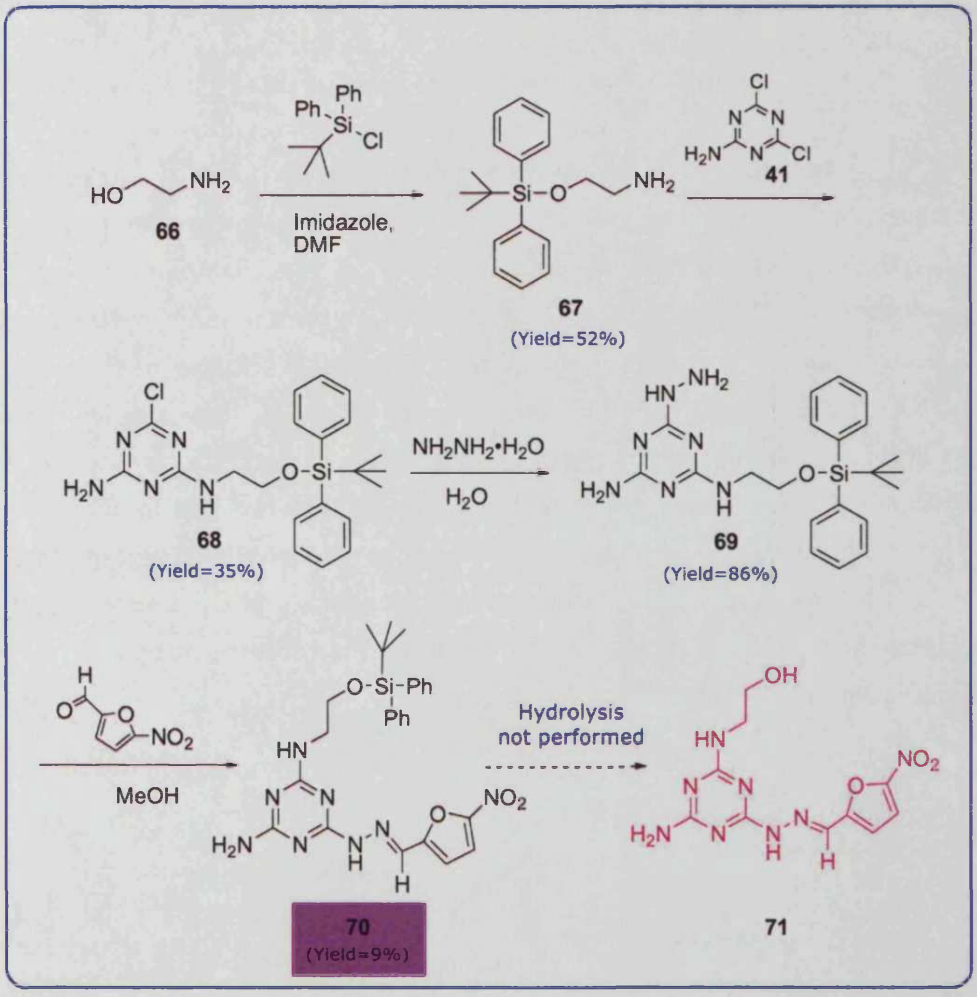

Scheme 3.39 Alternative route attempted for the synthesis of the hydrazone **71**.

Of the wide number of protecting groups for the hydroxyl function the *tert*-butyl-diphenyl-silyl chloride (TBDPS-Cl) was chosen as reagent for the protection. The utility of *tert*-butyldiphenylsilyl has been evaluated[97]. The corresponding tert-BDPSi ethers have much greater stability to different reaction conditions like to acids and to some bases like NaOH

[97] Hanessian, S.; Lavallee, P. Preparation and synthetic utility of tert-butyldiphenylsilyl ethers. *Can. J. Chem.* **1975**, *53*, 2975-2977.

(concentration up to 2N). At the same time the TBDP-silyl ether can be readly cleaved with reagents such as tetrabutylammonium fluoride (TBAF) or methanolic HCl. The ethanolamine (**66**) was therefore protected with *tert*-butyldiphenylsilyl chloride to give compound **67**. The selective protection of the hydroxyl over the amino group of the ethanolamine is due to the strong nature of the silicon-oxygen bond. The silyl protected ethanolamine **67** was then successfully inserted without difficulties onto the triazine ring to give the protected triazine **68** (scheme 3.39). The last chlorine was substituted with hydrazine hydrate to give the hydrazine product **69** which was converted to the silyl protected hydrazone **70** using standard methodology albeit in a poor yield (9%). Product **70** showed improved solubility compared with the previous synthesised hydrazones but unfortunately the negligible amount obtained and the difficulties encountered for the scale up did not allow us to carry on this route to the hydrolysis of the protective silyl group.

The route detailed in scheme 3.40 was repeated using the homologue propanolamine. The procedure used for the protection via silyl ether was modified using pyridine instead of imidazole and DMF[98]. The yields achieved were found to be improved compared to the previous route and were not affected by the scale up of the reactions.

3-Propanolamine (**72**) was converted into the silyl protected derivative **73** (84%) and then successively coupled with the 2-amino-4,6-dichloro-1,3,5-triazine (**4**) to give the intermediate **74** (45%). The last chlorine was displaced with hydrazine using standard conditions to give the triazinyl hydrazone **75** (52%) which was coupled with 5-nitro-2-furaldehyde (**1**) to give the silyl protected compound **76** in high yield (84%). Attempted cleavage of the silyl group using HCl (10M) was not successful. NMR analysis of the mixture showed the presence of hydrazone starting material and suggested that part of the product decomposed under these harsh conditions.

Although these initial results were disappointing, due to difficulties encountered with the synthesis of **77**, it was proposed that these two new silyl protected hydrazones could be evaluated for their biological activities.

[98] Wenninger, D.; Seliger, H. Synthesis and hybridization properties of modified oligonucleotides with PNA-DNA dimer blocks. Nucleosides & Nucleotides 1997, 16, 977-980.

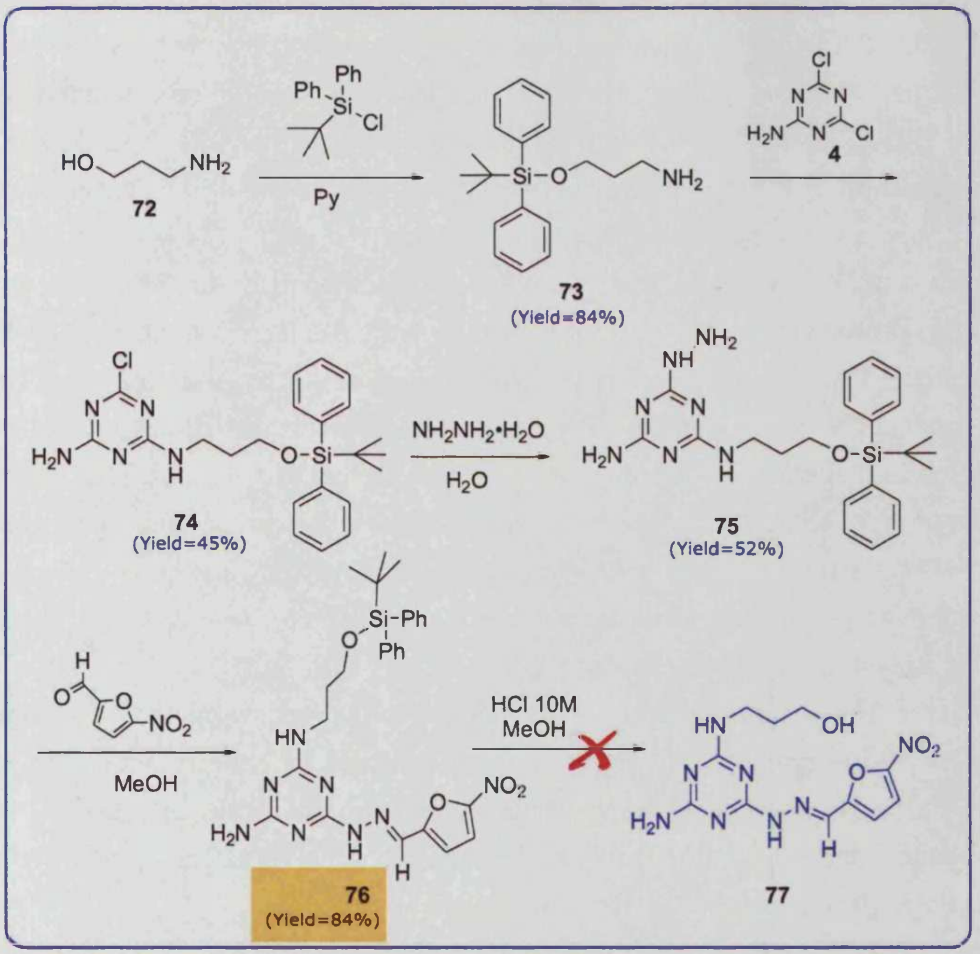

Scheme 3.40 Attempted synthesis of the hydrazone **77** via silyl protection of propanolamine.

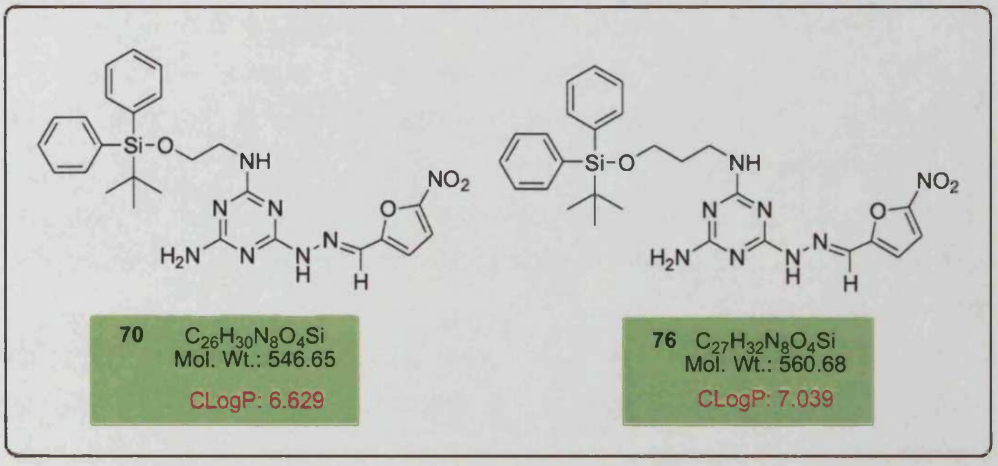

Scheme 3.41 Structure of TBDP-Silyl-protected hydrazones.

The predicted ClogP values are higher compared to the previous alkyl substituted derivatives and therefore these protected compounds could be

used to investigate the effects of the introduction of bulky lipophilic groups on the activity/affinity.

3.11 Dynamic behaviour of some 1,3,5-triazines:

Whilst investigating the route to compound **77** via protection of the hydroxyl group, we also decided to further study the behaviour of the substituted triazines which has previously hindered our work. We repeated some of the previous experiments and mostly focused our attention on the NMR data achieved. In particular, we observed that when a relatively bulky group was inserted on the triazine ring its NMR spectrum was characterised by the presence of extra signals that do not belong to the unwanted by-products, as we initially thought, but to the existence of tautomeric forms of the same triazine.

Recent work by Dìaz-Ortis and Valiente[99] has shown that bulky 1,3,5-triazines at room temperature can be detected as two or three tautomeric forms. They also used 2D-exchange spectroscopy studies in various solvents and at different temperatures to determine the equilibrium constants and the activation free energies of the restricted rotation about the amino-triazine bond.

If we consider a generic 2,4-substituted-6-chloro-1,3,5-triazine, it is possible to describe three dynamic processes (figure 3.11):

1) Tautomerism between amino and imino triazines [99];

2) E-Z isomerism of the imino tautomers[99];

3) the amino tautomers can show conformational isomerism due to restricted rotation about the amino triazine bond[99].

[99] Diaz-Ortis, A.; Elguero, J.; Foces-Foces, C.; De la Hoz, A.; Moreno, A.; Moreno, S.; Sànchez-Migallòn, A.; Valiente, G. Synthesis, structural determination and dynamic behaviour of 2-chloro-4,6-bis(pyrazolamino)-1,3,5-triazines. *Org. Biomol. Chem.* **2003**, 1, 4451-4457.

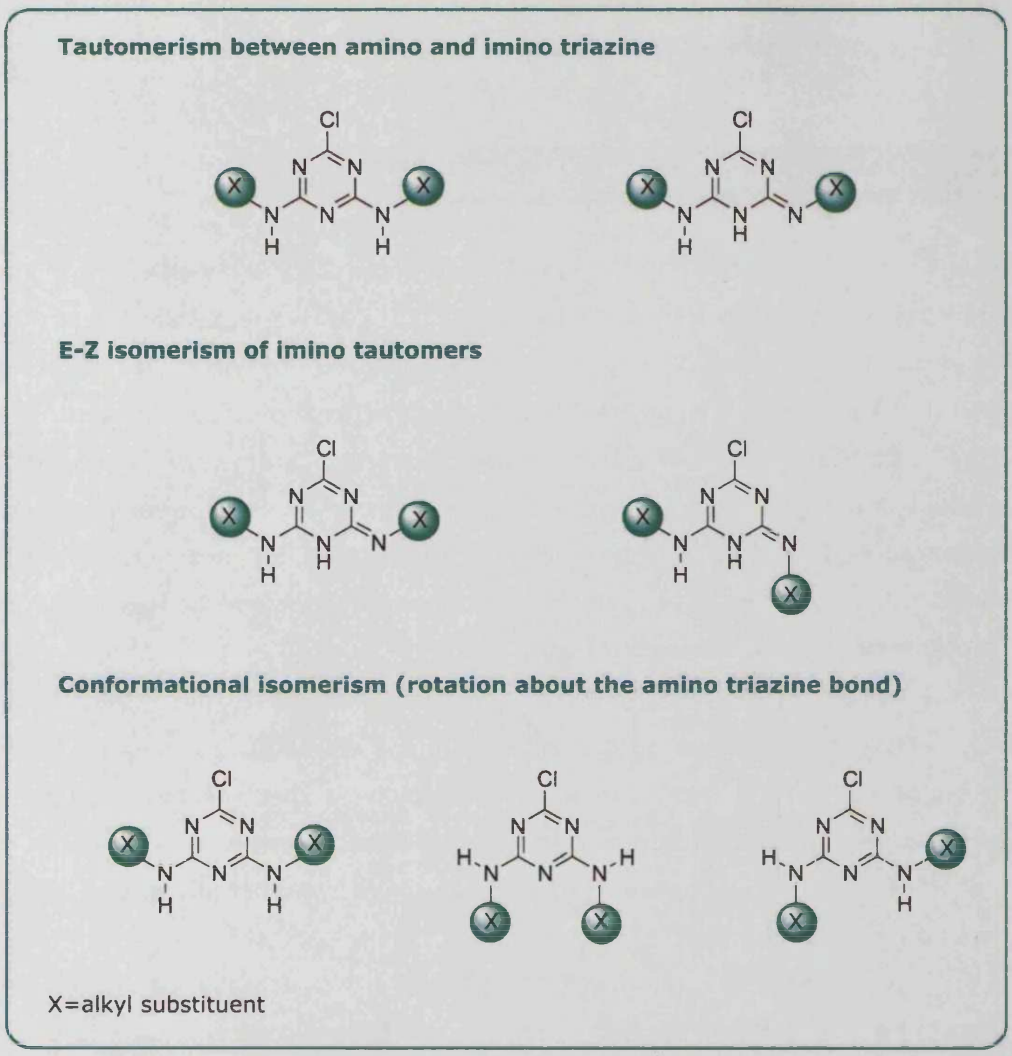

Figure 3.11 Example of some of the possible isomers of a bis-substituted diamino-triazine.

After taking into account these considerations some of the direct couplings with amino-alcohols were repeated. The analysis of the NMR at room temperature and at 100°C showed that the extra peaks are related to isomers of the same triazine derivate. Ethanolamine was chosen as model for our initial study. The reaction was repeated using different conditions: at 0°C to minimize the possible formation of by-product, which was unsuccessful and then, at room temperature which represents the standard conditions required for the displacement of the second chlorine. Scheme 3.42 and figure 3.12 summarize the experiments repeated, the outcome and the ^{13}C-NMR obtained at room temperature.

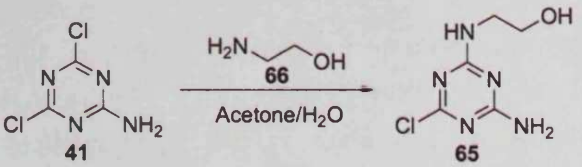

Base (equ.)	Temperature	Result	Yield
NaOH 2N 1equ	0°C	✗	—
NaOH until pH=10/11	rt	✓	75 %

Scheme 3.42 Synthesis of 2-hydroxyethyl-2,4-diamino-6-chloro-1,3,5-triazine.

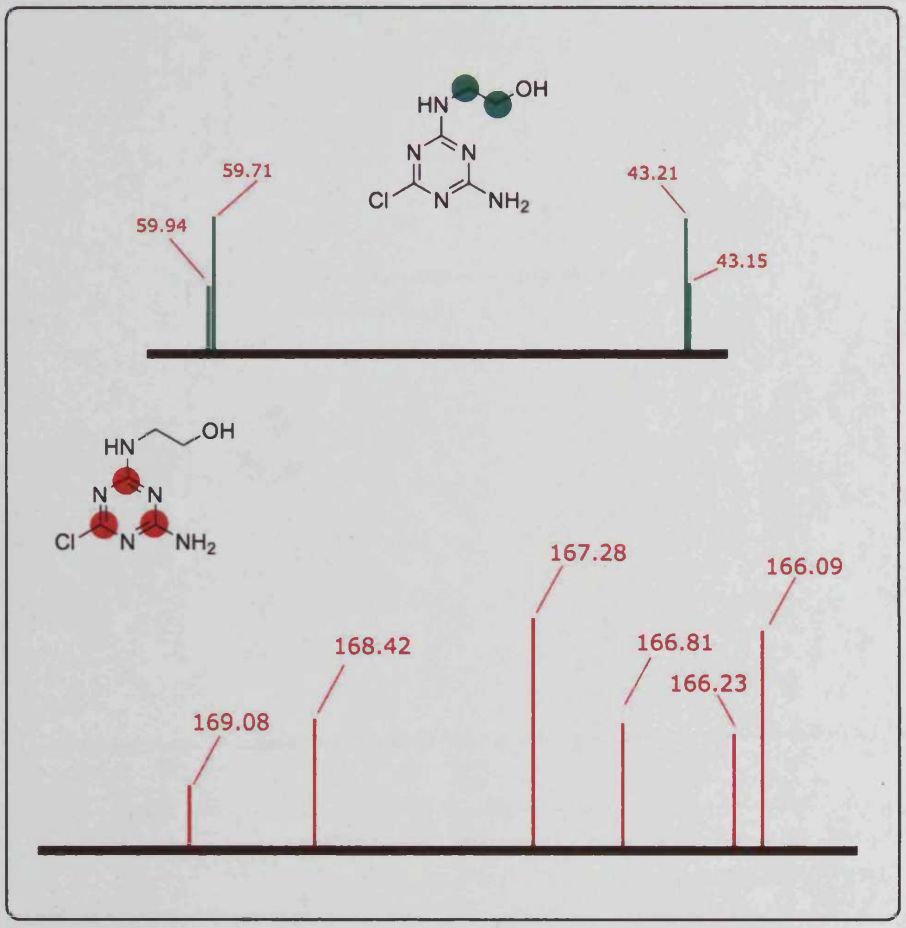

Figure 3.12 ^{13}C-NMR at room temperature (in order to facilitate the interpretation, the NMR has been drawn maintaining all the original settings).

The ^{13}C-NMR at room temperature shows splitting of the different carbons. To simplify, figure 3.12 shows the same ^{13}C-NMR depicted as two separated spectra: the upper one showing the signals related to the aliphatic carbons and the lower one which represents the signals associated with the triazine carbons. The split aliphatic carbons are separated from each other by a chemical shift of between 0.10 and 0.14 ppm whilst the split signals of the aromatic carbons are separated by chemical shifts values of up to 0.6 ppm.

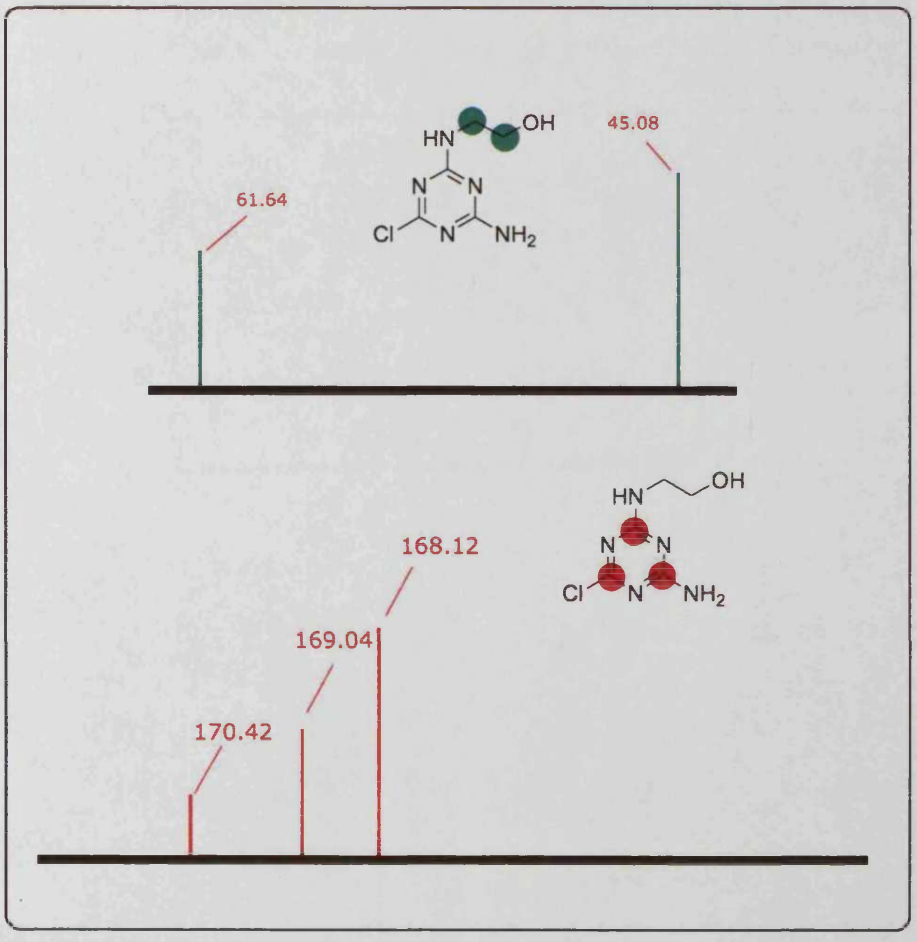

Figure 3.13 ^{13}C-NMR at 100°C. The NMR as been drawn to simplify the interpretation of the original.

At 100°C, as shown in figure 3.13, the splitting previously described for the aliphatic and aromatic carbons disappeared, confirming that the signals belonged to isomers of the same triazine compound. At this temperature the chemical shift of each peak is also shifted by a few units to higher fields.

The different rotamers and imino tautomers that can be considered to describe the behaviour of the hydroxy-ethyl-amino substituted triazine are shown in figure 3.14. For the imino form a E-Z isomerism is possible whilst a conformational isomerism can be associated with the amino form.

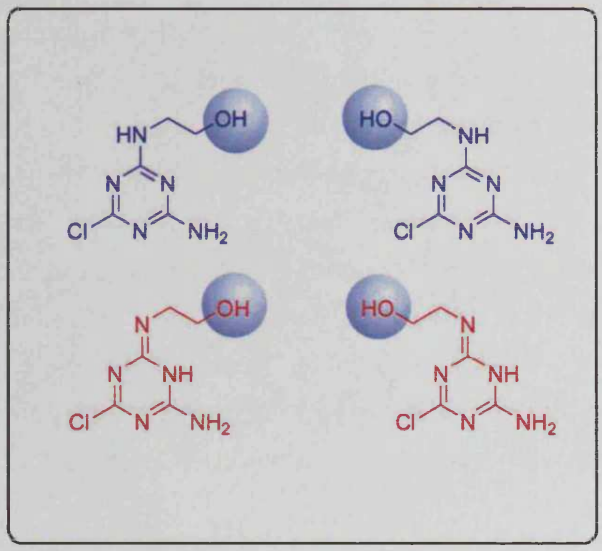

Figure 3.14 Possible isomers of the hydroxyethylamino substituted triazine.

The synthesis of the hydrazine derivative **78** was attempted (scheme 3.43) but as the product was not detected by MS electrospray analysis, and poor solubility handicapped purification attempts, it was not clear if this reaction had worked or not. The crude product **78** was used for the synthesis of the hydrazone **71** by coupling with 5-nitrofuraldehyde using standard conditions, however the formation of the product did not occur and this suggests that the first step had probably not worked.

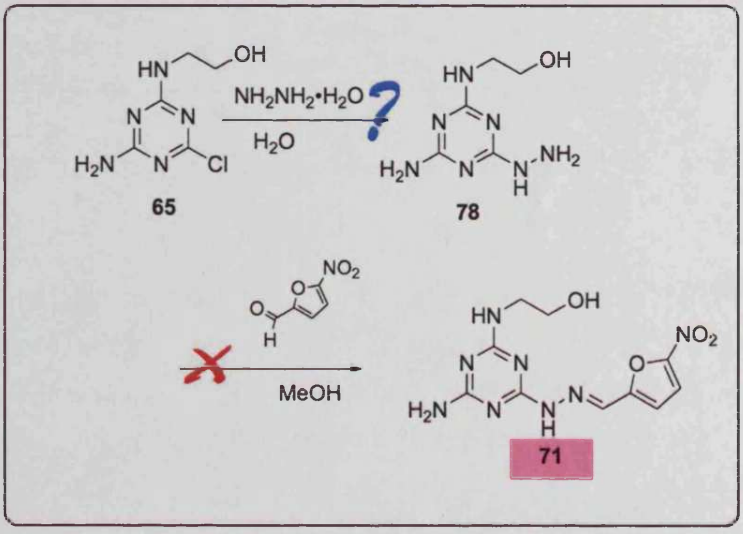

Scheme 3.43 Attempted formation of hydrazine **78** and hydrazone **71** derivatives.

3.12 Synthesis of hydroxypropyl substituted melamines:

The experiments previously carried out with the silyl-protected derivatives showed that 3-propanolamine not only appeared to be more reactive compared with ethanolamine but the solubility of its derivatives is also improved. The coupling of the propanolamine (**72**) with the dichlorotriazine intermediate **41** was carried out (scheme 2.44). The standard procedure using a water/acetone suspension of starting triazine **41** gave the formation of the product **79** with 31% yield. A new procedure was carried out using DMF and DIPEA as a base, these conditions are generally used for solid phase synthesis. By using this new procedure not only was the reaction time improved, but the yield was increased by 3 fold, as shown in scheme 3.44.

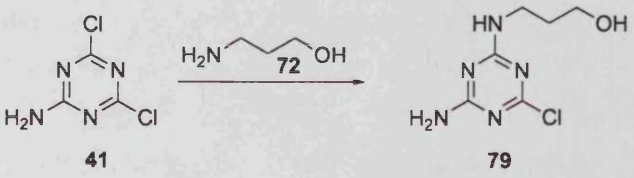

41 **79**

Solvent	Base	Result	Yield
H_2O/acetone	NaOH 2N (1.2 equ.)	✓	31%
DMF	DIPEA (1.2 equ.)	✓	91%

Scheme 3.44 Synthesis of 2-hydroxylpropyl-2,4-diamino-6-chloro-1,3,5-triazine (**79**).

The displacement of the last chlorine of the triazine derivative (**79**) with hydrazine does not seem to be significantly affected by the solvent conditions. In fact, the triazinyl-hydrazine (**80**) was successfully obtained by working either with water suspension or DMF solution, as summarised in scheme 3.45.

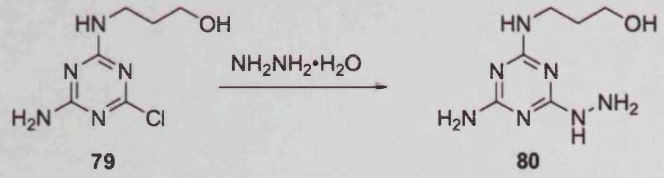

79 80

Solvent	Phase	Result
H_2O	suspension	✓
DMF	solution	✓

Scheme 3.45. Conditions used for the preparation of hydrazine derivative **80**.

The product **80** was used crude for the preparation of the hydrazone (**77**) by reaction with 5-nitrofuraldehyde. Compound **77** was purified by flash column chromatography eluting with DCM/MeOH (100/0 to 95/5) thus indicating that the introduction of the hydroxyl-alkyl functionality has greatly improved the solubility compared to the hydrazone lead compound (**6**). The predicted CLogP value shown on scheme 3.46 also confirms the increased hydrophilicity of the hydrazone **77** compared to the lead compound **6**. This result represented a big advance if we consider that that the solubility of the previous hydrazones made difficult their purification.

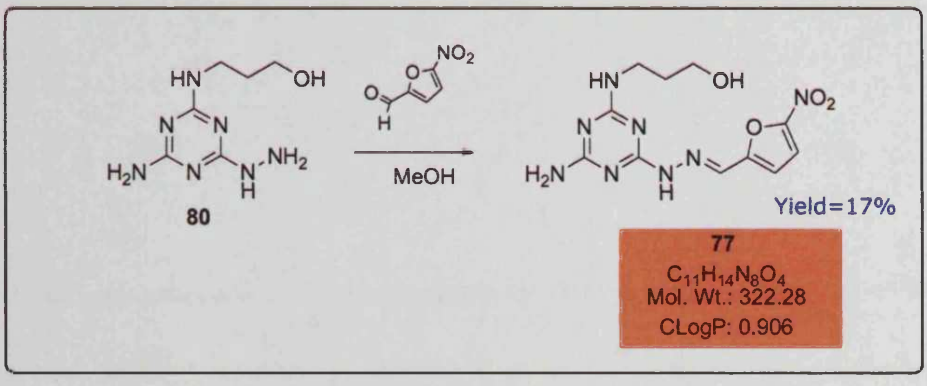

Scheme 3.46 Synthesis of hydrazone derivative **77**.

As also observed for some of the previous hydrazones, the NMR analysis of **77** shows the splitting of some of the signals. The ^{1}H-NMR in figure 3.15 shows the splitting of some characteristic broad singlet peaks of hydrazones.

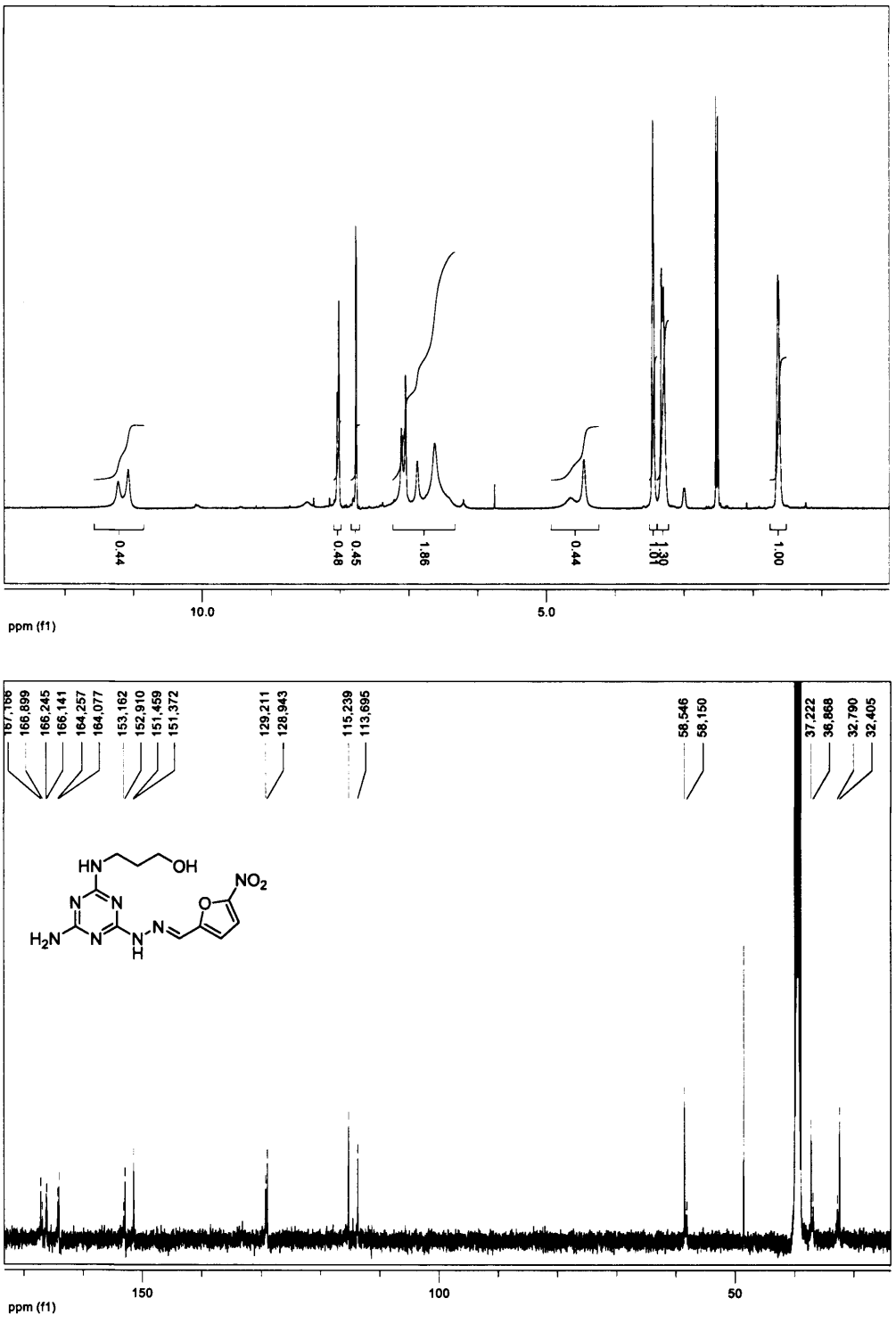

Figure 3.15 ^{1}H-NMR and 13C-NMR of hydrazone compound **77**.

The peak at 11.2 ppm, corresponding to the N-H of the hydrazone function, and the broad singlet of the hydroxyl function (4.5 ppm) are split into two signals of different intensity. The splitting of these peaks was not

usually observed for unhindered hydrazones. The peaks have been assigned with 2D-COSY experiment and with ACD Labs Vers 2.03.

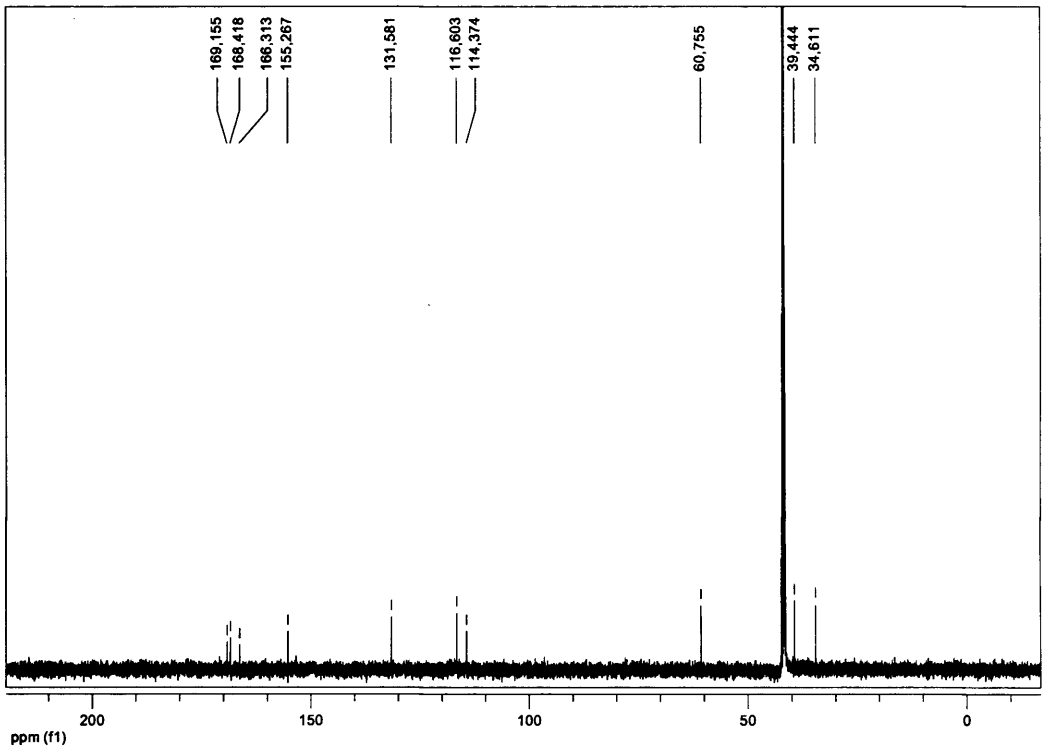

Figure 3.16 ^{13}C-NMR at 100°C of hydrazone compound **77**.

The ^{13}C-NMR analysis also shows splitting of the signals for most of the carbons (figure 3.15) of compound **77**. The splittings disappear when the ^{13}C-NMR is acquired at 100°C (figure 3.16), thus confirming these extra signals are due to tautomers/isomers of the compound **77**.

Having obtained compound **77** in good yield we next carried out modification of the free hydroxyl function by acetylation via acetic anhydride and DMAP in pyridine. The acetylated hydrazone **81** was obtained in 65% of yield. This ester derivative of the hydrazone **77** can be considered to be a prodrug compound (see chapter 5). We proposed that esterase hydrolysis will release the original hydrazone compound **77** and the advantage of this mechanism lies in the fact that the prodrug should exert the same trypanocidal effect but with greatly improved pharmacokinetic properties which are expected to increase the potency of the compound. However, further investigations and more derivatives are needed to further explore this field.

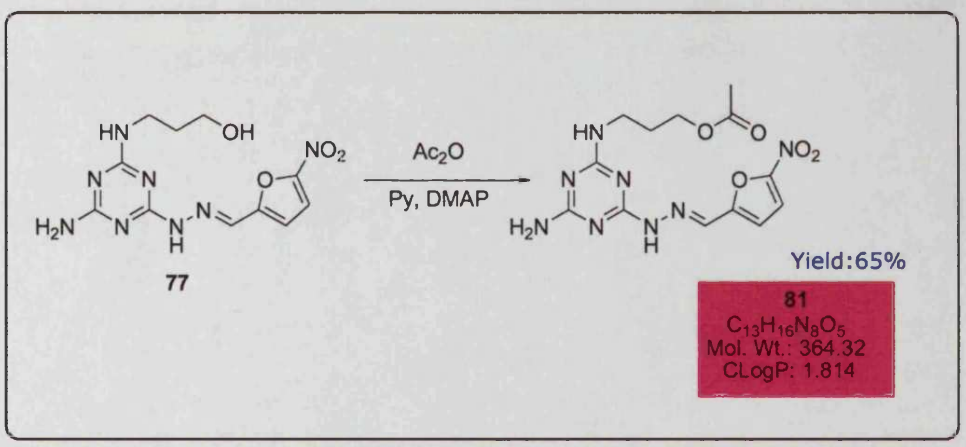

Scheme 3.47 Acetylation of hydrazone **77**.

3.13 Conclusions and future perspectives:

The *in vitro\in vivo* screening results which will be separately discussed in chapter 6 have given encouraging results indicating that this class of compounds should be further studied and expanded with new derivatives.

4. Results and Discussion II:

Amidine derivatives

Using the same approach described in the previous chapter, a series of nitroheterocycles compounds has been designed using a linker to connect the nitroheterocycles to the P2 recognition motif, which in this case is the benzamidine unit.

The chemistry and solubility of the amidine derivatives prepared proved to be an issue, and despite the different attempts and routes investigated, a reliable procedure for coupling the benzamidine to the nitroheterocycle is still needed. However, different procedures of synthesis of amidines were established and some interesting model compounds have been synthesised and assayed for their trypanocidal activity.

4.1 Design of amidine structures

The amidine function can be found as a part of many important chemical compounds with a large variety of properties also been investigated for their biological properties[100], [101]. Pentamidine has been described already in the previous chapter, as a drug containing a double amidine function which is effective not only against HAT but also against

[100] Patai, S. The Chemistry of Functional Groups: The Chemistry of Amidines and Imidates; Ed: Wiley and Sons, Vol.I, New York, 1975; 677 pp.

[101] Jarak, I.; Karminski-Zamola, G.; Pavlovic, G.; Popovic, Z. 4-Amino-N-isopropylbenzamidinium chloride ethanol solvate. *cta Crystallogr. C* **2005**, *C61*, o98-o100.

Pneumocystis carinii pneumonia (PCC) and which has also been evaluated for other infections such as Leishmania[102].

Using the same rationale described for the melamine derivatives in the previous chapter, the nitroheterocycle cytotoxic unit was linked to a new class of P2 substrate. It was planned to link the nitroheterocycle to the P2 substrate, the benzamidine.

As shown on figure 4.1 the amidine group is attached to a phenyl ring and, in order to have optimal binding to the P2 transporter, an electronegative group (X) is attached *para* to the amidine function. By using an oxygen or a nitrogen it is expected that the electron lone pair will contribute to the π-system. It was proposed that the trypanocidal moiety can be directly attached to the benzamidine or separated by a linker of variable length and chemical structure.

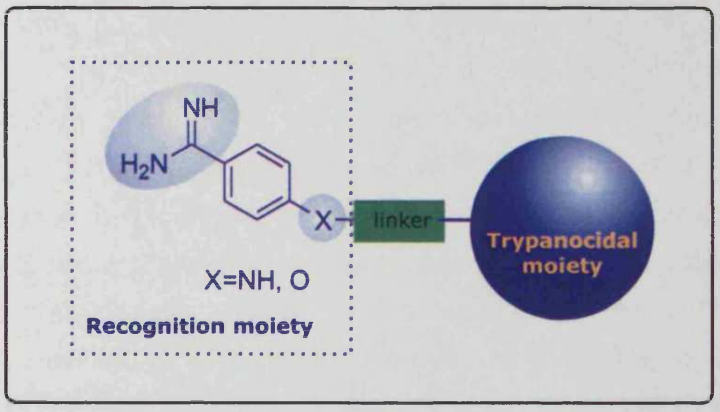

Figure 4.1 Design of a general benzamidine derivative carrying a cytotoxic moiety.

The chemistry of amidine derivatives has been explored in order to establish a robust and general method which is expected to be useful for the preparation of the types of compounds described in fig. 4.1.

[102] Tidwell, R. R.; Jones, S. K.; Geratz, J. D.; Ohemeng, K. A.; Cory, M.; Hall, J. E. Analogues of 1,5-bis(4-amidinophenoxy)pentane (pentamidine) in the treatment of experimental Pneumocystis carinii pneumonia. *J. Med. Chem.* **1990**, *33*, 1252-1257.

4.2 Synthesis and chemistry of amidines:

The synthesis of amidines generally proceeds through starting materials with an unsaturated carbon-nitrogen bond; the introduction of the second nitrogen is usually via action of ammonia or of primary or secondary amines[103].

This simple general scheme may proceed by two routes:

1) Transformation of nitriles by addition of amines (scheme 4.1):

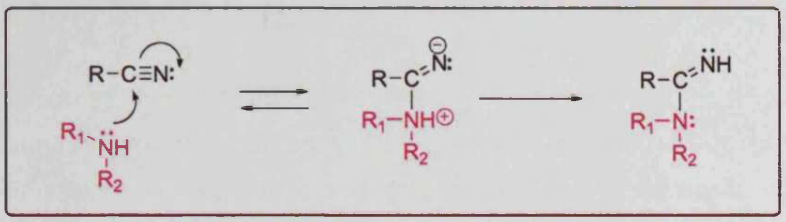

Scheme 4.1 Amidines by addition of amines to nitriles.

2) Substitution, by nucleophilic attack, on the carbon atom of amides or their derivatives (scheme 4.2):

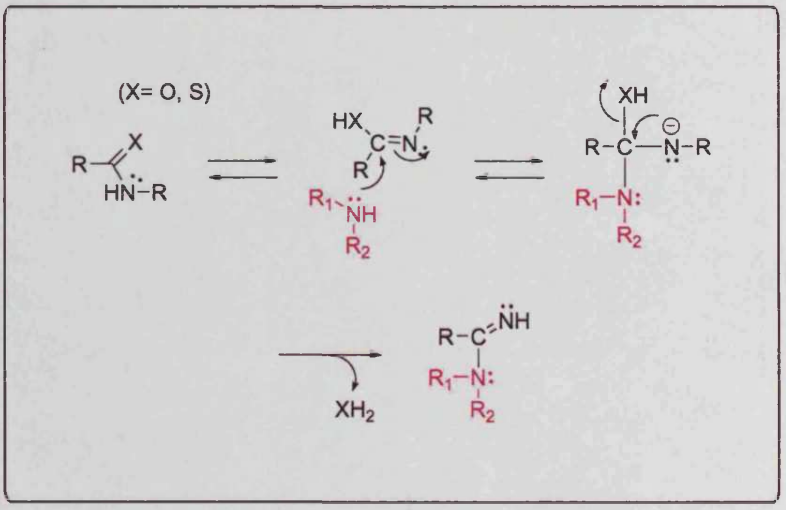

Scheme 4.2 Amidines by addition of amines to amides

In practise, these hypothetical equations hold for only a few particular examples and therefore whilst nitriles and amides are still the most frequent starting materials for synthesis of amidines, they must

[103] Gautier, J. A.; Miocque, M.; Farnoux, C. C. Preparation and synthetic uses of amidines. *Chemistry of Amidines and Imidates* **1975**, 283-348.

generally first be transformed into more reactive intermediates (scheme 4.3) such as imido esters (X=OR) or imidoyl halides (X= Hal):

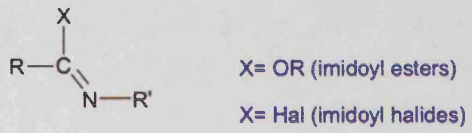

scheme 4.3 Structure of a reactive intermediates used for the synthesis of amidines

It is important to note that amidines can be involved in three different isomerism processes: geometrical isomerism (Figure 4.2a), rotational isomerism (Figure 4.2b) and prototropic isomerism (Figure 4.2c)[104] and these isomeric forms may greatly complicate ^{1}H and ^{13}C-NMR in a manner similar to that discussed for melamine compounds.

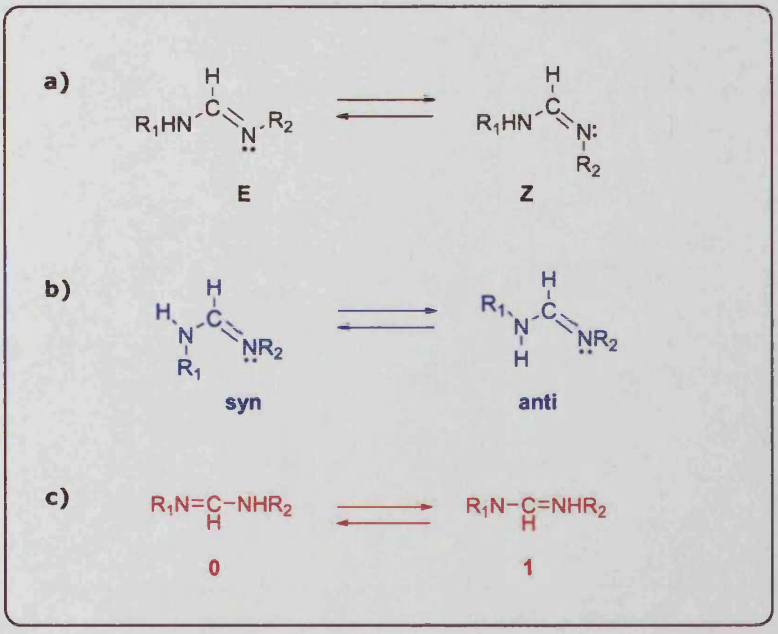

Figure 4.2 isomerism processes associated to the amidine compounds[104].

[104] Komber, H.; Limbach, H. H.; Bohme, F.; Kunert, C. NMR Studies of the Tautomerism of Cyclo-tris(4-R-2,6-pyridylformamidine) in Soltion and in the Solid State. *J. Am. Chem. Soc.* **2002**, *124*, 11955-11963.

☞ *The work described in the following section 4.3 is work carried out by a previous member of the group. This work is only being discussed herein to provide sufficient background to facilitate the understanding of our project and the work carried out by the author.*

4.3 Coupling of benzamidines with nitroimidazoles:

The first cytotoxic unit that was chosen at the beginning of the project was the nitroimidazole unit. Nitroimidazoles were chosen because the potent antiparasite activity of known nitroimidazoles such as megazol. However, as mentioned in the previous chapters, megazol not only has received attention for its potent trypanocidal activity but also for its toxicity, an issue that has prevented its further development[68].

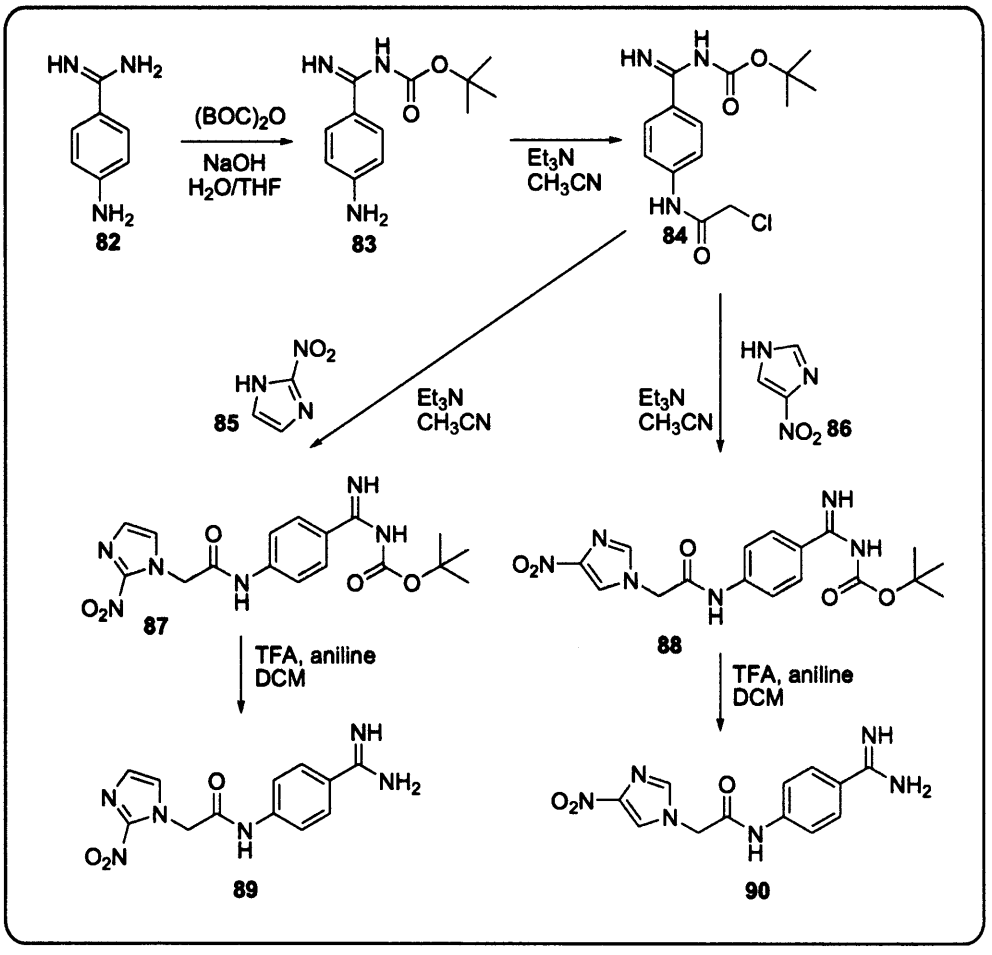

Scheme 4.4 synthesis of nitroimidazol-methyl-carbamoyl-benzamidines (**89**, **90**)[68].

Jimenez Bueno *et al.*[68] used 4-amino-benzamidine (**82**, scheme 4.4) as the starting material for the coupling of the P2 substrate with the nitroheterocycles. The benzamidine function was first protected with Boc anhydride to give intermediate **83**. Chloroacetyl chloride was coupled with the Boc protected benzamidine intermediate (**83**) using Et_3N as a base in acetonitrile solution to give the intermediate (**84**) which was subsequently coupled with either 2-nitroimidazole (**85**) or 4-nitroimidazole (**86**) using the same conditions to give the Boc protected nitroimidazole intermediates **87** and **88** respectively as shown in scheme 4.4. The subsequent deprotection with TFA and anisole in DCM gave the final nitroimidazole compounds **89** and **90** respectively[68].

In vitro screening showed that these compounds presented very low trypanocidal activity compared to the melamine nitrofuran derivatives. Therefore the nitrofuran cytotoxic unit was also considered for coupling with benzamidines as these results suggested the nitrofurans were more potent than the nitroimidazoles.

☞ *The work described from this part onwards is the work carried out to fulfil the requirements of the degree award.*

4.4 Chemistry of Benzamidines:

By substituting the nitrofurans with the nitroimidazoles we can generate a general model structure. Again the atom in *para* position should be an oxygen or a nitrogen[54] and the first two structures that we chose to carry (shown in figure 4.3) the nitrofuran ring connected to the benzamidine unit via an ether or an amino function, *para* to the amidine functionality (**91**, **92**).

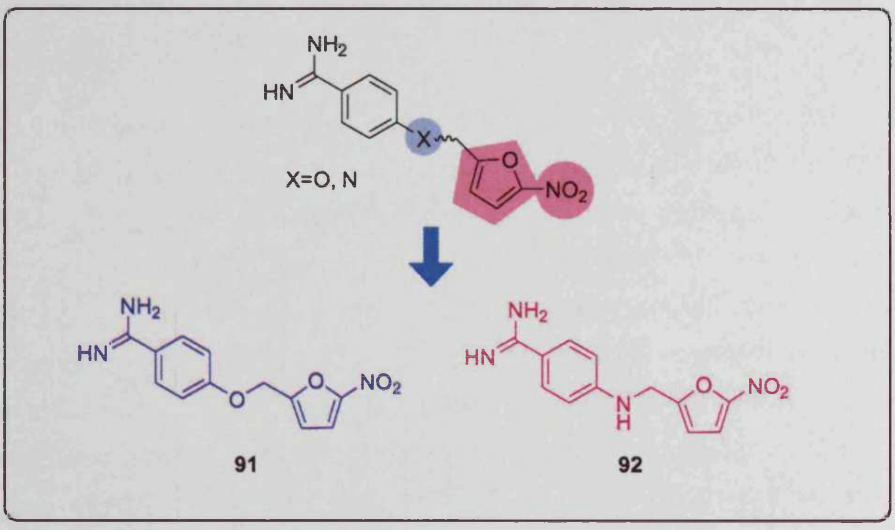

Figure 4.3 design of benzamidine derivatives linked to nitrofurans.

4.4.1 Benzamidines from nitriles via lithium hexamethyldisilazane:

In order to minimise solubility issues and to avoid unwanted further reaction of the amidine function, we have chosen to carry out our experiments keeping the nitrile functionality in place until the last step.

For the synthesis of derivative **91** we decided to use the starting materials 4-p-cyanophenol (**93**) and 2-bromomethyl-5-nitrofuran (**41**). Nucleophilic substitution of the bromine by the p-cyanophenol was successfully carried out after several attempts using dry THF and NaH as

base to give intermediate **94** in 43 % yield[105]. Washing the sodium hydride with hexane prior to reaction to remove the mineral oil did little to improve yield or purity.

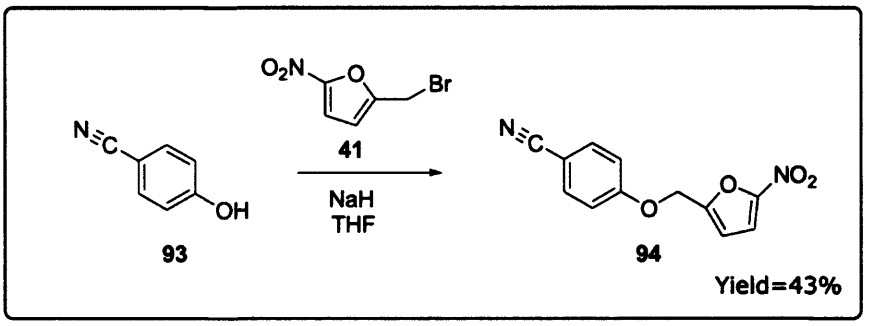

Scheme 4.5 Synthesis of 5-nitrofurfuryl-ether **94**.

A method to convert the nitrile to the amidine using lithium bis-trimethylsilylamide has been described in the literature[106, 107] and has been successfully repeated in these laboratories[108]. The conversion of the nitrile to the amidine function has been described in different works in the literature and is generally carried out using lithium 1,1,1,3,3,3-hexamethyldisilazane in dry THF at 0°C. The mechanism proceeds via nucleophilic addition of the hexamethyldisilazane to the nitrile to give an amidine lithium salt complex that is then hydrolised by HCl to give the free amidine as shown in scheme 4.6. The structure of the lithium-amidine complex intermediate has been characterised by Lappert *et al.*[106] Conversion of the nitrile intermediate **94** to the amidine derivative **91** was initially attempted using the described conditions which unfortunately did not yield the desired product in this case. Two different procedures were

[105] Mocelo, R.; Kováč, J. Aliphatic and Aromatic 5-nitro-2-furylamines and aromatic 5-nitrofurfuryl ethers. *Collect. Czech. Chem. C.* **1983**, *48*, 2682-2692.

[106] Lappert, M. F.; Slade, M. J.; Singh, A.; Atwood, J. L.; Rogers, R. D.; Shakir, R. Structure and Reactivity of Sterically Hindered Lithium Amides and Their Diethyl Etherates - Crystal and Molecular-Structures of $Li(N(SiMe_3)_2)(OEt_2)_2$ and $Li(NCMe_2CH_2CH_2CH_2CMe_2)_4$. *J. Am. Chem. Soc.* **1983**, *105*, 302-304.

[107] Thurkauf, A.; Hutchinson, A.; Peterson, J.; Cornfield, L.; Meade, R.; Huston, K.; Harris, K.; Ross, P. C.; Gerber, K.; Ramabhadran, *T.* V. 2-phenyl-4-(aminomethyl)-imidazoles as Potential Antipsychotic Agents, Synthesis and Dopamine D_2 Receptor Binding. *J. Med. Chem.* **1995**, *38*, 2251-2255.

[108] Boussard, C.; Klimkait, *T.*; Mahmood, N.; Pritchard, M.; Gilbert, I. H. Design, synthesis and evaluation of potential inhibitors of HIV gp120-CD4 interactions. *Bioorg. Med. Chem. Lett.* **2004**, *14*, 2673-2676.

also attempted: in the first attempt the lithium hexamethyldisilazane (LHMDS) used was a commercially available solution in dry ether whilst in the second attempt it was prepared *in situ*. MS and NMR analyses of the mixtures did not show the formation of the product and flash column chromatography of the crude mixture gave only the starting materials.

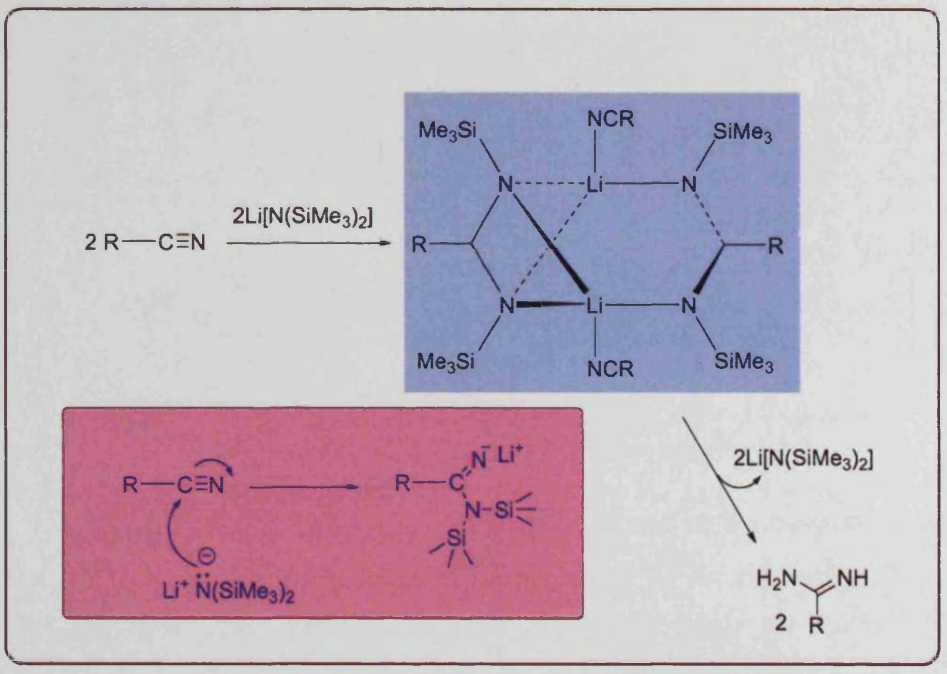

Scheme 4.6 Mechanism proposed for the conversion of a nitrile to amidine[106].

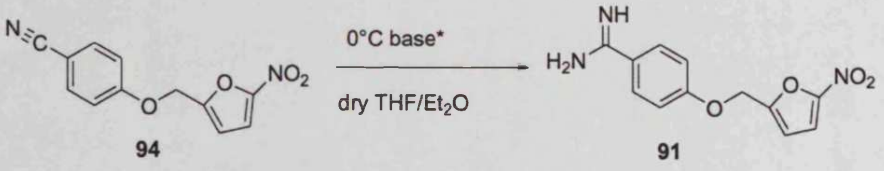

Base*	Result
Lithium 1,1,1,3,3,3-hexamethy-disalzane solution in Ether	✗
*n*BuLi + 1,1,1,3,3,3-hexamethyldisilazane	✗

Scheme 4.7 Attempted conversion of nitrile intermediate **94**

The failure of these initial reactions led us to propose that it was possible that the base could have reacted with the hydrogen in the α position to the

ether function. The acidity of the hydrogen at this position could be increased by the electron-withdrawing effect of the nitro group, which we propose can also be extended through the furan ring by conjugative effects (scheme 4.8).

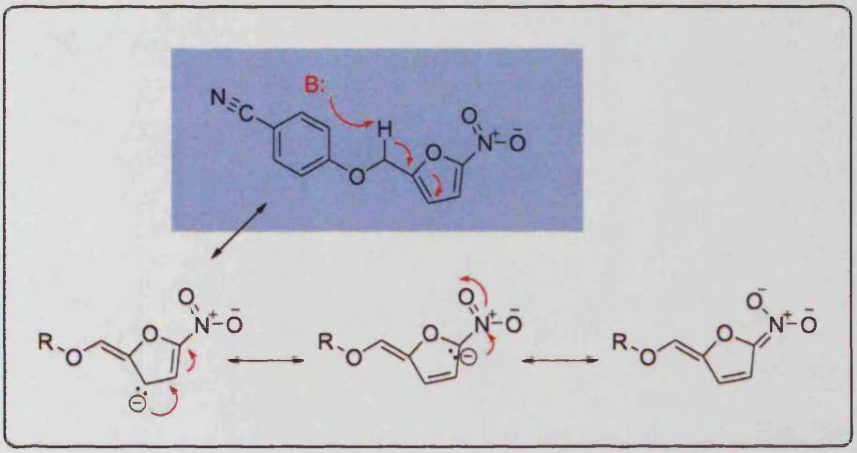

Scheme 4.8 Possible base mediated proton abstraction.

4.4.2 Benzamidine to nitrile via Alkyl-chloro-aluminium amides

Garigipati *et al.* [109] have described a one step preparation of an amidine by direct nucleophilic addition of an amine to the parent nitrile via aluminium amides. The alkylchloroaluminium amide can be conveniently generated from trimethyl aluminium and ammonium chloride or amine hydrochloride[110] as shown in scheme 4.9.

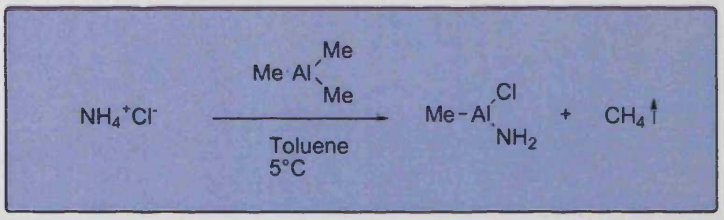

Scheme 4.9 Preparation of aluminium amide.

[109] Garigipati, R. S. An efficient conversion of nitriles to amidines. *Tetrahedron Lett.* **1990**, *31*, 1969-1972.

[110] Levin, J. I.; Turos, E.; Weinreb, S. M. An Alternative Procedure for the Aluminum-Mediated Conversion of Esters to Amides. *Synth. Commun.* **1982**, *12*, 989-993.

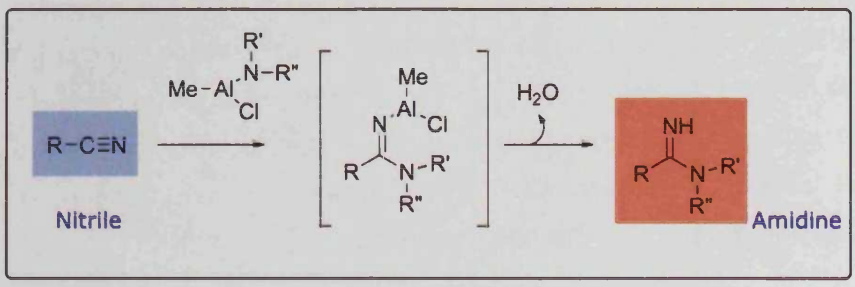

Scheme 4.10 nucleophilic addition of the aluminiumchloroamide to the nitrile.

The aluminiumchloroamide is subsequently added to the nitrile to afford the corresponding amidine derivative upon hydrolysis.

With this in mind, the intermediate **94** was reacted with the aluminiumchloroamide reagent, following the procedure described. As the outcome of the initial reaction was unclear by MS and NMR analyses we carried out various attempts including separate preparation of aluminiumchloroamide reagent which was then added to the reaction mixture in toluene or preparation of the aluminium reagent in situ followed by the addition of the nitrile intermediate **94**. Although MS analysis of the reaction mixtures showed the formation of a new product with the expected mass we were unable to isolate the desired product. Ion exchange chromatography (using gradient of HCl in propan-2-ol) and reversed phase silica gel (C18) column chromatography were carried out, but both methods failed to yield the desired compound and it was thought that the poor solubility (different extractions in organic solvents were performed) in organic solvent of the product contributed to the purification problems.

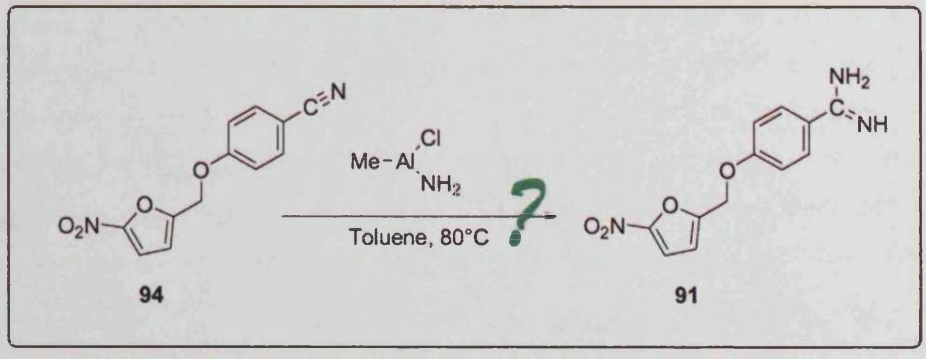

Scheme 4.11 Formation of amidine **91** via aluminiumchloroamide.

Having considered the difficulties encountered in the purification of **91** we decided it was necessary to convert the nitrile **94** in a manner which would minimise the purification issues. An alternative approach was found in the form of the Pinner reaction[111, 112], which involves reagents that can be easily removed from the reaction mixture.

4.4.3 Benzamidines from nitriles via the Pinner reaction:

The Pinner reaction [111, 112] proceeds through two steps:

1) transformation of the nitrile into an imido ester:

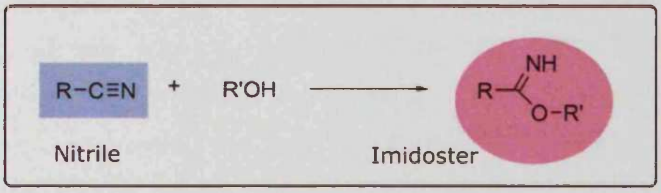

Scheme 4.12 Pinner reaction: formation of the imidoester intermediate

2) condensation with ammonia to give amidine:

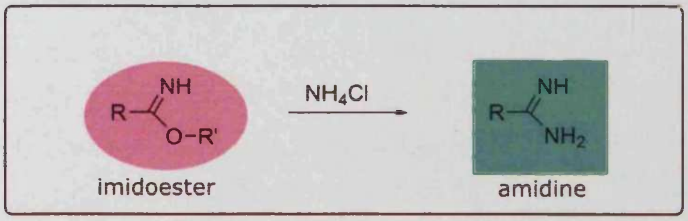

Scheme 4.13 Pinner reaction: formation of the amidine from the imidoester

Different variations of the Pinner reaction were attempted in order to convert nitrile **94** to amidine **91** and a summary of the attempts is shown on the following scheme 4.14. In the first attempt 7 equivalents of EtOH were used for the formation of the imidoester at 0°C[113] in chloroform as solvent. However as we did not yet know if the imidoester **95** would be detected by the MS method available to us and as the ^{1}H-NMR was also unclear we had to assume that the reaction had infact worked and carried

[111] Pinner, A.; Klein, F. *Ber. Deut. Chem. Ges.* **1877**, 10, 1889.

[112] Pinner, A. *Die Imidoäther und ihre Derivate*; Oppenheim: Berlin, **1892**.

[113] Dabak, K. Synthesis and protection of some amidines. *Turk. J. Chem.* **2002**, *26*, 547-550.

on. The supposed imdoester was treated with NH_4Cl in MeOH/water but MS and NMR analyses confirmed that the formation of the desired product did not take place.

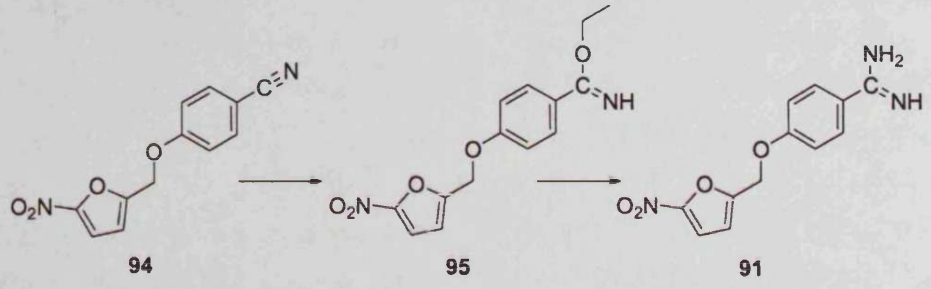

Imidoester formation		Amidine formation	
Conditions	**Result**	**Conditions**	**Result**
HCl(g) EtOH(7equ), $CHCl_3$ 0°C	✗	NH_4Cl (1.5 equ.) MeOH/H_2O (7/1)	✗
HCl(g), dry EtOH, 0°C, 24hrs	✓	NH_4Cl (1.5 equ.) MeOH/H_2O (7/1)	✗
Purification and isolation not obtained		NH_4Cl (3 equ.) MeOH/H_2O (7/1)	✓
		NH_4OH 7M in MeOH	✓

Scheme 4.14 Summary of the attempts carried out for the conversion of the nitrile **94**.

The first step of the Pinner reaction was modified by bubbling HCl(g) through the mixture of the nitrile derivative dissolved in dry ethanol at 0°C[114] for 24 hrs. TLC, MS and NMR analyses confirmed the formation of the imidoester intermediate **95** had occured using this method. The conversion of the imidoester into the amidine was attempted using various procedures as described on scheme 4.14. We found that the formation of the amidine occurs when increasing the number of equivalents of NH_4Cl from 1.5 to 3. Unfortunately, in this case, the product could not be isolated pure from the mixture possibly due to problems with unwanted chloride salt byproducts. Therefore the conversion of the imidoester was repeated using a solution of ammonia in methanol (7M). In these conditions MS analysis showed that the formation of the amidine probably

[114] Presnell, S. R.; Patil, G. S.; Mura, C.; Jude, K. M.; Conley, J. M.; Bertrand, J. A.; Kam, C. M.; Powers, J. C.; Williams, L. D. Oxyanion-mediated inhibition of serine proteases. *Biochemistry* **1998**, *37*, 17068-17081.

occurs together with the unwanted transesterification of the ethanol imidoester to a methanol imidoster (**96**, scheme 4.15). This gave rise to a mixture, which again hindered the purification of the desired product **91**.

It appeared that the poor solubility of the product in organic solvents was again a major hindrance to purification and with this in mind we proposed that *in situ* Boc protection of the crude mixture could be a way to modify the solubility of the desired amidine **91**. It was expected that the Boc protection of the amidine functionality would increase the lipophilicity of the product (**97**, scheme 4.15) and its solubility in organic solvents thus facilitating its separation from the mixture. The Boc protection was carried out by treating the crude reaction mixture from scheme 4.14 with Boc anhydride and NaOH in THF and water solution[115]. Unfortunately this reaction did not work and consequently we were unable to isolate the amidine **91** from the complex mixture.

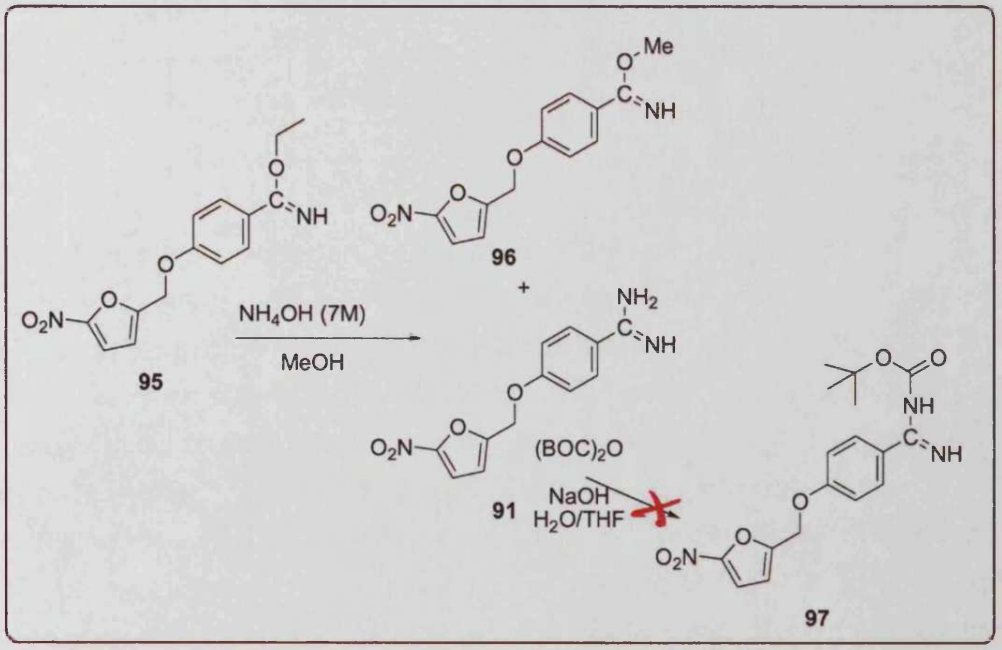

Scheme 4.15 Alternative strategy attempted to isolate the benzamidine **91**.

[115] Pons, J. F.; Fauchere, J. L.; Lamaty, F.; Molla, A.; Lazaro, R. A constrained diketopiperazine as a new scaffold for the synthesis of peptidomimetics. *Eur. J. Org. Chem.* **1998**, 853-859.

4.4.4 An alternative route for the synthesis of the furfurylether-benzamidine:

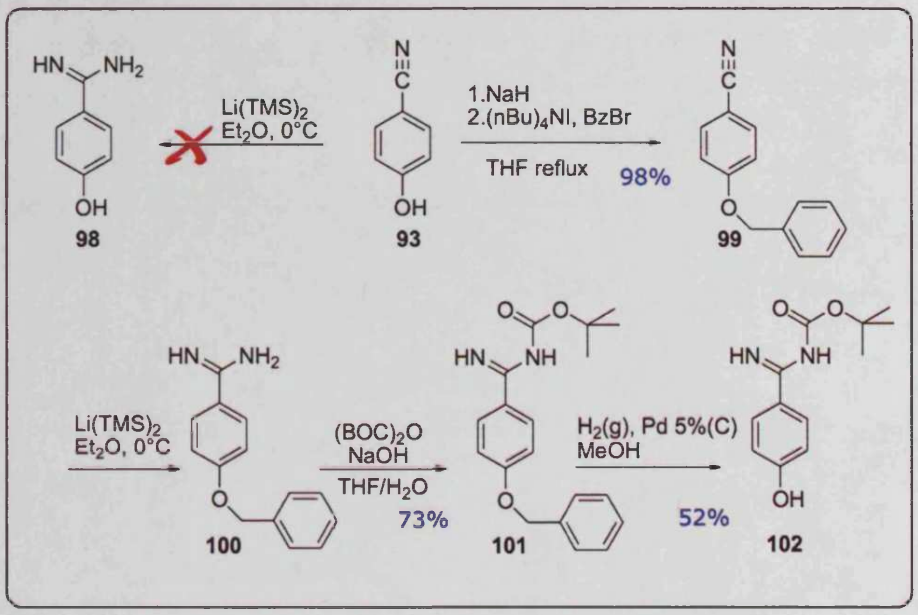

Scheme 4.16 Alternative route via Boc protection of amidine group.

After efforts to purify the product **91** failed we decided to consider an alternative route to synthesis of the benzamidine. As it was expected that the nitro group might affect the reactivity of these derivatives we therefore decided to build the amidine function on the protected p-cyanophenol (**93**) fragment with a view to coupling the free phenol function to the nitrofuran unit, as the last step. The direct conversion of the nitrile function of p-cyanophenol (**93**) to amidine (**98**) was unsuccessfully attempted via lithium 1,1,1,3,3,3-hexamethyldisilazane in dry ether. However by protection of the phenolic hydroxyl as a benzyl ether[116] (98% yield), it was possible to convert the nitrile **99** to the corresponding amidine **100** using the procedure previously described[106, 107]. Again problems with purification led to Boc protection as a strategy for product isolation from the mixture[115]. Standard protection using $(Boc)_2O$/NaOH in H_2O/THF gave compound **101** in 73% yield. The solubility of the product as compound **101** was dramatically improved in organic

[116] Czernecki, S.; Georgoulis, C.; Provelenghiou, C. Nouvelle method de benzylation d'hydroxyles glucidiques encombres. *Tetrahedron Lett.* **1976**, 3535-3536.

solvents and the isolation of the product was obtained by simple extraction with ethyl acetate. Purity of the product **101** was confirmed by NMR analysis, as detailed in scheme 4.17 and the benzyl protective group was then cleaved by bubbling hydrogen gas into an ethanolic solution of the intermediate **101** with 5% Pd on activated charcoal to yield the Boc protected intermediate **102** in 52% yield.

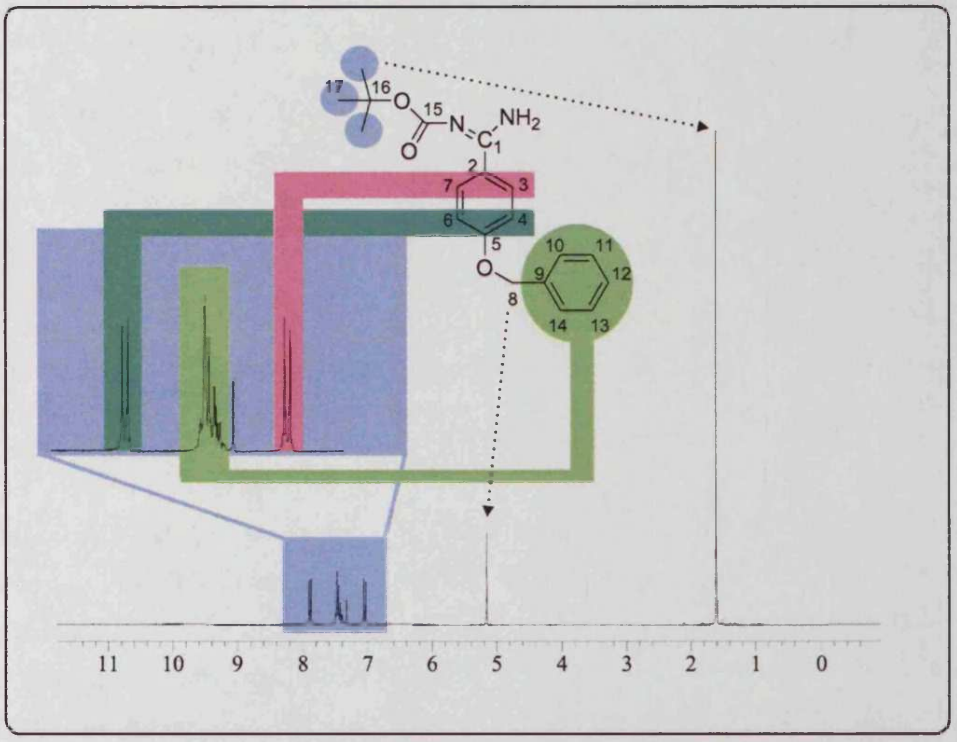

Scheme 4.17 1H-NMR ($CDCl_3$) of the Boc-protected intermediate 101.

The coupling of the Boc protected intermediate **102** with bromomethyl-5-nitrofuran was attempted using two sets of conditions, as detailed below in scheme 4.18. Our initial attempt was carried out as a THF suspension using NaH as base whilst the second attempt was carried out as an acetonitrile suspension with K_2CO_3 as base (scheme 4.18). In both cases MS analysis did not show the formation of the expected product and attempted purification of the crude reaction mixture by flash column chromatography (DCM:MeOH=100:0 to 80:20) gave only the starting material **102**.

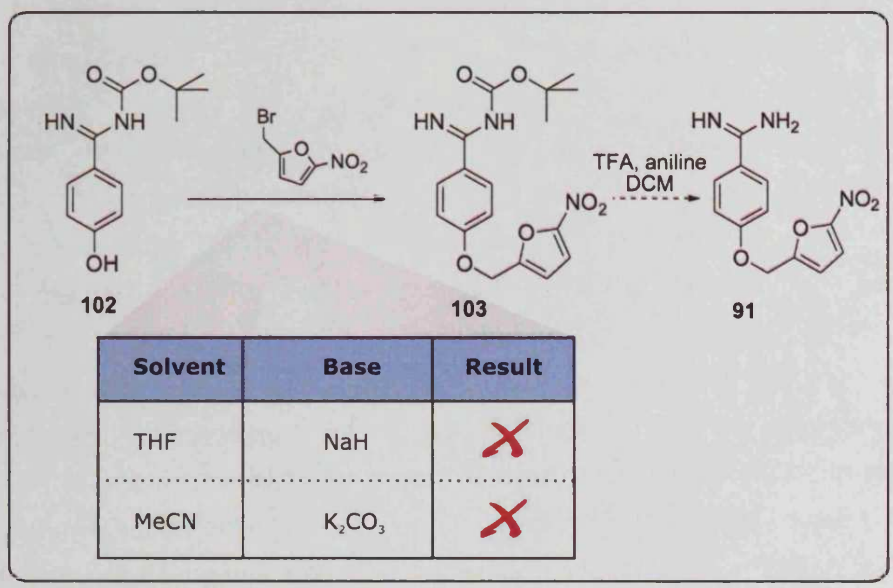

Solvent	Base	Result
THF	NaH	✗
MeCN	K_2CO_3	✗

Scheme 4.18 Attempted coupling of 2-bromomethyl-5-nitrofurane

4.4.5 Synthesis of p-substituted benzamidines:

By taking into account the failure of the previous reactions and also considering the successful coupling of the *p*-p-cyanophenol with 2-bromomethyl-5-nitrofuran (scheme 4.5), we can propose that the presence of the amidine function may for some as yet undetermined reasons prevent the coupling reaction of **102** with the nitrofuran derivative.

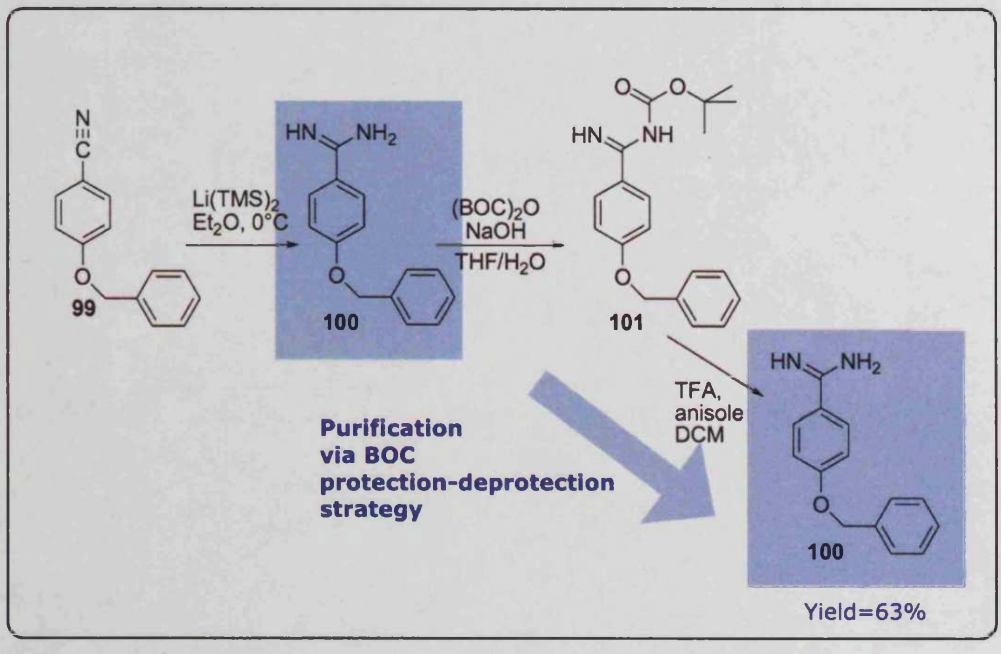

Scheme 4.19 Synthesis of p-benzyl-oxy-benzamidine (**100**).

However, having had some success with our benzyl and Boc protection/deprotection strategy (scheme 4.16) we therefore decided to utilise this methodology in an approach to synthesise some p-substituted-oxy-benzamidines. Some m-substituted benzamidines (see chapter 7) had already been synthesised by a previous member of our group but did not show significant *in vitro* activity against the different *Trypanosoma* species[108].

The first *para*-substituted benzamidine was synthesised in collaboration with the project student Siân Dukes using the Bz/Boc protection/deprotection route established by the author (scheme 4.19).

Benzyl protection of p-cyanophenol (**93**) followed by treatment with LHMDS gave the p-substituted benzamidine **100** (scheme 4.19). Standard Boc protection followed by extraction and standard deprotection using TFA and anisole in DCM solution[117] gave the p-substituted-benzamidine **100** in 63% yield. We have successfully used our Boc protection/deprotection strategy to access the previously unobtainable benzamidine **100**.

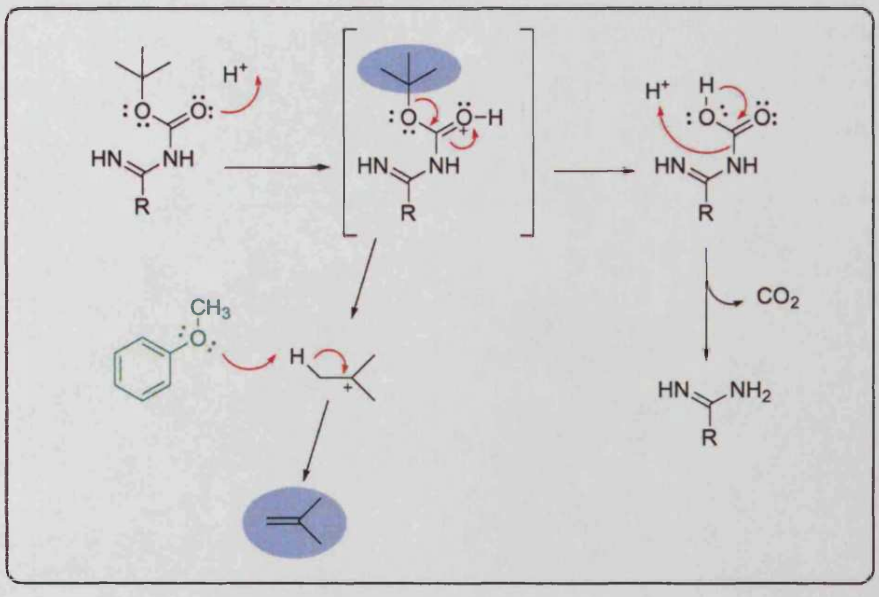

Scheme 4.20 Proposed mechanism for Boc-deprotection.

[117] Jarowicki, K.; Kocienski, P. Protecting groups. *J. Chem. Soc. Perk. T. 1* 1998, 4005-4037.

It is interesting to note the role of anisole in the deprotection step as scavenger[118] of the highly reactive *tert*-butyl cations which are liberated from the reaction. This prevents the generation of unwanted side products via alkylation, as shown in the mechanism detailed on scheme 4.20.

The *in vitro* activity of **100** against *Trypanosoma* species was evaluated. This has been compared with the meta analogues and will be discussed separately in chapter 7.

From our experiments we can note that the synthesis of the *para* substituted benzamidines appears to be hindered by its lower reactivity compared to the meta analogues and furthermore its low solubility in organic solvents handicaps the attempted purification of any product made. In contrast to this, the synthesis and purification of the meta-substituted benzamidine has not shown any difficulties and in order to explain these differences we proposed that differing electron-donating effects could be critical. In the *para*-substituted benzamidine the electron-donating resonance effect of the oxygen (alkoxyl- or aryloxy-) is transmitted to the amidine function through the aromatic ring whilst in the meta-substituted benzamidine it is not (scheme 4.21).

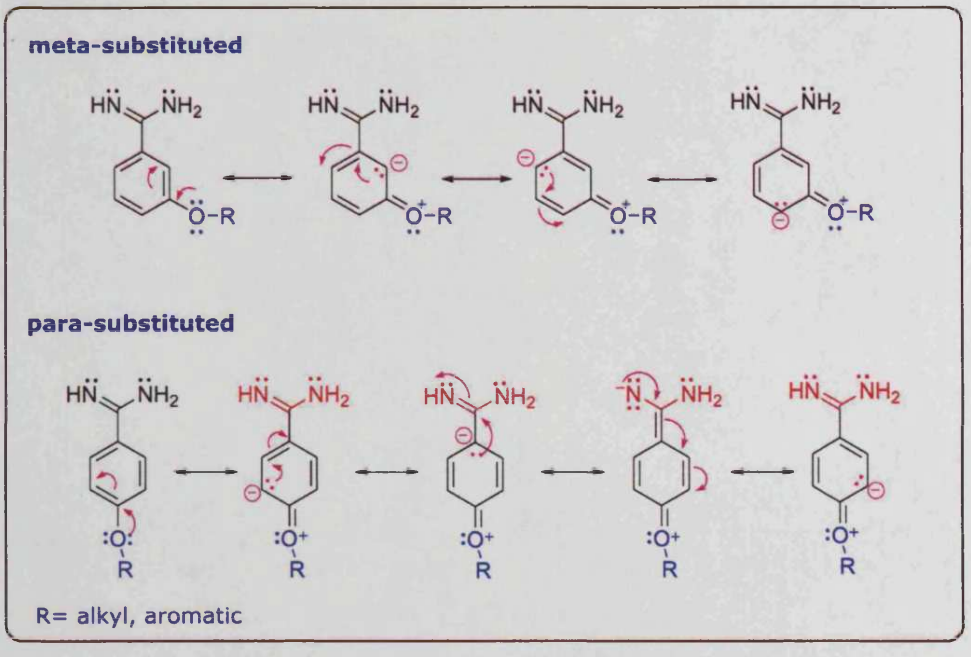

Scheme 4.21 Resonance effect of an electron-withdrawing group proposed for *para* and *meta* substituted benzamidines.

[118] Bodanszky, M. Alkyl esters of amino acids. *Int. J. Pept. Prot. Res.* **1984**, 23, 111.

From scheme 4.21 we can clearly see that in the case of the meta substitution the amidine is unaffected by resonance of the ring. In the *para* substitution this is not the case and this may be one of the reasons for problems encountered.

In collaboration with project student, Siân Dukes, we proposed to couple of an alkyl group to the benzamidine as a mean to establish a procedure for the coupling of the nitrofuran moiety to the benzamidine unit and to yield an interesting model compound. O-alkylation of Boc protected amidine **102** with heptyl iodide in THF, using NaH as base gave the heptyl-oxy-Boc-benzamidine (**105**) in 35% yield. The Boc group was subsequently removed using the standard conditions previously described for the benzyl derivative (**100**) to give the free p-heptyl-oxy-benzamidine derivative (**106**, scheme 4.22) in 95% yield. This model compound was also evaluated for its *in vitro* activity against *Trypanosoma* species and will be discussed in chapter 7.

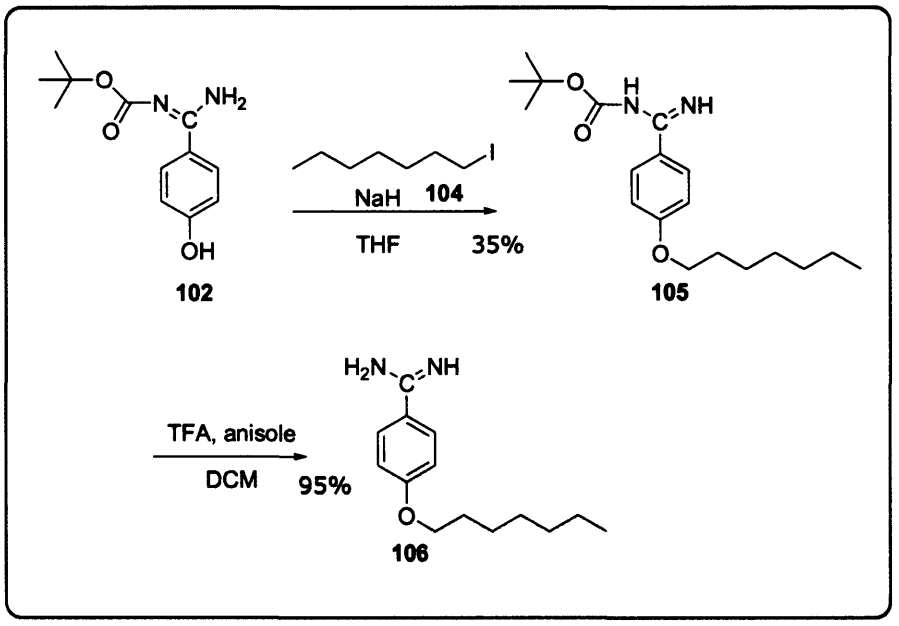

Scheme 4.22 Synthesis of p-heptyl-oxy-benzamidine (**106**)

The fact that the O-alkylation with **41** (Scheme 4.23) was only successful when the substrate contained a nitrile group is a very interesting result. Also the O-alkylation with **104** was successful in the presence of the

Boc protected amidine. This observed incompatibility suggests that further work on these reactions is warranted.

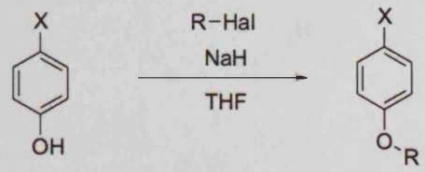

Group (X=)	Alkyl-halide	Outcome
Nitrile —C≡N	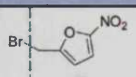 41	✓
BOC-amidine 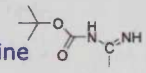	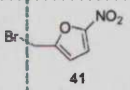 41	✗
BOC-amidine 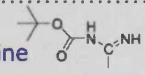	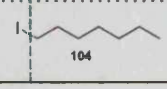 104	✓

Scheme 4.23 Results of different coupling using NaH in THF.

4.5 Approaches to p-substituted amino-benzamidines:

Having investigated the synthesis of benzamidines substituted with an oxygen in the *para* position we next investigated the use of p-amino-benzamidine (**82**) as a starting material to develop methodology in order to access model compounds eventually with a view to synthesising nitrofuran derivatives. The amino group is placed in the *para* position in order to have an electronegative atom in *para* position to the amidine moiety, as required for the interaction with the P2 transporter. Our early experiments suggested that the reactivity of this benzamidine starting material was probably handicapped by positioning of the amino function in *para* to the amidine. Further reactions and discussions concerning this starting material will be described in the next chapter (chapter 5).

Having successfully alkylated the p-hydroxy-benzamidine in scheme 4.23, we decided to investigate the reactivity of p-amino-benzamidine (**82**) with heptyl-iodine (**104**). Two different procedures were carried out, as shown in scheme 4.24: in a first attempt DBU was used as the base in ethanol at room temperature whilst in the second procedure the mixture was heated to reflux temperature. In both cases TLC and MS analyses did

not show the formation of the desired product **107** but only the presence of starting materials.

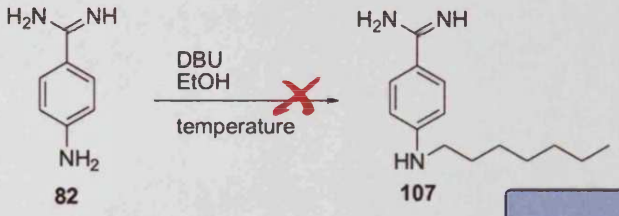

Temperature	Outcome
rt	✗
reflux	✗

Scheme 4.24 Attempted synthesis of p-heptyl-amino-benzamidine (**107**)

Another approach to form a *para*-substituted benzamidine would be Schiff's base formation between p-amino benzamidine and nitrofuraldehyde (scheme 4.25). p-Aminobenzamidine is supplied as the bis-hydrochloride salt. It is probable that as the aniline nitrogen is protonated, it has reduced nucleophilic properties. Therefore the reaction was carried out in the presence of different bases to increase the pH. However they led to formation of a thick black solid. TLC and MS analyses failed to show any required product. Only starting material was present. It is probable that the lack of reactivity is due to the poor nucleophilicity of the aniline amine.

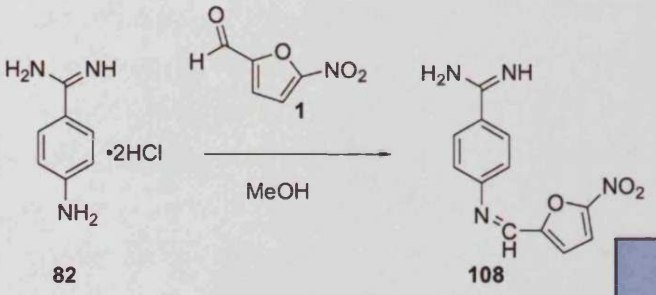

Base	Outcome
none	✗
NaOH 2N	✗
NH_4OH	✗
Phosphate buffer pH=7.2	✗

Scheme 4.25 Attempted synthesis of benzamidine **108**.

These problems with formaton of the imine led us back to the strategy successfully used for the p-hydroxybenzamidine (scheme 4.16). We therefore carried out the Boc protection of benzamidine **82** using the standard conditions[115] to give the intermediate **83** in 96% yield.

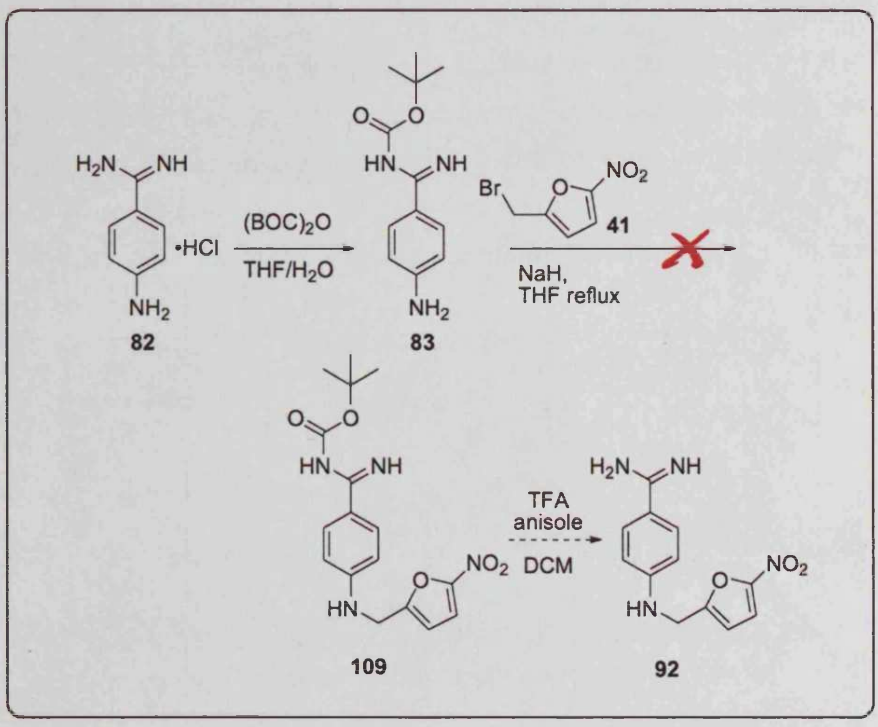

Scheme 4.26 Attempted synthesis of benzamidine **92** via Boc protection strategy.

Subsequent N-alkylation of **83** using **41** was attempted using standard NaH/THF conditions established in scheme 4.16, however we were unable to successfully obtain the desired Boc protected intermediate **109**. MS did not show the formation of the desired product.

The chemistry of Boc protected benzamidine **83** has been further investigated and will be further discussed on detail in chapter 5.

At this point it was clear that the synthesis of *para*-benzamidines attached to nitrofurans was a very challenging target. It was suggested that novel procedures were needed to be developed for this purpose and whilst the constraint of time prohibited further investigation by the Author into alternative routes to these compounds a search of the literature uncovered several interesting methods which could be of help for the development of new strategies to these compounds.

4.6 Synthesis of amidines: new methodologies:

4.6.1 Capdevielle's method for conversion of unactivated nitriles to amidines:

It has been observed that for an optimal conversion of the nitrile to amidine the first should be activated by electronegative substitution[119].

Capdevielle has reported a general preparation of amidines from unactivated nitriles[120, 121], via stoichiometric copper-(I)-chloride induced addition of various amines give amidines in good yields.

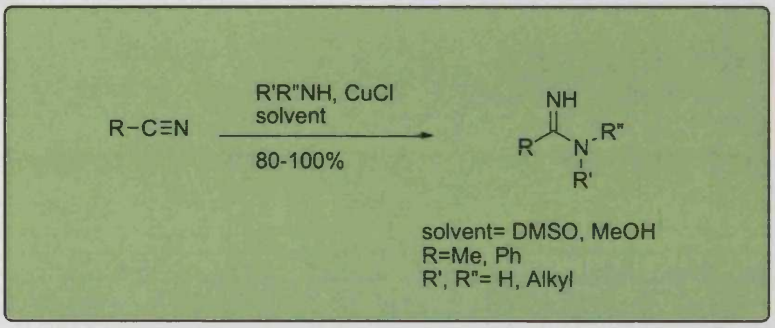

Scheme 4.27 Capdevielle's method of preparation of amidines.

4.6.2 Judkins: Amidines via benzamidoximes intermediates:

In Judkins' procedure[122] (scheme 4.28) the benzonitriles were first transformed into benzamidoximes and then reduced to benzamidines via palladium catalysed hydrogenolysis in acetic acid/anhydride mixture.

---

[119] Schaefer, F. C.; Krapcho, A. P. Pre*para*tion of amidine salts by reaction of nitriles with ammonium salts in the presence of ammonia. *J. Org. Chem.* **1962**, *27*, 1255-1258.

[120] Rousselet, G.; Capdevielle, P.; Maumy, M. Copper(I)-Induced Addition of Amines to Unactivated Nitriles - the 1st General One-Step Synthesis of Alkyl Amidines. *Tetrahedron Lett.* **1993**, *34*, 6395-6398.

[121] Yet, L. A Survey of Amidine Synthesis; Albany Molecular Research, Inc. Technical Reports.: Albany, NY, **2000**; pp 1-12.

[122] Judkins, B. D.; Allen, D. G.; Cook, *T.* A.; Evans, B.; Sardharwala, *T.* E. A versatile synthesis of amidines from nitriles via amidoximes. *Synth. Commun.* **1996**, *26*, 4351-4367.

palladium catalysed hydrogenolysis in acetic acid/anhydride mixture. Acetic anhydride acts as an acylating agent and is necessary in providing useful reaction rates for the hydrogenolysis step.

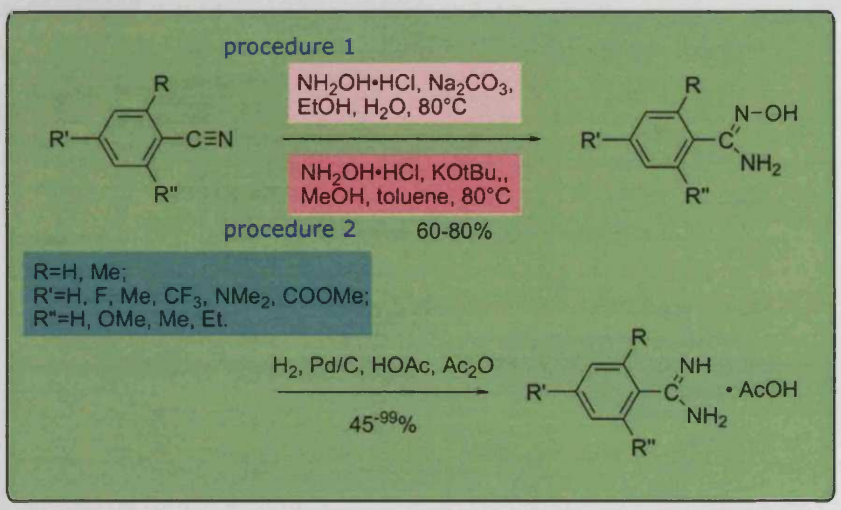

Scheme 4.28 Judkins's method of preparation of amidines.

4.6.3 Mioskowski: amidines via thioamides:

Mioskowski *et al.*[123] has prepared phenylthioamidates from nitriles in the presence of thiophenol and HBr. Nucleophilic addition of thiophenol to the nitrile leads to the formation of the thioamidate. Phenylthioamidates can be readily converted to amidine salts in the presence of various amines (scheme 4.29) and the thiophenol also acts as a good leaving group thus enhancing the nucleophilic substitution by the amine to give the corresponding amidine, as shown in scheme 4.29.

[123] Baati, R.; Gouverneur, V.; Mioskowski, C. An improved method for the preparation of amidines via thiophenylimidic esters. *Synthesis* **1999**, 927-929.

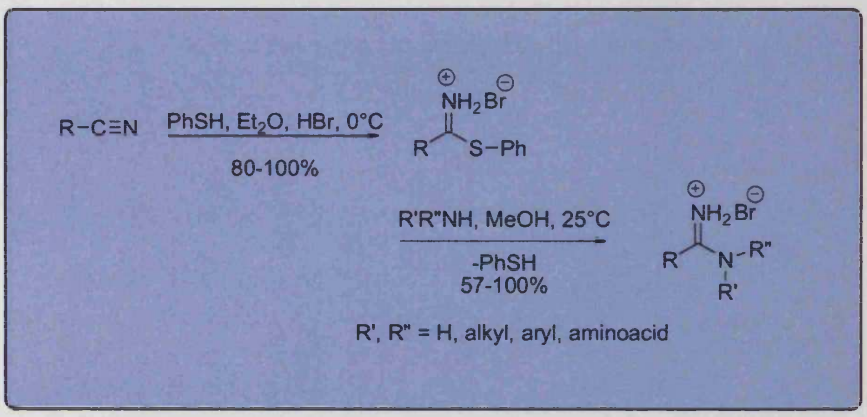

Scheme 4.29 Mioskowski procedure to convert nitriles to amidines.

4.6.4 Shäfer: amidines via N-acetyl-cysteine thioamidate

The Shäfer procedure[124] for the synthesis of amidines represents a new mild method which does not involve high temperatures, highly acidic, alkaline or strongly reducing conditions. In a first step N-acetylcysteine adds to the nitrile to form an imino-thioether intermediate (scheme 4.30). Catalytic regeneration of N-acetylcysteine by displacement with ammonia yields the amidine. In addition to its catalytic role, the N-acetylcysteine also acts by stabilising the amidine formed as the latter can decompose through loss of ammonia[124].

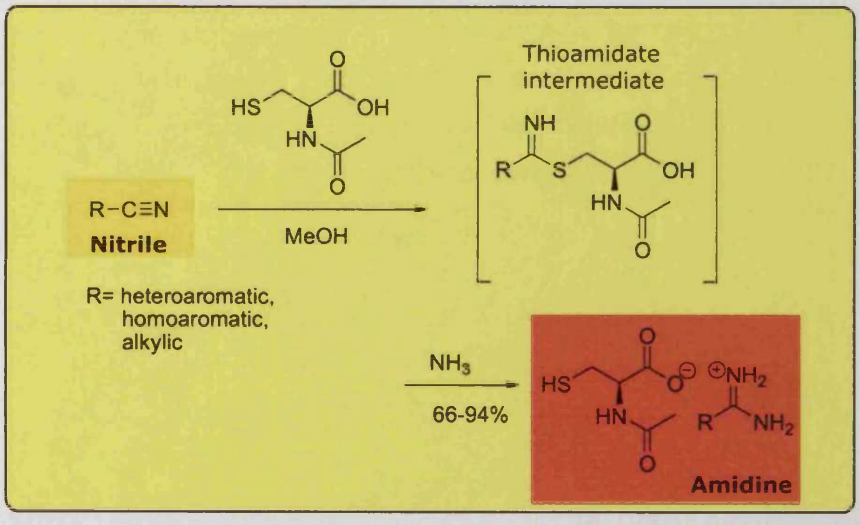

Scheme 4.30 Schäfer procedure via thioimidate.

[124] Lange, U. E. W.; Schafer, B.; Baucke, D.; Buschmann, E.; Mack, H. A new mild method for the synthesis of amidines. *Tetrahedron Lett.* **1999**, *40*, 7067-7070.

5. Results and Discussion III:

Prodrug Approach

The prodrug approach represents a new project we have recently started in our group. Triazines and benzamidines have again been considered as recognition moieties in order to exploit the P2 transporter as a target to selectively deliver a potential drug to the parasite. Following the delivery of the compound to the parasite the recognition motif should be cleaved off.

5.1 Prodrugs and their utility:

5.1.1 Definition of prodrug:

Albert[125] first used the term "prodrug" as referring to a pharmacologically inactive compound that is converted to an active drug through a metabolic biotransformation[126]. The activation of a prodrug can occur either by an enzymatic process or by a chemical process such as hydrolysis that does not involve the presence of an enzyme. The

[125] Albert, A. *Selective Toxicity*; Chapman & Hall: London, **1951**.

[126] Silverman, R. S. *The Organic Chemistry of Drug Design and Drug Action*; Academic Press, **1991**.

conversion of a prodrug to drug can occur at different pharmacokinetic stages and in specific targets in the body.

The main aims of a prodrug can be summarised as follow:

1) **Improvement of solubility**: the solubility of a drug can be modified by attaching different groups that can be metabolically cleaved;

2) **Absorption and Distribution**: Depending on the site of action, different groups can be linked in order to facilitate the concentration of the drug in a specific target site;

3) **Stability**: The structure of a drug can be modified in order to increase the stability to inactivation by metabolic processes;

4) **Prolonged release**: Modifications of the drug can prolong its release, maintaining a low concentration over a long period of time;

5) **Toxicity**: The toxicity of a drug can be modulated. The prodrug form can be administered in a non-toxic form that will be converted into the active, toxic form only at the site of action[126].

5.1.2 Types of prodrugs:

In a prodrug design the modifications carried out on a drug are usually made on the basis of known metabolic transformations many operated by the cytochrome P450 enzymes[126]. Harper[127] called this rational design approach "**drug latentiation**" in order to distinguish it from serendipity. Wermuth[128] subdivided this term into two different classes (scheme 5.1):

1) **Carrier-linked prodrug**: where an active drug is linked to a non-toxic carrier group through a labile bond. The carrier group can be cleaved enzymatically (e.g. esterase, amidase)[126]. A carrier-linked prodrug can be further subdivided into three classes:

- **bipartate**: when the carrier is directly linked to the drug;

[127] Harper, N. J. Drug latentiation. *J. Med. Pharmaceut. Ch.***1959**, 1, 467-500.

[128] Wermuth, C. G. (Briot, M.; Cautreels, W.; Roncucci, R.; Editors) *Drug Metabolism and Drug Design: Quo Vadis? Montpellier 26-27 November 1981*; **1983**; 381 pp.

- **tripartate** when the carrier is linked to a linker arm that is connected to the drug;
- **mutual prodrug** when two synergistic (in most cases) drugs are attached to each other and both are carriers of each other.

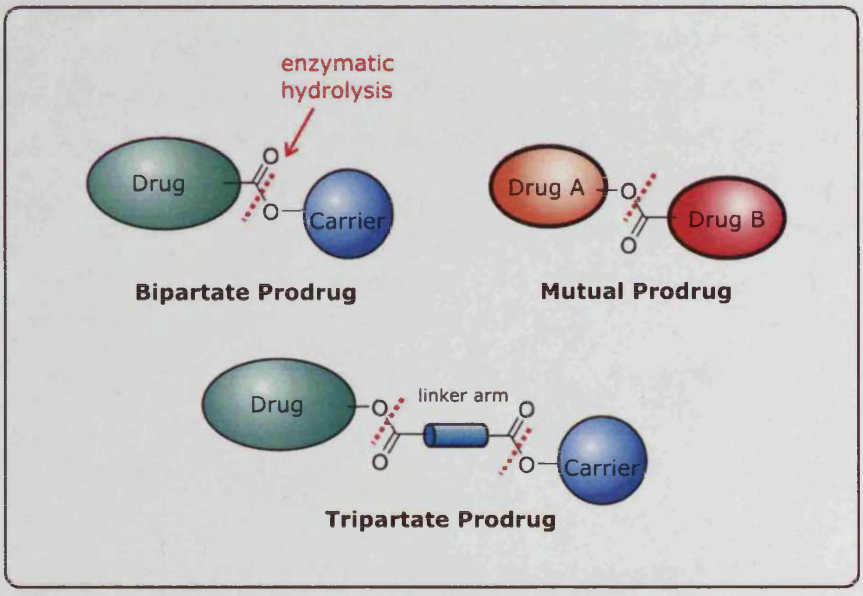

Scheme 5.1 Representation of carrier-linked prodrugs.

2) Bioprecursor: represents a compound that is activated to active drug after molecular modifications are carried out to it (e.g. oxidation reactions, scheme 5.2) and not by simple cleavage. In most cases a drastic structural change is required to unmask the desired group[126].

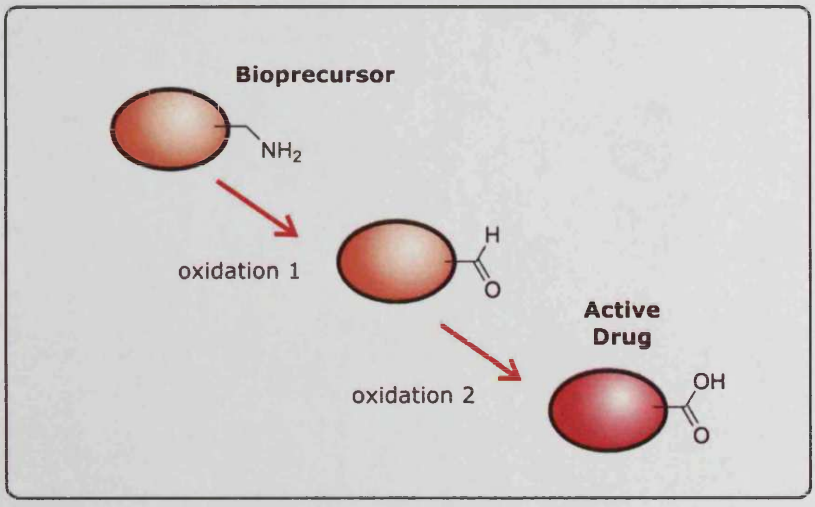

Scheme 5.2 Activation of a drug from its bioprecursor.

5.2 Prodrugs to selectively target Trypanosomes:

We proposed the carrier-linked prodrug model in the rational design of anti-trypanosomes prodrugs. Drugs could be linked to the P2 transporter recognition motif so that they are selectively taken up by trypanosomes. The carrier unit would have high affinity for the transporter and rapid uptake should occur. Once in the parasite the carrier could be cleaved by enzymatic hydrolysis by esterases in the case of an ester bond. The drug released into the parasite would then selectively exert its toxicity to its specific target in the parasite (scheme 5.3).

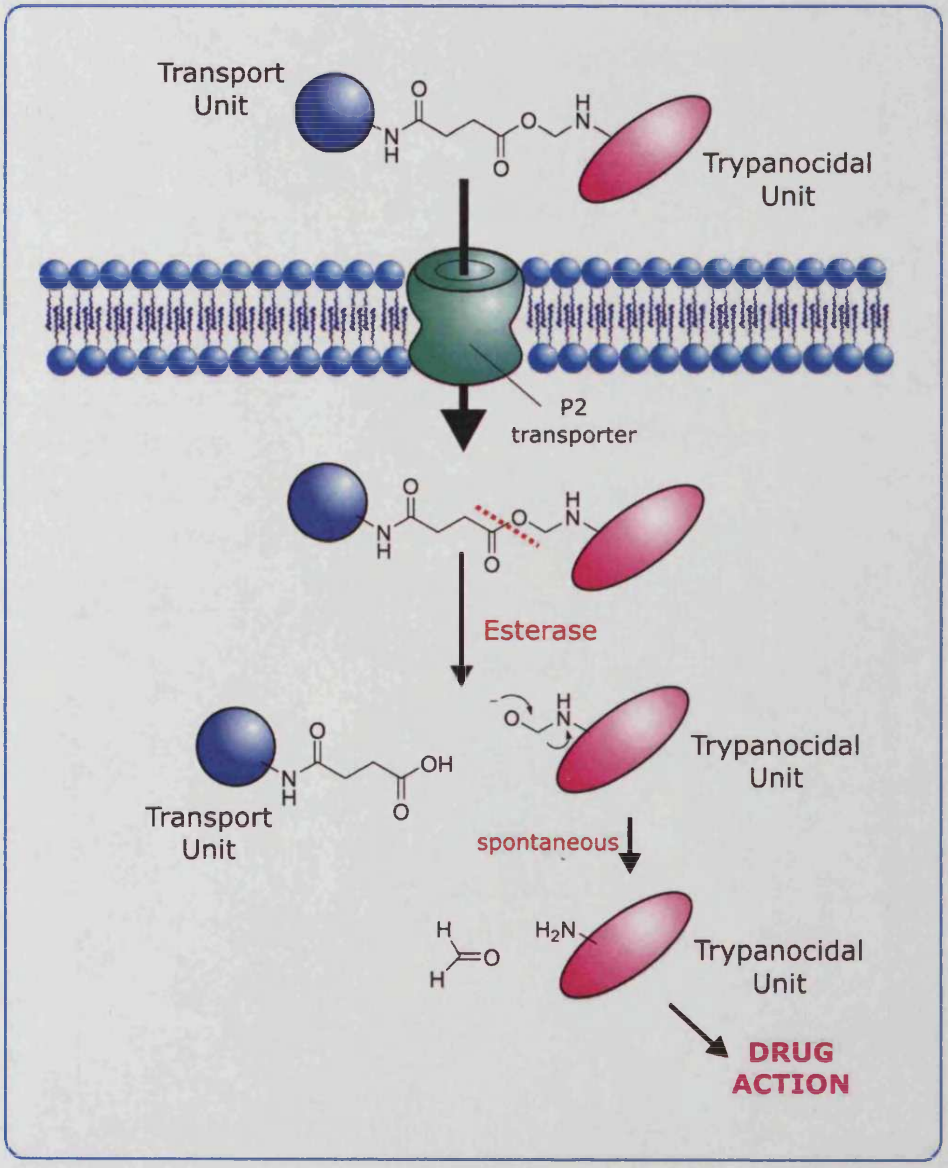

Scheme 5.3 Trypanocidal carrier-linked prodrug.

A tripartite carrier-linked prodrug, in this circumstance, represents an advantageous strategy, as it displaces the active drug further away from the site of enzymatic cleavage thereby reducing steric hindrance from the carrier as suggested by Ringsdorf[129]. The drug-linker connection must be designed so that it cleaves spontaneously after the carrier has been detached.

5.2.1 Therapeutic prospects of Target prodrug:

This prodrug strategy could potentially be applied to a wide series of trypanocidal agents that would normally not be taken efficiently up by the trypanosome.

It could be used for the delivery of current treatments such as DFMO. The carried-linked prodrug strategy could improve efficacy by minimising interactions with the host cells and enhancing uptake of the drug into trypanosomes. The selective drug delivery could reduce the dose required for a therapeutic effect and thus the toxicity associated with the pharmacological effect. As the transport unit will be cleaved *in vivo* from the active species, it will allow interaction of the drug with the molecular target and thereby reduce the risk of alteration of the activity of the drug by permanent attachment to the transport unit.

5.2.2 Considerations on Target Prodrug:

The release of formaldehyde from cleavage of the prodrug should be released into the parasite without giving rise to toxicity problems. The transport unit should be selectively released into the parasite thus circumventing related toxicity problems.

If we assume BBB uptake by passive diffusion, the high polarity of the transport unit could result in a poor bioavailability and inability of the drug to cross the blood brain barrier. In contrast to this hypothesis, these properties would not be affected if active transport is involved in the uptake.

---

[129] Ringsdorf, H. Structure and properties of pharmacologically active polymers. *J. Polym. Sci. Pol. Sym.* **1975**, *51*, 135-153.

5.3 Aims and Objectives:

The use of a prodrug approach represents a new strategy for selectively targeting trypanocides via the P2 transporter and would be a novel approach for the treatment of HAT.

The principal aim of this approach is represented by the design of a prodrug moiety to incorporate the P2 recognition motif as the carrier to selectively deliver cytotoxic agents to trypanosomes for the treatment of HAT. The carrier can be linked directly to the drug via an ester bond which could be cleaved *in vivo*.

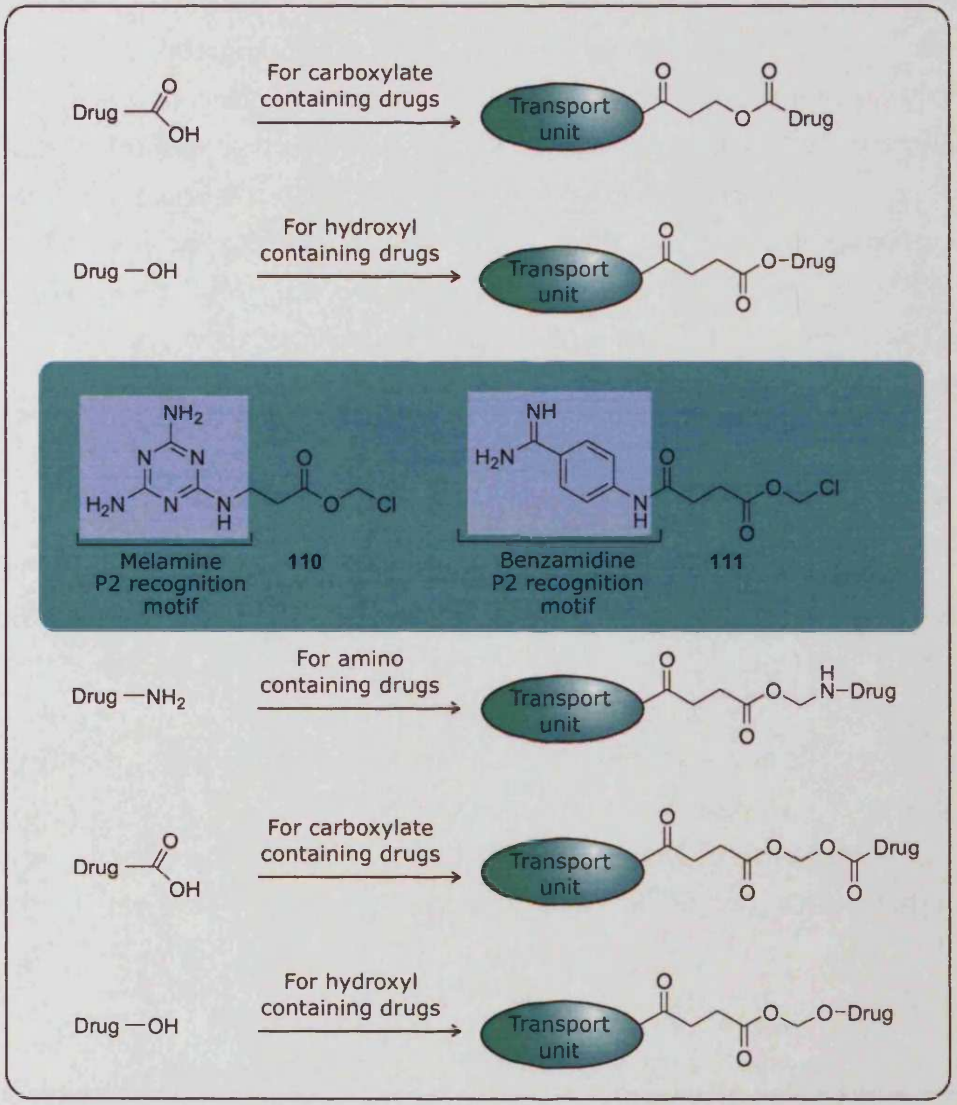

Scheme 5.4 Design of chloromethyl ester prodrugs bearing P2 recognition motifs[130].

Some bisphosphonates, such as alendronate (scheme 5.5) have been approved for use in humans by the FDA for osteoporosis, but also show significant antiparasitic activity. A further development of this method would be to attach a P2 recognition motif to the phosphonate of bisphosphonates such as alendronate, which should not only target the bisphosphonates to the trypanosomes, but also mask the negatively charged phosphonates.

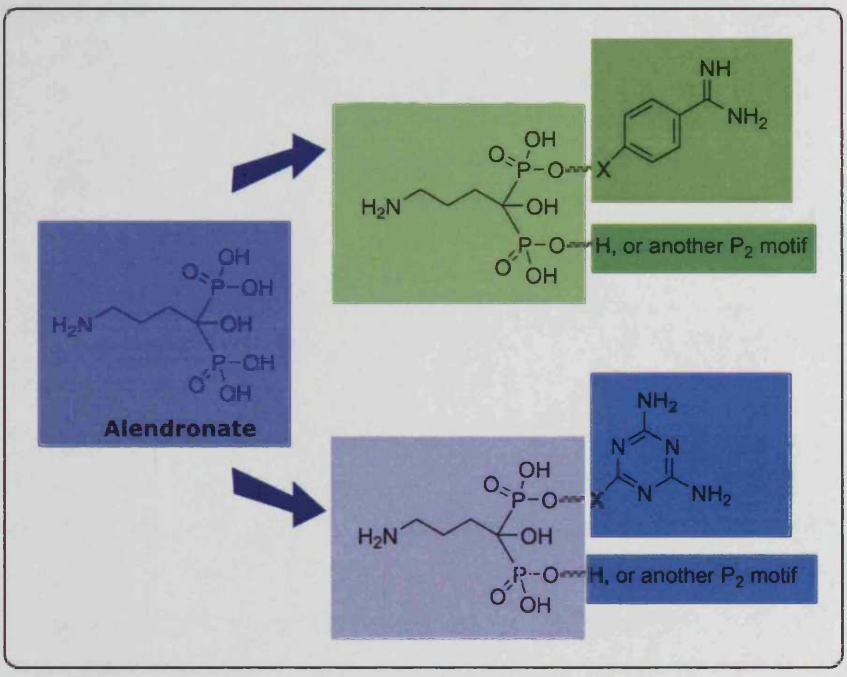

Scheme 5.5 Design of some bisphosphonate prodrugs derivative from alendronate.

Alendronate represents a versatile compound, where the phosphonate groups can be linked to one or two different P2 motifs.

The transporter should:

a) direct the drug to the parasite;

b) improve the uptake of the drug into the parasite;

c) mask the phosphonate.

The mechanism of action of alendronate and related bisphosphonates will be described further on in this chapter.

---

[130] Bodin, N. O.; Ekstrom, B.; Forsgren, U.; Jalar, L. P.; Magni, L.; Ramsay, C. H.; Sjoberg, B. Bacampicillin: a new orally well-absorbed derivative of ampicillin. *Antimicrob. Agents Chemother.***1975**, *8*, 518-525.

5.4 Prodrugs bearing a benzamidine moiety:

5.4.1 Attempted synthesis of benzamidine-chloromethyl esters

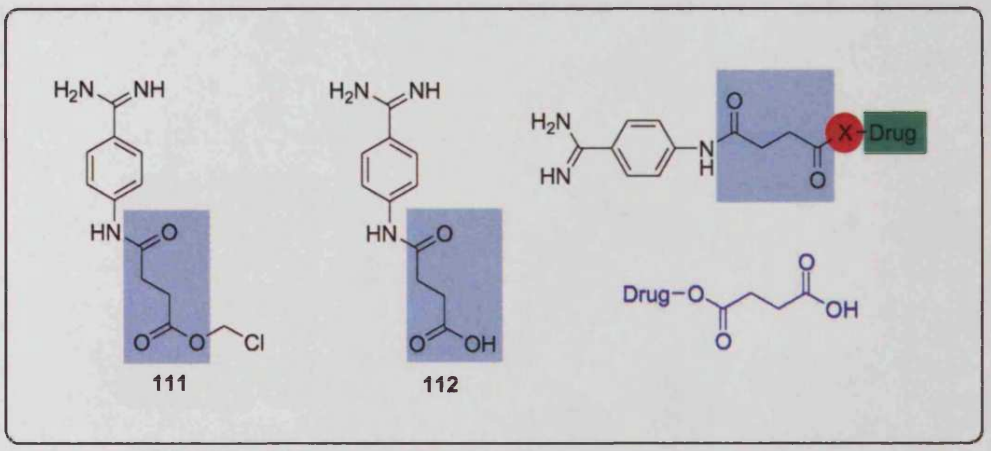

Scheme 5.6 Design of succinate esters prodrugs and their hydrolysis.

In collaboration with project student Lucy Rubij we decided to design a carrier linked prodrug bearing a benzamidine unit by linking prodrugs moieties such as compounds **111** and **112** (scheme 5.6). Succinic anhydride was used as a linker[131].

For the synthesis of benzamidine **111** we initially proposed the strategy shown in scheme 5.7. We thought that the protection of the amidine group was necessary, as it can be reactive towards electrophiles. The conversion to a carbamate effectively withdraws electron density from the N atom and renders it unreactive. This is required in order to direct further nucleophilic substitution reactions through the 4-amino group and not at the amidine group. The protection of 4-amino-benzamidine (**82**) has been described already on the previous chapter and can be carried out by using Boc anhydride in NaOH and THF to obtain protected benzamidine **83** in high yield.

[131] Carl, P.; Chakravarty, P. K.; Katzenellenbogen, J. A. A Novel Connector Linkage Applicable in Prodrug Design. *J. Med. Chem.* **1981**, 24, 479-480.

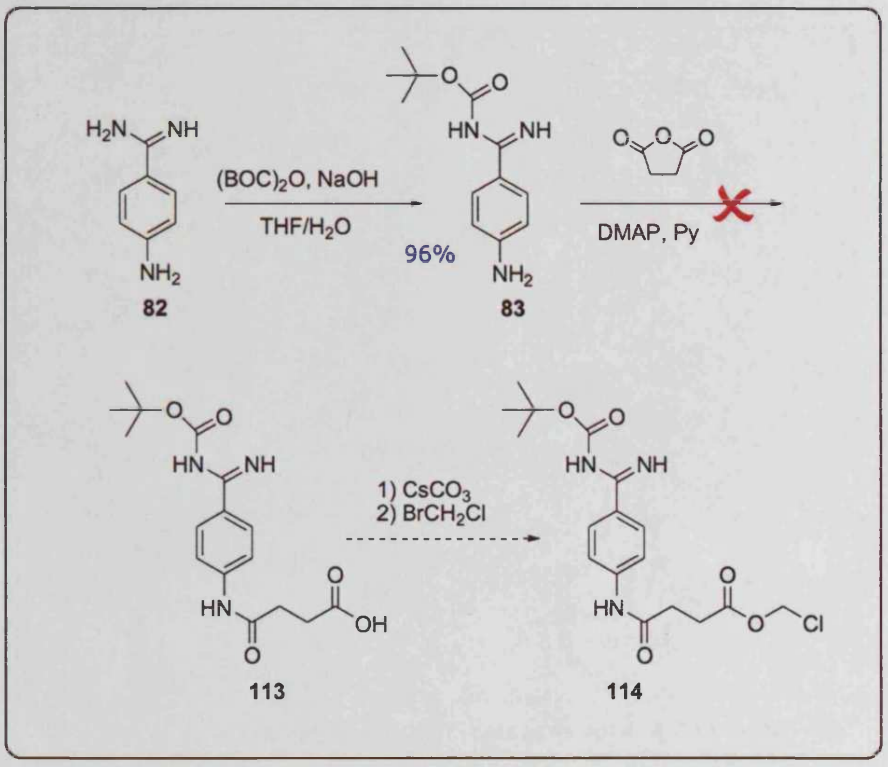

Scheme 5.7 Initial strategy followed for the synthesis of **114**.

In a second step benzamidine **83** was reacted with succinic anhydride in DMF, using DMAP as catalyst, following the conditions described by Zablocki *et al.*[132] TLC and MS analyses indicated that the reaction did not take place and only starting material was recovered from the reaction mixture. This can be due to a variety of factors. It is possible that the Boc protection of the amidine group contributes to the deactivation of the amino group in para position to the amidine reducing its nucleophilicity.

We proposed a modification of scheme 5.7 which represents an alterative route of synthesis of compound **111**.

[132] Zablocki, J. A.; Rico, J. G.; Garland, R. B.; Rogers, *T.* E.; Williams, K.; Schretzman, L. A.; Rao, S. A.; Bovy, P. R.; Tjoeng, F. S.; Lindmark, R. J.; Toth, M. V.; Zupec, M. E.; McMackins, D. E.; Adams, S. P.; Miyano, M.; Markos, C. S.; Milton, M. N.; Paulson, S.; Herin, M.; Jacqmin, P.; Nicholson, N. S.; Panzerknodle, S. G.; Haas, N. F.; Page, J. D.; Szalony, J. A.; Taite, B. B.; Salyers, A. K.; King, L. W.; Campion, J. G.; Feigen, L. P. Potent in-Vitro and in-Vivo Inhibitors of Platelet-Aggregation Based Upon the Arg-Gly-Asp Sequence of Fibrinogen - (Aminobenzamidino)Succinyl (Abas) Series of Orally-Active Fibrinogen Receptor Antagonists. *J. Med. Chem.* **1995**, *38*, 2378-2394.

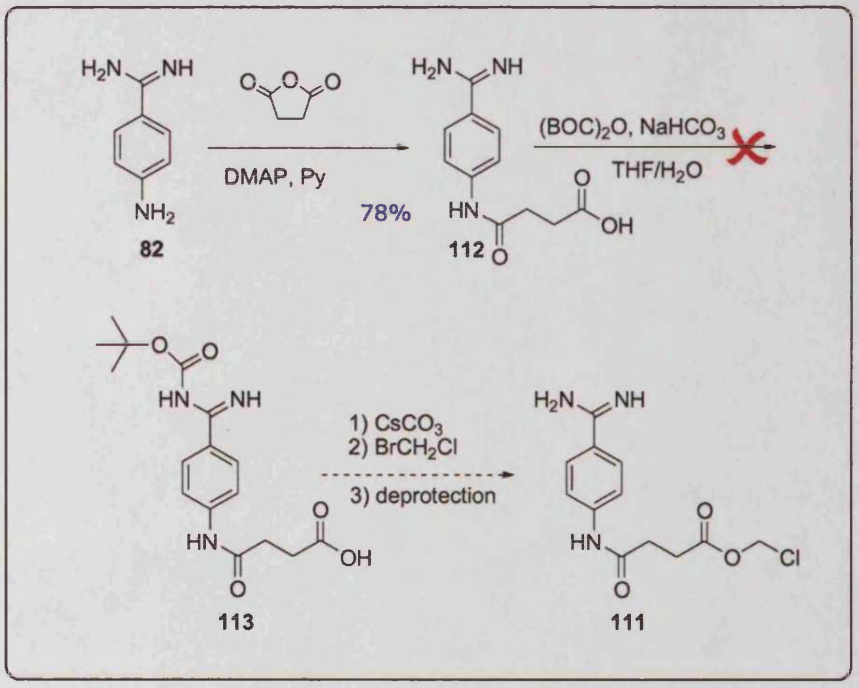

Scheme 5.8 Another strategy followed for the synthesis of **111**.

4-aminobenzamidine (**82**) was successively reacted with succinic anhydride to give amidine **112** in high yield (78%). This reaction has been previously reported in literature where the succinic anhydride was shown to react with the para-amino group[131]. It is interesting to observe that the unprotected amidine group could potentially also react with the succinic anhydride.

^{1}H-NMR of the pure compound **112** (figure 5.1) was compared with the ^{1}H-NMR of 4-amino-benzamidine (**82**), the amidine-Boc protected derivative (**83**) and a reference amidine compound from the literature[113]. The reference compound was not synthesised but its NMR data were considered for the purpose of the comparison. The results indicate that the reaction was likely to have occurred at the para-amino group to give **112**. ^{1}H-NMR of **112** shows only one peak for aromatic protons and coupling is not observed. The peak assigned to the amidine function is also of interest: two singlet peaks can be observed each corresponding to two protons; presumably the amidine is protonated giving four protons in total. The amidine reference compound also shows peaks with the same chemical shift but described as multiplet (table in figure 5.1). Compound **82** with the free amidine functionality presents similar chemical shifts for the amidine protons to those assigned to the amidine function in compound **112**. The

chemical shifts values for the amidine **82** and **112** are further downfield than **83**. This could possibly be due to the presence of the hydrochloride salt or simply due to the free amidine. All the compounds with the free aniline function, including the reference compound showed a peak around 6 ppm. The peak was not observed for **112** indicating that substitution was likely to have taken place.

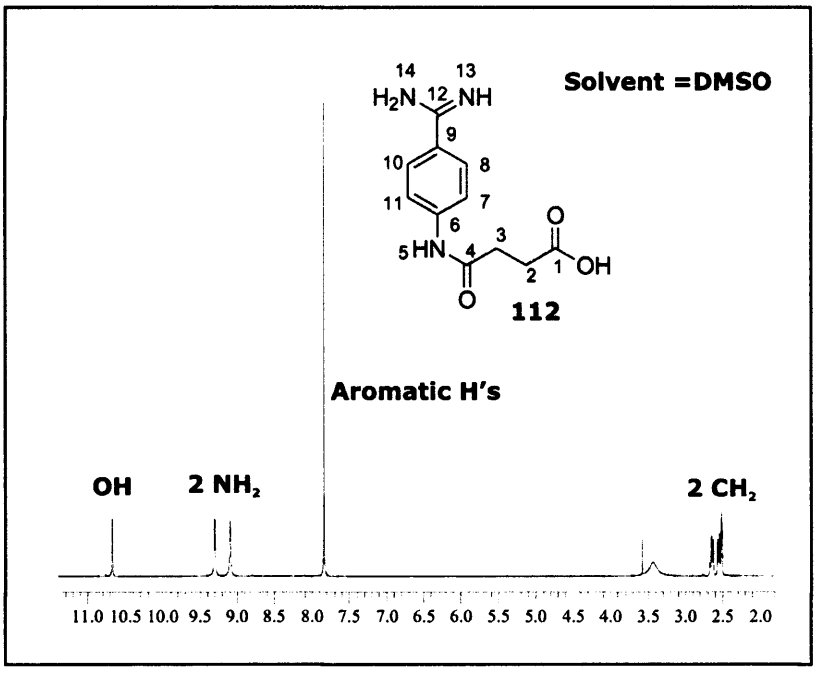

^{1}H-NMR (DMSO-d6, 300MHz)	**Compound 82** 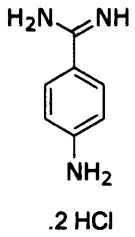 .2 HCl	**Compound 83** 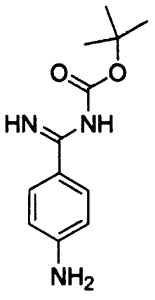	**Compound 112** 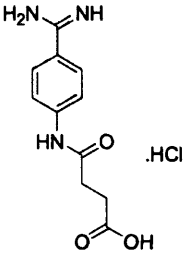 .HCl	**Reference compound*** 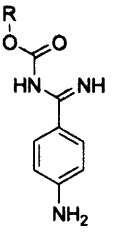 R= -CH_2Ph
Aromatic H's	**7.05** (d, 2H) and **7.84** (d, 2H)	**6.67** (d, 2H) and **7.74** (d, 2H)	**7.84** (s, 4H)	**6.51** (d, 2H) and **7.73** (d, 2H)
Amidine H's	**9.04** (s, 2H) and **9.23** (s, 2H)	**8.95** (bs, 2H)	**9.09** (s, 2H) and **9.30** (s, 2H)	**8.66** (m, 1H) and **9.11** (m, 1H)
4-amino H's	**6.27** (s, 3H)	**5.76** (s, 2H)	Not observed	**5.82** (s. 2H)

Figure 5.1 ^{1}H-NMR for benzamidine **112** and table of chemical shifts. *The reference compound was not synthesised but only considered for the purpose of comparison of the NMR data obtained.

Protection of benzamidine **112** using $(Boc)_2O$ and $NaHCO_3$ as the base was attempted. We proposed this step to prevent a possible chemical interference of the amidine function and the following coupling steps and at the same time to improve the solubility in organic solvents thus facilitating the purification. $NaHCO_3$ was used this time to avoid the cleavage of the succinamide group. TLC and MS analyses confirmed only the presence of starting material indicating that the reaction did not take place. Alternatively, since the mixture was acidified to generate the free acid for extraction it is possible that under these conditions the Boc group was hydrolysed.

In order to avoid a possible hydrolysis by the acidic conditions required for the extraction of the compound, the scheme 5.7 was further modified where the Boc protection was replaced by a protection with CbzCl using Na_2CO_3 as base. Cbz (benzyl-oxy-carbonyl) would be a suitable protecting group as it is widely used and can be easily cleaved using H_2 and a catalyst[133]. Another important feature of the Cbz group is that it is more stable under acidic conditions, compared to the Boc group.

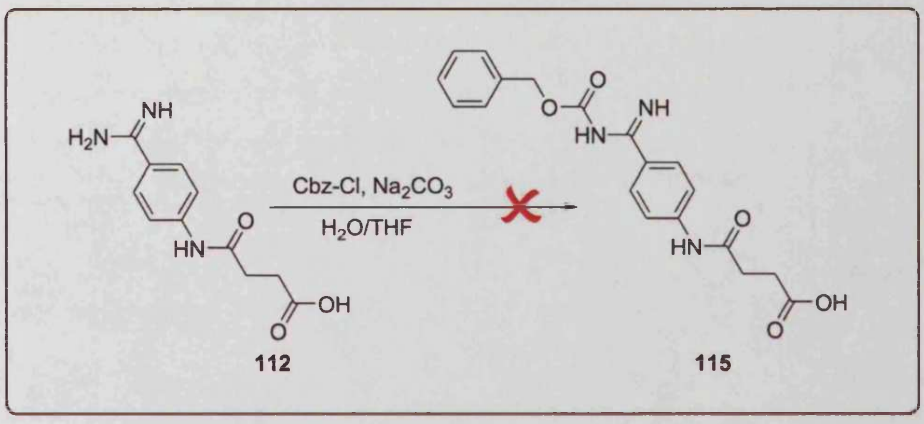

Scheme 5.9 Attempted Cbz protection of **112**.

Benzamidine **112** was reacted with Cbz-Cl. However TLC and MS analyses indicated that no reaction had occurred. The lack of reactivity of the amidine group suggested that it may not be necessary to protect this.

[133] Gomes, P.; Santos, M. I.; Trigo, M. J.; Castanheiro, R.; Moreira, R. Improved synthesis of amino acid and dipeptide chloromethyl esters using bromochloromethane. *Synth. Commun.* **2003**, *33*, 1683-1693.

Therefore we proposed that benzamidine **112** could be directly reacted with bromochloromethane in a two step synthesis according to Gomes *et al.*[133] to make the chloromethyl-ester. In the first step the caesium salt of **112** (**116**) is produced by addition of caesium carbonate until pH= 6.5 is reached. The caesium is used to increase the ionic character of the salt. The salt formed (**116**) is subsequently added to bromochloromethane in the dark using DMF as the solvent. As observed for the previous route TLC and MS analysis confirmed that the formation of the desired chloromethyl ester derivative did not occur. A variety of speculations can be made in order to explain the failure of this reaction:

1) interference or competition for reaction from the nucleophilic amidine groups;
2) failure to produce the caesium salt. In fact, the literature described the formation of the caesium salt for amino acids. It could be possible that for the benzamidine compound **112** the pH at which salt formation occurs may be different to that stated for the amino acid compounds;
3) unreactivity of compound **112** due to a possible conformation where the carboxylic group interacts with the aromatic rings via π-stacking interactions.

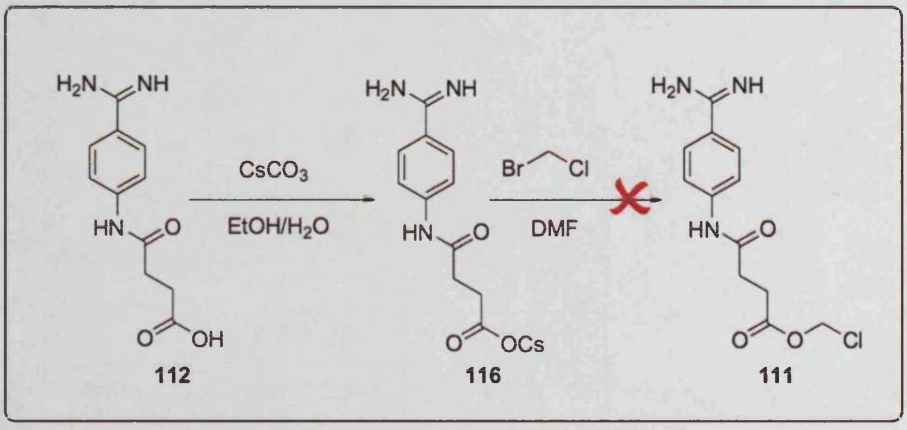

Scheme 5.10 Modification of scheme 5.8.

5.4.2 Attempted synthesis of amide pro-drugs:

Considering the failure of the different routes investigated for the synthesis of a benzamidine carrier linked prodrug, we proposed that the

succinic moiety could be linked to a trypanocidal amine directly via an amide bond and thus providing a strategy to link a P2 recognition motif to amino containing drugs. Amides, compared to esters, are less likely to be prodrugs as the amide bond is less susceptible to hydrolysis *in vivo*, with the exception of proteins. However some amides can be generated as activated amides with a higher susceptibility to enzymatic cleavage.

In order to optimise conditions to develop a suitable model for synthesis we carried out a series of procedures using benzylamine. We thought that once we found a successful method this could be extended to known drugs such as DFMO, generating an amide prodrug moiety bearing the P2 recognition motif.

The synthesis of the amide requires firstly the activation of the carboxylic acid to enable nucleophilic attack by the amine in order to form the amide. At room temperature the reaction of an amine with a carboxylic acid would simply form salts.

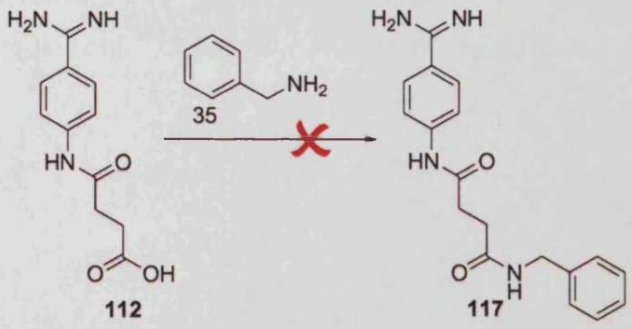

Method	Conditions used
A	DCC, DMF
B	HOBt, TBTU, DIPEA
C	DMAP, N-methylmorpholine, Isobutyl chloroformate, DIPEA
D	EDC, DMF

Scheme 5.11 Proposed routes of synthesis for amide prodrug model **117**.

Different coupling reagents were used for the generation of the amide model prodrug but the carboxylic function appeared to be highly deactivated in all the procedures used (scheme 5.11).

In the first method (method A, scheme 5.11) DCC was used. The mechanism of this reaction involves two main steps[134]. In a first step the DCC is added to the carboxylic acid to give a reactive acylating agent. This step is followed by the nucleophilic attack of the amine after which we have the formation of the amide compound and of dicyclohexylurea (scheme 5.12).

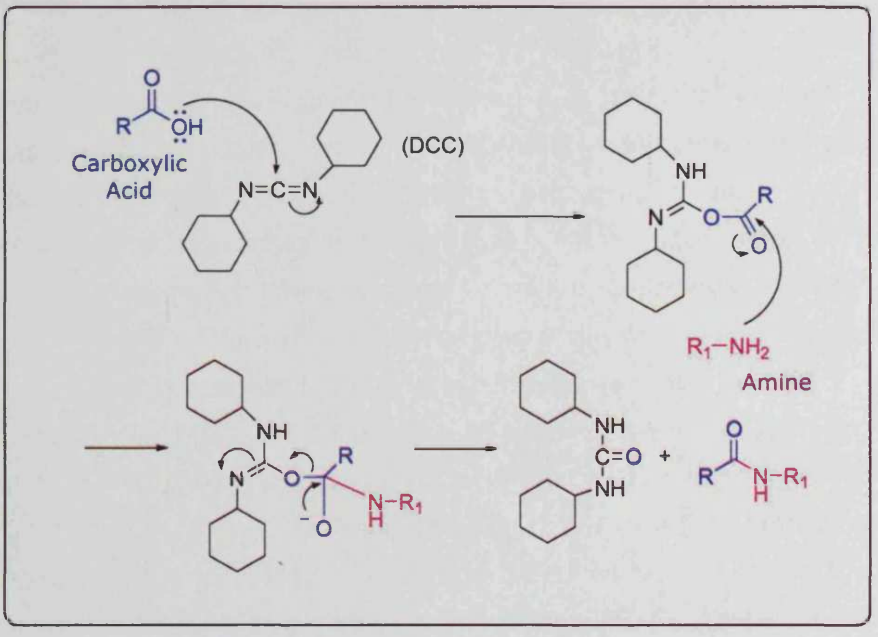

Scheme 5.12 Mechanism of amide formation activated by DCC.

TLC analysis showed only the presence of the starting material and MS analysis gave no peak corresponding to **117** but only a peak at 100% intensity corresponding to benzylamine (**35**).

The failure of the reaction could be attributed to poor reactivity of the carboxylic group or alternatively structural rearrangement of the reactive acylating agent may have occurred to give a compound that is no longer susceptible to aminolysis[134, 135]. Alternatively another reason of the

[134] McMurry. *Organic Chemistry*. 5th edition. Brooks/Cole: California, 2000

[135] Green, *T.* W. *Protective Groups in Organic Synthesis*. Wiley- Interscience: New York, 2004

failure could be accounted to possible interference in the mechanism by the benzamidine functionality.

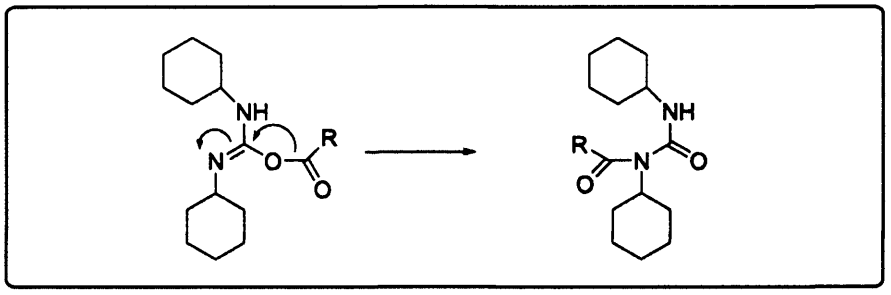

Scheme 5.13 Structural rearrangement of the reactive acylating reagent[135].

Another attempt was performed using EDC (ethyl-N,N-dimethyl-amino-propyl-carbodiimide) which is a water soluble carbodiimide. As described for the DCC reaction, the EDC mechanism proceeds through two steps (scheme 5.12). In a first step the carboxylic acid attacks the carbodiimide generating a highly reactive acylating agent. The amine subsequently attacks the acyl carbon thus generating the amide.

DMF was used as solvent since it has been described in literature that the best results are obtained when EDC is used in DMF solution[136]. However, MS and TLC analyses showed no peak corresponding to the desired product but only the starting material.

Another procedure was therefore attempted using TBTU and HOBt as coupling agents. TBTU should reacts readily with the acyl carbon to give an activated ester intermediate as shown in scheme 5.14. This coupling reagent has been found to be successful in sterically hindered couplings[136]. HOBt is used as an additive for the generation of the active acylating agent. The reaction was carried out using TBTU, HOBt and DIPEA, a tertiary base that is necessary to keep the carboxylic acid and the HOBt in the anionic form. As observed for the previous attempt the formation of the product was not observed using MS and TLC analyses.

[136] Jones, J. *Amino Acid and Peptide Synthesis.* 2nd Edition. Oxford University press: Oxford, 2002.

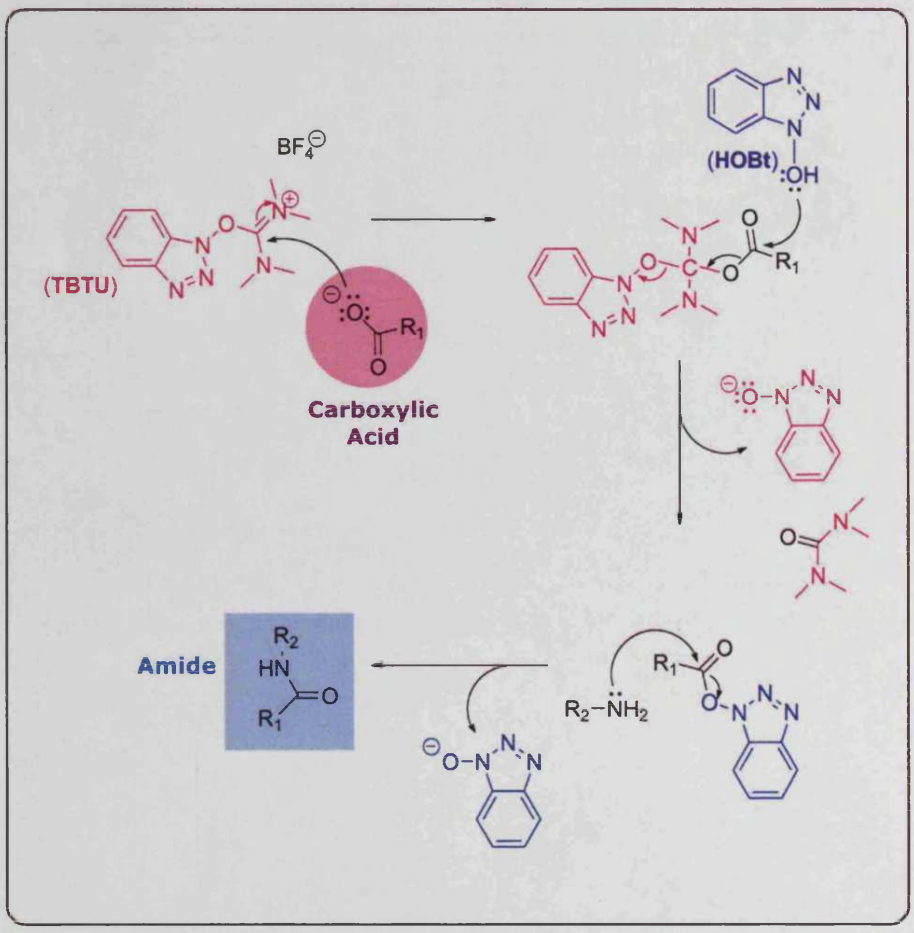

Scheme 5.14 Mechanism of amide formation using TBTU and HOBt.

The last attempt was carried out using a mixed anhydride method[131]. For the procedure N-methylmorpholine and isobutyl chloroformate were used together with DMAP as a catalyst and DIPEA as the base. The reaction was carried out carefully adding N-methylmorpholine and then isobutyl chloroformate in order to minimise its acylation with benzylamine. TLC analysis showed the formation of a complex mixture. A mixture of three components was obtained after purification with flash column chromatography. MS and NMR analyses indicated that the mixture did not contain the desired product **117**.

We proposed that the electron withdrawing effect of the benzamidine could affect the carboxylic acid function by reducing its reactivity.

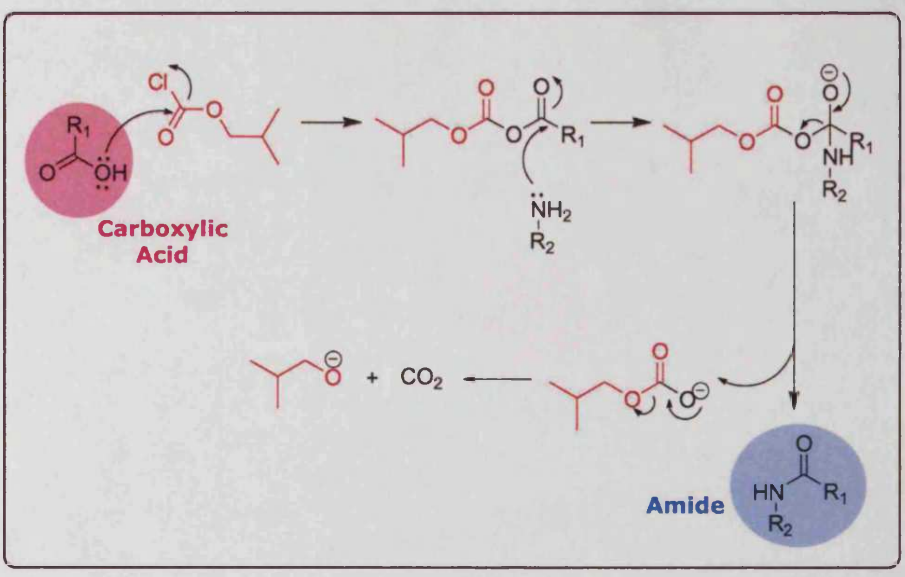

Scheme 5.15 Mechanism of amide formation using mixed anhydride method.

5.4.3 Synthesis of amide carrier linked pro-drugs: other attempts

After efforts to attach the terminal drug unit to the benzamidine P2 recognition motif we proposed another alternative route which consisted of modification of the linker. Following the procedure described in chapter 4 (scheme 4.4) with succinic anhydride, chloroacetyl-chloride (**118**) was reacted with the Boc protected benzamidine generating the amide intermediate **84**.

As an initial trypanocidal moiety we proposed to link 5-nitro-2-amino-thiazole and known drugs such as DMFO.

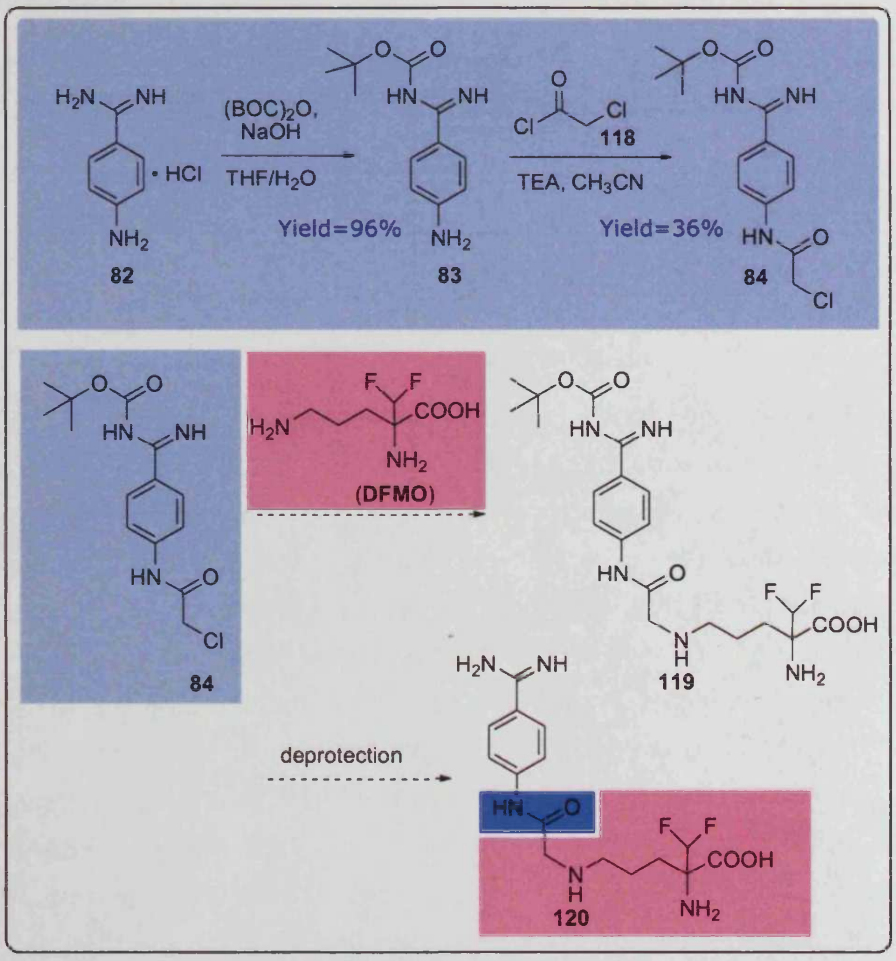

Scheme 5.16 Synthesis of chloroacetyl-amide derivative **84** and potential usage of DMFO.

In the first route the Boc protected benzamidine (**83**) was treated with chloroacetyl-chloride using TEA as base in CH_3CN giving **84** in 36% yield. The chloroacetyl-p-aminobenzamidine derivative (**84**) was then treated

with 5-nitro-2-aminothiazole (**32**) using TEA in CH_3CN under reflux. However, TLC and LRMS analyses did not show the formation of any new product (scheme 5.17).

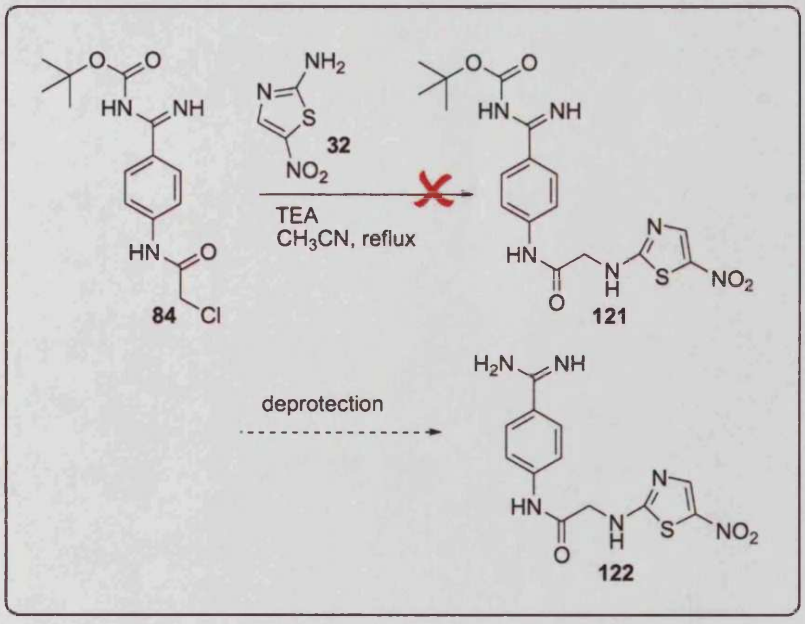

Scheme 5.17 Attempted synthesis of derivative **121**.

The low nucleophilicity of the amino group in compound **32** has been described already in chapter 3 (scheme 3.22, 3.23) and could be accounted for by the electron withdrawing effect of the nitro group transmitted through the heterocycle ring via resonance effect. However, we assumed that this amino group would be nucleophilic enough to displace an acylic chloride and we proposed an alternative route where the chloroacetyl-chloride is firstly coupled to the nitrothiazole **32** and in a second step to the protected p-amino-benzamidine (**83**).

5-nitro-2-aminothiazole (**32**) was treated with chloroacetyl-chloride (**118**) using TEA as base in CH_3CN. TLC and LRMS analyses showed the formation of a new product that was purified via column flash chromatography. NMR analysis confirmed that the new product was the desired one, obtained in 60% yield (scheme 5.18). It is interesting to observe that the amide linkage is inverted and attached to the heterocycle in contrast to the first route.

Nitrothiazole derivative **123** was subsequently treated with the Boc protected benzamidine (**83**) using the standard conditions TEA/CH_3CN. MS

and TLC analyses did not show the formation of the desired product. After purification of the mixture via column flash chromatography (DCM/MeOH =100:0 to 80:20) only the starting material was recovered.

This time the failure could be accounted for by the low nucleophilicity of the amino group, para to the amidine functionality. In fact, the electron withdrawing effect of the amidine could also be transmitted to the amino group via resonance effect through the aromatic ring.

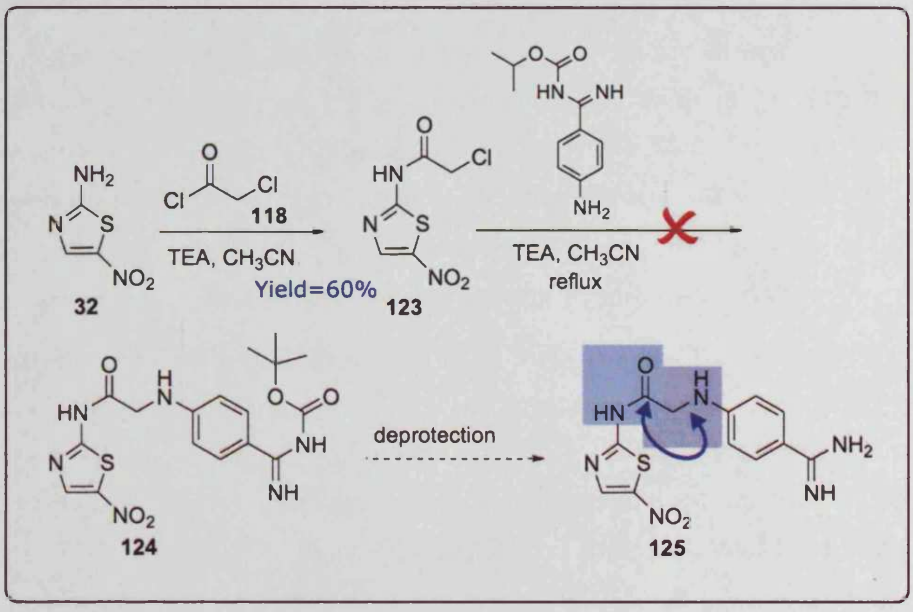

Scheme 5.18 An alternative route investigated for the synthesis of **125**.

5.5 Prodrugs bearing a melamine motif:

Considering the low reactivity of the carboxylic function linked to benzamidines, in collaboration with project student Lucy Rubij, we proposed that by replacing the benzamidine with a triazine we would expect less side reactions since the melamine functionality should be less reactive compared to the amidine.

As described for benzamidine derivatives we can design triazine carrier linked prodrugs where the linker used is represented by β-alanine (**126**) and where the drug is preferentially linked through an ester bond. Drugs bearing an hydroxyl functionality could be directly attached to the triazine structure **127** whilst either drugs bearing an amine or an hydroxyl functionality could be potentially linked to the chloro-methylester derivative **128** (scheme 5.20).

2,4-diamino-6-chlorotriazine (**4**) was reacted with β-alanine (**126**) as shown in scheme 5.19. The β-alanine was added at 80°C due to the lower susceptibility to aromatic nucleophilic substitution of the last chlorine of triazine compared to the first two. The water soluble derivative **127** was therefore precipitated by acidifying the mixture to pH=2. The free acid (**127**) was obtained as pure product in 45% yield.

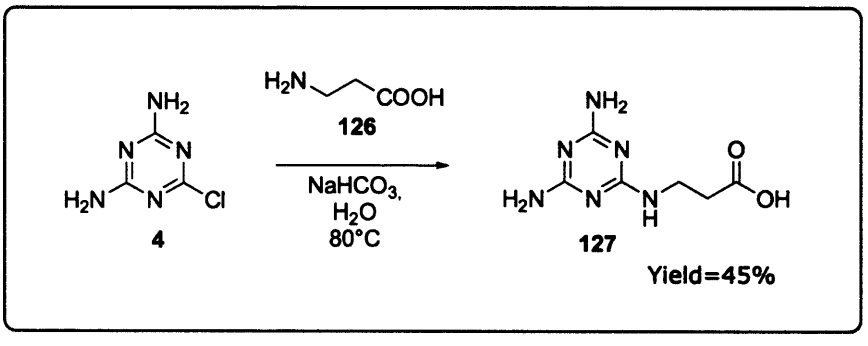

Scheme 5.19 Synthesis of 3-(4,6-diamino-[1,3,5]-triazin-2-yl)-amino-propionic acid.

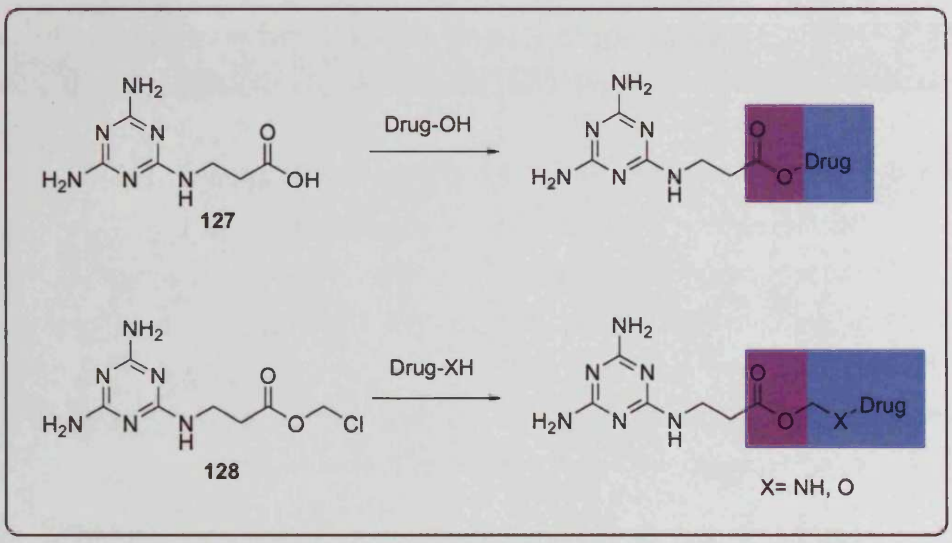

Scheme 5.20 Proposed structure of triazine carried linked prodrugs.

As attempted with the benzamidines compound **127** was reacted with bromo-chloro-methane repeating the same procedure as described in scheme 5.8 and 5.10. The synthesis of the amide prodrug model using different acylating agents was also repeated. The carboxylic acid derivative **127** was found again to be unreactive. TLC and MS analyses in both cases indicated the presence of starting material only, as was observed for the benzamidine analogue (**112**).

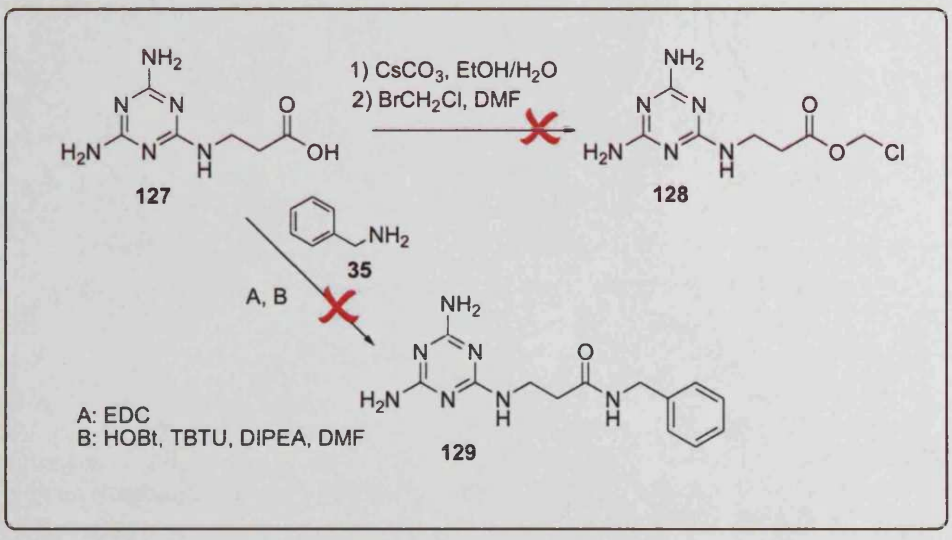

Scheme 5.21 Attempted synthesis of chloromethyl ester **128** and amide model **129**.

5.6 Alendronate: a new approach for the prodrug synthesis:

5.6.1 Bisphosphonates and their antiparasitic properties:

Bisphosphonates are a class of compounds known for their use in treating bone resorption diseases. Some of them have already been approved by the FDA for use in humans. Recently they have also been identified as potent antiparasitic agents against different species of parasites such as *Trypanosoma brucei*, *Leishmania donovani*, *Trypanosoma cruzi*, *Toxoplasma gondii* and *Plasmodium falciparum*[137, 138].

Bisphosphonate Compound	Name	Bisphosphonate Compound	Name
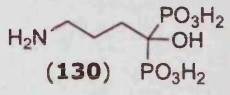 (130)	**Alendronate** (4-amino-1-hydroxybutane-1,1-bisphosphonate)	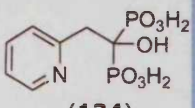 (134)	**o-Risedronate** 2-(3-pyridyl)-1-hydroxyethane-1,1-bisphosphonate
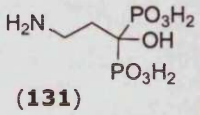 (131)	**Pamidronate** (3-amino-1-hydroxypropane-1,1-bisphosphonate)	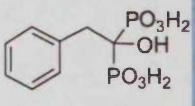 (135)	2-phenyl-hydroxyethane-1,1-bisphosphonate
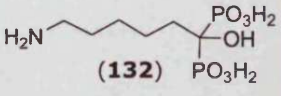 (132)	**Neridronate** (5-amino-1-hydroxyhexane-1,1-bisphosphonate)	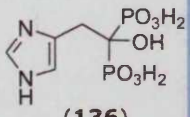 (136)	2-(4-imidazole)-1-hydroxyethane-1,1-bisphosphonate
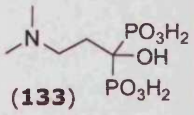 (133)	**Olpadronate** 3-(N,N-dimethyl)-amino-1-propane-1,1-bisphosphonate)	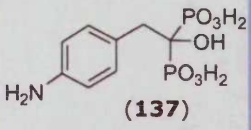 (137)	2-(4-aminophenyl)-hydroxyethane-1,1-bisphosphonate

Table 5.1 Structure of some bisphosphonates screened for antiparasitic activity.

[137] Martin, M. B.; Sanders, J. M.; Kendrick, H.; de Luca-Fradley, K.; Lewis, J. C.; Grimley, J. S.; Van Brussel, E. M.; Olsen, J. R.; Meints, G. A.; Burzynska, A.; Kafarski, P.; Croft, S. L.; Oldfield, E. Activity of bisphosphonates against *Trypanosoma brucei rhodesiense*. *J. Med. Chem.* **2002**, *45*, 2904-2914.

[138] Martin, M. B.; Grimley, J. S.; Lewis, J. C.; Heath, H. *T.*; Bailey, B. N.; Kendrick, H.; Yardley, V.; Caldera, A.; Lira, R.; Urbina, J. A.; Moreno, S. N. J.; Docampo, R.; Croft, S. L.; Oldfield, E. Bisphosphonates inhibit the growth of *Trypanosoma brucei*, *Trypanosoma cruzi*, Leishmania *donovani*, Toxoplasma gondii, and Plasmodium falciparum: A potential route to chemotherapy. *J. Med. Chem.* **2001**, *44*, 909-916.

Bisphosphonates such as alendronate, palmidronate and risendronate (Table 5.1) are structurally similar to a pyrophosphate except for the presence of an important difference: the oxygen bridge has been replaced with a C thus leading to a non hydrolysable structure[138]. This structure acts by inhibiting a key enzyme of the mevalonate-isoprenoid biosynthetic pathway[137].

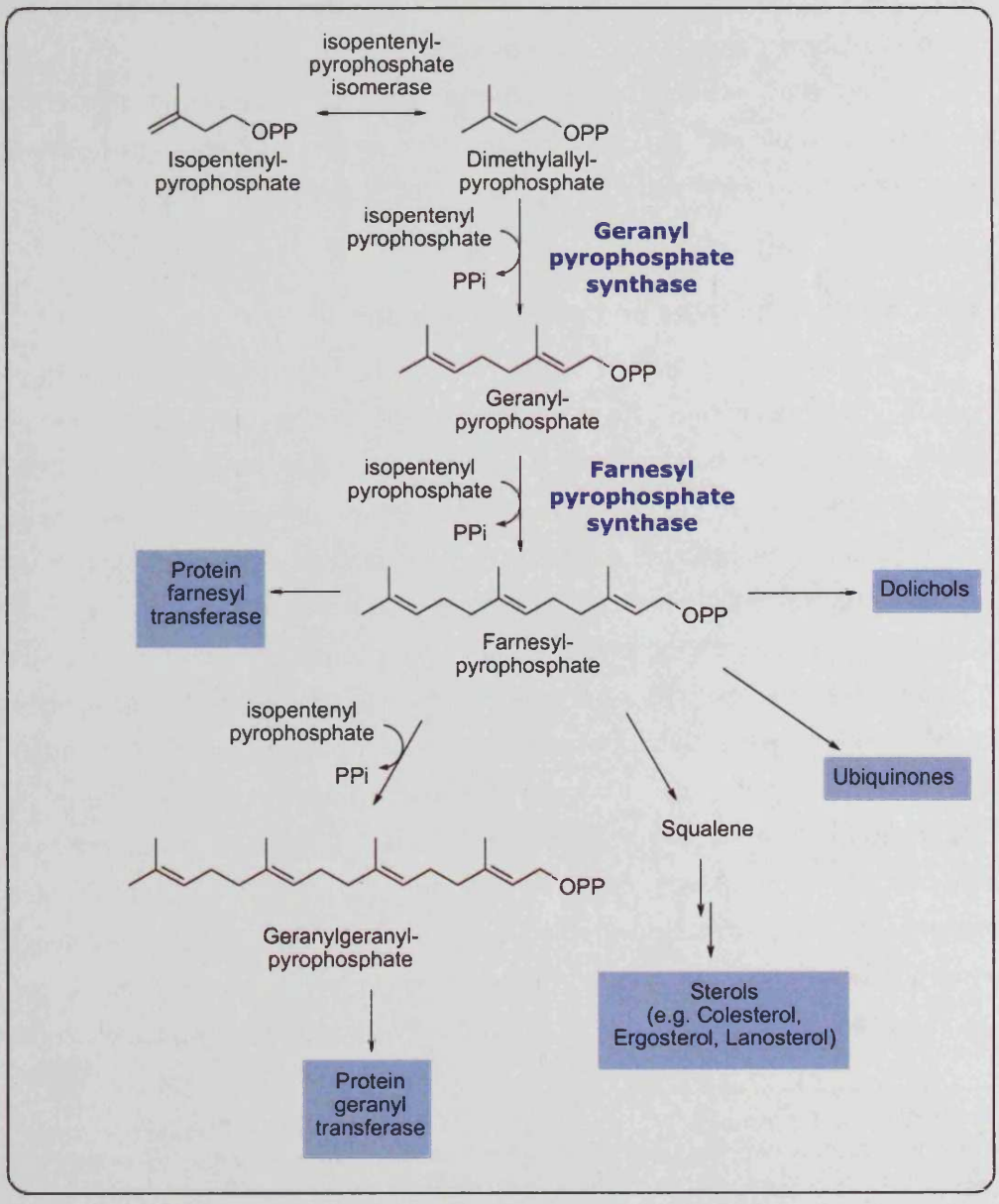

Scheme 5.22 The mevalonate/isoprene pathway and biosynthesis of isoprenoids and sterols.

Recent studies have shown that nitrogen-containing bisphosphonates, such as the ones previously mentioned, are competitive

inhibitors of farnesyl-pyrophosphate synthase (FPPS, scheme 5.22). This enzyme catalyses the condensation of dimethylallyl pyrophosphate (DMAPP) with isopentenyl pyrophosphate (scheme 5.22) to give geranyl pyrophosphate which subsequently condenses with another molecule of isopentenyl pyrophosphate (IPP) to give farnesyl pyrophosphate. This is an important intermediate that can be used for the synthesis of other important isoprenoids (some are essential for the *Trypanosoma brucei*), sterols (in some parasites) or ubiquinones.

Martin *et al.* have proposed that the potent nitrogen containing bisphosphonates act as (aza)-carbocation pyrophosphate intermediate analogues of the geranylpyrophosphate carbocation[139,140].

5.6.2 Bisphosphonates and prodrug design:

The interesting feature of the bisphosphonates that we proposed to exploit is the presence of the two phosphonate groups that could be ideally linked to P2 recognition units such as benzamidine and melamine in order to selectivity target the parasite. The design of these carrier linked prodrugs is represented in scheme 5.23. We proposed the bisphosphonate alendronate central core of the structure with a P2 recognition unit that could be linked directly or through a linker to the phosphonate. The other phosphonate could be either left free or attached to another P2 recognition motif. Alternatively this phosphonate could be also linked to another known trypanocidal drug. Considering the previously discussed Wermuth classification[128] of the prodrugs, this last bisphosphonate prodrug proposed, to some extent, could be considered a mutual prodrug. In fact not only the drug attached will exert a trypanocidal activity but this will act synergistically with the trypanocidal effect of the bisphosphonate. Some bisphosphonates showed good *in vitro* activity against *Trypanosoma brucei*

[139] Martin, M. B.; Arnold, W.; Heath, H. *T.*; Urbina, J. A.; Oldfield, E. Nitrogen-containing bisphosphonates as carbocation transition state analogs for isoprenoid biosynthesis. *Biochem. Biophys. Res. Commun.* **1999**, *263*, 754-758.

[140] Hosfield, D. J.; Zhang, Y. M.; Dougan, D. R.; Broun, A.; Tari, L. W.; Swanson, R. V.; Finn, J. Structural basis for bisphosphonate-mediated inhibition of isoprenoid biosynthesis. *J. Biol. Chem.* **2004**, *279*, 8526-8529.

rhodesiense: o-risendronate (**134**, table 5.1), for example, showed an IC_{50}= 220 nM, Olpadronate (**133**, table 5.1) an IC_{50}= 5.4 μM.

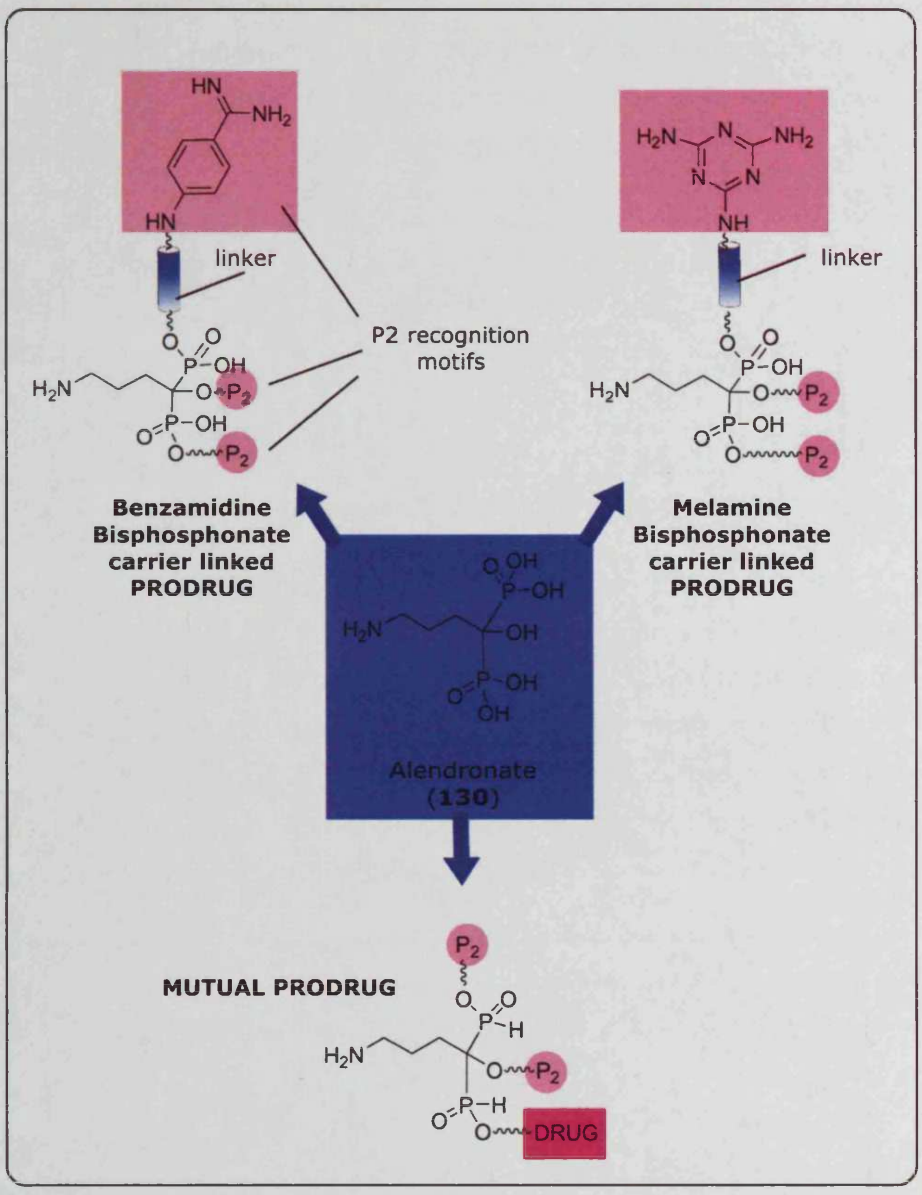

Scheme 5.23 Design of bisphosphonate carrier linked prodrugs.

Another important feature of these prodrugs is that by altering the structure of the bisphosphonate or the linker we expect to obtain a wide range of compounds with different solubility in water and in organic solvents.

This exciting new field has been taken into consideration just recently and will be a part of our future work. We have started to

investigate an efficient procedure for the synthesis of the bisphosphonate structure. Alendronate has been considered because its synthesis has been already described in different works by Kieczykowski *et al.*[141, 142]. The only method reported for the preparation of 4-amino-1-hydroxybutylidene-1,1-bisphosphonic acid (**130**, alendronate), reacts a 4-aminobutyric acid (GABA) with phosphorus trichloride and phosphorous acid.

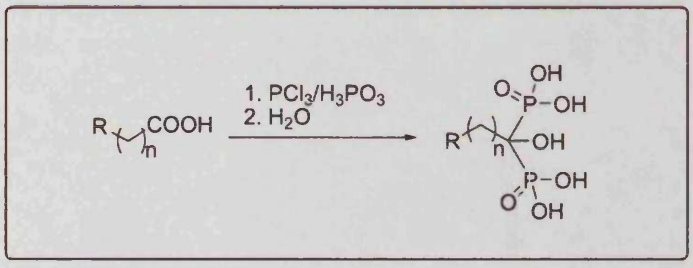

Scheme 5.24 General method of preparation of 1,1-bisphosphonates.

The procedure described was applied for the preparation of alendronate (**103**, scheme 5.25). The main step for the synthesis can be summarised as follow:

1) reaction of 4-aminobutyric acid (**138**) with a mixture of H_3PO_3 and PCl_3 in the presence of methansulfonic acid;
2) hydrolysis of the mixture maintaining the pH in the range of 4-10;
3) isolation of the product as bisphosphonic acid or its salt form.

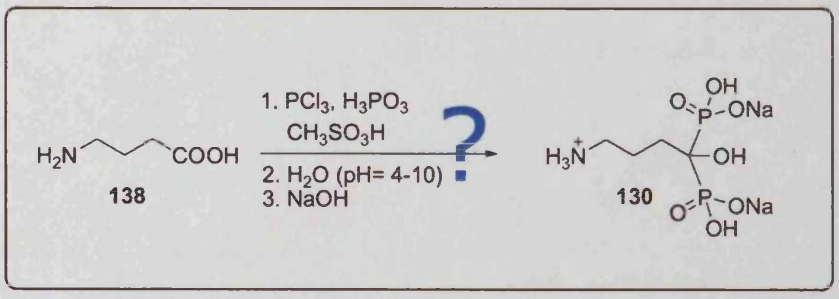

Scheme 5.25 Attempted preparation of alendronate (**130**).

[141] Kieczykowski, G. R.; Jobson, R. B.; Melillo, D. G.; Reinhold, D. F.; Grenda, V. J.; Shinkai, I. Preparation of (4-amino-1-hydroxybutylidene)bisphosphonic acid sodium salt, MK-217 (alendronate sodium). An improved procedure for the preparation of 1-hydroxy-1,1-bisphosphonic acids. *J. Org. Chem.* **1995**, *60*, 8310-8312.

[142] Kieczykowski, G. R. Process for preparing 4-amino-1-hydroxybutylidene-1,1-bisphosphonic acid (ABP) or salts thereof; Merck & Co., Inc., Rahway, N.J.: USA, Patent N. 5,019,651, **1991**; pp 1-6.

The outcome of the reaction attempted in these labs was unclear. MS analysis and ^{1}H-NMR/^{31}P-NMR analyses indicated that the formation of the product did not take place. One of the main problems we encountered was the difficulty to reproduce some conditions described in literature such as the circulation of brine at -10 °C through a reflux condenser for an overnight time[142]. Different variations of the procedure mentioned have been described[141] but were not investigated due to a constraint of time.

Another issue that should be taken into account is the lack of a known mechanism of reaction that would help us to understand the reaction procedure.

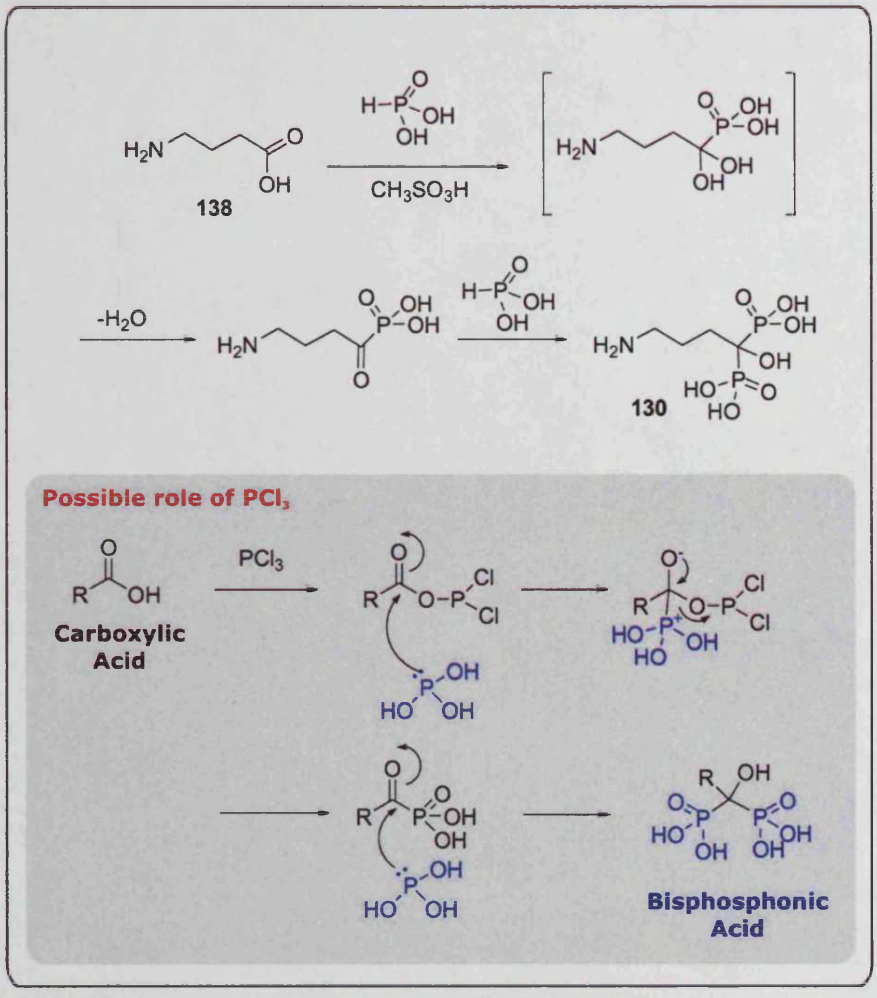

Scheme 5.26 Possible mechanism proposed for the conversion of the carboxylic acid to a 1,1-bisphosphonic acid.

We proposed that the process may be initiated by addition of the P-H bond of the H_3PO_3 to the carbonyl group as shown in scheme 5.26 but this is only a speculation and the mechanism is likely to be far more complex as the PCl_3, involved in the reaction, plays an important role that is still unclear. PCl_3 could react with the carboxylic acid generating an intermediate where the carbonyl carbon can be further attacked by H_3PO_3 thus generating the first phosphonic bond. The second phosphonic bond could be generated by the same mechanism generating the bisphosphonic acid (scheme 5.26).

6. Biological results:

Selected triazine and benzamidine derivatives presented in chapter 3 and 4 have been evaluated for their trypanocidal activity and will be discussed in this chapter. Some compounds prepared showed similar *in vitro* activities to melarsoprol, the principal drug used against late-stage HAT, with 50% growth inhibitory concentrations in the submicromolar range. Selected compounds were also evaluated for their *in vivo* activities in rodent models infected with *Trypanosoma brucei brucei* and *Trypanosoma brucei rhodesiense* showing pronounced activity and in two cases were curative.

Selected compounds were also tested against other Trypanosomatid pathogens such as *Leishmania donovani* and *Trypanosoma cruzi* and showed significant *in vitro* activities.

Part of the work discussed in this chapter has been recently published in Antimicrobial Agents and Chemotherapy (Stewart, M. L.; Bueno, G. J.; Baliani, A.; Klenke, B.; Brun, R.; Brock, J. M.; Gilbert, I. H.; Barrett, M. P. Trypanocidal activity of melamine-based nitroheterocycles. **2004**, *48*, 1733-1738)[63] and in Journal of Medicinal Chemistry (Baliani, A.; Bueno, G. J.; Stewart, M. L.; Yardley, V.; Brun, R.; Barrett, M. P.; Gilbert, I. H. Design and synthesis of a series of melamine-based nitroheterocycles with activity against trypanosomatid parasites. **2005**, *48*, 5570-5579)[44].

All the *in vitro* studies were carried out at the Institute of Biomedical and Life Sciences (Division of Infection & Immunity) in Glasgow and at the London School of Hygiene and Tropical Medicine. The *in vivo* studies were

carried out at the Swiss Tropical Institute in Basel. The genotoxicity studies were carried out at Dipartimento di Genetica Antropologia Evoluzione, Parma (Italy).

6.1 Triazine derivatives: Biology

6.1.1 Affinity for the P2 transporter:

In order to determine the ability of the compounds to interact with the P2 transporter, the K_i values against the P2-dependent adenosine uptake were determined. The K_i value gives an approximation of the affinity of the P2 transporter for the compounds. This value was obtained by measuring the ability of the compound to antagonise the uptake of radiolabeled adenosine[35]. Figure 6.1 shows typical inhibition curves that can be observed in an experiment using [^{3}H]-adenosine.

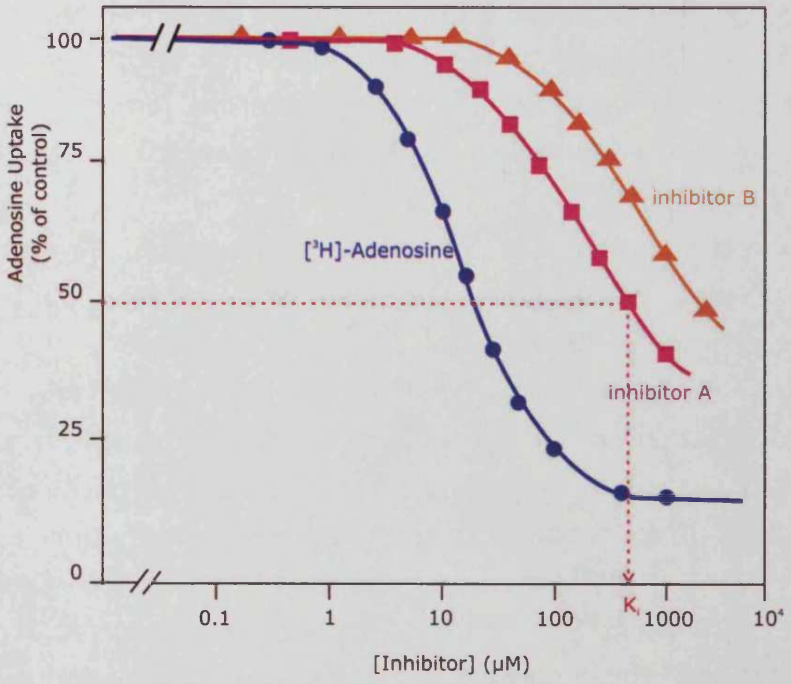

Figure 6.1 Transport assay of [^{3}H]-adenosine: the graph was drawn as a model to facilitate the understanding.

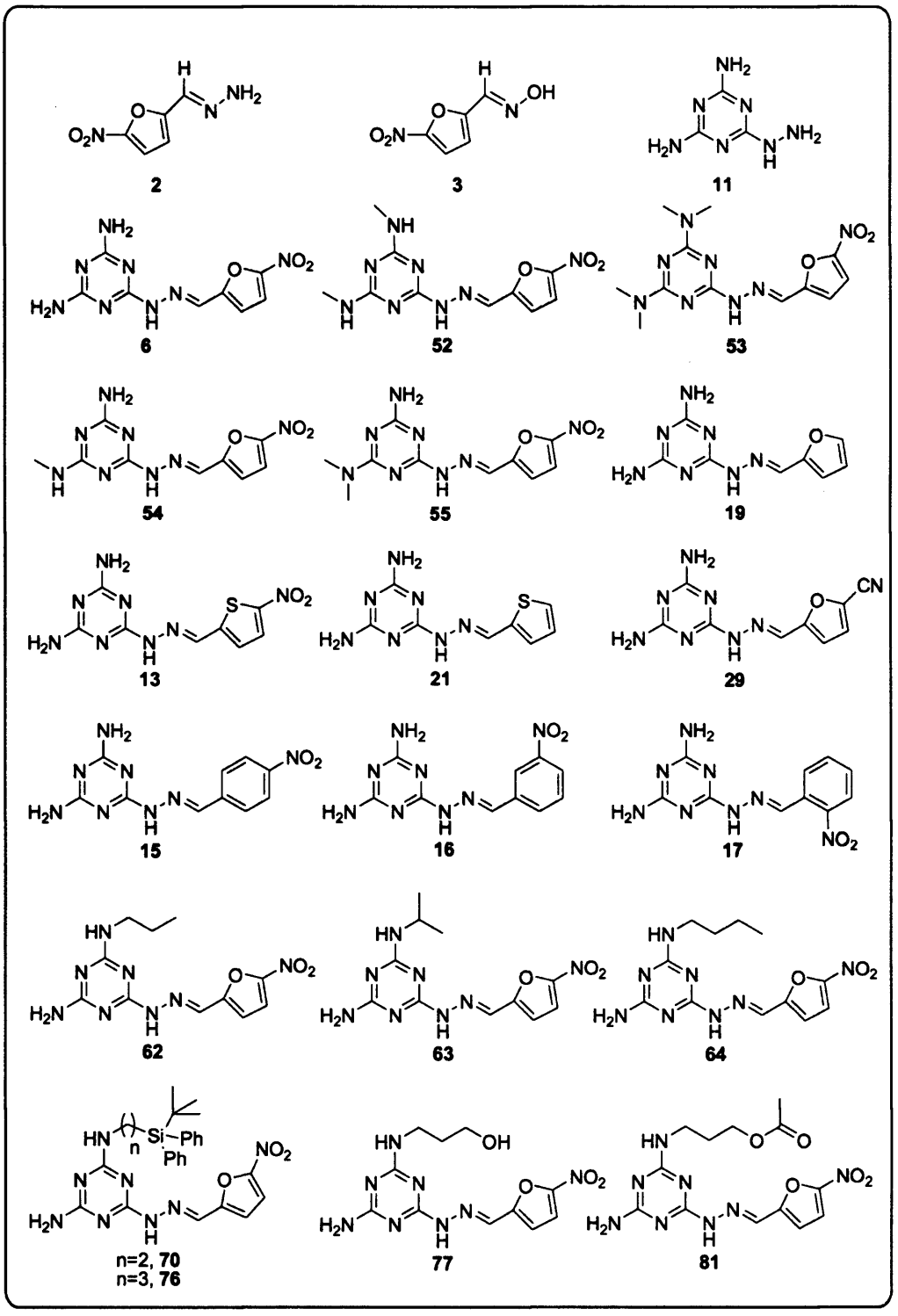

Scheme 6.1 Structure of compounds assayed and shown in table 6.1.

The IC_{50} values of the inhibitors can be simply obtained from the curves by reading the concentration of the inhibitor that inhibits the uptake of the 50% of radiolabelled adenosine. The experiment does not measure

the uptake of compounds through the P2 transporter but only gives a measure of the affinity of compounds for the P2 transporter. The compounds may be substrates themselves, or alternatively they may inhibit uptake of radiolabelled adenosine by inhibiting the P2 transporter.

As previously mentioned, the main routes for the uptake of adenosines in *T. brucei* are represented by the P1 and P2 transporter. The evaluation of the IC_{50} values for the P2 transporter without interference by the P1 transporter can be easily achieved by conducting the experiment with a large excess of inosine which saturates the P1 transporter.

			IC_{50} (μM)			
Compd	**MW**	***P2 uptake IC_{50} (μM)[a]***	***T.b.brucei AT1 wild type***	***T.brucei brucei AT1 knockout[b]***	***T. brucei rhodesiense***	***L6 cells[c]***
11	141.1	11.9	200	200	ND	ND
6	264.2	22.9	0.23	0.38	0.025	183
52	292.2	4.6	11.9	14.8	0.25	18.8
52*	292.2	ND	ND	ND	0.01	44.1
53	320.3	129	0.2	0.3	0.003	18.7
54	278.2	ND	0.13	0.06	0.018	48.9
55	292.2	ND	5.36	3.09	0.053	109.5
19	216.2	15.9	16.5	29.3	12.9	400
29	244.2	ND	ND	ND	46.27	ND
13	280.2	1.9	0.85	1.52	0.24	11.8
21	235.3	4.9	89	170	10.2	78.2
15	274.2	ND	75	75	29.9	ND
16	274.2	ND	75	75	52.88	ND
17	274.2	ND	75	75	36.47	ND
62	306.3	ND	ND	ND	0.021	17.3
63	306.3	ND	ND	ND	0.065	5.45
64	320.3	ND	ND	ND	0.023	18.32
70	546.6	ND	ND	ND	0.16	4.45
76	560.7	ND	ND	ND	0.037	7.38
77	322.3	ND	ND	ND	0.049	83.77
81	364.3	ND	ND	ND	0.048	74.65
2	155.1	404	1.18	1.26	2.3	20
3	156.1	300	23.5	13.7	2.3	20
Melarsoprol		1.2	0.053	0.12	0.006	7.8
Nifurtimox		ND	5.6	ND	1.5	68

a: Inhibition of adenosine uptake by the P2 transporter in *T. brucei brucei* 427. **b**: *T. brucei brucei AT1* knockout is a mutant with a non functional P2 transporter. **c**: L6 cells are rat skeletal myoblasts and are used as a measure of cytotoxicity to mammalian cells. **ND**: not determined. **52*** is compound 52 recrystallised and achieved with a better purity grade.

Table 6.1 *In vitro* activities of compounds against the P2 transporter, Blood stream *T. brucei*, and mammalian cells as a measure of toxicity.

From the results obtained it is clear that a melamine group is necessary for the affinity with the P2 transporter. Compounds without a

melamine group such as compounds **2** and **3** have relatively low affinity for the P2 transporter (IC_{50}= 404 μM and IC_{50}= 300 μM respectively). Compound **53** in which all the nitrogens on the melamine ring were methylated showed also a relatively low affinity (IC_{50} = 129 μM). For the other compounds evaluated, the IC_{50} values were all within about a log range of each other and were of a similar order as melarsoprol. The nitro heterocycle moiety was found to have a negligible effect on the affinity for the P2 transporter. The removal of the nitro group did not give any significant change of the affinity (compare **6** and **19** and compare **13** and **21**) whilst the replacement of the oxygen with a sulfur (compare **6** and **13** and compare **19** and **21**) gave a small increase in affinity. These results suggest that the melamine ring has a main role for the affinity with the P2 transporter compared to the nitroheterocycle unit. This can be observed in compound **11**, where the nitrofuran ring is absent and the affinity for the P2 transporter is relatively high (IC_{50} = 11.9 μM) compared to compound **6** with a nitrofuran ring (IC_{50} = 22.9 μM). These results are consistent with previously published literature findings[57, 144].

[144] Maeser, P.; Luescher, A.; Kaminsky, R. Drug transport and drug resistance in African Trypanosomes. *Drug Resistance Updates* **2003**, *362*, 281-290.

6.1.2 *In vitro* activities against *T. brucei*:

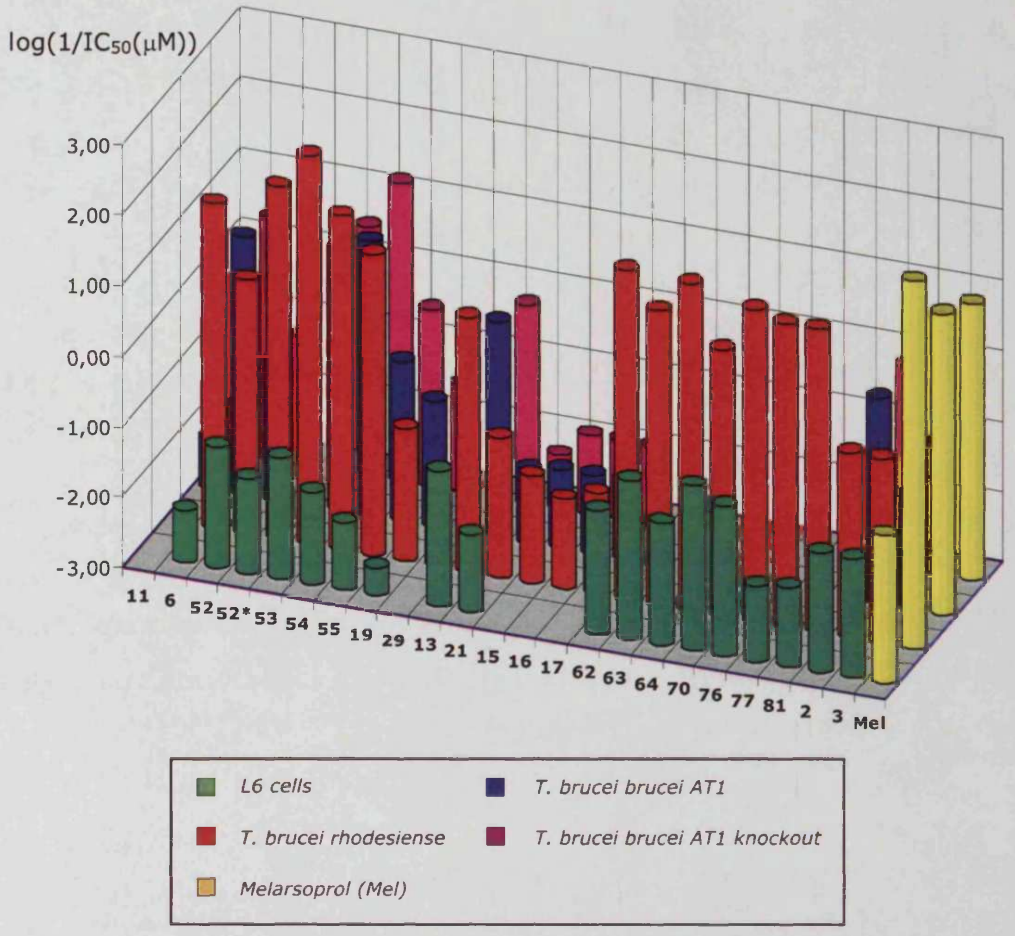

Figure 6.2 Activities of some selected triazines against *T. brucei* species. Standard drug, Mel. = Melarsoprol.

Table 6.1 shows the activities in μM of the compounds tested, expressed as IC_{50}, against *T. brucei brucei rhodesiense* and *T. brucei brucei*. In this last strain the activities were evaluated for the AT1 wild type and for the AT1 knockout. Together with these values are also represented the IC_{50} values for the P2 uptake and the L6 cells as a measure of cytotoxicity to mammalian cells.

Compounds were evaluated for their *in vitro* activities against *T. brucei* lines. In this study, in order to evaluate the mode of action and the role of the P2 transporter, we decided to compare the *T. brucei brucei* AT1 wild type with a *T. brucei* AT1 knockout mode. Compounds were also tested against *T. brucei rhodesiense*, the human pathogen, which is the causative agent of the acute HAT and against L6 cells. The L6 cells are rat

skeletal myoblasts and are usually used as a measure of cytotoxicity to mammalian cells. The *in vitro* results obtained for these compounds (scheme 6.1) are summarised in table 6.1 together with the P2 affinity previously described. The *in vitro* results have also been represented graphically (figure 6.2), where the activities are shown as $\log(1/IC_{50})$ so that the higher cylinders will represent the compounds with lower IC_{50} (higher activity) whilst the lower will represent compounds with higher IC_{50}.

Comparing the results for compounds against the wild type and the P2 knockout *T. brucei brucei* we can observe only a small reduction in activity for the knockout line. Some of our compounds as well as melarsoprol are 2 fold less active in the knockout line. However, the small difference of activity observed suggests that there are other routes other than the P2 transporter for the uptake of these compounds.

The activities of some compounds against *T. brucei brucei* were found to be lower than that observed for melarsoprol (IC_{50}= 53 nM) but still in the nanomolar range (**6**, IC_{50}= 230 nM; **53**, IC_{50}= 200 nM; **54**, IC_{50}=130 nM; **13**, IC_{50}=850 nM).

The activities obtained against the *T. brucei rhodesiense* line for a significant number of compounds were higher than that observed for the *T. brucei brucei* line. The difference probably reflects a range of activities against different strains of the *T. brucei* trypanosomes rather than a particular difference between non human pathogenic *T. brucei brucei* line and the human infectious *T. brucei rhodesiense* line. Against the *T. brucei rhodesiense* line melarsoprol showed an IC_{50} of 6 nM while **53** showed an IC_{50} of 3 nM. The IC_{50} values for a large number of the compounds were also in the nanomolar range (**6**, **52-55**, **13**, **62-64**, **70**, **76**, **77**, **81**).

By comparing the activities against *T. brucei rhodesiense* we proposed the following structure-activity relationships:

1. The absence of a melamine group in a compound is associated with a weak *in vitro* activity and also a weak selectivity to the mammalian L6 cells. Compound **2**, where only the nitrofuran moiety is retained, showed an IC_{50}=2.3 μM;
2. The complete removal of the nitrofuran moiety led to a loss of activity. Compound **11** showed a relatively high selectivity for the

P2 transporter but not show any activity against the *T. brucei brucei* line (IC_{50}=200 μM);

3. Compounds with a nitrofuran ring joined to a melamine ring showed potent *in vitro* activity (<53 nM observed for **6**, **52-55**, **13**, **62-64**, **70**, **76**, **77**, **81**);
4. Replacement of the oxygen with a sulfur led to a 10-fold loss in activity. A small increase in toxicity to L6 cells was also observed (compare **6** (IC_{50}=25 nM) with **13** (IC_{50}=240 nM));
5. The replacement of the nitro group by an hydrogen led to a significant loss of activity (compare **6** (IC_{50}=25 nM) with **19** (IC_{50}=12.9 μM) and compare **13** (IC_{50}=240 nM) and **21** (IC_{50}=10.2 μM);
6. The replacement of the nitro group with another electron-withdrawing group such as the nitrile group led to a loss of activity (**29**, IC_{50}=46.27 μM). This results suggests that more than an electron withdrawing effect is necessary for the activity;
7. The replacement of the nitrofuran ring with a non heterocycle structure such as nitrophenol also led to a loss of activity (**15-17**, IC_{50}> 30μM). Therefore the nitro group linked to an heterocycle moiety was found to be of crucial importance for the activity. The redox potential values associated with these structures could be a possible explanation to what observed and therefore need to be further investigated;
8. The nanomolar activity is maintained when the amino groups of the melamine ring are replaced with a different number and combination of methyl groups (**52-55**, IC_{50}<53nm) or with bulkier alkylic groups (**62**, IC_{50}=21 nm; **63**, IC_{50}=65 nm; **64**, IC_{50}=23 nm);
9. The introduction of functionalised chains in the melamine moiety such as 3-hydroxypropyl-, 3-acetoxypropyl- also maintained the activity in the nanomolar range (**77**, IC_{50}=49 nm; **81**, IC_{50}=48 nm).

Another important observation is that some nitro heterocycles (**6**, **54**, **55**) with relatively high *in vitro* activities were less toxic against mammalian cells than melarsoprol.

6.1.3 *In vitro* activities against *Trypanosoma cruzi* and *Leishmania donovani*:

Table 6.2 shows the activities (expressed as IC_{50} (μM)) of the compounds tested against *T. cruzi* and *L. donovani* (axenic amastigotes).

Table 6.2 *In vitro* activities against *T. cruzi* and *L. donovani*.

Compound	MW	IC_{50} [μM]	
		T.cruzi	*Leishmania donovani*
11	141.1	ND	ND
6	264.2	2.1	12.5
52	292.2	0.24	3.14
53	320.3	0.38	tox
54	278.2	0.39	0.75
55	292.2	0.29	tox
19	216.2	400	tox
29	244.2	122	ND
13	280.2	2.6	tox
21	235.3	85.84	tox
15	274.2	91.54	ND
16	274.2	328	ND
17	274.2	328	ND
62	306.3	1.06	ND
63	306.3	64.81	ND
64	320.3	1.17	ND
70	546.6	0.37	ND
76	560.7	89.2	ND
77	322.3	70.43	ND
81	364.3	36.73	ND
2	155.1	ND	tox
3	156.1	ND	tox
melarsoprol		0.006	7.8
Nifurtimox		1.5	68

Standards: For *T. cruzi*, Benznidazole, IC_{50}=1.435 μM; *L. donovani*, Miltefosine, IC_{50}= 1.16 μM: tox= toxic to macrophages thus precluding measurement of Leishmanicidal activity.

After the observation that our compounds retained their activities against the *T. brucei brucei* knockout line we proposed that together with the P2 transporter other routes were probably involved in the transport. Therefore we decided to test our compounds against parasites related to the *T. brucei* species such as *Trypanosoma cruzi* and *Leishmania donovani* (axenic amastigotes). In *T. cruzi*, the compounds were tested on intracellular amastigotes.

The activities obtained are shown in Table 6.2 and in figure 6.3 where they are compared with the activities of melarsoprol and nifurtimox.

Table 6.2 shows that except compound **54** (IC_{50}=0.75 μM), none of the compounds tested against *L. donovani* showed sub-micromolar activities *in vitro*. Moreover, some compounds were found to be toxic in macrophages and therefore the activity against *Leishmania* was precluded.

In vitro activities in sub-micromolar range against *T. cruzi* line were observed for compounds **52-55** (IC_{50}= 0.24, 0.38, 0.39, 0.29 μM respectively) and for compound **70** (IC_{50}= 0.37 μM).

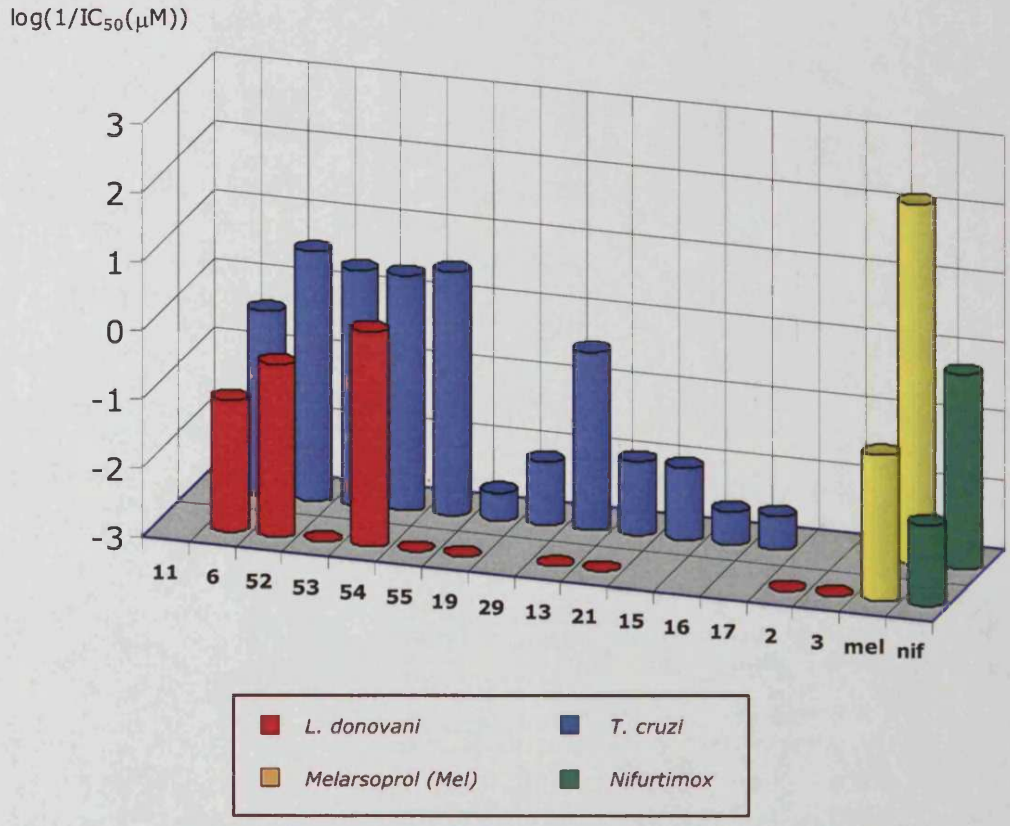

Figure 6.3 *In vitro* activities of some selected triazines against *T. cruzi* and *L. donovani*. The yellow cylinders represent melarsoprol (Mel) whilst the green cylinders represent nifurtimox (Nif).

6.1.4 *In vivo* activities in rodent models of infection:

Table 6.3 *In vivo* activities against *T. brucei brucei* model and *T. brucei rhodesiense* model[a].

Compound	Dose mg/Kg	*T. brucei brucei* (STIB 795 model)		*T. b. rhodesiense* (STIB 900 model)	
		Cured / Infected	Survival average (days)	Cured / Infected	Survival average (days)
6	4 x 20 i.p.	4/4	>60	1/4	35.25
53	4 x 20 i.p.	ND	ND	0/4	7.25
52	4 x 20 i.p.	0/4	5.25	ND	ND
54	4 x 20 i.p.	4/4	>60	2/4	>38.5
55	4 x 20 i.p.	0/4	18.3	ND	ND
Control (avrg)		0/4	7	0/4	6.5
Melarsoprol	4 x 1 i.p.	2/4	>60	0/4	21.25
	4 x 8 i.p.	ND	ND	4/4	>60
Pentamidine	4 x 5 i.p.	4/4	>60	ND	ND
	4 x 20	ND	ND	0/4	42.75

[a]The control represents the average of the controls for each experiments performed.

Selected compounds were evaluated in several rodent models of trypanosome infections. The compounds were initially examined in rodent models infected with *T. brucei brucei* STIB 795 infection at a dose of 20 mg/kg for 4 days i.p. (days 3 to 6). The mice are considered cured when no infection was found after 60 days. Compound **6** and compound **54** were able to cure all the 4 mice infected with this model. No overt sign of toxicity were observed in these mice. Compound **52** and **55** were not able to cure any of the mice infected at a dose of 20 mg/kg. However **55** increased the survival average of 18.3 days compared to the survival average of the control.

Having successfully treated this first acute model of infection we decided to test these compounds, at the same dose as for the previous test, in a more stringent test represented by the *T. brucei rhodesiense* STIB 900 model in rodents. This model is not cured by pentamidine (at the same dose), suramin, or any other drugs used for the treatment of the early stage. However the model responds to melarsoprol, a drug used for the late stage of the disease. Compound **6** cured only 1 of the 4 mice treated. The compound was given for 4 days at a dose of 20 mg/Kg. Compared to the untreated control animals the compound caused a significant increase of the life span (35 days) of the mice. Compound **54** cured 2 of the 4 mice treated at the same dose and also caused an

increase of life span of 38.5 days. Pentamidine, used at the same dosage, was not able to cure any mice infected with this model but only to increase the mice life span of 40 days.

The compounds, as for the *in vitro* testing, were assayed *in vivo* in mice model of *T. cruzi* (table 6.4).

Table 6.4 *In vivo* activities against a rodent model of Chagas disease for some selected compounds.

Compound	Dose mg/Kg	No doses	Route	Survival Time	% inhibition
53	15	5	i.p.	12.8	N.D.
6	25	5	i.p.	13	N.D.
54	50	5	i.p.	13	27.75
55	50	5	i.p.	14	44.95
Control	-			13	0.00
Benznidazole	45	5	oral	>30	100.00

Although the compounds tested were not able to cure the mice model, at a dose of 50 mg/Kg i.p. for 5 days, compounds **54** and **55** reduced the parasitaemia respectively of 28% and of 45% compared to the control.

Compound **54** was also tested in a rodent model of *Leishmania donovani*. At a dose of 40 mg/Kg i.p. for 5 days the compound did not cure any of the mice infected but reduced the parasitaemia of 28% compared to the control. The standard drug, pentostam, reduced the parasitaemia of 62% at a dose of 15mg/Kg for 5 days.

6.1.5 Mode of action studies:

Once evaluated the *in vitro* and *in vivo* activities of the compounds we investigated their mode of action. Two possible mechanisms of action of nitrofurans compounds are damage to DNA and oxidative damage.

A mechanism based on damage to DNA can be investigated by testing the different compounds in a mutant *T. brucei* line which is deficient in a DNA repair enzyme (RAD51). The wild type in presence of DNA damage is able to repair double-stranded DNA breaks. When an agent induces damage to DNA the mutant line ($RAD^{-/-}$) with a compromised repair mechanism will be more susceptible to damage than the wild type. Megazol (table 6.5) is known to exert its mode of action by damage to DNA[72]. The experiment conducted gives a proof of this mechanism of

action; thus, the RAD51$^{-/-}$ mutant is more sensitive to megazol with an IC_{50}=0.04±0.04 μM compared to that observed for the wild-type (IC_{50}=0.12±0.05 μM).

The oxidative damage produced by a compound can be evaluated by antagonising its activity with N-acetylcysteine (NAC), which reduces free radicals damage due to oxidative stress. Nifurtimox, a nitro heterocycle compound recently investigated for the treatment of melarsoprol refractory HAT and also registered for the treatment of the Chagas disease, appears to act via oxidative stress[145, 146]. Nifurtimox was also positive to the Ames test[147]. Table 6.5 shows that the mode of action of nifurtimox is antagonised by NAC. The activity against *T. brucei* wild type (IC_{50}=4.1±1.7 μM) is significantly reduced (IC_{50}=11.4±5.2 μM) culturing *T. brucei* wild type in presence of NAC suggesting the mode of action is not by DNA or oxidative damage.

Table 6.5 Activities of compounds against wild type, wild type and NAC and RAD$^{-/-}$ mutant *T. brucei*. The values are IC_{50} (μM).

Compound	54	6	Megazol	Nifurtimox	Benznidazole
Wild-type (427)	0.08±0.05	0.08±0.03	0.12±0.05	4.1±1.7	116.3 ±7.5
Wild-type (427) + NAC	0.09±0.04	0.12±0.05	0.13±0.06	11.4±5.2	116.3 ±13.6
RAD51$^{-/-}$ mutant	0.07±0.03	0.10±0.02	0.04±0.04	4.3±1.6	114.2±32

Benznidazole presents the lowest activity *in vitro*; moreover the activity is not pronounced in the RAD51$^{-/-}$ mutant and is not antagonised by NAC.

Compounds **54** and **6** showed similar activities against both the wild type and the RAD51$^{-/-}$ mutant, suggesting that their mechanism of action in *T. brucei* does not involve damage to DNA as observed for megazol. The activities are also similar when the wild type is compared with the same

[145] Docampo, R.; Stoppani, A. O. M. Generation of superoxide anion and hydrogen peroxide induced by nifurtimox in *Trypanosoma cruzi*. *Arch. Biochem. Biophys.* **1979**, *197*, 317-321.

[146] Moreno, S. N. J.; Mason, R. P.; Docampo, R. Reduction of nifurtimox and nitrofurantoin to free radical metabolites by rat liver mitochondria. Evidence of an outer membrane-located nitroreductase. *J. Biol. Chem.* **1984**, *259*, 6298-6305.

[147] Nagel, R.; Nepomnaschy, I. Mutagenicity of 2 Anti-Chagasic Drugs and Their Metabolic Deactivation. *Mutat. Res.* **1983**, *117*, 237-242.

cultured with NAC suggesting that their main mode of action cannot be related to the accumulation of reactive oxygen species.

6.1.6 Genotoxicity studies: the Comet assay

During early drug development, robust genotoxicity screening assays are required and are of crucial importance for the registration of a pharmaceutical compound[148, 149].

The single cell gel electrophoresis assay (Comet assay) represents a promising tool. It is rapid, simple to perform, requires only small amount of compound[150] and shows high sensitivity and specificity[151]. The Comet assay allows the detection of DNA breakage induced by genotoxic agents at single cell level such as individual mammalian and to some extent prokaryotic cells. The test is increasingly used in genotoxicity testing *in vitro* and is recommended for evaluating the genotoxic potential of compounds *in vivo*[151, 152].

DNA damaging reagents cause DNA fragmentation. In order to measure the sizes of DNA fragments within the cells in the Comet assay, it is necessary to convert DNA damage to DNA fragments by introducing breaks at the sites of DNA damage. Single strand breaks do not produce DNA fragments unless the two strands are separated. DNA unwinding can be obtained by increasing the pH to 12.1. However, other types of DNA

---

[148] Muller, *L.*; Kikuchi, Y.; Probst, G.; Schechtman, *L.*; Shimada, H.; Sofuni, *T.*; Tweats, D. ICH-harmonised guidances on genotoxicity testing of pharmaceuticals: evolution, reasoning and impact. *Mutat. Res.-Rev. Mutat. Res.***1999**, *436*, 195-225.

[149] Snyder, R. D. A review and investigation into the mechanistic basis of the genotoxicity of antihistamines. *Mutat. Res.-Rev. Mutat. Res.* **1998**, *411*, 235-248.

[150] Kiskinis, E.; Suter, W.; Hartmann, A. High throughput Comet assay using 96-well plates. *Mutagenesis* **2002**, *17*, 37-43.

[151] Tice, R. R.; Agurell, E.; Anderson, D.; Burlinson, B.; Hartmann, A.; Kobayashi, H.; Miyamae, Y.; Rojas, E.; Ryu, J. C.; Sasaki, Y. F. Single cell gel/comet assay: Guidelines for *in vitro* and *in vivo* genetic toxicology testing. *Environ. Mol. Mutagen.* **2000**, *35*, 206-221.

[152] Sasaki, Y. F.; Sekihashi, K.; Izumiyama, F.; Nishidate, E.; Saga, A.; Ishida, K.; Tsuda, S. The comet assay with multiple mouse organs: Comparison of comet assay results and carcinogenicity with 208 chemicals selected from the IARC monographs and USNTP carcinogenicity database. *Crit. Rev. Toxicol.* **2000**, *30*, 629-799.

damage, called alkali labile sites, are expressed when the DNA is treated with alkali at pH>13. There are several types of damage to DNA, other than direct fragmentation. For example, DNA base modification can occur. To identify these types of damage, breaks can be induced by appropriate glycosylases/endonucleases and the fragments thus produced can also be detected by Comet assay[153]. By controlling the conditions that produce nicks at the site of specific DNA lesions the Comet assay can be used to detect various classes of DNA damage.

Some selected compounds have been also studied *in vitro* to verify the drug-induced genotoxicity in human white blood cells. This model represents the *in vivo* drug susceptibility. The studies were also carried out for comparison in human chronic myelogenous leukemia K562 cells, a cell line widely used for *in vitro* drug-testing with the Comet assay[154, 155, 156].

Since free radicals could be produced during the treatment, the role of oxidative DNA damage was assessed by employing two enzymes: endonuclease III (Endo III) and formamidopyrimidine-DNA glycosylase (FPG). Endo III induces DNA strand breaks (detectable on the Comet assay) near oxidised pyrimidines[153]. FPG is involved in the first step of the base excision repair, removing specific modified bases from DNA thus creating an apurinic or apyrimidinic site (AP-site) that is subsequently cleaved by its AP lyase giving the formation of a gap in the DNA strand[157].

---

[153] Collins, A.; Dusinska, M.; Franklin, M.; Somorovska, M.; Petrovska, H.; Duthie, S.; Fillion, *L.*; Panayiotidis, M.; Raslova, K.; Vaughan, N. Comet assay in human biomonitoring studies: Reliability, validation, and applications. *Environ. Mol. Mutagen.* **1997**, *30*, 139-146.

[154] Buschini, A.; Alessandrini, C.; Martino, A.; Pasini, *L.*; Rizzoli, V.; Carlo-Stella, C.; Poli, P.; Rossi, C. Bleomycin genotoxicity and amifostine (WR-2721) cell protection in normal leukocytes vs. K562 tumoral cells. *Biochem. Pharmacol.* **2002**, *63*, 967-975.

[155] Di Francesco, A. M.; Mayalarp, S. P.; Kim, S.; Butler, J.; Lee, M. Synthesis and biological evaluation of novel diaziridinylquinone-acridine conjugates. *Anti-Cancer Drug.* **2003**, *14*, 601-615.

[156] Savickiene, J.; Gineitis, A. 3-Deazauridine triggers dose-dependent apoptosis in myeloid leukemia cells and enhances retinoic acid-induced granulocytic differentiation of HL-60 cells. *Int. J. Biochem. Cell Biol.* **2003**, *35*, 1482-1494.

[157] David-Cordonnier, M. H.; Boiteux, S.; O'Neill, P. Efficiency of excision of 8-oxo-guanine within DNA clustered damage by XRS5 nuclear extracts and purified human OGG1 protein. *Biochemistry* **2001**, *40*, 11811-11818.

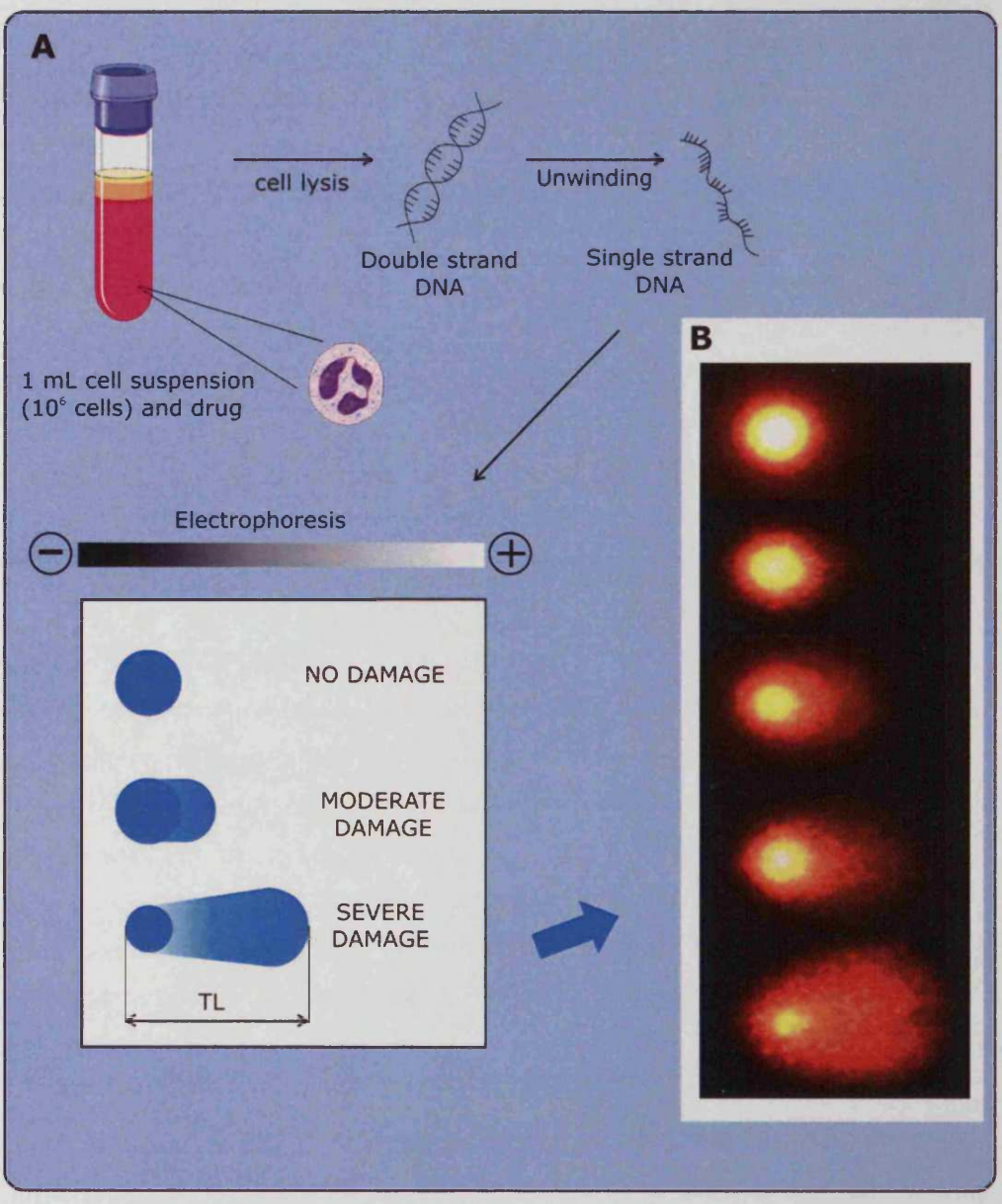

Figure 6.4 DNA strand break Comet assay. A. Principal steps of a Comet assay. B. Alkaline single cell-microgel-electrophoresis. The figure shows the different grades of DNA fragmentation in human mucosa cells. The fluorescent colour results from staining with ethidium bromide[158].

After the DNA unwinding in an electrophoretic alkaline buffer the electrophoresis is applied in the same buffer, the DNA is stained with ethidium bromide and analysed with a fluorescent microscope. The migration distance between the edge of the comet head and the end of tail

[158] GMSe Journal, available at:
http://www.egms.de/egms/servlet/Figure?id=cto000003&figure=f1&vol=2004-3

(figure 6.4, total length, TL) represents the value correlated to the genotoxic effects.

Compounds **6** and **54** were selected and tested with the Comet assay. A first experiment was conducted at pH>13 and benznidazole (BZ) was used to compare the effect observed. Figure 6.5 shows the experimental data for each drug and the relative regression lines: it is possible to see how the TL varies as a function of concentration of drug up to 10μg/mL. Compound **6** shows no significant effect at these doses. However compound **54** and benznidazole show a dose dependent increase in TL. This suggests as the concentration of compound/drug increases, the number of DNA alkali labile sites increases resulting with damage to DNA.

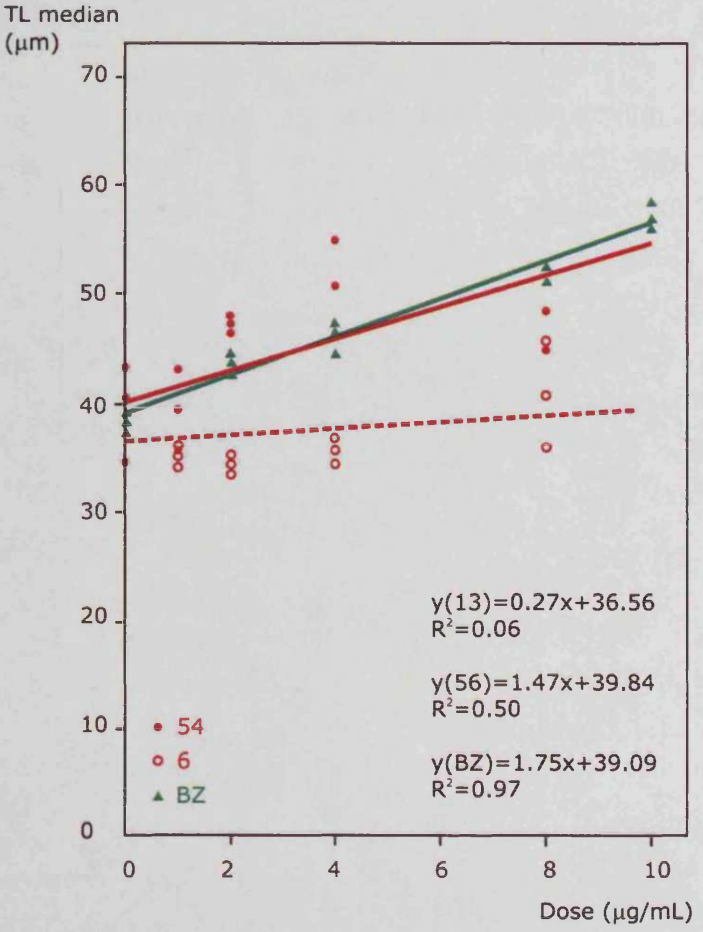

Figure 6.5 Comet assay (pH>13) on human leukocytes treated with **6**, **54** and benznidazole (37°C, 1h). Migration of DNA values, described by the median total length (TL) for each experiment point (50 cells per each of two replicates slides pr data point of each experiment) and regression lines are reported. Positive control (2mM EMS): TL=76.15±6.72 μm.

In leukocytes exposed to **54**, the "lowest effective dose" (LED) with a significant increase of DNA migration is 2μg/m*L*. At the highest concentration of the drug the TL does not significantly increase (figure 6.6). A similar behaviour can be observed in K562 cells with a LED=1μg/mL. Compound **6** was found to be unable to induce significant genotoxic effects. The atypical slope observed for compound **54** could be related two possible causes:

1. The toxicity increases at increasing doses, with induction of apoptotic/necrotic events with removal of cells with DNA damage, and a consequent under-estimation of the damage;

2. The mechanism of DNA damage of the drug could differ with the dose: induction of strand breaks and/or alkali labile sites (abasic sites, monoadducts, oxidative damage) at low doses and cross link formation (biadducts DNA-DNA, DNA-protein) at higher doses with inhibition of DNA migration.

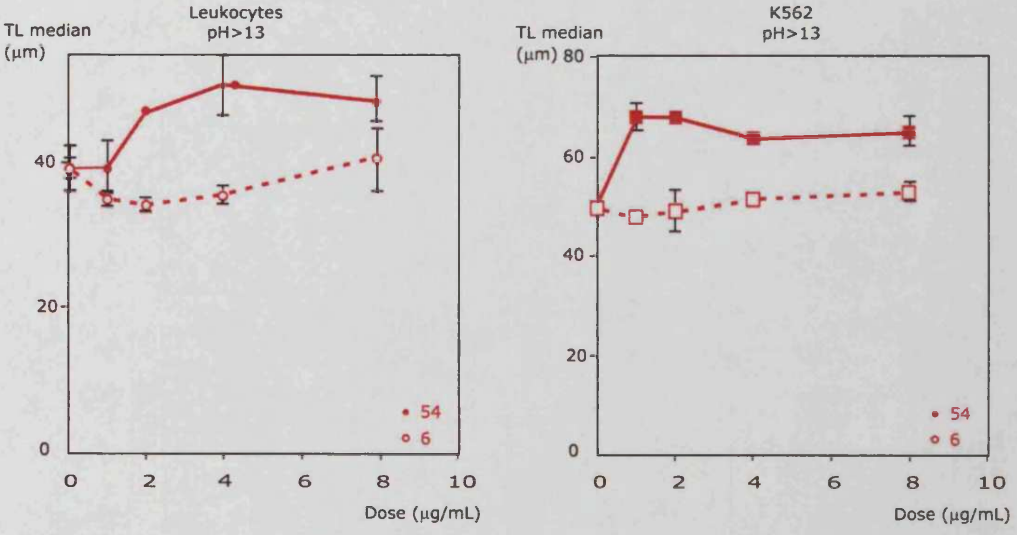

Figure 6.6 Comet assay (pH>13) on human leukocytes and K562 cells treated with **6** or **54** (37°C, 1h);migration of DNA as averaged median total length (mean ± SD of three independent experiments).

The DNA migration detected with the Comet assay at pH > 13 could be the results of strand breaks and/or alkali labile sites. In order to distinguish these different type of DNA damage, the Comet assay was performed at pH=12.1. At this pH, the DNA migration increase was not

significant for either compound (figure 6.7). These findings indicate that **54** mainly induced alkali labile sites (and eventually cross-links).

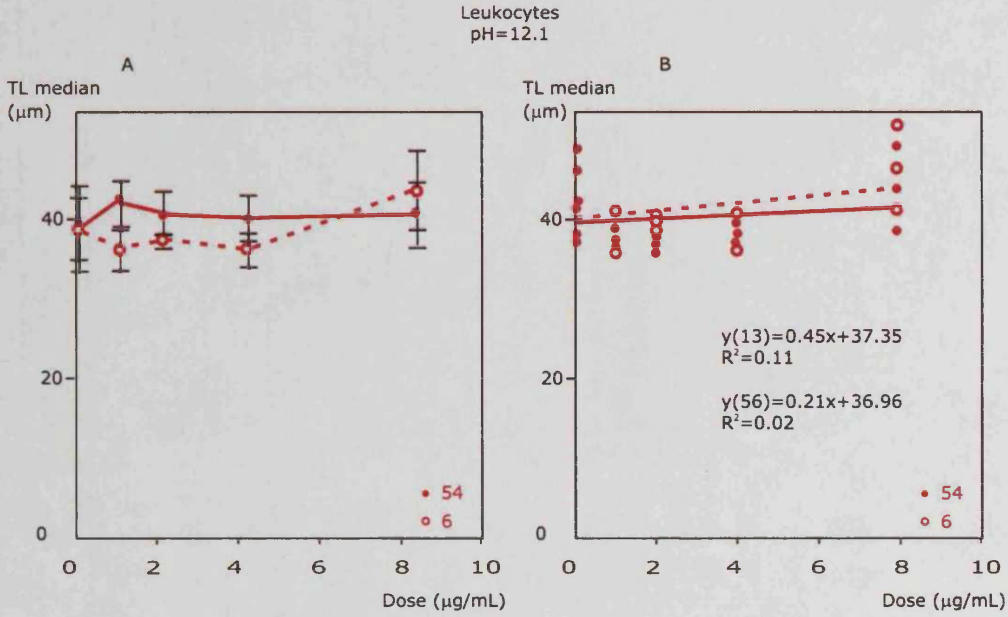

Figure 6.7 Dose-response relationship and regression analysis of DNA damage (Comet assay pH=12.1) induced on human fresh leukocytes by treatment with **6** and **54**. The DNA migration values are reported as: **A**) averaged median total length (TL); **B**) median TL for each experiment point and regression lines. Positive control (Bleomicine, 100mg/mL): TL=61.32±6.94mm.

In order to detect the amount of oxidised bases among the alkali-labile sites a modified protocol of the Comet assay was used. Following treatment with the compound, the cells are lysed and the nuclei treated with various endonucleases. DNA unwinding was then undertaken at pH=13 and 12.1. The results obtained (Figure 6.8 A) indicated that there was not detectable DNA base oxidation on cells treated with **6**. The finding for compound **54** (figure 6.8 B) showed:

1. At pH>13 the protocol using the two enzymes (FPG and ENDO III) did not detect significant increase of oxidised bases related to the drug exposure;
2. At pH=12.1 the Comet assay with ENDO III indicated the presence of oxidised bases with similar effects at the two tested doses (4 and 8 μg/mL).

A) Compound 6

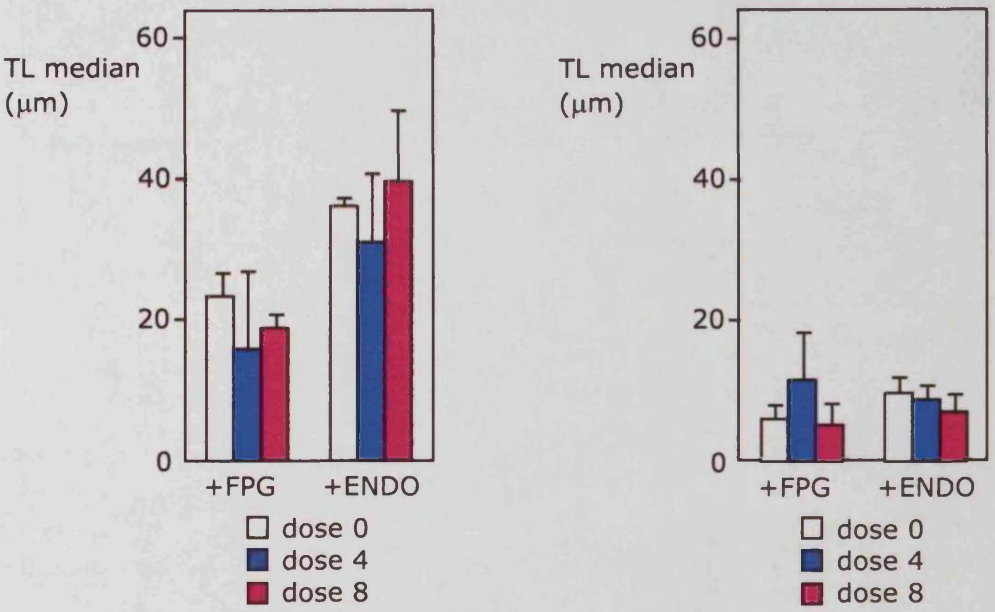

B) Compound 54

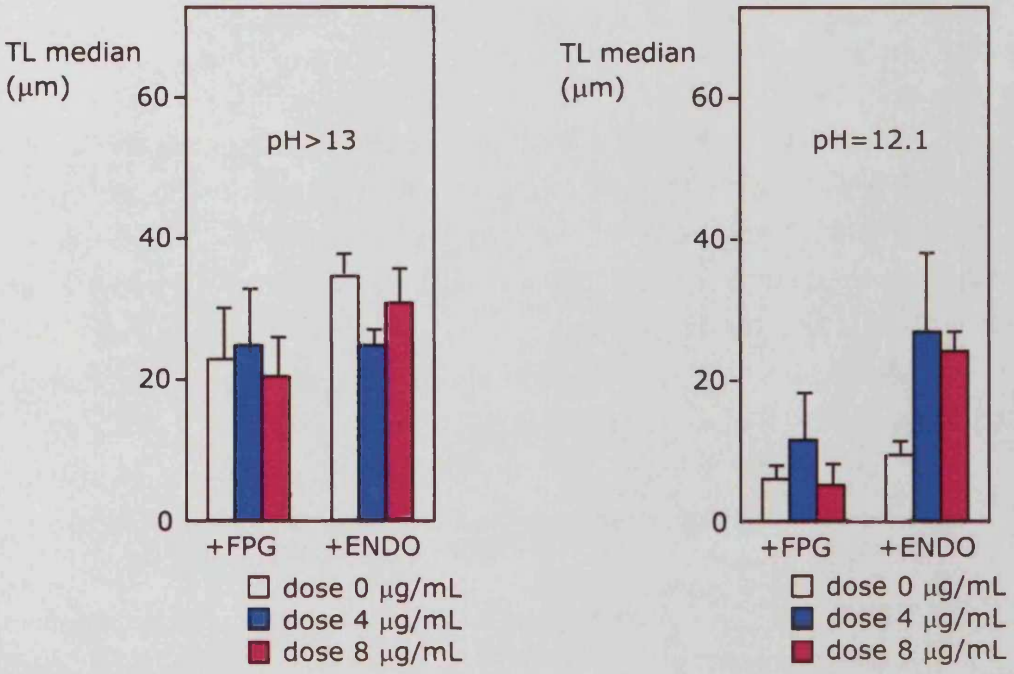

Figure 6.8 DNA damage induced in human leukocytes after treatment with compound **6** (A) or **54** (B) at different doses (0, 4, 8 μg/mL; 37°C, 1h). The Comet assay is modified by using bacterial repair endonucleases (Endo III) and formamidopyrimidine (FPG) for the detection of oxidised bases. Oxidised bases are expressed as DNA migration (TL) increase compared to the assay without enzymes.

In summary, for these compounds, compound **6** showed no mutagenic effects at the concentrations investigated. For compound **54** results suggest that there is oxidation of bases (shown by the DNA migration at pH=12 and by the DNA migration at pH>13) and possible cross-linking of DNA (observed at pH>13 without the enzymes and at pH=12 with ENDO III).

The interpretation of these genotoxicity studies suggests that compound **54** is probably mutagenic and therefore is not a good candidate for further optimisation. Unlikely, compound **6** was found not mutagenic at the doses tested. Tests at higher doses for this compound are needed. More compounds will be also tested with the Comet Assay and will be compared with these results.

6.2 Benzamidine derivatives: Biology

6.2.1 Affinity for the P2 transporter:

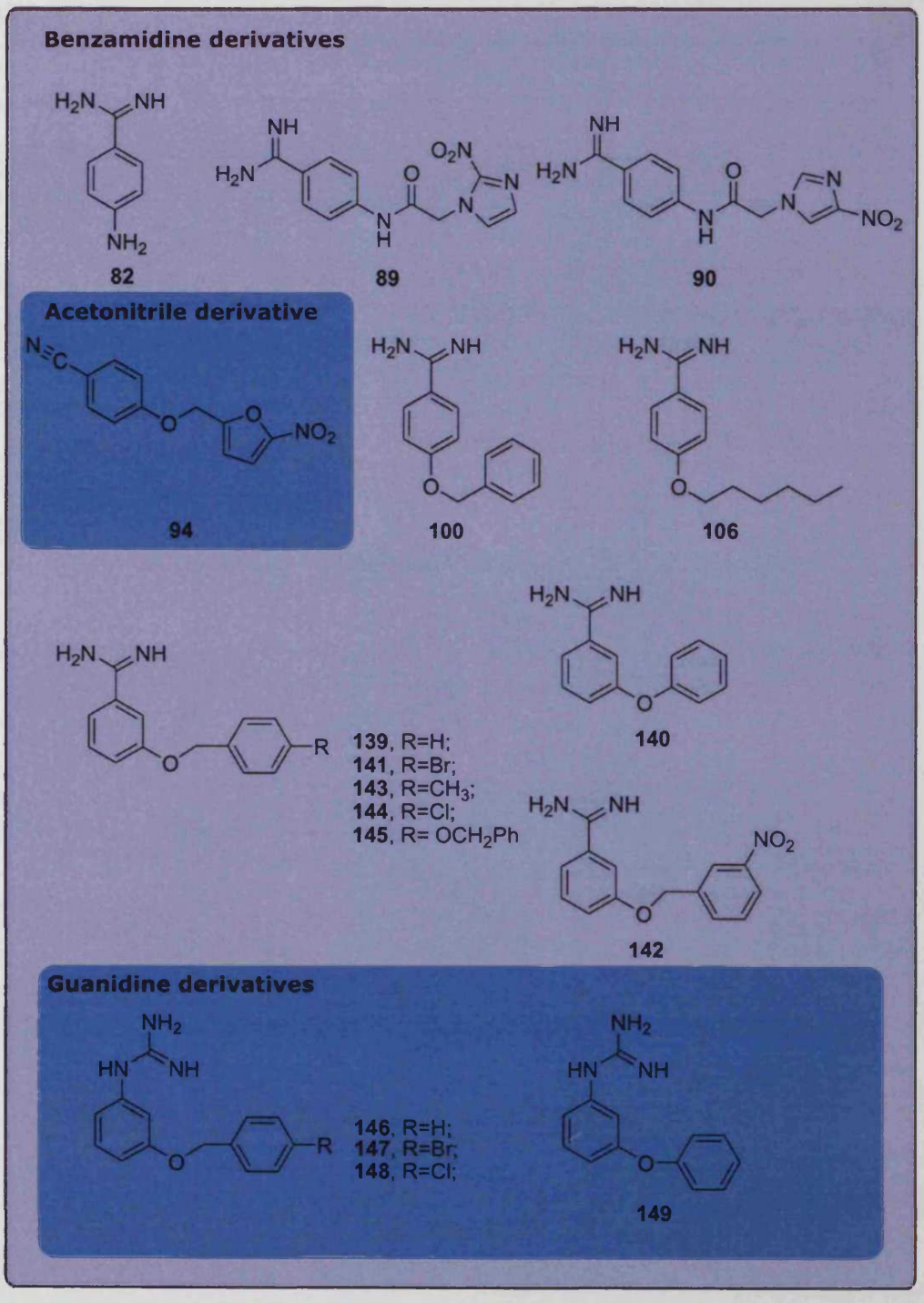

Scheme 6.2 Structure of compounds assayed and shown in table 6.6.

Compound	MW	P2 uptake IC_{50} (μM)[a]	IC_{50} (μM) *T.b. brucei*	*T. b. rhodesiense*	*L6 cells*[b]
82	208.1	0.38	54	12.8	167
89*	288.2	ND	ND	6.2	312
90*	288.2	ND	ND	79.8	312
94	244.2	ND	ND	0.77	27
100	340.3	ND	ND	3.44	ND
106	348.4	ND	ND	9.69	ND
139**	226.2	0.38	54	12.8	167
140**	212.2	0.38	56	31.1	203
141**	305.1	0.8	10	6.2	16.4
142**	271.2	0.33	68	49.8	129
143**	240.3	0.21	14	11.2	52
144**	260.7	1.01	13	8.4	46
145**	332.4	1.57	7	11.1	14.7
146**	277.7	8	109	81	71
147**	434.2	ND	ND	9.9	37
148**	389.7	ND	ND	32	14.6
149**	263.7	9.3	56	15.9	140
Melarsoprol		1.2	0.053	0.006	7.8

a: Inhibition of adenosine uptake by the P2 transporter in *T. brucei brucei* 427. **b**: L6 cells are rat skeletal myoblast and are used as a measure of cytotoxicity to mammalian cells. **ND**: not determined. * Compounds synthesised by Jimenez-Bueno, G. ** Compounds synthesised by Boussard, C.

Table 6.6 Affinity for P2 transporter and *in vitro* activities against *T. brucei* lines. Activities are shown in μM.

Selected benzamidine compounds were tested for their ability to interact with the P2 transporter of *T. brucei*. The majority of the benzamidine compounds tested showed IC_{50} values lower than melarsoprol (IC_{50}=1.2 μM) whilst compounds **144**, **145** showed values of a similar order of melarsoprol (IC_{50}=1.01 μM and 1.57 μM respectively). These results suggest that benzamidine compounds with an electronegative atom in *para* position have good affinity and are a good substrate for the P2 transporter.

6.2.2 *In vitro* activity against *T. brucei*:

The results suggest that these benzamidine compounds are less active than melamine derivatives at grown inhibition of *T. b. brucei*. However, nitrofuran derivatives of benzamidines are needed for a valuable comparison. As observed for the melamine compounds, there is no correlation between affinity for the P2 transporter and activity *in vitro* against the parasites.

Figure 6.9 showed the different *in vitro* results obtained against *T. brucei* lines and against *L6*-cells line as a model to investigate the toxicity

towards mammalian cells. The activity is reported as $\log(1/IC_{50})$ so that high cylinders represent compounds with high activity (low IC_{50} values). The activities obtained are in the micromolar range and therefore lower compared with the ones described for the triazine derivatives and melarsoprol (IC_{50}= 53 nM) were nanomolar activities were observed.

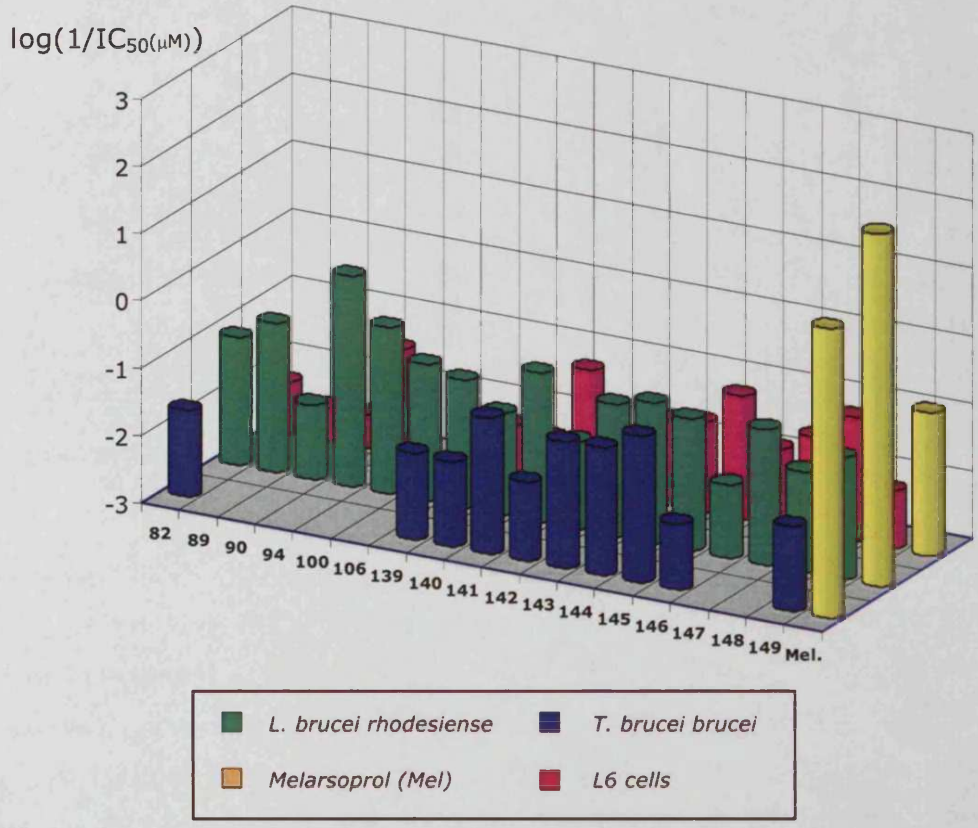

Figure 6.9 Activities of some selected benzamidines against *T. brucei* species.

Compound **94** showed a relatively good activity against *T. b. rhodesiense* line (IC_{50}=0.74 µM). This compound is a cyano-derivative and the only member of the group tested that does not carry an amidine function. The activity of this derivative could be accounted to the presence of the nitrofuran moiety. This result confirmed that the activity is not dependant on the interaction with the P2 transporter and that other transporters can be involved in the uptake. At the same time it suggests that a combination of benzamidines with a nitrofuran moiety in *para*-position could of interest in order to improve the activity against the *T.*

brucei line. The guanidine derivatives (**146-149**) did not show any significant *in vitro* activity against the *T. b. rhodesiense* line.

6.2.3 *In vitro* activities against parasites related to *T. brucei*:

Selected compounds were also tested against *T. cruzi* (trypomastigotes), *L. donovani* (axenic intracellular form) and *P. falciparum* (red blood cell stage). The IC_{50} values are shown on table 6.7. Some compounds (**141**, **145**, **106**) showed micromolar activities against *T. cruzi* similar to standard drug benznidazole (IC_{50}=1.435 μM).

Table 6.6 Affinity for P2 transporter and *in vitro* activities against *T. cruzi*, *L.donovani* (axenic amastigotes) and *P. falciparum* lines. Activities are shown in μM.

		IC_{50} (μM)			
Compound	**MW**	***T. cruzi***	***L. donovani***	***P. falciparum***	***L6 cells***
82	208.1	432	ND	65.2	ND
89*	288.2	162	104	35	312
90*	288.2	312	104	20.8	312
94	244.2	16.8	Tox	6.39	27
100	340.3	51.4	ND	14.8	ND
106	348.4	5.16	ND	2.78	ND
139**	226.2	62.3	Tox	7.4	167
140**	212.2	17.4	Tox	10.9	203
141**	305.1	7.5	Tox	1.3	16.4
142**	271.2	33.9	Tox	5.2	129
143**	240.3	13.3	Tox	3.1	52
144**	260.7	12.6	Tox	2.7	46
145**	332.4	5.4	6	4.8	14.7
146**	277.7	16.6	Tox	14.7	71
147**	434.2	8.5	Tox	22.7	37
148**	389.7	31.3	>15	>26	14.6
149**	263.7	16.7	Tox	27.8	140
Melarsoprol		0.006	7.8	ND	ND
Benznidazole		1.435	ND	ND	ND

Activities are shown in μM. Standards: *T. cruzi*, Benznidazole, IC_{50}=1.435 μM; *L. donovani*: Miltefosine, IC_{50}=1.16 μM. Tox= toxic to macrophages thus precluding measurement of leishmanicidal activities.* Compounds synthesised by Jimenez-B. G.; ** Compounds synthesised by Boussard C.

All the compounds tested against *L. donovani* (axenic amastigotes), except **145** that showed a micromolar activity (IC_{50}= 6μM), were found to be toxic to macrophages thus precluding the evaluation of their leishmanicidal activity.

The majority of the compound tested showed micromolar activities against *P. falciparum*. The highest activities were observed for compounds **141** (IC_{50} = 1.3 μM), **143** (IC_{50} = 3.1 μM) and **144** (IC_{50} = 2.7 μM).

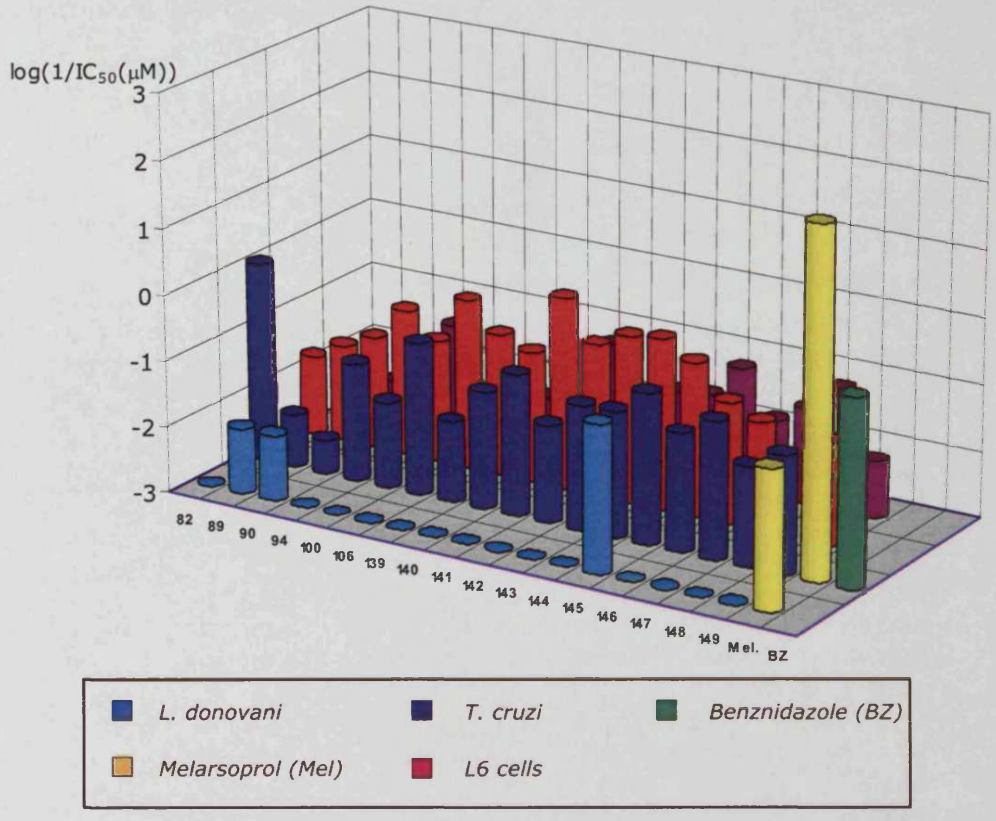

Figure 6.10 Activities of selected benzamidines against *L. donovani*, *T. cruzi* and *P. falciparum*.

6.3. Conclusions:

In summary, most of the melamine-nitrofurans synthesised showed potent *in vitro* activity against *T. b. rhodesiense* to the same order of magnitude as melarsoprol.

Some compounds showed also sub-micromolar activities against *T. cruzi*. Compound **54** showed sub-micromolar *in vitro* activity also against *L. donovani*.

Compound **6** and compound **54** retained trypanocidal effect in mice curing all the 4 mice infected with the STIB 795 *T. b. brucei* model and respectively 1 and 2 of the 4 mice infected with the STIB 900 T. b. rhodesiense model. These compounds were therefore evaluated for their potential genotoxic effects. Compound **6** showed no mutagenic effects whilst compound **54** is probably mutagenic.

Compound **6** represents a good candidate for further optimisation and therefore will be tested at higher doses.

7. Conclusions:

We have reported the design and the synthesis of different compounds as drugs against *T.brucei spp.*, the causative agent for African sleeping sickness.

The compounds were designed by attaching a toxic moiety to a P2 recognition motif in order to exert the toxicity selectively to parasite and minimise side effects in humans.

We have prepared melamine-nitrofuran conjugates that showed potent activity against T.*brucei rhodesiense* to the same order of magnitude as melarsoprol and that are significantly more active that nifurtimox, which is currently undergoing trials for HAT.

It is not possible to correlate the affinity of the P2 transporter and the trypanocidal activity (however melamine is required); other transporters may be involved in the uptake of these compounds;

In addition to *in vitro* activity, several melamine-nitrofurans retained trypanocidal effect in mice. Two compounds, **6** and **54**, were able to cure an animal model of trypanosomiasis (*T. brucei brucei* STIB795) and one the compounds was able to have a significant effect on another more stringent model of infection, *T. brucei rhodesiense* STIB900.

Mode of action studies indicated that the mechanism of action of compound **6** does not involve damage to DNA in trypanosomes, indicating that it will not be mutagenic in mammalian cells, thus greatly improving the chances that this compound can proceed to clinical trials against trypanosomiasis.

Some compounds showed also considerable activity against *T. cruzi in vitro* and some reduction in parasitaemia *in vivo*.

These compounds represent new leads for further evaluation for HAT and should also be considered as leads in developing novel drugs against Chagas disease.

Compounds bearing a benzamidine moiety as P2 recognition motif have been considered. The solubility and the chemistry of these derivatives represented an issue for the development of a valid procedure of synthesis of benzamidines linked to nitroheterocycles. However, some methodologies of synthesis of amidines have been established and some interesting model compounds have been synthesised. The *in vitro* results of these model compounds against the *T. brucei spp*. indicated that the presence of the nitrofuran moiety is essential for the activity and suggests that linking a benzamidine with a nitrofuran moiety in para position could greatly improve the activity.

The carrier-linked prodrug strategy, incorporating P2 recognition motifs, represents theoretically a valid tool to selectively target trypanocidal agents to trypanosomes. Interesting intermediates bearing P2 motifs have been synthesised and could be coupled to known drugs to generate interesting ester prodrugs.

8. Experimental Section I:

Triazine Derivatives

8.1 General remarks:

IR spectra were recorded at a FT-IR spectrometer 1600 from Perkin Elmer using the Diffuse Reflectance Accessory from Spectra Tech. (Refl.), a potassium bromide pellet (KBr), or methylene chloride solution of the compound between potassium bromide single crystals (film). The band positions were characterised by their wave numbers (ν/cm-1), intensity (strong, medium, weak, broad), and assignment.

Mass spectra were recorded at a Platform II mass spectrometer (Micromass) from Fisons. High resolution mass spectra were performed respectively on a Waters ZQ4000 and a Finningan MAT 95XP at EPSRC National Mass Spectrometry Service centre in the Chemistry department, University of Wales Swansea, Swansea, Wales, UK.

Purification by column chromatography was performed on Sorbosil C60A silica-gel-40-60 μm from Merck. In some cases higher flow rates were maintained by using a slight pressure. Qualitative thin-layer chromatography (TLC) was done on pre-coated aluminium sheets Silica gel 60 F254 from Merck. Compounds were detected either with iodine, ninhydrin or 254 nm UV-light. Purification by reversed phased was

performed on silica gel 100 C18. Qualitative thin layer chromatography reversed phased (TLC-RP) TLC was performed on pre-coated aluminium sheets Silica gel RP-18 F254 nm UV-light.

Purification by ion exchange chromatography was performed on a Dowex 50WX2-200 resign using HCl gradient (1M to 6M). To purify 100 mg (0.15 - 0.2 mmol, 0.6 – 0.8 mequ) of a sample 10 mL Dowex 50WX2-200 resign were suspended in 2N hydrochloric acid for 15 min and filled into a column. The resign was washed with 50 mL 5N hydrochloric acid followed by water until the eluate was neutral against pH-paper. The sample was submitted as diluted aqueous solution or suspension and elution was carried out with approximately 50 mL water, 200-400 mL 2N hydrochloric acid, 50 mL 4N hydrochloric acid, and 300 mL 5N hydrochloric acid in 2-propanol. The progress of elution was followed by determining the UV-absorption of the undiluted 10-20 mL fractions at 240 nm.

Melting points were determined with a Gallenkamp melting point apparatus and are not corrected.

Solvents and reagents were purchased from chemical companies and used without further purification. Dry solvents were purchased in sure sealed bottles stored over molecular sieves.

^{1}H-NMR spectra were recorded at a Bruker 300 MHz and 500 MHz spectrometers using the applied solvent simultaneously as internal standard. Chemical shifts (δ) are given in ppm together with the relative frequency, assignment, the coupling constants (nJ(H,H)/Hz) and the multiplicity: singlet (s), broad singlet (bs), doublet (d), triplet (t), quartet, quintuplet, sextet, septuplet, multiplet (m), broad multiplet (bm).
ACD Lab ver. 2.03 and Chemdraw Ultra 8.0 software were used for the assignment of the peaks.
Chemical shifts for AB-systems are directly deduced from Mestre-C ver. 4.5.9 free software program.
^{13}C-NMR spectra were recorded at a Bruker 300 MHz NMR spectrometer using the applied solvent simultaneously as internal standard. Chemical shifts (δ) are given in ppm.

DMSO-d_6/TFA was used in some experiments as solvent for some insoluble compounds and represents a mixture of DMSO-d_6 in which two drops of TFA were added.

For some peaks, the * after the number was used to describe the extra peak associated to tautomerism.

In some cases, the numbering and the nomenclature system used for the drawn structures in the following chapters are not referring to IUPAC nomenclature in order to aid the NMR interpretation.

Triazine Derivatives

8.2 Synthesis of Amino-dichloro-triazines:

8.2.1 Synthesis of 2-amino-4,6-dichloro-[1,3,5]-triazine (43)[90]:

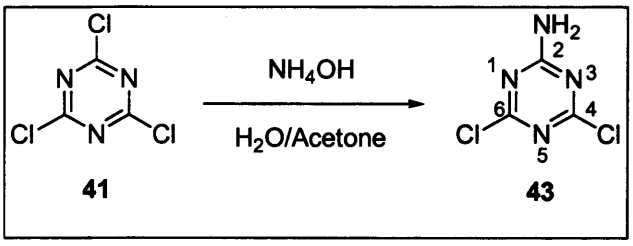

41 43

Cyanuric chloride (**41**, 2.5g 99%, 13.5 mmol) was dissolved in acetone (19 mL) and poured into 20 mL of ice-water (HPLC grade) to form a very fine suspension. Ammonium hydroxide solution (27 mL 1N, 27 mmol) was added dropwise carefully maintaining the temperature between 0°C and 5°C. The mixture was stirred 30 min at 0°C and additional 30 min at room temperature. The precipitate was filtered off, washed with cold water (4 x 15 mL) and dried over P_2O_5 under high vacuum giving 1.588 of a pure white solid.

Yield: 71%.

mp: 223-225°C.

LRMS (ES^+): m/z 165.7 ($(M+H)^+$, 60%).

^{1}H-NMR (DMSO-d6, 300 MHz): δ 8.59 (bs, 2H).

^{13}C-NMR (DMSO-d6, 75 MHz): δ 167.3 (C4 and C6), 169.5 (C2).

8.2.2 Synthesis of 2-hydroxyethyl-amino-4,6-dichloro-[1,3,5]-triazine (65a)

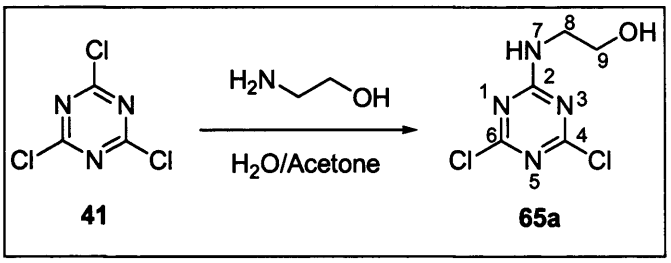

8.2.2.1 Attempted synthesis: Method A:

Cyanuric chloride (**41**, 1 g 99%, 5.42 mmol) was dissolved in acetone (HPLC grade, 10 mL) and poured into 10 mL of ice-water to form a very fine suspension. The suspension was left stirring for 10 min at -10°C and then ethanolamine (662.1 mg 99%, d= 1.012, 0.65 mL, 10.84 mmol) was added dropwise carefully maintaining the temperature at -10°C. The mixture was left stirring for 30 min at -10°C and for further 2hrs at room temperature. The suspension turned into a clear solution. TLC-RP (CH_3CN/H_2O=50/50) analysis showed the formation of two new products. The solvent was partially concentrated under reduced pressure until the formation of a white precipitate. The precipitate was filtered off and dried over high vacuum. MS showed the presence of the expected product and ^{13}C-NMR showed together with the expected product the presence of the two starting materials. The attempts to remove the starting materials from the products (washing the precipitate with different solvents) failed and the reaction was repeated following the procedure as described on the following method B.

8.2.2.1 Synthesis: Method B:

Cyanuric chloride (10 g 99%, 53.68 mmol) was dissolved in acetone HPLC grade (50 mL) and poured into 100 mL of ice-water to form a very fine suspension. The suspension was left stirring for 10 min at -10°C and then ethanolamine (3.93 mg 99%, d= 1.012, 3.88 mL, 64.41 mmol) was added dropwise carefully maintaining the temperature at -10°C. The mixture was left stirring for 30 min at -10°C and for further 2hrs at room temperature.

The suspension turned into a clear solution. TLC-RP (CH_3CN/H_2O=50/50) analysis showed the formation of two new products. The solvent was concentrated under reduced pressure until the formation of a white precipitate. The precipitate was filtered off, washed with MeOH and dried over high vacuum. MS showed the presence of the expected product. ^{13}C-NMR showed together with the expected product the presence of the two starting materials. The solid was washed several times with acetone. After the filtration further solid was separated from the solvent (acetone). The solid was filtered and dried over high vacuum giving 2.002 g of pure product.

Yield: 18%

LRMS (ES^-): m/z 208.0 ($(M-H)^-$, 50%).

^{1}H-NMR (DMSO-d6, 300 MHz): δ 3.34 (quartet, 2H, *J*= 5.81 Hz, H-C8), 3.49 (t, 2H, *J*= 5.81 Hz, H-C9), 5.20 (bs, 1H, OH), 9.09 (bs, 1H, H-N7).

^{13}C-NMR (DMSO-d6, 75 MHz): δ 43.6 (C8*), 43.8 (C8), 57.8 (C9*), 59.1 (C9), 165.8 (C4 and C6), 169.7 (C2*), 169.7 (C2).

8.3 Synthesis of diamino-triazines:

8.3.1 Synthesis of N^2-methyl-2,4-diamino-6-chloro-[1,3,5]-triazine (46):

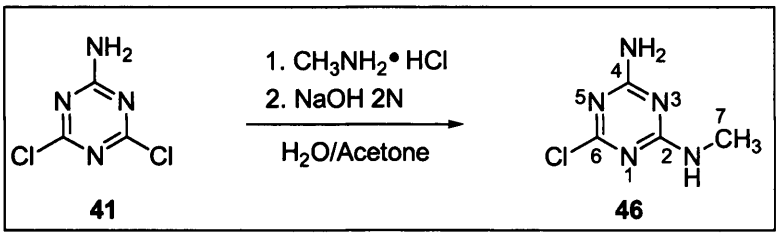

2-amino-4,6-dichloro-triazine (600 mg, 3.63 mmol) was dissolved in acetone (8 mL) and poured into 10 mL of water to form a very fine suspension. A solution of methylamine hydrochloride (247.5 mg 99%, 3.63 mmol) in 2 mL of water was added with temperature control at 0°C. NaOH solution (3.6 mL, 2N) was added dropwise carefully maintaining the temperature between 0°C and 5°C. After stirring for 24 hrs at room temperature the precipitate was filtered off, washed with water (2x15 mL) and dried over P_2O_5 giving 478mg of a white solid.

Yield: 82%

mp: 236-238 °C

LRMS (ES^+): m/z 159.8 ($(M+H)^+$, 20%).

^{1}H-NMR (DMSO-d6, 300 MHz) δ 2.75 (d, 3H, *J*=4.75Hz), 7.32 (bs, 2H, NH_2), 7.37 (m, 1H, H-N2).

^{13}C-NMR (DMSO-d6, 75 MHz) δ 27.6 (C7), 166.4 (C6), 167.3 (C2), 169.1 (C4).

8.3.2 Synthesis of N^2,N^2-dimethyl-2,4-diamino-6-chloro-[1,3,5]-triazine (47):

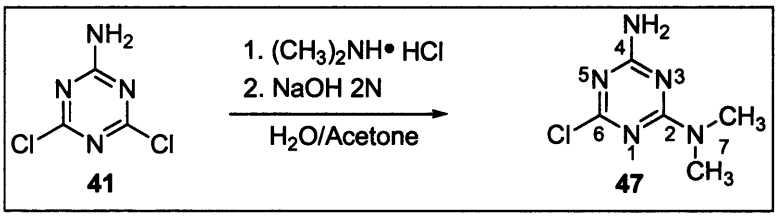

2-amino-4,6-dichloro-triazine (600 mg, 3.63 mmol) was dissolved in acetone (8 mL) and poured into 10 mL of water to form a very fine suspension. A solution of dimethylamine hydrochloride in 2 mL of water was added with temperature control at 0°C. NaOH solution (3.6 mL, 2N) was added dropwise carefully maintaining the temperature between 0 °C and 5°C. After stirring for 24 hrs at room temperature the precipitate was filtered off, washed with water (2x15 mL) and dried over P_2O_5 giving 511 mg of white solid.

Yield: 81 %

mp: 217-219 °C

LRMS (ES^+):m/z= 173.9 ($(M+H)^+$, 80%).

^{1}H NMR (DMSO-d6, 300 MHz) δ 3.05 (s, 6H, H-C7), 7.28 (bs, 2H, NH_2).

^{13}C NMR (DMSO-d6, 75 MHz) δ 36.2 (C7), 36.3 (C7'), 165.3 (C6), 166.9 (C2), 168,7 (C4).

8.3.3 Synthesis of N^2,N^4-dimethyl-2,4-diamino-6-chloro-[1,3,5]-triazine (44):

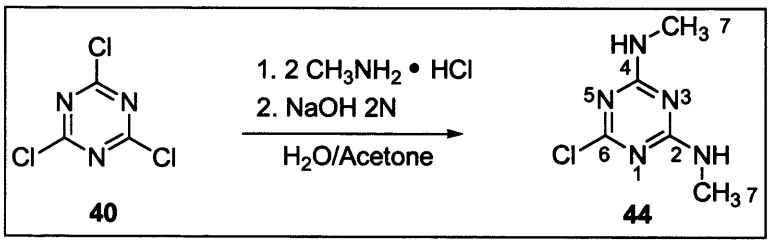

Cyanuric chloride (5.0 g, 27 mmol) was dissolved in 35 mL of acetone and poured into 50 mL of ice-water to form a very fine suspension. A solution

of methylamine hydrochloride (3.66 g, 54 mmol) in 20 mL of water was added with temperature control at 0°C. NaOH 2N (54 mL, 108 mL) was added dropwise carefully maintaining the temperature between 0°C and 5°C. The mixture was stirred 30 min at room temperature and additional 60 min at 50°C. The precipitate was filtered off, washed with water (3x 25 mL) and acetone (2x 25 mL). After drying over calcium chloride under high vacuum, 4.2 g of product was obtained as white powder.

Yield: 89%.

mp: 302-303 °C.

LRMS (ES^+): m/z = 174 ($(M+H)^+$, 15%).

^{1}H-NMR (300MHz, DMSO-d_6/TFA): δ 2.78 (3m, 6H, H-C7), 8.45 (4m, 2H, H-N2 and H-N4).

^{13}C-NMR (75 MHz, DMSO-d_6/TFA): δ 27.9 (C7), 159.5 (C2), 165.5 (C4).

8.3.4 Synthesis of N^2,N^2,N^4,N^4-tetramethyl-2,4-diamino-6-chloro-[1,3,5]-triazine (45):

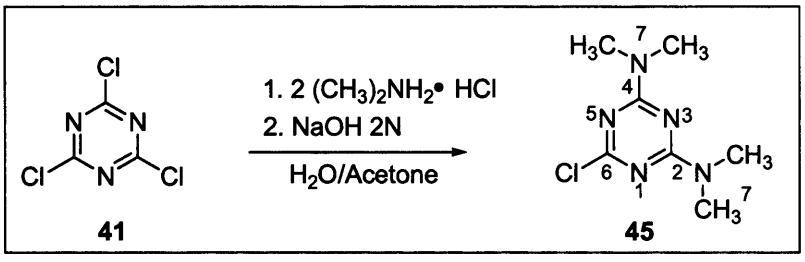

Cyanuric chloride (5.0 g, 27 mmol) was dissolved in 35 mL of acetone and poured into 50 mL of ice-water to form a very fine suspension. A solution of dimethylamine hydrochloride (4.42 g, 54 mmol) in 20 mL of water was added with temperature control at 0°C. NaOH 2N (54 mL, 108 mL) was added dropwise carefully maintaining the temperature between 0°C and 5°C. The mixture was stirred 30 min at room temperature and additional 60 min at 50°C. The precipitate was filtered off, washed with water (4x 30 mL) and dried under vacuum over calcium chloride giving 4.9g of pure product as white powder.

Yield: 90%.

mp: 72-74 °C

LRMS (ES^+): m/z = 174 ($(M+H)^+$, 15%).

^{1}H-NMR (DMSO-d_6/TFA, 300 MHz): δ 3.03 (2s, 12H, H-C7).

^{13}C-NMR (DMSO-d_6/TFA, 75 MHz): δ 36.7 (C7), 165.2 (C6), 169.0 (C2 and C4).

8.3.5 Synthesis of N^2-propyl-2,4-diamino-6-chloro-[1,3,5]-triazine (56):

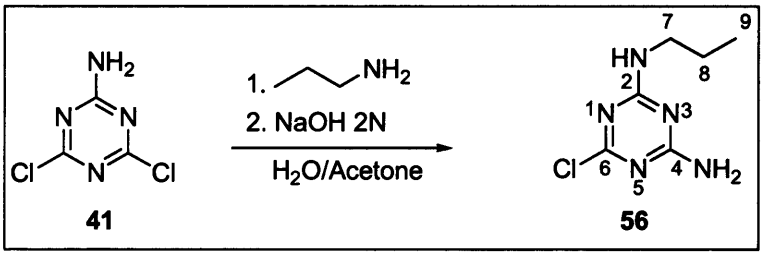

2-amino-4,6-dichloro-triazine (500 mg, 3.03 mmol) was dissolved in acetone (6 mL) and poured into 6 mL of water to form a very fine suspension. A solution of propylamine (182.7 mg 98%, d=0.71, 0.26 mL, 3.03 mmol) was added followed by the addition of NaOH 2N (1.5 mL, 3.6 mmol) and maintaining the temperature on the range 0°C/5°C. The mixture was left stirring for 1 hr at 0°C and overnight at room temperature. The precipitate was filtered off, washed with water (2x15 mL) and dried over P_2O_5 giving 431mg of a white solid.

Yield: 76%

mp: 156-158 °C

LRMS (ES^+) m/z = 188.1 ($(M+H)^+$, 100%).

^{1}H-NMR (DMSO-d6, 300 MHz) δ 0.89 (t, 3H, *J*=7.39 Hz, H-C9), 1.48 (m, 2H, H-C8), 3.15 (m, 2H, H-C7), 6.96-7.82 (3m, 3H, 2 H-N4, H-N2).

^{13}C-NMR (DMSO-d6, 75 MHz) δ 8.6 (C9*), 8.7 (C9), 22.3 (C8), 22.6 (C8*), 42.2 (C7), 42.3 (C7*), 165.9 (C6), 166.1 (C6*), 166.8 (C4*), 167.3 (C4), 168.4 (C2), 169.1 (C2*).

8.3.6 Synthesis of N^2-butyl-2,4-diamino-6-chloro-[1,3,5]-triazine (58):

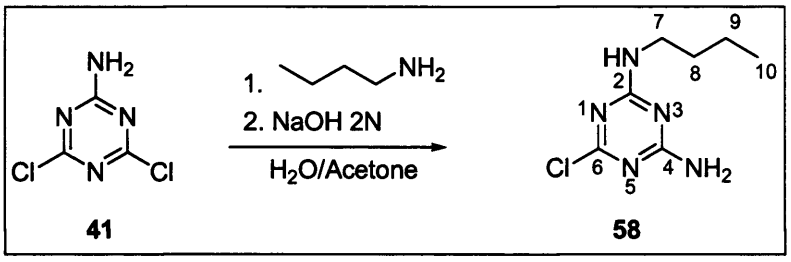

2-amino-4,6-dichloro-triazine (500 mg, 3.03 mmol) was dissolved in acetone (6 mL) and poured into 6 mL of water to form a very fine suspension. A solution of butylamine (222.7 mg 99.5%, d=0.74, 0.3 mL, 3.03 mmol) was added followed by the addition of NaOH 2N (1.5 mL, 3.6 mmol) carefully maintaining the temperature on the range 0°C/5°C. The mixture was left stirring for 1 hr at 0°C and overnight at room temperature. The precipitate was filtered off, washed with water (2x15 mL) and dried over P_2O_5 giving 577 mg of a white solid.

Yield: 94%

mp: 133-135 °C

LRMS (EI): m/z = 202.1 (M^+, 100%).

^{1}H-NMR (DMSO-d6, 300 MHz) δ 0.87 (t, 3H, *J*=7.27 Hz, H-C10), 1.29 (sextet, 2H, *J*=7.27 Hz, H-C9), 1.45 (quintuplet, 2H, *J*=7.27 Hz, H-C8), 3.15 (m, 2H, H-C7), 6.98-7.79 (3m, 3H, 2 H-N4, H-N2).

^{13}C-NMR (DMSO-d6, 75 MHz) δ 14.0 (C10), 19.8 (C9*), 19.9 (C9), 31.1 (C8), 31.5 (C8*), 40.1 (C7*), 41.2 (C7), 165.9 (C6), 166.1 (C6*), 166.8 (C4*), 167.3 (C4), 168.4 (C2), 169.1 (C2*).

8.3.7 Attempted synthesis of N^2-isoproyl-2,4-diamine-6-chloro-[1,3,5]-triazine (57):

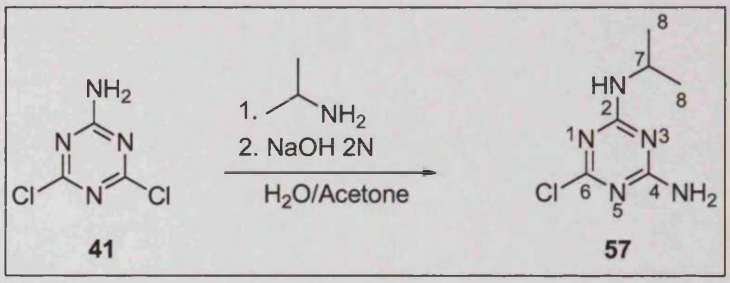

2-amino-4,6-dichloro-triazine (500 mg, 3.03 mmol) was dissolved in acetone (6 mL) and poured into 6 mL of water to form a very fine suspension. A solution of isopropylamine (180 mg 99.5%, d=0.694, 0.26 mL, 3.03 mmol) was added followed by the addition of NaOH 2N (1.5 mL, 3.6 mmol) and carefully maintaining the temperature on the range 0°C/5°C. The mixture was left stirring for 1 hr at 0°C and then overnight at room temperature. The precipitate was filtered off, washed with water (2x15 mL) and dried over P_2O_5 giving 318 mg of a white solid. The NMR showed weak peaks in D_2O. The product was used as crude for the synthesis of the hydrazine intermediate.

8.3.8 Attempted synthesis of N^2-hydroxyethyl-6-chloro-2,4-diamino-[1,3,5]-triazine *via* 2-hydroxyethyl-amino-4,6-dichloro-[1,3,5]-triazine (65):

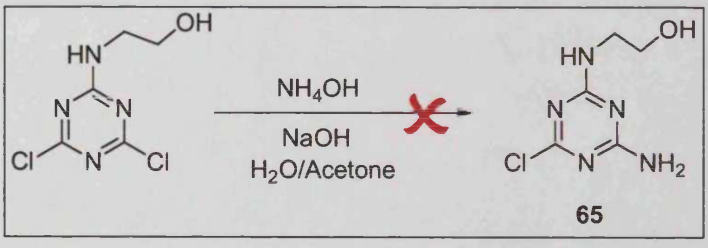

2-hydroxyethylamino-4,6-dichloro-[1,3,5]-triazine (1g, 4.76 mmol) was dissolved in acetone (12 mL) and then poured into ice-water (15 mL) to get a very fine suspension that become a solution after few min. The solution was left stirring at -5÷-10°C for 10 min and then NH_4OH 1N (5 mL, 4.76 mmol) was added dropwise followed by the addition of NaOH 2N (5mL, 10 mmol) carefully maintaining the temperature below 0°C. After 45

min the solution turned into a suspension and the temperature was left to rise to room temperature. The precipitate was filtered off and dried over high vacuum giving 516 mg of white solid. MS analysis as well as the NMR analysis did not show any peak corresponding to the expected product. The solvent from the solution after the wash was partially concentrated under vacuum and Et_2O was added giving the formation of a precipitate. The solid was filtered off and dried over high vacuum giving 128 mg of product. NMR analysis of the product was difficult to perform due to solubility problems. MS analysis showed weak signals and only a strong one corresponding to the starting material. The experiment was therefore performed using the alternative route described in the following procedure.

8.3.9 Synthesis of N^2-hydroxyethyl-6-chloro-2,4-diamino-[1,3,5]-triazine (65) via cyanuric chloride:

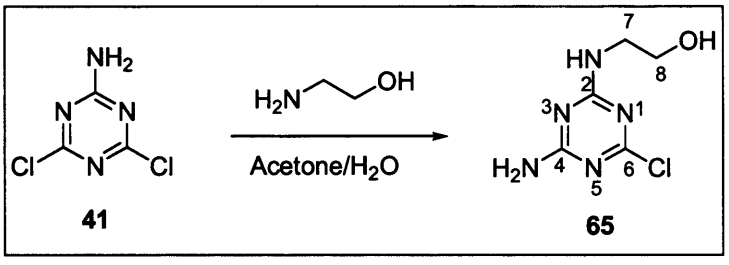

8.3.9.1 Attempted synthesis: Method A

2-amino-4,6-dichloro-[1,3,5]-triazine (400 mg, 2.42 mmol) was dissolved/suspended in acetone (5 mL) and then poured into ice-water (6 mL) to get a very fine suspension. Ethanolamine (147.8 mg, d= 1.012, 0.15 mL, 2.42 mmol) was added dropwise followed by the addition of NaOH 2N (1.21 mL, 2.42 mmol) maintaining the temperature below 5°C. The precipitate was filtered off, washed with cold water (2 x 10 mL) and cold EtOH (2 x 10 mL) and dried under high vacuum giving 322 mg of a white solid. TLC-RP (H_20/CH_3CN = 50/50) analysis showed only a weak spot of a new product and MS analysis did not show any peak corresponding to the expected product. ^{13}C-NMR showed the presence of extra peaks leading to the conclusion that a complex mixture of insoluble products was formed.

8.3.9.2 Synthesis: Method B

2-amino-6-chloro-[1,3,5]-triazine (200 mg, 1.21 mmol) was dissolved/suspended in acetone (2.5 mL) and then poured into ice-water (2.5 mL) to get a very fine suspension. NaOH 2N was added dropwise until pH=10÷11 carefully maintaining the temperature below 5°C. Ethanolamine (73.9 mg, d= 1.012, 0.075 mL, 1.21 mmol) was added dropwise and the mixture was left stirring for 30 min at 0°C and for further 2 hrs at room temperature. TLC-RP (H_20/CH_3CN = 50/50) analysis showed the formation of a new product with higher rf compared to the starting material. The precipitate was filtered off, washed with cold water (2 x 10 mL) and dried under high vacuum giving 172 mg of white solid. The ^{13}C-NMR performed at 100°C showed that the extra signals observed on the previous experiment were removed and were due to a splitting of the signals of the carbons. The product was used for the preparation of the corresponding hydrazine derivative.

Yield: 75%

^{1}H-NMR (DMSO-d6, 500 MHz): δ 3.28 (ddt, 2H, J_{8-9}= 6.14 Hz, J_{8-10}=5.54Hz, J_{8-7}=5.74Hz, H-C8), 3.49 (ddt, 2H, J_{9-8}= 6.14 Hz, J_{9-10}=5.54Hz, J_{9-7}=5.74Hz, H-C9) 4.70 (tt, 1H, J=5.54 Hz, OH), 7.00-7.30 (bm, 2H, 2 H-N2), 7.50 (2t, 1H, J=5.74Hz, H-N7).

^{13}C-NMR (DMSO-d6, 75 MHz): δ 42.7 (C8*), 42.8 (C8), 59.3 (C9), 59.5 (C9*), 165.7 (C6), 165.8 (C6*), 166.4 (C2*), 166.9 (C2), 168.0 (C4), 168.7 (C4*).

^{13}C-NMR, 100°C (DMSO-d6, 125 MHz): δ 45.1 (C8), 61.6 (C9), 168.1 (C6), 169.0 (C2), 170.4 (C4).

8.3.10 Preparation of 2-N-{[3-(*t*-butyl-diphenylsilyl)-oxy]-ethyl}-6-chloro-(2,4-diamino)-[1,3,5]-triazine

8.3.10.1 Synthesis of 2-N-[3-(t-butyl-diphenylsilyl)-oxy]-ethylamine (67)

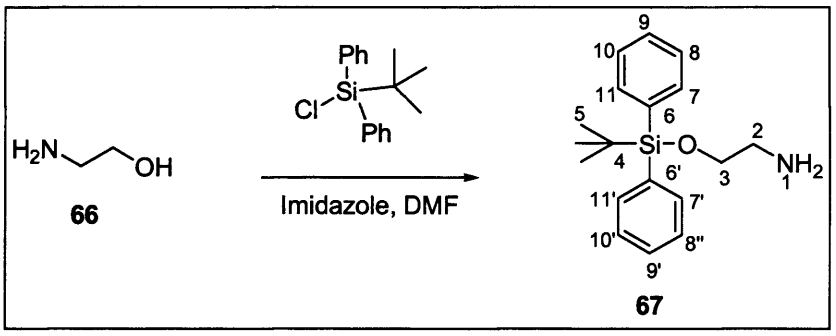

Imidazol (8.86 g 98%, 127.68 mmol), *tert*-butyl-chlorodiphenyl-silane (TBDPS) (16.53 g 98%, d=1.568, 10.54 mL, 58.93 mmol) were mixed together and dissolved in anhydrous DMF (20 mL) and **66** (3 g, 49.11 mmol) was added dropwise to the solution with stirring and under nitrogen. The mixture was left stirring at room temperature overnight until complete reaction. The solvent was removed under vacuum and the crude oil was purified by flash chromatography eluting with DCM / MeOH/NH_4OH (100:0:0 to 98:2:2) to give 7.6 g of pure product as a yellow oil.

Yield: 52%

LRMS (ES^+):m/z = 314.1 ($(M+H)^+$, 100%), 598.9 ($(2M+H)^+$, 50%).

^{1}H-NMR ($CDCl_3$, 300 MHz) δ 1.07 (s, 9H, H-C5), 1.70 (bs, 2H, NH_2), 2.81 (t, 2H, *J*= 5.32 Hz, H-C2), 3.68 (t, 2H, *J*= 5.32 Hz, H-C3), 7.41 (m, 6H, H-C8,10, H-C9, H-C8',10', H-C9'), 7.69 (m, 4H, H-C7,11, H-C7',11').

^{13}C-NMR ($CDCl_3$, 75 MHz) δ 19.7 (C4), 27.3 (C5), 44.7 (C2), 66.6 (C3), 128.1 (C8,8',10,10'), 130.1 (C9,9'), 134.1 (C6,6'), 135.9 (C7,7',11,11')

8.3.10.2 Synthesis of 2-N-{[3-(*t*-butyl-diphenylsilyl)-oxy]-ethyl}-6-chloro-(2,4-diamino)-[1,3,5]-triazine (68)

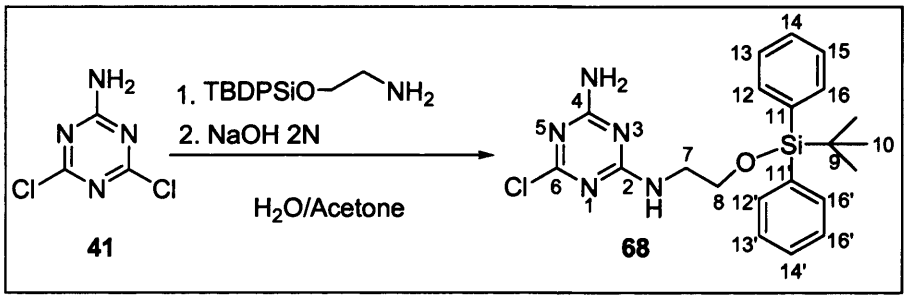

2-amino-4,6-dichloro-triazine (270 mg, 1.64 mmol) was dissolved in acetone (3.5 mL) and poured into 5 mL of water to form a very fine suspension. 3-[(*t*-butyl-diphenylsilyl)-oxy]-ethylamine was dissolved in water (1.5 mL) and was added dropwise to the suspension followed by the addition of NaOH 2N (0.9 mL, 1.8 mmol). The temperature during the addition was maintained on the range 0°C/5°C. The mixture was left stirring for 30 min at 0°C and for further 1.30 hr at room temperature. The precipitate was filtered off, washed with MeOH and dried over P_2O_5 giving 245 mg of a white pure solid.

Yield: 35%

mp: 95-97 °C

^{1}H-NMR (DMSO-d6, 300 MHz) δ 0.98 (s, 9H, H-C10), 3.46 (t, 2H, *J*= 5.59 Hz, H-C7), 3.71 (m, 2H, *J*= 5.59 Hz, H-C8), 7.10-7.80 (3m, 3H, 2 H-N4, H-N2), 7.42 (m, 6H, H-C13,15, H-C14, H-C13',15', H-C14'), 7.61 (m, 4H, H-C12,16, H-C12',16').

^{13}C-NMR (DMSO-d6, 75 MHz) δ 19.1 (C9), 26.59 (C10), 42.5 (C7*), 42.6 (C7), 62.3 (C8), 62.6 (C8*), 128.2 (C_{meta}), 130.1 (C_{para}), 133.4 (C11 and 11'), 135.4 (C_{orto}), 166.3 (C6), 166.5 (C6*), 166.9 (C4*), 167.0 (C4), 168.5 (C2).

8.3.11 Preparation of 2-N-{[3-(*t*-butyl-diphenylsilyl)-oxy]-propyl}-6-chloro-(2,4-diamino)-[1,3,5]-triazine

8.3.11.1 Synthesis of 2-N-[3-(t-butyl-diphenylsilyl)-oxy]-propylamine (73)

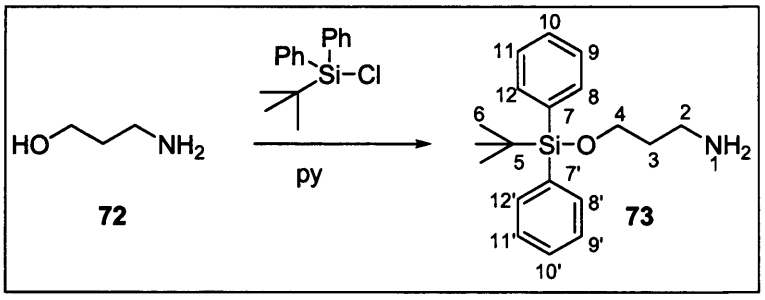

3-amino-1-propanol (1.2 g, 97%, 15.4 mmol) was dissolved in anhydrous pyridine (7mL) and TBDP chloride (5.11 g 98%, d= 1.074, 4.75 mL, 18.58 mmol) was slowly added to the solution. The mixture was stirred overnight at room temperature and under nitrogen. The mixture was then concentrated under reduced pressure and the crude oil was purified by flash chromatography eluting with DCM/MeOH (100:0 to 90:10) to give 4.1 g of pure product.

Yield: 84%

mp: 119-120 °C

LRMS (CI^+): m/z 314.1 ($(M+H)^+$, 100%).

^{1}H-NMR ($CDCl_3$, 500 MHz) δ 1.08 (s, 9H, H-C6), 2.05 (m, 2H, H-C2), 3.22 (t, 2H, *J*= 7.52 Hz, H-C2), 3.77 (t, 2H, *J*= 5.42 Hz, H-C4), 7.41 (m, 6H, H-C9,11, H-C10, H-C9',11', H-C10'), 7.69 (m, 4H, H-C8,12, H-C8',12').

^{13}C-NMR ($CDCl_3$, 125 MHz) δ 19.2 (C5), 26.9 (C6), 30.6 (C3), 30.0 (C2), 61.2 (C4), 127.8 (C9,9',11,11'), 129.8 (C10,10'), 133.1 (C7,7'), 135.5 (C8,8',12,12')

8.3.11.2 Synthesis of 2-N-{[3-(*t*-butyl-diphenylsilyl)-oxy]-propyl}-6-chloro-(2,4-diamino)-[1,3,5]-triazine (74)

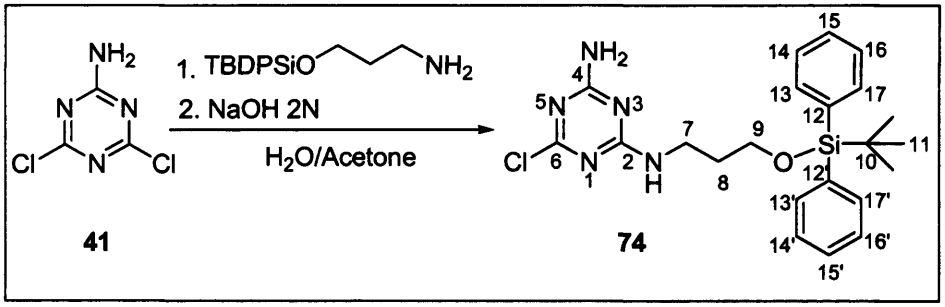

2-amino-4,6-dichloro-triazine (500 mg, 3.03 mmol) was dissolved in acetone (8 mL) and poured into 10 mL of water to form a very fine suspension. 3-[(*t*-butyl-diphenylsilyl)-oxy]-propylamine was dissolved in water (2 mL) and was added dropwise to the suspension followed by the addition of NaOH 2N (1.5 mL, 3.6 mmol). The temperature during the addition was maintained on the range 0°C/5°C. The mixture was left stirring for 30 min at 0°C and then left stirring overnight at room temperature. The precipitate was filtered off, washed with water and dried over P_2O_5 giving 604 mg of a white pure solid.

Yield: 45%

mp: 132-134 °C

LRMS (CI^+) m/z = 442.3 ($(M+H)^+$, 70%), 444.3 ($(M+H+^{37}Cl)^+$, 25%).

^{1}H-NMR (DMSO-d6, 500 MHz) δ 0.99 (s, 9H, H-C11), 1.77 (quintuplet, 2H, *J*= 6.61 Hz, H-C8), 3.34 (m, 2H, H-C7), 3.70 (m, 2H, H-C9), 7.00-7.53 (3m, 2H, 2 H-N4), 7.43 (m, 6H, H-C14,16, H-C15, H-C14',16', H-C15'), 7.61 (m, 4H, H-C13,17, H-C13',17'), 8.57 (m, 1H, H-N2).

^{13}C-NMR (DMSO-d6, 125 MHz) δ 18.7 (C10), 26.5 (C11*), 26.6 (C11), 31.3 (C8), 31.8 (C8*), 36.9 (C7*), 37.1 (C7), 61.1 (C9*), 61.3 (C9), 127.5 (C*meta**), 127.8 (C*meta*), 129.1 (C*para**), 129.7 (C*para*), 133.2 (12 and 12'), 134.4 (C*orto**) 134.9 (C*orto*), 165.6(C6), 166.4 (C6*), 166.9 (C4*), 168.0 (C4), 169.2 (C2).

8.3.12 Synthesis of N^2-hydroxypropy-6-chloro-2,4-diamino-[1,3,5]-triazine (79):

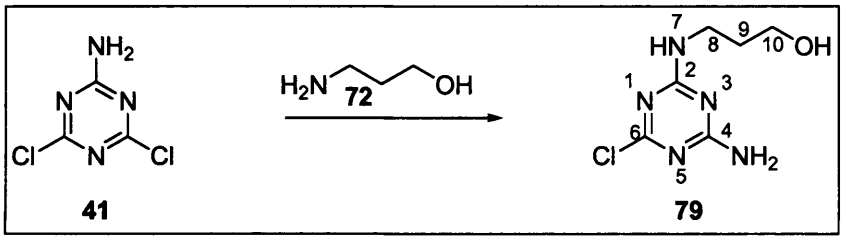

8.3.12.1 Attempted synthesis: Method A

2-amino-4,6-dichloro-[1,3,5]-triazine (500 mg, 3.03 mmol) was dissolved/suspended in acetone (6 mL) and then poured into ice-water (6 mL) to get a very fine suspension. 3-amino-propanol (234.6 mg, d= 0.986, 0.24 mL, 3.03 mmol) was added dropwise followed by the addition of NaOH 2N (2.3 mL, 4.54 mmol) carefully maintaining the temperature on the range 0÷-5°C. The mixture was left stirring for 30 min at 0÷-5°C and overnight at room temperature. The mixture (colloidal solution) was concentrate under vacuum and the solid triturated with water. The solid was then filtered, washed with water and dried under high vacuum giving 193 mg of a white product. The mass spectra analysis did not show any signal corresponding to the expected product. However the product was used for the preparation of the corresponding hydrazine derivative as described on § 8.4.12.1.

Yield: 31%

^{1}H-NMR (DMSO-d6, 300 MHz): δ 1.60 (m, 2H, H-C9), 3.23 (m, 2H, H-C8), 3.42 (m, 2H, H-C10) 4.47 (bs, 1H, OH), 6.00-7.40 (bm, 2H, 2 H-N2), 7.68 (2t, 1H, *J*=5.45 Hz, H-N7).

^{13}C-NMR (DMSO-d6, 125 MHz): 32.3 (C9*), 32.6 (C9), 37.8 (C8), 58.7 (C10), 165.9 (C6), 166.7 (C4*), 167.3 (C4), 168.4 (C2).

8.3.12.2 Attempted synthesis: Method B

2-amino-4,6-dichloro-[1,3,5]-triazine (1.2 mg, 7.2 mmol) was dissolved/suspended in acetone (15 mL) and then poured into ice-water

(15 mL) to get a very fine suspension. 3-amino-propanol (546 mg, d= 0.986, 0.55 mL, 7.2 mmol) was added dropwise followed by the addition of NaOH 2N (5.4 mL, 10.8 mmol). The mixture was left stirring for 3 hrs at room temperature, overnight at 50°C and for further 8 hrs at 70°C. TLC-RP (CH_3CN/H_2O = 50/50) showed still the presence of starting material. The solvent was removed under vacuum. The solid was washed with ice-water and dried under high vacuum giving 505 mg of white solid. NMR analysis showed together with the product the presence of starting material and other impurities.

8.3.12.3 Synthesis: Method C:

2-amino-4,6-dichloro-[1,3,5]-triazine (1.5 mg, 9.09 mmol) was dissolved in DMF (20 mL) at -20°C and 3-amino-propanol (690 mg 99%, d= 0.986, 0.69 mL, 9.09 mmol) was added dropwise to the solution maintaining the temperature around -20°C. DIPEA (Diisopropylethylamine) (1.76g 99.5%, d=0.742, 2.38mL, 13.6 mmol) was added dropwise to the previous mixture at -20°C. The temperature was left rise to room temperature and the reaction was left stirring for 2hrs. The solvent was removed under vacuum and the oil obtained was washed with DCM to give a lumpy white solid which was ground by using a pestle and mortar. The solid was dissolved in the minimum amount of DMF and then added dropwise DCM with stirring to get a fine precipitate. The fine white solid was filtered off, washed with DCM and dried under high vacuum at 40°C giving 1.68 g of a white product.

Yield: 91%

^{1}H-NMR (DMSO-d6, 500 MHz): δ 1.60 (quintuplet, 2H, J= 4.46 Hz, H-C9), 3.25 (quintuplet, 2H, J=6.46Hz, H-C8), 3.43 (t, 2H, J= 6.46 Hz, H-C10), 4.40 (bs, 1H, OH), 7.07-7.28 (bm, 2H, 2 H-N2), 7.55-769 (2t, 1H, *J*=5.50 Hz, H-N7).

^{13}C-NMR (DMSO-d6, 125 MHz): 31.9 (C9), 32.2 (C9*), 37.4 (C8), 37.5 (C8*), 58.3 (C10), 58.4 (C10*), 165.5 (C6), 166.9 (C2), 167.9 (C4).

8.4 Synthesis of diamino-[1,3,5]-triazin-2-yl hydrazines:

8.4.1 Synthesis of 4,6-diamino-[1,3,5]-triazin-2-yl-hydrazine (11):

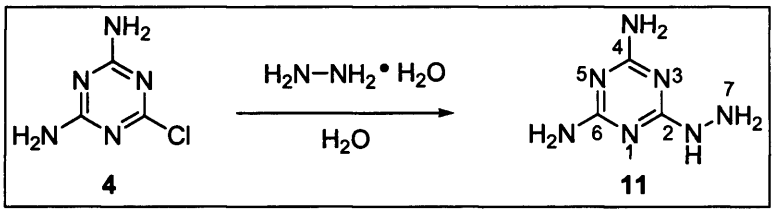

Hydrazine hydrate (4.32g, 4.2 mL, 86.4 mmol) was added dropwise to a suspension of 2,4-diamino-6-chloro-[1,3,5]-triazine (2.5g, 17.7 mmol) in water (20 mL). The mixture was stirred overnight at 85°C and then stopped. The white solid was filtered off and washed with 300 mL of water. The solid was then dried under high vacuum to give 1.78g of pure product.

Yield: 72%

mp: 271-272°C

LRMS (ES+):m/z 141.8 $[(M+H)^+$,30%], 163.9 $[(M+Na)^+$, 15%]

^{1}H-NMR (DMSO-d6, 300 MHz) δ 4.09 (bs, 2H, NH_2), 6.19 (bs, 4H, 2 H-N4 and 2 H-N6), 7.72 (bs, 1H, H-N2).

^{13}C-NMR (DMSO-d6, 75 MHz) δ 167.2 (C2), 168.8 (C4 and C6).

8.4.2 Synthesis of N^4-methyl-4,6-diamino-[1,3,5]-triazin-2-yl-hydrazine (50):

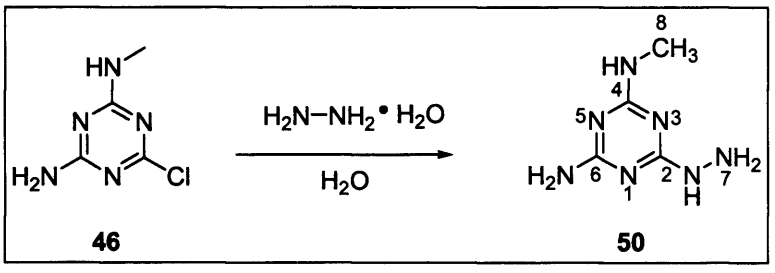

N^2-methyl-2,4-diamino-6-chloro-[1,3,5]-triazine (400 mg, 2.51 mmol) was suspended in water (5 mL) and hydrazine hydrate (d = 1.03, 0.61 mL, 12.55 mmol) was added dropwise in the suspension. The mixture was left

stirring for 1hr at room temperature and then overnight at 85 °C. The mixture was filtered off, washed with water (2 x 20 mL) and dried under high vacuum over P_2O_5 giving a 117 mg of a white pure solid.

Yield: 30%.

mp: 215-217°C.

LRMS (ES^+): m/z 156 ($(M+H)^+$, 90%)).

^{1}H NMR (DMSO-d6, 300 MHz) δ 2.72 (d, 3H, H-C8), 4.06 (bs, 2H), 6.38 (m, 3H) 7.71 (m, 1H, H-N2).

^{13}C NMR (DMSO-d6, 75 MHz) δ 27.5 (C8), 166.7 (C6), 168.4 (C2).

8.4.3 Synthesis of N^4,N^6-dimethyl-4,6-diamino-[1,3,5]-triazin-2-yl-hydrazine (48):

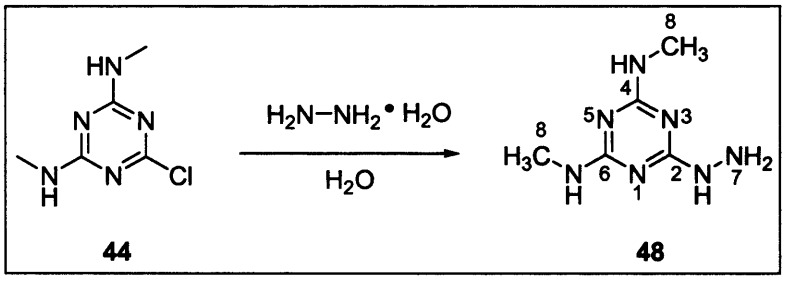

44 48

Hydrazine hydrate (0.7g, d=1.03, 0.68 mL, 13.9 mmol) was added dropwise to a suspension of N^2,N^4-dimethyl-6-chloro-2,4-diamino-[1,3,5]-triazine (500 mg, 2.88 mmol) in 10 mL of ethanol. The reaction mixture was stirred at 90 °C for 3 hours and at room temperature overnight. The solvent was evaporated and the white solid was washed with water (2x2mL), ethanol (2x2 mL) and ether (3x3mL). The compound was dried under high vacuum giving 470 mg of pure product.

Yield: 96%.

LRMS (ES^+) m/z 170 ($(M+H)^+$, 100%).

^{1}H-NMR (CD_3OD, 300 MHz,): δ 2.7 (s, 6H, H-C8), 4.05 (bs, 2H, 2 H-N7), 6.55 (bs, 2H, H-N4, H-N6), 7.65 (bt, 1H, H-N2).

^{13}C-NMR (CD_3OD, 75 MHz,): δ 27.5 (C8), 166.2 (C2), 168.0 (C4 and C6).

8.4.4 Synthesis of N^4,N^4-dimethyl-4,6-diamino-[1,3,5]-triazin-2-yl-hydrazine (51):

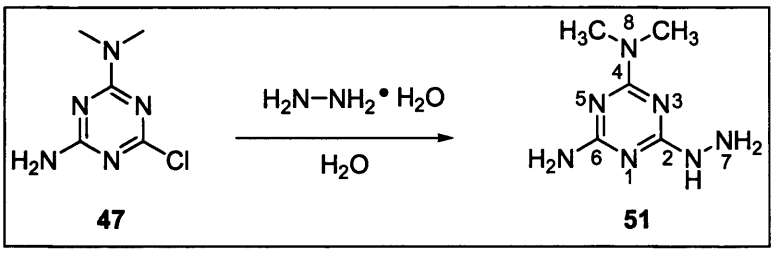

47 51

N^2,N^2-dimethyl-2,4-diamino-6-chloro-[1,3,5]-triazine (450 mg, 2.59 mmol) was suspended in water (5 mL) and hydrazine hydrate (d = 1.03, 0.63 mL, 12.95 mmol) was added dropwise in the suspension. The mixture was left stirring for 1hr at room temperature and overnight at 85 °C. The mixture was filtered off, washed with water (2 x 20 mL) and dried under high vacuum over P_2O_5 giving 280 mg of a white pure solid.

Yield: 64%.

LRMS (ES^+): m/z 170 ($(M+H)^+$, 100%).

mp: 230-232 °C.

^{1}H-NMR (DMSO-d6, 300 MHz) δ 3.02 (s, 6H, H-C8), 4.08 (bs, 2H, 2 H-N7), 6.46 (bs, 2H, 2 H-N6) 7.66 (s, 1H, H-N2).

^{13}C-NMR (DMSO-d6, 75 MHz) δ 35.9 (C8), 165.9 (C4), 166.9 (C2), 168.4 (C6).

8.4.5 Synthesis of N^4,N^4,N^6,N^6-tetramethyl-4,6-diamino-[1,3,5]-triazin-2-yl-hydrazine (49)

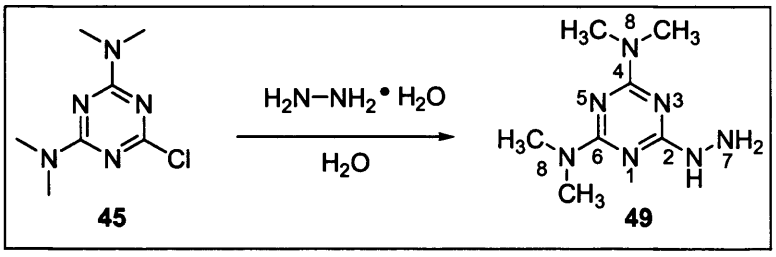

45 49

Hydrazine hydrate (0.302g, d=1.03, 0.29 mL, 6.3 mmol) was added dropwise to a solution of N^2,N^2,N^4,N^4-tetramethyl-2,4-diamino-6-chloro-

[1,3,5]-triazine (250 mg, 1.24 mmol) in 2 mL of ethanol. The reaction mixture was stirred at 85 °C for 3 hours. The solution was reduced under vacuum and the white solid was filtered off, washed with water (3x3mL) and dried under high vacuum giving 162 mg of a white pure solid.

Yield: 66%.

LRMS (ES^+): m/z 198 ($M+H^+$, 100%).

^{1}H-NMR (300 MHz, CD_3OD) δ 3.1 (s, 12H, H-C8).

^{13}C-NMR (75 MHz, CD_3OD): δ 36.7 (C8), 167 (C4 and C6), 170 (C2).

8.4.6 Synthesis of N^4-n-propyl-4,6-diamino-[1,3,5]-triazin-2-yl-hydrazine (59):

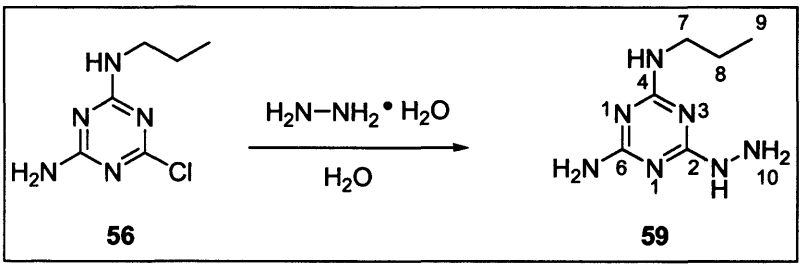

56 59

N^2-propyl-2,4-diamino-6-chloro-[1,3,5]-triazine (409 mg, 2.17 mmol) was suspended in water (8mL) and hydrazine hydrate (343.04 mg, d=1.03, 0.52 mL, 10.85 mmol) was added dropwise into the suspension at room temperature. The mixture was left stirring overnight at 85 °C. The precipitate was filtered and dried under high vacuum giving 282 mg of a white pure product.

Yield: 52%

mp: 109-111°C

LRMS (EI^+): m/z 183.1 (M^+, 40%).

^{1}H-NMR (DMSO-d6, 300 MHz) δ 0.85 (t, 3H, *J*=7.33 Hz, H-C9), 1.47 (m, 2H, H-C8), 3.14 (m, 2H, H-C7), 4.56 (bs, 2H, H-N10), 6.94-7.85 (3m, 3H, H-N4, H-N2, 2 H-N6).

^{13}C-NMR (DMSO-d6, 75 MHz) δ 8.7 (C9), 22.9 (C8), 23.0 (C8*), 41.9 (C7), 42.0 (C7*), 166.2 (C2), 166.7 (C6), 168.5 (C4).

8.4.7 Synthesis of N^4-n-butyl-4,6-diamino-[1,3,5]-triazin-2-yl-hydrazine (61):

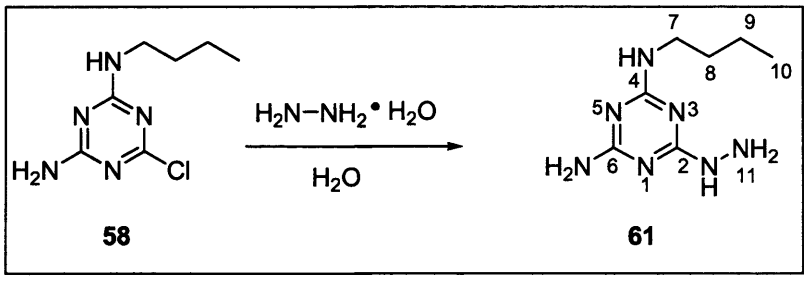

58 61

N^2-butyl-2,4-diamino-6-chloro-[1,3,5]-triazine (552 mg, 2.74 mmol) was suspended in water (10mL) and hydrazine hydrate (685.6 mg, d=1.03, 0.66 mL, 13.7 mmol) was added dropwise into the suspension at room temperature. The mixture was left stirring overnight at 85 °C. The precipitate was filtered and dried under high vacuum giving 281 mg of a white pure product.

Yield: 52%

mp: 114-117 °C

LRMS (CI^+): m/z 198.2 ($(M+H)^+$, 40%).

^{1}H-NMR (DMSO-d6, 300 MHz) δ 0.86 (t, 3H, *J*=6.99 Hz, H-C10), 1.28 (sextet, 2H, *J*=6.99 Hz, H-C9), 1.43 (m, 2H, H-C8), 3.18 (m, 2H, H-C7), 4.29 (bs, 2H, H-N11), 6.95-7.93 (3m, 3H, H-N4, H-N2, 2 H-N6).

^{13}C-NMR (DMSO-d6, 75 MHz) δ 14.2 (C10), 19.9 (C9), 31.9 (C8), 39.9 (C7), 166.2 (C2), 168.4 (C4).

8.4.8. Preparation of N^4-isopropyl-4,6-diamino-[1,3,5]-triazin-2-yl-hydrazine (60):

8.4.8.1 Attempted synthesis:

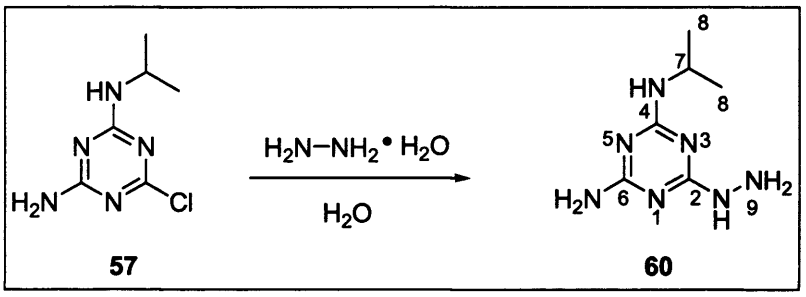

57 60

Crude N^2-isopropyl-2,4-diamino-6-chloro-[1,3,5]-triazine (250 mg, 1.33 mmol) was suspended in water (5mL) and hydrazine hydrate (335.8 mg, d=1.03, 0.33 mL, 6.65 mmol) was added dropwise into the suspension at room temperature. The mixture was left stirring overnight at 85 °C. The precipitate was filtered and dried under high vacuum giving 53 mg of crude product. The MS did not show any peak corresponding to the product and 1H-NMR. However the product was used as crude for the preparation of the corresponding 5-nitrofuraldehyde hydrazone.

8.4.8.2 Synthesis:

Pure N^2-isopropyl-2,4-diamino-6-chloro-[1,3,5]-triazine from Aldrich (750 mg, 3.99 mmol) was dissolved in EtOH (9mL) and hydrazine hydrate (599 mg, d=1.03, 0.58 mL, 8.67 mmol) was added dropwise into the suspension at room temperature. The mixture was left stirring overnight at 85 °C. The solvent was removed under vacuum until the formation of white crystals. The solid was filtered off and washed with cold EtOH and dried over high vacuum giving 180 mg of pure product. The remaining solution was concentrated under high vacuum and EtOAc was added until the precipitation of further product. The solid was filtered off and dried over high vacuum giving 356 mg of pure product.

Yield: 73%

mp: 106-107 °C

LRMS (EI^+): m/z 183.0 (M^+, 20%).

^{1}H-NMR (D_2O, 300 MHz) δ 1.04 (d, 6H, *J*=6.40 Hz, H-C8), 3.85 (septuplet, 1H, *J*=6.40 Hz, H-C7).

^{13}C-NMR (D_2O, 75 MHz) δ 22.2 (C8), 42.5 (C7), 164.6.

8.4.9 Synthesis of N^4-hydroxyethyl-4,6-diamino-[1,3,5]-triazin-2-yl-hydrazine (68):

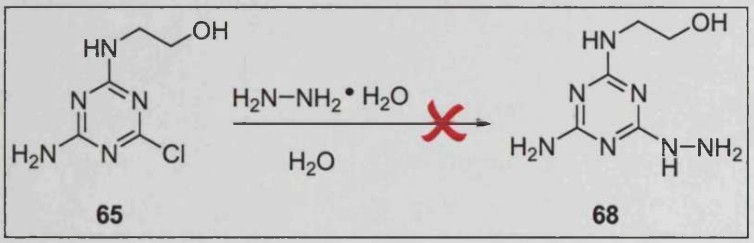

N^2-hydroxyethyl-6-chloro-2,4-diamino-[1,3,5]-triazine (200 mg, 1.05 mmol) was suspended in water (3.5mL) and hydrazine hydrate was added dropwise to the mixture at room temperature and with stirring. The reaction was left stirring for 6 hrs at 85°C and then left cooling down to room temperature. TLC-RP (H_2O/CH_3CN = 50/50) analysis showed the formation of a new product together with the starting material. The suspension was filtered and the precipitate was washed with cold H_2O and dried under high vacuum giving 115 mg of white solid. The product, unlike the starting material, was soluble in MeOH but the MS analysis gave only a weak peak with small intensity corresponding to the expected product together with a strong peak corresponding to the starting material (226= starting material+K^+). The attempt to purify the product failed and therefore the crude product was used for the preparation of the corresponding hydrazone.

8.4.10 Synthesis of 2N-{[3-(*t*-butyl-diphenylsilyl)-oxy]-ethyl}-(4,6-diamino)-[1,3,5]-triazin-2-yl-hydrazine (69):

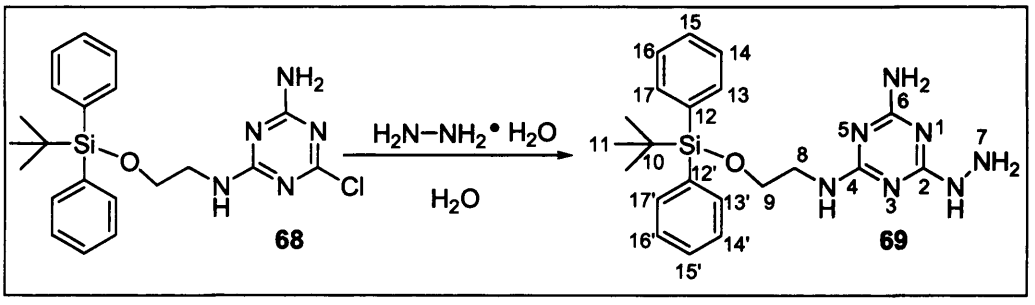

2N-{[3-(*t*-butyl-diphenylsilyl)-oxy]-ethyl}-6-chloro-(2,4-diamino)-[1,3,5] - triazine (235 mg, 0.55 mmol) was suspended in water (3.5 mL) and hydrazine hydrate (138 mg, d=1.03, 0.13 mL, 2.75 mmol) was added dropwise to the suspension. The mixture was left stirring overnight at 75°C. The product was then filtered, washed with water and dried under high vacuum over P_2O_5 giving 200 mg of a white pure product.

Yield: 86%

mp: 80-82 °C

LRMS (ES^+): m/z 424.1 ($(M+H)^+$, 100%),

^{1}H-NMR (DMSO-d6, 300 MHz) δ 0.96 (s, 9H, H-C11), 3.45 (m, 2H, H-C8), 3.71 (m, 2H, H-C9), 6.20-7.20 (3m, 3H, H-N4, 2H-N6), 7.43 (m, 6H, H-C14,16, H-C15, H-C14',16', H-C15'), 7.62 (m, 4H, H-C13,17, H-C13',17'), 7.69 (m, 1H, H-N2).

^{13}C-NMR (DMSO-d6, 75 MHz) δ 19.1 (C10), 26.9 (C11*), 27.0 (C11), 42.4 (C8), 42.6 (C8*), 62.3 (C9), 62.6 (C9*), 128.1 (C_{meta}*), 128.2 (C_{meta}), 130.1 (C_{para}), 133.4 (12 and 12'), 135.4 (C_{orto}), 166.2 (C4).

8.4.11 Synthesis of 2N-{[3-(*t*-butyl-diphenylsilyl)-oxy]-propyl}-(4,6-diamino)-[1,3,5]-triazin-2-yl-hydrazine (75):

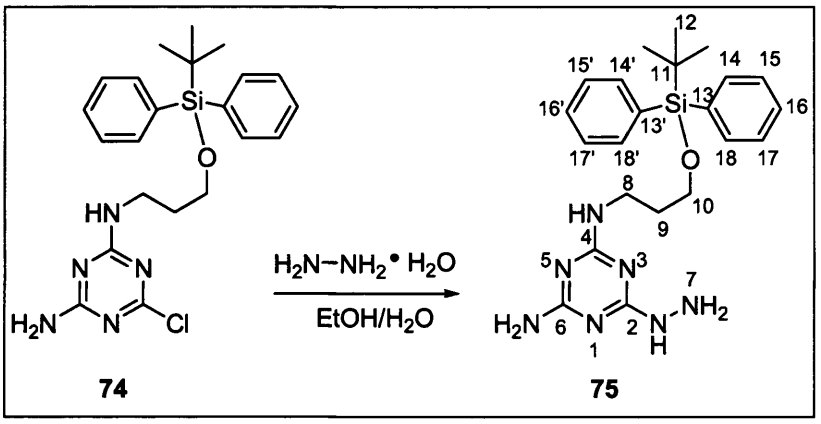

74 **75**

2N-{[3-(*t*-butyl-diphenylsilyl)-oxy]-propyl}-6-chloro-(2,4-diamino)-[1,3,5] -triazine (550 mg, 1.24 mmol) was suspended in EtOH (7 mL) and hydrazine hydrate (186.2 mg, d=1.03, 0.18 mL, 3.72mmol) was added dropwise to the suspension. The mixture was left stirring overnight at 75°C. The product was then filtered, washed with EtOH and water and dried under high vacuum over P_2O_5 giving 281 mg of a white pure product.

Yield: 52%

mp: 234-237 °C

LRMS (CI^+): m/z 438.4 ($(M+H)^+$, 40%),

^{1}H-NMR (DMSO-d6, 500 MHz) δ 0.99 (s, 9H, H-C12), 1.77 (quintuplet, 2H, *J*= 6.30 Hz, H-C9), 3.35 (m, 2H, H-C8), 3.70 (t, 2H, *J*= 6.30 Hz, H-C10), 4.08 (bs, 2H, 2 H-N7), 5.98-6.57 (3m, 3H, H-N4, 2 H-N6), 7.44 (m, 6H, H-C15,17, H-C16, H-C15',17', H-C16'), 7.62 (m, 4H, H-C14,18, H-C14',18'), 7.69 (m, 1H, H-N2).

^{13}C-NMR (DMSO-d6, 125 MHz) δ 18.7 (C11), 26.5 (C12*), 26.6 (C12), 32.2 (C9), 36.9 (C8), 61.7 (C10), 127.5 (C_{meta}*), 127.8 (C_{meta}), 129.1 (C_{para}*), 129.7 (C_{para}), 133.3 (13 and 13'), 134.4 (C_{orto}*) 135.0 (C_{orto}), 167.9 (C4).

8.4.12 Synthesis of N^4-hydroxypropyl-4,6-diamino-[1,3,5]-triazin-2-yl-hydrazine (80):

8.4.12.1 Synthesis method A:

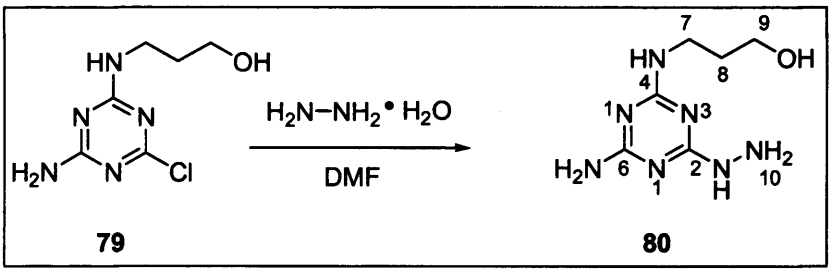

79 80

N^2-hydroxypropyl-6-chloro-2,4-diamino-[1,3,5]-triazine (180 mg, 0.88 mmol) was suspended in water (3 mL) and hydrazine hydrate (220.2 mg, d=1.03, 0.21 mL, 4.4 mmol) was added dropwise to the suspension at room temperature and with stirring. The mixture was left stirring overnight at 85°C and then left cooling down to room temperature. The solution was concentrated under vacuum and the white solid was washed with cold water and dried under high vacuum giving 230 mg of a crude solid.

LRMS (ES^+): m/z 200.1 ($(M+H)^+$, 50%).

^{1}H-NMR (DMSO-d6, 300 MHz): δ 1.63 (m, 2H, H-C8), 3.27 (m, 2H, H-C7), 3.43 (t, 2H, J= 6.10 Hz, H-C9), 5.70-6.70 (bm, 4H, 2 H-N6, H-N2, H-N4).

^{13}C-NMR (DMSO-d6, 75 MHz): 32.9 (C8), 37.4 (C7), 58.3 (C9), 166.2 (C2).

8.4.12.2 Synthesis method B:

N^2-hydroxypropyl-6-chloro-2,4-diamino-[1,3,5]-triazine (400 mg, 1.96 mmol) was dissolved in DMF (6 mL) and hydrazine hydrate (196.2 mg, d=1.03, 0.19 mL, 3.92 mmol) was added dropwise to the solution at room temperature and with stirring. The mixture was left stirring for 3 hrs at 85°C and then left cooling down to room temperature. The solution was concentrated under vacuum and the white solid was washed with cold water and dried under high vacuum giving 390 mg of crude solid. NMR analysis of the crude in D_2O showed deuterium exchange with some of the

NH group of the triazine and the presence of DMF that could not be removed due to solubility of the product in H_2O.

^{1}H-NMR (D_2O, 500 MHz): δ 1.75 (m, 2H, H-C8), 3.05 (bs, 2H, 2 H-N10), 3.36 (m, 2H, H-C7), 3.60 (m, 2H, H-C9), 8.0 (bm, 1H, H-N, D-exchange)

^{13}C-NMR (D2O, 125 MHz): 31.4 (C8), 37.2 (C7), 37.3 (C7*), 59.0 (C9), 59.1 (C9*), 162.4 (C2), 162.7 (C2*), 168.9 (C4).

8.5 Synthesis of triazinyl-hydrazones:

8.5.1 Synthesis of 5-nitro-2 furaldehyde (4,6-diamino)-[1,3,5]-triazin-2-yl-hydrazone (6):

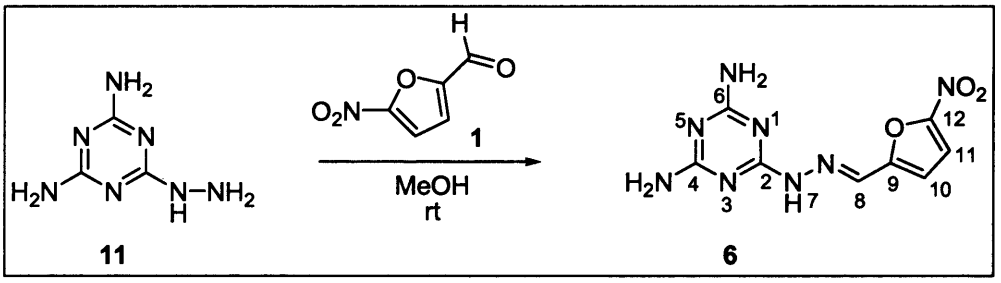

A mixture of 2-hydrazino-4,6-diamino-1,3,5-triazine (149.50 mg, 1.06 mmol) and 5-nitrofuraldehyde (150.00 mg, 1.06mmol) was dissolved in methanol (5 mL). The suspension was left stirring overnight at room temperature. The reaction mixture was filtered and the yellow precipitate was washed with methanol and dried under vacuum at 40°C. The crude product was recrystallised from water to yield 100.5 mg of a pure yellow solid.

Yield: 36%.

mp: >350°C

IR: νN–H =3313.9 cm-1, νC=N at 1631.9 cm-1, νC–NO_2 at 1537.8 cm-1, νC–N at 809.3.

LRMS (ES+): m/z 265 ($(M+H)^+$, 100%), 287 ($M+Na^+$, 80%).

HRMS (ES+): Calcd for $C_8H_9N_8O_3^+$ ($M+H^+$): 265.0792; Found: 265.0799.

Anal. Calcd for $C_8H_9N_7O{\cdot}2H_2O$: C, 37.6, H 5.1, N, 38.4. Found: C, 37.3, H, 4.0, N, 38.7.

^{1}H-NMR (DMSO-d6, 300 MHz) δ 6.51 (bs, 4H, 2 NH_2), 7.05 (d, J= 3.84 Hz, 1H, H-C10) 7.78 (d, J= 3.84 Hz, 1H, H-C11), 8.00 (s, 1H, H-C8), 11.25 (s, 1H, H-N7).

^{13}C-NMR (DMSO-d6, 75 MHz) δ 114.2 (C-11) , 115.6 (C-10), 129.4 (C-8), 151.8 (C-9), 153.2 (C-12), 164.9 (C-4 and C-6), 167.7 (C-2).

8.5.2 Synthesis of 5-Nitro-thiophen-2-carbaldehyde (4,6-diamino)-[1,3,5]-triazin-2-yl-hydrazone (13):

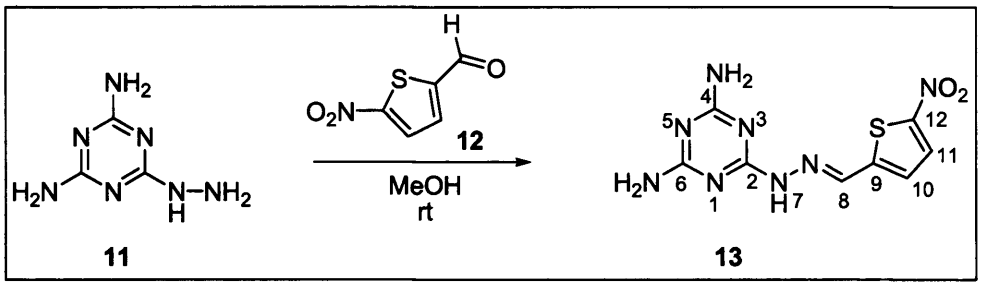

A mixture of 2-hydrazino-4,6-diamino-1,3,5-triazine (150 mg, 1.06 mmol) and 5-nitro-2-thiophene-carboxaldehyde (166.58 mg, 1.06 mmol) was suspended in methanol (5 mL). The suspension was left stirring for two days at room temperature. The reaction mixture was filtered and the brown precipitate was washed with MeOH and then dried under vacuum at 40°C. The crude product was recrystallised from H_2O/EtOH (5:1) to give 76mg of a pure brown solid.

Yield: 25%.

mp: >350°C.

LRMS (ES+): m/z 281 ($(M+H)^+$, 100%), 303 ($(M+Na)^+$, 10%).

HRMS (ES+): calcd mass for $C_8H_9N_8O_2S^+$ ($M+H^+$): 281.0569. Found: 281.0572.

Anal. Calcd for $C_8H_8N_8O_2S \cdot 1H_2O$: C, 32.2, H, 3.4, N, 37.6, S, 10.7. Found: C, 32.7, H, 2.9, N, 35.9, S, 10.3.

^{1}H-NMR (DMSO-d6, 300 MHz) δ 6.50 (bs, 4H, 2 x NH_2), 7.36 (d, J= 4.29 Hz, 1H, H-C10), 8.08 (d, J= 4.29 Hz, 1H, H-C11), 8.25 (s, 1H, H-C8), 11.10 (s, 1H, H-N7).

^{13}C-NMR (DMSO-d6, 75 MHz) δ 127.6 (C11), 131.1 (C10), 134.9 (C8), 148.7 (C9), 149.7 (C12), 164.8 (C4 and C6), 167.6 (C2).

8.5.3 Synthesis of 2-furaldehyde (4,6-diamino)-[1,3,5]-triazin-2-yl-hydrazone (19):

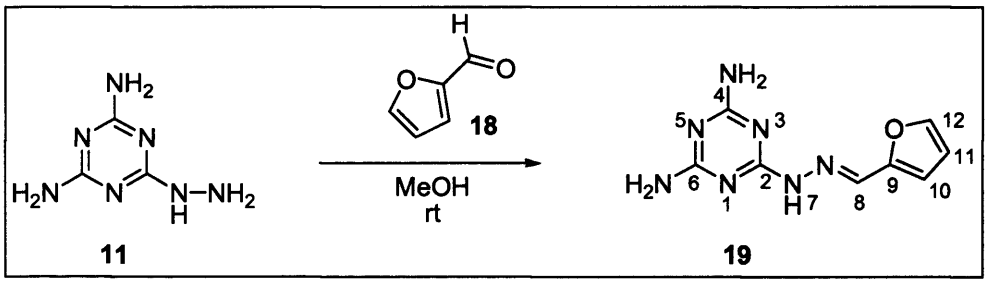

A mixture of 2-hydrazino-4,6-diamino-1,3,5-triazine (150 mg, 1.06 mmol) and 2-furaldehyde (102.88 mg, 1.06 mmol) was suspended in MeOH (5 mL). The suspension was left stirring overnight at room temperature. The mixture was filtered and the brown solid was washed with MeOH and then dried under vacuum at 40°C. The crude product was recrystallised from H_2O/MeOH (5%) to give 133 mg of a pure brown solid.

Yield: 58%.

mp: 281-283 °C.

LRMS (ES+): m/z 219 $((M+H)^+$, 241,9 $(M+Na)^+)$.

HRMS: Calcd mass for $C_8H_{10}N_7O^+$ $(M+H^+)$: 220.0941. Found: 220.0941.

Anal. Calcd for $C_8H_9N_7O{\cdot}2H_2O$: C, 37.6, H 5.1, N, 38.4. Found: C, 37.3, H, 4.0, N, 38.7.

^{1}H-NMR (DMSO-d6, 300 MHz) δ 6.38 (bs, 4H, 2 x NH2), 6.57 (m, 1H, H-C12), 6.69 (d, J= 3.29 Hz, 1H, H-C11), 7.76 (m, 1H, H-C10), 7.94 (m, 1H, H-C8), 10.56 (s, H-N7).

^{13}C-NMR (DMSO-d6, 75 MHz) δ 111,5 (C-11), 112.2 (C-10), 131.8 (C-8), 144.3 (C-12), 150.5 (C-9), 165.0 (C-4 and C-6), 167.7 (C-2).

8.5.4 Synthesis of Thiophen-2-carbaldehyde (4,6-diamino)-[1,3,5]-triazin-2-yl-hydrazone (21):

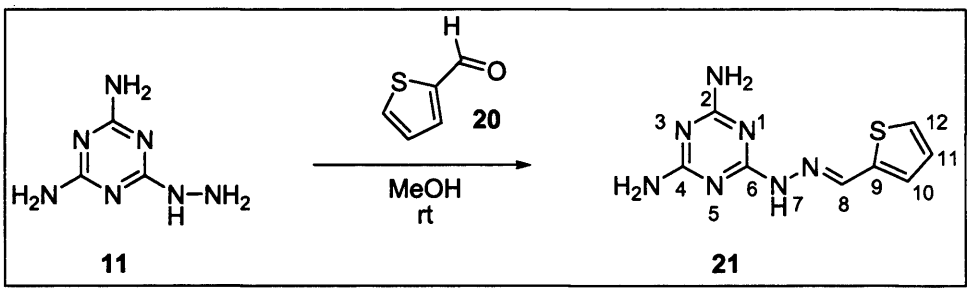

A mixture of 2-hydrazino-4,6-diamino-1,3,5-triazine (150 mg, 1.06 mmol) and 2-thiophene-carboxaldehyde (121.31 mg, 1.06 mmol) was suspended in methanol (5 mL). The suspension was left stirring overnight at room temperature. The mixture was filtered and the brown solid was washed with methanol and dried under vacuum at 40°C. The crude product was recrystallised from water-ethanol (10%) to give 95 mg of a pure brown-yellow solid.

Yield: 38%.

mp: 309-310°C.

LRMS (ES+): m/z 236 ($(M+H)^+$, 100%).

HRMS (ES+): calcd mass for $C_8H_{10}N_7S^+$ ($M+H^+$): 236.0713. Found: 236.0717.

Anal. Calcd for $C_8H_9N_7S \cdot 0.7H_2O$; C, 38.8, H, 4.2, N, 39.5, S, 12.9. Found: C, 39.0, H, 3.9, N, 39.1, S, 12.5.

^{1}H-NMR (DMSO-d6, 300 MHz) δ 6.38 (bs, 4H, 2 NH_2), 7.07 (s, 1H, H-C12), 7.25 (s, 1H, H-C11), 7.53 (s, 1H, H-C10), 8.25 (s, 1H, H-C8), 10.53 (s, 1H, H-N7).

^{13}C-NMR (DMSO-d6, 75 MHz) δ 127.6 (C10), 127.9 (C11), 129.1 (C8), 137.3 (C9), 140.2 (C12), 164.9 (C2 and C4), 167.6 (C6).

8.5.5 Synthesis of 5-nitro-2 furaldehyde (N^4-methyl-4,6-diamino)-[1,3,5]-triazin-2-yl-hydrazone (54):

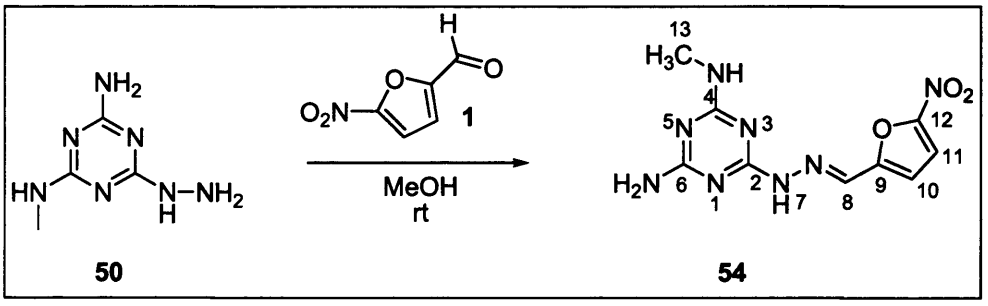

5-nitrofuraldehyde (90mg, 0.58 mmol) and 2-hydrazino-4-N-methyl-4,6-diamino-1,3,5-triazine (81.82 mg, 0.58 mmol) were mixed together, suspended in MeOH (5 mL) and the suspension was left stirring overnight. The mixture was reduced under vacuum giving 120 mg of brown solid. The solid was recrystallised from H_2O/MeOH (35 mL: 20 mL) giving 83 mg of a dark yellow solid.

Yield: 51%.

mp: 261-263°C.

LRMS (ES^+): m/z: 279.2 ($(M+H)^+$, 50%), 301.1 ($(M+Na)^+$, 100%).

HRMS: Calcd mass for $C_9H_{11}N_8O_3^+$ ($M+H^+$): 279.0949; Found: 279.0951.

Anal. Calcd. ($C_9H_{10}N_8O_3 \cdot 0.4\ H_2O \cdot 0.02$ HCl) C, H, Cl; calcd: N, 38.4. Found: N, 37.9.

^{1}H-NMR (DMSO-d6, 300 MHz) δ 2.77 (s, 3H, H-C13), 6.77 (bs, 3H, H-N4, 2H-N6), 7.07 (s, 1H, H-C10), 7.78 (d, J= 4.02 Hz, 1H, H-C11), 8.01 (s, 1H, H-C9), 11.10 (s, 1H, H-N7).

^{13}C-NMR (DMSO-d6, 75 MHz) δ 27.6 (C-15) , 114.0 (C-10), 115.6 (C-11), 129.5 (C-8), 151.8 (C-9), 153.3 (C-12), 166.9 (C-2).

8.5.6 Synthesis of 5-nitro-2 furaldehyde (N^4,N^6-dimethyl-4,6-diamino)-[1,3,5]-triazin-2-yl-hydrazone (55):

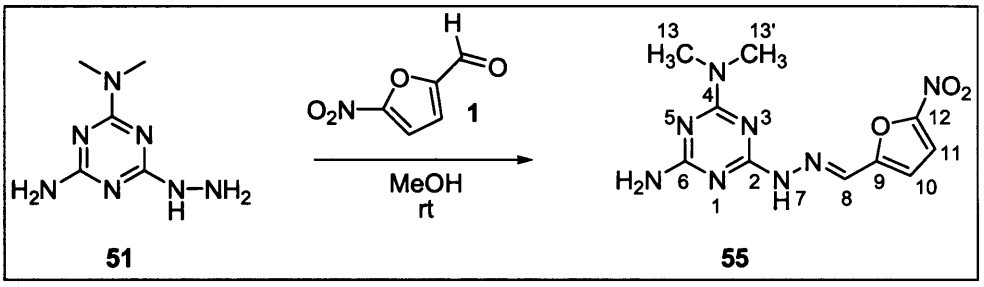

5-Nitrofuraldehyde (246 mg, 99%, 1.45 mmol) and 2-hydrazino-4-N,N-dimethyl-4,6-diamino-1,3,5-triazine (204.56 mg, 1.45 mmol) were suspended in MeOH (5 mL) and left stirring overnight. The mixture was reduced under vacuum giving 120 mg of brown solid. The solid was recrystallised from H_2O/MeOH (30 mL: 20 mL) giving 336 mg of a light brown solid.

Yield: 80%.

mp: 264-266°C

LRMS (ES^+): m/z 293.1 ($(M+H)^+$, 20%), 315.1 ($(M+Na)^+$, 100%).

HRMS: Calcd mass for $C_{10}H_{13}N_8O_3^+$ ($M+H^+$): 293.1105. Found: 293.1110.

Anal. Calcd for $C_{10}H_{12}N_8O_3 \cdot 0.02$ HCl: C, 41.0, H, 4.1, N, 38.2, Cl, 0.2; Found: C, 41.3, H, 4.2, N, 38.0, Cl, 0.5.

^{1}H-NMR (DMSO-d6, 300 MHz) δ 3.11 (s, 6H, H-C13 and H-C13'), 6.75 (bs, 2H, 2H-N6), 7.11 (d, 1H, J=3.84 Hz, H-C10), 7.82 (d, J= 3.84 Hz, 1H, H-C11), 8.08 (s, 1H, H-C8), 11.21 (s, 1H, H-N7).

^{13}C-NMR (DMSO-d6, 75 MHz) δ 36.1 (C-13 and C-13'), 113.8 (C-10), 115.6 (C-11), 129.4 (C-8), 151.8 (C-9), 153.4 (C-12), 164.5 (C-6), 166.0 (C-4), 167.5 (C-2).

8.5.7 Synthesis of 5-nitro-2 furaldehyde (N^4,N^6-dimethyl-4,6-diamino)-[1,3,5]-triazin-2-yl-hydrazone (52):

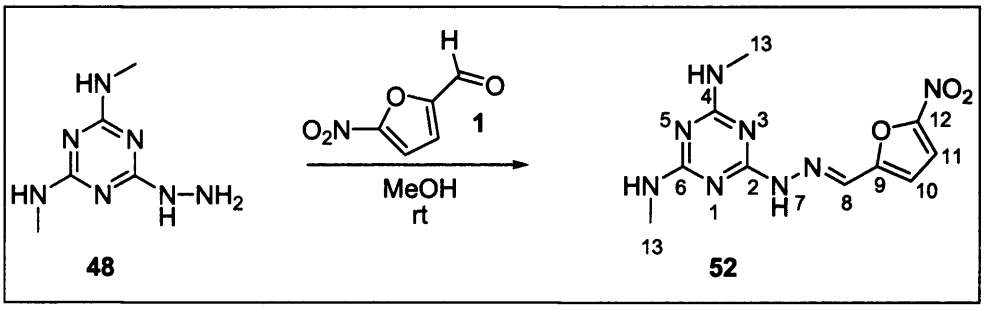

A mixture of N^4,N^4,N^6,N^6-tetramethyl-2,4-diamino)-[1,3,5]-triazin-2-yl-hydrazine (180 mg, 1.06 mmol) and 5-nitro-2-furaldehyde (150 mg, 1.06 mmol) was dissolved in 10 mL of EtOH. The reaction mixture was left stirring overnight at room temperature and the solvent was evaporated under vacuum. The yellow crude product was recrystallised by H_2O/MeOH giving 220 mg of yellow product.

Yield: 71%

mp: 258-260°C.

LRMS (ES^+): m/z 293.1 ($(M+H)^+$, 100%), 315.2 ($(M+Na)^+$, 20%).

HRMS: Calcd mass for $C_{10}H_{13}N_8O_3^+$ ($M+H^+$): 293.1105. Found: 293.1104.

Anal. Calcd for $C_{10}H_{12}N_8O_3 \cdot 0.4\ H_2O$; C, 40.1, H, 4.3, N, 37.4. Found C, 40.5, H, 4.1, N, 36.7.

^{1}H-NMR (DMSO-d6, 300 MHz) δ 2.70, 2.65 (2s, 6H, H-C13 and H-C13*), 6.60-7.23 (bm, 2H, H-N4, H-N6), 7.05 (s, 1H, H-C10), 7.78 (d, 1H, H-C11), 7.90,8.05 (2s, 1H, H-C8 and H-C8*), 11.06, 11.20 (2 bs, 1H, H-N7 and H-N7*).

^{13}C NMR (DMSO-d6, 75 MHz) δ 27.4 (C-13), 27.6 (C13*), 113.9 (C-10), 115.6 (C-11), 129.0 (C-8*), 129.4 (C-8), 151.8 (C-9), 153.3 (C12), 164.1 (C-2), 166.4 (C4* and C6*), 166.6 (C4 and C6).

8.5.8 Synthesis of 5-nitro-2 furaldehyde (N^4,N^4,N^6,N^6,-tetramethyl-4,6-diamino)-[1,3,5]-triazin-2-yl-hydrazone (53):

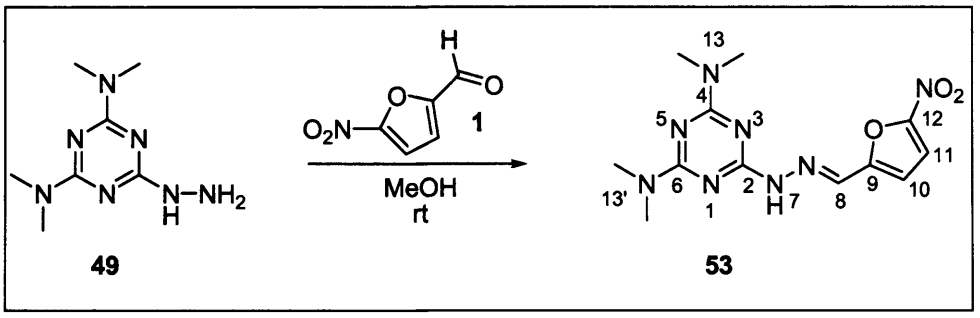

49 **53**

A mixture of N^4,N^4,N^6,N^6-tetramethyl-4,6-diamino-[1,3,5]-triazin-2-yl-hydrazin (201 mg, 1.01 mmol) and 5-nitro-2-furaldehyde (143 mg, 1.02 mmol) was dissolved in 10 mL of ethanol. The reaction mixture was allowed to stir overnight at room temperature and then the solvent was evaporated under vacuum. The residue was purified by column chromatography (1-5% MeOH/DCM) giving 187 mg of a white pure solid.

Yield:58%

HRMS: calcd mass for $C_{12}H_{17}N_8O_3^+$ ($M+H^+$): 321.1424, found: 321.1421.

^{1}H-NMR (DMSO-d6, 300 MHz) δ 3.21 (s, 12H), 7.04 (m, 1H), 7.44 (m, 1H), 7.92 (s, 1H), 9.05 (bs, 1H).

^{13}C-NMR (DMSO-d6, 75 MHz) δ 36.5 (C-13), 111.1 (C-10), 114.2 (C-11), 129.4 (C-8), 153.5 (C-9), 164.1 (C-2), 165.8 (C4 and C-6).

8.5.9 Synthesis of 4-nitro-benzaldehyde (4,6-diamino)-[1,3,5]-triazin-2-yl-hydrazone (15):

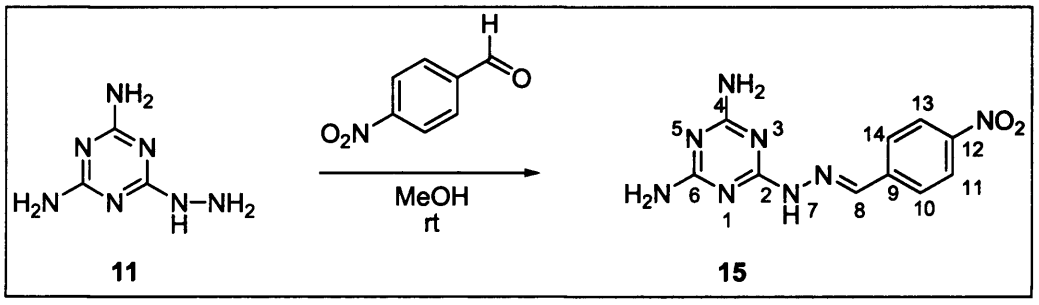

2-hydrazin-4,6-diamino-1,3,5-triazine (328.23 mg, 2.32 mmol) and p-nitro-benzaldehyde (357.75mg, 98%, 2.32 mmol) were suspended in MeOH (5 mL) and the suspension was left stirring overnight. The mixture was reduced under vacuum giving a yellow solid. The solid was recrystallised from H_2O/MeOH (120 mL: 200 mL) giving 493 mg of a yellow solid.

Yield: 77%.

mp: 321-322 °C.

LRMS (EI): m/z 274 (M^+, 100%).

HRMS: Calcd mass for $C_{10}H_{11}N_8O_2^+$ ($M+H^+$): 275.0999. Found: 275.1004.

Anal. Calcd for $C_{10}H_{10}N_8O_2 \cdot 1.1\ H_2O \cdot 0.03$ HCl: C, 40.7, H, 4.2, N, 37.9, Cl, 0.4. Found: C, 40.6, H, 3.4, N, 37.6, Cl, 0.1.

^{1}H-NMR (DMSO-d6, 300 MHz) δ 6.50 (bs, 4H, 2 NH_2), 7.86 (d, 2H, J=8.78 Hz, H-10 and H-C14), 8.18 (s, 1H, H-C8), 8.28 (d, 1H, J= 8.78 Hz, H-C11 and H-C13), 10.98 (s, 1H, H-N7).

^{13}C-NMR (DMSO-d6, 75 MHz) δ 124.4 (C-11 and C-13), 127.3 (C-10 and C-14), 139.3 (C-8), 142.0 (C-9), 147.3 (C-12), 165.1 (C-2), 167.7 (C-4 and C-6).

8.5.10 Synthesis of 3-nitro-benzaldehyde (4,6-diamino)-[1,3,5]-triazin-2-yl-hydrazone (16):

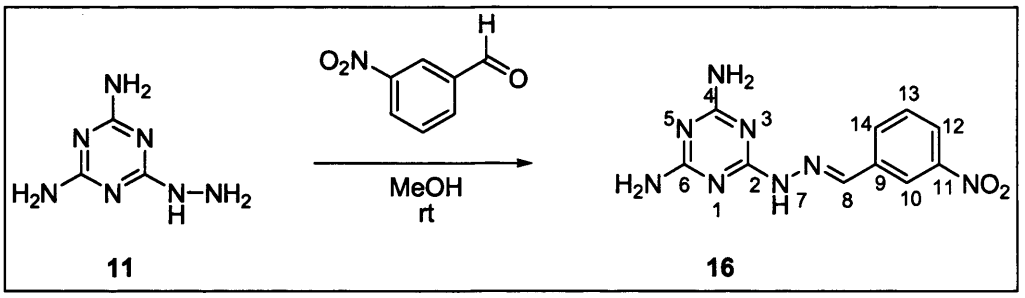

2-hydrazin-4,6-diamino-1,3,5-triazine (331.6 mg, 2.35 mmol) and m-nitro-benzaldehyde (358.71mg, 98%, 2.35 mmol) were suspended in MeOH (5 mL) and the suspension left stirring overnight. The mixture was reduced under vacuum giving a green solid. The solid was recrystallised from H_2O/MeOH (170 mL: 50 mL) giving 83 mg a light green solid.

Yield :13%.

mp: > 345 °C.

LRMS (EI): 274 (M^+, 100%).

HRMS: Calcd mass for $C_{10}H_{11}N_8O_2^+$ ($M+H^+$): 275.0999. Found: 275.0999.

Anal. Calcd for $C_{10}H_{10}N_8O_2 \cdot 8.5\ H_2O \cdot 0.1$ HCl: C, 27.8, H, 6.3, N, 26.0, Cl, 0.8. Found: C 27.5, H 2.7, N, 26.2, Cl 1.0.

^{1}H-NMR (DMSO-d6, 300 MHz) δ 6.50 (bs, 4H, 2 NH_2), 7.72 (m, 1H, H-C13), 8.01 (d, 1H, H-C14), 8.20 (m, 2H, H-C10 and H-C12), 8.47 (s, 1H, H-C8), 10.85 (s, 1H, H-N7).

^{13}C-NMR (DMSO-d6, 75 MHz) δ 120.0 (C-10), 123.3 (C-12), 130.7 (C-13), 133.3 (C-14), 137.4 (C-9), 139.4 (C-8), 148.6 (C-11) 165.2 (C-2), 167,7 (C-4 and C-6).

8.5.11 Synthesis of 2-nitro-benzaldehyde (4,6-diamino)-[1,3,5]-triazin-2-yl-hydrazone (17):

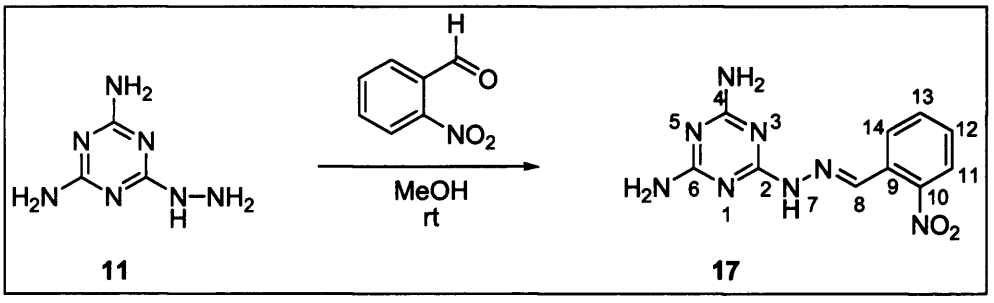

2-hydrazin-4,6-diamino-1,3,5-triazine (328.23 mg, 2.32 mmol) and o-nitro-benzaldehyde (357.75mg, 98%, 2.32 mmol) were suspended in MeOH (5 mL) and the suspension was left stirring overnight. The mixture was reduced under vacuum giving a yellow solid. The solid was recrystallized from H_2O/MeOH (120 mL/80 mL) giving 107 mg of a yellow solid.

Yield: 17%.

mp: 288-291°C.

LRMS (EI): m/z 274 (M^+, 100%).

HRMS: Calcd mass for $C_{10}H_{11}N_8O_2^+$ ($M+H^+$): 275.0999. Found: 275.1001.

Anal. Calcd for $C_{10}H_{10}N_8O_2 \cdot 4.5\ H_2O \cdot 0.02$ HCl: C, 33.7, H, 5.4, N, 31.5, Cl, 0.2. Found: C, 33.9,. H, 3.1, N, 29.7, Cl, 0.4.

^{1}H-NMR (DMSO-d6, 300 MHz) δ 6.45 (bs, 4H, 2 NH_2), 7.62 (m, 1H, H-C14), 7.78 (m, 1H, H-C11), 8.09 (m, 2H, H-C12 and H-C13), 8.48 (m, 1H, H-C8), 10.98 (s, 1H, H-N7).

^{13}C-NMR (DMSO-d6, 75 MHz) δ 124.9 (C-14), 127.8 (C-13), 129.8 (C-12), 129.9 (C-9) 133.7 (C-11), 136.5 (C-8), 147.9 (C-10) 165.2 (C-2), 167,7 (C-4 and C-6).

8.5.12 Synthesis of 5-cyano-2 furaldehyde (4,6-diamino)-[1,3,5]-triazin-2-yl-hydrazone (29):

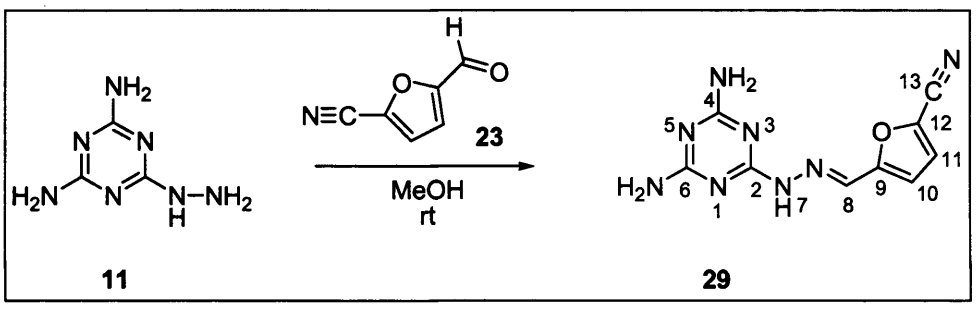

6-hydrazino-2,4-diamino-1,3,5-triazine (98.7 mg, 0.70 mmol) and 5-cyanofuraldehyde (crude 85mg, 0.70 mmol) were mixed together, suspended with MeOH (3 mL) and the mixture was left stirring overnight. The mixture was concentrated under vacuum giving a light brown solid. The solid was recrystallised by H_2O/MeOH (10 mL/15 mL) giving 22 mg of a light brown solid.

Yield: 13%.

mp: >350°C.

IR shows –CN at 2229.7 cm^{-1}.

LRMS (ES^+): m/z 245 ($(M+H)^+$, 100).

HRMS: calcd mass for $C_9H_9N_8O^+$ ($M+H^+$): 245.0894. Found: 245.0893.

Anal. Calcd for $C_9H_8N_8O \cdot 1.5H_2O \cdot 0.1$ HCl: C, 39.3, H, 4.1, N, 40.8, Cl, 1.3. Found C, 37.8, H, 3.4, N, 41.1, Cl, 1.2.

^{1}H-NMR (DMSO-d6, 300 MHz) δ 6.52 (bs, 4H, 2 NH_2), 6.96 (d, *J*= 3.76 Hz, 1H, H-C10) 7.71 (d, *J*= 3.76 Hz, 1H, H-C11), 8.04 (s, 1H, H-C8), 10.95 (bs, 1H, H-N7).

^{13}C-NMR (DMSO-d6, 75 MHz) δ 111.8 (C10), 112.3 (C13), 124.7 (C11), 125.5 (C12), 129.7 (C8), 155.3 (C9), 165.0 (C2), 167,7 (C4 and C6).

8.5.13 Synthesis of 5-nitro-2 furaldehyde (N^4,propyl-4,6-diamino)-[1,3,5]-triazin-2-yl-hydrazone (62):

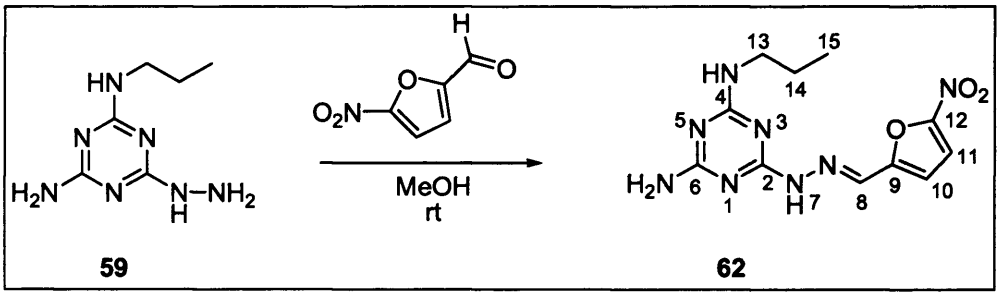

59 62

5-Nitrofuraldehyde (203.7 mg, 99%, 1.43 mmol) and 6 N^4-propyl-4,6-diamino-1,3,5-triazin-2-yl-hydrazine (264 mg, 1.34 mmol) were suspended in MeOH (5 mL) and left stirring overnight at room temperature. The mixture was filtered and washed several times with MeOH. The yellow product was dried over high vacuum giving 282 mg of pure product.

Yield: 64%

mp: 236-238 °C

LRMS (EI^+): m/z = 306.2 (M^+, 10%).

HRMS: Calcd mass for $C_{11}H_{15}N_8O_3^+$ ($M+H^+$): 307.1262. Found: 307.1261.

Anal. Calcd for $C_{11}H_{14}N_8O_3 \cdot 0.5\ H_2O \cdot 0.08$ HCl: C, 41.5, H, 4.8, N, 35.2, Cl, 0.9; Found: C, 41.9, H, 4.5, N, 34.9, Cl, 0.6.

^{1}H-NMR (DMSO-d6, 500 MHz) δ 0.86 (t, 3H, *J*=7.32 Hz, H-C15), 1.49 (m, 2H, H-C14), 3.18 (m, 2H, H-C13), 6.41-7.13 (m, 3H, H-N4, 2H-N2), 7.05 (d, 1H, *J*=3.45 Hz, H-C10), 7.76 (d, 1H, *J*=3.45 Hz, H-C11), 8.00-8.04 (2s, 1H, H-C8), 11.15 (bs, 1H, H-N7).

^{13}C-NMR (DMSO-d6, 125 MHz) δ 8.4 (C15), 22.3 (C14), 22.5 (C14*), 41.7 (C13), 113.6 (C10), 114.0 (C10*), 115.2 (C11), 128.9 (C8), 129.2 (C8*), 151.4 (C9), 152.9 (C12), 164.0 (C4), 164.2 (C4*), 166.0 (C2), 166.9 (C6), 167.1 (C6*).

8.5.14 Preparation of 5-nitro-2 furaldehyde (N^4,isopropyl-4,6-diamino)-[1,3,5]-triazin-2-yl-hydrazone (63):

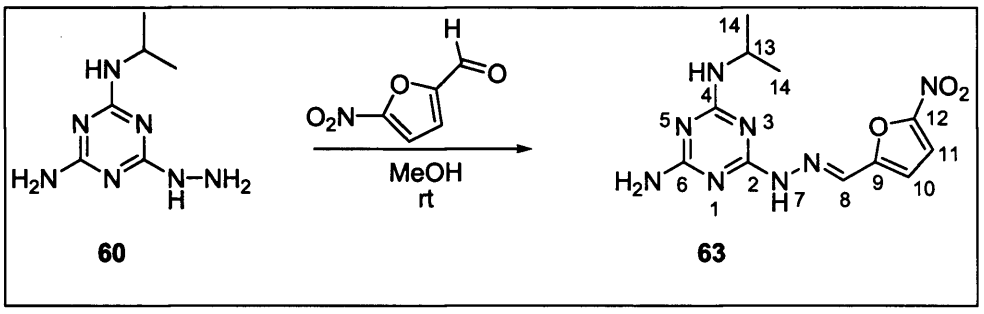

8.5.14.1 Attempted synthesis:

5-Nitrofuraldehyde (32.78 mg, 99%, 0.28 mmol) and crude N^2-isopropyl-4,6-diamino-[1,3,5]-triazin-2-yl-hydrazine from exp. § 8.4.8.1 (53 mg, 0.28 mmol) were suspended in MeOH (2 mL) and the suspension left stirring overnight at room temperature. ^{1}H-NMR and ^{13}C-NMR did not show any peaks related to the product but only N^2-isopropyl-2,4-diamine-6-chloro-[1,3,5]-triazine used as starting material on the previous experiments.

8.5.14.2 Synthesis:

5-Nitrofuraldehyde (92.6 mg, 99%, 0.65 mmol) and N^4-isopropyl-4,6-diamino-[1,3,5]-triazin-2-yl-hydrazine (120 mg, 0.65 mmol) were suspended in MeOH (3 mL) and the suspension left stirring overnight at room temperature. The mixture was filtered and recrystallised by EtOH. The yellow product was dried over high vacuum giving 50 mg of pure product.

Yield: 25%

mp: 178-180 °C

LRMS (ES^+) m/z 307.11 ($(M+H)^+$, 100%), 329.2 ($(M+Na)^+$, 20%).

HRMS: Calcd mass for $C_{11}H_{15}N_8O_3^+$ ($M+H^+$): 307.1262. Found: 307.1258.

Anal. Calcd for $C_{11}H_{14}N_8O_3 \cdot 2\ H_2O \cdot 0.2\ CH_2Cl_2 \cdot EtOH$: C, 38.5, H, 5.7, N, 29.0, Cl, 3.7; Found: C, 38.6, H, 4.2, N, 29.6, Cl, 4.0.

^{1}H-NMR (DMSO-d6, 500 MHz) δ 1.17 (d, 6H, *J*= 6.22 Hz, H-C14), 4.10 (m, 1H, H-C13), 7.15-9.18 (m, 3H, H-N4, 2H-N2), 7.85 (m, 1H, H-C10), 8.20 (s, 1H, H-C11), 8.25-8.30 (2s, 1H, H-C8), 13.0 (bs, 1H, H-N7).

^{13}C-NMR (DMSO-d6, 500 MHz) δ 22.0 (C14), 42.7 (C13), 114.4 (C10), 114.5 (C10*), 115.5 (C11), 134.4 (C8), 151.7 (C9), 151.8 (C9*), 152.0 (C12).

8.5.15 Synthesis of 5-nitro-2 furaldehyde (N^4,butyl-4,6-diamino)-[1,3,5]-triazin-2-yl-hydrazone (64):

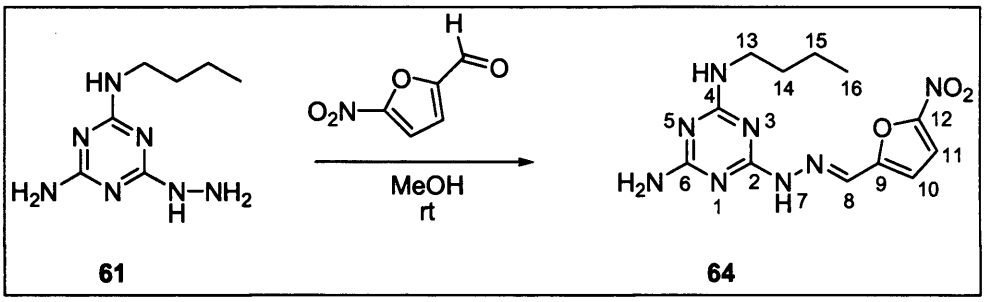

61 64

5-Nitrofuraldehyde (191 mg, 99%, 1.34 mmol) and N^4-butyl-4,6-diamino-1,3,5-triazin-2-yl-hydrazine (264 mg, 1.34 mmol) were suspended in MeOH (5 mL) and left stirring overnight at room temperature. The mixture was filtered and washed several times with MeOH. The yellow product was dried over high vacuum giving 317 mg of pure product.

Yield: 73%

mp: 226-228°C

LRMS (EI^+) m/z 320.2 (M^+, 10%).

HRMS: Calcd mass for $C_{12}H_{17}N_8O_3^+$ ($M+H^+$): 321.1418. Found: 321.1415.

Anal. Calcd for $C_{12}H_{16}N_8O_3 \cdot 0.5\ H_2O \cdot 0.05$ HCl: C, 43.5, H, 5.2, N, 33.8, Cl, 0.5; Found: C, 43.9, H, 4.9, N, 33.5, Cl, 0.7.

^{1}H-NMR (DMSO-d6, 500 MHz) δ 0.88 (t, 3H, *J*=7.28 Hz, H-C16), 1.30 (m, 2H, H-C15), 1.47 (m, 2H, H-C14), 3.22 (m, 2H, H-C13), 6.58-7.13 (m, 3H, 2 H-N4, H-N2), 7.04 (d, 1H, *J*=3.20 Hz, H-C10), 7.77 (d, 1H, *J*=3.20 Hz, H-C11), 8.00-8.04 (2s, 1H, H-C8), 11.06 (bs, 1H, H-N7).

^{13}C-NMR (DMSO-d6, 125 MHz) δ 13.7 (C16), 19.6 (C15), 30.6 (C14), 31.2 (C14*), 40.0 (C13), 113.6 (C10), 114.0 (C10*), 115.2 (C11), 128.9 (C8), 129.1 (C8*), 151.4 (C9), 152.9 (C12), 164.0 (C4), 164.2 (C4*), 166.0 (C2), 166.9 (C6), 167.1 (C6*).

8.5.16 Synthesis of 5-nitro-2 furaldehyde (N^4-hydroxyethyl-4,6-diamino)-[1,3,5]-triazin-2-yl-hydrazone (72):

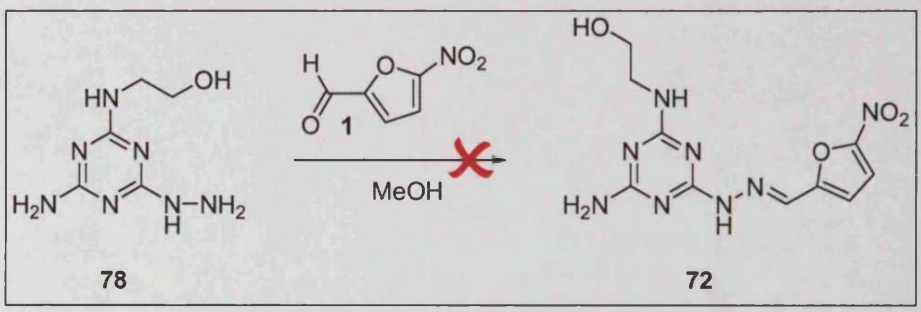

Crude N^4-hydroxyethyl-4,6-diamino-[1,3,5]-triazin-2-yl-hydrazine from exp §8.4.9 and 5-nitrofuraldehyde were mixed together and dissolved in MeOH (4 mL). The mixture was left stirring overnight at room temperature. The solvent of the clear solution was partially concentrated under reduced pressure and a precipitate was formed after the addition of acetone to the mixture. The product was filtered off and dried under high vacuum. MS analysis did not show any peak corresponding to the expected product. The NMR analysis also did not show any characteristic signal corresponding to the expected hydrazone.

8.5.17 Synthesis of 5-nitro-2 furaldehyde {N^4-[3-(*t*-butyl-diphenylsilyl)-oxy]-ethyl}-(4,6-diamino)-[1,3,5]-triazin-2-yl-hydrazone (70):

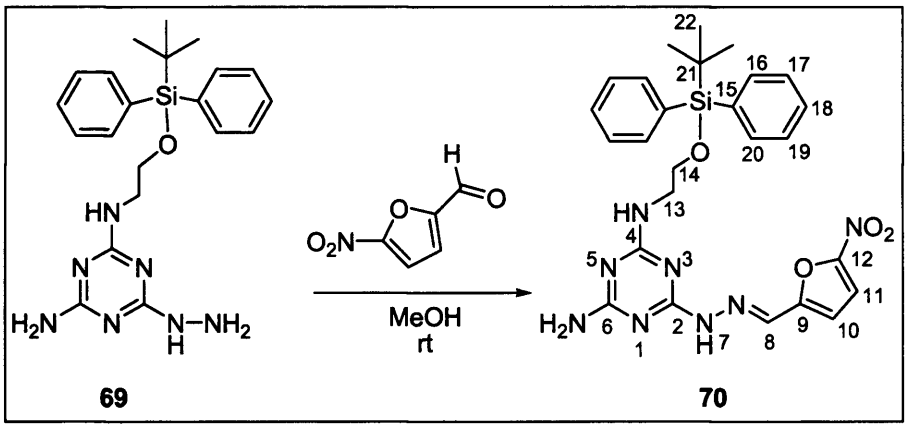

5-Nitrofuraldehyde (57.0 mg, 99%, 0.40 mmol) and N^4-{[3-(*t*-butyl-diphenylsilyl)-oxy]-ethyl}-4,6-diamino-[1,3,5]-triazin-2-yl-hydrazine (170 mg, 0.40 mmol) were suspended in MeOH (5 mL) and left stirring overnight at room temperature. The mixture was filtered and washed with cold EtOH and with Et_2O. The product was dried over high vacuum giving 20 mg of pure product.

Yield: 9%

mp: 163-165°C

LRMS (ES^+): m/z 547.5 ($(M+H)^+$, 100%)

HRMS: Calcd mass for $C_{26}H_{30}N_8O_4SiNa^+$ ($M+Na^+$): 569.2057. Found: 569.2069.

^{1}H-NMR (DMSO-d6, 300 MHz) δ 0.99 (s, 9H, H-C22), 3.48 (m, 2H, H-C13), 3.73 (m, 2H, H-C14), 6.40-7.00 (3m, 3H, 2 H-N6, H-N4), 7.43 (m, 6H, H-C17,19, H-C17',19', H-C18 and H-C18'), 7.63 (m, 4H, H-C16,20 and H-C16',20'), 7.76 (d, 1H, *J*=3.24 Hz, H-C10), 7.84 (d, 1H, *J*=3.24 Hz, H-C11), 8.02 (s, 1H, H-C8), 11.10 (bs, 1H, H-N7).

^{13}C-NMR (DMSO-d6, 75 MHz) δ 19.1 (C22), 26.9 (C21), 42.4 (C13), 62.8 (C14), 114.4 (C10), 115.6 (C11), 120.1 (C8), 128.2 (C_{meta}), 130.1 (C_{para}), 133.5 (C15 and C15'), 135.4 (C_{orto}), 151.8 (C12), 166.6 (C2).

8.5.18 Synthesis of 5-nitro-2 furaldehyde {N⁴-[3-(*t*-butyl-diphenylsilyl)-oxy]-propyl}-(4,6-diamino)-[1,3,5]-triazin-2-yl-hydrazone (76):

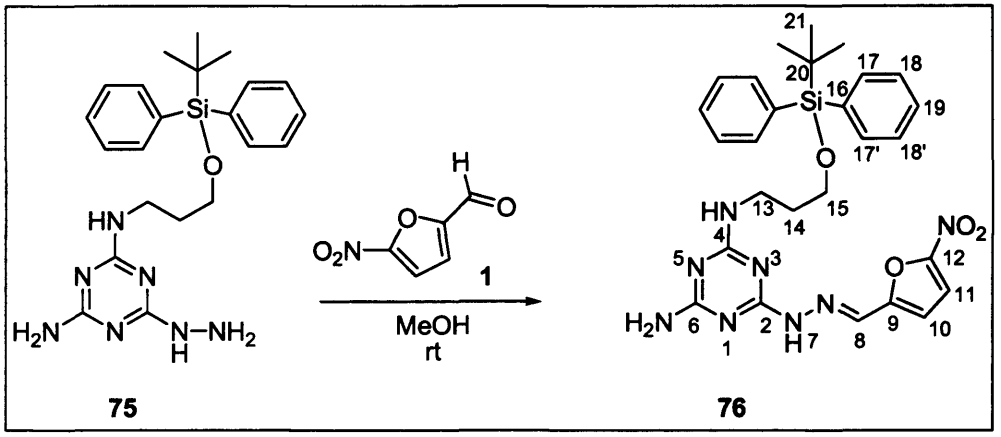

5-Nitrofuraldehyde (81.2 mg, 99%, 0.57 mmol) and N⁴-{[3-(*t*-butyl-diphenylsilyl)-oxy]-propyl}-4,6-diamino-[1,3,5]-triazin-2-yl-hydrazine (250 mg, 0.57 mmol) were suspended in EtOH (5 mL) and left stirring at room temperature. The yellow colour turned into a dark orange colour after 30 mins. The mixture was left stirring overnight at room temperature and then was filtered and washed with cold EtOH and with Et_2O. The product was dried over high vacuum giving 264 mg of pure product.

Yield: 84%.

mp: >320 °C.

LRMS (ES^+): m/z 561.3 ($(M+H)^+$, 100%).

HRMS: Calcd mass for $C_{27}H_{33}N_8O_4Si^+$ ($M+H^+$): 561.2389. Found: 561.2390.

^{1}H-NMR (DMSO-d6, 500 MHz) δ 0.99 (s, 9H, H-C21), 1.81 (t, 2H, *J*= 6.23 Hz, H-C15), 3.40 (m, 2H, H-C14), 3.72 (t, 2H, *J*= 6.23 Hz H-C13), 5.95-6.85 (bm, 3H, 2 H-N6, H-N4), 7.05 (d, 1H, *J*=3.59 Hz, H-C10), 7.43 (m, 6H, 2 H-C18, H-C19 and 2 H-C18'), 7.62 (m, 4H, 2 H-C17 and 2 H-C17'), 7.77 (d, 1H, *J*=3.59 Hz, H-C11), 8.05-8.10 (2 s, 1H, H-C8), 11.10 (bs, 1H, H-N7).

^{13}C-NMR (DMSO-d6, 125 MHz) δ 18.7 (C20), 19.6 (C15), 26.6 (C21), 36.9 (C15), 56.0 (C14), 61.5 (C13), 115.1 (C10), 115.2 (C11), 127.8 (C18 and C18'), 129.7 (C8), 133.2 (C19), 134.9 (C17 and C17'), 151.4 (C9), 152.9 (C12), 166.1 (C2).

8.5.19 Synthesis of 5-nitro-2 furaldehyde {[N^4-(3-hydroxypropyl-amino)-4,6-diamino-[1,3,5]-triazin]-2-yl}-hydrazone (77)

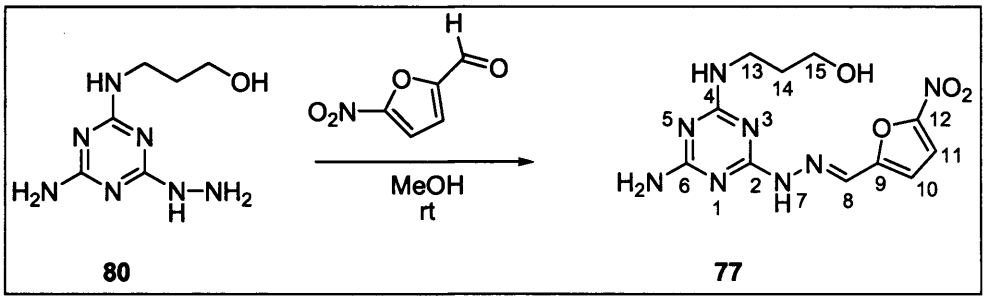

80 77

Crude N^4-(3-hydroxy-propyl)-2,4-diamino-1,3,5-triazin-2-yl-hydrazine (1.466 g, 14.72 mmol) was dissolved in MeOH (10 mL) and 5-nitrofuraldehyde (2.096 g, 99%, 14.72 mmol), previously dissolved in MeOH (10 mL), was added to the solution. The solution turned into a suspension after 30 mins. The mixture was left stirring at room temperature for 2 hrs. The solvent was then removed under vacuum and the solid purified by flash chromatography (2 x 200mL DCM 100%, 2 x 200mL MeOH 0.5% in DCM, 2 x 200 mL MeOH 1% in DCM) giving 417 mg of pure orange product.

Yield: 17%

mp: 143-145°C

LRMS (ES^+):m/z 323.12 ($(M+H)^+$, 100%).

HRMS: Calcd mass for $C_{11}H_{15}N_8O_4^+$ ($M+H^+$): 323.1211. Found: 323.1211.

Anal. Calcd for $C_{11}H_{14}N_8O_4 \cdot 0.2$ MeOH·0.2 HCl: C, 40.0, H, 4.5, N, 33.3, Cl, 2.1; Found: C, 39.7, H, 4.5, N, 33.6, Cl, 1.6.

^{1}H-NMR (DMSO-d6, 500 MHz) δ 1.64 (m, 2H, H-C15), 3.34 (m, 2H, H-C14), 3.44 (m, 2H, H-C13), 4.46-4.65 (2 bs, 1H, O-H), 6.32-7.11 (bm, 3H, NH_2, H-N4), 7.05 (d, 1H, *J*=2.84 Hz, H-C10), 7.77 (d, 1H, *J*=2.84 Hz, H-C11), 8.02-8.04 (2s, 1H, H-C8), 11.08-11.23 (2 bs, 1H, H-N7).

^{13}C-NMR (DMSO-d6, 125 MHz) δ 32.4 (C15), 32.7 (C15*), 36.9 (C14), 37.2 (C14*), 58.5 (C13), 113.7 (C10), 115.2 (C11), 128.9 (C8), 129.2 (C8*), 151.5 (C9), 152.9 (C12), 164.0 (C4), 166.1 (C2), 167.1 (C6).

^{13}C-NMR 100°C (DMSO-d6, 125 MHz) δ 34.6 (C15), 60.7 (C13), 114.4 (C10), 116.6 (C11), 131.6 (C8), 153.5 (C9), 155.3 (C12), 166.3 (C4), 168.4 (C2), 169.2 (C6).

8.5.20 Synthesis of 5-nitro-2 furaldehyde [N^4-(3-acetyl-oxy)-propyl]-4,6-diamino-[1,3,5]-triazin-2-yl-hydrazone (81)

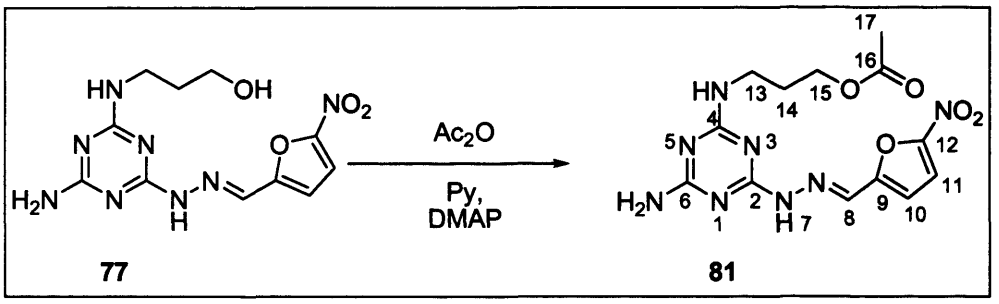

77 81

5-nitro-2 furaldehyde [N^4-(3-hydroxypropyl)-4,6-diamino-[1,3,5]-triazin]-2-yl-hydrazone (117 mg, 0.36 mmol) was suspended in dry pyridine (5 mL) and acetic anhydride (39.8 mg, d=1.08, 0.04 mL, 0.39 mmol) was added to the suspension at 0°C. The mixture was left stirring for 30 min and DMAP (catalytic, 10 mg) was then added. The temperature was left stirring at room temperature for 20 min. The reaction was quenched with MeOH and the solvent was removed under vacuum. The crude was purified by flash chromatography (200 mL DCM %, 2 x 100 mL 2% MeOH in DCM, 2 x 100 mL 5% MeOH in DCM) giving 85 mg of pure orange product.

Yield: 65%

mp: 142-144 °C

LRMS (ES^+): m/z 365.13 ($(M+H)^+$, 100%).

HRMS: Calcd mass for $C_{13}H_{17}N_8O_5^+$ ($M+H^+$): 365.1316. Found: 365.1331.

Anal. Calcd for $C_{13}H_{16}N_8O_5 \cdot 0.5$ MeOH $\cdot 0.05$ HCl: C, 42.4, H, 4.7, N, 29.3, Cl, 0.5; Found: C, 42.8, H, 4.5, N, 29.2, Cl, 0.4.

^{1}H-NMR (DMSO-d6, 500 MHz) δ 1.81 (t, 2H, *J*= 6.33 Hz, H-C14), 2.01 (s, 3H, H-C17), 3.25 (m, 2H, H-C13), 4.04 (t, 2H, *J*=6.33 Hz), 6.40-7.58 (bm, 3H, NH_2, H-N4), 7.05 (s, 1H, H-C10), 7.77 (d, 1H, *J*=3.93 Hz, H-C11), 8.01,8.04 (2s, 1H, H-C8), 11.08,11.16 (2 bs, 1H, H-N7).

^{13}C-NMR (DMSO-d6, 125 MHz) δ 20.6 (C17), 20.7 (C17*), 28.2 (C14), 28.4 (C14*), 36.9 (C13), 37.1 (C13*), 61.7 (C15), 61.8 (C15*), 113.7 (C10), 114.4 (C10*), 115.2 (C11), 116.0 (C11*), 129.0 (C8), 151.5 (C9), 152.9 (C12), 164.0 (C4), 166.1 (C2), 167.1 (C6), 170.4 (C16).

8.6 Modification of furan unit:

8.6.1 Preparation of 5-cyano-furaldehyde (23):

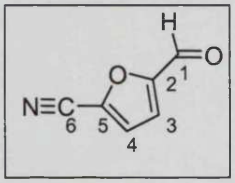

8.6.1.1 Method A: Attempted synthesis from cyanofuran (22):

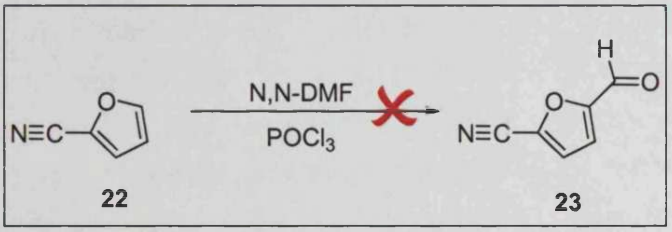

$POCl_3$ (0.23 mL, 99%, d= 1.675, 2.53 mmol) was added dropwise to N,N-DMF (0.53 mL, d= 0.948, 6.33 mmol) at 0°C with stirring and under nitrogen. The temperature was then allowed to rise to room temperature and the mixture was left stirring for 30 min. The reaction was cooled down to 0°C and cyanofuran (0.19 mL, d=1.064, 2.11 mmol) was added dropwise to the previous solution. The mixture was left stirring at 0°C for 1 hr and then overnight at room temperature. The reaction was stopped and cooled down in an ice bath. TLC analysis (DCM 100%) showed the formation of two products with rf respectively 0.3 and 0.5. The LRMS analysis showed a peak at 121.5 corresponding to the desired product. Water (20 mL) was added followed by the dropwise addition of NaOH 2N until pH basic. The water layer was extracted with Et_2O (3 x 25 mL). The organic layers were combined together, dried with $MgSO_4$ and concentrated under vacuum giving 263 mg of a yellow oil. The attempt to purify the mixture by using flash chromatography (DCM/MeOH, 100:0 to 80:20) failed and the product could not be isolated.

8.6.1.2 Method B: Attempted synthesis from 5-hydroxymethyl-2-furaldehyde (24) *via* 5-hydroxy-methyl-2-furaldoxime (25):

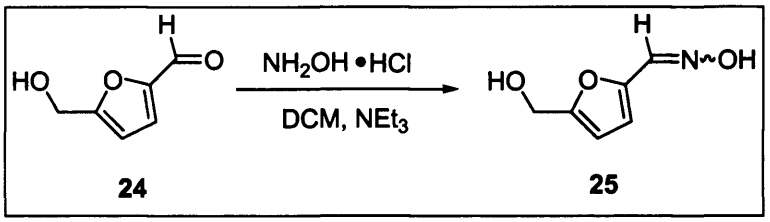

24 **25**

Hydroxylamine hydrochloride (121.4 mg 99%, 1.73 mmol) was slowly added to solution of 5-hydroxymethyl-2-furaldehyde (200 mg 99%, 1.57 mmol) in anhydrous chloroform (5 mL) and anhydrous triethylamine (0.48 mL, d= 0.727, 3.45 mmol) with stirring, under nitrogen and at 5°C. The temperature was kept below 5°C during the addition and then was left to rise to room temperature. The mixture was left stirring for 3 hrs and then stopped once the TLC analysis (DCM/MeOH = 85:15) showed no further formation of product. The solvent was concentrated under reduced pressure and the residue was used for the following step.

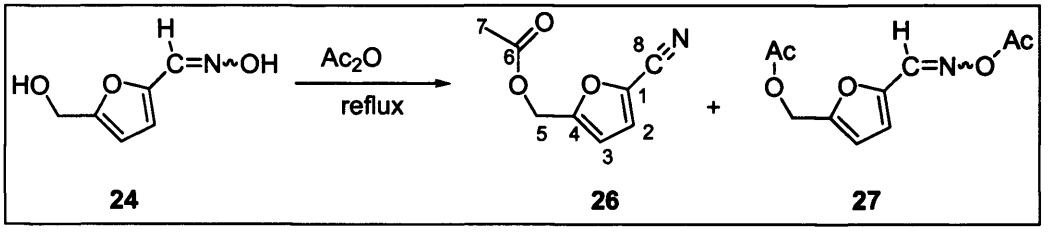

24 **26** **27**

Crude 5-hydroxy-methyl-2-furaldoxime was dissolved in Ac_2O (7 mL) and the solution was left stirring under nitrogen and at 140 °C for 3 hrs. The TLC analysis (Hexane/EtOAc = 50:50) showed the formation of a product with rf 0.88. The reaction was then stopped and carefully poured into ice-water (10 mL). $NaHCO_3$ and NaOH were added until complete hydrolysis of the Ac_2O. The water layer was extracted with EtOAc (4x15mL), the organic layers were dried over $MgSO_4$ and concentrated under vacuum to give 221 mg of a pale yellow oil. The crude oil was then purified by flash chromatography (hexane/EtOAc, 95:5 to 80:20) giving 121 mg of pure (5-cyanofuran-2-yl)methyl acetate and 65 mg of bis-acetate-product.

IR:-CN at 2232.9 cm^{-1}, -C=O at 1744.3 cm^{-1}.

^{1}H-NMR (MeOD, 300 MHz) δ 2.07 (s, 3H, H-C7), 5.04 (s, 2H, H-C5), 6.35 (d, 1H, *J*= 3.56 Hz, H-C3), 7.04 (d, 1H, *J*= 3.56 Hz, H-C2).

^{13}C-NMR (MeOD, 75 MHz) δ 21.0 (C7), 57.7 (C5), 18.6 (C8), 112.0 (C3), 123.2 (C2), 126.7 (C1), 155.2 (C4), 170.6 (C6).

Synthesis of 5-hydroxy-2-furonitrile (28):

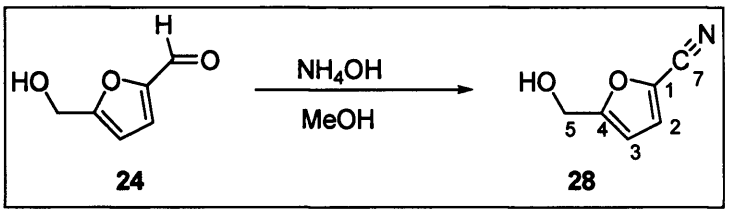

Aqueous ammonia (1mL, 25%) was added to (5-cyanofuran-2-yl)methyl acetate (103mg, 0.61 mmol) in MeOH (1 mL) at room temperature with stirring. After 2 hrs TLC analysis showed the complete reaction and the solvent was concentrated under reduced pressure. The residue was dissolved with EtOAc (10 mL) and the solution was washed with water. The organic layers were collected together, dried with $MgSO_4$ and concentrated under vacuum to give a yellow oil. The crude oil was purified by preparative chromatography (EtOAc/Hexane = 60/40) giving 14 mg of pure 5-hydroxy-2-furonitrile.

Yield: 19%

LRMS (ES^-): 122.0 [$(M-H)^-$, 50%], 245.1 [$(2M-H)^-$, 100%]

^{1}H-NMR (MeOD, 300 MHz) δ 4.55 (s, 2H, H-C5), 6.50 (d, 1H, *J*= 3.56 Hz, H-C3), 7.24 (d, 1H, *J*= 3.56 Hz, H-C2).

^{13}C-NMR (MeOD, 75 MHz) δ 57.7 (C5), 110.2 (C3), 112.8 (C7), 124.8 (C2), 126.8 (C1), 162.7 (C4).

8.6.1.3 Method C: Attempted synthesis from 5-hydroxymethyl-2-furaldehyde (24):

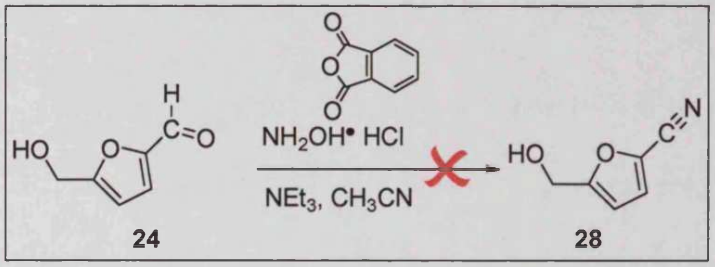

Anhydrous triethylamine (0.60 mL, 4.31 mmol) and 5-hydroxymethyl-2-furaldehyde (500mg 99%, 3.92 mmol) were added to a solution of hydroxylamine hydrochloride (302.4 mg, 99%, 4.31 mmol) in anhydrous acetonitrile (40 mL) at 0°C and under nitrogen. The mixture was left stirring for 30 min at 0°C. The reaction was then heated to reflux temperature for 24 hrs but the formation of the product was not observed.

8.6.1.4 Method D: Attempted synthesis *via* 5-hydroxy-methyl-2-cyanofuran (28):

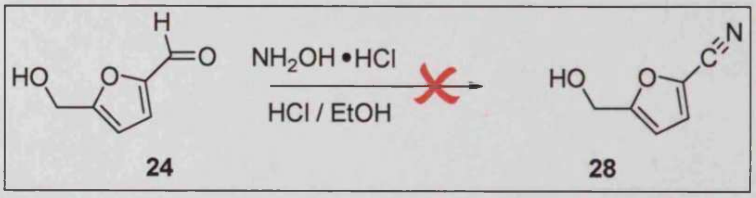

5-hydroxymethyl-2-furaldehyde (500mg, 99%, 3.92 mmol), hydroxylamine hydrochloride (329.9 mg 99%, 4.70 mmol) and HCl conc (3 drops) were mixed together in anhydrous EtOH (4mL) and the mixture was left stirring at reflux temperature. After 30 min polymerisation may occurred and the reaction mixture turned into a black thick slurry.

8.6.1.5 Method E: Attempted synthesis *via* 5-hydroxy-methyl-2-cyanofuran (28):

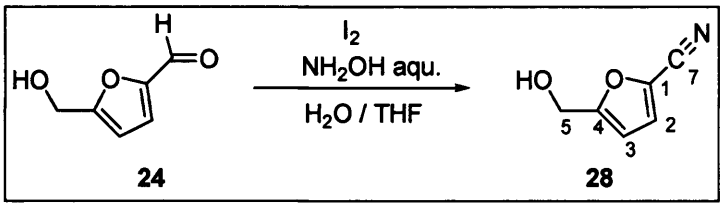

Iodine (279.75 mg 99.8%, 1.1 mmol) was added to a solution of 5-hydroxymethyl-2-furaldehyde (127.38 mg 99%, 1 mmol) in ammonia (10 mL, 25%) and THF (1mL) at room temperature and with stirring. The dark solution after 1 hr became colourless (light yellow), as indication that the reaction is complete. TLC analysis (EtOAc/Hexane=60:40) also confirmed the complete reaction. $Na_2S_2O_3$ (5 mL 5%) was added to reduce the excess of iodine and to quench the reaction. The water layer was extracted with Et_2O (4 x 30 mL). The organic layers were dried with $MgSO_4$ and concentrated under vacuum giving 98 mg of a pale yellow oil.

Yield: 80%.

IR: –CN at 2233.0 cm^{-1}.

^{1}H-NMR (MeOD, 300 MHz) δ 4.58 (s, 2H, H-C5), 6.53 (d, 1H, *J*= 3.56 Hz, H-C3), 7.26 (d, 1H, *J*= 3.56 Hz, H-C2).

^{13}C-NMR (MeOD, 75 MHz) δ 57.7 (C5), 110.2 (C3), 112.9 (C7), 124.9 (C2) 126.8 (C1), 162.7 (C4).

8.6.1.6 Oxidation of 5-hydroxy-methyl-2-cyanofuran to 5-cyano-2-furaldehyde:

8.6.1.6.1 Method A: Attempted oxidation with pyridinium chlorochromate (PCC):

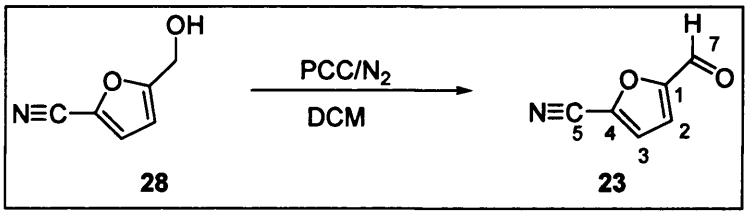

28 23

5-hydroxymethyl-2-cyanofuran (85 mg, 0.69 mmol) in anhydrous DCM (2mL) was added to a solution of pyridinium chlorochromate (PCC, 226.6 mg, 98%, 1.03 mmol) in anhydrous DCM (4 mL) under nitrogen. The mixture was left stirring at room temperature and under nitrogen for 3 hrs. The precipitate was filtered off and washed with Et_2O. The organic layers were combined together, dried over $MgSO_4$ and the solvent was reduced under reduced pressure. The crude solid was purified with flash chromatography eluting with EtOAc/Hexane (0:100 to 0:80). The amount of desired product obtained was negligible (<10mg).

8.6.1.6.2 Method B: Attempted oxidation via Swern oxidation:

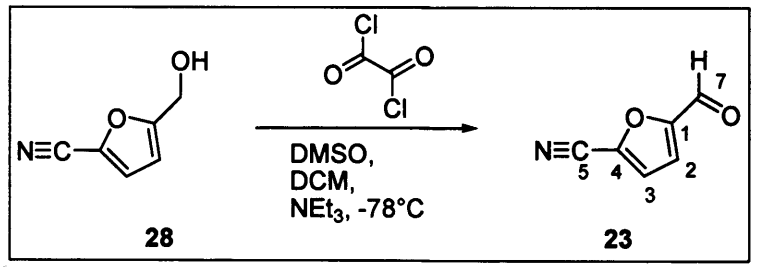

28 23

Oxalyl chloride (0.1 mL, d= 1.477, 1.1 mmol) was dissolved in dry DCM and the solution was cooled to -78°C with stirring and under nitrogen. Anhydrous DMSO (0.17 mL, d= 1.101, 2.4 mmol) was dissolved in anhydrous DCM (0.5 mL) and added dropwise to the previous solution carefully maintaining the temperature below -75°C. After the addition, the reaction was left stirring for 30 min at -78°C. 5-hydroxymethyl-2-cyanofuran (123.11 mg, 1 mmol) was dissolved in anhydrous DCM (2.5

mL) and was added dropwise to the mixture at -78°C. The mixture was left stirring for further 30 min at -78°C and then anhydrous triethylamine was added dropwise. The reaction was left stirring under nitrogen and at room temperature for 4 hrs. TLC analysis and ^{1}H-NMR and ^{13}C-NMR confirmed the formation of the aldehyde. The mixture was then washed with H_2O (2 x 10 mL), $NaHCO_3$ saturated solution (2 x 15 mL) and HCl 1N solution (2 x 15 mL). The organic layer was dried with $MgSO_4$ and the solvent concentrated under vacuum giving 85 mg of crude product which was used for the synthesis of the corresponding hydrazone (§8.5.12).

8.7 Attempted synthesis of 5-nitrothiazol-2-yl-[1,3,5]-triazine:

8.7.1 Method A:

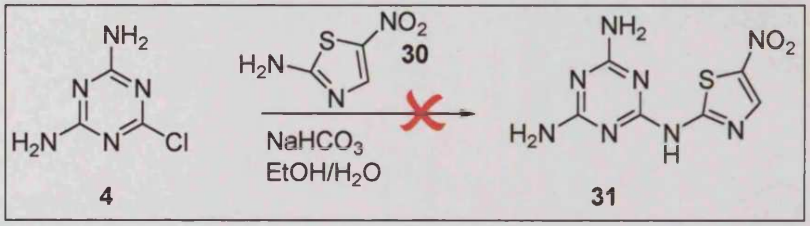

6-chlor-2,4-diamino-[1,3,5]-triazine (200 mg 95%, 1.30 mmol), 2-amino-5-nitrothiazole (252.6 mg, 97%, 1.69 mmol) and $NaHCO_3$ (142 mg, 1.69 mmol) were mixed together and suspended in water (20 mL) and abs. EtOH (20 mL). The mixture was left stirring at 80 °C for 24 hrs. TLC analysis (ammonia 2M in MeOH) showed the formation of product in the base line. MS analysis did not show any peaks related to the desired product. The mixture was left cooling down and the solvent concentrated under vacuum. The residue was washed with water and recrystallised from water-methanol giving 98 mg of a light brown solid. ^{1}H-NMR and ^{13}C-NMR did not show any peak corresponding to the expected product.

8.7.2 Method B:

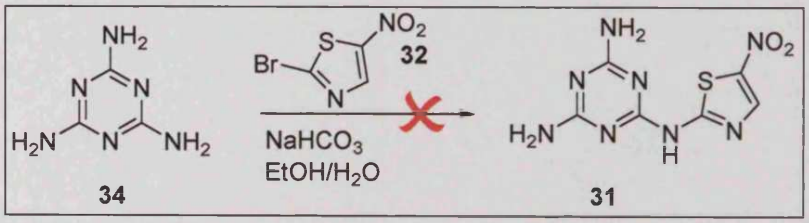

2-bromo-5-nitrothiazole (400 mg 98%, 1.88 mmol), melamine (310.8 mg 99%, 2.44 mmol) and $NaHCO_3$ were mixed together and suspended in water (20 mL) and abs. EtOH (20 mL). The mixture was left stirring at 80°C for 24 hrs. TLC (DCM/CH_3OH = 80:20) showed the formation of three products. The reaction was stopped and the mixture was extracted

with EtOAc (3 x 30 mL). The organic layers were collected together, dried with $MgSO_4$ and concentrated under vacuum. MS analysis did not show any peak related to the expected product. The solid was purified twice by flash chromatography eluting with DCM/CH_3OH (100:0 to 80:20). ^{1}H-NMR and ^{13}C-NMR confirmed that none of the products recovered corresponded to the desired one.

8.7.3 Method C:

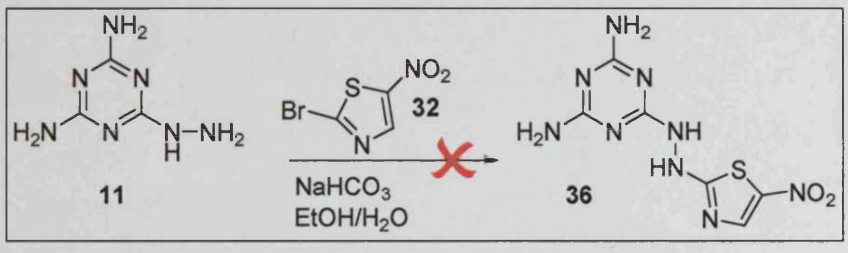

A mixture of 2-bromo-5-nitrothiazole (400 mg 98%, 1.88 mmol), 4,6-diamino-[1,3,5]-triazin-2-yl-hydrazine (344 mg, 2.44 mmol) and $NaHCO_3$ (204.98mg, 2.44 mmol) in water (20 mL) and abs. ethanol (20 mL) was left stirring overnight at room temperature and for 6 hrs at 80°C. MS analysis did not show any peaks corresponding to the expected compound. The attempts to purify the mixture by flash chromatography also failed.

9. Experimental Section II:

Amidine Derivatives

9.1 Synthesis of 5-nitrofuran-2-yl-benzamidines

9.1.1 Synthesis of 4-[O-[5-(nitrofuran-2-yl)-methyl]-oxy-]-benzamidine *via* 4-(5-Nitro-furan-2-yl-methoxy)-benzonitrile (91):

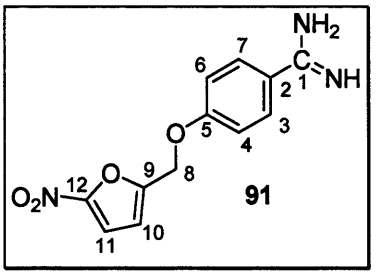

9.1.1.1 Synthesis of 4-(5-Nitro-furan-2-yl-methoxy)-benzonitrile (94):

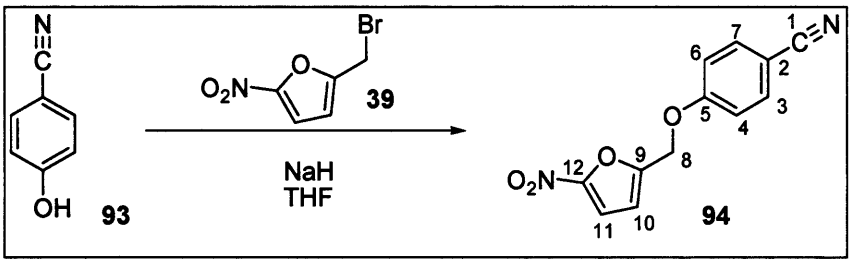

Method A: attempted synthesis:

A NaH dispersion was previously washed with dried hexane in order to remove the mineral oil. Cyanophenol (0.29 g 95%, 2.35 mmol) in anhydrous THF (2 mL) was added to a suspension of NaH (123.6 mg 60%, 3.09 mmol) in anhydrous THF (3 mL). The mixture was stirred at 15°C and under nitrogen. The excess of NaH was filtered off after 1hr 30 mins and 2-bromomethyl-5-nitrofuran (0.5g 97%, 2.35 mmol) in anhydrous THF (4 mL) was added to the solution at room temperature. The reaction was left stirring overnight at room temperature. TLC (DCM/MeOH= 98/2) and the MS analyses did not show the formation of the desired product.

Method B: attempted synthesis:

Cyanophenol (0.29 g 95%, 2.35 mmol) in anhydrous THF (2 mL) was added to a suspension of NaH (123.6 mg 60%, 3.09 mmol) in anhydrous THF (3 mL) at 15°C with stirring and under nitrogen. The excess of NaH was filtered off after 1 hr 30 mins and 2-bromomethyl-5-nitrofuran (0.5g 97%, 2.35 mmol) in anhydrous THF (4 mL) was added to the solution at room temperature. The reaction was left stirring overnight at room temperature. As well as observed for the previous method, TLC (DCM/MeOH= 98/2) and the MS analyses did not show the formation of the desired product.

Method C: Synthesis:

Cyanophenol (0.87 g 95%, 7.05 mmol) in anhydrous THF (6 mL) was added to a suspension of NaH (370.8 mg 60%, 9.27 mmol) in anhydrous THF (9 mL) at 15°C, with stirring and under nitrogen. After 1 hour a solution of 2-Bromomethyl-5-nitrofuran (1.5g 97%, 7.05 mmol) in anhydrous THF (12 mL) was added at room temperature. The reaction was left stirring overnight at room temperature. The solvent was removed under vacuum and the crude mixture was purified by flash chromatography eluting with Hexane/EtOAc (100:0 to 80:20), giving 747 mg of pure product as a brown solid. 701 mg of product were recrystallised from Hexane/EtOAc (50/50) giving 276 mg of pure product as a brown needle crystals.

Yield= 43%
mp= 106-107 °C
LRMS (ES^+) m/e: 267.1 ($(M+H)^+$, 100%).
HRMS: Calcd mass for $C_{12}H_9N_2O_4^+$ ($M+H^+$): 267.0382; Found: 267.0377.
Anal. Calcd. ($C_{12}H_8N_2O_4 \cdot 1/3\ H_2O$): C, 57.6, H, 3.5, N, 11.2; Found: C, 58.1, H, 3.3, N, 11.3.
^{1}H-NMR ($CDCl_3$, 300 MHz): δ 5.17 (s, 2H, H-C8), 6.74 (d, 1H, *J*=3.66 Hz, H-C10), 7.08 (d, 2H, *J*=8.42 Hz, H-C4,C6), 7.34 (d, 1H, *J*=3.66, H-C11), 7.68 (d, 2H, *J*=8.42 Hz, H-C3,C7).

^{13}C-NMR ($CDCl_3$, 75 MHz): δ 62.5 (1, C-8), 105.9 (C-2), 112.5 (C-10), 113.4 (C-11), 115.8 (C-4 and C-6), 119.2 (C-1), 134.6 (C-3 and C-7), 152.3 (C-12), 161.1 (C-9).

9.1.2 Attempted synthesis of 4-[O-[5-(nitrofuran-2-yl)-methyl]-oxy-]-benzamidine (91) from corresponding nitrile derivative:

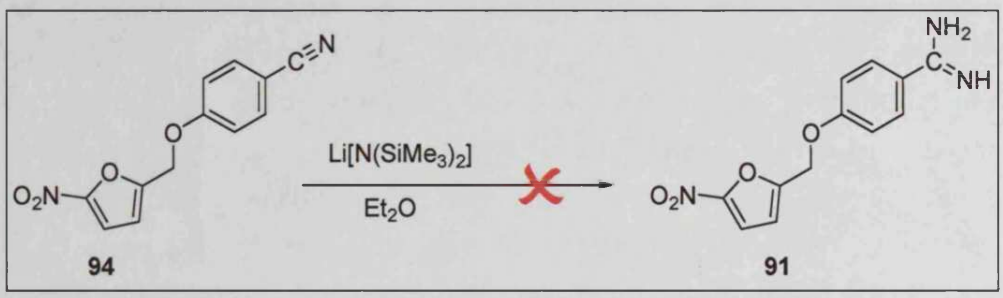

9.1.2.1 Method A: attempted synthesis:

A solution of lithium 1,1,1,3,3,3-hexamethyldisilazane was prepared *in situ,* by a dropwise addition of nBuLi (0.42 mL 2.5M, d=0.693, 1.06 mmol) to a solution of 1,1,1,3,3,3-hexamethyldisilazane (0.22 mL, d=0.765, 1.06 mmol) in anhydrous ether (2mL) at 0°C with stirring and under nitrogen. 4-(5-Nitro-furan-2-yl-methoxy)-benzonitrile (150 mg, 0.53 mmol) was dissolved in anhydrous THF (3mL) at 0°C and added dropwise to the solution previously prepared. The temperature was left to rise to room temperature and the reaction was left stirring overnight. The mixture was cooled and quenched by adding aqueous HCl. A black precipitated was observed. The mixture was diluted with water (100 mL) and Et_2O (15 mL) was added. The aqueous layer was basified with NaOH 3N and several organic extractions were performed (EtOAc, DCM, Et_2O were used). TLC and MS analyses of the fractions suggested that the product was not present. The water layer was concentrate under vacuum and the solid was purified by flash chromatography (Hexane/EtOAc= 100/0 to 70:30). TLC (Hexane/EtOAc= 60:40 + ninhydrin stain) and MS analyses of the different fractions confirmed that the formation of the expected product did not occur.

9.1.2.2 Method B: attempted synthesis:

4-(5-Nitro-furan-2-yl-methoxy)-benzonitrile (150 mg, 0.61 mmol) in anhydrous THF (1 mL) and anhydrous Et_2O (1 mL) was added dropwise to a solution of lithium 1,1,1,3,3,3-hexamethyldisilazane (1.22 mL 1.0M, d=0.891, 1.22 mmol) in anhydrous Et_2O (2 mL) at O°C with stirring and under nitrogen. The temperature was left to rise to room temperature and the reaction was left stirring overnight. The mixture was cooled and quenched with aqueous HCl (0.25 M, 70 mL). HCl 2M (2 mL) was added and the mixture was diluted with water (50 mL) and Et_2O (20 mL). The aqueous layer was made basic with NaOH 3N and the ether layer was discarded. Several extractions were performed (EtOAc, DCM, Et_2O were used). TLC (Hexane/EtOAc= 60:40 + ninhydrin stain) and MS analyses of the different fractions confirmed that the formation of the expected product did not occur.

9.1.2.3 Method C: attempted synthesis via Aluminium amide:

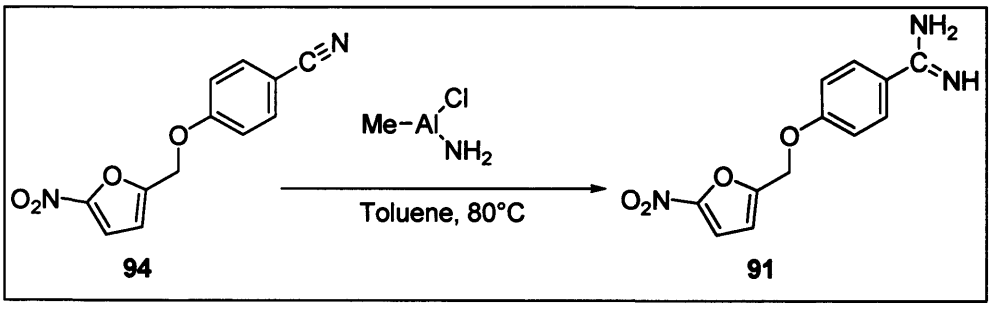

Preparation of Aluminium amide reagent 0.67M:

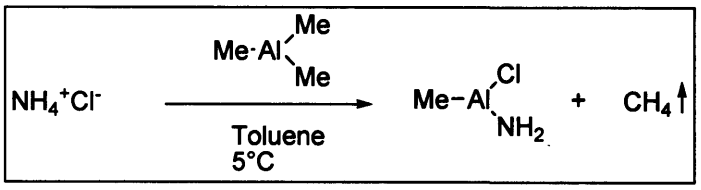

10 mL of a 2M solution of trimethyl-aluminium in toluene were slowly added to a suspension of ammonium chloride (1.06g, 0.02 mol) in 20 mL of anhydrous toluene at 5°C. After the addition was complete, the reaction was stirred under nitrogen for 2 hrs at room temperature until the gas evolution had ceased.

9.1.2.3.1 Procedure A:

1.83 mL of a 0.67M solution of hydrochloride aluminium amide was added to a solution of 4-(5-Nitro-furan-2-yl-methoxy)-benzonitrile (100 mg, 0.41 mmol) in anhydrous toluene (4 mL) and the mixture was left stirring overnight under nitrogen at 50°C and then at 80°C for 3 hrs. TLC analysis (Hexane/EtOAc=65:35) showed the formation of a product on the base line that becomes pink when stained with ninhydrin. The reaction was then left cooling down to room temperature and the aluminium complex was decomposed by carefully pouring the mixture into a slurry of silica gel (2g) in chloroform. The mixture was stirred for 5 mins and then was filtered. The filtercake was washed with 20 mL of methanol and the filtrate was concentrated under vacuum giving a mixture with silica. The attempts to extract the expected product from the mixture (propan-2-ol was used in order to extract the product without dissolving the silica) failed and the reaction was repeated following the procedure B.

9.1.2.3.1 Procedure B:

Trimethyl-aluminium (1.38 mL, 2.0M in toluene, 2.76 mmol) was added to a suspension of ammonium chloride in toluene (147.63 mg, 2.76 mmol) at 5°C with stirring and under nitrogen. After the complete addition and when the gas evolution was ceased, the temperature was left to rise to room temperature and 4-(5-Nitro-furan-2-yl-methoxy)-benzonitrile (195 mg, 0.79 mmol) was added. The mixture was left stirring overnight at 80°C and then stopped and left cooling down to room temperature. The aluminium complex was decomposed by carefully pouring the mixture into a slurry of silica gel (2g) in chloroform. The mixture was stirred for 10 mins and then was filtered. The filtercake was washed with chloroform and then with propan-2-ol in order to avoid the dissolution of the silica but, as well as observed on the previous procedure, all the attempts to isolate the product failed.

9.1.2.3.3 Procedure C:

Trimethyl-aluminium (3.59 mL, 2.0M in toluene, 7.17 mmol) was added to a suspension of ammonium chloride in toluene (383.52 mg, 7.17 mmol in 7 mL of toluene) at 5°C under stirring and under nitrogen atmosphere. After the complete addition and when the gas evolution was ceased, the temperature was left to rise to room temperature and 4-(5-Nitro-furan-2-yl-methoxy)-benzonitrile (500 mg, 2.05 mmol) was added. The mixture was left overnight at 80°C and then stopped and left cooling down to room temperature. The aluminium complex was decomposed by carefully pouring the mixture in 80 mL of aqueous HCl. The water layer was extracted with EtOAc (3 x 30mL) until complete elimination of the starting material. The water layer was then concentrated under vacuum and the solid divided in two batches. The first batch was purified by flash chromatography using reversed phase silica gel 100_{C18} and H_2O/CH_3CN as eluent. The second batch was purified by ion exchange chromatography (the resin was previously treated as previously described on §11.1) using a gradient of HCl in propan-2-ol (0N to 6N). Unfortunately in both cases the the product could not be isolated.

9.1.3 Attempted synthesis of 4-[O-[5-(nitrofuran-2-yl)-methyl]-oxy-]-benzamidine (91) via formation of imidoester:

9.1.3.1 Method A: attempted synthesis:

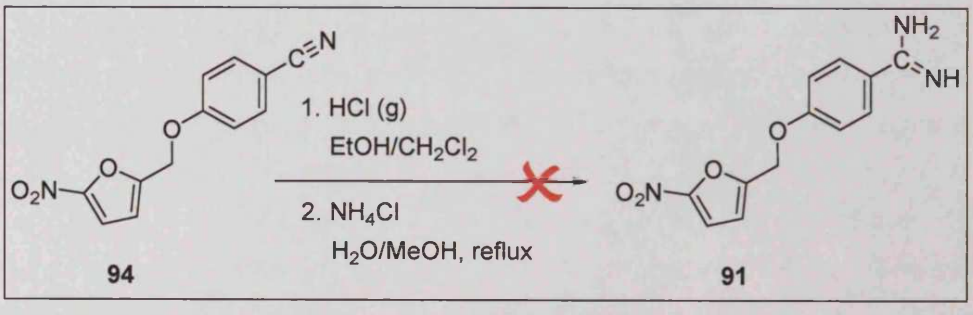

4-(5-Nitro-furan-2-yl-methoxy)-benzonitrile (295 mg, 1.21mmol) was dissolved in anhydrous chloroform (8 mL) and absolute EtOH (0.5 mL, 8.57 mmol) was added to the suspension with stirring. The mixture was cooled down to 0°C, saturated with dry HCl (g) under nitrogen and was kept

refrigerated at 0°C for 24 hrs. The solvent was removed under reduced pressure and Et_2O was added until the formation of brown crystals. The crystals were dissolved in cold water (5mL) and 3 mL of K_2CO_3 were added. The mixture was stirred for 5 mins at room temperature and then extracted with EtOAc. The organic phases were collected together, dried with $MgSO_4$ and the solvent was removed under vacuum giving a dark brown solid. The solid was then dissolved in water/methanol (3.5mL/1mL) with ammonium chloride (97.1 mg, 1.81 mmol) and heated to reflux for 5 hrs. The mixture was concentrated under vacuum and the residue dissolved in acetone giving a grey-white precipitate. MS and NMR analyses of the precipitate did not confirm the formation of the desired product.

9.1.3.2 Method B: attempted synthesis:

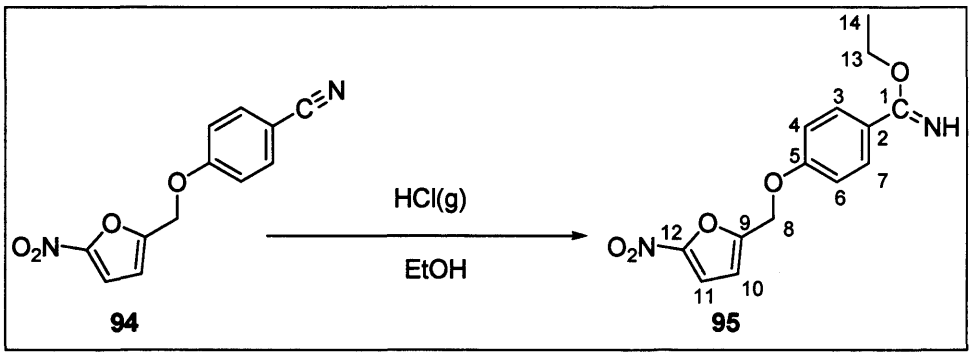

4-(5-Nitro-furan-2-yl-methoxy)-benzonitrile (180 mg, 0.73 mmol) was dissolved in absolute ethanol (3 mL) and the mixture was saturated with HCl (g) at 0°C and under nitrogen. The mixture was left stirring and at 0°C for 8hrs and stored overnight in a refrigerator. TLC analysis (Hexane/EtOAc=50/50) showed the complete reaction of the starting material and the formation of a new product. The MS [LRMS (ES^+)m/z= 291, $(M+H)^+$] and NMR analyses confirmed the formation of the imidoester. The mixture was concentrated under vacuum and the crude product was used without further purifications in the following procedures for the synthesis of the corresponding benzamidine.

9.1.3.2.1 Attempted conversion of the imido ester to benzamidine (procedure A)

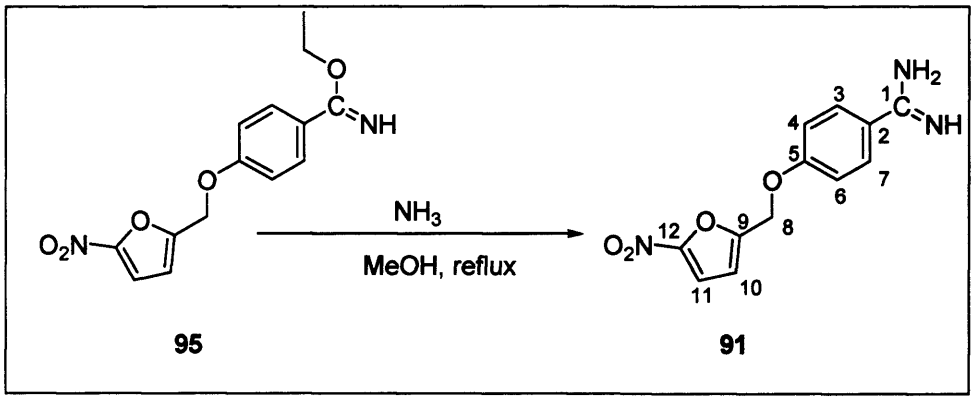

95 **91**

The crude imidoester (60 mg, 0.21mmol) was dissolved in NH_4OH 2M in MeOH (4mL) and the solution was heated to reflux and left stirring and temperature overnight. The TLC analysis (Hexane/EtOAc= 50/50) showed the complete reaction of the starting material and the MS analysis showed a peak at 262 ($M+H^+$) corresponding to the expected benzamidine product. However, the product could not be isolated from the mixture since the attempts to purify it from the crude mixture have failed.

9.1.3.2.2 Attempted conversion of the imido-ester to benzamidine (procedure B)

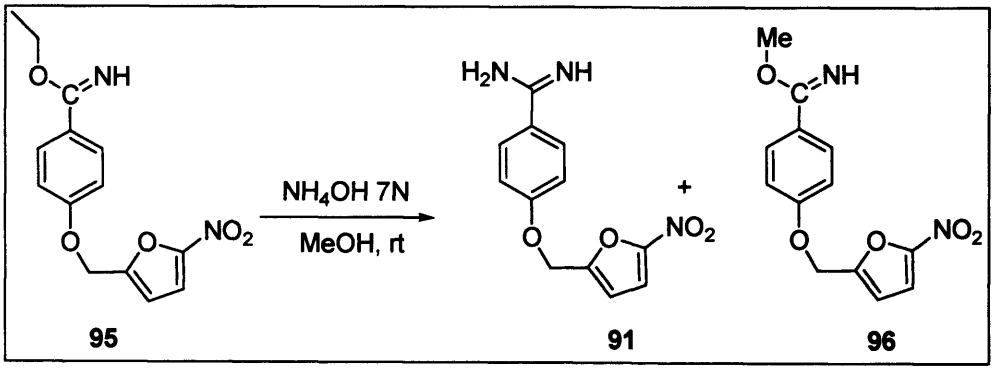

95 **91** **96**

The crude imidoester (68mg, 0.2 mmol) was dissolved in NH_4OH 7N in MeOH (5mL) and was left stirring at room temperature for 3 hrs. MS analysis showed a peak of the expected product at 262 ($M+H^+$), together with a peak at 277 ($M+H^+$) corresponding to the imido-methyl ester indicating that trans-esterification with MeOH occurred. As well as

observed for the previous experiment, the product could not be isolated from the mixture.

In order to facilitate the purification of the benzamidine product Boc-protection of the mixture was performed as described.

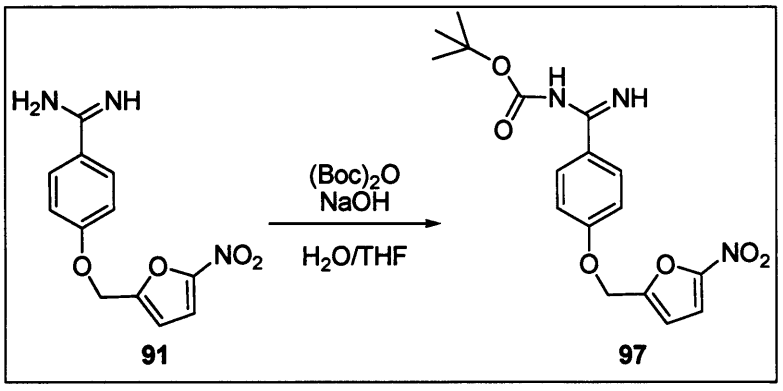

91 **97**

The mixture was concentrated under vacuum, dissolved in H_2O (10 mL) and THF (10 mL) and cooled down to 0°C. NaOH 3N was added (2,45 mL, 7.35 mmol) followed by the dropwise addition of Boc anhydride (462 mg 99%, 2.1 mmol) previously dissolved in THF (2 mL). The temperature was left to rise to room temperature and the mixture was left stirring for 1 day. TLC analysis showed the presence of two new products but MS analysis of the mixture did not confirm the presence of the expected Boc derivative of the benzamidine compound. The THF layer was removed under vacuum and the water layer was extracted with EtOAc. The organic phases, containing the two products were collected together, dried over $MgSO_4$ and concentrated under vacuum. The mixture was purified by preparative chromatography eluting with EtOAc/Hexane (50/50) giving respectively 15 mg and 30 mg of the two new products. MS and NMR analyses of the two product showed that none corresponded to the expected product.

9.1.4 Attempted synthesis of 4-[O-[5-(nitrofuran-2-yl)-methyl]-oxy-]-benzamidine: an alternative route from p-cyanophenol

9.1.4.1 Attempted synthesis of p-hydroxybenzamidine (98):

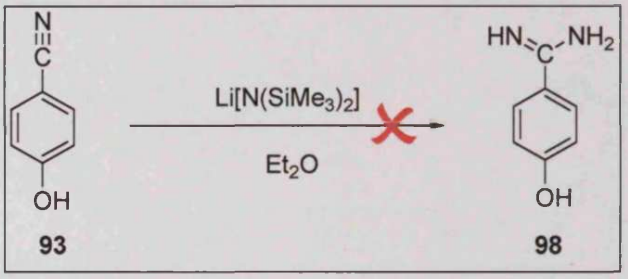

p-Cyanophenol (500 mg 99%, 4.15 mmol) was added to a solution of lithium 1,1,1,3,3,3-hexamethyldisilazane (8.3 mL 1.0M, d=0.891, 8.3 mmol) in anhydrous Et_2O at 0°C under nitrogen and with stirring. The solution was then left stirring for 20 hrs at room temperature. The mixture was cooled down and HCl 1N was added dropwise until acidic pH. The ether layer was washed with acidic water and discarded. The water layers were collected together but TLC and MS analyses showed only the presence of starting material and the formation of the expected product did not occur.

9.1.4.2 Synthesis of p-benzyl-4-cyanophenol (99):

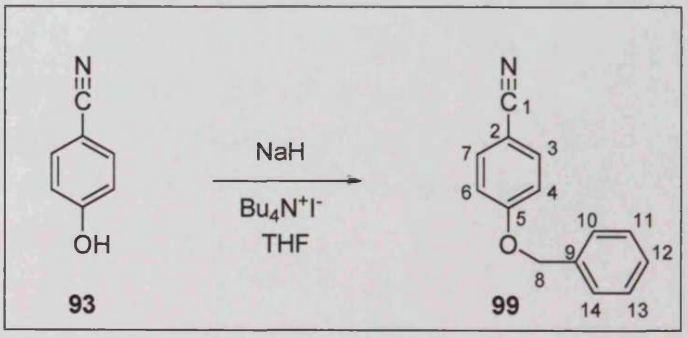

9.1.4.2.1 Attempted synthesis: method A

NaH (176 mg 60%, 4.4 mmol) was slowly added to a solution of p-cyanophenol (500 mg 99%, 4 mmol) in anhydrous THF (10 mL) at room temperature, with stirring and under nitrogen. The reaction was left stirring for 30 mins and then tetrabutylammonium iodide (14.77 mg, 0.04

mmol) and benzyl bromide (767.93 mg 98%, 4.4 mmol) were added to the mixture. The reaction was left stirring overnight at room temperature. TLC analysis (Hexane/EtOAc=75/35) did not show any formation of expected product. Method B was therefore considered for the synthesis.

9.1.4.2.2 Synthesis p-benzyl-4-cyanophenol: method B

NaH (1.056 g 60%, 26.31 mmol) was slowly added to a solution of 4-cyanophenol (3 g, 23.92 mmol) in anhydrous THF (60 mL) at room temperature with stirring and under nitrogen. The reaction was left stirring for 30 mins and then tetrabutylammonium iodide (369.4 mg, 0.24 mmol) and benzyl bromide (4.591 g 98%, 26.31 mmol) were added to the mixture. The reaction heated to reflux and left stirring for 5 hrs until complete reaction of the starting material. The mixture was poured into a solution of diluted HCl. The water layer was extracted with EtOAc. The organic layers were combined together and concentrated under vacuum. The crude product was purified by flash chromatography eluting with Hexane/EtOAc (100:0 to 80/20) giving 4.900 g of pure product as a white solid.

Yield: 98 %
mp: 85-86°C
LRMS (ES^+): m/z 232 $(M+Na)^+$, 35%), 441 ($(2M+Na)^{+,}$ 10%).
^{1}H-NMR (MeOD, 300 MHz) δ 5.16 (s, 2H, H-C8), 7.14 (d, 2H, *J*= 8.96 Hz, H-C3, H-C5), 7.33-7.46 (m, 5H, H-C10-14), 7.64 (d, 2H, *J*= 8.96 Hz, H-C2, H-C6).
^{13}C-NMR (MeOD, 75 MHz) δ 71.7 (C8), 105.3 (C1), 117.3 (C3 and C5), 120.4 (C7), 129.1 (C11 and C13), 129.6 (C12), 130.0 (C10 and C14), 135.5 (C2 and C5), 138.1 (C9), 164.1 (C4).

9.1.4.3 Synthesis of 4-[O-(benzyloxy]-benzamidine (100):

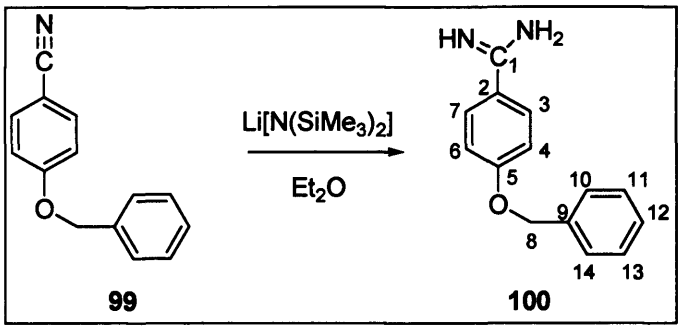

p-benzyl-4-cyanophenol (2 g, 9.5 mmol) was dissolved in Et_2O (5mL) and anhydrous THF (10 mL) and added at 0°C to a solution of lithium hexamethyldisilazane (3.82 mL 1M in THF, 3.82 mmol,) in dry Et_2O (70 mL) with stirring and under nitrogen. The temperature was left to rise to room temperature and the mixture was left stirring under nitrogen for 20 hrs. The mixture was carefully poured into a solution of diluted HCl. The water layer was extracted with EtOAc (3x50 mL). The organic layers were combined together and concentrated under vacuum. The product was not further purified but used as crude in the following step.

9.1.4.4 BOC protection of the 4-O-(benzyloxy)-benzamidine (101):

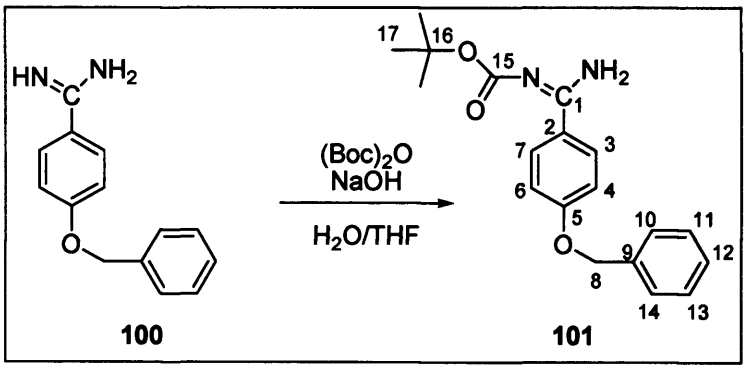

A water solution of crude 4-[O-(benzyl-)-oxy]-benzamidine was neutralised with NaOH 3N and was added to THF (100 mL) and water (100 mL) followed by the addition of further NaOH (23.75 mL 3N, 71.25 mmol). The

mixture was cooled down to 0°C and a solution of di-*tert*-butyldicarbonate (3.11 g, 14.25 mmol) in THF (20 mL) was added dropwise. After complete addition the mixture was left stirring for 12 hrs at room temperature. The organic layer was removed under vacuum and the remaining water layer was extracted with EtOAc (4 x 65 mL). The organic phases were collected together, dried with $MgSO_4$ and concentrated under vacuum giving a crude solid. The solid was triturated using hexane giving 2.251g of product as a pure white solid.

Yield: 73%

LRMS (ES^+): m/z 327 ($(M+H)^+$, 100 %), 349 ($(M+Na)^+$, 20 %).

^{1}H-NMR (MeOD, 300 MHz) δ 1.53 (s, 9H, H-C17), 5.15 (s, 2H, H-C8), 7.07 (d, 2H, *J*= 9.15 Hz, H-C4, H-C6), 7.28-7.50 (m, 5H, H-C10-C14), 7.81 (d, 2H, *J*= 9.15 Hz, H-C3, H-C7).

^{13}C-NMR (MeOD, 75 MHz) δ 28.9 (C17), 71.5 (C8), 80.7 (C16), 116.2 (C4 and C6), 128.7 (C2), 129.0 (C11 and C13), 129.4 (C12), 130.0 (C3 and C7), 131.0 (C10 and C14), 138.6 (C5), 163.7 (C1).

9.1.4.5 Synthesis of N'-(O-tert-butoxycarbonyl)-4-hydroxy-benzamidine (102):

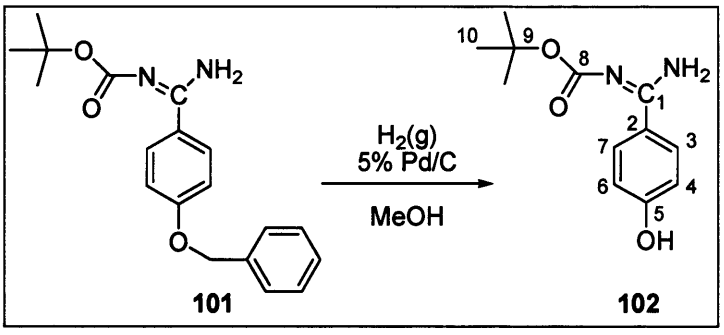

Boc protected 4-[O-(benzyl-)-oxy]-benzamidine (2.2 g, 6.13 mmol) was dissolved in anhydrous methanol (80 mL). Palladium 5% on activated charcoal was added (1 g) and the reaction was left stirring and under hydrogen at room temperature. After 1 h 30 mins the catalyst was filtered off and the solution was concentrated under vacuum giving the crude product as an oil. The oil was triturated with Et_2O giving the pure product

as a white crystals that was filtered and dried under high vacuum giving 750 mg of pure solid.

Yield: 52%

LRMS (ES+): m/z 237.1 ($(M+H)^+$,100%), 259.1 ($(M+Na)^+$, 20%), 473.0 ($(2M+H)^+$, 25%).

^{1}H-NMR (MeOD, 300 MHz) δ 1.53 (s, 9H, H-C10), 6.84 (d, 2H, *J*= 8.87, H-C4, H-C6), 7.73 (d, 2H, *J*= 8.87 Hz, H-C3, H-C7).

^{13}C-NMR (MeOH, 75 MHz) δ 28.9 (C10), 80.6 (C9), 116.7 (C4 and C6), 126.7 (C2), 131.1 (C3 and C7), 163.4 (C5), 165.1 (C1), 170.3 (C8).

9.1.4.6 Attempted synthesis of 4-O-[(5-nitrofuran-2yl)-methyl]-N'-(O-tert-butoxycarbonyl)-4-hydroxy-benzamidine (97):

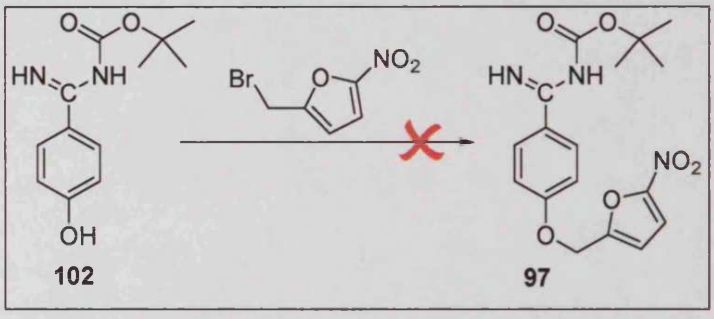

9.1.4.6.1 Method A:

NaH (20 mg 60%, 0.50 mmol) and N'-[(O-tert-butyl-oxy-)-carbonyl]-4-hydroxy-benzamidine (100 mg, 0.42 mmol) were suspended together in anhydrous THF (10 mL) and the suspension was left stirring for 30 mins at room temperature under nitrogen. 2-Bromomethyl-5-nitrofuran in anhydrous THF (10 mL) was added dropwise to the suspension and the mixture was left refluxing for 5 hrs and overnight at room temperature. TLC (EtOAc: Hexane = 30:70) analysis of the mixture showed mainly starting material. The MS of the mixture did not show any peak corresponding to the expected product. The mixture was concentrated under vacuum and purified by flash chromatography (MeOH/DCM = 0:100 to 7.5:92.5) but only starting material was recovered.

9.1.4.6.2 Method B:

A solution of 2-bromomethyl-5-nitrofuran (214 mg 97%, 1.01 mmol) in acetonitrile (8 mL) was added dropwise to a suspension of N'-[(O-tert-butyl-oxy-)-carbonyl]-4-hydroxy-benzamidine (200 mg, 0.84 mmol) and K_2CO_3 (464.4 mg, 3.36 mmol) in dry acetonitrile (8mL) under nitrogen. The mixture was left stirring overnight. TLC analysis (DCM/MeOH=85/20) showed the formation of a new product but MS analysis did not show any peak corresponding to the expected product. The mixture was purified by flash chromatography eluting with DCM/MeOH (100/O to 80/20) but NMR analysis of the fractions recovered showed that the formation of the desired product did not occur.

9.2 Synthesis of p-substituted benzamidines:

9.2.1 Synthesis of 4-benzyloxy-benzamidine (100):

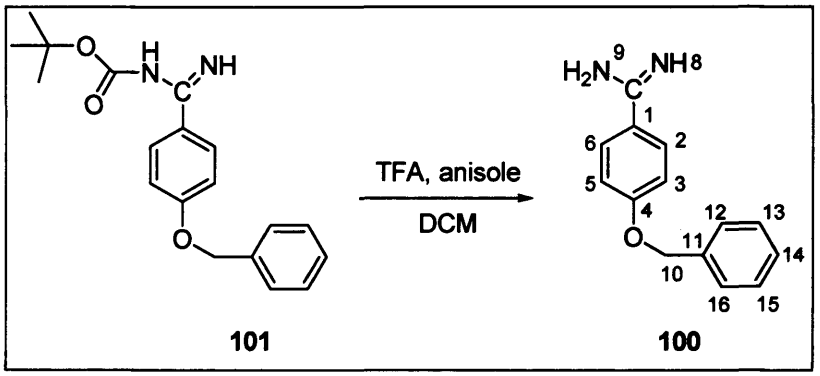

101 **100**

Boc protected 4-[O-(benzyl-)-oxy]-benzamidine (80mg, 0.245mmol) was dissolved in DCM (3mL) and trifluoroacetic acid (0.19ml, 2.45 mmol) together with anisole (0.08ml, 0.735mmol) were added to the solution at 0°C. The temperature was allowed to rise to room temperature and the reaction was left stirring for 30 minutes. The mixture was concentrated under vacuum. Diethyl ether was added to the mixture until formation of a precipitate. The precipitate was filtered off and washed with diethyl ether to afford 35 mg of 4-Benzyloxy-benzamide as a white crystalline solid.

Yield: 63%.

mp: 259-261°C.

LRMS (ES^+): m/z 227.1 ($(M+H)^+$, 100%).

^{1}H-NMR (300 MHz, MeOD): δ 5.22 (s, 2H, H-C10), 7.21 (d, 2H, *J* = 9.0 Hz, H-C2 and H-C6), 7.34 -7.47 (m, 5H, H-C12-16), 7.80 (d, 2H, *J* = 9.0 Hz, H-C3 and H-C5).

^{13}C-NMR (75 MHz, MeOD): δ 71.8 (C10), 117.1 (C3 and C5), 121.6 (C 1), 129.1 (C2 and C6), 129.6 (12 and C16), 130.0 (C14), 131.4 (C 13 and C15), 138.1 (C11), 165.3 (C4)

9.2.2 Synthesis of 4-O-heptyloxy-N'-[(O-*tert*-butyl-oxy-)-carbonyl]-benzamidine (105):

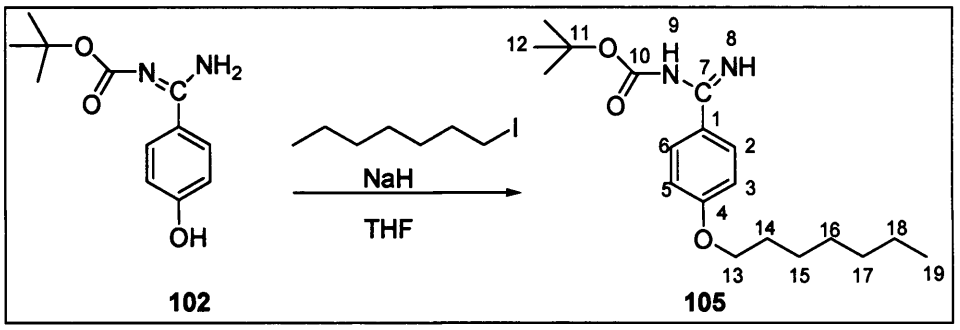

A solution of N'-[(O-tert-butyl-oxy-)-carbonyl]-4-hydroxybenzamidine (40mg, 0.169 mmol) in dry THF (0.5 mL) was added to a solution of NaH (7 mg 60%, 0.186mmol) in dry THF (1.5 mL) at 0° and left to stir for 30 minutes. Then heptyl-iodide (0.03ml, 0.186 mmol) was slowly added and the mixture was allowed to warm to room temperature. The mixture was heated under reflux for 2 hours and then left to stir at room temperature overnight. The reaction mixture was concentrated under vacuum to give a yellow solid. The solid was purified by column chromatography using hexane/EtOAc (97:3 v/v) as eluent. The fractions collected were concentrated under vacuum to afford 20 mg of pure product as a white solid.

Yield: 35%.

LRMS (ES^+): m/z 335.0 ($(M+H)^+$, 5%), 668.7 ($(2M+H)^+$, 100%).

^{1}H-NMR (300 MHz, MeOD): δ 0.87-0.95 (m, 3H, H-C19), 1.45 (s, 8H, H-C14, H-C15, H-C16, H-C17), 1.54 (s, 9H, H-C12), 1.74-1.85 (m, 2H, H-C14), 4.05 (t, 2H, H-C13), 7.0 (d, 2H, *J*= 9.0 Hz, H-C3 and H-C5), 7.8 (d, 2H, *J*= 9.0 Hz, H-C2 and C6).

^{13}C-NMR (75 MHz, MeOD): δ 14.8 (C19), 24.1 (C18), 27.5 (C17), 29.1 (C12), 30.6 (C16), 30.7 (C15), 33.4 (C14), 80.6 (C11), 115.7 (C3 and C5), 128.3 (C1), 130.9 (C2 and C6), 164.2 (C4).

9.2.3 Synthesis of 4-O-heptyloxy-benzamidine (106):

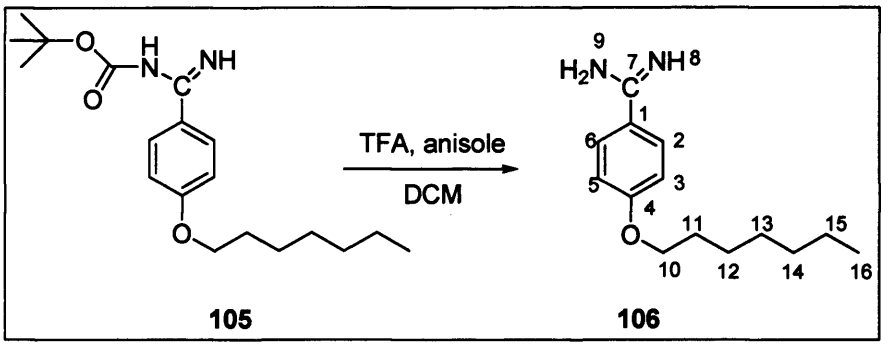

105 106

4-O-heptyloxy-N'-[(O-*tert*-butyl-oxy-)-carbonyl]-benzamidine (30mg, 0.09 mmol) was dissolved in DCM (1.2 mL) and trifluoroacetic acid (0.07ml, 0.9 mmol) together with anisole (0.03ml, 0.27mmol) were added at 0°C. The mixture was allowed to warm to room temperature and left to stir for 30 minutes. A TLC (hexane/ethyl acetate 70:30) showed the some starting material in the reaction mixture, so further trifluoroacetic acid (0.05ml) was added and the reaction was left to stir for a further 30 minutes. The mixture was then concentrated under vacuum to give a brown solid. This was then washed with diethyl ether to give 32mg 4-Heptyloxy-benzamidine as an off-white solid.

Yield: 95%.

mp: 235-238°C.

LRMS(ES^+): m/z 235.1 ($(M+H)^+$, 100%)

^{1}H NMR (300 MHz, MeOD): δ 0.93 (m, 3H, H-C16), 1.32-1.56 (m, 8H, H-C12-15), 1.78-1.87 (m, 2H, H-C11), 4.11 (t, 2H, H-C10), 7.13 (d, 2H, *J*= 9.0 Hz, H-C3 and H-C5), 7.79 (d, 2H, *J*= 9.0 Hz, H-C2 and H-C6).

^{13}C-NMR (75 MHz, MeOD): δ 14.6 (C16), 24.0 (C15), 27.4 (C14), 30.5 (C13 and C12), 33.3 (C11), 70.1 (C10), 116.6 (C3 and C5), 131.4 (C2 and C6), 163.2 (C7).

9.3 Synthesis of derivatives of 4-aminobenzamidine:

9.3.1 Attempted synthesis of 4-Heptylamino-benzamidine (107):

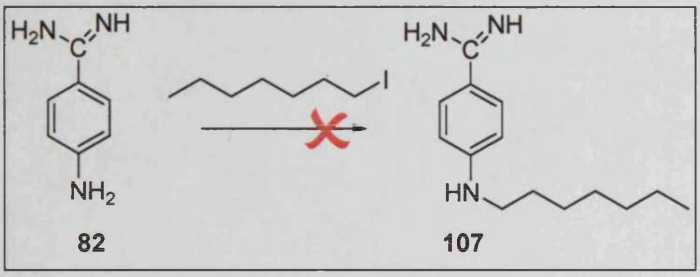

82 107

9.3.1.1 Procedure A

DBU (0.7ml, 4.51mmol) was added dropwise to a mixture of 4-aminobenzamidine dihydrochloride (300mg, 1.44 mmol) and ethanol (4 mL) and left stirring until homogenous. Then heptyliodide (0.3ml, 1.69 mmol) was slowly added to the mixture. The mixture was then left stirring overnight. A TLC analysis (hexane/ethyl acetate 70:30) and MS analysis showed only starting material to be present and the product had not been obtained.

9.3.1.2 Procedure B

Procedure A was followed for this reaction with the exception of the reaction mixture being heated under reflux. Mass spectra data obtained showed that the resulting product was a complex mixture that did not give any peaks corresponding to the estimated molecular weight of the desired product.

9.3.2 Attempted synthesis of 4-{[(5-nitrofuran)-2-yl]-methylene}-amino-benzamidine (108):

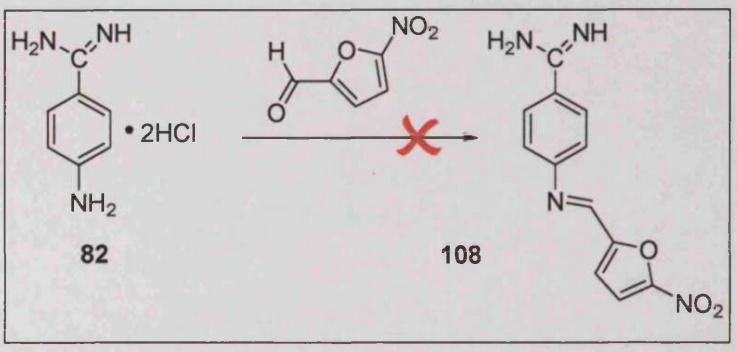

9.3.2.1 Method A

A mixture of 4-amino-benzamidine (218.49 mg 98%, 1.05 mmol) and 5-nitrofuraldehyde (150 mg 99%, 1.05 mmol) were suspended in MeOH (5 mL) and the suspension was left stirring and at room temperature overnight. The reaction was concentrated under vacuum and the yellow-orange solid was purified using reverse phase chromatography (SiO_2 reverse phase C_{18}) using H_2O/CH_3CN as eluent. MS and NMR analysis of the fractions showed that the formation of the expected product did not occur.

9.3.2.2 Method B

4-amino-benzamidine (218.49 mg 98%, 1.05 mmol) was neutralised with NaOH. Upon addition of the neutralised benzamidine to the 5-nitro-furaldehyde (150 mg 99%, 1.05 mmol) in MeOH (5 mL) a thick black solid formed. It was likely that the black solid is a result of polymerisation.

9.3.2.3 Method C

4-amino-benzamidine (218.49 mg 98%, 1.05 mmol) was neutralised with NH_4OH. As well as observed in the previous experiment, upon addition of

the neutralised benzamidine to the 5-nitro-furaldehyde (150 mg 99%, 1.05 mmol) in MeOH (5 mL) a thick black solid formed.

9.3.2.4 Method D

4-amino-benzamidine (109.24 mg 98%, 0.52 mmol) was neutralised and dissolved in a phosphate buffer at pH 7.2. Upon addition of the neutralised 4-amino-benzamidine to the 5-nitro-furaldehyde (75 mg 99%, 0.52 mmol) in MeOH (3 mL) a thick black solid formed.

9.3.3 Attempted synthesis via Boc-protection of 4-amino-Benzamidine:

9.3.3.1 N-(O-*tert*-butoxycarbonyl)-4-amino-benzamidine (83)[115]:

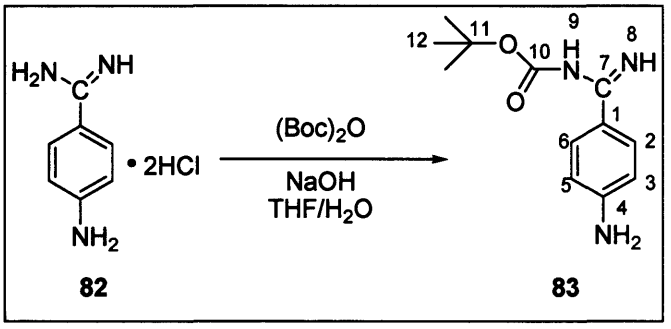

82 83

p-Aminobenzamidine dihydrochloride (2.04g 98%, 9.6 mmol) was suspended in THF (50 mL) and water (10 mL). The HCl was neutralised with NaOH 3N and then 3 further NaOH 3N was added (9.6 mL, 28.8 mmol). The solution was cooled down to 0°C and a solution of Boc-anhydride (3.175g 99%, 14.4 mmol) in THF (30 mL) was added dropwise. The mixture was left stirring at room temperature for 3 hrs. The THF layer was removed under vacuum and the remaining water solution was extracted with EtOAc (3x100 mL). The organic phases were collected together, dried over $MgSO_4$ and concentrated under vacuum giving 2.17g of pure product as light yellow crystals.

Yield: 2.170 g, 96%

LRMS(ES^+): m/z 236.2 ($(M+H)^+$, 100%), 258 ($(M+Na)^+$, 20 %), 471.1 $(2M+H)^+$, 20%), 492.9 ($(2M+Na)^+$, 25%).

^{1}H-NMR (MeOD, 300 MHz) δ 1.53 (s, 9H, H-C12), 6.68 (d, 2H, *J*= 8.78 Hz, H-C3, H-C5), 7.64 (d, 2H, *J*= 8.78 Hz, H-C2, H-C6).

^{13}C-NMR (MeOD, 75 MHz) δ 29.0 (C12), 80.3 (C11), 115.1 (C3 and C5), 123.5 (C1), 130.8 (C2 and C6), 154.2 (C7), 165.5 (C4), 170.4 (C7).

9.3.3.1 Attempted synthesis of 4-N-[(5-nitrofuran-2yl)-methyl]-N'-(O-*tert*-butoxycarbonyl)-4-amino-benzamidine (109):

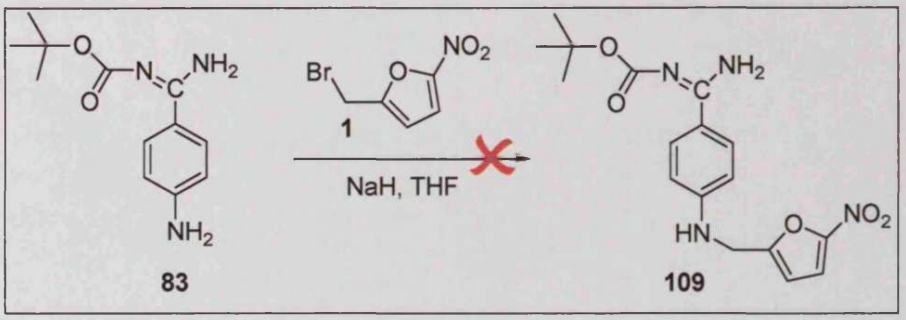

NaH (34.8 mg 60%, 0.87 mmol) and Boc-protected p-aminobenzamidine (172 mg, 0.73 mmol) were suspended together in anhydrous THF (15 mL) and the suspension was left stirring at room temperature and under nitrogen for 1hr and 30 mins. 2-Bromomethyl-5-nitrofuran in anhydrous THF (15 mL) was added dropwise to the suspension and the mixture was left at room temperature for 2 hrs, then left refluxing for 2 hrs and at room temperature overnight. TLC analysis of the mixture (EtOAc: Hexane = 40:60) showed the presence of new products. The MS analysis of the mixture did not show any peak corresponding to the desired product. The mixture was concentrated under vacuum and purified by flash chromatography eluting with EtOAc/Hexane (EtOAc/Hexane = 0:100 to 20:80) but starting materials were just recovered.

10. Experimental Section III:

Prodrug Approach

10.1 Prodrugs of Triazines:

10.1.1 Synthesis of 3-(4,6-diamino-[1,3,5]-triazin-2-yl)-amino-propionic acid (127):

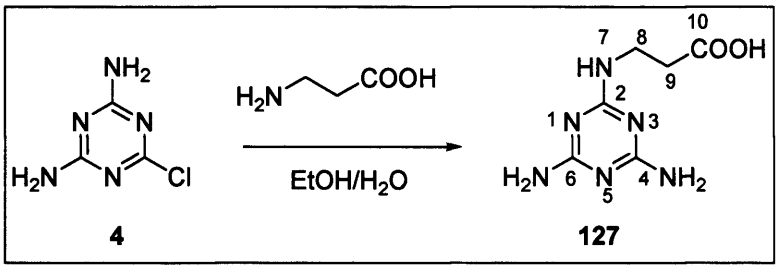

4 **127**

2,4-diamino-6-chloro-triazine (1.00 g, 6.87 mmol), β-alanine (0.92 g, 10.31 mmol) and $NaHCO_3$ (1.15 g, 10.31 mmol) were mixed together and suspended in $EtOH/H_2O$ (1/1, 160 mL). The suspension was left stirring overnight at 100°C. The mixture was acidified with dilute HCl to pH=2 and a white precipitate formed. The precipitate was filtered and washed with water then dried under high vacuum giving 0.61 g of a white solid.

Yield: 45%

mp: 292-295 °C

LRMS (ES^+): 199.2 ($(M+H)^+$, 100%)

^{1}H-NMR (DMSO-d6, 300 MHz): δ 2.50 (t, 2H, J=6.90 Hz, H-C9), 3.43 (dt, 2H, J_d=5.89 Hz, J_t=6.90 Hz, H-C8), 7.80-8.80 (3m, 5H, $2NH_2$, N-H), 12.5 (bs, 1H, .

^{13}C-NMR (DMSO-d6, 75 MHz): δ 33.7 (C9), 36.7 (C8), 147.2 (C2), 158.8 (C4 and C6), 172.9 (C10).

10.1.2 Attempted synthesis of 3-(4,6-Diamino-[1,3,5]triazin-2-yl-amino)-propionic acid chloromethyl ester (128):

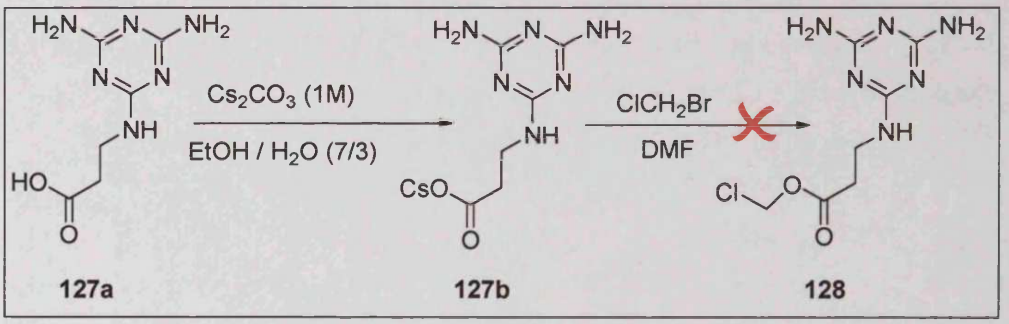

Step 1

3-(4,6-diamino-[1,3,5]-triazine-2-yl)-amino-propionic acid (0.15 g, 0.76 mmol) was suspended in ethanol/ water 7:3 v/v (5 mL). Aqueous caesium carbonate (1 M) was slowly added dropwise until the pH=6.5. The solvents were removed under vacuum and the caesium salt obtained was dried and used in the following step.

Step 2

Bromochloromethane (5 mL) was slowly added to **127b** in dry DMF (3 mL) in the dark. The reaction mixture was stirred in the dark at room temperature under a nitrogen atmosphere for 20 hrs. Reverse phase TLC (acetonitrile/ water 50:50) analysis indicated that the starting material was present in the mixture. LRMS showed no peak corresponding to the desired product and the reaction was unlikely to have taken place.

10.1.3 Attempted synthesis of 3-(4,6-diamino-[1,3,5]-triazin-2-ylamino)-N-benzylpropanamide (129):

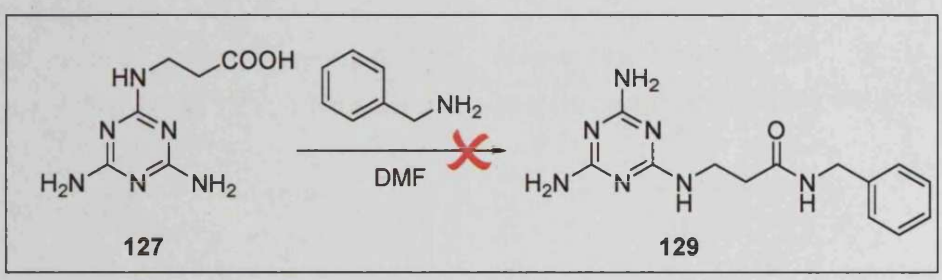

127 129

10.1.3.1 Method A:

3-(4,6-diamino-[1,3,5]-triazine-2-yl)-amino-propionic acid (0.15 g, 0.76 mmol) and EDC (0.27g, 1.7 mmol) were added to dry DMF (14 mL) with stirring and under nitrogen. Benzylamine (0.12 g, 1.14 mmol) was added and the mixture was stirred under nitrogen at rt for 24 hrs. TLC-RP analysis (H_2O/CH_3CN 50/50) showed only the presence of starting material and the formation of the product did not occur.

10.1.3.2 Method B:

3-(4,6-diamino-[1,3,5]-triazine-2-yl)-amino-propionic acid (0.15 g, 0.76 mmol), HOBt (0.12 g, 0.89 mmol) and TBTU (0.29 g, 0.91 mmol) were dissolved in dry DMF (4 mL) under nitrogen and with stirring. DIPEA (0.35 g, 2.69 mmol) was added and the mixture stirred under nitrogen for 30 mins. Benzylamine (0.16 g, 1.52 mmol) in dry DMF (4 mL) was added and the reaction mixture was stirred under nitrogen at rt for 24 hrs. TLC-RP (H_2O/CH_3CN 50/50) showed still the presence of starting material and the formation of a small amount of new product. MS analysis confirmed that the product was not the one expected and the reaction did not occur.

10.2 Prodrugs of Benzamidines:

10.2.1 Attempted synthesis of 3-[N-*tert*-butoxycarbonyl-(4-amidino-phenyl-carbamoyl)]-propanoic acid (113) (method A):

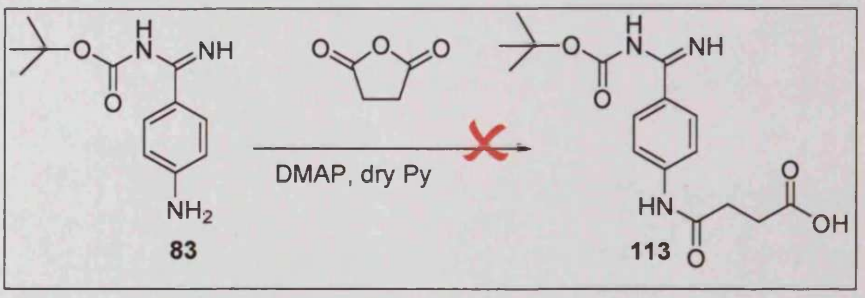

BOC protected benzamidine (0.20 g, 0.85 mmol) was added to dry DMF (1.2 mL). Dry pyridine (0.8 mL), then, succinic anhydride (0.09 g, 0.85 mmol) followed by DMAP (0.01 g, 0.08 mmol) were added to the reaction mixture. The reaction mixture was stirred and heated to 100 °C under nitrogen atmosphere for 3 hrs. A cream precipitate formed and was filtered and washed with water (2 x 100 mL), acetonitrile (2 x 100ml) and ether (2 x 100 mL). LRMS (ES^-) analysis of the precipitate gave no peak corresponding to the desired product. TLC (MeOH/ CH_2Cl_2 15:85) analysis indicated a complex mixture consisting of unknown impurities and starting material.

10.2.2 Synthesis of 3-(4-amidinophenylcarbamoyl)-propanoic acid (112)[132]:

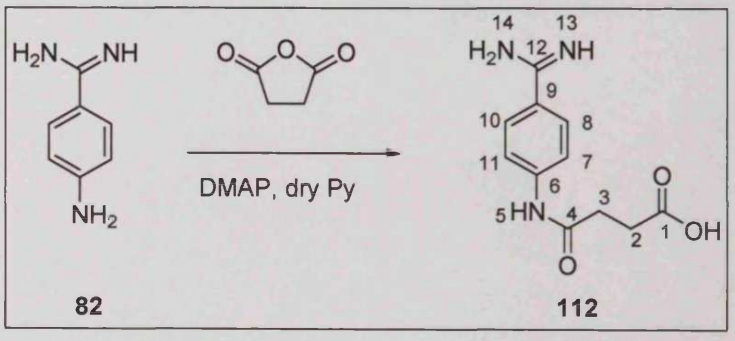

4-Aminobenzamidine dihydrochloride (1.00 g, 4.80 mmol) was added to dry DMF (4 mL). Dry pyridine (4 mL), then, succinic anhydride (0.48 g, 4.80 mmol) followed by DMAP (0.06 g, 0.48 mmol) were added to the reaction mixture. The reaction mixture was stirred and heated to 100 °C at reflux under nitrogen atmosphere for 1 hr. A cream precipitate formed and was filtered and washed with water (2 x 100 mL), acetonitrile (2 x 100ml) and ether (2 x 100 mL). The precipitate was suspended in 4N HCl and dioxane (4 mL). The reaction mixture was stirred for 2 hrs at room temperature then filtered and dried under high vacuum to give 880 mg of pure product.

Yield: 78%

mp= 258-260°C

LRMS (ES+): m/z= 236.2 ($(M+H)^+$, 100 %).

^{1}H-NMR (DMSO-d6, 300 MHz) δ 2.55 (t, 2H, *J*= 5.94 Hz, H-C2), 2.65 (t, 2H, *J*=5.94 Hz, H-C3), 7.84 (s, 4H, Ar-H), 9.09 (s, 2H, NH_2), 9.30 (s, 2H, 2 H-N), 10.67 (s, 1H, OH).

^{13}C-NMR (DMSO-d6, 75 MHz) δ 28.1 (C3), 31.5 (C2), 118.7 (C7, C11), 121.7 (C9), 129.6 (C8, C10), 144.7 (C6), 165.2 (C12), 171.4 (C4), 174.1 (C1).

10.2.3 Attempted synthesis of 3-[N-*tert*-butoxycarbonyl-(4-amidino-phenyl-carbamoyl)]-propanoic acid (113) (method B)

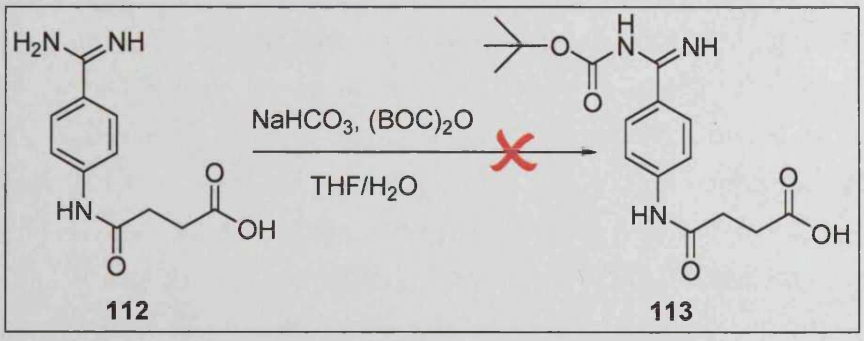

112 113

3-(4-amidinophenylcarbamoyl)-propanoic acid (0.15 g, 0.64 mmol) was suspended in 2:1 THF/water (5ml). The solution was stirred and sodium hydrogen carbonate was added. $(BOC)_2O$ (1.57 g, 7.20 mmol) in THF (15

mL) was slowly added dropwise. The reaction mixture was stirred for 3 hrs at room temperature. The reaction mixture was acidified with dilute HCl to pH 4 . The THF was removed *in vacuo* and the remaining water solution extracted with EtOAc (3 x 50 mL). Reversed phase TLC (acetonitrile/water 50:50) analysis of the organic layer showed starting material only. LRMS analysis indicated no peak corresponding to the desired product but only a peak at 20% intensity corresponding to the starting material.

10.2.4 Attempted Synthesis of 3-[N-benzyloxy-carbonyl-(4-amidino-phenyl-carbamoyl)]-propanoic acid (117):

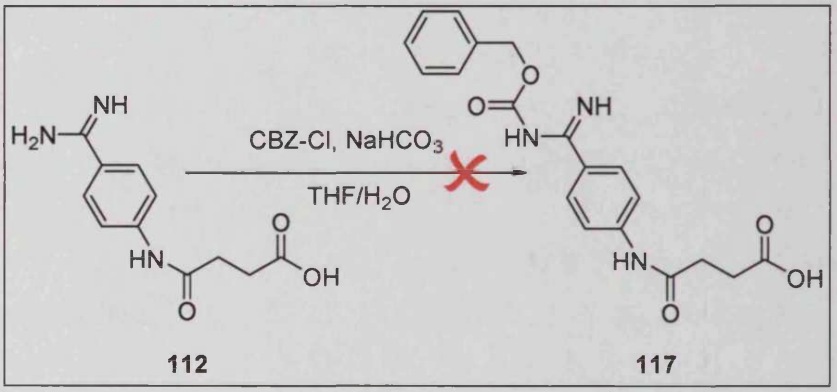

112 117

Sodium hydrogen carbonate (0.34 g, 3.2 mmol) in water (3mL) was added to 3-(4-amidinophenylcarbamoyl)-propanoic acid (0.15 g, 0.64 mmol). The reaction mixture was cooled to 0 °C and stirred for 10 min. THF (2 mL) was added followed by the addition of CBZ-Cl (0.14 mL, 0.96 mmol). The reaction mixture was stirred at 0 °C for 30 min and then at room temperature for 1 hr. The reaction mixture was then acidified with dilute HCl to pH 2 and extracted with EtOAc. The organic layer was dried over $MgSO_4$ and concentrated. TLC (MeOH/ CH_2Cl_2 5:95) analysis showed a mixture containing CBZ-Cl and possible product. LRMS analysis indicated no peak corresponding to the desired product but a peak at 20% intensity corresponding to the reagent CBZ-Cl. The NMR analysis confirmed that CBZ-Cl and unknown impurities had been extracted and indicates that the reaction was unlikely to have taken place.

10.2.5 Synthesis of 3-(4-amidinophenylcarbamoyl)-propanoic acid chloromethyl ester (111):

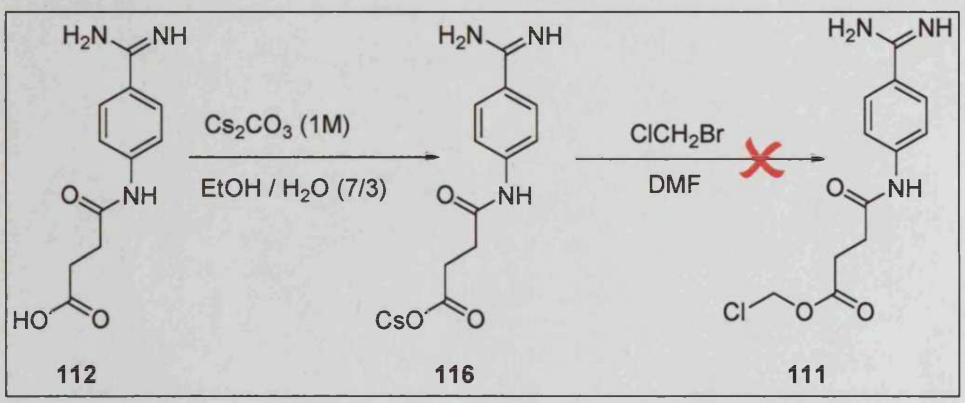

Step 1

3-(4-amidinophenylcarbamoyl)-propanoic acid (0.15 g, 0.64 mmol) was suspended in ethanol/water 7:3 v/v (5 mL). Aqueous caesium carbonate (1 M) was slowly added dropwise to the suspension until pH=6.5. The solvents were removed under vacuum and the caesium salt obtained was dried and used in the following step.

Step 2

Bromochloromethane (3 mL) was slowly added to **116** in dry DMF (3 mL) in the dark. The reaction mixture was stirred in the dark at room temperature under nitrogen atmosphere for 20 hrs. Reverse phase TLC (acetonitrile/ water 50:50) analysis indicated that starting material was present in the mixture. MS analysis showed no peak corresponding to **111** and only a peak at 10% intensity corresponding to starting material indicating that the reaction did not take place.

10.2.6 Attempted synthesis of N-Benzyl-N'-(4-amidino-phenyl)-succinamide (117)

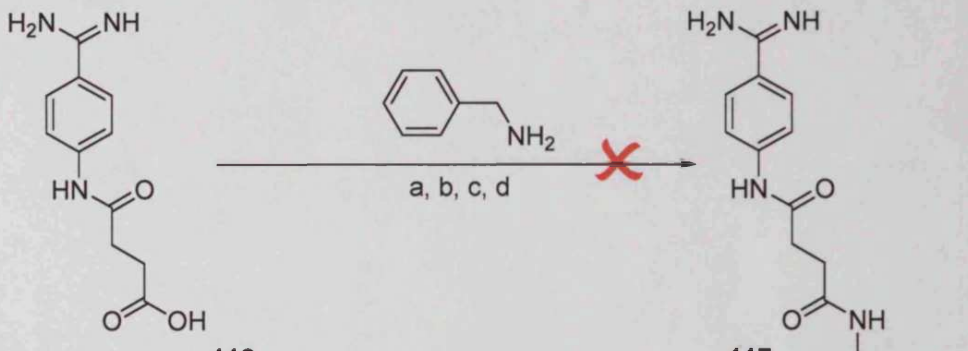

112 **117**

a: DCC / DMF
b: HOBT / TBTU / DIPEA / DMF
c: DMAP / N-methylmorpholine / Isobutyl chloroformate / DIPEA / DMF
d: EDC / DMF

Method A

3-(4-amidinophenylcarbamoyl)-propanoic acid (0.15 g, 0.64 mmol) and DCC (0.40 g, 1.92 mmol) were dissolved in dry DMF (8 mL). Benzylamine (0.21 g, 1.92 mmol) was added and the reaction mixture and was stirred under nitrogen at room temperature for 24 hrs. TLC ($MeOH/CH_2Cl_2$ 40:60) analysis indicated one component corresponding to starting material. LRMS analysis indicated no peak corresponding to the desired product but only a peak corresponding to the benzylamine.

Method B

3-(4-amidinophenylcarbamoyl)-propanoic acid (0.15 g, 0.64 mmol), HOBT (0.10 g, 0.75 mmol) and TBTU (0.25 g, 0.77 mmol) were dissolved in dry DMF (4 mL). DIPEA (0.29 g, 2.27 mmol) was added and the solution stirred under nitrogen for 30 min. Benzylamine (0.14 g, 1.28 mmol) in dry DMF (4 mL) was added. The reaction mixture was stirred under nitrogen at room temperature for 24 hrs. Aqueous NaOH was added dropwise until pH=12. Water (50 mL) was added and the solution extracted with EtOAc (3 x 50 mL). TLC ($MeOH/CH_2Cl_2$ 20:80) analysis of the organic phase indicated a complex mixture consisting of three components. LRMS gave no peak corresponding to the desired compound.

Method C

3-(4-amidinophenylcarbamoyl)-propanoic acid (0.15 g, 0.64 mmol) was added to dry DMF (5 mL). N-methylmorpholine (0.08 g, 0.64 mmol) and isobutyl chloroformate (0.08 g, 0.58 mmol) were added. The mixture was stirred under nitrogen for 5 mins. Benzylamine (0.14 g, 1.28 mmol), DIPEA (0.1 mL) and a catalytic amount of DMAP (1.5 mg) were added. The reaction mixture was stirred under nitrogen at room temperature for 24 hrs. The reaction mixture was concentrated under vacuum and then purified by column chromatography (CH_2Cl_2 100% initially then to MeOH 7% in CH_2Cl_2). TLC analysis indicated a complex mixture of three components after purification and LRMS indicated no peak corresponding to the desired product. NMR analysis also indicated that the isolated mixture was unlikely to be **117**.

Method D:

3-(4-amidinophenylcarbamoyl)-propanoic acid (0.15 g, 0.64 mmol) and EDC (0.23 g, 1.15 mmol) was added to dry DMF (10 mL). Benzylamine (0.10 g, 0.96 mmol) was added. The reaction mixture was stirred under nitrogen at room temperature for 24 hrs. Reverse phase TLC (Acetonitrile/ water 50:50) indicated starting material and that no reaction had occurred. LRMS indicated a peak at 263.2 at 100% intensity that could not be explained.

10.2.7 Synthesis of {[4-(2-Chloro-acetylamino)-phenyl]-imino-methyl}-carbamic acid tert-butyl ester (84)

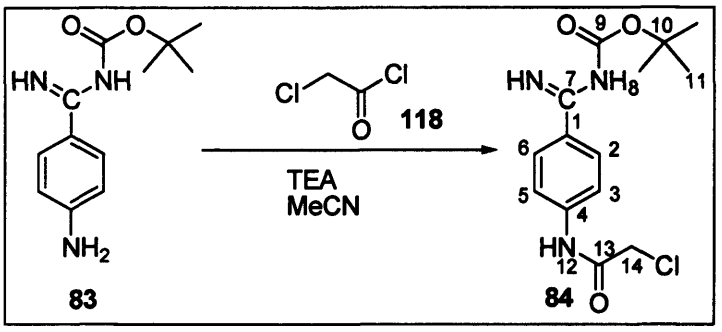

A solution of chloroacetyl-chloride in MeCN (12 mL) was added dropwise at 0°C to a solution of Boc-protected 4-aminobenzamidine (1,5 g, 6.38 mmol) and TEA (0,9 mL, d=0.727, 6.38 mmol) in acetonitrile (24 mL). The mixture was left stirring at 0°C under nitrogen for 1 hr and then at room temperature overnight. The solvent was evaporated under vacuum and the solid was recrystallised from MeOH (15 mL). The crystals were filtered, washed with cold MeOH and then dried under high vacuum giving 717 mg of pure product.

Yield:36%

LRMS (ES+): m/z= 312.1 ($(M+H)^+$, 30 %), 314 ($(M+^{37}Cl+H)^+$,10%).

^{1}H-NMR ($CDCl_3$, 300 MHz) δ 1.55 (s, 9H, H-C11), 4.30 (s, 2H, H-C14), 7.72 (d, 2H, *J*= 8.68 Hz, H-C2, H-C6), 7.95 (d, 2H, *J*= 8.68 Hz, H-C3, H-C5).

^{13}C-NMR ($CDCl_3$, 75 MHz) δ 29.1 (C11), 44.5 (C14), 80.9 (C10), 121.0 (C3 and C5), 130.1 (C2 and C6), 132.1 (C7), 143.2 (C9), 168.0 (C13).

10.2.8 Attempted synthesis of (Imino-{4-[2-(5-nitro-thiazol-2-yl-amino)-acetyl-amino]-phenyl}-methyl)-carbamic acid tert-butyl ester (84a)

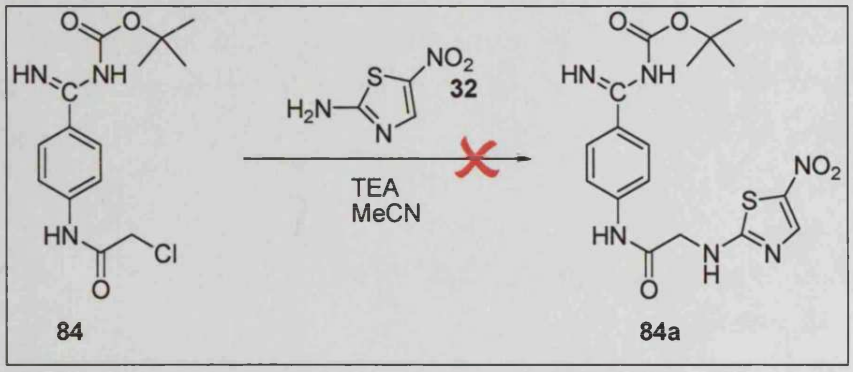

A mixture of 2-amino-5-nitro-thiazole (56.86 mg, 0.38 mmol) and TEA (0.09 mL, 0.64 mmol) in dry acetonitrile (2 mL) were added dropwise to a solution of {[4-(2-Chloro-acetylamino)-phenyl]-imino-methyl}-carbamic acid tert-butyl ester (100 mg, 0.32 mmol) in dry acetonitrile (4 mL) at room temperature and under nitrogen. The mixture was refluxed for 3 hrs and then left stirring overnight at room temperature. TLC and MS analyses did not show the formation of the expected product indicating that the reaction likely did not occur.

10.2.9 Synthesis of 2-chloro-N-(5-nitrothiazol-2-yl)-acetamide (123):

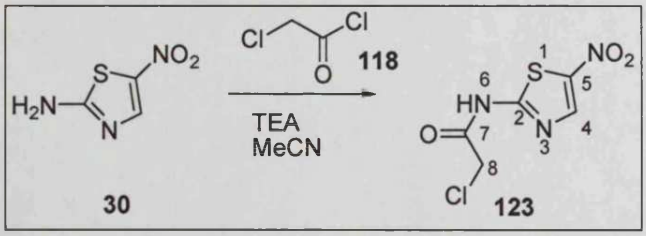

A solution of chloroacetyl-chloride in dry acetonitrile (15 mL) was added dropwise to a suspension of 2-amino-5-nitro-thiazole (1.5g 97%, 10.02 mmol) in dry acetonitrile (15 mL) and TEA (1.38 mL, d=0.727, 10.02 mmol) at 0°C, under nitrogen and with stirring. After the gas formation has

ceased the temperature was left to rise to room temperature and the mixture was left stirring overnight. The mixture was then concentrated under vacuum and then purified by column flash chromatography (DCM:MeOH =100:0 to 97:3). The yellow solid was triturated with Et_2O followed by addition of petroleum ether. The solid was filtered, washed with petroleum ether and dried over high vacuum giving 1.335g of pure compound as light yellow crystals.

Yield: 60%

LRMS (ES^-): m/z 219.9 ($(M-H)^-$, 100 %), 222.1 (40%).

mp: 145-148 °C.

^{1}H-NMR ($CDCl_3$, 300 MHz) δ 1.55 (s, 9H, H-C11), 4.30 (s, 2H, H-C14), 7.72 (d, 2H, *J*= 8.68 Hz, H-C2, H-C6), 7.95 (d, 2H, *J*= 8.68 Hz, H-C3, H-C5).

^{13}C-NMR ($CDCl_3$, 75 MHz) δ 43.0 (C8), 142.7 (C4), 163.1 (C2), 168.5 (C7).

10.2.10 Attempted synthesis of Imino-{4-[(5-nitro-thiazol-2-yl)-carbamoyl-methyl-amino]-phenyl}-methyl)-carbamic acid tert-butyl ester (122):

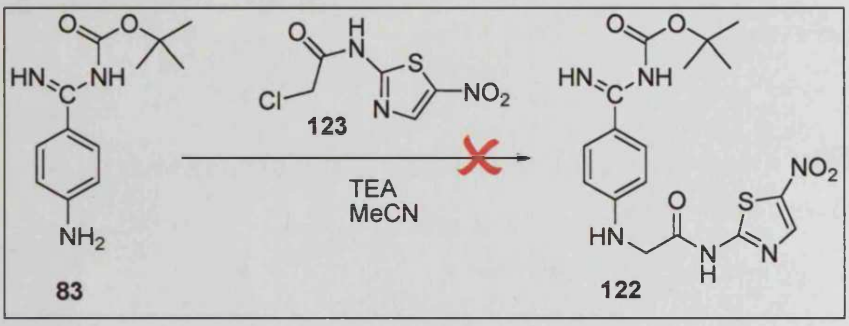

10.2.4.1 Method A:

A solution of 2-chloro-N-(5-nitrothiazol-2-yl)-acetamide (100 mg, 0.45 mmol) in acetonitrile (2 mL) was added dropwise at room temperature to a suspension of Boc-protected 4-amino-benzamidine (136 mg, 0.58 mmol) and TEA (0.1 mL, d=0.727, 0.58 mmol) in dry acetonitrile (2.5 mL) with stirring and under nitrogen. The mixture was left stirring overnight at room temperature. TLC analysis showed that the reaction did not take place therefore the mixture was left stirring for a whole day. The solvent was concentrated under vacuum and flash chromatography of the mixture was performed eluting with DCM/MeOH (100:0 to 80:20). The starting material was the only fraction recovered and MS of the minor fractions recovered showed that the formation of the expected product did not take place.

10.2.4.2 Method B:

A solution of 2-chloro-N-(5-nitrothiazol-2-yl)-acetamide (100 mg, 0.45 mmol) in dry acetonitrile (2 mL) was added dropwise at room temperature to a suspension of Boc-protected 4-amino-benzamidine (136 mg, 0.58 mmol) and TEA (0.1 mL, d=0.727, 0.58 mmol) in dry acetonitrile (2.5 mL) with stirring and under nitrogen. The mixture was refluxed under nitrogen for 5 hrs and overnight at room temperature. The MS analysis did not

confirm the presence of the desired product. The solvent was concentrated under vacuum and purification by flash chromatography (DCM: MeOH = 100:0 to 75:25) was performed. As well as observed for method A, starting material was only recovered from the mixture and the reaction did not take place.

10.2.11 Attempted synthesis of 3-(5-Nitro-thiazol-2-ylcarbamoyl)-propionic acid (30a):

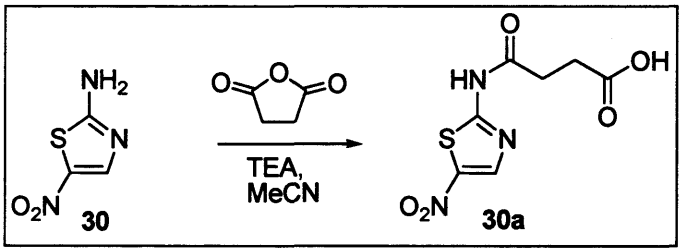

A solution of succinic anhydride (2.002 g 99%, 10.02 mmol) in dry acetonitrile (15 mL) was added dropwise to a suspension of 2-amino-5-nitro-thiazole (1.5 g 97%, 10.02 mmol) and TEA (1,38 mL, d=0.727, 10.02 mmol) in anhydrous acetonitrile (15 mL) at 0°C. The solution was left stirring at room temperature and under nitrogen. MS (ES^-) analysis showed the formation of the desired product with peak corresponding to $(M-H)^-$ and $(2M-H)^-$. The mixture was treated with HCl and the solid was filtered and washed with H_2O and acetone. Different attempts to purify the mixture were performed but the desired product could not be recovered from the mixture.

10.3 Prodrugs of Bisphosphonic acid:

10.3.1 Attempted synthesis of 4-amino-1-hydroxybutylidene-bisphosphonic acid sodium salt Sodium Alendronate (130)[141, 142]:

10.3.1.1 Method A[141, 142]:

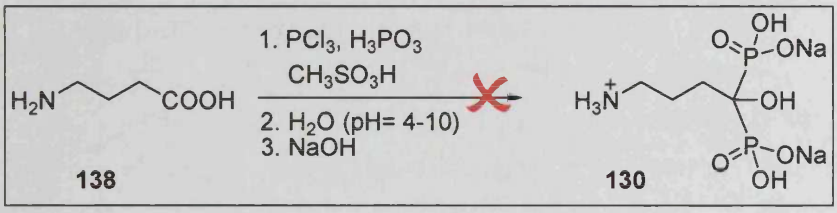

4-aminobutyric acid (1.031g 97%, 10 mmol) was added into methansulfonic acid (8 mL, 99.5%) followed by the addition of H_3PO_3 (1.65g 99.5%, 20 mmol) under nitrogen. PCl_3 (4 mL, d=1.574, 45 mmol) was then added dropwise to the mixture and the reaction was left stirring at 65°C for 5hrs under nitrogen. Since the reaction becomes self heating above 85°C the temperature was not allowed to get above 65°C. The mixture was left cooling down to room temperature and left stirring overnight under nitrogen. The clear colourless solution was cooled to 25°C and quenched into ice-water (10 mL) with vigorous stirring and the solution was refluxed for 5hrs. The solution was then cooled down to 25°C and the pH was adjusted to 4 by using a solution of NaOH 50%. The resulting solution was left stirring at 0-5°C. A small portion of the mixture was treated with EtOH and a precipitated was achieved. Neither the MS analysis nor the ^{1}H-NMR and ^{31}P-NMR analyses of the precipitated and of the solution confirmed the formation of the desired product.

10.3.1.2 Method B[141, 142]:

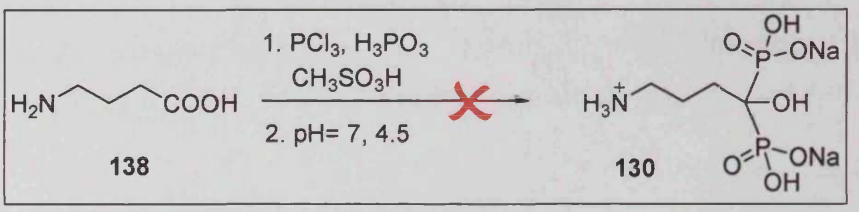

A 50 mL flask was connected with a condenser through which was circulated brine at -5÷-10 °C by using a pump (Grant LTD 6). The system was also connected with a trap and to a caustic scrubber and also was flushed and left under nitrogen. 4-aminobutyric acid (1.031g 97%, 10 mmol) was added into methansulfonic acid (8 mL, 99.5%) followed by the addition of H_3PO_3 (1.65g 99.5%, 20 mmol) under nitrogen. PCl_3 (4 mL, d=1.574, 45 mmol) was then added dropwise to the mixture. The gas formation was observed in the gas scrubber but was not as intense as observed on method A. The mixture was heated at 65°C and left stirring for 5hrs under nitrogen and then left cool down to room temperature. The reaction mixture was quenched over 35 minutes by adding it dropwise to a solution of 1 g Na_2HPO_4 in 100 mL of water, at pH=7. The pH was maintained between 6.0 and 7.0 by adding 25% NaOH carefully maintaining the temperature below 25°C. Once the quench was complete, the pH was adjusted to 7.0 and the solution concentrated to 50 mL by atmospheric distillation (100-104°C) over three hours. The pH was then adjusted to 4.3 by using a buffer $CH_3COOH\backslash CH_3COONa$. The solution was left stirring overnight at room temperature and a precipitate was formed. The suspension was stirred for two hours at 0°C and then filtered. The precipitated was dried over high vacuum. MS analysis and ^{1}H-NMR/^{31}P-NMR analyses indicated that the formation of the product did not occur.

11. Appendix 1:

11.1 *In Vitro* Assays:

11.1.1 P2 transporter affinity measurements:

Parasites purified from blood were stored on ice in Carter's buffered saline solution[45]. Transport assays used the centrifugation through oil technique, which is routinely used in analyses.[54, 59, 63, 67, 159.]

Radiolabeled adenosine (0.5 μM) uptake via P2 was measured in the presence of 1 mM inosine that blocks the P1 transporter[45]. Compounds were assayed for affinity for the P2 transporter by using labelled adenosine fixed at 0.5 μM and a range of inhibitor concentrations. IC_{50} values were calculated using the Grafit 4.0 Software (Erithacus) by plotting inhibitory value against concentration of inhibitor.

11.1.2 *T. brucei brucei* , *T. brucei rhodesiense* and cytotoxicity:

Activity of compounds was determined for *T. brucei rhodesiense* trypomastigotes of STIB 900. This stock was isolated in 1982 from a

[159] Barrett, M. P.; Fairlamb, A. H.; Rousseau, B.; Chauviere, G.; Perie, J. Uptake of the nitroimidazole drug megazol by African trypanosomes. *Biochem. Pharmacol.* **2000**, *59*, 615-620.

human patient in Tanzania. Minimum essential medium (50 µL) supplemented with 2-mercaptoethanol and 15% heat-inactivated horse[160] serum was added to each well of a 96-well microtiter plate. Serial drug dilutions were prepared covering a range from 90 to 0.123 µg/ml.

Then, 50 µL of a trypanosome suspension was added to each well, and the plate incubated at 37°C under a 5%CO_2 atmosphere for 72 hrs. Alamar Blue (10 µL) was then added to each well, and incubation continued for a further 2 to 4 hrs. The plate was then read in a Spectramax Gemini XS microplate fluorometer (Molecular Devices Corp., Sunnyvale, Calif.) by using an excitation wavelength of 536 nm and an emission wavelength of 588 nm. Fluorescence development was expressed as a percentage of the control, and the 50% inhibitory concentration (IC_{50}) values were determined. Cytotoxicity was assessed by using the same assay and rat skeletal myoblasts (L-6 cells)[161].

To investigate whether transport of these compounds through the P2 transporter is necessary for activity, compounds were assayed against the *T. brucei brucei* trypomastigotes using either the wild type or P2 knockout mutants (*TbAT1*$^{-/-}$)[58]. The Alamar Blue assay[161] was also used to determine IC_{50} values against wild-type lines and the *TbAT1*$^{-/-}$ derivative. To determine whether DNA damage was associated with trypanocidal activity the Alamar Blue assay was also used to determine IC_{50} values against the *RAD51*$^{-/-}$ deletion mutant[162].

11.1.3 *Trypanosoma cruzi*:

Rat skeletal myoblasts (L-6 cells) were seeded in 96-well microtiter plates at 2000 cells/well/100µl in RPMI 1640 medium with 10% FBS and 2 mM L-glutamine. After 24 hrs 5000 trypomastigotes of *T. cruzi* (Tulahuen

[160] Baltz, *T.*; Baltz, D.; Giroud, C.; Crockett, J. Cultivation in a semi-defined medium of animal infective forms of *Trypanosoma brucei*, *T.* equiperdum, *T.* evansi, *T. rhodesiense* and *T. gambiense*. *EMBO J.* **1985**, *4*, 1273-1277.

[161] Raz, B.; Iten, M.; Grether-Buhler, Y.; Kaminsky, R.; Brun, R. The Alamar Blue assay to determine drug sensitivity of African trypanosomes (*T.b. rhodesiense* and *T.b. gambiense*) *in vitro*. *Acta Trop.* **1997**, *68*, 139-147.

[162] McCulloch, R.; Barry, J. D. A role for RAD51 and homologous recombination in *Trypanosoma brucei* antigenic variation. *Genes Dev.* **1999**, *13*, 2875-2888.

strain C2C4 containing the μ-galactosidase (Lac Z) gene) were added in 100 μL per well with 2x of a serial drug dilution. The plates were incubated at 37°C in 5% CO_2 for 4 days. Then the substrate CPRG/Nonidet was added to the wells. The colour reaction, which developed during the following 2-4 hrs, was read photometrically at 540 nm. From the sigmoidal inhibition curve IC_{50} values were calculated.

11.1.4 *Leishmania donovani*:

Mouse peritoneal macrophages were seeded in RPMI 1640 medium with 10% heat-inactivated FBS into Lab-tek 16 chamber slides. After 24 h *Leishmania donovani* amastigote were added at a ratio of 3:1 (amastigotes to macrophages). The medium containing free amastigotes was replaced by fresh medium 4 h later. Next day the medium was replaced by fresh medium containing different drug concentration. The slides were incubated at 27 °C under a 5 % CO_2 atmosphere for 96 h. Then the medium was removed, the slides fixed with methanol and stained with Giemsa. The ratio of infected to non-infected macrophages was determined microscopically, expressed as percentage of the control and the IC_{50} value calculated by linear regression.

11.1.5 *P. falciparum*:

Plasmodium falciparum 3D7 cultures were mantained in RPMI 1640 medium (Sigma, UK) 37°C, 5% CO_2 in 5% hematocrit. Synchronised ring stage cultures were prepared at 1% parasitemia and 50μl added per well, the top test drug final concentration being 30μg/ml. After 24 hours incubation, 37°C, 5% CO_2 5μl (^{3}H)-hypoxanthine was added (0.2μCi/well) [Desjardins *et al.*, 1979, O'Neill *et al.*, 1985] and plates were shaken for 1 minute and then incubated for 48 hours. The plates were freeze/thawed rapidly, harvested and dried. (^{3}H)-hypoxanthine uptake was measured using a microbeta counter (Wallac 1450).

11.2 *In Vivo* Assays:

11.2.1 *T. brucei*:

Female NMRI mice weighting 22 to 25 g were infected with cryopreserved stabilates of *T. brucei brucei* STIB 795 (derivate of strain 427[163]) or *T. brucei rhodesiense* STIB 900. Each mouse was infected intraperitoneally with 2 to 4 x 10^4 bloodstream forms. Melarsoprol (Arsobal; Aventis) acted as standard drug and was diluted with sterile distilled water to an appropriate concentration. Groups of four mice were treated on days 3, 4, 5 and 6 intraperitoneally with 20 mg/Kg. A control group remained untreated. The parasitaemia of all animals was checked on day 7 and 10 postinfection and every second day thereafter until 60 days. Death of animals was recorded to calculate the mean survival time. Surviving and aparasitemic mice were considered cured at 60 days and then euthanized.

11.2.2 *T. cruzi*:

20g, female BALB/c mice (Charles Rivers Ltd, UK) were infected intraperitoneally with 2 x 10^4 trypomastigotes in 0.2 mL, harvested from the blood of a passage mouse. Infected mice were randomly sorted into groups of five. After 5 days tail blood was examined for potency of infection – the number of trypomastigotes in 10 microscope field was noted. Dosing commenced for 5 consecutive days. Tail blood was examined 2 days after the end of treatment and at 7 day intervals on any surviving mice.

11.2.3 *L. donovani*:

20g, female BALB/c mice were infected, via a lateral tail vein, with 2 x 10^7 freshly isolated amastigotes of L. donovani HU3. Seven days post infection a mouse was necropsied to check for potency of infection and dosing commenced. The experimental compound was given at 40 mg/Kg intraperitoneally for 5 consecutive days. 14 days post infection all mice

[163] Cunningham, M. P.; Vickerman, K. Antigenic analysis in the *Trypanosoma brucei* group, using the agglutination reaction. *T. Roy. Soc. Trop. Med. H.* **1962**, *56*, 48-59.

were necropsied and liver impression smears made. Parasite load was determined by Giemsa staining the smears and microscopic evaluation of the number of amastigotes per liver cell (LDU). The percentage inhibition was calculated in comparison to uninfected control mice. A positive control of 15 mg Sb^V/Kg was also included.

11.3 Genotoxicity *studies*:

11.3.1 Cell types

Heparin-anticoagulated peripheral blood was obtained by venipuncture from consenting healthy non-smoker donors. In order to isolate leukocytes, the blood was maintained at 37°C for 5′ in a erylysis buffer (155 mM NH_4Cl, 5 mM $KHCO_3$, 0.005 mM Na_2EDTA, pH 7.4), centrifuged and washed with PBS, and finally resuspended (~10^6 cells/mL) in RPMI-1640 medium (Gibco).
The K562 cell line was maintained in the suspension culture in RPMI-1640 supplemented with 10% (v/v) foetal bovin serum (FBS, Stem Cell Technologies) and L-glutamine (2 mM). Exponentially growing K562 cells, washed with PBS and resuspended (~10^6 cells/mL) in RPMI-1640 medium, were used throughout this study.

11.3.2 Cell treatment

Appropriate volumes of **54**, **6**, and benznidazole, as a known antiprotozoal drug, were added to an Eppendorf tube containing cell suspension (10^6 cells) at final volume of 1 m*L*. The cells were treated for 1 hour at 37°C and then washed twice in PBS.

11.3.3 Cytotoxicity assays

Toxicity was checked immediately after exposure. Cell survival was determined by the carboxyfluorescein diacetate (FDA)/ethidium bromide (EtBr)-assay[164]. A freshly prepared solution consisting of 30 µL FDA in acetone (5mg/mL), 200 µL EtBr in PBS (200 µg/mL), and 4.88 mL of PBS as used. 40 µL of cell suspension (equivalent to about $5x10^5$ cells) was mixed with 10 µL of the staining solution, maintained at 37°C for 5 min.

[164] Merk, O.; Speit, G. Detection of crosslinks with the comet assay in relationship to genotoxicity and cytotoxicity. *Environ. Mol. Mutagen.* **1999**, *33*, 167-172.

The cells were counted (200 cells per data point) under a fluorescent microscope (FDA/EtBr blue filter): viable cells appear green-fluorescent, whereas orange-stained nuclei indicated dead cells.

11.3.4 Comet assay:

The Comet assay was performed only with viability ≥ 70% (Tice 2000), basically according to Singh (Singh *et al.*, 1988) with minor modifications: cell lysis at 4°C overnight (2.5M NaCl, 10 mM Na_2EDTA, 10 mM Tris-HCl, 1% Triton X-100 and 10% DMSO, pH 10), DNA unwinding for 40 min in a electrophoretic alkaline buffer (1mM Na_2EDTA, 300 mM NaOH, 0°C, pH>13 or pH= 12.1), electrophoresis for 30 min, (0.78 V/cm, 300 mA) at 0°C in the same buffer, neutralisation (0.4 M Trs-HCl, pH 7.5). DNA was stained with 100 µL ethidium bromide (2 µg/mL) before the examination at 400X magnification under a Leika DMLB fluorescent microscope (excitation filter BP 515-560 nm, barrier filter LP 580 nm) using an automatic image analysis system (Cometa release 2.1 – Sarin). The migration distance between the edge of the comet head and the end of the tail (total lenght, TL) provided representative data on genotoxic effects. The samples were coded and evaluated blind (50 cells per each of the two replicate slides per data point). All the tests were performed at least three times. EMS (2mM), an alkylating compound, was used as positive control for the comet assay at pH>13; bleomycin, a radiomimetic antitumoral drug, was selected as positive control for the comet assay at pH=12.1 since is a free radical-based DNA damaging agent that also induces DNA strand breaks[154]. Additionally, after processing slides in the Comet assay, the occurrence of cells showing completely fragmented chromatin ("hedgehogs" or "clouds" or "ghost cells"[165] i.e. non-detectable cell nuclei wich represent cellular toxic events, i.e. apoptotic and/or necrotic cells[166],

[165] Hartmann, A.; Elhajouji, A.; Kiskinis, E.; Poetter, F.; Martus, H. J.; Fjallman, A.; Frieauff, W.; Suter, W. Use of the alkaline comet assay for industrial genotoxicity screening: comparative investigation with the micronucleus test. *Food Chem. Toxicol.* **2001**, *39*, 843-858.

[166] Bacso, Z.; Everson, R. B.; Eliason, J. F. The DNA of annexin V-binding apoptotic cells is highly fragmented. *Cancer Res.* **2000**, *60*, 4623-4628.

[167, 168], was assessed as a further indicator of cytotoxicity. These cells are not evaluated by image analysis but are recorded separately.

11.3.4 Comet assay for detection of oxidised bases:

This type of Comet assay is used to detect specific classes of DNA damage. By using lesion specific DNA glycosylases/endonucleases, specific DNA base modifications are converted to strand breaks. These strand breaks are then detected by comet assay at pH 12.1 r >13. By comparing the DNA migration in enzyme treated and buffer treated slides, interpretation can be easily be made. The comet assay, with the modification of an extra step after lysis in which DNA is digested with a lesion-specific enzyme, is performed according to Collins *et al*[153]. Briefly, after cell lysis, slides were washed three times with enzyme buffer (0.1 KCl, 0.5 mM Na_2EDTA, 40 mM HEPES (4-(2-hydroxythyl)-1-piperazineethanesulfonic acid), 0.2 mg/mL bovine serum albumin, pH 8 with KOH) and incubated with endonuclease III (which converts oxidised pyrimidines to single strand breaks) or formamidopyrimidine glycolase (FPG), which recognises altered purines, in this buffer (or in buffer alone as control, detecting only strand breaks and alkali-labile sites). Hydrogen peroxide (25 μM), an oxidant stress inducer, was used as positive control. Endonuclease III (endo III) and FPG were isolated from bacteria containing over-producing plasmids (Collin's Laboratory, Rowett Research Institut, Bucksburn, Aberdeen, UK).

The gels without the enzyme treatment provide an estimate of only DNA strand breaks (pH=12.1) and alkali labile sites too (pH>13). At pH=12.1, the enzyme-treated gels reveal strand breaks and oxidised bases (SB + OX). Assuming a linear dose response, subtraction of (SB) from (SB + OX) gives a measure of oxidised bases.

---

[167] Meintières, S.; Nesslany, F.; Pallardy, M.; Marzin, D. Detection of ghost cells in the standard alkaline comet assay is not a good measure of apoptosis. *Environ. Mol. Mutagen.* **2003**, *41*, 260-269.

[168] Chandna, S. Single-cell gel electrophoresis assay monitors precise kinetics of DNA fragmentation induced during programmed cell death. *Cytom. Part A*, **2004**, *61A*, 127-133.

An SPSS 11 (SPSS Inc., Chicago, IL, USA) statistical package has been applied. Statistical differences between controls and treated samples are first determined with non-parametric Wilcoxon rank-sum test for each experiment[169]. The mean values from the repeated experiments are used in a one-way analysis of variance test. If a significant F-value ($P<0.05$) was obtained, a Dunnett's C multiple comparison analysis is conducted.

[169] Anderson, D.; Yu, *T.* W.; Phillips, B. J.; Schmezer, P. The Effect of Various Antioxidants and Other Modifying Agents on Oxygen-Radical-Generated DNA-Damage in Human-Lymphocytes in the Comet Assay. *Mutat.Res.* **1994**, *307*, 261-271.

12. Appendix 2:

Publications

Baliani, A.; Bueno, G. J.; Stewart, M. L.; Yardley, V.; Brun, R.; Barrett, M. P.; Gilbert, I. H. Design and synthesis of a series of melamine-based nitroheterocycles with activity against trypanosomatid parasites. *J. Med. Chem.* **2005**, *48*, 5570-5579.

Stewart, M. L.; Bueno, G. J.; Baliani, A.; Klenke, B.; Brun, R.; Brock, J. M.; Gilbert, I. H.; Barrett, M. P. Trypanocidal activity of melamine-based nitroheterocycles. *Antimicrob. Agents Chemother.* **2004**, *48*, 1733-1738.

ANTIMICROBIAL AGENTS AND CHEMOTHERAPY, May 2004, p. 1733–1738 Vol. 48, No. 5
0066-4804/04/$08.00+0 DOI: 10.1128/AAC.48.5.1733–1738.2004

Trypanocidal Activity of Melamine-Based Nitroheterocycles

Mhairi L. Stewart,[1] Gorka Jimenez Bueno,[2] Alessandro Baliani,[2] Burkhard Klenke,[2] Reto Brun,[3] Janice M. Brock,[1] Ian H. Gilbert,[2] and Michael P. Barrett[1]*

Division of Infection and Immunity, Institute of Biomedical and Life Sciences, University of Glasgow, Glasgow G12 8QQ,[1] and Welsh School of Pharmacy, Cardiff University, Cardiff CF10 3XF,[2] United Kingdom, and Swiss Tropical Institute, CH-4002 Basel, Switzerland[3]

Received 24 September 2003/Returned for modification 31 October 2003/Accepted 21 January 2004

A series of nitroheterocyclic compounds were designed with linkages to melamine or benzamidine groups that are known substrates of the P2 aminopurine and other transporters in African trypanosomes of the brucei group. Several compounds showed in vitro trypanotoxicity with 50% inhibitory concentrations in the submicromolar range. Although most compounds interacted with the P2 transporter, as judged by their ability to inhibit adenosine transport via this carrier, uptake through this route was not necessary for activity since *TbAT1*-null mutant parasites, deficient in this transporter, retained sensitivity to these drugs. One compound, a melamine-linked nitrofuran, also showed pronounced activity against parasites in mice. Studies into the mode of action of this compound indicated that neither reductive, nor oxidative, stress were related to its trypanocidal activity ruling out a genotoxic effect in *T. brucei*, distinguishing it from some other, mammalian cell toxic, trypanocidal nitroheterocycles.

There is an urgent need for the development of new drugs to treat human African trypanosomiasis, owing to poor clinical efficacy and toxic side effects of current drugs and a growing problem of resistance at a time when the disease has become resurgent (25).

In order to exert trypanocidal activity, drugs must first enter the parasites or else act on essential plasma membrane-associated targets. An unusual aminopurine transporter, termed the P2 transporter, is one of several that can carry purine nucleosides and bases into these cells (27, 37). The P2 transporter recognizes adenine and adenosine as substrates, but it can also transport melamine (triazine) derivatives and benzamidine derivatives that include several known drugs used against the African trypanosomiases (Fig. 1) (4, 11, 14).

Other transporters can also carry drugs into trypanosomes and contribute to their selectivity (15). A better understanding of these routes of uptake and the design of agents that can be delivered to trypanosomes via these portals offers one route to urgently needed trypanocidal drugs. We have previously reported approaches to selectively deliver compounds to trypanosomes using the P2 transporter (6, 23, 38). The principal of this approach was to attach P2 recognition motifs (in particular the melamine unit) to cytotoxic agents. The cytotoxic agents first selected were polyamine analogues, which are known to be cytotoxic to trypanosomes (26, 32). Several series of compounds were prepared and some of the compounds were shown to have high activity against *Trypanosoma brucei* trypomastigotes (23). However, they were too toxic in mammals for use in vivo.

Alternate cytotoxic moieties to couple to the P2 recognition motifs have now been considered. Nitroaromatic compounds are of particular interest. Nitroheterocycles have long been known to be effective against trypanosomes. Throughout the 1950s and 1960s a variety of compounds, notably furacin (nitrofurazone), were used in clinical trials (1, 19). In spite of good antitrypanosomal activity, toxicity issues prevented further development of nitrofurazone. A nitrofuran, nifurtimox, however, was licensed for use against Chagas' disease caused by *Trypanosoma cruzi* (36). Nifurtimox is also active against *T. brucei* and has been used in treating melarsoprol refractory trypanosomiasis (25, 33). The World Health Organization and Bayer are currently engaged in efforts to extend the license for nifurtimox for routine use against human African trypanosomiasis (7). A nitroimidazole, megazol, has recently received attention for its potent trypanocidal activity (9, 17), although toxicity issues (34) have stifled further development. Reports of novel trypanocidal nitroheterocycles continue to appear (8, 30), which emphasizes the fact that trypanosomes are particularly sensitive to this class of compound.

Given the potent trypanocidal activity of various nitroheterocycles, but the disadvantageous impact of host toxicity, selectively targeting nitroheterocycles to the trypanosome's interior could greatly increase their therapeutic index. We have therefore set out to produce a number of nitroheterocycles carrying either a melamine ring or a benzamidine moiety aiming to facilitate selective uptake into trypanosomes via the P2 and other transporters and circumvent host toxicity. Trypanocidal nitroheterocycles appear to be optimally active if attached to a second moiety, possibly because of steric requirements in binding to particular enzymes with nitroreductase activity. Consequently, both delivery across the plasma membrane and targeting to the active sites of particular enzymes could be bestowed by coupling nitroheterocycles to melamine or benzamidine moieties.

* Corresponding author. Mailing address: Institute of Biomedical and Life Sciences, Division of Infection and Immunity, University of Glasgow, The Joseph Black Building, Glasgow G12 8QQ, United Kingdom. Phone: (44) 141-330-6904. Fax: (44) 141-330-6904. E-mail: m.barrett@bio.gla.ac.uk.

MATERIALS AND METHODS

Chemistry. The compounds were prepared from the 2,4-diamino-6-chlorotriazines by displacement of the chlorine by hydrazine, followed by condensation

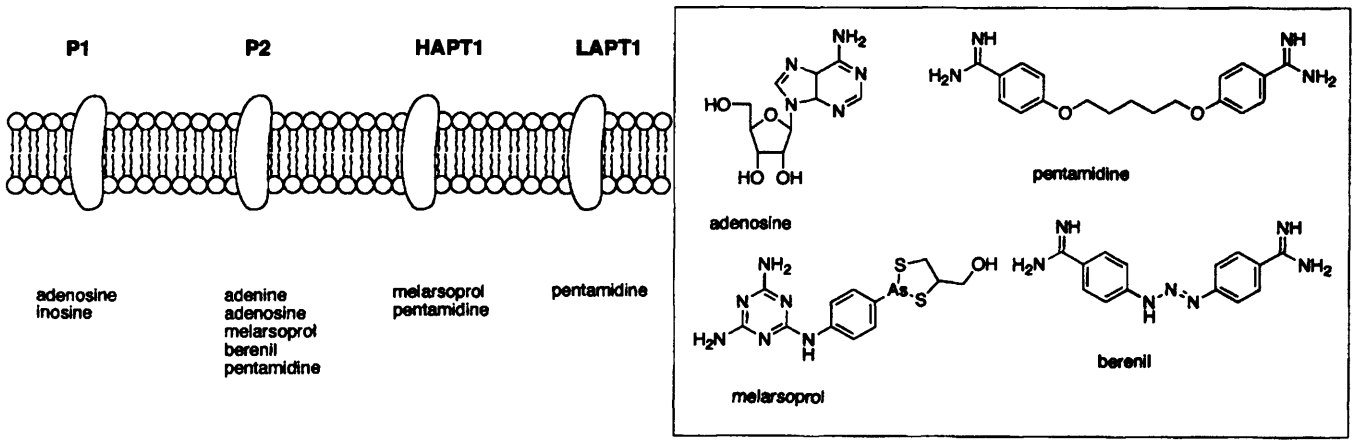

FIG. 1. Uptake of triazines and benzamidines into *T. brucei*. The left-hand side of the diagram shows the known routes of uptake of diamidines and melaminophenyl arsenicals into *T. brucei*. P2 is the product of the *TbAT1* gene and encodes an unusual transporter capable of nucleoside and nucleobase uptake. It recognizes a motif also present on diamidine- and melamine-based drugs. These are shown on the right hand side of the diagram. Pentamidine enters via two additional transporters: HAPT1 and LAPT1. The uptake routes of selected triazine- and benzamidine-derived drugs is depicted.

with the appropriate nitrofuraldehyde (Fig. 2). Synthesis was handicapped by the insolubility of the reagents and products. For control purposes, nitrofurans 4 and 5 were also screened.

The synthesis of benzamidine derivatives of the imidazoles are shown in Fig. 3. The starting point was 4-aminobenzamide (compound 6). The amidine functionality was protected with a BOC protecting group, which allowed derivatization of the aniline position with chloroacetyl chloride. The intermediate compound 8 was then coupled with either 2-nitroimidazole or 4-nitroimidazole, which followed by deprotection gave the required products 11 and 12.

Biological assays. (i) Cultivation of parasites. Bloodstream-form *T. brucei brucei* (strain 427) (13) was cultivated in HMI-9 medium containing 20% fetal calf serum (22) at 37°C in a humidified CO_2 environment. The bloodstream-form *RAD51*$^{-/-}$ deletion mutant (29) derived from strain 427 was a gift from R. McCulloch (University of Glasgow), and these cells were cultured in HMI-9 medium with 20% fetal calf serum supplemented with puromycin (1 mg/ml) and bleomycin (2 μg/ml), which select for the respective genes giving resistance to these antibiotics targeted to the *RAD51* loci of the *T. brucei* genome.

N-Acetylcysteine (NAC) has been used frequently as an antagonist of oxidative stress in different cellular systems since it reacts readily with a number of the reduced oxygen species produced during oxidative stress (2, 12). When administered at 0.5 mM, no detrimental effect on trypanosomes was induced by this compound in in vitro assays.

For uptake analysis bloodstream-form parasites were grown to peak parasitemia (10^9 cells per ml of blood) in Wistar rats and then purified from blood by using DEAE anion-exchange chromatography (24).

(ii) P2 transporter affinity measurements. Parasites purified from blood were stored on ice in Carter's buffered saline solution (11). Transport assays used the centrifugation through oil technique, which is routinely used in analyses (5, 11, 14, 15, 23, 38). Radiolabeled adenosine (0.05 μM) uptake via P2 was measured in the presence of 1 mM inosine that blocks the P1 transporter (11). Compounds

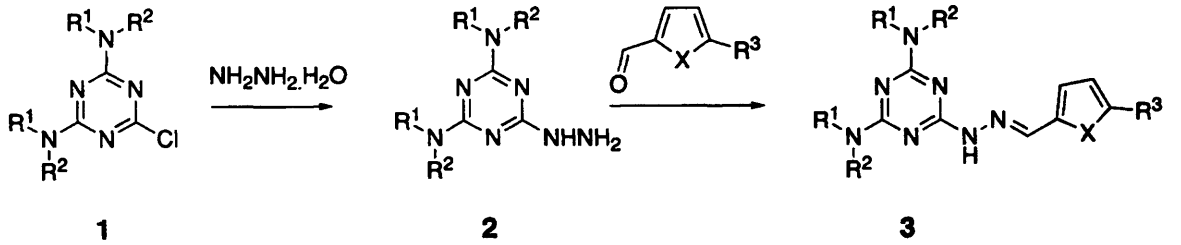

1

2

3

1a, $R^1 = R^2 = H$
1b, $R^1 = H$, $R^2 = Me$
1c, $R^1 = R^2 = Me$

2a, $R^1 = R^2 = H$
2b, $R^1 = H$, $R^2 = Me$
2c, $R^1 = R^2 = Me$

3a, $R^1 = R^2 = H$, $R^3 = NO_2$, X = O
3b, $R^1 = R^2 = H$, $R^3 = NO_2$, X = S
3c, $R^1 = R^2 = H$, $R^3 = H$, X = O
3d, $R^1 = R^2 = H$, $R^3 = H$, X = S
3e, $R^1 = H$, $R^2 = Me$, $R^3 = NO_2$, X = O
3f, $R^1 = R^2 = Me$, $R^3 = NO_2$, X = O

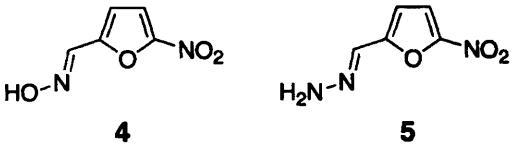

4 5

FIG. 2. Preparation of compounds from 2,4-diamino-6-chlorotriazines by displacement of the chlorine by hydrazine, followed by condensation with the appropriate nitrofuraldehyde.

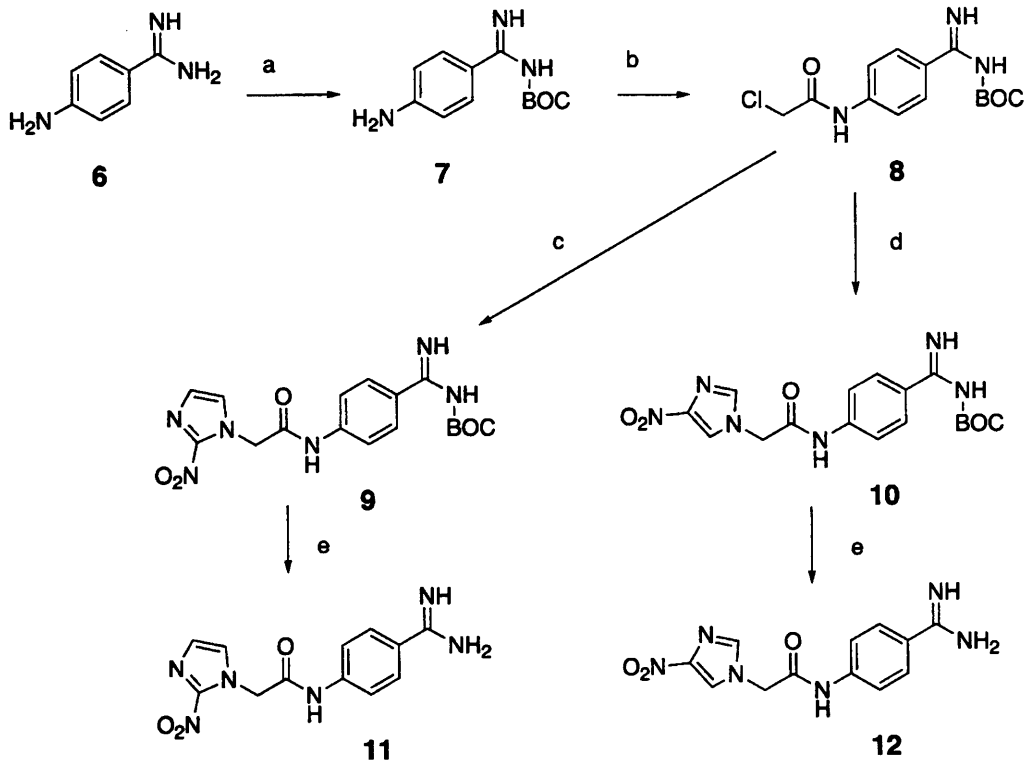

FIG. 3. Synthesis of benzamidine derivatives of the imidazoles. Lettered arrows: a, $(BOC)_2O$, NaOH, THF/H_2O; b, chloroacetyl chloride, Et_3N, MeCN; c, 2-nitroimidazole, Et_3N, MeCN; d, 4-nitroimidazole, Et_3N, MeCN; e, TFA, anisole, DCM.

were assayed for affinity for the P2 transporter by using three separate concentrations of adenosine and a range of inhibitor concentrations. The data were plotted by using the competitive inhibition algorithm of the Grafit 4.0 software (Erithacus). Plots were viewed by eye to verify inhibition type (Table 1).

(iii) In vitro activities against parasites and cytotoxicity. Activity of compounds was determined for *T. brucei rhodesiense* trypomastigotes of STIB 900. This stock was isolated in 1982 from a human patient in Tanzania. Minimum essential medium (50 μl) supplemented with 2-mercaptoethanol and 15% heat-inactivated horse serum (3) was added to each well of a 96-well microtiter plate. Serial drug dilutions were prepared covering a range from 90 to 0.123 μg/ml. Then, 50 μl of a trypanosome suspension was added to each well, and the plate incubated at 37°C under a 5% CO_2 atmosphere for 72 h. Alamar Blue (10 μl) was then added to each well, and incubation continued for a further 2 to 4 h. The plate was then read in a Spectramax Gemini XS microplate fluorometer (Molecular Devices Corp., Sunnyvale, Calif.) by using an excitation wavelength of 536 nm and an emission wavelength of 588 nm (35). Fluorescence development was expressed as a percentage of the control, and the 50% inhibitory concentration (IC_{50}) values were determined. Cytotoxicity was assessed by using the same assay and rat skeletal myoblasts (L-6 cells).

To investigate whether transport of these compounds through the P2 trans-

TABLE 1. Activities of compounds against the P2 transporter and against various strains of *T. brucei* trypomastigotes[a]

Compound	K_i, P2 uptake (μM)	*T. brucei brucei AT1* wild type (IC_{50} [μM])	*T. brucei brucei AT1* knockout (IC_{50} [μM])	*T. brucei rhodesiense* (IC_{50} [μM])	L-6 cells (IC_{50} [μM])
2a	11.9	>200	>200	ND	ND
2b	59.3	>200	>200	ND	ND
3a	22.9	0.23	0.38	0.025	183
3b	1.9	0.85	1.52	0.24	11.8
3c	15.9	16.5	29.3	12.9	>400
3d	4.9	89	170	10.2	78.2
3e	4.6	11.9	14.8	0.25	18.8
3f	129	0.2	0.3	0.003	18.7
4	–[b]	1.1	1.2	0.68	40.4
5	404	23.5	13.7	2.3	20.0
9	13.09	111	119	ND	ND
10	3.65	>200	>200	ND	ND
11	1.58	>200	191	6.2	>300
12	2.88	>200	>200	79.8	>300
Melarsoprol	1.2	0.053	0.12	0.006	7.8
Nifurtimox	ND	5.6	ND	1.5	68

[a] *T. brucei AT1* Knockout is a mutant with a nonfunctional P2 transporter. ND, not determined.
[b] –, No inhibition.

porter is necessary for activity, compounds were assayed against the *T. brucei brucei* trypomastigotes using either the wild type or P2 knockout mutants (*TbAT1*$^{-/-}$) (28). The Alamar Blue assay (35) was also used to determine IC_{50} values against wild-type lines and the *TbAT1*$^{-/-}$ derivative. To determine whether DNA damage was associated with trypanocidal activity the Alamar Blue assay was also used to determine IC_{50} values against the *RAD51*$^{-/-}$ deletion mutant.

(iv) In vivo activities. Female NMRI mice weighing 22 to 25 g were infected with cryopreserved stabilates of *T. brucei brucei* STIB 795 (derivative of strain 427 (13) or *T. brucei rhodesiense* STIB 900. Each mouse was infected intraperitoneally with 2 to 4 × 10^4 bloodstream forms. Melarsoprol (Arsobal; Aventis) acted as a standard drug and was diluted with sterile distilled water to an appropriate concentration. Groups of four mice were treated on days 3, 4, 5, and 6 intraperitoneally with 20 mg/kg. A control group remained untreated. The parasitemia of all animals was checked on day 7 and 10 postinfection and every second day thereafter until day 60. Death of animals was recorded to calculate the mean survival time. Surviving and aparasitemic mice were considered cured at 60 days and then euthanized.

RESULTS

Activities of melamine nitroheterocycles against *T. brucei* in vitro. Table 1 shows the in vitro activities of a number of nitroheterocyclic compounds versus *T. brucei rhodesiense* and *T. brucei brucei* and a *TbAT1*$^{-/-}$ derivative that is deficient in P2 transport. It is noteworthy that all compounds are substantially more active against the *T. brucei rhodesiense* line in vitro than against *T. brucei brucei*. This observation has been made for a number of other compounds. In vitro, compound 3f (see Fig. 3) is of similar activity as melarsoprol against *T. brucei rhodesiense*, whereas in the *T. brucei* model melarsoprol is somewhat more active than any of the new compounds. However, a number of compounds (notably compounds 3a and 3f) did show pronounced in vitro activity against these parasites.

Role of the P2 transporter in activity. The compounds were designed with the intention of eliciting selective uptake into trypanosomes via the P2 transporter. Loss of the P2 transporter can be a key determinant of drug resistance. In order to determine the ability of these compounds to interact with that transporter, K_i values (which give an approximation to the affinity for the compounds) against P2-dependent adenosine uptake were determined. Most of the compounds did interact with the transporter, as judged by their ability to inhibit adenosine uptake; however, there was no correlation between the sensitivity of trypanosomes to these compounds and their apparent affinity for the transporter (Table 1). Toxic activities were also measured against a parasite line that had been rendered deficient in P2 transporter activity through knockout of the *TbAT1* gene that encodes the transporter. In no instance was an increase in sensitivity to the nitroheterocyclic compounds of >2-fold observed. This indicates that the activity of these compounds is, for the most part, not dependent upon the P2 transporter, although it is possible that other transporters may be involved in the uptake of compounds.

Compounds 2a and 2b, melamine-based binding units, were not active against trypanosomes, and they showed moderate affinity for the P2 transporter. The lack of activity of these compounds indicates that the nitrofuran group present on 3a and 3e is necessary for trypanocidal activity when coupled to a second aromatic group. In general, the benzamidine-coupled nitroimidazole compounds showed less trypanocidal activity than did the melamine-coupled nitrofurans.

TABLE 2. Activities of compounds against RAD51$^{-/-}$ mutant *T. brucei* in the presence or absence of NAC[a]

Compound(s)	Mean IC_{50} (μM) ± SD (n = 3)	
	Wild type	RAD51$^{-/-}$ mutant
Megazol	0.18 ± 0.012	0.034 ± 0.004
Megazol + NAC	0.20 ± 0.018	0.032 ± 0.001
Nifurtimox	5.6 ± 0.48	4.8 ± 0.67
Nifurtimox + NAC	14.35 ± 2.1	12.3 ± 2.2
3a	0.32 ± 0.03	0.36 ± 0.06
3a + NAC	0.34 ± 0.02	0.34 ± 0.04

[a] The effect of 0.5 mM NAC was assessed by adding this to wild-type cells only prior to the addition of drug.

In vivo activity in mice. Selected compounds were evaluated in several rodent models of trypanosome infection. Compounds 3a, 3e, and 3f were examined in rodent models infected with *T. brucei brucei* STIB 795 and *T. brucei rhodesiense* STIB 900. Neither compound 3e nor compound 3f was effective in vivo at 20 mg/kg. Compound 3a, however, cured the STIB 795 *T. brucei brucei* model mice (four of four mice all cured, as defined by no infection at 60 days) at a dose of 20 mg/kg given for 4 days (days 2 to 5). No overt signs of toxicity were observed in these mice. Having successfully treated an acute stage model, the more stringent *T. brucei rhodesiense* STIB 900 model was then tested in rodents. This model is not cured by pentamidine, suramin, or any other drugs active against early stage disease, although it does respond to melarsoprol, which is used in late-stage disease. It is thought that parasites may leave the vasculature early in a STIB 900 infection so that drugs must penetrate extravascular compartments to effect radical cure. As such, STIB 900 infection is perceived to represent a good model for determining likely outcomes of drugs in late-stage models, while providing the advantage of enabling experiments to be conducted within 2, rather than 6, months. Given intraperitoneally at 20 mg/kg for 4 days, compound 3a cured only one of the four mice as defined by their remaining infection free at 60 days. The compound did, however, promote a significant increase in life span of the mice from 8 days for untreated control animals to 35 days for the treated animals. In comparison, in the assay for the STIB 900 model, pentamidine was not curative in any of a group of four mice when given intraperitoneally at 20 mg/kg for 4 days, although the average life expectancy was extended to 43 days.

Genotoxicity is not associated with trypanocidal activity. It is important to determine whether DNA damage plays a role in activity of nitroheterocyclic trypanocides. For example, the principal stumbling block in the development of another nitroheterocycle, megazol, for use in trypanosomiasis therapy related to its propensity to induce mutations in DNA. Megazol is positive in Ames tests (20) and mutagenic in mammalian cell tests (34). Trypanosomes deficient in their own DNA repair enzymes are also hypersensitive to megazol, indicating that the genotoxic effects of this drug are also manifest in these cells (18). A *T. brucei* mutant deficient in a DNA repair enzyme (RAD51) was tested for susceptibility to megazol, to nifurtimox, and to compound 3a. The *RAD51*$^{-/-}$ line was more susceptible than wild-type to megazol but not to compound 3a or to nifurtimox (Table 2), indicating that megazol, but not nifurtimox or compound 3a, induces DNA damage in trypano-

somes. Culture of *T. brucei* in the presence of 0.5 mM NAC reduces free radical damage due to oxidative stress. Although the activity of nifurtimox was antagonized by NAC, that of compound 3a was not, indicating that induction of oxidative stress might not be responsible for the trypanocidal activity of this compound.

DISCUSSION

The chemotherapy of human African trypanosomiasis recently reached the crisis point (25). The lack of surveillance has led to a resurgence of the disease in sub-Saharan Africa (25). Treatment failures with melarsoprol, the principal drug used against late stage disease, have also increased sharply in recent years (10). New drugs are urgently needed.

Trypanosomes have long been known to be highly susceptible to a number of nitroheterocyclic compounds. The nitrofuran furacin was used in several trials in the 1950s and 1960s (1, 19), but its development halted when it became clear that it was responsible for severe toxic side effects. Another nitrofuran, nifurtimox, was registered for use against *T. cruzi* that causes Chagas' disease in Latin America (36). Nifurtimox is also active against *T. brucei*, and this compound has been used against melarsoprol refractory sleeping sickness as a monotherapy (33) or in combination with melarsoprol (25), and a license extension to allow its use for this indication is currently being sought. Nifurtimox, too, has been linked to important side effects.

Since African trypanosomes live free in the bloodstream and cerebrospinal fluid, and not intracellularly, it is possible to exert selectively toxic effects against parasites, but not against host cells, by selectively targeting compounds to the parasite's interior by the use of transporter proteins present in the parasite membrane (21). The P2 aminopurine transporter has been shown to be responsible for the uptake of the melamine-based arsenicals and diamidine classes of drugs. The reason for this relates to the substrate recognition motif of this transporter that is capable of recognizing melamine and benzamidine rings in addition to 6-aminopurine samples. We have previously reported a series of toxic polyamine analogues that possess the P2 transporter recognition motif in the form of melamine groups and shown some of these to have a high activity against *T. brucei* (6, 23, 38).

Given the susceptibility of *T. brucei* to nitroheterocycles but the difficulties in taking such compounds through clinical development due to toxicity issues, we considered the possibility of enhancing the therapeutic index of representatives of this class of molecule by linking nitrofurans and nitroimidazoles to the melamine and benzamidine P2 recognition motifs, respectively.

A number of such compounds were derived. The activity of these compounds is not dependent on uptake via the P2 transporter. First, no correlation between affinity for the P2 transporter, as measured by the ability of these molecules to inhibit uptake of adenosine via this route, and trypanocidal effect was noted. Moreover, it was demonstrated that parasites lacking the P2 transporter were not substantially less sensitive to these compounds than wild-type cells. It is not currently known what routes the compounds do take into the cell. It is plausible that other transporters could be involved in uptake or that the general lipophilic character of the agents could enable uptake through passive diffusion as is the case for the nitroimidazole megazol (5). This observation has an important corollary. It implies that loss of the P2 transporter, an event that appears to occur relatively easily (4, 11, 27), will not lead to resistance to this class of compound. However, in the absence of selective uptake, the reasons for selective activity against the trypanosome compared to the mammalian host are not certain.

Several of the compounds showed pronounced trypanocidal activity. The best compound, 3a, showed in vitro IC_{50} values against *T. brucei* of 0.23 μM and against *T. brucei rhodesiense* of 0.025 μM. In comparison, nifurtimox has an in vitro IC_{50} value of 5.6 μM against *T. brucei* and 1.5 μM against *T. brucei rhodesiense*. Compound 3a is therefore some 20-fold better in terms of in vitro efficacy than this rival nitroheterocycle that is in use clinically (Table 1). Crucially compound 3a was able to cure mice infected with *T. brucei rhodesiense* when given at 20 mg/kg for 4 days. In the difficult to cure *T. brucei rhodesiense* STIB 900 model, the same treatment schedule resulted in cure of one of four animals with a mean survival of 35 days (untreated controls had a mean survival of 8 days). The good trypanocidal activities in vitro and in rodent models seen for this class of compound suggest that further investigations into novel derivatives might yield even better trypanocidal agents, and further studies are planned.

Many nitroheterocyclic drugs are believed to exert their activity through either reductive stress or oxidative stress. In the case of reductive stress, single electron reduction of the nitro group is believed to create a highly reactive radical, derivatives of which can then form covalent bonds with numerous cellular macromolecules, including DNA. Oxidative stress is believed to arise from reduced oxygen intermediates that arise once oxygen accepts electrons from the reduced nitro group (16). We have developed assays using trypanosomes that give insight as to whether reductive or oxidative stress underlies the activity of these compounds (18). Reductive stress can be assessed by measuring the susceptibility of DNA repair-deficient trypanosomes to toxic agents. Oxidative stress can be assessed by determining the ability of NAC to antagonize an agent's activity, since this compound interacts with several reactive oxygen intermediates.

Using the RAD51 knockout line and NAC assay system, we have shown that the nitroimidazole-thiadazole megazol exerts its activity through reductive stress as *RAD51* knockout parasites, which are deficient in DNA repair and hypersensitive to this drug (18). These cells are not hypersensitive to the nitrofuran nifurtimox. The action of nifurtimox, however, is antagonized by NAC, whereas that of megazol is not. It therefore appears that megazol acts through reductive stress, whereas nifurtimox acts through oxidative stress (16, 18). Compound 3a does not have any enhanced activity against the *RAD51* knockout cells, which indicates that this compound may not exert its activity through reductive stress. Moreover, NAC fails to antagonize the activity of compound 3a. This could indicate that the agent does not act through oxidative stress. These results are important, given that the development of the nitroimidazole megazol was arrested when it became clear that the compound was genotoxic in mammalian cells, an activity also apparent in trypanosomes (18). Nifurtimox is also toxic to mammals, probably through events related to oxidative stress

(31). Compound 3a is notable in that it apparently does not act through either reductive or oxidative stress in trypanosomes.

It is noteworthy that the activity against L6 cells in vitro is 2 to 3 orders of magnitude lower than against trypanosomes. Moreover, no overt adverse effects became apparent in mice challenged with the drug up to 100 mg kg^{-1}. It is possible that the action of compound 3a occurs independently of reduction of the nitro group. In this case, the chances of the compound's passing stringent tests on mammalian cell toxicity would be greatly enhanced. Such testing has yet to be performed but, based on the data reported here, further studies into the efficacy and toxicology of this important lead compound are justified.

ACKNOWLEDGMENTS

This study was funded by a grant from the Wellcome Trust and the UNDP/World Bank/WHO Special Programme for Research and Training in Tropical Diseases. We thank the Welsh School of Pharmacy for funding (A.B.).

We also thank Elke Gobright and Guy Riccio for excellent technical assistance and Richard McCulloch (University of Glasgow) and Enock Matovu (LIRI, Uganda) for the generous provision of the *RAD51*$^{-/-}$ and *TbAT1*$^{-/-}$ *T. brucei* lines, respectively. The EPSRC National Mass Spectrometry Centre in Swansea is acknowledged for accurate mass spectrometry.

REFERENCES

1. **Apted, F. I. C.** 1960. Nitrofurazone in the treatment of sleeping sickness due to *Trypanosoma rhodesiense*. Trans. R. Soc. Trop. Med. Hyg. **54**:225–228.
2. **Aruoma, O. I., B. Halliwell, B. M. Hoey, and J. Butler.** 1989. The antioxidant action of *N*-acetylcysteine: its reaction with hydrogen peroxide, hydroxyl radical, superoxide, and hypochlorous acid. Free Radic. Biol. Med. **6**:593–597.
3. **Baltz, T., D. Baltz, C. Giroud, and J. Crockett.** 1985. Cultivation in a semidefined medium of animal infective forms of *Trypanosoma brucei*, *T. equiperdum*, *T. evansi*, *T. rhodesiense*, and *T. gambiense*. EMBO J. **4**:1273–1277.
4. **Barrett, M. P., and A. H. Fairlamb.** 1999. The biochemical basis of arsenical-diamidine cross-resistance in African trypanosomes. Parasitol. Today **15**: 136–140.
5. **Barrett, M. P., A. H. Fairlamb, B. Rousseau, G. Chauviere, and J. Perie.** 2000. Uptake of the nitroimidazole drug megazol by African trypanosomes. Biochem. Pharmacol. **59**:615–620.
6. **Barrett, M. P., and I. H. Gilbert.** 2002. Perspectives for new drugs against trypanosomiasis and leishmaniasis. Curr. Top. Med. Chem. **2**:471–482.
7. **Barrett, M. P., R. J. S. Burchmore, A. Stich., J. O. Lazzari, A. C. Frasch, J. J. Cazzulo, and S. Krishna.** 2003. The trypanosomiases: divergent parasitic diseases arising from a common genus. Lancet **362**:1469–1480.
8. **Borowy, N. K., R. T. Nelson, H. Hirumi, R. Brun, H. K. Waithaka, D. Schwartz, and A. Polak.** 1988. Ro 15–0216: a nitroimidazole compound active in vitro against human and animal pathogenic African trypanosomes. Ann. Trop. Med. Parasitol. **82**:13–19.
9. **Bouteille, B., A. Marie-Daragon, G. Chauviere, C. de Albuquerque, B. Enanga, M. L. Darde, J. M. Vallat, J. Perie, and M. Dumas.** 1995. Effect of megazol on *Trypanosoma brucei brucei* acute and subacute infections in Swiss mice. Acta Trop. **60**:73–80.
10. **Brun, R., R. Schumacher, C. Schmid, C. Kunz, and C. Burri.** 2001. The phenomenon of treatment failures in human African trypanosomiasis. Trop. Med. Int. Health **6**:906–914.
11. **Carter, N. S., and A. H. Fairlamb.** 1993. Arsenical-resistant trypanosomes lack an unusual adenosine transporter. Nature **361**:173–175.
12. **Cotgreave, I. A.** 1997. *N*-Acetylcysteine: pharmacological considerations and experimental and clinical applications. Adv. Pharmacol. **38**:205–227.
13. **Cunningham, M. P., and K. Vickerman.** 1962. Antigenic analysis in the *Trypanosoma brucei* group using the agglutination reaction Trans. R. Soc. Trop. Med. Hyg. **56**:48–59.
14. **de Koning, H. P., and S. M. Jarvis.** 1999. Adenosine transporters in bloodstream forms of *Trypanosoma brucei brucei*: substrate recognition motifs and affinity for trypanocidal drugs. Mol. Pharmacol. **56**:1162–1170.
15. **de Koning, H. P.** 2001. Uptake of pentamidine in *Trypanosoma brucei brucei* is mediated by three distinct transporters: Implications for cross-resistance with arsenicals. Mol. Pharmacol. **59**:586–592.
16. **Docampo, R., and Stoppani, A. O. M.** 1979. Generation of superoxide anion and hydrogen peroxide induced by nifurtimox in *Trypanosoma cruzi*. Arch. Biochem. Biophys. **197**:317–321.
17. **Enanga, B., M. Keita, G. Chauviere, M. Dumas, and B. Bouteille.** 1998. Megazol combined with suramin: a chemotherapy regimen which reversed the CNS pathology in a model of human African trypanosomiasis in mice. Trop. Med. Int. Health **3**:736–741.
18. **Enanga, B., M. Ariyanayagam, M. Stewart, and M. P. Barrett.** 2003. Activity of megazol, a trypanocidal nitroimidazole, is associated with DNA damage. Antimicrob. Agents Chemother. **47**:3368–3370.
19. **Evens, F., K. Niemegeers, and A. Packchanian.** 1957. Nitrofurazone therapy of *Trypanosoma gambiense* sleeping sickness in man. Am. J. Trop. Med. Hyg. **6**:665–678.
20. **Ferreira, R. C., and L. C. Ferreira.** 1986. CL 64,855, a potent anti-*Trypanosoma cruzi* drug, is also mutagenic in the *Salmonella*/microsome assay. Mem. Inst. Oswaldo-Cruz **81**:49–52.
21. **Hasne, M.-P., and M. P. Barrett.** 2000. Drug uptake via nutrient transporters in *Trypanosoma brucei*. J. Appl. Microbiol. **89**:697–701.
22. **Hirumi, H., and K. Hirumi.** 1989. Continuous cultivation of *Trypanosoma brucei brucei* bloodstream forms in a medium containing a low concentration of serum protein without feeder cell layers. J. Parasitol. **75**:985–989.
23. **Klenke, B., M. Stewart, R. Brun, M. P. Barrett, and I. H. Gilbert.** 2001. Synthesis and biological evaluation of s-triazine substituted polyamines as potential new anti-trypanosomal drugs. J. Med. Chem. **44**:3440–3452.
24. **Lanham, S. M., and D. G. Godfrey.** 1970. Isolation of salivarian trypanosomes from man and other mammals using DEAE-cellulose. Exp. Parasitol. **28**:521–534.
25. **Legros, D., G. Ollivier, M. Gastellu-Etchegorry, C. Paquet, C. Burri, J. Jannin, and P. Buscher.** 2002. Treatment of human African trypanosomiasis: present situation and needs for research and development. Lancet Infect. Dis. **2**:437–440.
26. **Marton, L. J., and A. E. Pegg.** 1995. Polyamines as targets for therapeutic intervention. Annu. Rev. Pharmacol. Toxicol. **35**:55–91.
27. **Maser, P., C. Sutterlin, A. Kralli, and R. Kaminsky.** 1999. A nucleoside transporter from *Trypanosoma brucei* involved in drug resistance. Science **285**:242–244.
28. **Matovu, E., M. L. Stewart, F. Geiser, R. Brun, P. Mäser, L. M. P. Wallace, R. J. S. Burchmore, K. K. C. Enyaru, M. P. Barrett, R. Kaminsky, T. Seebeck, and H. P. de Koning.** 2003. The roles of the *Trypanosoma brucei* P2 adenosine transporter (TbAT1) in drug uptake and resistance determined through gene knockout. Eukaryot. Cell **2**:1003–1008.
29. **McCulloch, R., and J. D. Barry.** 1999. A role for RAD51 and homologous recombination in *Trypanosoma brucei* antigenic variation. Genes Dev. **13**: 2875–2888.
30. **Millet, R., L. Maes, V. Landry, C. Sergheraert, and E. Davioud-Charvet.** 2002. Antitrypanosomal activities and cytotoxicity of 5-nitro-2-furancarbohydrazides. Bioorg. Med. Chem. Lett. **12**:3601–3604.
31. **Moreno, S. N. J., Mason, R. P., and Docampo, R.** 1984. Reduction of nifurtimox and nitrofurantoin by intact rat liver mitochondria. Evidence of an outer membrane-located nitroreductase. J. Biol. Chem. **259**:6298–6305.
32. **Muller, S., G. H. Coombs, and R. D. Walter.** 2001. Targeting polyamines of parasitic protozoa in chemotherapy. Trends Parasitol. **17**:242–249.
33. **Pepin, J., F. Milord, F. Meurice, L. Ethier, L. Loko, and B. Mpia.** 1992. High-dose nifurtimox for arseno-resistant *Trypanosoma brucei gambiense* sleeping sickness: an open trial in central Zaire. Trans. R. Soc. Trop. Med. Hyg. **86**:254–256.
34. **Poli, P., M. Aline de Mello, A. Buschini, R. A. Mortara, C. Northfleet de Albuquerque, S. da Silva, C. Rossi, and T. M. Zucchi.** 2002. Cytotoxic and genotoxic effects of megazol, an anti-Chagas' disease drug, assessed by different short-term tests. Biochem. Pharmacol. **64**:1617–1627.
35. **Raz, B., M. Iten, Y. Grether-Buhler, R. Kaminsky, and R. Brun.** 1997. The Alamar Blue assay to determine drug sensitivity of African trypanosomes (*T. b. rhodesiense* and *T. b. gambiense*) in vitro. Acta Trop. **68**:139–147.
36. **Rodriques-Coura, J., and S. L. de Castro.** 2002. A critical review on Chagas disease chemotherapy. Mem. Inst. Oswaldo-Cruz **97**:3–24.
37. **Sanchez, M. A., R. Tryon, J. Green, I. Boor, and S. M. Landfear.** 2002. Six related nucleoside nucleobase transporters from *Trypanosoma brucei* exhibit distinct biochemical functions. J. Biol. Chem. **277**:21499–21504.
38. **Tye, C. K., G. Kasinathan, M. P. Barrett, R. Brun, V. E. Doyle, A. H. Fairlamb, R. Weaver, and I. H. Gilbert.** 1998. An approach to use an unusual adenosine transporter to selectively deliver polyamine analogues to trypanosomes. Bioorg. Med. Chem. Lett. **8**:811–816.

Design and Synthesis of a Series of Melamine-based Nitroheterocycles with Activity against Trypanosomatid Parasites

Alessandro Baliani,[†] Gorka Jimenez Bueno,[†] Mhairi L. Stewart,[‡] Vanessa Yardley,[§] Reto Brun,[||] Michael P. Barrett,[‡] and Ian H. Gilbert*,[†]

Welsh School of Pharmacy, Redwood Building, Cardiff University, King Edward VII Avenue, Cardiff CF10 3XF, United Kingdom; Institute of Biomedical and Life Sciences, Division of Infection & Immunity, University of Glasgow, Glasgow G12 8QQ, United Kingdom; London School of Hygiene and Tropical Medicine, Keppel Street, London, WC1E 7HT, United Kingdom; and Swiss Tropical Institute, Socinstrasse 57, CH-4002 Basel, Switzerland

Received February 24, 2005

The parasites that give rise to human African trypanosomiasis (HAT) are auxotrophs for various nutrients from the human host, including purines. They have specialist nucleoside transporters to import these metabolites. In addition to uptake of purine nucleobases and purine nucleosides, one of these transporters, the P2 transporter, can carry melamine derivatives; these derivatives are not substrates for the corresponding mammalian transporters. In this paper, we report the coupling of the melamine moiety to selected nitro heterocycles with the aim of selectively delivering these compounds to the parasites. Some compounds prepared have similar in vitro trypanocidal activities as melarsoprol, the principal drug used against late-stage HAT, with 50% growth inhibitory concentrations in the submicromolar range. Selected compounds were also evaluated in vivo in rodent models infected with *Trypanosoma brucei brucei* and *T. brucei rhodesiense* and showed pronounced activity and in two cases were curative without overt signs of toxicity. Compounds were also tested against other trypanosomatid pathogens, *Leishmania donovani* and *Trypanosoma cruzi*, and significant activity in vitro was noted for *T. cruzi* against which various nitro heterocycles are already registered for use.

Introduction

Parasitic trypanosomatids cause a number of important diseases, including human African trypanosomiasis (HAT), Chagas disease, and the leishmaniases. HAT is caused by the protozoan parasites *Trypanosoma brucei gambiense* and *T. brucei rhodesiense* and is endemic in sub-Saharan Africa, where it is a major health problem.[1] The current drugs used for the treatment of the infection are unsatisfactory, due to poor blood−brain barrier permeability, toxicity, and increasing problems due to resistance.[2,3] Chagas disease is caused by *Trypanosoma cruzi*, and no drugs are currently registered that are totally active against these parasites, particularly at the chronic stage of infection.[4] The leishmaniases represent a spectrum of diseases which are caused by several species of leishmania[5] and for which chemotherapy is also difficult.[6]

When present in the human host, the parasites require nutrients from the host. To achieve this, *T. brucei* encodes a number of transporters for uptake of essential nutrients, which are expressed in the clinically relevant bloodstream form of the parasite. One of the nutrient classes that the parasites sequester from the host are the purines. Carter and Fairlamb[7] first described an unusual purine transporter from *T. brucei* that has been designated the P2 transporter. This purine transporter shows significant differences to the corresponding mammalian transporters. The parasites also contain a more general purine uptake system, designated the P1 transporter, which in fact comprises the activities of a number of different transporters.[8] The normal substrates for the P2 transporter are adenosine and adenine. However, in addition to this, other motifs such as melamines and benzamidines (Figure 1) have been shown to be substrates for this transporter, which differs from the case of mammalian transporters.[2,7] Results of structure−activity relationship studies have indicated the following requirements for uptake through the P2 transporter: an amidine moiety, an aromatic ring, and an electronegative heteroatom. These features can be seen in substrates for the P2 transporter shown in Figure 1.[2,9] Melarsoprol and pentamidine have been shown to be substrates of the P2 transporter, and this is one of the mechanisms by which these trypanocidal agents are concentrated in the parasite.[3] Loss or mutation of the P2 transporter has been implicated in resistance to melarsoprol and also some diamidines in laboratory studies.[2,3,10] It is possible that the increased incidence of treatment failure in the field[11] is related to the emergence of drug resistance in this setting too.

Recently it has been shown that the situation is more complex than originally thought. Loss of the P2 transporter only causes a small (50%) decrease in susceptibility of parasites to melarsoprol, although this small decrease may be sufficient to explain the clinical resistance of this drug. The small decrease in susceptibility to melarsoprol of the parasite indicates that there are additional modes of uptake of melarsoprol into the parasite, and it has been shown that there are other transporters involved in uptake of melamine and ben-

* Corresponding author. Tel: +44 29 2087 5800. Fax: +44 29 2087 4149. E-mail: gilbertih@cf.ac.uk.
[†] Cardiff University.
[‡] University of Glasgow.
[§] London School of Hygiene and Tropical Medicine.
[||] Swiss Tropical Institute.

10.1021/jm050177+ CCC: $30.25
Published on Web 07/29/2005

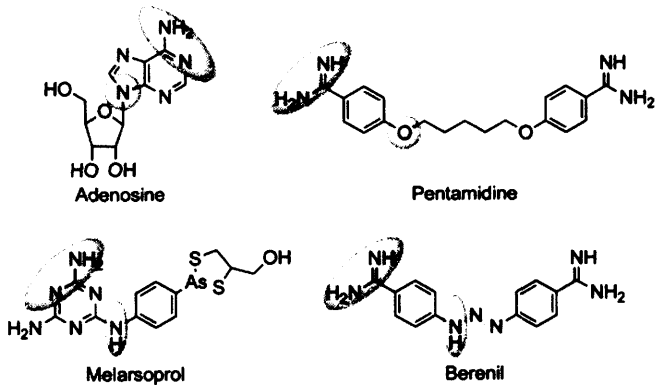

Figure 1. Substrates of the P2 transporter. The amidine and electronegative heteroatom are highlighted on each structure.

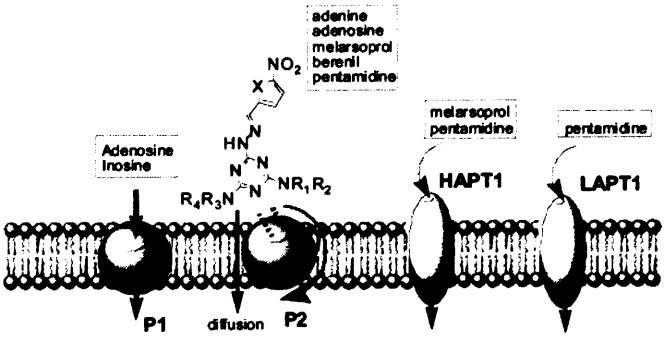

Figure 2. The known routes of uptake of diamines and melaminophenyl arsenicals into *T. brucei*. The P2 transporter is also represented interacting with a melamine-nitrofuran compound (**6a**), whose transport through the membrane is probably facilitated by the transporter and passive diffusion.

zamidine motifs into parasites (Figure 2).[9,12] In particular at least two other transporters have been identified for pentamidine uptake, designated "HAPT1" (high-affinity pentamidine transporter) and "LAPT1" (low-affinity pentamidine transporter). The transporter HAPT1 is possibly also responsible for uptake of melarsoprol. The normal physiological roles of LAPT1 and HAPT1 are certainly unknown. It is possible that other transporters are also involved in uptake of these motifs as well; for example, another purine nucleoside transporter, an *S*-adenosylmethionine transporter, has been reported.[13] However it is clear that these motifs are selectively taken up into parasites.

The presence of the P2 transporter with its particular substrate specificity presents an opportunity in the field of drug design. This could be achieved by attaching trypanocidal compounds to motifs that are substrates of the P2 transporter.[14,15] Then both the P2 recognition motif and trypanocidal agent should be selectively taken up into the parasite. To study this, we have investigated the coupling of the P2 recognition motif, melamine, to the polyamine analogues. Polyamine analogues are toxic to *T. brucei*.[16,17] We have reported the coupling of polyamine analogues to the melamine moiety and prepared compounds that showed potent trypanocidal activity and good selectivity on a cellular level.[14] However, the compounds turned out to be toxic in animal models. Therefore, we have selected an alternate trypanocidal moiety for attachment to the melamine and benzamidine delivery moiety, nitroaromatics. Nitroaromatic compounds have been shown to have potent activity against a variety of microbes. Of particular

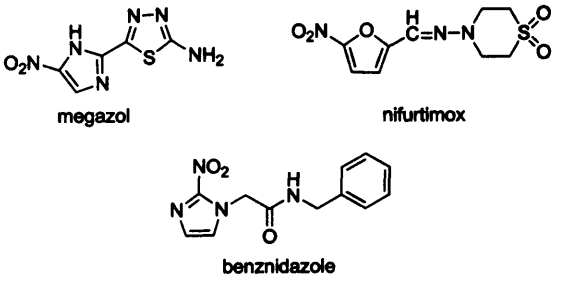

Figure 3. Structure of some known nitro heterocycles having activity against *T. brucei* and or *T. cruzi*.

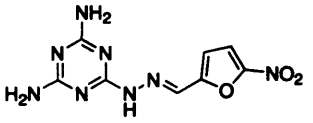

6a

Figure 4. The structure of the lead compound.

relevance, nifurtimox and benznidazole (Figure 3) are nitro heterocycles used for treatment of Chagas disease, which is caused by the related organism *T. cruzi*. In addition, nifurtimox is being considered as a potential treatment for melarsoprol refractory African trypanosomiasis.[18,19] A key problem with nitroaromatics is that some, but not all, compounds in this class are mutagenic.[20,21] We decided to couple nitroaromatics to the melamine motif, with the aim of selectively delivering these compounds to the parasites. Rapid and selective delivery of these compounds to the parasites should give selective accumulation in the parasite and minimize side effects, possibly allowing reduced doses. We have recently described the activity of some compounds in which we have linked a nitro heterocycle to a melamine delivery motif.[12] In this current paper we report the preparation of these initial compounds and some new compounds plus a detailed analysis of the structure–activity relationships.

As nitro heterocycles are the only drugs currently registered against Chagas disease, we considered it of interest to test the new compounds against *T. cruzi*. *Leishmania* parasites too share substantial similarity to the other trypanosomatids belonging to the same taxonomic order and here too new drugs are required, thus we also tested for activity against *Leishmania*.

Chemistry

The general structure of our lead compound, **6a**, is shown in Figure 4.[12] In this compound the melamine motif is linked to the nitro heterocycle via a hydrazone.

We proposed to investigate the following structure–activity relationships: (i) addition of methyl substitutents to the melamine, to alter the lipophilic properties of the molecules; (ii) replacement of the oxygen in the nitro heterocycle with sulfur, to modify the electronic properties of the nitro heterocycle and lipophilic properties of the molecule; (iii) investigation of the necessity of the nitro group, by replacement of the nitro group with a hydrogen or another electron-withdrawing group.

The triazines described were synthesized starting from cyanuric chloride (2,4,6-trichloro-1,3,5-triazine) (**1**) and different nucleophiles. The chlorine atoms of cyanuric chloride can be replaced successively by substituted or nonsubstituted amino groups. The nucleophiles

Scheme 1[a]

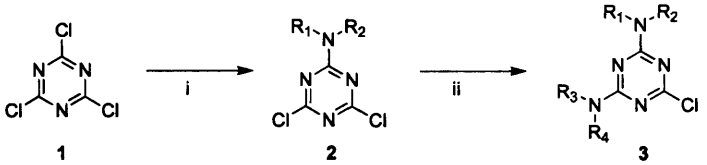

2a, $R_1 = R_2 = H$ (71%)
2b, $R_1 = H$, $R_2 = CH_3$
2c, $R_1 = R_2 = CH_3$

3a, $R_1 = R_2 = R_3 = R_4 = H$
3b, $R_1 = R_3 = H$, $R_2 = R_4 = CH_3$ (89%)
3c, $R_1 = R_2 = R_3 = R_4 = CH_3$ (90%)
3d, $R_1 = R_2 = R_3 = H$, $R_4 = CH_3$ (82%)
3e, $R_1 = R_2 = H$, $R_3 = R_4 = CH_3$ (81%)

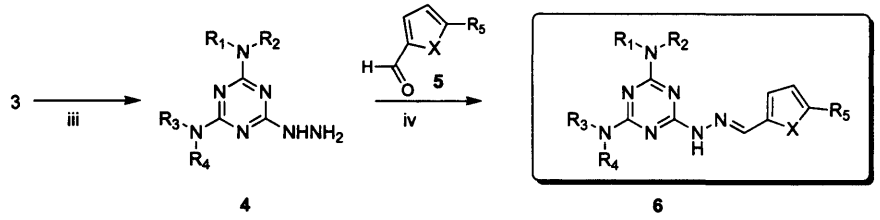

4a, $R_1 = R_2 = R_3 = R_4 = H$ (72%)
4b, $R_1 = R_3 = H$, $R_2 = R_4 = CH_3$ (96%)
4c, $R_1 = R_2 = R_3 = R_4 = CH_3$ (66%)
4d, $R_1 = R_2 = R_3 = H$, $R_4 = CH_3$ (30%)
4e, $R_1 = R_2 = H$, $R_3 = R_4 = CH_3$ (64%)

6a, $R_1 = R_2 = R_3 = R_4 = H$, $R_5 = NO_2$, X = O (36%)
6b, $R_1 = R_3 = H$, $R_2 = R_4 = CH_3$, $R_5 = NO_2$, X = O (71%)
6c, $R_1 = R_2 = R_3 = R_4 = CH_3$, $R_5 = NO_2$, X = O (58%)
6d, $R_1 = R_2 = R_3 = H$, $R_4 = CH_3$, $R_5 = NO_2$, X = O (51%)
6e, $R_1 = R_2 = H$, $R_3 = R_4 = CH_3$, $R_5 = NO_2$, X = O (80%)
6f, $R_1 = R_2 = R_3 = R_4 = H$, $R_5 = H$, X = O (58%)
6g, $R_1 = R_2 = R_3 = R_4 = H$, $R_5 = CN$, X = O (13%)
6h, $R_1 = R_2 = R_3 = R_4 = H$, $R_5 = NO_2$, X = S (25%)
6i, $R_1 = R_2 = R_3 = R_4 = H$, $R_5 = H$, X = S (38%)

[a] (i) R_1R_2NH, acetone/H_2O, rt; (ii) R_2R_3NH, 2 N NaOH, acetone/H_2O, rt; (iii) NH_2NH_2, H_2O, reflux; (iv) aryl aldehyde, MeOH, rt. The yields are shown in brackets.

can selectively displace the different chlorines by controlling the reaction temperature.[22] In general, the first chlorine can be displaced while the temperature is maintained below 0 °C, the second between 25 and 50 °C, and the third substitution at 67 °C.[23] Another important factor that has to be considered for the preparation of the different derivatives is the nature of the reactive group and the order of entry of the group. When different amino groups were introduced, the less reactive amine was introduced before the more reactive one.

The reactions, in most cases, were carried out in aqueous suspensions, since the products precipitate from solution, simplifying their isolation.[24] To increase the reactivity and the yield, the cyanuric chloride was previously dissolved in acetone and then poured into ice–water to get a very fine suspension. The direct reaction of cyanuric chloride with ammonia, methylamine, and dimethylamine gave the 2-substituted-4,6-dichloro-1,3,5-triazines (**2a–c**) (Scheme 1).[25,26]

The 2,4-disubstituted-6-chloro-1,3,5-triazines (**3a–e**) were obtained by reaction of a further amine with the 2-substituted-4,6-dichloro-1,3,5-triazine in the presence of base (NaOH or $NaHCO_3$). The displacement of the last chlorine by the hydrazine was achieved by further increasing the temperature to 85 °C, affording the hydrazine derivatives (**4**) in good yields.[27] The first set of hydrazones (**6a–i**) were prepared by reaction of the hydrazine derivatives (**4**) with 5-nitro-2-furaldeyde, affording the corresponding 4,6-disubstituted-2-(5-nitrofurfurylidenehydrazino)-1,3,5-triazines (**6a–e**). The products had a low solubility in most organic solvents, except DMSO. However purification was achieved by recrystallization from methanolic and ethanolic water solutions.

Scheme 2[a]

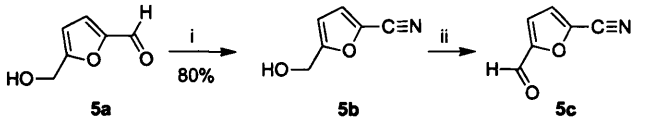

[a] (i) I_2, NH_3, THF/H_2O, rt; (ii) oxalyl chloride, DMSO, NEt_3 CH_2Cl_2, −78 °C.

Amended data is presented for compound **6b** to that originally presented;[12] this compound was remade and repurified.

With the purpose of improving the solubility and evaluating the pharmacological importance of the redox potentials of the heteroaromatic rings, the hydrazine (**4a**) was coupled with 5-nitro-2-thiophenecarboxaldehyde to prepare the thiophene analogue (**6h**).

To investigate the pharmacological role of the nitro group in these compounds, compounds without a nitro group were prepared. Replacement of the nitro with a hydrogen was achieved by coupling the hydrazine **4a** with 2-furaldehyde or 2-thiophenecarboxaldehyde to give the related hydrazones (**6f**, **6i**). The solubility observed for all these compounds was slightly improved and the recrystallization was achieved using the conditions described for the previous hydrazones.

We were also interested to replace the nitro with a cyano group, as this is electron-withdrawing, like the nitro. To do this, we required the 5-cyano-substituted 2-furaldehyde. This compound was synthesized as showed in Scheme 2. 5-Hydroxymethyl-2-furaldehyde (**5a**) was used as starting material. The aldehyde function was successfully converted in nitrile by using iodine in aqueous ammonia. The reaction seems to proceed via oxidation of aldimine with iodine to give an N-iodo aldimine intermediate, which eliminates an HI

Scheme 3[a]

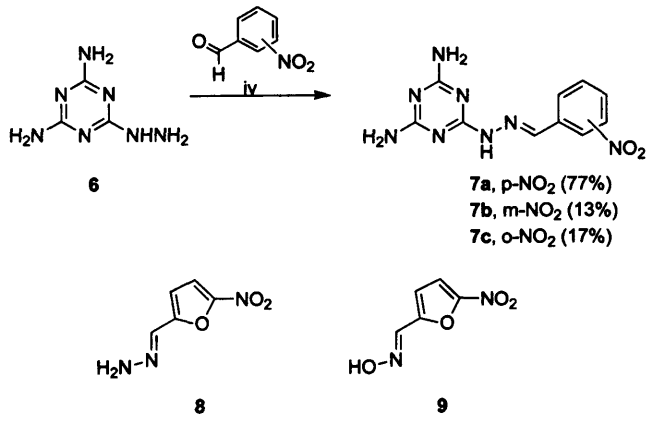

[a] (iv) Methanol, rt.

molecule in ammonia solution to afford the nitrile product (**5b**) in good yield (80%).[28] The hydroxyl group was then oxidized to the aldehyde **5c** via Swern oxidation.[29]

The three isomers of nitrobenzaldehyde (**7a–c**) have also been used to synthesize hydrazones where the heterocyclic ring has been replaced with a nonheterocyclic structure.

Biology

The activity of the compounds was evaluated in a variety of different models.

Affinity for the P2 Transporter. Compounds were evaluated for their ability to interact with the P2 aminopurine transporter of *T. brucei* (Table 1). This was achieved by measuring their ability to antagonize the uptake of radiolabeled adenosine.[10] In addition to uptake through the P2 transporter, the other main route of adenosine uptake is through the P1 system. To differentiate transport through the P1 and P2 systems, the experiments were conducted in the presence of a large excess of inosine, which saturates the P1 transporter. Thus, adenosine uptake will only occur through the P2 transporter. It is important to note that this experiment does not actually measure uptake of compounds through the P2 transporter, but it does give a measure of the affinity of compounds for the P2 transporter.

The results suggest that compounds without a melamine group have relatively low affinity for the P2 transporter (compound **9** has IC_{50} = 404 μM), as would be anticipated. Also compound **6c** in which all the nitrogens on the melamine ring were methylated showed poor affinity (IC_{50} = 129 μM). The other compounds assayed showed IC_{50} values all within about a log range of each other that were of a similar order as melarsoprol. Changes to the nitrofuran ring gave very small changes to the apparent affinity for the P2 transporter: thus, removal of the nitro group (compare **6a/6f** and **6h/6i**) gave virtually no change in affinity, while replacement of the oxygen with a sulfur gave a small increase in affinity (compare **6a/6h** and **6f/6i**). This suggests that the primary determinant of affinity for the P2 transporter is the melamine ring and the nitro heterocycle has a limited effect on affinity. This is consistent with previous reports in the literature.[2-15]

Activities against *T. brucei* in Vitro. Compounds were tested against several *T. brucei* lines in vitro. The *T. brucei brucei* AT1 wild type and a TbAT1 knockout line were compared to study the effects of the P2 transporter on the activity of the compounds (the TbAT1 gene encodes the P2 transporter). A strain of *T. brucei rhodesiense*, the causative agent of acute HAT, was also studied. Compounds were also assayed against mammalian L6 cells as a measure of cellular toxicity toward mammalian cells.

Very similar results were seen with compounds against both the wild type and P2 knockout *T. brucei brucei*. There was a slight reduction in activity for the knockout line, on the order of 2-fold less active, for many compounds. This was observed for melarsoprol as well as our compounds. This reduction in activity is not very significant and suggests that there are routes other than the P2 transporter for uptake of these compounds. Melarsoprol was the most active compound against *T. brucei brucei* (IC_{50} = 53 nM). However, some of the nitro heterocycles prepared showed only slightly reduced activity against *T. brucei brucei*, notably **6a**, **6c**, **6d**, **6h** (IC_{50} = 230, 200, 130, and 850, respectively).

Compounds were more potent against the *T. brucei rhodesiense* line studied here than against the *T. brucei brucei* line, although very similar trends were seen within the different species. These probably reflect a range of activities against different strains of the *T. brucei* trypanosomes in general rather than a particular difference between the nonhuman pathogenic *T. brucei brucei* line and the human infectious *T. brucei rhodesiense* line. Thus, melarsoprol had an IC_{50} against *T. brucei rhodesiense* of 6 nM, while **6c** had an IC_{50} of 3 nM. A significant number of our compounds had IC_{50} values in the nanomolar range (**6a**, **6b**, **6c**, **6d**, **6e**, and **6h**). Compound **6c** was the most active compound in our series in cellular assays.

In comparing all activities the following structure–activity relationships can be observed:

(1) Compounds without a melamine structure (**8** and **9**) showed weak activity (IC_{50} = 2.3 μM) and also weak selectivity compared to the mammalian L6 cells.

(2) Compounds with a nitrofuran ring joined to a melamine ring showed potent in vitro activity (**6a–e**).

(3) Replacement of the oxygen with a sulfur led to a 10-fold loss in activity and a small increase in toxicity to L6 cells.

(4) Compounds in which the nitro group was replaced by a hydrogen had significant loss in activity (compare **6a/6f** and **6h/6I**).

(5) Replacement of the nitro group with another electron-withdrawing group, the nitrile group, led to loss of activity (**6g**), implying that more than an electron-withdrawing effect is necessary for activity.

(6) Complete removal of the nitro heterocycle caused loss of activity (**4a**).

(7) Replacement of the nitrofuran with a nitrophenol also led to loss of activity (**7a–c**).

(8) A number of the nitro heterocycles were markedly less toxic against mammalian cells than melarsoprol; of particular note are **6a**, **6d**, and **6e**.

Activities against *Trypanosoma cruzi* and *Leishmania donovani*. An interesting point noted from the data on in vitro activities against *T. brucei brucei* was the fact that compounds retained activity despite the loss of the P2 transporter. This indicates that routes

Table 1. In Vitro Activities of Compounds against the P2 Transporter, Bloodstream *T. brucei*, and Mammalian Cells as a Measure of Toxicity[d]

			IC_{50}, μm			
compd	MW	P2 uptake[a]	*T. brucei brucei* AT1 wild type	*T. brucei brucei* AT1 knockout[b]	*T. brucei rhodesiense*	L6 cells[c]
4a	141.1	11.9	>200	>200	ND	ND
6a	264.2	22.9	0.23	0.38	0.025	183
6b	292.2	ND	ND	ND	0.010	44.1
6c	320.3	129	0.2	0.3	0.003	18.7
6d	278.2	ND	0.13	0.06	0.018	48.9
6e	292.2	ND	5.36	3.09	0.053	109.5
6f	216.2	15.9	16.5	29.3	12.9	>400
6g	244.2	ND	ND	ND	46.27	ND
6h	280.2	1.9	0.85	1.52	0.24	11.8
6i	235.3	4.9	89	170	10.2	78.2
7a	274.2	ND	>75	>75	29.9	ND
7b	274.2	ND	>75	>75	52.88	ND
7c	274.2	ND	>75	>75	36.47	ND
8	155.1	404	23.5	13.5	2.3	20
9	156.1	300	1.18	1.26	0.68	40
melarsoprol		1.2	0.053	0.12	0.006	7.8
nifurtimox		ND	5.6	ND	1.5	68

[a] Inhibition of adenosine uptake by the P2 transporter in *T. brucei brucei* 427. [b] *T. brucei brucei* AT1 knockout is a mutant with a non functional P2 transporter. [c] L-6 cells are rat skeletal myoblasts and are used as a measure of cytotoxicity to mammalian cells. ND, not determined. [d] Data for compounds **4a**, **6a**, **6c**, **6f**, **6h**, **6i** has been reported previously,[12] but is included here for comparative purposes. Amended data for **6b** is presented.

Table 2. In Vitro Activities of Compounds against Intracellular Amastigotes of *T. cruzi* and *L. donovani*[a]

Compound	MW	*T. cruzi* (IC_{50} [μM])	*Leishmania donovani* (IC_{50} [μM])
4a	141.1	ND	ND
6a	264.2	2.1	>12.5
6b	292.2	0.24	3.14
6c	320.3	0.38	tox
6d	278.2	0.39	0.75
6e	292.2	0.29	tox
6f	216.2	>400	tox
6g	244.2	122	ND
6h	280.2	2.6	tox
6i	235.3	85.84	tox
7a	274.2	91.54	ND
7b	274.2	328	ND
7c	274.2	328	ND
8	156.1	ND	tox
9	156.1	ND	tox
Melarsoprol		0.006	7.8
Nifurtimox		1.5	68

[a] Standards: For *T. cruzi*, Benznidazole, IC_{50} = 1.435 μM; *L. donovani*: Miltefosine, IC_{50} = 1.16 μM: tox − toxic to macrophages thus precluding measurement of leishmanicidal activity.

other than the *T. brucei* specific transporter clearly exist for these compounds. This prompted us to also test for activity against the related pathogens *T. cruzi* and *L. donovani*.

As shown in Table 2 activities against *T. cruzi* were observed for compounds **6b**−**e**, with activities in the submicromolar range. None of the compounds showed sub-micromolar activities in vitro against *L. donovani*, except for compound **6d**, with an IC_{50} of 0.75 μM.

In Vivo Activity in Rodent Models of Infection. Selected compounds were evaluated in several rodent models of *T. brucei* group infection. Compounds **6a**, **6b**, **6d**, and **6e** were examined in rodent models infected with *T. brucei brucei* STIB 795 at a dose of 20 mg/kg for 4 days ip (days 3−6). The mice are considered cured when no infection was found at 60 days. Compounds **6a** and **6d** were able to cure the STIB 795 *T. brucei brucei* model mice, where four mice of four were all cured. No overt signs of toxicity were observed in these mice. Compounds **6b** and **6e** were not curative in vivo at a dose of 20 mg/kg.

Table 3. In Vivo Activities of Compounds against *T. brucei brucei* Model and *T. b. rhodesiense* Model[a]

		T. brucei brucei (STIB 795 model)		*T. b. rhodesiense* (STIB 900 model)	
Compound	Dose mg/Kg	Cured/ Infected	Survival average (days)	Cured/ Infected	Survival average (days)
6a[b]	4 × 20 i.p.	4/4	>60	1/4	35.25
6c[b]	4 × 20 i.p.	ND	ND	0/4	7.25
6b	4 × 20 i.p.	0/4	5.25	ND	ND
6d	4 × 20 i.p.	4/4	>60	2/4	>38.5
6e	4 × 20 i.p.	0/4	18.3	ND	ND
Control (avrg)		0/4	7	0/4	6.5
Melarsoprol	4 × 1 i.p.	2/4	>60	0/4	21.25
	4 × 8 i.p.	ND	ND	4/4	>60
Pentamidine	4 × 5 i.p.	4/4	>60	ND	ND
	4 × 20	ND	ND	0/4	42.75

[a] The control represents the average of the controls for each experiments performed. [b] These data was presented previously,[12] but is included here for comparative purposes.

The compounds were also tested with *T. brucei rhodesiense* STIB 900 model in rodents, which is a more stringent test. For example, pentamidine, one of the drugs currently used for early stage HAT, was not able to cure this model at this dose. However, this model responds to melarsoprol, a drug currently in use for the treatment of the late stage. In the STIB 900 model, parasites appear to leave the vasculature system early so that drugs must penetrate extravascular compartments to effect radical cure. Therefore, this in vivo test represents a good model for evaluating likely outcomes of drugs in late-stage models.

As already described in our previous work,[12] compound **6a** was given intraperitoneally at 20 mg/kg for 4 days and cured only one mouse of four. However, the compound caused a significant increase in life span of the mice to 35 days compare to the 7 days for the untreated control animals. Pentamidine did not cure any of the four mice but increased the life span to 43 days.

Some compounds were also investigated for their in vivo activities in mice model infected with *T. cruzi*.

Table 4. In Vivo Activities against a Rodent Model of Chagas Disease for Some Selected Compounds

Compound	Dose mg/Kg	No of doses	Route	Survival Time	% inhibition
6c	15	5	i.p.	12.8	N. D.
6a	25	5	i.p.	13	N. D.
6d	50	5	i.p.	13	27.75
6e	50	5	i.p.	14	44.95
Control	-			13	0.00
Benznidazole	45	5	p.o.	>30	100.00

Although none of the compounds evaluated was able to cure the model mice, compounds **6d** and **6e** were able to reduce parasitaemia, the latter by 45%. Compound **6d** was investigated in a rodent model of leishmaniasis (*L. donovani*-infected mice). The compound had a moderate effect. When dosed at 40 mg/kg intraperitoneally for 5 days, there was 28% reduction in parasitaemia, compared to the control. With the standard drug, pentostam, there was a 62% reduction in parasitaemia compared to the control when dosed at 15 mg/kg for 5 days.

Mode of Action Studies. We have previously reported mode of action studies[12] and have repeated these studies now also including **6d** and the nitroimidazole benznidazole, too. Two possible mechanisms of action of the compounds are damage to DNA and oxidative damage.

First, to investigate damage to DNA, experiments were undertaken with a *T. brucei* mutant deficient in a DNA repair enzyme (RAD51). This mutant is compromised in its ability to repair double-stranded DNA breaks; thus, agents that induce such damage are more active against these mutants than against wild-type cells. Megazol (see Figure 3 for structure) is a heterocycle that exerts its mode of action by damage to DNA. Thus the RAD51$^{-/-}$ line was more susceptible than wild type to megazol[30] (Figure 3). However, compound **6a** showed similar activity against both the wild-type and RAD51$^{-/-}$, indicating that the mode of action does not involve damage to DNA in the same manner as megazol, although other types of DNA damage cannot be ruled out. Benznidazole has markedly lower activity against *T. brucei* in vitro than other compounds and shows no additional activity in the RAD51 deficient cell line. Compound **6d** shows a very similar profile to **6a**.

Nifurtimox (Figure 3) is another nitro heterocycle that is currently registered for treatment of Chagas disease and is being investigated for the treatment of melarsoprol refractory HAT. Nifurtimox is believed to act via oxidative stress.[31,32] Thus, culturing the *T. brucei* in the presence of *N*-acetylcysteine, which reduces free radical damage due to oxidative stress, antagonizes the mode of action of nifurtimox. This effect was not seen in the case of **6a** nor **6d**, suggesting that the main mode of action is not due to accumulation of high levels of reactive oxygen species within compartments that are targeted by *N*-acetylcysteine. More subtle effects associated with oxidative damage, however, cannot be ruled out.

Discussion

In this paper, we report results on a group of trypanocidal nitro heterocycles identified during work aiming to induce selective toxicity through selective uptake of compounds into *T. brucei* using nucleoside transporters. The compounds prepared were investigated for their ability to antagonize uptake of radiolabeled adenosine through the P2 transporter. This assay does not give proof that the compounds are internalized through the transporter, but does indicate that many of the compounds showed good affinity for the P2 transporter, as they compete with adenosine in binding to the transporter. However, there was no correlation between affinity for the P2 transporter and activity in vitro against intact parasites. In addition to this, there are no remarkable changes in the sensitivity when the in vitro activities against the *T. brucei brucei* model are compared with the activities against the *T. brucei brucei* knockout line (i.e., deficient in P2 transporter activity). Therefore, it is not possible to directly correlate the affinity of the P2 transporter and the trypanocidal activity. Passive diffusion or other transporters may be involved in the uptake of the compounds.[33] However, compound **8**, which lacked a melamine group and had poor affinity to the P2 transporter, showed weak activity against the parasites, suggesting that the melamine group is required for uptake, or else in interactions with enzymes involved in either activation or directly in the mode of action of the compounds. Future research should focus on learning more about roles of the melamine moiety.

Interestingly, **6c** showed poor affinity for the P2 transporter but marked in vitro activity against *T. brucei brucei* and *T. brucei rhodesiense*. In compound **6c**, all the hydrogen atoms on the amino group have been replaced by methyl groups. The lack of affinity of this compound for the P2 transporter could possibly be explained by a requirement for substrates of the P2 transporter to have an H-bond donor. Compound **6c** showed much higher solubility in a variety of solvents than other compounds, and this may allow rapid passive diffusion, which may account for high activity against the parasites. It is clear that the melamine moiety (with at least some NH bonds) is selectively concentrated within the parasite, but the route of uptake is not exclusively through the P2 transporter. This is important, since loss of the P2 transporter can induce resistance to drugs that enter cells exclusively via this route. The fact that other routes of uptake exist for the melamine nitroheterocycles means that resistance resulting from simple loss of the P2 transporter should not be an issue.

Some of the compounds prepared showed potent activity against *T. brucei rhodesiense*, of the same order as melarsoprol (**6a**, IC_{50} = 25 nM; **6b**, IC_{50} = 10 nM **6c**, IC_{50} = 3 nM; **6d**, IC_{50} = 18 nM; **6e**, IC_{50} = 53 nM; **6h**, IC_{50} = 240 nM, melarsoprol, IC_{50} = 6 nM). In addition, some of these compounds showed lower toxicity against mammalian (L6) cells than melarsoprol, although further work is required to show that these compounds would have better selectivity/therapeutic indices. Compound **6a** gave an IC_{50} value of 0.025 μM against *T. brucei rhodesiense*, which is 60-fold better than nifurtimox (1.5 μM) that is clinically in use against Chagas' disease[34] and in trial against melarsoprol refractory trypanosomiasis.[18,19]

We decided to investigate the roles of both the nitro group and the furan ring. The nitro group is a strong

Table 5. Activities[a] of Compounds against Wild Type, Wild-type with NAC and RAD51$^{-/-}$ Mutant *T. brucei*

Compound	6d	6a	megazol	nifurtimox	benznidazole
Wild-type (427)	0.08 ± 0.05	0.08 ± 0.03	0.12 ± 0.05	4.1 ± 1.7	116.3 ± 7.5
Wild-type (427) + NAC	0.09 ± 0.04	0.12 ± 0.05	0.13 ± 0.06	11.4 ± 5.2	116.3 ± 13.6
RAD51$^{-/-}$ mutant	0.07 ± 0.03	0.10 ± 0.02	0.04 ± 0.04	4.3 ± 1.6	114.2 ± 32

[a] Values are IC_{50} (μM).

electron-withdrawing group and also can be involved in the generation of free radicals. Replacement of the nitro with a hydrogen (**6f**) or by another electron-withdrawing group such as the nitrile (**6g**) led to an inactive compound, indicating the importance of the nitro group itself. Replacement of the nitrofuran with a nitrophenyl gave significant loss of activity. Even replacement of the oxygen with sulfur (**6h**) gave reduced activity, suggesting that perhaps the redox potential of the nitrofuran is important for the mode of action of these compounds.

Nitro heterocycles often work through free-radical mechanisms, so genotoxicity represents a main issue in the development of new trypanocidal nitro heterocyclic compounds. Megazol, a nitro heterocyclic compounds, was found to be mutagenic in mammalian cell tests[35] and also positive in the Ames test.[36] It has been found that the trypanocidal activity of megazol was related to its ability to induce mutations in DNA; trypanosomes deficient in their own DNA repair enzymes (the RAD51$^{-/-}$ line) are hypersensitive to this compound. However, the RAD51$^{-/-}$ line showed susceptibility similar to that of wild-type parasites to compound **6a**. This suggests that **6a** has a different mode of action to megazol. Another nitro heterocycle, nifurtimox (which is also positive in the Ames test[37]), appears to work by oxidative stress, as can be seen by antagonizing the compound with *N*-acetylcysteine. Compound **6a** was not antagonized by *N*-acetylcysteine, indicating that its mode of action is not by oxidative stress. These findings may indicate that the compounds do not work by damage to DNA or oxidative stress, both of which are implicated in positive Ames tests. Further studies are continuing in this area.

In addition to in vitro activity, several compounds retained trypanocidal effect in mice. Compounds **6a** and **6d** were able to cure mice infected with *T. brucei brucei* at a dose of 20 mg/kg for 4 days. It is noteworthy that addition of methyl groups to the melamine NH_2 groups reduces activity both in vitro and in vivo. Addition of one methyl group to one of the amino groups (**6d**) yields a compound with slightly better activity in vitro and activity is retained in vivo. However, addition of an extra methyl to the same nitrogen (**6e**) or a methyl to the other amino (**6b**) led to loss of activity in vivo at the dose tested. The fact that trypanocidal activity in each case was barely altered by the presence of the P2 transporter indicates that the relative activity of these compounds is not related to their ability to interact with that transporter. It is noteworthy that the most active compound in vitro, **6c**, was inactive in vivo at the dose tested, highlighting the role of pharmacokinetic issues, beyond simple antiparasite activity, on in vivo trypanocidal capability.

Compound **6a** was also tested with the more stringent *T. brucei rhodesiense* STIB 900; using the same treatment schedule, it cured only one of four animals infected with a mean survival of 35 days compare to the untreated controls that had a mean survival of 8 days.

The discovery that the nitro heterocycles were active against *T. brucei* regardless of the presence of the P2 transporter prompted us to test the compounds against other pathogenic trypanosomatids that do not possess this transporter. Considerable activity was noted against amastigote *T. cruzi* in vitro within mammalian cells. Several compounds were several-fold more active than the registered drug, nifurtimox, in vitro. However, all failed to cure mice in vivo, although some compounds also led to a reduction in parasitaemia in vivo, highlighting the lead status of these new molecules for use in Chagas therapy.

In the case of *Leishmania*, none of the compounds were particularly active against the intracellular amastigotes, except for compound **6d**. A modest activity was found for this compound in a rodent model of disease.

Conclusion

We have prepared some melamine-nitrofuran conjugates that have potent activity against *T. brucei rhodesiense* on the same order of magnitude as melarsoprol and that are significantly more active than nifurtimox, which is currently undergoing trials for HAT. Two of the compounds were able to cure an animal model of trypanosomiasis (*T. brucei brucei* STIB795) and one of the compounds was able to have a significant effect on the course of another model of infection (*T. brucei rhodesiense* STIB900). The fact that the mode of action of **6a** does not appear to involve DNA damage in trypanosomes might indicate that it will be not mutagenic in tests in mammalian cells, thus greatly improving the chances that this compound or its derivatives can proceed to clinical trials against trypanosomiasis. These compounds represent exciting new leads for further evaluation for HAT. Moreover, some compounds also showed considerable activity against *T. cruzi* in vitro and some reduction in parasitaemia in vivo, indicating that this class of molecule should also be considered as a lead in developing novel drugs against Chagas disease.

Experimental Section

P2 Transporter Affinity Measurements. Parasites purified from blood were stored on ice in Carter's buffered saline solution.[7] Transport assays used the centrifugation-through-oil technique, which is routinely used in analyses.[9,14,15,33,38] Radiolabeled adenosine (0.5 μM) uptake via P2 was measured in the presence of 1 mM inosine, which blocks the P1 transporter.[7] Compounds were assayed for affinity for the P2 transporter by using labeled adenosine fixed at 0.5 μM and a range of inhibitor concentrations. IC_{50} values were calculated using the Grafit 4.0 Software (Erithacus) by plotting inhibitory value against concentration of inhibitor.

In Vitro Activities against *T. brucei brucei and T. brucei rhodesiense* and Cytotoxicity. The activity of compounds was determined for *T. brucei rhodesiense* trypomastigotes of STIB900. This stock was isolated in 1982 from a human patient in Tanzania. Minimum essential medium (50 μL) supplemented with 2-mercaptoethanol and 15% heat-

inactivated horse serum[39] was added to each well of a 96-well microtiter plate. Serial drug dilutions were prepared covering a range from 90 to 0.123 μg/mL. Then, 50 μL of a trypanosome suspension was added to each well, and the plate incubated at 37 °C under a 5%CO_2 atmosphere for 72 h. Alamar Blue (10 μL) was then added to each well and incubation continued for a further 2–4 h. The plate was then read in a Spectramax Gemini XS microplate fluorometer (Molecular Devices Corp., Sunnyvale, CA) by using an excitation wavelength of 536 nm and an emission wavelength of 588 nm.[40] Fluorescence development was expressed as a percentage of the control, and the 50% inhibitory concentration (IC_{50}) values were determined. Cytotoxicity was assessed by using the same assay and rat skeletal myoblasts (L-6 cells).

To investigate whether transport of these compounds through the P2 transporter is necessary for activity, compounds were assayed against the *T. brucei brucei* trypomastigotes using either the wild type or P2 knockout mutants (*TbAT1*$^{-/-}$).[41] The Alamar Blue assay[40] was also used to determine IC_{50} values. To determine whether DNA damage was associated with trypanocidal activity, the Alamar Blue assay was also used to determine IC_{50} values against the *RAD51*$^{-/-}$ deletion mutant.[42]

In Vitro Activities against *Trypanosoma cruzi*. Rat skeletal myoblasts (L-6 cells) were seeded in 96-well microtiter plates at 2000 cells/well/100 μL in RPMI 1640 medium with 10% FBS and 2 mM L-glutamine. After 24 h, 5000 trypomastigotes of *T. cruzi* (Tulahuen strain C2C4 containing the β-galactosidase (Lac Z) gene) were added in 100 μL per well with 2× of a serial drug dilution. The plates were incubated at 37 °C in 5% CO_2 for 4 days. Then the substrate CPRG/Nonidet was added to the wells. The color reaction, which developed during the following 2–4 h, was read photometrically at 540 nm. From the sigmoidal inhibition curve IC_{50} values were calculated.

Activities against *L. donovani*. Mouse peritoneal macrophages were seeded in RPMI 1640 medium with 10% heat-inactivated FBS into Lab-tek 16 chamber slides. After 24 h *L. donovani* amastigotes were added at a ratio of 3:1 (amastigotes to macrophages). The medium containing free amastigotes was replaced by fresh medium 4 h later. The next day the medium was replaced by fresh medium containing different drug concentrations. The slides were incubated at 27 °C under a 5% CO_2 atmosphere for 96 h. When the medium was removed, the slides were fixed with methanol and stained with Giemsa. The ratio of infected to noninfected macrophages was determined microscopically, expressed as percentage of the control, and the IC_{50} value was calculated by linear regression.

In Vivo Biological Activity against *T. brucei*. Female NMRI mice weighting 22–25 g were infected with cryopreserved stabilates of *T. brucei brucei* STIB 795 (derivate of strain 427[43]) or *T. brucei rhodesiense* STIB 900. Each mouse was infected intraperitoneally with (2–4) × 10^4 bloodstream forms. Melarsoprol (Arsobal; Aventis) acted as standard drug and was diluted with sterile distilled water to an appropriate concentration. Groups of four mice were treated on days 3, 4, 5, and 6 intraperitoneally with 20 mg/kg. A control group remained untreated. The parasitemia of all animals was checked on day 7 and 10 postinfection and every second day thereafter until 60 days. Death of animals was recorded to calculate the mean survival time. Surviving and aparasitemic mice were considered cured at 60 days and then euthanized.

In Vivo Activity for *T. cruzi*. Female BALB/c mice weighing 20 g (Charles Rivers Ltd, UK) were infected intraperitoneally with 2 × 10^4 trypomastigotes in 0.2 mL, harvested from the blood of a passage mouse. Infected mice were randomly sorted into groups of five. After 5 days tail blood was examined for patency of infection: the number of trypomastigotes in 10 microscope field was noted. Dosing commenced for five consecutive days. Tail blood was examined 2 days after the end of treatment and at 7 day intervals on any surviving mice.

Chemistry. General. Chemicals were purchased from Aldrich and Fluka and were used without further purification. Dry solvents were generally purchased from Fluka in sure-seal bottles and stored over molecular sieves. Qualitative thin-layer chromatography (TLC) was performed on precoated aluminum sheets silica gel $60F_{254}$ from Merck. Melting points were determined with a Gallenkamp melting point apparatus and are not corrected. ^1H and ^{13}C NMR data were recorded on a Bruker Avance DPX 300 MHz NMR spectrometer, with tetramethylsilane as the internal standard and deuterated solvents purchased from Goss unless stated otherwise. Infrared (IR) spectra were recorded on a Perkin-Elmer 1600 FT-IR spectrometer. Mass Spectra were recorded at a Platform II mass spectrometer (Micromass) from Fisons. Ionization was achieved in the positive electrospray mode using a mixture of acetonitrile/water (1:1) or MeOH (HPLC grade) as mobile phase. High-resolution mass spectra were recorded by the National Mass Spectrometry Service Centre in Swansea with a MAT 900 XLT high resolution double focusing mass spectrometer from Finnigan using the same ionization procedure. Combustion analyses were performed by the analytical and chemical consultancy services MEDAC Ltd. The triazine derivatives, as observed in other work,[44] often present a problem in analysis. The problem was mainly found to be for the microanalysis of the nitrogen content.

5-Nitro-2-furaldehyde (4,6-Diamino)-[1,3,5]-triazin-2-ylhydrazone (6a). A mixture of **4a** (149.50 mg, 1.06 mmol) and 5-nitrofuraldehyde (150.00 mg, 1.06 mmol) was dissolved in methanol (5 mL). The suspension was left stirring overnight at room temperature. The reaction mixture was filtered and the yellow precipitate was washed with methanol and dried under vacuum at 40 °C. The crude product was recrystallized from water to get 100.5 mg of a pure yellow solid. Yield: 100.5 mg, 36%. mp: >350 °C. IR: ν_{N-H} 3313.9 cm^{-1}, $\nu_{C=N}$ 1631.9 cm^{-1}, ν_{C-NO_2} 1537.8 cm^{-1}, ν_{C-N} 809.3. LRMS (ES^+): *m/z* 265 (M + H^+, 100%), 287 (M + Na^+, 80%). HRMS (ES^+): calcd for $(C_8H_9N_8O_3)^+$ 265.0792, found 265.0799. ^1H NMR (300 MHz, DMSO-d_6): δ 6.51 (bs, 4H), 7.05 (d, J = 3.84) 7.78 (d, J = 3.84 Hz), 8.00 (s, 1H), 11.25 (s, 1H). ^{13}C NMR (75 MHz, DMSO-d_6): δ 114.2, 115.6, 129.4, 151.8, 153.2, 164.9, 167.7.

5-Nitro-2-furaldehyde (N^4,N^6-Dimethyl-4,6-diamino)-[1,3,5]-triazin-2-ylhydrazone (6b). Compounds **4b** (180 mg, 1.06 mmol) and 5-nitrofuraldehyde (142.5 mg, 1.06 mmol) were suspended in MeOH (10 mL). The suspension was left stirring overnight. The reaction was reduced under vacuum. The yellow solid was then recrystallized from H_2O/MeOH (50/50 mL). Yield: 220 mg, 71%. LRMS (ES^+): *m/z* 293.1 ((M + $H)^+$, 100%), 315.2 (M + Na^+, 20%). HRMS: calcd mass for $(C_{10}H_{13}N_8O_3)^+$ 293.1105, found 293.1104. ^1H NMR (300 MHz, DMSO-d_6): δ (mixture of the two geometric isomers) 3.36 (m, 6H), 7.05 (bs, 2H) 7.23 (bs, 1H), 7.78 (m, 1H), 11.06 (s, 1H), 11.20 (s, 1H). ^{13}C NMR (75 MHz, DMSO-d_6): δ (mixture of the two geometric isomers) 27.4, 27.6*, 113.9, 115.6, 129.0, 129.4*, 151.8, 153.3, 164.1, 166.4, 166.6*. Anal. ($C_{10}H_{12}N_8O_3 \cdot 0.4H_2O$) C, H, N.

5-Nitro-2-furaldehyde (N^4,N^4,N^6,N^6-Tetramethyl-4,6-diamino)-[1,3,5]-triazin-2-ylhydrazone (6c). A mixture of **4c** (201 mg, 1.01 mmol) and 5-nitro-2-furaldehyde (143 mg, 1.02 mmol) was dissolved in 10 mL of ethanol. The reaction mixture was allowed to stir overnight at room temperature and the solvent was evaporated under vacuum. The residue was purified by flash column chromatography (gradient from 1 to 5% MeOH/DCM). Compound **6c** was isolated as a clear white solid. Yield: 187 mg, 58%. HRMS: calcd mass for $(C_{12}H_{17}N_8O_3)^+$ 321.1424, found 321.1421. ^1H NMR (300 MHz, DMSO-d_6): δ 3.21 (s, 12H), 7.04 (m, 1H), 7.44 (m, 1H), 7.92 (s, 1H), 9.05 (bs, 1H). ^{13}C NMR (75 MHz, DMSO-d_6): δ 36.5, 111.1, 114.2, 129.4, 153.5, 164.1, 165.8.

5-Nitro-2-furaldehyde (N^4-Methyl-4,6-diamino)-[1,3,5]-triazin-2-ylhydrazone (6d). 5-nitrofuraldehyde (90 mg, 0.58 mmol) and **3d** (81.82 mg, 0.58 mmol) were mixed together and suspended in MeOH (5 mL), and the suspension was left stirring overnight. The mixture was reduced under vacuum, giving 120 mg of brown solid. The solid was recrystallized from

H_2O:MeOH (35 mL:20 mL), giving a dark yellow solid. Yield: 83 mg, 51%. Mp: 261–263 °C. LRMS (ES^+): *m/e* 279.2 ($M + H^+$, 50%), 301.1 ($M + Na^+$, 100%). HRMS: calcd mass for $(C_9H_{11}N_8O_3)^+$ 279.0949, found 279.0951. ^1H NMR (300 MHz, DMSO-d_6): δ 2.77 (s, 3H), 6.77 (bs, 3H), 7.07 (s, 1H), 7.78 (d, J = 4.02), 8.01 (s, 1H), 11.10 (s, 1H). ^{13}C NMR (75 MHz, DMSO-d_6): δ 27.6, 114.0, 115.6, 129.5, 151.8, 153.3, 166.9. Anal. ($C_9H_{10}N_8O_3 \cdot 0.4H_2O \cdot 0.02HCl$) C, H, Cl; calcd: N, 38.4. Found: N, 37.9.

5-Nitro-2-furaldehyde (N,$^4N^4$-Dimethyl-4,6-diamino)-[1,3,5]-triazin-2-ylhydrazone (6e). 5-Nitrofuraldehyde (246 mg, 99%, 1.45 mmol) and **3e** (204.56 mg, 1.45 mmol) were suspended in MeOH (5 mL) and left stirring overnight. The mixture was reduced under vacuum, giving 120 mg of brown solid. The solid was recrystallized from H_2O:MeOH (30 mL: 20 mL), giving a light brown solid. Yield: 336 mg, 80%. Mp: 264–266 °C. LRMS (ES^+): *m/z* 293.1 ($(M + H)^+$, 20%), 315.1 ($M + Na^+$, 100%). HRMS: calcd mass for $(C_{10}H_{13}N_8O_3)^+$ 293.1105, found 293.1110. ^1H NMR (300 MHz, DMSO-d_6): δ 3.11 (s, 6H), 6.75 (br s, 3H), 7.11 (d, 1H, J = 3.84), 7.82 (d, J = 3.84), 8.08 (s, 1H), 11.21 (s, 1H). ^{13}C NMR (75 MHz, DMSO-d_6): δ 36.1, 113.8, 115.6, 129.4, 151.8, 153.4, 164.5, 166.0, 167.5. Anal. ($C_{10}H_{12}N_8O_3 \cdot 0.02HCl$) C, H, N, Cl.

2-Furaldehyde (4,6-Diamino)-[1,3,5]-triazin-2-ylhydrazone (6f). A mixture of **4a** (150 mg, 1.06 mmol) and 2-furaldehyde (102.88 mg, 1.06 mmol) was suspended in MeOH (5 mL). The suspension was left stirring overnight at room temperature. The mixture was filtered and the brown solid was washed with methanol and then dried under vacuum at 40 °C. The crude product was recrystallized from H_2O/MeOH (5%) to give a pure brown solid. Yield: 133 mg, 58%. Mp: 281–283 °C. LRMS (ES^+): *m/z* 219 ($M + H)^+$, 241.9 ($M + Na)^+$. HRMS: calcd mass for $(C_8H_{10}N_7O)^+$ 220.0941, found 220.0941. ^1H NMR (300 MHz, DMSO-d_6): δ 6.38 (bs, 4H), 6.57 (m, 1H), 6.69 (d, J = 3.29 Hz, 1H), 7.76 (m, 1H), 7.94 (m, 1H), 10.56 (s, 1H). ^{13}C NMR (75 MHz, DMSO-d_6): δ 111.5, 112.2, 131.8, 144.3, 150.5, 165.0, 167.7.

5-Cyano-2-furaldehyde (4,6-Diamino)-[1,3,5]-triazin-2-ylhydrazone (6g). Compounds **4a** (98.7 mg, 0.70 mmol) and crude **5c** (85 mg, 0.70 mmol) were mixed together and suspended with MeOH (3 mL), and the suspension was left stirring overnight. The mixture was reduced under vacuum, giving a light brown solid. The solid was recrystallized from H_2O:MeOH (10 mL:15 mL), giving a light brown solid. Yield: 22 mg, 13%. Mp: >350 °C. IR: ν_{CN} 2229.7 cm^{-1}. LRMS (ES^+): *m/z* 245 ($(M + H)^+$, 100). HRMS: calcd mass for $(C_9H_9N_8O)^+$ 245.0894, found 245.0893. ^1H NMR (300 MHz, DMSO-d_6): δ 6.52 (bs, 4H), 6.96 (d, J = 3.76 Hz, 1H) 7.71 (d, J = 3.76 Hz, 1H), 8.04 (s, 1H), 10.95 (s, 1H). ^{13}C NMR (75 MHz, DMSO-d_6): δ 111.8, 112.3, 124.7, 125.5, 129.7, 155.3, 165.0, 167,7.

5-Nitrothiophene-2-carbaldehyde (4,6-Diamino)-[1,3,5]-triazin-2-ylhydrazone (6h). A mixture of **4a** (150 mg, 1.06 mmol) and 5-nitro-2-thiophenecarboxaldehyde (166.58 mg, 1.06 mmol) was suspended in methanol (5 mL). The suspension was left stirring for 2 days at room temperature. The reaction mixture was filtered and the brown precipitate was washed with MeOH and then dried under vacuum at 40 °C. The crude product was recrystallized from water and ethanol (5:1) to give a pure brown solid. Yield: 75.7 mg, 25%. Mp: >350 °C. LRMS (ES^+): *m/z* 281 ($(M + H)^+$, 100%), 303 ($(M + Na)^+$, 10%). HRMS (ES^+): calcd mass for $(C_8H_9N_8O_2S)^+$ 281.0569, found 281.0572. ^1H NMR (300 MHz, DMSO-d_6): δ 6.50 (br s, 4H), 7.36 (d, J = 4.29 Hz, 1H), 8.08 (d, J = 4.29 Hz, 1H), 8.25 (s, 1H), 11.10 (s, 1H). ^{13}C NMR (75 MHz, DMSO-d_6): δ 127.6, 131.1, 134.9, 148.7, 149.7, 164.8, 167.6.

Thiophene-2-carbaldehyde (4,6-Diamino)-[1,3,5]-triazin-2-ylhydrazone (6i). A mixture of **4a** (150 mg, 1.06 mmol) and 2-thiophenecarboxaldehyde (121.31 mg, 1.06 mmol) was suspended in methanol (5 mL). The suspension was left stirring overnight at room temperature. The mixture was filtered and the brown solid was washed with methanol and dried under vacuum at 40 °C. The crude product was recrystallized from water–ethanol (10%) to give a pure brown-yellow solid. Yield: 95 mg, 38%. Mp: 309–310 °C. LRMS (ES^+): *m/z* 236 ($(M + H)^+$, 100%). HRMS (ES^+): calcd mass for $(C_8H_{10}N_7S)^+$ 236.0713, found 236.0717. ^1H NMR (300 MHz, DMSO-d_6): δ 6.38 (br s, 4H), 7.07 (m, 1H), 7.25 (m, 1H), 7.53 (m, 1H), 8.25 (s, 1H), 10.53 (s, 1H). ^{13}C NMR (75 MHz, DMSO-d_6): δ 127.6, 127.9, 129.1, 137.3, 140.2, 164.9, 167.6. Anal. ($C_8H_9N_7S \cdot 0.7H_2O$) C, H, N, S.

4-Nitrobenzaldehyde (4,6-diamino)-[1,3,5]-triazin-2-ylhydrazone (7a). Compounds **4a** (328.23 mg, 2.32 mmol) and **iv-a** (357.75 mg, 98%, 2.32 mmol) were suspended in MeOH (5 mL), and the suspension was left stirring overnight. The mixture was reduced under vacuum, giving a yellow solid. The solid was recrystallized from H_2O:MeOH (120 mL:200 mL), giving a yellow solid. Yield: 493 mg, 77%. Mp: 321–322 °C. LRMS (EI): *m/z* 274 (M^+, 100%). HRMS: calcd mass for $(C_{10}H_{11}N_8O_2)^+$ 275.0999, found 275.1004. ^1H NMR (300 MHz, DMSO-d_6) δ 6.50 (br s, 4H), 7.86 (d, 2H, J = 8.78), 8.18 (s, 1H), 8.28 (d, J = 8.78 Hz, 1H), 10.98 (s, 1H). ^{13}C NMR (75 MHz, DMSO-d_6) δ 124.4, 127.3, 139.3, 142.0, 147.3, 165.1, 167.7. Anal. ($C_{10}H_{10}N_8O_2 \cdot 1.1H_2O \cdot 0.03HCl$) C, N, Cl calcd: H, 4.2. Found: H, 3.4.

3-Nitrobenzaldehyde (4,6-Diamino)-[1,3,5]-triazin-2-ylhydrazone (7b). Compounds **4a** (331.6 mg, 2.35 mmol) and **iv-b** (358.71 mg, 98%, 2.35 mmol) were suspended in MeOH (5 mL), and the suspension was left stirring overnight. The mixture was reduced under vacuum, giving a green solid. The solid was recrystallized from H_2O:MeOH (170 mL:50 mL), giving a light green solid. Yield: 83 mg, 13%. Mp: > 345 °C. LRMS (EI): *m/z* 274 (M^+, 100%). HRMS: calcd mass for $(C_{10}H_{11}N_8O_2)^+$ 275.0999, found 275.0999. ^1H NMR (300 MHz, DMSO-d_6): δ 6.50 (bs, 4H), 7.72 (m, 1H), 8.01 (d, 1H), 8.20 (m, 2H), 8.47 (s, 1H), 10.85 (s, 1H). ^{13}C NMR (75 MHz, DMSO-d_6): δ 120.0, 123.3, 130.7, 133.3, 137.4, 139.4, 148.6, 165.2, 167,7.

2-Nitrobenzaldehyde (4,6-Diamino)-[1,3,5]-triazin-2-ylhydrazone (7c). Compounds **4a** (328.23 mg, 2.32 mmol) and **iv-c** (357.75 mg, 98%, 2.32 mmol) were suspended in MeOH (5 mL), and the suspension was left stirring overnight. The mixture was reduced under vacuum, giving a yellow solid. The solid was recrystallized from H_2O:MeOH (120 mL:80 mL,) giving a yellow solid. Yield: 107 mg, 17%. Mp: 288–291 °C. LRMS (EI): *m/z* 274 (M^+, 100%). HRMS: calcd mass for $(C_{10}H_{11}N_8O_2)^+$ 275.0999, found 275.1001. ^1H NMR (300 MHz, DMSO-d_6): δ 6.45 (bs, 4H), 7.62 (m, 1H), 7.78 (m, 1H), 8.09 (m, 2H), 8.48 (m, 1H), 10.98 (s, 1H). ^{13}C NMR (75 MHz, DMSO-d_6): δ 124.9, 127.8, 129.8, 129.9, 133.7, 136.5, 147.9, 165.2, 167,7.

Acknowledgment. We would like to acknowledge the Welsh School of Pharmacy (A.B.), the Wellcome Trust (G.J., M.S.), and the UNDP/World Bank/WHO Special Program for Research and Training in Tropical Diseases (R.B.) for funding. We also would like to acknowledge the EPSRC National Mass Spectrometry Service Centre for the accurate mass spectroscopy.

Supporting Information Available: Experimental procedures and spectral data for compounds **2–5** and microanalytical data. This material is available free of charge via the Internet at http://pubs.acs.org.

References

(1) http://www.who.int/tdr
(2) Barrett, M. P.; Fairlamb, A. H. The biochemical basis of arsenical-diamidine crossresistance in African trypanosomes. *Parasitol. Today* **1999**, *15*, 136–140.
(3) Maeser, P.; Luescher, A.; Kaminsky, R. Drug transport and drug resistance in African trypanosomes. *Drug Resistance Updates* **2003**, *6*, 281–290.
(4) Barrett, M. P.; Burchmore, R. J.; Stich, A.; Lazzari, J. O.; Frasch, A. C.; Cazzulo, J. J.; Krishna, S. The trypanosomiases. *Lancet* **2003**, *362*, 1469–80.
(5) Herwaldt, B. L. Leishmaniasis. *Lancet* **1999**, *354*, 1191–1199.
(6) Croft, S. L.; Yardley, V. Chemotherapy of Leishmaniasis. *Curr. Pharm. Des.* **2002**, *8*, 319–342.
(7) Carter, N. S.; Fairlamb, A. H. Arsenical-resistant trypanosomes lack an unusual adenosine transporter. *Nature* **1993**, *361*, 173–176.

(8) Landfear, S. M.; Ullman, B.; Carter, N. S.; Sanchez, M. A. Nucleoside and nucleobase transporters in parasitic protozoa. *Eukaryot. Cell.* **2004**, *3*, 245–254.
(9) De Koning, H. P.; Jarvis, S. M. Adenosine transporters in bloodstream forms of *Trypanosoma brucei brucei*: Substrate recognition motifs and affinity for trypanocidal drugs. *Mol. Pharmacol.* **1999**, *56*, 1162–1170.
(10) Carter, N. S.; Berger, B. J.; Fairlamb, A. H. Uptake of diamidine drugs by the P2 nucleoside transporter in Melarsen-sensitive and -resistant *Trypanosoma brucei brucei*. *J. Biol. Chem.* **1995**, *270*, 28153–28157.
(11) Brun, R.; Schumacher, R.; Schmid, C.; Kunz, C.; Burri, C. The phenomenon of treatment failures in human African trypanosomiasis. *Trop. Med. Int. Health* **2001**, *6*, 906–914.
(12) Stewart, M. L.; Jimenez Bueno, G.; Baliani, A.; Klenke, B.; Brun, R.; Brock, J. M.; Gilbert, I. H.; Barrrett, M. P. Trypanocidal activity of melamine-based nitroheterocycles. *Antimicrob. Agents Chemother.* **2004**, *48*, 1733–1738.
(13) Goldberg, B.; Rattendi, D.; Llyod, D.; Sufrin, J. R.; Bacchi, C. J. Effects of intermediates of methionine metabolism and nucleoside analogues on A-adenosylmethionine transport by *Trypanosoma brucei brucei* and a drug resistant *Trypansoma brucei rhodesiense*. *Biochem. Pharmacol.* **1998**, *56*, 95–103.
(14) Tye, C.-K.; Kasinathan, G.; Barrett, M. P.; Brun, R.; Doyle, V. E.; Fairlamb, A. H.; Weaver, R.; Gilbert, I. H. An approach to use an unusual adenosine transporter to selectively deliver polyamine analogues to trypanosomes. *Bioorg. Med. Chem. Lett.* **1998**, *8*, 811–816.
(15) Klenke, B.; Stewart, M.; Barrett, M. P.; Brun, R.; Gilbert, I. H. Synthesis and Biological Evaluation of s-Triazine Substituted Polyamines as Potential New Anti-Trypanosomal Drugs. *J. Med. Chem.* **2001**, *44*, 3440–3452.
(16) Muller, S.; Coombs, G. H.; Walter, R. D. Targeting polyamines of parasitic protozoa in chemotherapy. *Trends Parasitol.* **2001**, *17*, 242–249.
(17) Marton, L. J.; Pegg, A. E. Polyamines as targets for therapeutic intervention. *Annu. Rev. Pharmacol.* **1995**, *35*, 55–91.
(18) Legros, D.; Ollivier, G.; Gastellu-Etchegorry, M.; Paquet, C.; Burri, C.; Jannin, J.; Buscher, P. Treatment of human African trypanosomiasis – present situation and needs for research and development. *Lancet Infect. Dis.* **2002**, *2*, 437–440.
(19) Pepin, J.; Milord, F.; Meurice, F.; Ethier, L.; Loko, L.; Mpia, B. High-dose nifurtimox for arseno-resistant *Trypanosoma brucei gambiense* sleeping sickness: An open trial in central Zaire. *T. R. Soc. Trop. Med. H.* **1992**, *86*, 254–256.
(20) Purohit, V.; Basu, A. K. Mutagenicity of Nitroaromatic Compounds. *Chem. Res. Toxicol.* **2000**, *13*, 673–692.
(21) Korbelik, M.; Horvat, D. The mutagenicity of nitroaromatic drugs: effect of metronidazole after incubation in hypoxia in vitro. *Mutat. Res* **1980**, *78*, 201–207.
(22) Goi, M. Reactivities of cyanuric chloride derivatives. I. Displacement reactions of substituted 2,4-bis(anilino)-6-chloro-s-triazines with benzylamine. *Yuki Gosei Kagaku Kyokaishi* **1960**, *18*, 327–331.
(23) de Hoog, P.; Gamez, P.; Driessen, W. L.; Reedijk, J. New polydentate and polynucleating N-donor ligands from amines and 2,4,6-trichloro-1,3,5-triazine. *Tetrahedron Lett.* **2002**, *43*, 6783–6786.
(24) Goi, M. Reactivities of cyanuric chloride derivatives. II. Displacement reactions of 2-chloro-4-substituted 6-anilino-s-triazines with benzylamine. *Yuki Gosei Kagaku Kyokaishi* **1960**, *18*, 332–336.
(25) Diels, O. Zur Kenntnis der Cyanurverbindungen. *Ber. Dtsch. Chem. Ges.* **1899**, *32*, 691–702.
(26) H. Koopman, J. D. Investigation on Herbicides I. 2-(substituted amino)-4,6-dichloro-1,3,5-triazines. *Recl. Trav. Chim. Pays-Bas* **1958**, *77*, 235–240.
(27) Simmonds, R. J.; Stevens, M. F. G. Triazines and Related Products 0.25. Methods for the Attachment of Sugar Residues to Cyto-Toxic 1,3,5-Triazines. *J. Chem. Soc., Perkin Trans. 1* **1982**, 1821–1825.
(28) Talukdar, S.; Hsu, J. L.; Chou, T. C.; Fang, J. M. Direct transformation of aldehydes to nitriles using iodine in ammonia water. *Tetrahedron Lett.* **2001**, *42*, 1103–1105.
(29) Omura, K.; Swern, D. Oxidation of alcohols by "activated" dimethyl sulfoxide. A preparative, steric and mechanistic study. *Tetrahedron* **1978**, *34*, 1651–1660.
(30) Enanga, B.; Ariyanayagam, M. R.; Stewart, M. L.; Barrett, M. P. Activity of megazol, a trypanocidal nitroimidazole, is associated with DNA damage. *Antimicrob. Agents Chemother.* **2003**, *47*, 3368–3370.
(31) Docampo, R.; Stoppani, A. O. M. Generation of superoxide anion and hydrogen peroxide induced by nifurtimox in *Trypanosoma cruzi*. *Arch. Biochem. Biophys.* **1979**, *197*, 317–321.
(32) Moreno, S. N. J.; Mason, R. P.; Docampo, R. Reduction of nifurtimox and nitrofurantoin to free radical metabolites by rat liver mitochondria. Evidence of an outer membrane-located nitroreductase. *J. Biol. Chem.* **1984**, *259*, 6298–6305.
(33) De Koning, H. P. Uptake of pentamidine in *Trypanosoma brucei brucei* is mediated by three distinct transporters: Implications for cross-resistance with arsenicals. *Mol. Pharmacol.* **2001**, *59*, 586–592.
(34) Rodriques Coura, J.; de Castro Solange, L. A critical review on Chagas disease chemotherapy. *Mem. I. Oswaldo Cruz* **2002**, *97*, 3–24.
(35) Poli, P.; de Mello, M. A.; Buschini, A.; Mortara, R. A.; de Albuquerque, C. N.; da Silva, S.; Rossi, C.; Zucchi, T. Cytotoxic and genotoxic effects of megazol, an anti-Chagas' disease drug, assessed by different short-term tests. *Biochem. Pharmacol.* **2002**, *64*, 1617–1627.
(36) Ferreira, R. C.; Ferreira, L. C. CL 64,855, a potent anti-*Trypanosoma cruzi* drug, is also mutagenic in the Salmonella/microsome assay. *Mem. I. Oswaldo Cruz* **1986**, *81*, 49–52.
(37) Nagel, R.; Nepomnaschy, I. Mutagenicity of 2-antichagasic drugs and their metabolic deactivation. *Mutat. Res.* **1983**, *117*, 237–242.
(38) Barrett, M. P.; Fairlamb, A. H.; Rousseau, B.; Chauviere, G.; Perie, J. Uptake of the nitroimidazole drug megazol by African trypanosomes. *Biochem. Pharmacol.* **2000**, *59*, 615–620.
(39) Baltz, T.; Baltz, D.; Giroud, C.; Crockett, J. Cultivation in a semi-defined medium of animal infective forms of *Trypanosoma brucei*, *T. equiperdum*, *T. evansi*, *T. rhodesiense* and *T. gambiense*. *EMBO J.* **1985**, *4*, 1273–1277.
(40) Raz, B.; Iten, M.; Grether-Buhler, Y.; Kaminsky, R.; Brun, R. The Alamar Blue assay to determine drug sensitivity of African trypanosomes (*T.b. rhodesiense* and *T.b. gambiense*) in vitro. *Acta Tropica* **1997**, *68*, 139–147.
(41) Matovu, E.; Stewart, M. L.; Geiser, F.; Brun, R.; Maeser, P.; Fallace, L. J. M.; Burchmore, R. J.; Enyaru, J. C. K.; Barrett, M. P. Mechanisms of arsenical and diamidine uptake and resistance in *Trypanosoma brucei*. *Eukaryotic Cell* **2003**, *2*, 1003–1008.
(42) McCulloch, R.; Barry, J. D.; A role for RAD51 and homologous recombination in *Trypanosoma brucei* antigenic variation. *Gene Dev.* **1999**, *13*, 2875–2888.
(43) Cunningham, M. P.; Vickerman, K. Antigenic analysis in the *Trypanosoma brucei* group, using the agglutination reaction. *T. R. Soc. Trop. Med. H.* **1962**, *56*, 48–59.
(44) Shaefer C.; Dagfrid H. H.; Thurston, T. J. D., J. R. Cyanuric Chloride Derivatives. I. Aminochloro-s-triazines. *J. Am. Chem. Soc.* **1951**, *73*, 2981–2983.

JM050177+